

**First International Meeting
on
Wind Turbine Noise: Perspectives for Control
Berlin 17th and 18th October 2005**

**PERFORMANCE AND NOISE FROM A
WALL-MOUNTED WIND MILL DRIVING A
REFRIGERATOR/HEAT PUMP UNIT**

K. Asfar , H. Radaydeh, and B. Shaddad
Department of Mechanical Engineering
Jordan University of Science and Technology
P.O.Box 3030
Irbid – Jordan
E-Mail: kasfar@just.edu.jo

ABSTRACT

A six-blade wind turbine, four-meters in diameter, is wall mounted on top of a 11-m high residential building. The power obtained from this wind mill is used to drive a compressor of a vapor-compression cycle refrigerator/heat pump. The idea behind this system is that this unit accepts the variability in wind power delivered to the compressor. The unit uses refrigerant R134a as the working fluid. The evaporator of the unit is housed in an insulated room to provide cooling. The condenser of the unit is housed in another insulated compartment in order to provide heating. The unit performance and noise generated from this unit for varying wind speeds is studied to evaluate the effect of generated noise on residents and environment. The unit was found to have a high overall coefficient of performance and acceptable noise levels.

INTRODUCTION

The present work deals with a wind mill system proposed for residential areas. It is hard for engineers to find an empty lot in those areas where conventional steel-tower-mounted wind mills could be erected. Hence, a wall-mounted system is proposed to be installed on roof tops or walls of buildings. Such system can be installed on top of buildings where enough wind is available to operate the wind mill. The preferred installation site is on the rim of the

external wall found on most concrete-walled buildings (normally one meter high above the roof level). In this paper, a six-blade wind turbine, four-meters in diameter, is wall mounted on top of an 11-m high residential building, Figure 1. This proposed technique has several advantages such as: the low cost of construction (no expensive steel tower is needed), saving of farmland for agricultural purposes, and the close distance from the power generation site to the power consumption site. The mechanical power obtained from this wind mill is used to drive a compressor of a vapor-compression cycle refrigerator/heat pump unit. It can be used also for generating electric power when needed. The idea behind this system is that this unit accepts the variability in wind power delivered to the compressor. If strong wind blows the compressor will deliver more of the compressed vapor to the condenser. If wind speed decreases, less vapor is delivered. Hence, there is no harm in fluctuating wind speed as opposed to the electric power generation which requires more or less a sustained wind speed or a complex control circuit to stabilize the output.

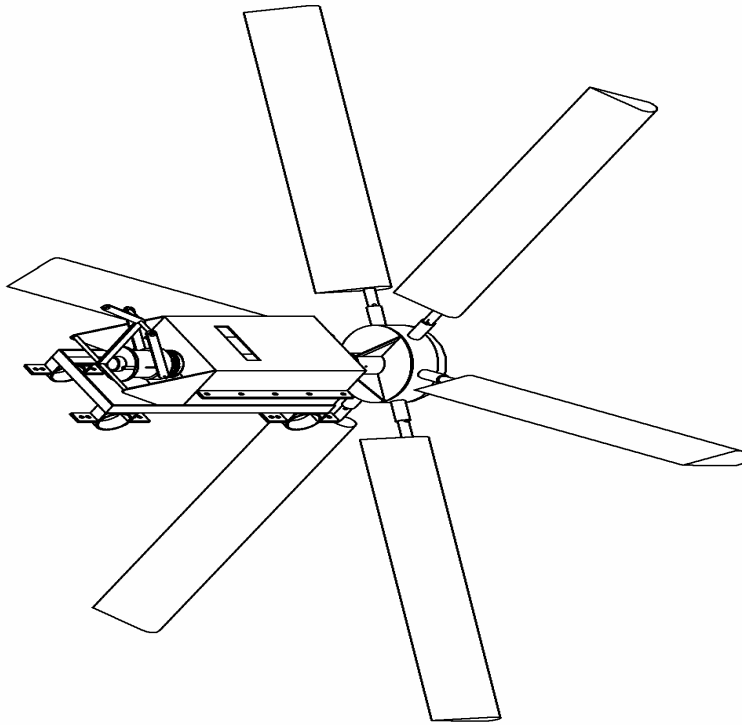


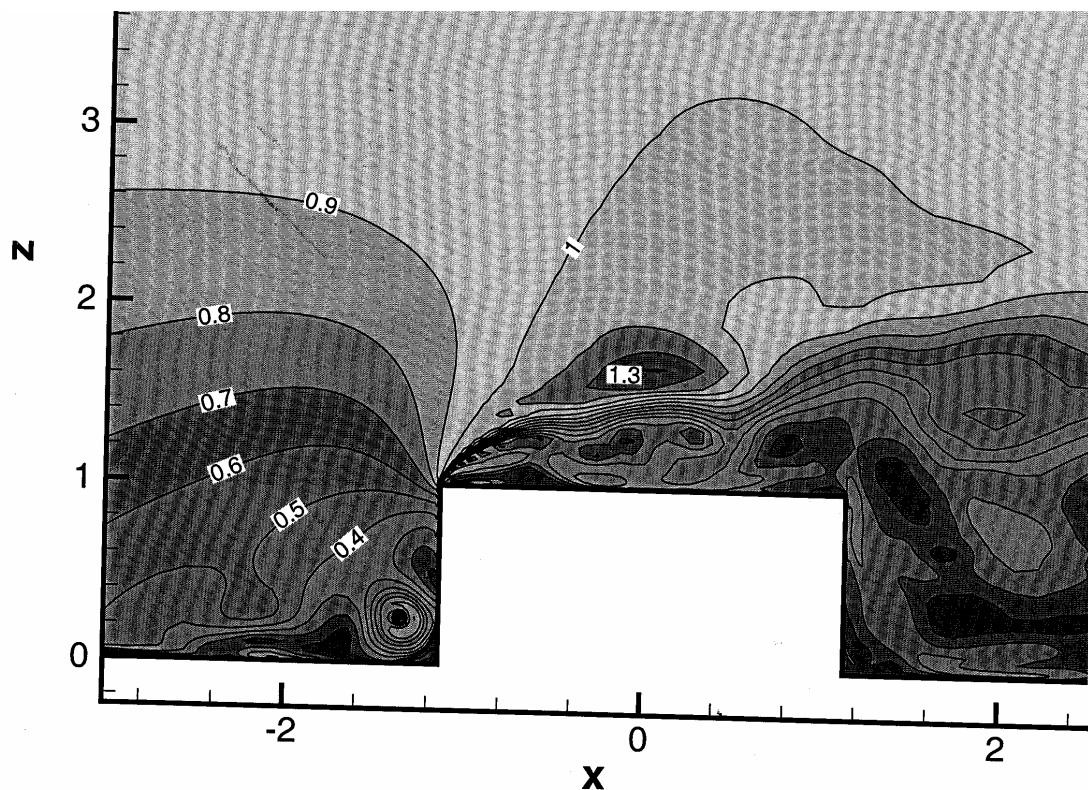
Figure 1. An isometric view of the wall-mounted wind mill.

The unit uses refrigerant R134a as the working fluid. The evaporator of the unit is housed in an insulated room to provide cooling. The condenser of the unit is housed in another insulated compartment in order to provide heating. This configuration is reserved only for experimental purposes. If the setup is meant to be used only as a refrigerator, the condenser unit is installed in the open air so that the wind takes care of the cooling of the condenser. The evaporator in this case is kept in the compartment to be cooled. Thermocouples and indicators are

provided for each compartment. The compressor of the unit used is similar to compressors used in automotive applications due to the fact that it is designed to accommodate variable speed power input coming from an engine. The unit performance and noise generated from this unit for varying wind speeds is studied to evaluate the effect of generated noise on residents. The unit was found to have a high overall coefficient of performance and acceptable noise levels. Emphasis in this paper will be on noise generation and measurement.

WIND FLOW SIMULATION

Wind velocity contours around a cubic building were obtained by computational fluid dynamics simulation and showed the possibility of mounting wind mills on walls of buildings at a location similar to the site of the experiment without sacrificing much reduction in wind power. This is shown in Figure 2. It is clear from the simulation that it is feasible to install a wind mill on top of the walled-roof of a building facing the wind.



In this case, the plane of the rotor should be away from the wall by a small distance. This way, the upper half of the rotor is completely "in" the wind while the other half is in the area backed by the wall. As is obvious from the simulation, the wind speed in this region is slightly reduced due to the blockage effect of the building. The figure also shows the possibility of installing a tower on top of the building, if desired, to increase the effectiveness of the wind mill. In this case, the tower has to be quite high in order to obtain a satisfactory performance. This is a

much more expensive option although from the point of view of noise it is a desirable option.

WIND TURBINE NOISE

The noise generated by wind turbines is from two sources. One is the aerodynamic noise caused by the movement of the rotor blades relative to the air, and would commonly be described as a 'swish'. This noise is largely unavoidable. It relates to the shape of the blades, and increases with wind speed and turbulence. Aerodynamic noise is not audible over long distances and as wind speed increases, is drowned by the noise of the wind itself. This type of noise is not a major cause of complaints. The second type is mechanical noise caused by the operation of the gearbox within the turbine. This category also encompasses the noise of electrical equipment in the generator. Complaints occur about the persistent tonal quality of this type of noise presumably as a result of the operation of the gears. Careful design, siting, and operation and the use of acoustic enclosures and gearless turbines continue to mitigate the impact of mechanical noise. For the proposed system and application, a third part comes into the scene. It is the aerodynamic noise generated by wind blowing past buildings. This type can vary considerably with wind direction. Sometimes, the slight change in wind direction results in a sizeable increase or decrease in the background noise due to wind-structure interaction.

In the current system, no gear box is used. Instead, a pulley system and belt is adopted since it has a quieter operation. The only source of mechanical noise is the compressor (generator) which is used in the system as a power absorption unit.

NOISE MEASUREMENTS

The location of the wind mill was chosen to face the prevalent wind direction (western wind) on top of a building (11 meters high). The average wind speed in the area is 5 m/sec. The noise measurement was taken at a point 4 meters behind the wind mill and at a 30 cm. Height from the floor (the wall height on which the wind mill was installed) is 1 meter. This point was chosen such that we minimize the noise generated from direct wind effect on the microphone. The measuring instrument was a portable sound level meter (B&K). A wind screen is also used with the device. For every test, the background noise is first measured without the windmill rotation. The blades are rotated to be aligned with the wind. Next, the blades are put back to its power position and measurements are taken. Each test is carried out as long as the wind speed is nearly constant. Later on, various data points are matched (the background noise and the total noise for the same wind speed. Many points had to be taken in order to be able to do a good job in matching. The mechanical noise of the compressor and the rotating parts

is found by subtracting the background noise from the total noise. The following table (Table 1) shows the relationship between the average wind speed (meter/second) and the generated noise (in dB).

Table 1. Noise levels behind the wind mill.

Average Wind Speed	Total Noise level	Corrected Windmill Noise Level
3	45	44
4	48	46
5	53	51
6	58	55
7	63	60

Measurements inside the building were made directly in the room below the roof using the same sound level meter. Readings were on the average lower than the above values by about 10 dB. The roof is insulated thermally by a 5-cm layer of poly Urethane- cement mix which acts as an acoustic absorber as well.

CONCLUDING REMARKS

We have shown in this work the feasibility of installing wind mills on top of buildings and using the generated mechanical power for operating a refrigerator/heat pump unit directly. The advantages of the proposed setup are numerous such as low cost, reliability,....etc. On the other hand, noise from this installation is within acceptable limits and can be reduced further by proper design of the setup.

References:

[1] Cheremisinoff, Nicholas P., Fundamentals of Wind Energy. Ann Arbor: Ann Arbor Science Publishers, Inc. 1978.

[2] J. Shigley, C. Mischke, and E. Budynas, "Mechanical Engineering Design" 7th. Edition ,2001.

[3] Robert L. Mott " Machine Elements In Mechanical Design" ,Third Edition, Prentice Hall, 1999..

[4] S. Kalpakjian, and S. Schmidt "Manufacturing Engineering and Technology" Fourth Edition, November, 2000.

[5] R. C. Hibbeler " Engineering Mechanics Dynamics", Ninth Edition, Prentice Hall, New Jersey, 2001.

[6] Dunn P. Peter ," Renewable Energies: Conversion and Application" (IEE energy series).

First International Meeting on Wind Turbine Noise: Perspectives for Control Berlin 17th and 18th October 2005

Regulation of Wind Turbine Noise in the Western United States

Mark Bastasch
CH2M HILL
825 NE Multnomah St.
Suite 1300
Portland, OR 97232
USA
Mark.Bastasch@ch2m.com

Introduction

The United States does not have federally enforceable environmental noise requirements and only a few states have noise regulations. Therefore, the noise requirements of commercial-scale energy projects, including wind farms, may vary from one jurisdiction to another. The permitting process which imposes noise requirements also varies from state to state. For example, large renewable and fossil fueled projects in Oregon require a permit from the State and undergo a detailed environmental review by the State. Other states, like California and Washington, do not require a state permit for renewable energy projects; the local jurisdiction (city or county) is the lead permitting agency. At least one state, Oregon, recently revised its noise requirements to specifically address noise from wind farms. The substantive acoustical requirements for commercial scale wind projects in the Western United States will be discussed briefly. The goal of this paper is not a critical assessment of various noise regulations; rather it is to present the varying regulatory requirements.

Federal Environmental Noise Policy

The National Environmental Policy Act of 1969 (NEPA)¹, requires “Federal agencies to include in their decision-making processes appropriate and careful consideration of all environmental effects of proposed actions, analyze potential environmental effects of proposed actions and their alternatives for public understanding and scrutiny, avoid or minimize adverse effects of proposed actions, and restore and enhance environmental quality as much as possible.” NEPA requires an Environmental Impact Statement (EIS) be prepared when “The Federal action may directly or through induced development have a significant adverse effect upon local ambient air quality, *local ambient noise levels*, surface water or groundwater quality or quantity, water supply, fish, shellfish, wildlife, and their natural habitats.” It is important to note that NEPA does not specify a threshold for “significant adverse effect” for noise and that NEPA is only triggered when there is a “federal action” such as the issuance of a federal permit.

While there are no federal regulations that limit overall environmental noise levels, there are federal guidance documents that address environmental noise and regulations for specific sources (for example, aircraft or federally funded highways).

The only energy facility specific requirements are those of the Federal Energy Regulatory Commission (FERC) which regulates interstate electrical transmission lines, natural gas, and petroleum pipelines. The FERC limits specifically address compressor facilities associated with pipelines under its jurisdiction and limits the noise to 55 dBA Day-Night Level (DNL) in noise sensitive areas².

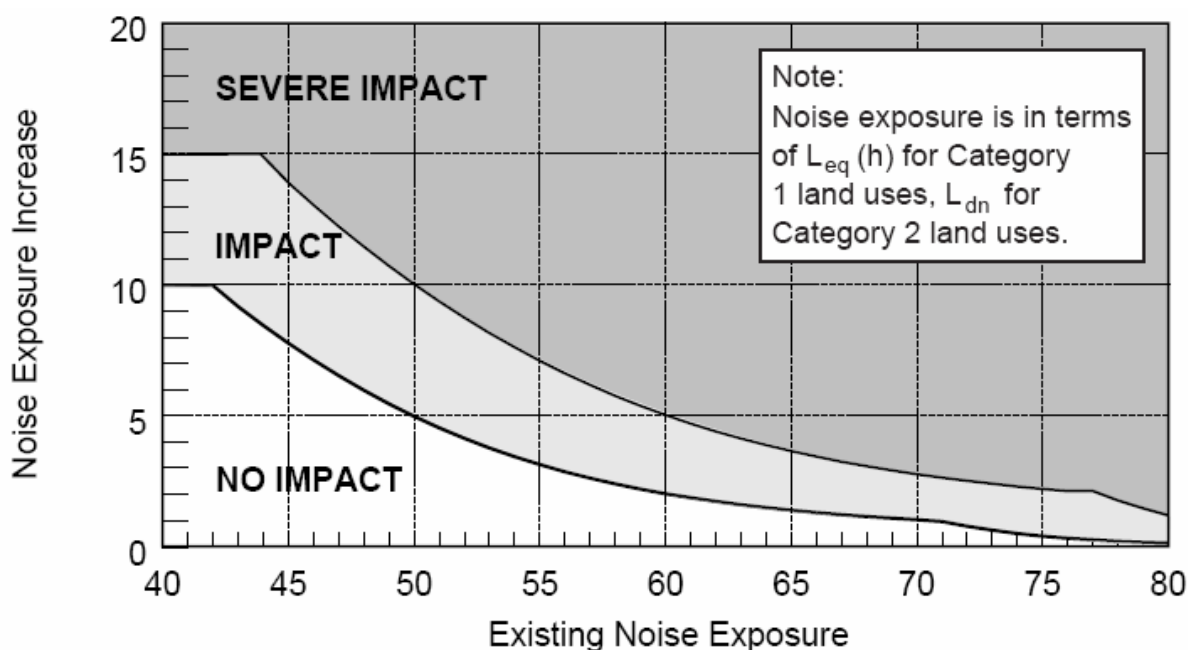
There are also federal highway and aircraft guidelines/regulations established by the Federal Highway Administration (FHWA)³ and Federal Aviation Administration (FAA)⁴ respectively. A summary of federal guidelines/regulations is presented in Table 1.

TABLE 1
Summary of Federal Guidelines/Regulations for Exterior Noise (dBA)

Agency	L_{eq}	DNL
Federal Energy Regulatory Commission (FERC)	[49]	55
Federal Highway Administration (FHWA)	67	[67]
Federal Aviation Administration (FAA)	[59]	65
U.S. Department of Transportation—Federal Rail and Transit Authorities (FRA & FTA) ^{5,6}	Sliding scale, refer to Figure X	Sliding scale, refer to Figure X
U.S. Environmental Protection Agency (EPA) ⁷	[49]	55
U.S. Department of Housing and Urban Development (HUD) ⁸	[59]	65

Note: Brackets [59] indicate calculated equivalent standard. Because FHWA regulates peak noise level, the DNL is assumed equivalent to the peak noise hour.

FIGURE 1
FRA & FTA Allowable Increase in Cumulative Noise Level.
(Note: Residential uses are included in Category 2)



Bureau of Land Management Programmatic EIS

The U.S. Department of the Interior (DOI), Bureau of Land Management (BLM) is the federal agency charged with managing federal public lands and is responsible for the development of wind energy resources on BLM-administered lands. Approximately 500 megawatts (MW) of wind energy is currently installed on federal public lands administered by the BLM. The BLM recently prepared a programmatic EIS in accordance with the requirements of NEPA to establish a “Wind Energy Development Program”⁹. Several key findings/statements relevant to assessing noise impacts of a wind project are quoted below:

- At many wind energy project sites on BLM-administered lands, large fluctuations in broadband noise are common, and even a 10-dB increase would be unlikely to cause an adverse community response.
- For a typical rural environment, background noise is expected to be approximately 40 dB(A) during the day and 30 dB(A) at night (Harris 1979), or about 35 dB(A) as DNL (Miller 2002).
- The EPA guideline recommends a day-night sound level (L_{dn}) of 55 dB(A) to protect the public from the effect of broadband environmental noise in typically quiet outdoor and residential areas (EPA 1974). This level is not a regulatory goal but is “intentionally conservative to protect the most sensitive portion of the American population” with “an additional margin of safety.”
- Geometric spreading only, results in a sound pressure level of 58 to 62 dB(A) at a distance of 50 meters (164 feet) from the turbine, which is about the same level as conversational speech at a 1-meter (3-foot) distance. At a receptor approximately 2,000 feet (600 meters) away, the equivalent sound pressure level would be 36 to 40 dB(A) when the wind is blowing from the turbine toward the receptor. This level is typical of background levels of a rural environment.
- To estimate combined noise levels from multiple turbines, the sound pressure level from each turbine should be estimated and summed. Different arrangements of multiple wind turbines (e.g., in a line along a ridge versus in clusters) would result in different noise levels; however, the resultant noise levels would not vary by more than 10 dB.
- Wind-generated noise would increase by about 2.5 dB(A) per each 3 feet per second (ft/s) (1 meter per second [m/s]) wind speed increase (Hau 2000); the noise level of a wind turbine, however, would increase only by about 1 dB(A) per 3 ft/s (1 m/s) increase.
- In general, if the background noise level exceeds the calculated noise level of a wind turbine by about 6 dB(A), the latter no longer contributes to a perceptible increase of noise. At a wind speed of about 33 ft/s (10 m/s), wind-generated noise is higher than aerodynamic noise. In addition, it is difficult to measure sound from modern wind turbines above a wind speed of 26 ft/s (8 m/s) because the background wind-generated noise masks the wind turbine noise at that speed (DWIA 2003).
- Proponents of a wind energy development project should take measurements to assess the existing background noise levels at a given site and compare them with the anticipated noise levels associated with the proposed project.

- Noise generated by turbines, substations, transmission lines, and maintenance activities during the operational phase would approach typical background levels for rural areas at distances of 2,000 feet (600 meters) or less and, therefore, would not be expected to result in cumulative impacts to local residents.

While the above are not regulations, they provide detail on how BLM will assess the “significance” of noise impacts on individual projects and provide guidelines on how individual projects will need to address noise.

Western State Regulations

Table 2 summarizes which western states have noise requirements. Only 4 of the 11 states listed have state noise regulations applicable to wind energy projects. The applicable requirements of Washington, Oregon, California and Colorado will be more thoroughly discussed in the following sections.

TABLE 2
Summary of Western States Regulatory Requirements Potentially Applicable to Wind Energy Projects

State	Regulatory Citation
Arizona	No primary statutory authority
California	Health and Safety Code, Division 28, Noise Control Act, § 46000 et seq. (requires local agencies to develop regulations)
Colorado	Noise Abatement (CRS 25-12-101 et seq.)
Idaho	No primary statutory authority
Montana	No primary statutory authority
Nevada	Prevention of Excessive Noise (NRS 244.363, only addresses transportation noise)
New Mexico	No primary statutory authority
Oregon	Noise Control (ORS 467.010 et seq.)
Utah	No primary statutory authority
Washington	Noise Control (RCW 70.07.010 et seq.)
Wyoming	No primary statutory authority

Note: Local jurisdictions may have noise regulations applicable to wind energy facilities.

Source: Adapted from “Wind Energy Final Programmatic Environmental Impact Statement (EIS),” Bureau of Land Management (BLM) 2005

State of Washington

Wind projects in Washington State are not required to but may choose to submit a permit application to the Washington State Energy Facility Site Evaluation Council (EFSEC or Council) which “provides a ‘one-stop’ siting process for major energy facilities in the State of Washington. If a project is approved, EFSEC specifies the conditions of construction and operation, issues permits in lieu of any other individual state or local agency authority, and manages an environmental and safety oversight program of facility and site operations”¹⁰. Similar state energy siting agencies also exist in Oregon and California. Their purposes include streamline permitting and review by staff familiar with issues associated with energy projects, while also providing an authority that is potentially more insulated from politics than elected county officials.

Washington EFSEC requires that a permit application:

- Describe and quantify the background noise environment that would be affected by the energy facility. The number of locations used for assessment of the existing noise environment shall be commensurate with the type of energy facility being proposed, the impacts expected, and the presence of high density receptor locations in the vicinity of the proposed site.
- Identify and quantify the impact of noise emissions resulting from construction and operation of the energy facility, using appropriate state-of-the-art modeling techniques, and including impacts resulting from low frequency noise;
- Identify local, state, and federal environmental noise impact guidelines;
- Describe the mitigation measures to be implemented to satisfy WAC 463-62-030;
- Describe the means the applicant proposes to employ to ensure continued compliance with WAC 463-62-030.

Washington Administrative Code (WAC) 463-62-030 refers to WAC Section 173-60, which contains the noise standards for Washington State. Local jurisdictions are allowed to develop independent state-approved noise standards. It is primarily the urban communities such as Seattle that have done so. The State's noise limits are based on the environmental designation for noise abatement (EDNA) which is defined as "an area or zone (environment) within which maximum permissible noise levels are established." There are three EDNA designations, which roughly correspond to residential, commercial/recreational, and industrial/agricultural uses:

- Class A: Lands where people reside and sleep (such as residential)
- Class B: Lands requiring protection against noise interference with speech (such as commercial/recreational)
- Class C: Lands where economic activities are of such a nature that higher noise levels are anticipated (such as industrial/agricultural)

Table 3 summarizes the maximum permissible levels applicable to noise received at noise sensitive areas (Class A EDNA) and at industrial/agricultural areas (Class C EDNA) from an industrial facility (Class C EDNA).

TABLE 3
State of Washington Noise Regulations

Statistical Descriptor	Maximum Permissible Noise Levels (dBA) from a Class C EDNA		
	Class A EDNA Receiver		Class C EDNA Receiver ¹
	Daytime (7 a.m. – 10 p.m.)	Nighttime (10 p.m. – 7 a.m.)	Anytime
L _{eq}	60	50	70
L ₂₅	65	55	75
L _{16.7}	70	60	80
L _{2.5}	75	65	85

The regulations lack clear guidance when the receptor is a farmhouse on agricultural land. Is that receptor a Class C EDNA because of the “economic activity” or is it a Class A EDNA because “people reside and sleep” there? What the author has suggested and Washington EFSEC has accepted in several permit applications (but not formally adopted), is assessing the property line as a Class C EDNA and the area around the home as a Class A EDNA. Effectively this results in a 70 dBA limit at the property line and a 50 dBA limit at the home. Others have suggested that the entire parcel be treated as a Class C EDNA subject to a 70 dBA limit, thus on smaller parcels noise levels at homes may exceed the 50 dBA level. Note that the regulations also do not specify equivalent sound level (L_{eq}) as the metric, rather they have identified “maximum permissible noise levels” which are allowed to be exceeded a certain amount of time by the specified amounts (L_{25} , $L_{16.7}$, and $L_{2.5}$).

It is important to note that 173-60-50(6) WAC states, “Nothing in these exemptions is intended to preclude the Department from requiring installation of the best available noise abatement technology consistent with economic feasibility.” However, the author is unaware of any project, where this has been implemented, requiring more restrictive noise limits.

Neither the Washington State noise regulations nor the EFSEC permitting guidelines specifically address changes in ambient noise levels resulting from a project. WAC 173-60 is silent on this matter while EFSEC doesn’t provide specific guidance on how to quantify background noise or impacts. On several recent projects FRA & FTA DNL criteria shown in Figure 1 have been suggested by EFSEC’s noise consultant as an appropriate way to address changes in ambient noise levels.

The Washington State Environmental Policy Act (SEPA), requires all State governmental agencies to consider all of the environmental impacts of a proposed development. SEPA is Washington State’s version of federal NEPA. SEPA contains a checklist of questions pertaining to all potential areas of environmental impacts, including noise. The purpose of the checklist is to provide information to help identify impacts and to help the agency decide whether a more comprehensive EIS is required. The checklist requires the following be answered with respect to noise:

1. What types of noise exist in the area which may affect your project (for example: traffic, equipment, operation, other)?
2. What types and levels of noise would be created by or associated with the project on a short-term or a long-term basis (for example: traffic, construction, operation, other)? Indicate what hours noise would come from the site.
3. Proposed measures to reduce or control noise impacts, if any:

Projects that are permitted outside of the Washington EFSEC process and through a SEPA checklist (with the local City or County as the lead permitting agency) therefore do not necessarily need to address the existing noise levels or change in noise levels, but would be required to comply with the State and local noise regulations.

State of Oregon

The Oregon noise regulations (Oregon Administrative Rule [OAR] Chapter 340 Division 35) contain two noise standards that are generally referred to as the “Table 8 test” and the “ambient degradation test” (other portions of the rules address octave, third-octave band and tonal limits). The “Table 8 test” refers to Table 8 of the

rule (reproduced here as Table 4), which limits the maximum permissible statistical noise levels generated by a project. The “Table 8” limits are similar to the limits in Washington State. Unlike Washington, the “ambient degradation test” specifically limits the increase in the existing L_{10} or L_{50} to a maximum of 10 dBA.

TABLE 4
Oregon’s Table 8 Limits¹⁰: Maximum Permissible Levels for New Industrial and Commercial Noise Sources

Statistical Descriptor	Daytime (7 a.m. – 10 p.m.) (dBA)	Nighttime (10 p.m. – 7 a.m.) (dBA)
L_{50}	55	50
L_{10}	60	55
L_1	75	60

Source: OAR 340-35-035

The “ambient degradation test” proved to be the greatest impediment in permitting wind energy facilities, and the motivation for recent modifications to the noise rule. The “ambient degradation test” required monitoring to determine existing noise levels, resulted in large setbacks from landowners who may be indifferent to the increase in noise and who may directly benefit from project royalties.

In at least one instance the ambient degradation rule as administered by Oregon EFSEC prevented a landowner from legally re-occupying a dwelling on her land notwithstanding the fact that she stated she does not find the noise bothersome. In another case, a home was vacated because the landowner was concerned that occupation would adversely impact or complicate the landowner’s chances of being included in a large wind development.

With the support of the Governor’s Office of Sustainability, the Oregon Department of Energy (ODOE) established a joint rule with the Oregon Department of Environmental Quality (DEQ) to amend the existing noise rule to explicitly address noise standards for wind turbines. This is the only state noise rule that the author is aware of that explicitly addresses wind turbine noise. The substantive issues raised during the rule making proceedings will each be discussed briefly. A more thorough discussion on this subject can be found in Reference ¹¹.

Establishing Minimum Existing Ambient Levels. The relatively calm conditions that are ideal for establishing existing noise levels for other industrial noise sources are not necessarily representative of the existing noise levels when a wind turbine would be expected to generate power and noise. Thus a correlation between background noise level (at the receiver location) and wind speed (preferably at hub height at the proposed turbine location) is necessary to establish the existing noise levels. This creates several challenges given the “large variations in measured noise levels due to the wind speed dependence of the background noise and wind effects at the microphone¹²”. Addressing these issues requires extensive monitoring, which has proved to be challenging and costly in terms of both equipment and time and requires a statistical method to analyze the collected data to be legislated to ensure that project proponents and/or opponents do not unfairly skew the results.

To avoid these difficulties, the new rule establishes a minimum background L_{50} of 26 dBA. This was based in part on field measurements conducted for a Site

Certificate application and in part because the resulting limit of 36 dBA is generally consistent with British and Australian guidance^{13,14}.

Similar to both the British and Australian guidelines, the proposed changes to the Oregon rule will allow the project developer to submit evidence that the actual existing level is more than 26 dBA. Given the level of effort required to conclusively demonstrate the existing noise levels, it is unlikely that many projects in Oregon will pursue this option.

Establishing Landowner Consent. One of the more significant changes was to allow affected landowners to consent to waive the ambient rule on their properties. The “Table 8” limits—namely an L₅₀ of 50 dBA—still apply at the properties of consenting landowners. Landowners who choose not to consent are still governed by the ambient degradation limit of 10 dBA, when used with the assumed ambient of 26 dBA results in a project limit of 36 dBA.

It is very often the case that nearby residents are involved in the project and are not concerned with noise increases near their homes as a result of the wind facility. Many landowners, including one audiologist, provided testimony at public hearings held during the rule making process to substantiate this. Annoyance from changes in ambient noise levels is subjective, and rural landowners can be fairly accepting of noise from agriculture, forestry, and other natural resource development. “Different individuals have different sensitivities to different types of noise and this probably reflects differences in expectations and attitude...depending almost entirely on personal preferences, lifestyles and attitudes of the listeners and on the context in which the sound is heard¹⁵.” In many situations the resident potentially affected by noise also would benefit financially from leasing land to the wind development project. Texas rancher and wind project landowner, Louis Woodward, is quoted in a Public Citizen brochure: “Yep, they make some noise, but it’s the soothing sound of money being made.”

The new rule allows all affected landowners the option of entering into a consent agreement. “If landowners want to agree to this level of noise for compensation, I see no reason to deny them this ability to do so...this is a reasonable compromise since it provides some flexibility for wind for willing landowners, while maintaining the noise degradation standards for those unwilling to waive this standard¹⁶.” This provides certainty needed for financing both large and small wind projects.

Incorporating IEC 16400-11. Historically wind projects were required to demonstrate that the Table 8 limits were complied with under the maximum operating conditions, typically around 25 m/s. For obvious reasons, this was typically a modeling demonstration. In addition, compliance with the ambient degradation test was determined under cut-in conditions as this was the period where the potential maximum increase was thought to occur.

Most if not all turbine manufacturers provide sound power level data determined in accordance with International Electrotechnical Commission’s (IEC) International Standard IEC 61400-11, *Wind Turbine Generator Systems – Part 11: Acoustic Noise Measurement Techniques*¹⁷. This IEC method establishes the acoustic reference wind speed of 8 m/s at 10-meter height. Although often misunderstood, this does not require that a measurement is made with 8 m/s winds at a height of 10 meters. Rather, the 10-meter height is part of IEC’s calculations to standardize the results for comparison of different turbines and different hub heights.

The new rule requires the maximum sound power level, determined in accordance with IEC 61400-11, be used to demonstrate compliance with both Table 8 and the ambient degradation limits. It should be made clear that this is not necessarily at the acoustic reference conditions of 8 m/s winds at 10-meter height; rather, it is the maximum sound power level determined between cut-in and the wind speed that results in 95 percent of the rated electrical power. This ensures that the maximum sound power level is used for prediction purposes and that measurements (if required) would be conducted when the hub height wind speeds correspond to the maximum noise emissions.

Referencing the maximum sound power level also ensures that variable-speed turbines are not preferentially treated. While the typical difference between minimum and maximum operating sound power levels is less than 4 dBA for a constant-speed turbine, the sound power level of a variable-speed turbine increases rapidly with only slight increases in wind speed. The difference between the minimum and maximum operating sound power level for a variable-speed turbine can exceed 12 dBA (and was cited to be as great as 23 dBA¹⁸). Under the previous method of determining ambient degradation at cut-in windspeeds, variable speed turbines lower cut-in wind speeds gave them a distinct advantage. By referencing the maximum sound power level and IEC 61400-11, the new rule ensures that the noise level of nonconsenting landowners will remain 36 dBA under even the loudest operating conditions, regardless of turbine type.

The development community also tried unsuccessfully to add a distance criteria based on the turbines maximum sound power level. This would eliminate the need for acoustical models, provide absolute certainty with respect to noise compliance.

State of California

While the State of California has a similar state permitting body for energy projects to that of Washington and Oregon, the California Energy Commission (CEC) was established with jurisdiction solely over thermal projects 50 MW or greater (geothermal, fossil, and nuclear fueled)¹⁹. California does not have a state level noise regulation such as in Oregon or Washington. A Model Noise Ordinance was drafted by the State to assist cities and counties develop their own noise regulations; however, it has no legal standing. Each city or county is also required to have a General Plan that establishes long-term planning and land use policy including noise compatibility which is to be updated every 20 years. Therefore, the primary regulatory noise limits for wind farms in California are local ordinances and General Plans.

In addition to the local ordinance or general plan requirements, the Californian Environmental Quality Act (CEQA, similar to SEPA in Washington State or the Federal NEPA) requires that the project assess if it will result in:

- Exposure of persons to or generation of noise levels in excess of standards established in the local general plan or noise ordinance or applicable standards of other agencies?
- A substantial permanent increase in ambient noise levels in the project vicinity above levels existing without the project?
- A substantial temporary or periodic increase in ambient noise levels in the project vicinity above levels existing without the project?

CEQA is quiet on what constitutes a significant increase. Rather the CEQA lead agency (typically the County or City) may establish their own thresholds of significance. Often they do not, and it is up to the permittee to determine an appropriate methodology for determining if an increase is significant. The California Energy Commission (CEC) Staff concluded that a potential for a significance noise impact exists where the noise of the project exceeds the background noise (L_{90}) by 5 dBA or more. It is important to note that the potential for an impact does not mean that there is an impact. Rather, it means that the project noise levels need further evaluation. CEC staff have not uniformly applied their L_{90} -based criteria, and that in at least one case the CEC commissioners overturned staffs L_{90} -based recommended threshold for one that was LDN based.

A summary of local noise regulations in various California counties follows. Note that a few counties specifically address wind turbine noise. Note that these are not complete regulatory citations and regulations are subject to change.

Riverside County—Riverside County establishes two thresholds for noise, one for permitting and another for operational compliance. An acoustical study is not required by the County when permitting a project where a 2,000-foot setback is maintained on projects consisting of 10 turbines or less or 3,000 feet when there are more than 10 turbines. When these setbacks are not maintained, the acoustical study must document wind project noise to be less than or equal to 55 dBA. Unless a more restrictive limit is established, operational noise (compliance measurements) is limited to 60 dBA.

Solano County—In a recent permit for a wind project, PPM Energy's Shiloh project, Solano County limited a wind projects noise to 50 dBA CNEL or 44 dBA L_{eq} . It appeared to presume that level would be met if a 2,000-foot setback was maintained, but the County maintained the 50 dBA CNEL or 44 dBA L_{eq} level as enforceable upon receipt of a complaint.

City of Fairfield—Located within Solano County, the City's nighttime noise property line standard is 45 dBA L_{eq} and 65 dBA L_{max} .

Kern County—The Kern County General Plan requires proposed commercial and industrial uses or operations to be designed or arranged so that they will not subject residential or other noise sensitive land uses to exterior noise levels in excess of 65 dB L_{dn} and interior noise levels in excess of 45 dB L_{dn} . For wind projects, [Chapter 19.64 WIND ENERGY \(WE\) COMBINING DISTRICT](#) of the Kern County Code establishes a not-to-exceed level of 50 dBA and an $L_{8,3}$ of 45 dBA. It also establishes for a waiver provided that the affected property owners consent and a permanent noise easement is recorded with the County.

Fresno County—The Fresno County noise ordinance establishes a nighttime L_{50} limit of 45 dBA.

Alameda County—The Alameda County Noise Ordinance (Section 6.60.040) establishes a nighttime L_{50} noise limit of 45 dBA.

Contra Costa County—For wind projects [Chapter 88-3 WIND ENERGY CONVERSION SYSTEMS](#) of the County Code establishes a maximum noise limit of 65 dBA at the property line. The noise element of the general plan states that noise levels up to 60 dBA L_{dn} are normally acceptable at residential receptors.

Morro Bay—The Morro Bay General Plan establishes a nighttime limit of 45 dBA L_{eq} .

City and County of San Francisco—The basic noise level criteria for most residential land uses are that the average noise level caused by the source shall not exceed 50 dBA at nighttime (10 p.m. to 7 a.m.), or 55 dBA in daytime (7 a.m. to 10 p.m.). In the absence of specific noise standards, Section 2901.11 states that producing a noise level that exceeds the ambient noise level by 5 dBA or more when measured at the receiving property line is a violation.

County of San Bernardino—For residential property, the San Bernardino general plan establishes nighttime performance standards of 45 dBA L_{eq} and 65 dBA L_{max} . The noise performance standards adopted in Chapter 9 (Section 87.0905 of the County Code) are the same as those specified in the General Plan.

Monterey County—The Monterey County General Plan states that 45 to 55 dBA CNEL is normally acceptable. The Monterey County Noise Ordinance basically states that “No person shall...operate any machine...which produces a noise level exceeding 85 dBA measured at fifty feet...”

Santa Cruz County—The Santa Cruz County General Plan limits nighttime noise to 45 dBA L_{eq} , 65 dBA L_{max} . If the ambient L_{eq} is 35 dBA or less, the allowable levels are reduced by 5 dBA to 40 dBA L_{eq} and 65 dBA L_{max} .

San Joaquin County—The San Joaquin County noise ordinance establishes a nighttime limit of 45 dBA L_{eq} and 65 dBA L_{max} .

Sacramento County—The Sacramento County Noise Ordinance limits nighttime hours to a maximum exterior level of 50 dBA L_{50} . Compliance with the noise standards is measured immediately within the property line of any affected residentially designated lands or residential land use.

State of Colorado

The Colorado noise regulations, Title 25 (Health) Article 12 (Noise Abatement), state that noise radiating from a property line in excess of 50 dBA at night in a residential area constitutes a public nuisance. It also states that activities shall be conducted to ensure noise is “not objectionable due to intermittence, beat frequency or shrillness” and contains a 5 dBA penalty for “periodic, impulsive or shrill” noises. None of these qualitative terms are defined. Compliance measurements are required to be made when the wind speed does not exceed 5 miles per hour (2.2 meters per second). Noise associated with agricultural operations is not regulated. There are also over 340 local jurisdictions within Colorado that may have additional noise requirements.

Conclusions

In the United States, noise is primarily regulated at the state or local level. Many western states have no noise regulations. Local regulations can vary dramatically, even when they specifically address wind turbines. Local requirements are also free to exceed federal guidance. Most noise regulations establish absolute noise limits, relative limits that regulate increases over existing are few and typically not well defined.

Appendix—Oregon Noise Rule for Wind Turbines

Additions to the Oregon rule to address wind turbines are **bold underlined**, there were no deletions.

http://arcweb.sos.state.or.us/rules/OARs_300/OAR_340/340_035.html

Oregon Administrative Record (OAR) 340-035-0035 Noise Control Regulations for Industry and Commerce

(1) Standards and Regulations:

(a) Existing Noise Sources. No person owning or controlling an existing industrial or commercial noise source shall cause or permit the operation of that noise source if the statistical noise levels generated by that source and measured at an appropriate measurement point, specified in subsection (3)(b) of this rule, exceed the levels specified in Table 7, except as otherwise provided in these rules.

(b) New Noise Sources:

(A) New Sources Located on Previously Used Sites. No person owning or controlling a new industrial or commercial noise source located on a previously used industrial or commercial site shall cause or permit the operation of that noise source if the statistical noise levels generated by that new source and measured at an appropriate measurement point, specified in subsection (3)(b) of this rule, exceed the levels specified in Table 8, except as otherwise provided in these rules. **For noise levels generated by a wind energy facility including wind turbines of any size and any associated equipment or machinery, subparagraph (1)(b)(B)(iii) applies.**

(B) New Sources Located on Previously Unused Site:

(i) No person owning or controlling a new industrial or commercial noise source located on a previously unused industrial or commercial site shall cause or permit the operation of that noise source if the noise levels generated or indirectly caused by that noise source increase the ambient statistical noise levels, L_{10} or L_{50} , by more than 10 dBA in any one hour, or exceed the levels specified in Table 8, as measured at an appropriate measurement point, as specified in subsection (3)(b) of this rule, **except as specified in subparagraph (1)(b)(B)(iii).**

(ii) The ambient statistical noise level of a new industrial or commercial noise source on a previously unused industrial or commercial site shall include all noises generated or indirectly caused by or attributable to that source including all of its related activities. Sources exempted from the requirements of section (1) of this rule, which are identified in subsections (5)(b) - (f), (j), and (k) of this rule, shall not be excluded from this ambient measurement.

(iii) For noise levels generated or caused by a wind energy facility:

(I) The increase in ambient statistical noise levels is based on an assumed background L_{50} ambient noise level of 26 dBA or the actual ambient background level. The person owning

the wind energy facility may conduct measurements to determine the actual ambient L₁₀ and L₅₀ background level.

(II) The “actual ambient background level” is the measured noise level at the appropriate measurement point as specified in subsection (3)(b) of this rule using generally accepted noise engineering measurement practices. Background noise measurements shall be obtained at the appropriate measurement point, synchronized with windspeed measurements of hub height conditions at the nearest wind turbine location. “Actual ambient background level” does not include noise generated or caused by the wind energy facility.

(III) The noise levels from a wind energy facility may increase the ambient statistical noise levels L₁₀ and L₅₀ by more than 10 dBA (but not above the limits specified in Table 8), if the person who owns the noise sensitive property executes a legally effective easement or real covenant that benefits the property on which the wind energy facility is located. The easement or covenant must authorize the wind energy facility to increase the ambient statistical noise levels, L₁₀ or L₅₀ on the sensitive property by more than 10 dBA at the appropriate measurement point.

(IV) For purposes of determining whether a proposed wind energy facility would satisfy the ambient noise standard where a landowner has not waived the standard, noise levels at the appropriate measurement point are predicted assuming that all of the proposed wind facility’s turbines are operating between cut-in speed and the wind speed corresponding to the maximum sound power level established by IEC 61400-11 (version 2002-12). These predictions must be compared to the highest of either the assumed ambient noise level of 26 dBA or to the actual ambient background L₁₀ and L₅₀ noise level, if measured. The facility complies with the noise ambient background standard if this comparison shows that the increase in noise is not more than 10 dBA over this entire range of wind speeds.

(V) For purposes of determining whether an operating wind energy facility complies with the ambient noise standard where a landowner has not waived the standard, noise levels at the appropriate measurement point are measured when the facility’s nearest wind turbine is operating over the entire range of wind speeds between cut-in speed and the windspeed corresponding to the maximum sound power level and no turbine that could contribute to the noise level is disabled. The facility complies with the noise ambient background standard if the increase in noise over either the assumed ambient noise level of 26 dBA or to the actual

ambient background L₁₀ and L₅₀ noise level, if measured, is not more than 10 dBA over this entire range of wind speeds.

(VI) For purposes of determining whether a proposed wind energy facility would satisfy the Table 8 standards, noise levels at the appropriate measurement point are predicted by using the turbine's maximum sound power level following procedures established by IEC 61400-11 (version 2002-12), and assuming that all of the proposed wind facility's turbines are operating at the maximum sound power level.

(VII) For purposes of determining whether an operating wind energy facility satisfies the Table 8 standards, noise generated by the energy facility is measured at the appropriate measurement point when the facility's nearest wind turbine is operating at the windspeed corresponding to the maximum sound power level and no turbine that could contribute to the noise level is disabled.

340-035-0110

Suspension of Commission and Department Responsibilities

In 1991, the Legislative Assembly withdrew all funding for implementing and administering ORS Chapter 467 and the Department's noise program. Accordingly, the Commission and the Department have suspended administration of the noise program, including but not limited to processing requests for exceptions and variances, reviewing plans, issuing certifications, forming advisory committees, and responding to complaints. Similarly, the public's obligations to submit plans or certifications to the Department are suspended.

TABLE A1

Oregon's Table 8 Limits¹: Maximum Permissible Levels for New Industrial and Commercial Noise Sources

Statistical Descriptor	Daytime (7 a.m. – 10 p.m.) (dBA)	Nighttime (10 p.m. – 7 a.m.) (dBA)
L ₅₀	55	50
L ₁₀	60	55
L ₁	75	60

Source: OAR 340-35-035

TABLE A2
Oregon's Median Octave Band Standards for Industrial and Commercial Noise Sources

Octave Band Center Frequency (Hz)	Daytime (7 a.m.-10 p.m.)	Nighttime (10 p.m.–7 a.m.)
31.5	68	65
63	65	62
125	61	56
250	55	50
500	52	46
1000	49	43
2000	46	40
4000	43	37
8000	40	34

Source: OAR 340-35-035

References

- 1 United States Code of Federal Regulations Title 40 Part 6.
- 2 *Guidance Manual for Environmental Report Preparation*. Federal Energy Regulatory Commission. (August 2002). Viewed online at <http://www.ferc.gov/industries/gas/enviro/erpman.pdf>
- 3 United States Code of Federal Regulations Title 23 Part 772.
- 4 United States Code of Federal Regulations Title 18 Part 150.
- 5 *High-Speed Ground Transportation Noise and Vibration Impact Assessment*. U. S. Department of Transportation, Federal Railroad Administration (December 1998). Available online at http://www.fra.dot.gov/downloads/RRDev/nvman1_75.pdf
- 6 *Transit Noise and Vibration Impact Assessment*. U. S. Department of Transportation, Federal Transit Administration (April 1995). Available online at <http://ntl.bts.gov/data/rail05/rail05.html>
- 7 *Information on Levels of Environmental Noise Requisite to Protect Public Health and Welfare with an Adequate Margin of Safety*, EPA-550/9-74-004, EPA. U.S. Environmental Protection Agency (March 1974)
- 8 United States Code of Federal Regulations Title 24 Part 51B.
- 9 *Final Programmatic Environmental Impact Statement on Wind Energy Development on BLM-Administered Lands in the Western United States*. U.S. Department of Interior, Bureau of Land Management (June 2005). Available online at <http://windeis.anl.gov/eis/index.cfm>
- 10 <http://www.efsec.wa.gov/>

-
- 11 *Revising Oregon's Noise Regulations for Wind Turbines*. Bastasch, M. Proceedings of NOISE-CON 2004. Baltimore, MD (July 2004).
 12. *Acoustics-Measurement, prediction and assessment of noise and wind turbine generators*. Draft for public comment. (Standards Australia. March 31, 2004).
 13. Noise Working Group. *The Assessment & Rating of Noise from Wind Farms*. ETSU-R-7. (September 1996).
 14. *Environmental Noise Guidelines: Wind Farms*. Environmental Protection Authority of South Australia. (February 2003).
 15. *Recommendations for an Expanded Environmental Noise Impact Assessment and Mitigation Process*. L. Finegold. *Proceedings of InterNoise 02*. Dearborn, MI. (2002).
 - 16 *Draft Hearings Officer Report to the Oregon Environmental Quality Commission On Noise Rulemaking Standards for Wind Energy Facilities*. Prepared by Michael W. Grainey, Director of the Oregon Department of Energy. March 22, 2004. Viewed online April 15, 2004, at http://www.energy.state.or.us/renew/Wind/Noise/Hearing_Officer_Report.pdf.
 17. *Wind Turbine Generator Systems – Part 11: Acoustic Noise Measurement Techniques*, International Standard IEC 61400-11:1998(E) (International Electrotechnical Commission, Geneva, Switzerland, 1998).
 18. G.P. van den Berg, "Effects of the wind profile at night on wind turbine sound", *J. Sound Vibr.*, Article In Press, (accepted September 2003).
 - 19 <http://www.energy.ca.gov/commission/index.html>

First International Meeting
on
Wind Turbine Noise: Perspectives for Control
Berlin 17th and 18th October 2005

UNDERWATER NOISE EMISSIONS OF OFFSHORE
WIND TURBINES

K. Betke³, K.-H. Elmer², J. Gabriel¹, W.-J. Gerasch², R. Matuschek³, T. Neumann¹

1: Deutsches Windenergie Institut GmbH (DEWI), Wilhelmshaven, Germany, t.neumann@dewi.de

2: Institut für Statik und Dynamik, Univ. Hannover, (ISD), Hannover, Germany, wj.gerasch@isd.uni-hannover.de

3: Institut für technische und angewandte Physik GmbH (itap), Oldenburg, Germany, betke@itap.de

Summary

In the German North Sea and Baltic Sea, claims of wind farms are planned with several hundred turbines of up to 5 MW each. Furthermore, several research platforms are installed in the sea to determine possible effects of future offshore wind turbines on fish and diving mammals.

Both operation and construction of offshore wind turbines induce underwater noise, but especially the use of pile drivers for erecting wind turbines will result in substantial underwater noise energy.

Extensive measurements and numerical FE-simulations of monopiles and jacket foundations under construction result in maximum underwater sound pressure levels of more than 200 dB re 1 μ Pa nearby during pile driving and in considerable noise levels several ten kilometres away. This noise has possible effects on marine life, but is not known enough till now to formulate acoustic emission limits and assessment procedures.

The aims of these investigations are:

- to build a database of extensive measurements of background noise, turbine construction noise and turbine operating noise,
- to develop forecasting hydrosound models of offshore wind converters using Finite-Element-Methods and analytical and semi-empirical methods,
- to study the generation, radiation and attenuation of underwater noise for future noise reduction methods during pile driving,
- to determine the impact area of offshore wind farms on marine life,
- to develop recommendations for acoustic emission limits for offshore wind farms in cooperation with biologists and
- to develop standard procedures for the determination and assessment of underwater noise emissions.

Introduction

In Germany, several large offshore wind farms are planned in the North Sea and the Baltic Sea, each with several hundred turbines of up to 5 MW.

Offshore wind energy technology is a new technology created by the merging of classical wind energy technology and classical offshore technology. Wind speeds are considerably higher over the sea as compared to onshore sites, but also the cost per installed kW will increase when moving offshore. The rapid development of wind energy use in Germany is accompanied by an increase of the installed power per wind turbine.

So there are many open problems and questions concerning the technical realization on one hand and the various possible environmental impacts of future offshore wind farms on the marine fish and diving mammals.

The Institute for Structural Analysis (ISD) of the University of Hannover, the German Wind Energy Institute (DEWI) in Wilhelmshaven, and the Institute for Technical and Applied Physics (itap) in Oldenburg are partners in a project on: 'Standard Procedures for the Determination and Assessment of Noise Impact on Sea Life by Offshore Wind Farms' which is funded by the German Federal Ministry of Environment (BMU).

The aim of this project is to study the generation, radiation and attenuation of underwater noise, to develop forecasting hydrosound models of offshore wind converters and future noise reduction methods during pile driving, to determine the impact area of offshore wind farms, to allow the formulation of recommendations for acoustic emission thresholds for offshore wind farms in cooperation with biologists and to develop standard procedures for the determination and assessment of noise emissions.

The operation and in particular the construction of offshore wind converters induce considerable underwater noise emissions. It is assumed that small whales and seals could be affected by noises from machines and vessels, piling and installation of the wind turbines. Piling, in particular using hydraulic hammers creates high frequency noise with considerable sound power levels. Currently only little knowledge about the effects of different noises to marine life is available. With a view to determining the effects on the marine flora and fauna and structural design aspects, the research platforms FINO1 (**Fig. 1**) and 'Amrumbank West' (**Fig. 2**) are erected in the North Sea.



Fig.1 Research Platform FINO1



Fig.2 Research Platform Amrumbank West under construction

Measurements of the underwater noise during construction of offshore research platforms and numerical investigations are used to develop future forecasting hydrosound models of offshore wind converters.

1. MECHANICAL SYSTEMS

Monopile foundations represent the most commonly used solution in conventional offshore industries.

The piles are driven into the sea ground by means of a vibrating or piling hammer. Piles are also used to fix tripod and jacket foundations after **Fig. 3**.

For the investigation of the complex process of noise generation, radiation and attenuation of noise in the sea, Finite-Element-Methods and Finite-Difference-Models are used.

Analytical, mathematical and physical models are developed to calculate the noise radiation of monopile tubes of offshore wind converters during operation and construction and to take into account the influences from sea surface and sea floor on the attenuation of underwater noise in the shallow water.

Fig. 4 shows the system with the tube or monopile in the shallow water. This system with the dynamic axial force $F(t)$ at the top of the cylindrical tube is symmetrical with respect to rotation. The dynamic response of the tube is described by the axial displacement $u(z)$ and the radial displacement $w(z)$.

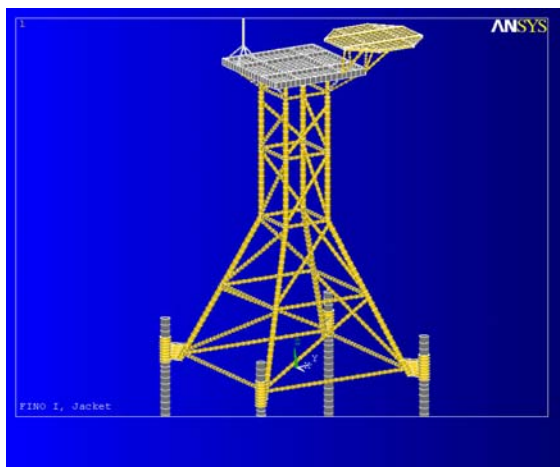


Fig. 3 FINO1 foundation with piles.

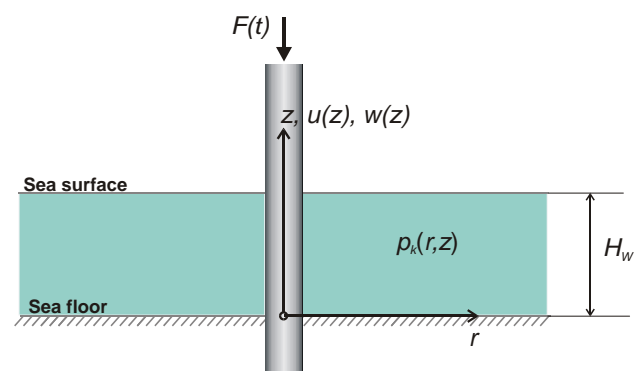


Fig. 4 System of monopile in shallow water

2. NUMERICAL SIMULATION AND MEASURING OF CONSTRUCTION NOISE

Both operation and construction of offshore wind turbines induce underwater noise but the impact of pile drivers on the piling will result in substantial noise energy propagation within the acoustically shallow water.

As an example of this the noise of the FINO1 platform was simulated and measured during the pile driving.

Fig. 5 shows the system of the FINO1 platform with pile and pile driver. The pile of length $l = 37.5\text{m}$ has stepped cross sections and thickness of the wall between

40 and 18mm. These sections cause reflections of the impact wave beside the reflections at both ends of the tube. The answer of the pile system in the shallow water of 28m to the impact of the pile driver is symmetrical with respect to rotation.

Numerical simulations of pile driving, radiation of underwater noise and the propagation of noise are done based on the symmetrical Finite-Element model after **Fig. 6** and using the FE-program ANSYS.

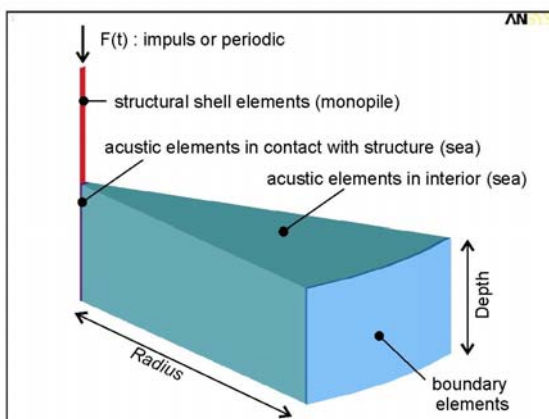


Fig. 6 System of monopile and water.

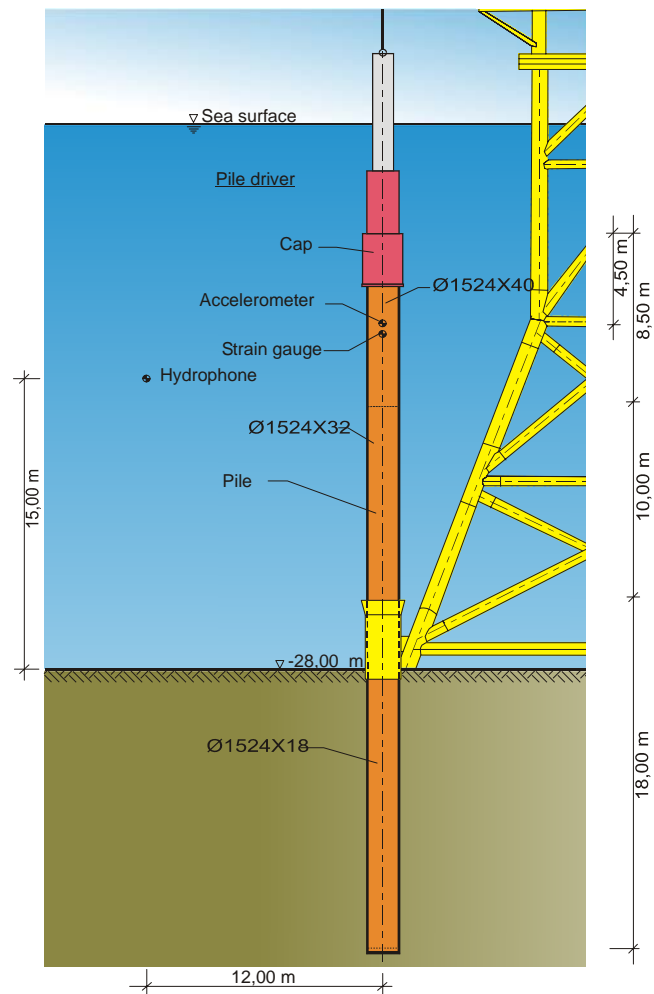


Fig. 5 Foundation of the FINO1 platform with the hydraulic hammer driving the pile into the ground.

To get reliable results from numerical simulations of the complex mechanism of transient dynamic noise generation and radiation of noise, it is necessary to know the amount and the time function of the impact force as the driving force of the system.

The characteristic number of a pile driver is the maximum impact energy of the hammer. The piles of the FINO1 foundation with a diameter of 1.50 m were driven into the ground by a hydraulic hammer IHC 280 with nominal energy of 280 kNm. To get the real energy of an impact, accelerations and strain rate of a pile were measured near the driving point at the top of the tube.



The offshore construction site is to be seen in **Fig.7** with the offshore working platform and the crane in the middle of the picture and the FINO1 platform under construction on the right side.

Fig. 7 Offshore working platform with crane and pile. On the right side: FINO1 platform under construction.

The sign on the upper end of the hanging pile is the location of the acceleration pick ups and the wire strain gauges. They are fixed below the pile driver cap.

Numerical simulations of the first impacts of the pile driver show that the resulting traveling wave within the pile is reflected several times at the stepped cross sections and at both ends of the pile.

Measurements show that there is nearly no influence of the soil when driving in the first 5 m and there is only a small amount on energy radiation into the ground that cause damping to the traveling wave.

This is a transient wave propagation problem, not a vibration problem and the numerical model is only a free-free tube as the pile system with stepped cross sections after **Fig. 5** and with low damping rate. The pile sinks into the ground by each reflected wave at the bottom of the pile. The impact energy of the hydraulic pile driver IHC 280 with maximum energy of 280 kNm was set to nominal 70 kNm with a pulse rate of about 40 per minute.

Numerical simulations yield hydrodynamic pressure at a distance of 12m and 13m depth of more than 22000 Pa after **Fig. 9** and a typical peak sound pressure level of $L_{\text{peak}} = 206.8$ dB with respect to $1 \mu\text{Pa}$.

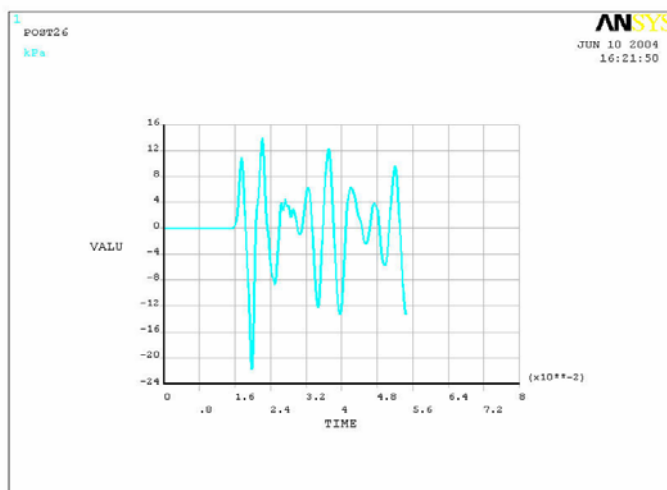


Fig.9 Numerical sound pressure at 12 m distance of 22000 Pa. Peak sound pressure level of $L_{\text{peak}} = 206.8$ dB with respect to $1 \mu\text{Pa}$.

This is in good agreement to measured results of the underwater noise peak level during pile driving of 205.8 dB re $1 \mu\text{Pa}$ in **Fig. 10** although the considered frequency range of the numerical model is limited to frequencies below 400 Hz.

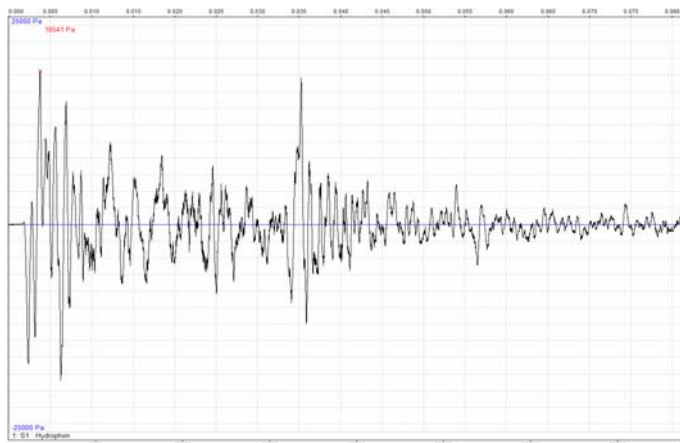


Fig.10 Measured sound pressure at 12 m distance with a peak sound pressure level of $L_{\text{peak}} = 205.8$ dB re $1 \mu\text{Pa}$.

Fig. 10 also shows in the middle of the time function peak values from bumping effects of the driven pile and the pile sleeve of the FINO1 foundation in **Fig.11**. In this case they are not responsible to the measured high underwater sound pressure level of 205.8 dB.

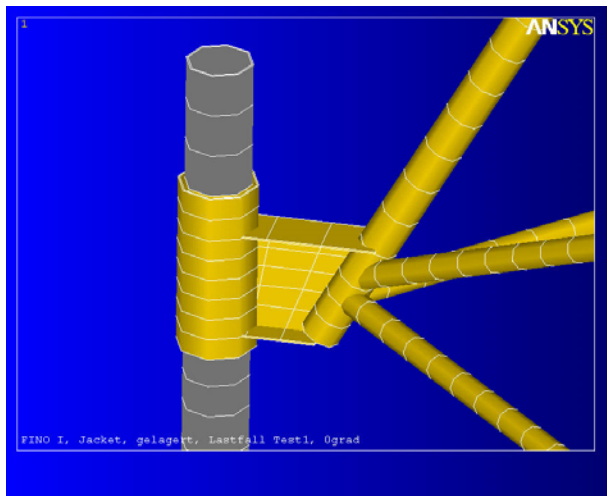


Fig.11 Pile and pile sleeve of FINO1 foundation

3. MEASURING OF TURBINE OPERATING NOISE

Vibration of the turbine's gear box and generator is guided downwards and radiated as sound from the tower wall (**Fig. 12**). Sound radiation by surface waves is difficult to compute and to predict, in particular for complicated boundary conditions. Hence, measurements on an already existing offshore wind turbine were made.

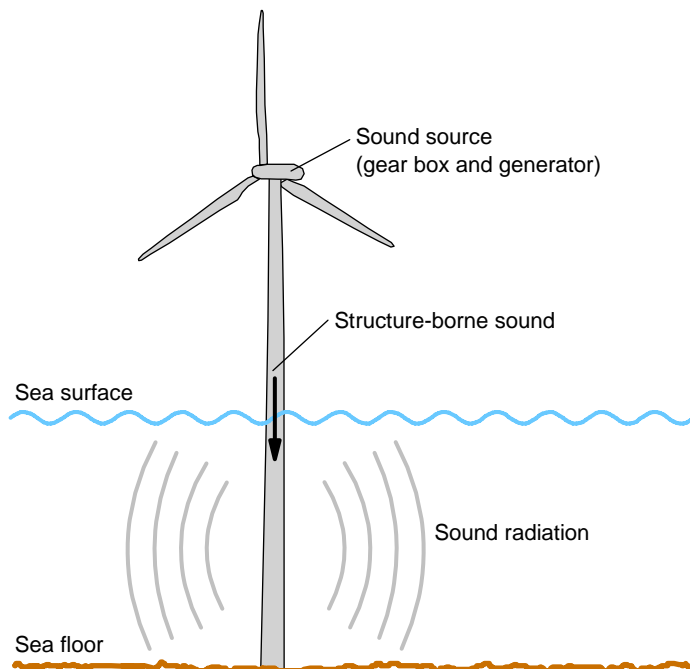


Fig. 12: Mechanism of underwater noise generation by an offshore wind turbine

The measurement setup is shown in **Fig. 13**. Since access to the turbine is only possible at low wind speeds, an automatic recording was made over a one month period.

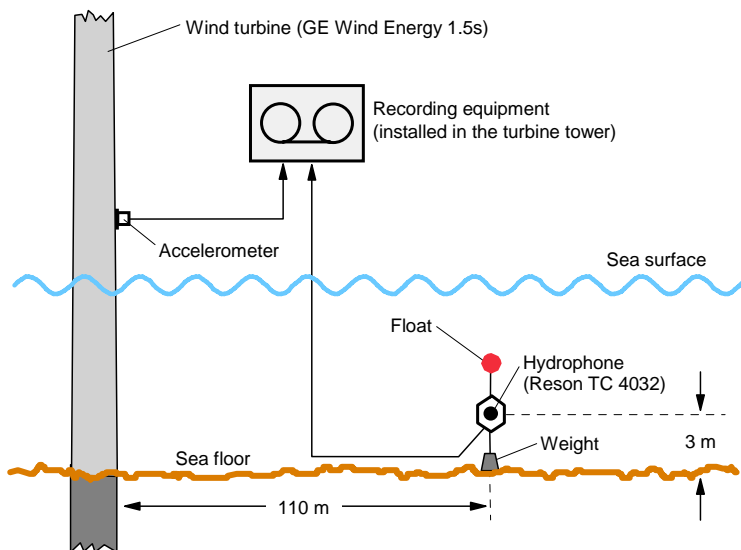


Fig. 13: Measurement setup for monitoring underwater noise induced by an offshore wind turbine. Water depth was about 10 m.

At every full hour, 20 minutes of underwater sound and tower wall vibration were recorded to hard disk. The accelerometer position – approx. 10 m above sea level and perpendicular to the wall – was chosen after preliminary measurements with several sensor positions above and below sea level. Wind and electric power values were taken from the turbine’s routine log files.

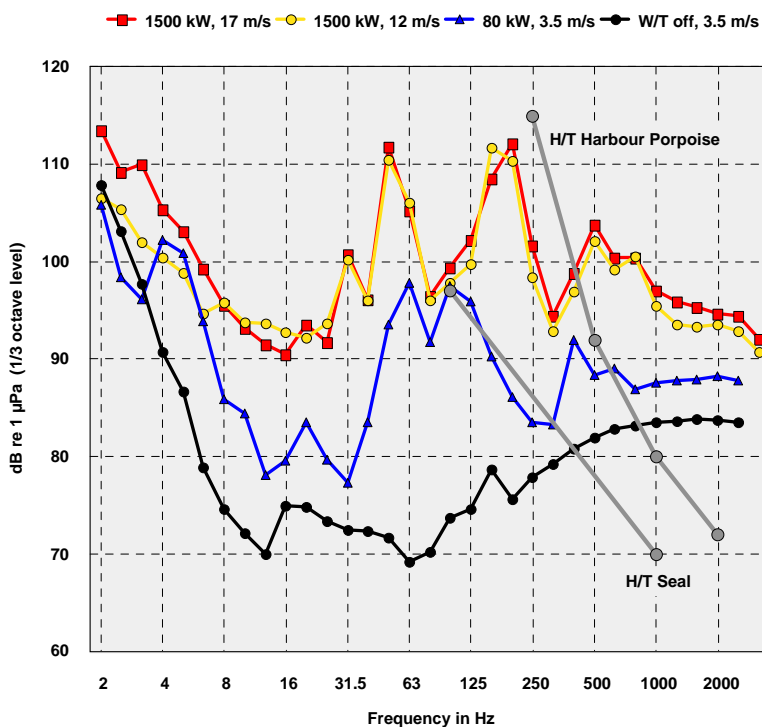


Fig. 14: Underwater sound pressure levels (1/3rd octave spectra) recorded at 110 m distance from the turbine for different turbine states. Wind speeds refer to hub height (nacelle anemometer). Low frequency parts of hearing thresholds for two marine mammals are shown for comparison

Some acoustic spectra are shown in **Fig. 14**. At low wind speeds, the generator runs at about 1100 rpm, but rises rapidly to the nominal value of 1800 rpm, which is reached at 700 kW. Turbine rated power is 1500 kW. Hence there are mainly two acoustic spectra (caused by two different sets of tooth mesh frequencies), one for low wind speeds, and one for moderate and strong wind.

The sound levels found here will certainly not cause damage to the hearing organ of marine animals, but might affect their behavior in the vicinity of a turbine. However, somewhat higher tower vibration levels than for this turbine type have been measured onshore on several 2 to 2.5 MW turbines. If set up offshore, these turbine models are likely to produce higher underwater noise levels than those of **Fig. 14**. On the other hand, the larger the turbine, the lower the tooth mesh frequencies, radiation efficiency of surface wave declines towards low frequencies, while hearing thresholds increase. At present, it is not clear if the underwater noise from offshore wind turbine will influence the behavior of marine animals.

4. PROPAGATION DAMPING IN WATER

The level of the immissions expected in the vicinity of future wind farms, but also around construction activities, depend to a large extent on the decline of sound pressure levels with increasing distance from the source of emission.

For the calculation of this propagation damping, an easy-to-use model for the decline of sound pressure levels in the North Sea and the Baltic Sea is needed, for example as used by Thiele [2]. Unfortunately there are hardly any measurements available for the North Sea and the Baltic Sea that could be used for verification and, if necessary, modification, of this model. During the first project phase, measurements were carried out in the Mecklenburg Bight up to a distance of 2 km from the source of acoustic noise, but this single measurement is not sufficient for a model verification.

In order to achieve a satisfactory accuracy and planning reliability for future predictions of acoustic noise impact on the marine environment, extensive measurements were carried out in connection with the privately funded second research platform in the North Sea (Amrum Bank) in the spring of this year. The acoustic noise immissions caused by the construction activities were recorded at six different locations. The measurement with the least distance from the acoustic noise source took place at close range, only 25m from the pile-driving action. At medium range, immissions were measured at three different locations (400, 800 and 1600m), complemented by measurements at 18,000m and 36,000m. In the medium range between 400 and 18,000m the measurements were taken from a ship chartered for the purpose, whereas the measurement at 36km was made by means of a buoy with automatic recording system.

In contrast to the FINO1 platform, the Amrumbank platform has been founded on a large monopile of approx. 3-4m thickness, with a pile-driving depth of approx. 20m. By comparison, the 4 FINO1 piles only had a diameter of 1.5m each, and the pile-driving depth was about 30m.

Fig. 15 shows the acoustic noise immission levels measured during the complete pile-driving action. The diagram shows the short-term peak level as well as the continuous equivalent sound pressure level L_{eq} averaged over 60 seconds. The measurement

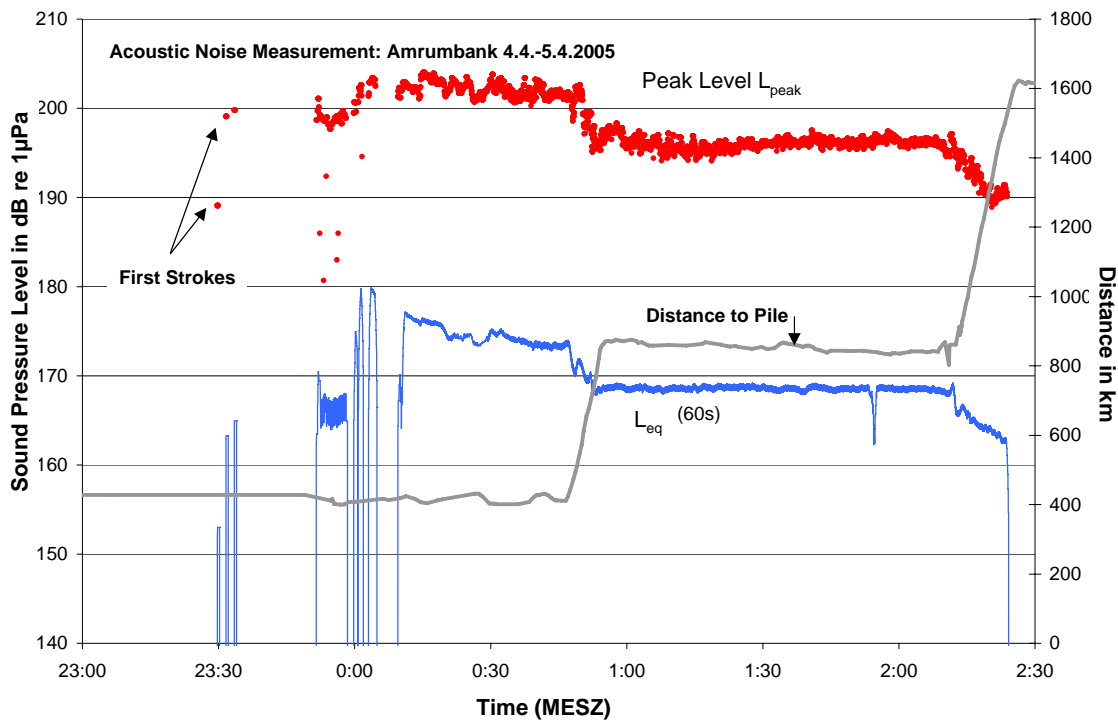


Fig. 15: Curve of the acoustic peak level L_{peak} and the continuous equivalent sound pressure level $L_{eq}(60s)$ at different locations.

started at 23:30 (MESZ) at a distance of 400m, towards 0:45 the distance was increased to 800m, and towards the end of the pile-driving action at 2:15 the distance was doubled once again to 1600m. With each change of distance, the levels decreased by approx. 5-6 dB. Apart from that the levels remained relatively constant for the duration measured.

The time between two blows was approximately 3-4 seconds. The energy per blow was more than twice as high compared to the FINO1 platform (approx. 1Hz) with a clearly lower blow rate. On the whole the levels measured were higher than at the FINO construction site. At a distance of 400m peak levels of over 200 dB (re 1µPa) were measured which is 10dB higher than the 190dB (re 1µPa) measured at the FINO1 platform at a similar distance. The continuous equivalent sound pressure levels show similar differences with 175 dB at the Amrumbank and 165dB at the FINO1 platform. A noticeable difference to the FINO1 measurement is the fact that there is no decrease of the level towards the end of the pile-driving action. A reason for this could be the constant area of contact of the monopile with the water, whereas at FINO1 the piles were lowered into the seabed.

The evaluation of the measurement data shows an average propagation damping of 5.5dB in **Fig. 15** for each doubling of distance, which was also established in other measurements in the North Sea [3]. With higher frequencies especially at large distances - in line with the Thiele formula - a stronger damping is noticed. However the damping altogether is approx. 1dB higher than according to Thiele and in comparison to the measurements carried out in the Baltic Sea. This seems to indicate a different behaviour in North Sea and Baltic Sea, which however has to be confirmed by further measurements. The pile-driving for FINO2 in the Baltic Sea scheduled at the end of this year would provide a suitable opportunity.

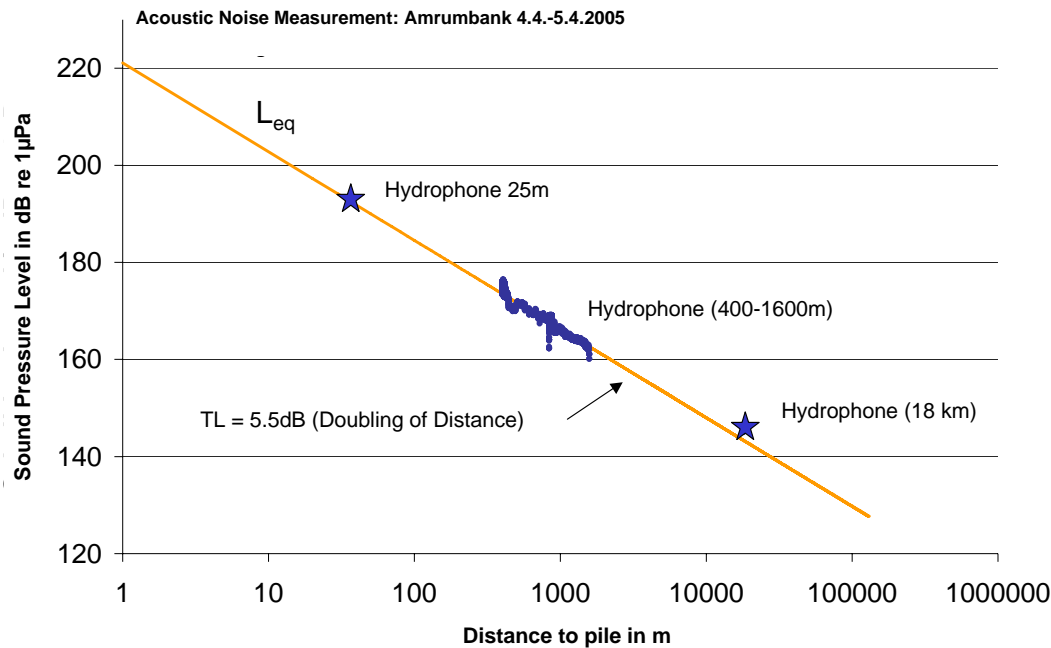


Fig. 16: Measured noise propagation attenuation in the North Sea.

5. ACKNOWLEDGEMENT

The research project to which this report is referring has been funded by the Federal Ministry for the Environment, Nature Conservation and Nuclear Safety, funding code 0329947. The contents of this article are the authors' responsibility.

References

CRI, DEWI, ITAP (2004): Standardverfahren zur Ermittlung und Bewertung der Belastung der Meeresumwelt durch die Schallimmission von Offshore-Windenergieanlagen. BMU-Projekt (FKZ 0327528A). Bundesministerium für Umwelt, Naturschutz und Reaktorsicherheit, Berlin

K. BETKE, M. SCHULTZ-VON GLAHN, R. MATUSCHEK (2004): Underwater noise emissions from offshore wind turbines. DAGA'04 (30. Deutsche Jahrestagung für Akustik). Deutsche Gesellschaft für Akustik e.V. (DEGA)

K.-H. ELMER, W.-J. GERASCH (2004): Numerical simulation and measurement of underwater noise during pile driving of offshore wind converters; International Symposium on Numerical Simulation of Environmental Problems, November 22 –23, Okayama University, Japan.

T. NEUMANN, J.GABRIEL, W.-J. GERASCH, K.-H. ELMER, M. SCHULTZ-VON GLAHN, K. BETKE (2005): Standards for the assessment of acoustic emissions of offshore wind farms. DEWI-Magazin Nr. 26, Februar 2005.

R. THIELE (2002): Mitteilung beim Fachgespräch zum UBA-Projekt „Vermeidung und Verminderung von Belastungen der Meeresumwelt durch Offshore-Windenergieanlagen im küstenfernen Bereich der Nord- und Ostsee“ am 15.01.2002.

**First International Meeting
on
Wind Turbine Noise: Perspectives for Control
Berlin 17th and 18th October 2005**

Masking of Sound from Wind Turbines by Vegetation
Noise

Karl Bolin
Royal Institute of Technology / Marcus Wallenberg Laboratory
Teknikringen 8
SE-100 44 Stockholm
Sweden
+46-(0)8 790 92 02
+46-(0)70 628 33 42
kbolin@kth.se

Abstract

This paper investigated the masking of wind turbine sound by wind induced vegetation noise. Turbulent properties of the wind was modeled and connected to a developed method of predicting vegetation noise. Sound and wind velocity measurements have been performed at a downwind forest edge. At this site masking occurred at frequencies above 500 Hz at a wind velocity of 3.5 m/s. However, no general deduction of the masking potential can be concluded from the results and hence case studies of different sites should be conducted in order to estimate the masking potential.

1 Introduction

In the issue of noise annoyance generated by wind turbines, masking by ambient noise can potentially make wind turbine sound less disturbing or possibly even inaudible. At wind turbine sites in rural areas the main natural source of noise arises from the whistling of the wind in the surrounding vegetation. This sound is also, as wind turbine noise, increasing with increasing wind speed. It is consequently of great interest to investigate the sound from the wind blowing through vegetation and its potential of masking sound from nearby wind farms.

Among today's noise annoyance assessments in different countries the British method [1] is considered particularly interesting due to its comparison with background noise level measurements in order to establish threshold levels of turbine noise. The ambient noise level is correlated to the wind velocity and compared to the corresponding wind farms sound pressure level. This method would consequently yield good results when the spectral shapes from turbines and background noise are similar and the temporal fluctuation of the background noise is limited. However the above conditions are not always fulfilled, consequently the audibility of the wind turbine can not be correctly computed if wind turbulence is disregarded. Fégeant proposed a semi-empirical analytical prediction model of vegetation noise in [2] and [3] for different tree species and vegetation geometries. This analysis was validated for cases of non-turbulent flow. Further work by Fégeant [4] stressed the importance of wind turbulence causing variations in the level of vegetation noise. However the number of test sites were limited and measurements have only been performed at wind speeds of 7 m/s and below, confirmation of the theory above these conditions is considered necessary in order to be able to also assess the masking probability at higher wind speeds.

The objectives of this paper are to discretize and further validate the Fégeant model and couple this to a wind turbulence model. The semi-analytical solutions are replaced by discrete equivalents, better suited to deal with turbulent flow and increased complexity of the terrain. These adjustments are performed in order to prepare for psycho-acoustic tests of the masking potential of vegetation sound on wind turbine noise. Validations of the model are also performed. Comparisons between measured data and predictions of the new model have been conducted with satisfying results.

2 Vegetation noise

The semi-empirical analytical model developed by Fégeant and presented in [2] and [3] is by the authors knowledge the only prediction method of vegetation noise published. As this model is analytical it is not suitable to combine with the chaotic nature of wind turbulence. To circumvent this predicament a discrete vegetation noise model based on

the research by Fégeant is developed and combined with a stochastic turbulence model in order to evaluate the fluctuations of vegetation sound caused by variations of wind speed.

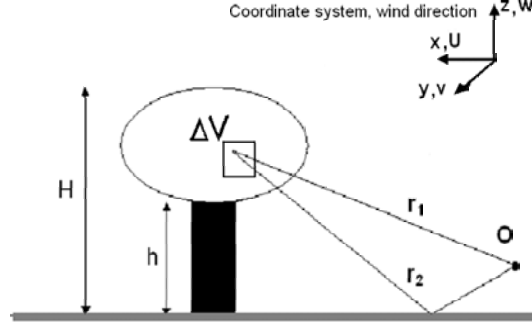


Figure 1: Geometry of vegetation source and observer position \mathbf{O} .

Prediction of vegetation noise is, to the authors knowledge, restricted to the analytical model of Fégeant [2] and [3]. To combine this model with a turbulence model it is necessary to discretize it. The effective pressure fluctuations can be calculated by Equation 1

$$p_{eff}(f)^2 = \frac{\rho c}{4\pi} \sum_{n=1}^N \sum_{m=1}^M \sum_{o=1}^O J_{mno}(f, \mathbf{r}) \Delta W_{mno}(f, \mathbf{r}) \quad (1)$$

where f is the frequency, \mathbf{r} is the vector from the source to the receiver, ρ is the air density, c the sound speed, (m, n, o) represent indices in the (x, y, z) directions respectively,

$J(f, \mathbf{r})$ shown in equation (2) represent the propagation of a spherical sound source along the rays \mathbf{r}_1 and \mathbf{r}_2 shown in figure 1.

$$J_{mno}(f) = \left| \frac{e^{-jkr_{1mno}}}{r_{1mno}} + R \frac{e^{-jkr_{2mno}}}{r_{2mno}} \right|^2 \quad (2)$$

where $k = -i\alpha$, α is the attenuation coefficient calculated according to ISO 9613 [5] and [6]. R is the reflection coefficient described in [2].

The acoustic power of the source from volume element $(\Delta x_m, \Delta y_n, \Delta z_o)$ is denoted

$$\Delta W_{mno}(f, \mathbf{r}) = AS(\mathbf{r})u^{2\chi}\Gamma(f)\Delta x_m, \Delta y_n, \Delta z_o \quad (3)$$

An analytical expression of the normalized frequency spectrum were given in [2] for deciduous species equation

$$\Gamma_d(f) = C_1 f^{-1} + C_2 e^{-C_3 \frac{(f-f_m)^2}{f_m^2}} \quad (4)$$

The coefficients $C_{1,2,3}$ and f_m are given in [3] for different tree species. For coniferous species, a dipole source Equation 5 is derived in [2] as

$$\Gamma_c(f) = e^{-\lambda \log^2(\frac{f}{f_0})} \quad (5)$$

where λ is a constant and f_0 is the velocity dependent Strouhal frequency.

3 Wind models

3.1 Mean wind

Wind velocity models of flow in and around vegetation have received considerable attention in the field of boundary layer meteorological research. Amongst others Panovsky and Dutton [7] and Kaimal and Finnigan [8] wrote excellent books in the subject and explained flow inside tree canopies. In the paper of Cionco [9] the flow in an infinite forest is

$$u(z) = u_H e^{a(z/H-1)} \quad (6)$$

as in the paper by Fégeant [2] this model is also assumed to be valid in the upwind forest edge case.

In the case of downwind forest edges and single trees the vertical velocity profile of the free field is propagating a distance of approximately $2H$ inside the canopy according to smoke visualizations performed by Miller [10]. The profile is depending on the atmospheric conditions and is modeled in The German Air Quality Guideline “TA-Luft” [11] by

$$u(z) = u_{ref} \left(\frac{z}{z_{ref}} \right)^m \quad (7)$$

where u_{ref} is the mean wind velocity at height z_{ref} and m varies from 0.09 to 0.41 for very unstable to very stable atmospheric conditions respectively. These two velocity profiles of different atmospheric conditions normalized at $u(z = 10) = 1$ m/s are shown in figure 2(a). Although the integral $\int_{z=0}^{20} u(z) dz$ varies less than 4% between extreme conditions the resulting change in sound pressure level figure 2(b) is about 3 dB for an edge of aspens with trunk height of 8 m, tree height of 17 m and at a wind speed of 2.5 m/s. Hence it is concluded that different atmospheric conditions might have significant impact on the vegetation noise, according to results from simulations.

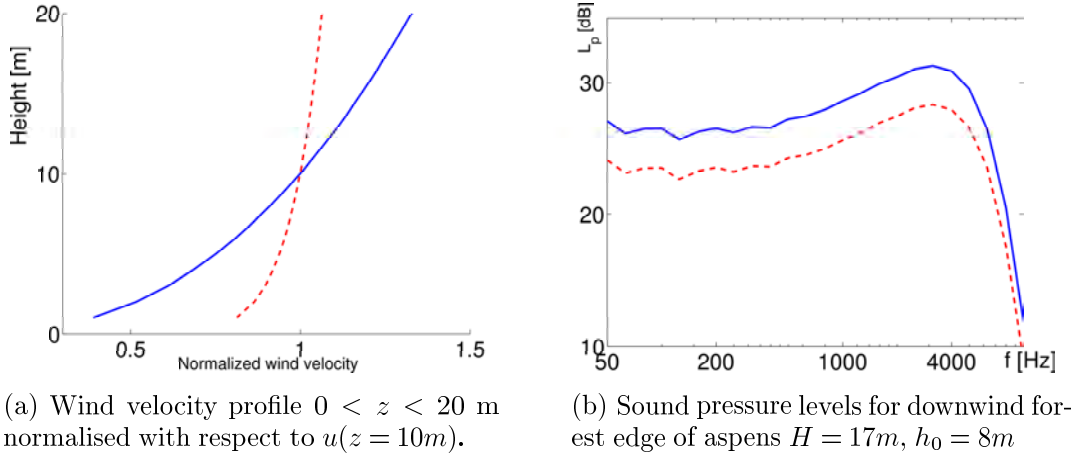


Figure 2: Vertical wind speed profiles for very stable (—) respectively very unstable (- - -) atmospheric conditions.

3.2 Turbulence

Variations in the wind speed and consequent sound pressure variations are important to the masking issue. Wind turbulence in and around vegetation canopies has been attracting attention from a number of researchers (see [12], [13] and [14] among others). The statistical properties assigned to turbulence in complex terrain differs from the one of flat and smooth surfaces. This fact should be considered when investigating the fluctuations of sound level generated by the turbulent eddies. In the report [4] a one dimensional turbulence model was proposed but flows orthogonal to the mean wind direction were omitted, hence it is considered of interest to investigate if a three dimensional model significantly changes the temporal variations in vegetation sound compared to a one dimensional model.

The chaotic nature of wind turbulence can be modeled as a stochastic process correlated in space and time. In order to extract time series of wind velocities the Sandia method [15] and [16] is applied. This algorithm uses the power spectral density of the turbulence and fixed points in space as input, this combined with series of random number produces space- and time-correlated series of wind velocity fluctuations and is therefore fully compatible with the discrete vegetation noise model. This simulation technique was proposed in [4], however as this model was not coupled to a vegetation noise model. Fluctuations of vegetation noise could not be predicted in these simulations. The aim of the turbulence model is to capture the characteristics in the low frequency domain, defined in [8] as the energy containing sub range. Turbulence at higher frequencies rapidly breaks down to high frequency eddies, hence this region is not necessary to consider as these gusts are small enough to be estimated by the mean velocity, even in small canopies. To describe the temporal variations of wind a power spectrum density is used, see [8] for details and explanation of this distribution. It is essential that a power spectral density adjusted to complex terrain is used in the simulation in order to obtain correct temporal fluctuations

of the wind. Standard spectrums in use are the von Karman and the Kaimal spectrum but as both of these assume flat, smooth and uniform terrain, not only in the interesting area but several kilometers upwind, hence another spectrum is needed that is adjusted to irregular terrain. Tieleman presents a three dimensional spectral model in the paper [17] adapted to complex terrain described in all three directions \hat{x} equation 8, \hat{y} equation 9 and \hat{z} equation 10 respectively.

$$\frac{nPSD_u(n)}{PSD_u^2} = \frac{40.42f}{(1 + 60.62f)^{5/3}} \quad (8)$$

$$\frac{nPSD_v(n)}{PSD_v^2} = \frac{13.44f}{(1 + 20.16f)^{5/3}} \quad (9)$$

$$\frac{nPSD_w(n)}{PSD_w^2} = \frac{3.28f}{(1 + 4.92f)^{5/3}} \quad (10)$$

where $n = f(U/z)$ is a normalized frequency, PSD_n^2 is the variance in the \hat{n} direction these are given by the relationship $(PSD_n/U_*)^2 = 6.25, 4$ and 1.56 for $n = u, v$ and w , respectively. The friction velocity U_* can be calculated by

$$U_* = \frac{0.4U}{\log(z/z_0)} \quad (11)$$

Comparisons between the spectrums of Kaimal and Tieleman are shown in figure 3.

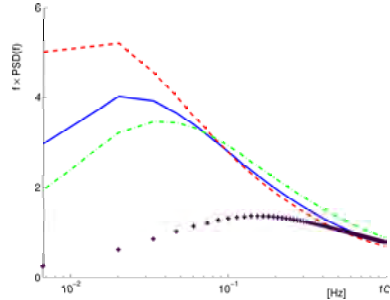


Figure 3: Power Spectrum Density of Kaimal (—) and Tieleman (- - -), (-.-) and (+) for the (u,v,w) components shows that the peak frequency is lower in the PSD in the mean wind direction this results in time series with stronger low frequency fluctuations.

4 Masking and Loudness index

Masking, by definition of American Standards Association (1960) is "the process by which the threshold of audibility for one sound is raised by the presence of another masking

sound". The wind turbine sound is referred to as the "signal" and the vegetation noise is denoted "masker" in this text. Partial masking occurs when the signal is stronger than the masker but still reduce the perceived loudness of the signal. In the current application this is interesting at the first few octave bands as the turbine sounds are estimated to be higher than the masker at these frequencies.

In order to describe the loudness perceived by the human hearing system the physical quantities of sound is not an appropriate measure. The objective sensation of loudness has considerable intra-personal variations and it is therefore a difficult task to model the magnitude of loudness correctly. Several methods of calculating loudness has been suggested among others the Zwicker and Fastl [18] and the Moore [19]. In this paper the ISO 532A [20] standard is used to calculate the loudness index in the unit sones. The difference of the loudness index between the wind turbine and the vegetation noise $N_D = N_{WT} - N_{Veg}$ is assumed to be a measure of the experienced loudness of the wind turbine.

The time depending noise annoyance assessment in [18], page 322-327, uses the percentile loudness N_5 to estimate the perceived disturbance. This limit marks the sound level that is reached or exceeded 5% of the time. In analogy with this method the masking potential should be evaluated with respect to vegetation noise level of N_{95} to yield the values of the signal to noise ratio exceeded 5% of the time.

5 Measurements

5.1 Equipment

The measurement setup consisted of one cup anemometer mounted on a pole, 10 m high, and a weather station registering humidity and temperature. In the sound measurement 1/2" microphones connected to a digital analyzer SONY PC216Ax was used. In order to decrease the pseudo-noise generated by wind blowing into the microphone the free microphone technique with microphones protected by a foam windscreen 10 cm in diameter were applied. Recordings were performed in the frequency range between 43.2 Hz and 11200 Hz.

5.2 Sites

New measurements as well as results from [3] have been analyzed in order to investigate the validity of the discrete model and to compare it to the analytical equivalent.

The third octave band sound pressure levels from [3] measurements of a downwind forest edge of aspens with the height 17 meters and the microphone placed 50 meters from the

edge (site 4 in [3]). Another downwind forest edge consisting of with the height 10 meters and the microphone placed 40 meters from the edge (site 5 in [3])

A new set of measurements were performed to investigate the temporal fluctuations of vegetation noise. The results shown in [4] are presented in octave band and the first set of measurements was performed into a shelterbelt of elms, a tree species not modeled in any known literature and hence impossible to simulate accurately. At a second site, consisting of aspen, spruce and pine trees, the exact vegetation geometry and meteorological data is not reported. Therefore, new measurements were considered necessary. Data were collected from a forest edge consisting of spruces. The geometry of the site is shown in figure 4. Meteorological conditions were as follows, temperature $T = 10^{\circ}C$, relative humidity $H_R = 82\%$, atmospheric pressure was not measured and is approximated to 1 atm and the atmospheric condition was considered moderately unstable.

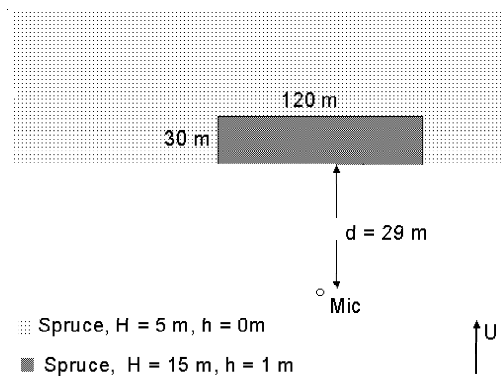


Figure 4: Geometry of forest edge of spruces.

5.3 Results

Measurements and predictions of from [3] are shown in figures 5(a) and 6(a). Calculations of their respective loudness index are shown in figures 5(b) and 6(b). To investigate the signal to noise ratio between the wind turbine sound and the vegetation noise a typical wind turbine sound generated by the software from [21] have been plotted in these figures.

The sound pressure levels of 5(a) and 6(a) shows that better estimations of the measurements with the discrete model compared to the analytical method used by Fégeant. This is especially true in the region around 500 Hz to 1 kHz which is the interesting range were the wind turbine sound and vegetation sound will be of approximately equal magnitude. However, as the fluctuations of vegetation noise is not taken into account these conclusions should be questionable.

The loudness index estimations in 5(b) and 6(b) displays that in stationary conditions masking is probable to occur above 400 Hz in the former site and above 500 Hz in the latter estimation.

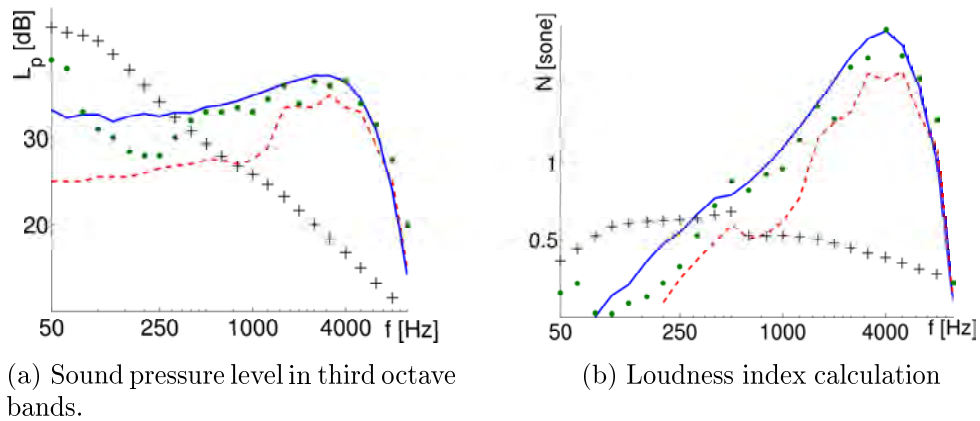


Figure 5: Sound pressure level and loudness index from the edge of aspens at $u = 3.3$ m/s. (●) Measurement, (—) Prediction by Bolin, (- - -) Prediction by Fégeant, (+) Prediction of wind turbine sound by Lindblom.

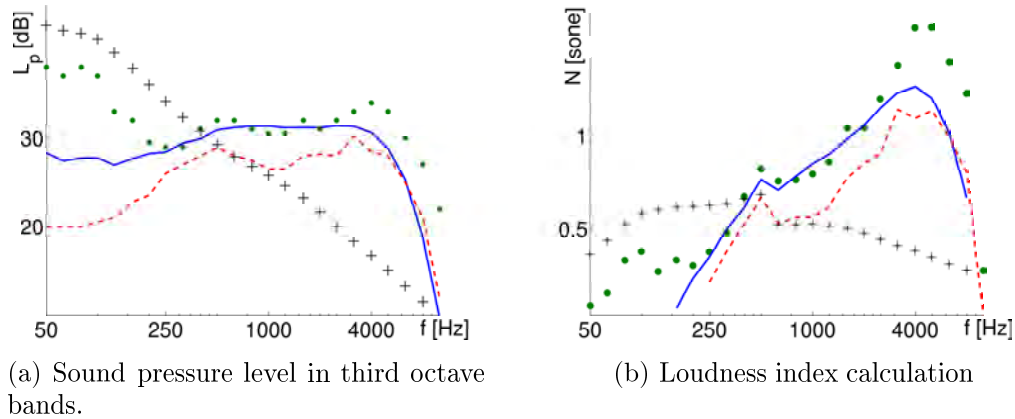


Figure 6: Sound pressure level and loudness index from the edge of aspens, pines and spruces at $u = 4.4$ m/s. (●) Measurement, (—) Prediction by Bolin, (- - -) Prediction by Fégeant, (+) Prediction of wind turbine sound by Lindblom.

Figure 7(a) and 7(b) shows measurements and prediction of the spruce forest edge. It can be observed that the estimations accuracies are increasing above 500 Hz. In 7(a) wind turbine sound is shown, it is shown that masking should occur at frequencies above 500 Hz in this specific case.

Table 1 shows the measured and estimated standard deviations of the spruce edge. These data are closely corresponding to each other, but the first third octave frequency band standard deviation is underestimated in both cases. It should be noted that the smaller standard deviations of the latter case compared to the former is inconsistent with the expectations and theory but could be explained by the short time series used in both analyze and simulation. The use of short periods of time is due to the presence of disturbances in the measurements and due to lack of computational power in the data from the simulation.

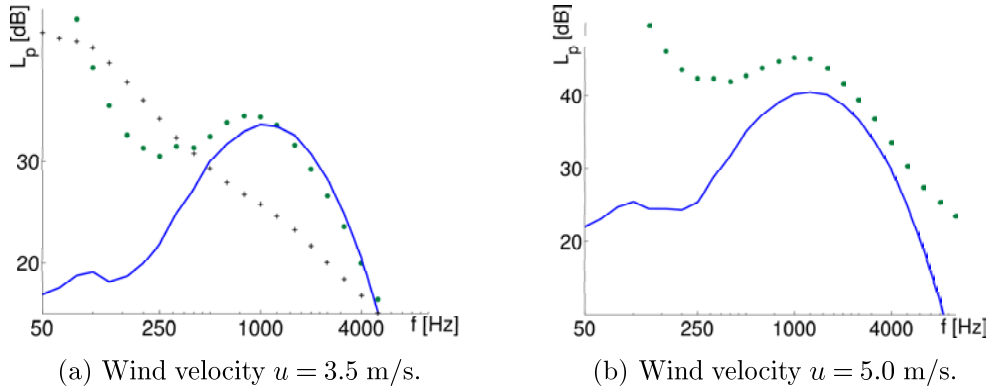


Figure 7: Sound pressure level, spruce forest edge. (\bullet) Measurement, (—) Prediction by Bolin, (+) Prediction of Wind turbine sound according to Lindblom

	u (m/s)	63 Hz (dB)	125 Hz (dB)	250 Hz (dB)	500 Hz (dB)	1 kHz (dB)	2 kHz (dB)	4 kHz (dB)
U=3.5 m/s								
Measured σ_X	1.9	8.4	7.6	7.1	6.5	6.7	7.2	7.9
Estimated σ_X	1.8	6.1	6.3	6.7	6.8	6.9	7.1	7.3
U=5.0 m/s								
Measured σ_X	1.1	7.3	6.6	6.4	5.7	5.7	6.2	6.4
Estimated σ_X	0.93	5.2	5.4	5.8	5.6	5.6	5.8	6.0

Table 1: Measured and estimated standard deviations at spruce forest edge at wind velocity $u = 3.5$ m/s and $u = 5.0$ m/s.

6 Conclusion

One of the objectives of this paper was to improve the Fégeant prediction model and to combine it to a turbulence model. As shown, the discrete prediction method estimate the measurements with higher accuracy than the analytical method and can easily be coupled to a stochastic three-dimensional turbulence model. However, different atmospheric conditions can influence the predicted sound level and must therefore be taken into account when modeling vegetation noise. Further more the number of computations to generate time series of vegetation noise is very large and hence only short time series can be obtained. Unfortunately, this results in turbulence statistics that are not completely reliable

The loudness index difference equation in section 4 may only be used in conditions where $L_{WT} \sim L_{Veg}$ this equation is otherwise invalid but as these nonlinear effects are not completely understood future work is planned to quantify this phenomena in the wind turbine case.

It can be concluded that the temporal variations of vegetation noise have drastic effect

on the masking potential. Still, psycho-acoustic tests have not yet been performed it is considered difficult to quantify the perceived masking potential as the evaluated percentile theory has been modified and conclusions from this model should be used with care.

No general deduction of masking can be concluded, therefore case studies in different environments and meteorological conditions should be conducted in order to estimate the masking potential of wind turbine sound by vegetation noise.

References

- [1] R Meir et al. The assessment and rating of noise from wind farms. Technical report, ETSU, Department of Trade and Industry, 1996.
- [2] O Fégeant. Wind-induced vegetation noise. part 1: A prediction model. *Acta Acoustica*, 85, 1999.
- [3] O Fégeant. Wind-induced vegetation noise. part 2: Field measurements. *Acta Acoustica*, 85, 1999.
- [4] O Fégeant. Masking of wind turbine noise: Influence of wind turbulence on ambient noise fluctuations. Technical Report 2002:12, Department of Civil and Architectural Engineering, Royal Institute of Technology, Sweden, 2002.
- [5] *ISO/DIS 9613-1: Attenuation of sound during propagation outdoors- Part 1: Atmospheric absorption.*
- [6] *ISO/DIS 9613-2: Attenuation of sound during propagation outdoors- Part 2: General method of calculation.*
- [7] H Panovsky and J Dutton. *Atmospheric Turbulence*. John Wiley & Sons, New York, 1984.
- [8] J C Kaimal and J J Finnigan. *Atmospheric Boundary Layer Flows*. Oxford University Press, New York, 1994.
- [9] R C Cionco. A wind profile index for canopy flow. *Boundary Layer Meteorology*, 3, 1972.
- [10] D Miller. The two dimensional energy budget of a forest edge with field measurement of a forest edge with field measurement of a forest parking lot interface. *Agricultural meteorology*, 2:53–78, 1980.
- [11] *TA-Luft, Erste Allgemeine Verwaltungsvorschrift zum Bundes-Immissionsschutzgesetz- Technische Anleitung zur Reinhaltung der Luft (First general directive to the federal immission protection act- Technical guideline for clean air)*. (in German).

-
- [12] R Cionco. Intensity of turbulence within canopies with simple and complex roughness elements. *Boundary Layer Meteorology*, 2:453–465, 1972.
- [13] D Baldocchi and T Meyers. A spectral and lag-correlation analysis of turbulence in a deciduous forest canopy. *Boundary Layer Meteorology*, 45:31–58, 1988.
- [14] B Amiro. Comparison of turbulence statistics within three boreal forest canopies. *Boundary Layer Meteorology*, 51:345–364, 1990.
- [15] P S Veers. Modeling stochastic wind loads on vertical axis wind turbines. Technical Report SAND83-1909, Sandia National Laboratories, 1984.
- [16] P S Veers. Three-dimensional wind simulation. Technical Report SAND88-0152, Sandia National Laboratories, 1988.
- [17] H W Tieleman. Universality of velocity spectra. *Journal of wind engineering and industrial dynamics*, 56, 1995.
- [18] E Zwicker and H Fastl. *Psychoacoustics: Facts and Models*. Springer, second edition, 1999.
- [19] B C J Moore. *Psychology of Hearing*. Academic Press, fifth edition, 2003.
- [20] *ISO/DIS 532A: Method for calculating loudness level*.
- [21] C Lindblom. Prediction code for wind turbin noise. Master’s thesis, KTH/FKT, 2002.

**First International Meeting
On
Wind Turbine Noise: Perspectives for Control
Berlin 17th and 18th October 2005**

**The Use of 10 m Wind Speed Measurements in the Assessment
of Wind Farm Developments**

Paul Botha BSc (Mech) Eng, MSc Eng
Wind Technical Specialist
Meridian Energy Limited
PO Box 10-840, Wellington, New Zealand
Email: paul.botha@meridianenergy.co.nz

Summary

Most wind turbine manufacturers provide the sound power level (L_{WA}) of their turbines in accordance with IEC61400-11 [1]. This requires the L_{WA} to be reported against a wind speed at a height of 10 m above ground level (agl). Since the turbine source noise is given at 10 m agl, noise predictions and planning limits are often also undertaken against wind speeds at a height of 10 m agl. This use of a 10 m reference height for wind speed measurements during acoustic measurements of wind turbines seems largely historic and may have been appropriate for the tower heights at the time. Today's wind turbines are generally much taller and the reference height of 10 m is perhaps no longer appropriate.

The relationship between the wind speed at a height of 10 m and that at the hub height of a turbine (the wind speed profile or wind shear) is not constant and is not simply a function of the site surface roughness, Z_0 , as expressed by the logarithmic wind speed profile and used in the IEC 61400-11 standard. The site wind speed profile is dependent on the site topography, wind direction and atmospheric conditions.

This paper examines the wind speed profiles at four sites that have the same surface roughness, based on a physical examination of the site. Two of the sites are in flat terrain in Australia and two in complex terrain in New Zealand. It shows that as the wind speed profiles vary significantly between the four sites and with time of day at a given site, the use of surface roughness to determine wind speeds for wind farm acoustic assessment can lead to errors.

The paper proposes that hub-height wind speeds should be used for the entire acoustic assessment of both wind turbines (sound power level determination) and wind farms (prediction and measurement), and outlines the advantages of this approach.

1. Introduction

The majority of standards and guidelines [1,2,3,4] that set out procedures to determine the sound power level (L_{WA}) of a wind turbine, require that the results be reported against a wind speed at a height of 10 m above ground level (agl). The first version of IEC 61400-11 required that the results be reported at 8 m/s at 10 m agl and this was referred to as the reference conditions. The 2002 version of this same standard requires the results to be reported at wind speeds of 6 to 10 m/s, all referenced to a height of 10 m above ground level.

Since the sound power level of a wind turbine is reported against a wind speed at 10 m agl, this same wind speed measurement height is often used when predicting noise from a proposed wind farm development. In many instances it also becomes a wind speed measurement height against which planning conditions are assessed.

This paper outlines the typical steps in assessing the noise from a wind farm which are influenced by the assumptions made on the wind speed variations with height (wind speed profile). Measured wind speed records have been analysed in order to make a comparison against theoretical wind speed profiles.

2. The typical phases in wind farm noise assessments and the 10 m wind speed reference height

Typically there are three distinct phases required to complete the assessment of the noise from wind farms. These are:

- I. Wind turbine manufacturers measure and provide the sound power level of their turbines. These are typically measured in accordance with IEC 61400-11.
- II. Wind farm developers undertake wind farm noise predictions using the sound power level information provided by the wind turbine manufacturers and a suitable noise propagation model.
- III. Local authorities require that the wind farm developer demonstrates compliance with the limits placed on the wind farm development, through measurements conducted after the wind farm is operational.

As the sound power level of a wind turbine is dependent on its power output, and therefore the hub height wind speed, it is important that the height above ground level of the wind speed measurement, in each of the three phases above, is clearly defined and consistent. Typically most noise predictions and assessments are done relative to a wind speed at 10 m agl, primarily because this is the height of the wind speed required to be reported by IEC 61400-11 [1]. Other guidelines and standards such as AWEA [2] and IEA [3] also require sound power level measurements to be reported against a wind speed at 10 m agl.

At the time that these standards and guidelines were first developed, wind turbine hub heights were significantly lower than they are today. As a consequence, the

uncertainty in determining a hub height wind speed, at 30 m or 40 m, from a 10 m wind speed to was not significant. Hub heights of wind turbines today are significantly greater and turbine hub heights in excess of 70 m are common for megawatt class turbines.

Additionally, measurements taken for wind resource monitoring purposes have shown that the relationship between hub height wind speeds (40 m to 80 m) and the wind speed at 10 m is not constant and dependent on surface roughness alone. Atmospheric stability, wind direction and the topographical changes in the vicinity of a wind turbine will also influence the rate of change in wind speed with height above ground level.

3. The IEC 61400-11 sound power level measurement procedure

During the measurement of a wind turbine's sound power level, as per IEC 61400-11:2002, wind speeds can be derived in one of two ways.

- I. Method 1. Determination of the wind speed from the electric output and the power curve.
- II. Method 2. Determination of the wind speed with an anemometer positioned between 10 m and the wind turbine hub height.

Method 1 is the preferred method and is mandatory for certification and declaration of measurements. It is interesting to note that this method suggests that it is preferable to use a power curve measured in accordance with IEC61400-12 [5] and preferably for the same wind turbine. IEC61400-12 requires a hub height anemometer to be used for the derivation of the power curve and therefore if both preferences of Method 1 of IEC61400-11 are being complied with, it is very likely that a hub height anemometer would be situated nearby.

Irrespective of which method is used to determine the wind speeds in accordance with IEC61400-11, an anemometer is required (of height between 10m and hub height) to determine the wind speeds while the wind turbine is shut-down. The shut-down measurements are used to determine the background noise levels in order to make a correction for the background noise levels while the wind turbine is operating.

Assuming the preferred method of wind speed derivation is used under IEC 61400-11 (Method 1), the hub height wind speeds (derived from the power curve) are then converted to 10 m high wind speeds simply using the reference surface roughness Z_{0ref} of 0.05 m. If wind speed measurements are recorded at any height between 10 m and hub height, they are corrected to hub height using the site roughness length Z_0 and then converted to 10 m wind speeds using the reference surface roughness Z_{0ref} of 0.05m. Note that these 'two' conversions are done together using equation (7) in IEC 61400-11:2002.

In effect, the 10 m reference wind speeds against which the sound power levels are reported are reliant on the relationship between the 10 m and hub height wind

speeds being well defined by the visual assessment of the site surface roughness. This is not always the case as is discussed in Section 6.

4. Shortcomings of the IEC61400-11 methodology

In IEC61400-11, where wind speed measurements are corrected to hub height using the surface roughness, there is a probability that they are not consistent with the wind speed derived from the power curve. Where any wind speed measurements are derived from an anemometer at a height other than at hub height (Method 2) their absolute value may not be entirely correct as the logarithmic extrapolation method is not precise. The logarithmic wind speed profile assumed can have an effect on the reported sound power level, irrespective of which method of wind speed determination is used.

Since the preferred method of wind speed determination in IEC61400-11 is via the wind turbine power curve, it only requires the acoustic assessment of the wind turbine up to a wind speed of 95% of rated power. The correlation between the sound power level of the turbine and the electrical output is low beyond the rated power of the turbine. This is a shortcoming of the Standard as there are some wind turbines which have an increased sound power level when the turbine reaches rated power and starts to limit its power output. If hub height wind speed measurements were mandatory, the wind speed range against which the sound power levels were reported, could be extended.

5. The logarithmic wind speed profiles

The logarithmic wind speed profile that is used to extrapolate wind speeds from one height to another (as in IEC61400-1) is defined as follows:

$$V = V_{\text{ref}} * \ln(Z/Z_0) / \ln (Z_{\text{ref}} / Z_0) \quad \dots\dots\dots\text{equation (1)}$$

Where

V = wind speed at height Z
 V_{ref} = wind speed at height Z_{ref}
 Z = height above ground level
 Z_0 = surface roughness

Clearly this equation describes the relationship between two different height wind speeds as a function of the surface roughness alone. While this function may be appropriate on an average basis (e.g. over a year) it is not as robust when converting 10 m high wind speeds to their hub height equivalents for the purposes of sound power level certification or assessment. This is discussed further in Section 6.

6. Wind profile examination

To investigate the variation of the logarithmic wind speed profile, data for a year at three sites and data for 8 months at a fourth site have been analysed. For all four sites 10-minute wind data records at hub height (50 m to 80 m) have been monitored simultaneously with wind speeds typically at a height of 10 m and in one case 15 m. The sites were situated in both New Zealand and Australia and covered both flat and complex terrain.

The four sites at which data has been monitored and analysed are listed in Table 1.

Site Name	Wind speed measurement heights	Data period	Location	Topography
Site 1	80 m, 10 m	1 year	Australia	Flat site
Site 2	50 m, 10 m	1 year	Australia	Flat site
Site 3	70 m, 15 m	8 months	New Zealand	Complex terrain
Site 4	40 m, 10 m	1 year	New Zealand	Complex terrain

Table 1. Data at which wind speed profiles were examined

For each of the 4 sites, the mean wind speeds at the two heights were used to calculate the theoretical site surface roughness based on equation 1. Using the calculated surface roughness for the site, the logarithmic wind speed profile was drawn for each of the four sites and is shown in Figure 1. The calculation of the site surface roughness was then repeated using only the day time data (06h00 to 22h00) and the night time data (22h10 to 05h50). Each of the logarithmic profiles were added to the charts in Figure 1.

In addition to the calculated logarithmic profiles, the wind speed profiles based on the observed site surface roughness ($Z_0 = 0.03\text{m}$), which were used for wind flow modelling, and the IEC61400-11 reference surface roughness $Z_0 = 0.05\text{m}$ have been plotted. The calculated surface roughness values are listed in Table 2.

Site Name	All time	Day time	Night time	Observed from terrain
Site 1	0.1741	0.0513	0.7834	0.03
Site 2	0.1262	0.0499	0.4752	0.03
Site 3	0.0011	0.0006	0.0029	0.03
Site 4	0.0007	0.0005	0.0014	0.03

Table 2. Calculated surface roughness lengths from site measurements

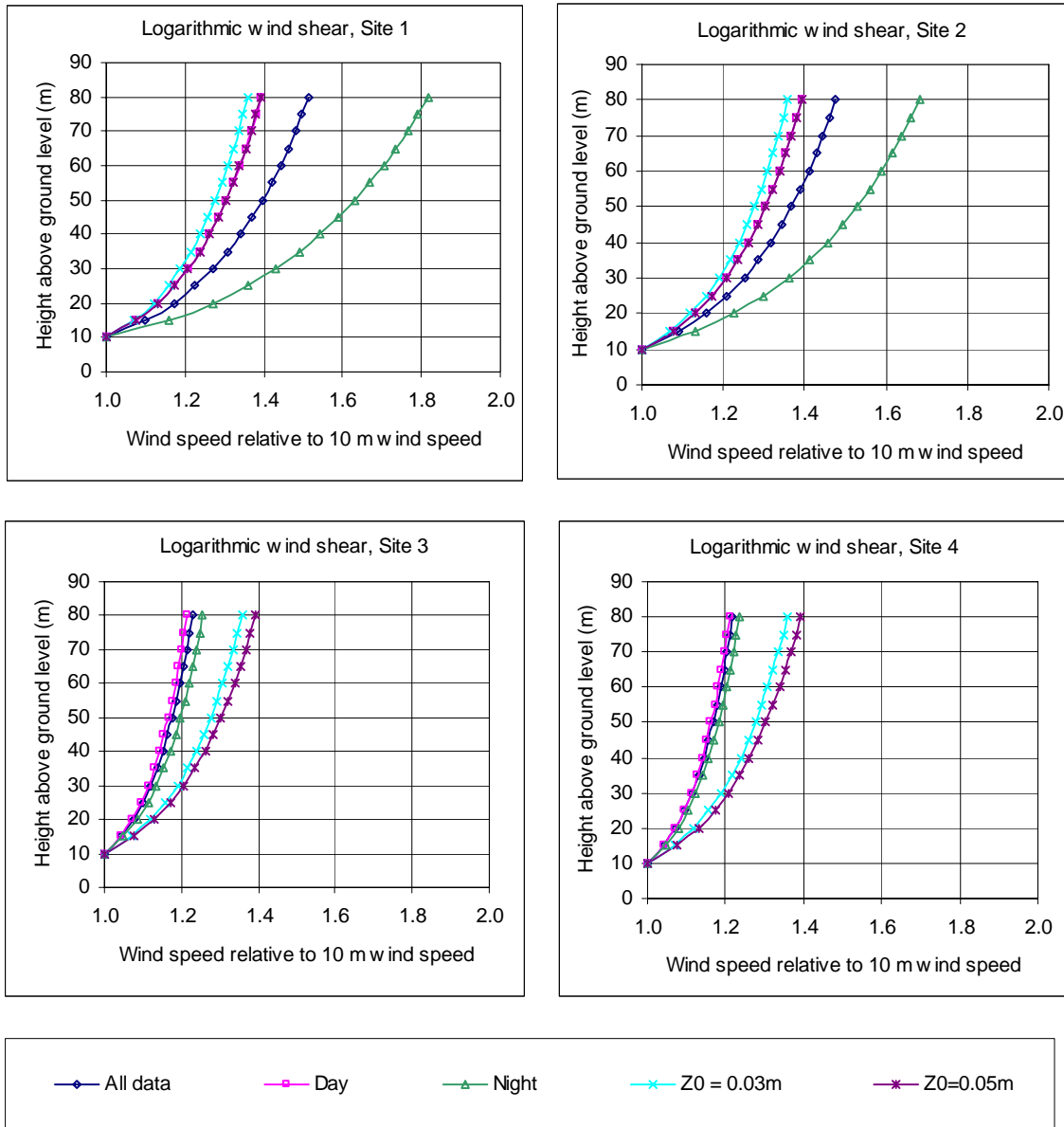


Figure 1. Logarithmic wind speed profiles at 4 different sites.

Some observations that can be made from the results shown in Figure 1 are:

- In all cases the wind speed profile based on the observed site surface roughness is different to the measured “all data” wind profile.
- Using the wind speed profile based on the estimated site surface roughness significantly under-estimates the hub height wind speed at night at the two Australian sites (flat terrain).
- The wind speed profile based on the estimated site surface roughness is similar to the measured day time wind speed profile for the two Australian sites.
- There is a significant difference between the day and night profiles at the two Australian sites.

- The estimated site surface roughness over-estimates the hub height wind speed at both New Zealand sites (complex terrain sites).
- There is very little difference between the day and night wind speed profiles at the two New Zealand sites.
- In all cases, the differences that are identified are greater for higher wind turbine hub heights.

From Figure 1 it is evident that the actual wind speed profile at a particular site is not simply a function of the estimated surface roughness but is dependant on both atmospheric conditions (stability) and the site topography and wind direction.

7. The influence of wind speed height in noise propagation modelling

When noise modelling is undertaken for a potential wind farm site, the wind speed for which the results have been produced needs to be stated. If a developer is undertaking and presenting wind farm noise predictions for a given hub height wind speed, they simply use the L_{WA} of the turbine, provided in accordance with IEC61400-11 and correct the wind speed to hub height using the reference surface roughness $Z_0 = 0.05m$. For example, for a 70 m hub height wind turbine, the IEC61400-11 10 m reported wind speeds translate to those in Table 3. This is in effect the reverse of how the wind speeds were initially derived from the wind turbine power curve.

Reference Wind speed (at 10 m) (m/s)	70m hub height wind speed (m/s)
6	8.2
7	9.6
8	10.9
9	12.3
10	13.7

Table 3. 70 m equivalent wind speeds based on $Z_{0,ref} = 0.05m$

If the developer is calculating and presenting wind farm noise predictions with reference to 10 m high wind speeds, they are required to convert the IEC61400-11 wind speeds to hub height (again using $Z_0 = 0.05m$) and then correct them a second time to a site specific 10 m wind speed value using the site specific surface roughness or the measured wind speed profile. Representing the noise predictions as a function of a 10 m value creates uncertainties where the wind speed profile at the site varies between day and night. One solution would be to provide two sets of predictions, one for each wind speed profile, however this can be eliminated if noise predictions are done for a specific hub height wind speed.

It should be noted that if the wind speeds, at which predictions are made, are converted to 10 m wind speeds, they are only valid for times when the relationship

between wind speed at hub height and 10 m are as per those used in their conversion. As shown in Section 6, the relationship between wind speeds at two different levels is not constant and can vary by time of day, wind direction and site topography.

Clearly there are advantages in presenting wind farm noise predictions as a function of the hub height wind speed as the predictions will always be valid for the stated wind speed. Additionally it doesn't rely on the estimate of the site surface roughness when presenting the results.

There have been two papers [6,7] published that suggest that wind farm noise predictions are inaccurate especially under stable atmospheric conditions, which can occur at some locations more frequently at night. As shown in Figure 1, the wind speed profile often varies between day and night at some sites and furthermore the profile varies between sites which appear to have the same surface roughness. In the Rhede wind farm example referenced in [6,7] it is perhaps not so much that the noise predictions were inaccurate but that the assumptions made on the wind speed profile were inaccurate for the reasons outlined above. If the wind farm was required to meet a planning limit based on a hub height wind speed rather than a 10 m high wind speed this would have required the wind farm to meet the planning noise limit irrespective of the site wind speed profile.

From the analysis completed in Section 6 and shown in Figure 1, for an 80 m hub height wind speed of 15 m/s at night, the error in the hub height wind speed estimate could have been 3.6 m/s. This in turn would have led to an error in the sound power level assumption, the extent to which would have been dependant on the particular turbine type being used.

8. Setting limits based on hub height wind speed rather than 10 m

As has been shown in Section 6 the relationship between the wind speed at 10 m agl and hub height may not be constant at a particular site. Likewise, for sites of the same surface roughness the wind speed profiles can be quite different. It is important also to note that it is the hub height wind speed and not the 10 m wind speed that dictates the sound power level of a wind turbine.

Where noise limits are placed on a wind farm and are assessed against a 10 m wind speed measurement height, the wind farm developer needs to be aware of the actual relationship between the 10 m wind speed and that at hub height for a range of atmospheric conditions to ensure that the noise levels are met under the range of wind speed profiles experienced at the site.

An approach that is used in the UK [8], New Zealand [9], Australia [10] and the Netherlands [11], is to set the wind farm limit as a function of the background noise level that exists prior to the wind farm being installed. This typically requires background levels to be measured prior to the wind farm installation and background plus wind farm levels to be measured once the wind farm is operational. In both cases, the noise levels are plotted against wind speeds recorded simultaneously with

the noise measurements. Ideally these wind speeds measurements should be those at the hub height of the wind turbines, however a height of 10 m is regularly used. Again this height appears to be adopted only since the wind turbine sound power levels are listed against 10 m high wind speeds. These could just as easily be plotted against hub height wind speeds.

In cases where the background noise levels are plotted against hub height wind speed, the noise measurements should include the representative range of wind speed profiles experienced at the site. Typically, best practice is to divide the data (and therefore the compliance limit) into day and night too. Furthermore if the background noise levels are plotted against the site hub height site wind speed, it eliminates the problems that occur at sites where the wind speed profile changes due to atmospheric stability, wind direction and site topography.

9. Conclusions

The historical use of 10 m high wind speed measurements for the acoustic assessment of both wind turbines and wind farms has the ability to create inaccuracies and sometimes confusion around sound power levels, noise predictions and even demonstration of wind farm compliance. The use of 10 m high wind speed measurements appears to be largely historic and there are advantages in using hub height wind speeds throughout the noise assessment process.

In the determination of the sound power level of a wind turbine in accordance with IEC61400-11, the use of the surface roughness to determine the hub height wind speed has the ability to introduce errors into the measurement procedure. Hub height wind speeds should be required and these could be obtained either from the nacelle anemometer or, if possible, a hub height anemometer that was used in the measurement of the power-curve of the wind turbine. Consideration should also be given to determining the sound power level of turbines to beyond their rated power, since some wind turbines increase their sound power level once they start to control their power output.

For wind farm noise compliance measurements the hub height wind speed can be derived from either the power curve of the operational wind turbine, the nacelle anemometer or a wind farm meteorological monitoring mast. Where hub height wind speeds are required prior to the wind farm installation, these are more reliably obtained from coincident measurements at two heights (e.g. 10 m and 50 m) rather than based on surface roughness wind speed corrections.

There are already wind turbine manufacturers that provide their sound power levels as a function of the hub height wind speed and to beyond rated power. There are advantages to developers in having that information and it would be beneficial if this was a mandatory requirement within IEC61400-11.

The continued use of a wind speed reference height of 10 m used in IEC61400-11 appears largely historical and with increasing turbine hub heights there are good reasons why this should now be changed.

References

1. Wind Turbine Generator Systems – Part 11: Acoustic Noise Measurement Techniques, IEC 61400-11, Second edition 2002.
2. AWEA Standard 2.1. 1989 “Procedure for Measurement of Acoustic Emissions from Wind Turbines Generator Systems” Volume 1: 1st tier.
3. Mackinnon, A and Henderson A R, Sound Power Measurement and Certification of Wind Turbines, Proceedings of the Institute of Acoustics, Vol 16, Part 1 (1994).
4. Recommended Practices for Wind Turbine Testing and Evaluation. 4, Acoustics, Measurement of Noise Emission from Wind Turbines, 3rd Edition 1994, IEA.
5. Wind Turbine Generator Systems – Part 12: Wind Turbine Power Performance Testing, IEC 61400-12, First edition 1998.
6. Effects of the Wind Profile at Night on Wind Turbine Sound, G.P van den Berg. Journal of sound and Vibration, 2003
7. Wind Turbines at Night: Acoustical Practice and Sound Research, Frits GP van den Berg. Euronoise Naples 2003.
8. The Assessment and Rating of Noise from Wind Farms, ETSU-R-97, Final Report 1996.
9. NZS 6808:1998, Acoustics- the Assessment and Measurement of Sound from Wind Turbine Generators. Standards New Zealand.
10. Wind Farms, Environmental Noise Guidelines. Environment Protection Authority of South Australia, February 2003.
11. Noise annoyance from wind turbines – a review, Eja Pedersen, Hogskolan I Halmstad. Naturvardsverket Swedish Environmental Protection Agency.

**First International Conference on
Wind Turbine Noise: Perspectives for Control
Berlin, Germany, 17-18 October 2005**

**TWO-MEDIUM THEORY OF AERODYNAMIC SOUND SOURCES
AND THE PRACTICAL PROBLEMS OF WIND TURBINE NOISE**

A. T. Fedorchenko

*Institute for Mathematical Modeling, Russian Academy of Sciences
125047 Moscow, Russia
E-mail: fedorch@rol.ru*

A number of practical problems of wind turbine noise are considered, mainly those associated with the sources of aerodynamic sound in high-unsteady flow near turbine blades. Unfortunately, the current level of comprehension of the key mechanisms of noise generation should be recognized insufficient, and so the efforts in inventing new means of noise reduction cannot be quite successful. In hindsight, during more than half century various versions of Lighthill's "acoustic analogy" were used to identify the aerodynamic noise sources, though the rigorous mathematical proofs have been given that this "well-recognized approach" is wrong. The radically new non-local two-medium theory of aerodynamic sound sources has been developed by the author, and its main properties are now discussed in connection with the analysis of aerodynamic noise sources close to wind turbine.

1. On aerodynamic noise of wind turbines

Wind generators, as the very attractive clean sources of energy [1], are widely used in many countries, and the today jumps in oil prices only enhance their attractiveness. However, no energy can be obtained without serious penalties. In particular, wind turbines generate noise through diverse mechanical and aerodynamic sources, and so the increasing research efforts are being now undertaken to reduce noise emitted by wind turbines [2-6]. The great variety of wind turbines have been invented: with vertical and horizontal axis (including those pointed upwind or downwind of the tower), combined turbines with counter-rotation, specific onshore and offshore ones, etc. Some turbines may have blades which can be pitched, and in the other ones the rotor speed can be regulated by following the wind changes. Anyway, when comparing different modern turbines with horizontal axis, one is able to conclude that upwind rotors may be quieter, especially when the rotational speeds and possible pitching are controlled.

The components of wind turbine noise could be roughly attributed to the following main types [3]: *tonal noise* (at discrete frequencies) caused by diverse mechanical and aerodynamic effects, *broadband noise* (at frequencies greater than 100 Hz), *low frequency noise* (in the range from 20 to 100 Hz, that is mostly associated with downwind turbines), and *impulsive noise* that may be caused by complex interaction of unsteady flows near the tower and turbine blades in downstream machines. The mechanical sources of noise (e.g., from gearbox and generator) are excluded from

consideration in this paper, and only the sources of aerodynamic noise are under discussion.

Aerodynamic noise sources arise in the high-unsteady vortical flow around wind turbine blades, and partly due to presence of tower. Aerodynamic broadband noise emitted by the flow close to rotor blades is typically dominant in the noise emission, and it increases with wind velocity, and respectively with the rotation speed. Various mechanisms of aerodynamic noise are roughly divided by some researchers into three groups: low frequency noise, inflow turbulence noise, and airfoil self-noise [3-6]. However, this classification is too ambiguous, because so far the key mechanisms of noise generation by unsteady flow remain unstudied, primarily due to the long use of wrong theoretical approaches by many researchers in their efforts to define accurately the aerodynamic sound sources of different nature. For instance, there is no ground for regarding the rotation of blades as a direct mechanism of low-frequency noise [6,7]; really, the true impact of rotation on sound generation could not be investigated within the “well-recognized” theoretical models of noise sources, because in fact all those models represent the branches of absurd “acoustic analogy”. Concerning the noise sources close to blades (due to flow instabilities in boundary layers, local separation effects, vortex shedding from the trailing edge, tip vortices, etc.) supposedly responsible for the main portion of “airfoil self-noise” [6], all these phenomena should be also completely understood before one could formulate any general conclusion on their true contribution to the overall noise emission. Complex flows around the tower and gearbox, as well as their interaction (including possible effects of acoustic feed-back) with the phenomena near blades, form a separate research direction. The influence of inflow turbulence on noise emission remains unstudied as well because no adequate theory of high-unsteady turbulent flows of compressible fluid has been created, and moreover, such a prospective theory cannot be incorporated into the traditional models of aerodynamic sound sources.

Of course, due to general progress in technology the modern wind turbines become much quieter, partly due to using some new approaches in designing rotor blades. For instance, serration of the rotor blade trailing edge and the new tip design have resulted in noise reduction, up to several dB in some cases [5,8]; nevertheless, these changes in the blade shape cannot be recognized as the best and universal remedy able to exclude any perceptible noise. It should be also noted that this approach is rather old, and so far it is not accompanied by the radical increase in comprehension of the key mechanisms of noise generation by turbulent separated flows. As a result, even after applying the known means of noise reduction the residual noise emission is able to cause very unpleasant effects, especially within the vast wind farms and when wind velocities are substantial. Sometimes the declared “excellent noise characteristics” of an offered wind turbine cause serious doubts, and generally these characteristics can be scarcely determined under all wind conditions. Really, the atmospheric medium, including its inherent turbulence, is too unpredictable as usual, and so it is difficult to take into account all flow regimes (e.g., the night effects [10]) and all internal interactions resulting in peculiar parts of noise spectrum.

As for the measurement of real noise emission, even this problem is still far from easy, though a number of quite effective methods have been developed for this [4,8, 9,11]. It is well known that no accurate measurement of the far sound field (e.g., by

microphone arrays) is unable to restore in unique manner the true distribution of noise sources just in the local zone of sound generation. To this should be added that no perfect acoustic probe is yet invented to measure all acoustic components of high-unsteady flow within the zone of intense noise generation; moreover, first one must understand how to distinguish the acoustic components from various kinds of disturbances in a high-unsteady flow. Also, the following sharp question is usually ignored: if the local sound source is a multi-component vector (see below Section 3), but not a simple scalar variable, then one should select the radically new, non-traditional set of flow parameters to be measured.

Thus, the above mentioned research problems are still of great current importance, and among those the correct definition of aerodynamic sound sources should be recognized as the crucial problem in aeroacoustics. In connection with the practical problems of wind turbine noise the topical research directions could be again marked out: investigation of noise sources in unsteady separated flows (especially in vortical flows close to turbine blades) through applying the newest experimental and theoretical methods, with possible consideration of interaction between flow induced structure vibration and wind noise, and eventually the development of more effective means of flow control (active or passive) aimed at noise reduction.

2. The main flaws in the current methods of TCAA

Diverse means of flow control aimed at drag and noise reduction play an increasingly important role in the development of new technologies. A considerable part of the related research work is traditionally concentrated in aerospace and military industry, but any practical achievements could be also readily adopted in many civil areas, including wind power engineering, that would give the substantial commercial gain. Nevertheless, it seems that visible, though rather modest, technological progress in numerous problems of noise reduction, that is now demonstrated by aerospace industries in the United States and the European Union, was attained primarily due to inventive activity based on the growing volume of practical experience, but not from the full comprehension of fundamental mechanisms of sound generation in high-unsteady flows. Obviously, any experimental research should be supported by solid theoretical basis, and so perhaps the technological accomplishments would be much more impressive if engineers could also possess an adequate theoretical knowledge of the key mechanisms of noise generation. One should also bear in mind the following delicate problem: if the newest research results are first obtained in aerospace or military industry, it may be difficult (because of evident reasons) to transfer them immediately into a certain civil field like the wind turbine design.

If one appreciates impartially the current posture of theoretical and computational aeroacoustics (TCAA) in all its branches, it is far from “the state of the art”, though the latter is often declared. The vast databases of numerical solutions, even three-dimensional, have been collected for various unsteady flows, but this has not yet caused a radical advance in comprehension of the sound generation phenomena, including those peculiar to wind turbines. Indeed, these solutions are usually able to show the integral flow field in which all kinds of disturbances are inseparable, and so a general non-linear theory of aerodynamic sound sources, which should be based on a proper procedure of flow decomposition, is urgently required as a necessary supplement to the classical equations of fluid mechanics written in terms of “total”

variables. If turbulent gas flows are under simulation, one should distinguish between the turbulent fluctuations (usually these are assumed to be “quasi-incompressible”) and the sound disturbances; here the problem of an adequate decomposition of all flow variables becomes most crucial, especially when the impact of fine-scale turbulence on noise emission is studied. The absence of perfect algorithm for this decomposition was the most feeble point of all the “well-adopted” approaches to the theory of aerodynamic sound.

In the author’s view, the wrong mathematical models are still used by many for the definition of aerodynamic sound sources, especially the vast family of Lighthill’s acoustic analogy [7,12,13,], probably due to its illusory simplicity. Although the falsity of diverse kinds of acoustic analogy was clearly proved in the author’s work [14], now it is relevant to enumerate again some delusions resulted from this approach:

- 1) Sound source Q , typically being the right-hand part of a single scalar high-order “inhomogeneous acoustic equation”, is a local function of flow variables (the velocity components, pressure and density) as well as of their temporal or spatial derivatives.
- 2) Sound source Q is directly determined by the Reynolds stress tensor, at least in subsonic flows, that may be obtained from the ready DNS-solution.
- 3) Sound sources in a free shear flow display quadrupole features.
- 4) There are many different formulae for Q (though some of them are not Galilean invariant), but all those yield the same far field (i.e., the notion of “non-radiating sources” was there introduced).
- 5) At low Mach numbers $Q \approx \rho_0 \nabla[\Omega \times \mathbf{u}_v]$, where $\Omega = \nabla \times \mathbf{u}_v$, $\nabla \mathbf{u}_v = 0$ [7]. This means that sound sources are concentrated only in the zone with non-zero vorticity, and then any unsteady irrotational flow does not generate sound.
- 6) Intensity of sound (including that emitted by jets and wakes) $I \approx AU^8$, $A = \text{const}$, U is the mean flow velocity (averaged over all the flow domain?).
- 7) “Thermal source of sound” $Q_t = -\nabla(T \nabla S)$, T is the gas temperature, S is the entropy (as if sound is emitted due to motion of “entropy spots” [15]).
- 8) Unsteady background flow can be approximated by a simple uniform procedure of averaging (e.g., in each point over a certain finite time period).
- 9) If unsteady background flow can be considered steady in a certain non-inertial (rotational) reference frame, it will generate sound.

In the author’s view, these groundless assertions, and some other ones, have exerted (and still continue to exert) the detrimental influence on the evolution of theoretical aeroacoustics, and thereby they retard the developing of new practical means for noise reduction.

3. On the basic concept of the two-medium theory of aerodynamic sound

A general two-medium theory of aerodynamic sound has been created by the author. This non-linear theory is based on the original decomposition of all five independent scalar variables of a high-unsteady flow into acoustic and non-acoustic components, and the special integro-differential operator Ψ has been designed to implement this. Within the general concept of this decomposition a certain initial-boundary-value problem posed with using the common system of non-linear gas-dynamics differential equations, originally written in terms of “total” variables, is split into the two separate, though interconnected, initial-boundary-value problems, which are governed by the closed systems of *integro-differential* equations: for the unsteady background flow (this new medium displays very unusual properties), and for the acoustic field. The

Galilean invariant non-local formulae are derived for sound sources in the acoustic system. Some simplified versions of the theory have been suggested as well.

This theory was first exposed in 1995 in the leading Russian journal [16] which, having been translated into English, was distributed worldwide by the American Institute of Physics. The theory was also presented at several international conferences and workshops held after 1995. However, the reaction of the “leaders of world aeroacoustics” on this theory is rather curious. In the past decade, even after work [14] issued, they were reluctant to discuss this new theory, and much less to apply it. They preferred to use the old and well-verified method: they did their best in silencing this theory, probably pursuing the primitive objective: everything should be retained as it is in aeroacoustics fundamentals. At the same time in a number of recent publications their authors tried to extol again the family of Lighthill’s acoustic analogy, in spite of the fact that its falsity was clearly proved in [14]. Fortunately, aeroacoustics represents the scientific field where the rigorous mathematical language can be used to describe the grounds of a certain model; therefore, a sufficient set of proofs was suggested to substantiate the new two-medium theory of aerodynamic sound as well as to refute the wrong previous approaches. The following fact should be also mentioned: during the rather long past period possible opponents were unable to find any serious mistake in this theory.

Within this theory the basic system of equations governing the flow of inviscid air (here without any forces or heat/mass sources in the volume) is written for the vector variable $\mathbf{Z}(\mathbf{r}, t) = \{Z_1, Z_2, Z_3, Z_4, Z_5\} = \{u_1, u_2, u_3, \beta, s\}$ as

$$d\mathbf{u}/dt + a^2 \nabla \beta = 0, \quad d\beta/dt + \nabla \mathbf{u} = 0, \quad ds/dt = 0, \quad (1)$$

where $d/dt = \partial/\partial t + (\mathbf{u}, \nabla)$, $\beta = \gamma^{-1} \ln p$, $\zeta = \xi + q/c_p$, p is the pressure, s is the specific entropy, $a^2 = \gamma p/\rho = \gamma RT = (\gamma - 1)h$, a is the adiabatic speed of sound, $h = c_p T$ is the specific enthalpy, $c_p = \text{const}$ is the specific heat at constant pressure. The equation of state $\mathfrak{A}(\beta, s, h) = 0$ can be taken as

$$a^2 = (\gamma - 1) h = \gamma \exp [(\gamma - 1)\beta + s/c_p]. \quad (2)$$

With using the closed system (1)-(2), that is hyperbolic in time and space, one can pose a certain initial-boundary-value problem for $\mathbf{Z}(\mathbf{r}, t)$, $\mathbf{r} \in G$, $t \in J_t$ by specifying the initial distributions $\mathbf{Z}(\mathbf{r}, 0)$ in the spatial domain G , and the boundary conditions on a certain surface Γ . It is generally assumed that the boundary surface Γ may be permeable or its parts can move along the normal \mathbf{n} , possibly changing the volume of finite domain G .

Further all components of vector \mathbf{Z} are exactly decomposed as

$$\mathbf{Z}(\mathbf{r}, t) = \mathbf{Z}_v(\mathbf{r}, t) + \mathbf{Z}_\alpha(\mathbf{r}, t),$$

and the flow decomposition implies two successive stages. First one should obtain a solution to a non-linear initial-boundary-value problem posed for the background-flow variable $\mathbf{Z}_v(\mathbf{r}, t)$ which at this stage is completely independent of the acoustic disturbances $\mathbf{Z}_\alpha(\mathbf{r}, t)$. The following closed system of equations is offered to govern the unsteady background flow:

$$\partial \mathbf{u}_v / \partial t + (\mathbf{u}_v, \nabla) \mathbf{u}_v + a_v^2 \nabla \beta_v = \eta_v (\mathbf{W} - \mathbf{u}_v), \quad (3)$$

$$\nabla \mathbf{u}_v + \partial \beta_v / \partial t + \mathbf{u}_v \nabla \beta_v = \eta_v, \quad (4)$$

$$\partial s_v / \partial t + \mathbf{u}_v \nabla s_v = 0, \quad (5)$$

$$\mathfrak{F}(\beta_v, s_v, a_v) = 0. \quad (6)$$

Now $a_v^2 = \gamma p_v / \rho_v = (\gamma - 1) h_v$, but in the background medium this amount has nothing in common with the true velocity of sound propagation in the basic gas medium. This system is supplemented by the relations

$$\eta_v = \Psi\{\beta_v\} = \partial \beta_v / \partial t + \mathbf{W} \nabla \beta_v - H,$$

$$\mathbf{W} = \mathbf{V} + \mathbf{\Omega} \times \mathbf{r}, \quad \nabla \mathbf{W} = 0, \quad \mathbf{V} = \mathbf{V}(t), \quad \mathbf{\Omega} = \mathbf{\Omega}(t), \quad H = H(t).$$

The definition of non-local operator Ψ , as well as the procedures for calculating \mathbf{W} and H , have been given in references [16,17].

At the second stage $\mathbf{Z}_v(\mathbf{r}, t)$ is taken as a known function in $G \times J_t$, and then one can derive the closed system of nonlinear equations for $\mathbf{Z}_\alpha(\mathbf{r}, t)$ [17], that complements system (3)-(6) to the basic system (1)-(2)

$$\begin{aligned} \partial \mathbf{u}_\alpha / \partial t + (\mathbf{u}_v + \mathbf{u}_\alpha, \nabla) \mathbf{u}_\alpha + (\mathbf{u}_\alpha, \nabla) \mathbf{u}_v + (\gamma - 1)(h_\alpha \nabla \beta_v + h_v \nabla \beta_\alpha + h_\alpha \nabla \beta_\alpha) \\ = -\eta_v (\mathbf{W} - \mathbf{u}_v), \end{aligned} \quad (7)$$

$$\partial \beta_\alpha / \partial t + (\mathbf{u}_v + \mathbf{u}_\alpha) \nabla \beta_\alpha + \mathbf{u}_\alpha \nabla \beta_v + \nabla \mathbf{u}_\alpha = -\eta_v, \quad (8)$$

$$\partial s_\alpha / \partial t + (\mathbf{u}_v + \mathbf{u}_\alpha) \nabla s_\alpha + \mathbf{u}_\alpha \nabla s_v = 0, \quad (9)$$

$$\mathfrak{F}(\beta_v + \beta_\alpha, s_v + s_\alpha, h_v + h_\alpha) = 0. \quad (10)$$

Thereby, the five-component vector of aerodynamic sound sources in equations (7)-(9), that depends on the evolution of \mathbf{Z}_v , is now written as

$$\mathbf{Q}_v = \{ -\eta_v (\mathbf{W} - \mathbf{u}_v), \quad -\eta_v, \quad 0 \}.$$

Thus, all components of the source vector \mathbf{Q}_v in the acoustic system (7)-(9) are defined along with minimizing the norm $J_\eta(t) = \|\eta_v\|_G^2$, the functions \mathbf{W} and H being determined implicitly by the whole field $\beta_v(\mathbf{r}, t)$ (see [17] for details). It is important that all components of this source are Galilean invariant.

A set of necessary requirements was posed before deriving these two systems which are of first-order like the basic system: all the newly defined sources of aerodynamic sound must be integrable square over the infinite flow domain, the formulae for such sources have to be Galilean invariant, the norms of these sources should be minimized so that the spurious pseudo-sound effects are eliminated, the relevant initial-boundary-value problems should conform to some important particular cases, and so on. The quite unusual non-local operator Ψ was designed just with the aim to

define the sound sources while all these requirements are met. At the same time the basic set of initial and boundary conditions must be accurately decomposed (in doing this one should minimize the norm of \mathbf{Z}_α by meeting the above requirements) to provide all necessary data for both initial-boundary-value problems.

As a result, two closed systems of *integro-differential* non-linear equations have been derived, for unsteady background flow $\mathbf{Z}_v(\mathbf{r}, t)$ and for acoustic field $\mathbf{Z}_\alpha(\mathbf{r}, t)$. The sound source \mathbf{Q}_v , which appears in the right-hand part of the acoustic system, depends on the field \mathbf{Z}_v in the whole domain G . Thereby, the traditional comprehension of sound-flow interactions, at least in inviscid gas media, should be radically revised after such a decomposition.

Diverse simplified versions of the theory were developed for particular flow conditions, and a number of analytical solutions was obtained to demonstrate the new physical effects this theory reveals, as well as the old myths it destroys. At the same time the special approximate models have been created for unsteady subsonic background flows at low Mach numbers [18,19], and then the *explicit* formula for the source \mathbf{Q}_v can be found. Also, a set of linearized versions of the theory has been suggested for specific aeroacoustic problems.

4. Comments on some unusual properties of the theory

Unfortunately, the volume of this brief paper is evidently insufficient for exposing all important details of this theory, and so these will be revealed in further publications. Nevertheless, some features of this theory should be now mentioned. By the way, just with the aim to emphasize the unusual properties of both media, the background flow (\mathbf{Z}_v) and the acoustic field (\mathbf{Z}_α), the title “two-medium theory” is used.

The local characteristic analysis of both systems has shown that the background flow medium represents a rather exotic “globally-compressible fluid” in which all sound waves are characteristically excluded, but all the rest of the dynamic processes can be well simulated; this implies the infinite speed of sound propagation, though the formally calculated value $a_v^2 = \gamma p_v / \rho_v$ is finite. It is important that all thermodynamic relations, including the equation of state, in the background flow medium are similar to those we have in the classical model of compressible flow, though the mechanism of sound wave propagation has been completely excluded in the former.

In the case of subsonic background flow ($M_v = |(\mathbf{u}_v - \mathbf{W})/a_v| < 1$) \mathbf{Z}_v -system displays the following local characteristic properties: partly elliptic (due to the infinite speed of sound), and partly hyperbolic, with the characteristics $dx_j/dt = u_j$. These properties resemble those one can find in the classical model of incompressible fluid flow. In two-dimensional *unsteady* supersonic background flow ($M_v > 1$), though all sound waves are there precluded as well, one can find the spatially hyperbolic properties like those in the classical model of *steady* supersonic flow.

At the second stage, when the variable $\mathbf{Z}_v(\mathbf{r}, t)$ is taken as a known function, \mathbf{Z}_α -system shows the combined hyperbolic properties which are responsible for the sound wave propagation along with the relevant effects of convection, and the source term \mathbf{Q}_v reflects the “collective” impact of the whole unsteady field \mathbf{Z}_v in G .

The invariant definition of Mach number has been found, and this enables one to classify better different flow types, even those without acoustics (e.g., steady flows).

Within other versions of this theory the externally specified mass/heat sources or mass forces (e.g., the gravity force in atmospheric flows [19]) can be considered as well. Under specific conditions these sources may be included only in the background flow equations, so that these terms are able to cause sound emission solely through changing the background flow structure. Thereby this theory has removed many ambiguities inherited from the classical acoustics.

The important general conclusion has been derived which departs radically from the opinions well accepted in aeroacoustics: the potential shell of a vortex can make the substantial contribution to the total strength of sound sources in unsteady background flow, because the evolution of pressure field p_v (that, of course, depends on the vorticity distribution) is most decisive within this model. Moreover, the initially irrotational background flow is able to become vortical after sound sources arise therein, for instance due to some changes in the boundary conditions.

Generally, this theory does enable one to understand better the classical concept of incompressible fluid, as well as its serious limitations, especially those associated with the non-trivial boundary conditions and the continuous mass/heat sources.

In contrast to the widespread delusion (Howe [15]) that the non-zero term $-\nabla(T\nabla s)$ should be regarded as a “thermal source of sound”, the entropy spots are able to move downstream without generating sound, at least in inviscid gas flows.

What is also very important, the processes of hydrodynamic instability in a compressible medium can be separately investigated within the background-flow system (3)-(6). Moreover, many significant effects of sound generation due to flow instability could be well studied within the special simplified versions of this theory.

5. On the non-locality of sound sources

At first sight it seems that the non-locality of this model is at variance with physical reality, because the local mechanism of sound propagation is taken as basic in classical acoustics, and so some comments should be given on this question. Actually, the non-local features arise when operator Ψ is applied to the pressure field $p_v(\mathbf{r}, t)$ with the aim to obtain $\{ \mathbf{V}, \Omega, H \}$. In doing this we assume that the sources of aerodynamic sound should be determined through a certain measure of the background flow unsteadiness, and such a measure is introduced by analyzing the distributions of static pressure p_v in unsteady background flow. However, the local values (i.e., in a definite point) of p_v , as well as the local values of derivatives $\partial p_v / \partial t$, $\partial p_v / \partial x_i$, cannot give the clear answer whether this point belongs to the unsteady flow (perhaps one can find another reference frame so that just in this point $\partial p_v / \partial t = 0$). Hence, an adequate measure of flow unsteadiness can be realized only through comparing the fluid motion in different points, or better in the whole flow domain under consideration; then the unique reference frame (generally non-inertial) can be determined for the whole flow domain so that the degree of flow structure unsteadiness will be mathematically associated with the minimum of a certain integral norm. Within this concept many specific factors (including the boundary conditions) may influence in non-local manner the local values of sound sources.

Now it is relevant to recall the problems of mathematical physics, in which the phenomena under simulation are depicted by elliptic or parabolic (e.g., the heat conduction processes considered in both time and space) partial differential equations. In all those models any local variation will influence instantly the whole spatial domain under consideration, but this effect embarrasses no one. Similarly, if the elliptic properties are partly introduced into our system of background flow equations, this means that these properties will be inherent in the formulae written for Q_{ν} , and then the elliptic features are *implicitly* conveyed to the acoustic system. This may look rather surprising because the classical system of equations for dynamics of inviscid gas possesses only hyperbolic characteristics, and it does not display any elliptic features. Nevertheless, in the author's view, this two-stage non-local approach seems to be the only way if one wishes to obtain an adequate theory of sound sources in high-unsteady flows. Anyway, all the previous attempts to create such a theory through using the classical local approaches proved to be absolutely unsuccessful, and this fact was convincingly explained in reference [14].

In the meantime one should recognize the fact that the uniqueness of the suggested procedure of flow decomposition cannot be proved in the most general case, and this question is intended for further consideration. Of course, one can try to decompose a certain unsteady flow in another manner, but it is very probable that such a "new" way will result in violation of some logical requirements from the basic set postulated in the above theory. By the way, a number of alternative ways were investigated by the author and eventually they were rejected as mistaken.

6. Conclusions

Thus, the quite general mathematical model of sound generation has been proposed that forms solid basis for many practical applications. This model is open for further improvements which may be introduced if an additional set of parameters is taken into account in more complex flows; anyway, one should minimize as possible both the norm of sound sources and the norm of acoustic disturbances within a definite initial-boundary-value problem, and the final result of such a minimization can be well estimated in the course of subsequent computational simulation.

This theory was successfully applied to the study of various aeroacoustic phenomena. The high-efficient computational codes were elaborated for the simulation of diverse unsteady flows. Primary attention was focused on the key mechanisms of sound generation in high-unsteady subsonic flows, both internal and free, acoustic feedback and self-excited oscillations in separated flows, non-linear interaction between small-scale turbulence and large-scale vortical motion in jets and wakes, etc. The substantial experience has been also accumulated in numerous practical problems. Some new means of flow control were developed, including those aimed at noise reduction. So this new theory are being now suggested as a promising way to comprehension of the main mechanisms of aerodynamic noise, and it could be much helpful in developing the most effective means of flow control aimed at noise reduction in wind turbines. To this should be added that the key phenomena of noise generation in turbulent flows close to wind turbines have not yet been completely investigated, and it is highly improbable that this gap can be filled with using the traditional theoretical approaches.

References

1. P. Gipe. *Wind energy comes of age*. Wiley, New York, 1995.
2. L. Beranek and I. L. Ver (1992). *Noise and vibration control engineering: principles and applications*. Wiley, New York.
3. S. Wagner, R. Bareib and G. Guidati (1996). *Wind turbine noise*. Springer, Berlin.
4. *Noise emission from wind turbines*. (1996), ETSU Report W/13/00503, UK.
5. H. Klug (2002). *Proceedings of the Forum Acusticum 2002, Sevilla, Spain*. Noise from wind turbines: standards and noise reduction procedures.
6. A. L. Rogers and J. F. Manwell (2004). *White Paper by the University of Massachusetts at Amherst*. Wind turbine noise issues.
7. M. E. Goldstein (1976). *Aeroacoustics*. McGraw-Hill, New York.
8. P. Sijtsma, S. Oerlemans and H. Holthusen (2001). *AIAA Paper 2001-2167*. Location of rotating sources by phased array measurements.
9. P. Migliore, J. Van Dam and A. Huskey (2004). *AIAA Paper 2004-1185*. Acoustic tests of small wind turbines.
10. G. P. Van den Berg (2004). *Journal of Sound and Vibration* **277**, 955-970. Effects of the wind profile at night on wind turbine sound.
11. S. Oerlemans and P. Migliore (2004). *AIAA Paper 2004-3042*. Aeroacoustic wind tunnel tests of wind turbine airfoils.
12. P. J. Morris and F. Farassat (2002). *NASA TR 2002-227*. The acoustic analogy and alternative theories for jet noise prediction..
13. P. J. Moriarty and G. Guidati (2005). *AIAA Paper 2005-2881*. Prediction of turbulent inflow and trailing-edge noise for wind turbines.
14. A. T. Fedorchenko (2000). *Journal of Sound and Vibration* **232**, 719-782. On some fundamental flaws in present aeroacoustic theory.
15. M. S. Hove (1975). *Journal of Fluid Mechanics* **71**, 625-673. Contribution to the theory of aerodynamic sound, with application to excess jet noise and the theory of the flute.
16. A. T. Fedorchenko (1995). *Doklady Akademii Nauk* **344**, 48-51 (In Russian; English translation: 1995 *Physics-Doklady* **40**, 487-490). On the nonlinear theory of aerodynamic sound sources.
17. A. T. Fedorchenko (2001). *AIAA Paper 2001-2250*. On the fundamental problem of flow decomposition in theoretical aeroacoustics.
18. A. T. Fedorchenko (1997). *Journal of Fluid Mechanics* **334**, 135-155. A model of unsteady subsonic flow with acoustics excluded.
19. A. T. Fedorchenko (1996). *Doklady Akademii Nauk* **351**, 633-636 (In Russian; English translation: 1996 *Physics-Doklady* **41**, 611-614). A non-local mathematical model of subsonic flow in the gravitational field.

**First International Meeting
On
Wind Turbine Noise: Perspectives for Control
Berlin 17th and 18th October 2005**

**MAPPING OF UPWIND AND DOWNWIND AIRBORNE
NOISE PROPAGATION**

GAMBA R., GARRIGUES S., SENAT C.

Gamba Acoustique & Associés

BP 163 – 31676 Labege cedex – France

Rene.gamba@acoustique-gamba.fr ; claudesenat@acoustique-gamba.fr

SUMMARY

Introduction	P.2
The ground considered as diffusing planes	P.2
Weather characteristics	P.5
The refraction influence	P.7
Comparison of the calculated results with measured results	P.8
Conclusion	P.12
Appendix	P.12
References	P.13

Introduction

In France, the noise impact of wind turbines is measured by what is called the “sound emergence”. This measured value must not be exceeded. Noise impact studies have to make predictions in order to ensure that this limit is not exceeded and if necessary indicate to wind farm developers how their projects can be modified to satisfy this requirement. These modifications often consist in decreasing the number of wind turbines in operation if the weather conditions would cause the legal limits to be exceeded. Therefore these conditions have to be identified as closely as possible.

Weather conditions have an impact on sound propagation and are one of the parameters which influence this “sound emergence”. The noise level may vary considerably upwind and downwind of a noise source. The models used for the impact assessment should take into account the weather conditions which are least propagators of noise emissions so that the operation of the wind turbines can be adjusted to suit these conditions. Thus, models which are defined for airborne noise emissions only (such as ISO 96-13) are not sufficient to cover these particular site characteristics. Moreover, in France, wind turbines are often installed on hilly terrain. The models must therefore take into account the influence of topography on sound propagation.

This paper describes a model which has been developed and used for making operational forecasts (short calculation, time, noise map plotting, etc.) suitable for use with wind-farms.

It differs from the conventional models of specular reflection in that it is based on the assumption that the sound waves are diffused on their reflection by the ground. We will describe this aspect of the model in the first part.

The meteorological characteristics are defined by temperature and wind speed changes at height. The orientation of the wind is also taken into account and is assumed to be constant at the height covered by the calculation. We will describe the method used to cover these parameters in the second part.

These characteristics enable the speed of sound propagation with height to be evaluated and the sound wave refraction to be deduced. This enables the sound wave curve to be evaluated. When the curved sound waves come into contact with the ground (taken into account together with its topography by the model) or any other type of obstacle, the model evaluates the diffraction and the sound energy which result. We will describe the calculation method in the third part.

Ultimately, the model allows the noise map to be plotted for complex topographies in both good and poor airborne noise propagating conditions (upwind and downwind). Measurements and calculations have been carried out in real situations and we describe them in the conclusion to this paper.

The ground considered as diffusing planes

The models for predicting the sound field based on specular reflection assumptions use infinitely smooth surfaces. However, in the case of rough surfaces and dimensions less than the wavelength, experiments have shown that specular reflection of the sound no longer applies. In France, wind turbines are generally

located in rural zones where the ground is seldom smooth and flat. To take account of these ground conditions, a diffuse reflection model has to be used.

Our model assumes [23], [25], [26] that the intensity of the noise at any point above the ground consists of two superposed components, a direct component consisting of the intensity of the noise emitted directly by the source, and a component of noise reverberated from the ground, buildings or other obstacles. The first component, which is easily determined, corresponds to the free field propagation of spherical waves, the theoretical model for which is well known. The second component (reverberated noise) requires the assimilation of the floor and any walls of buildings as point sources (virtual) the directivity of which takes account of the diffusion assumption.

The directivity factor of the diffused reflection used by our model is:

$$Q(\theta)=4\cos\theta$$

Each component of a surface which receives energy retransmits it towards all the surface components. Let us examine two components dS and dS' centred respectively on x and x' ,

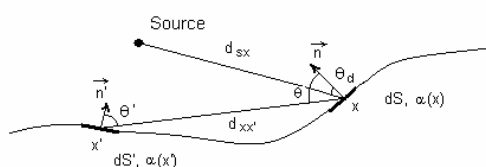


Figure 1: influence of a ground element on another one

These elements are both characterized by their absorption coefficients $\alpha(x)$ and $\alpha(x')$. The surface density of incident power on dS , noted $dI(x)$ and induced by dS' , is:

$$dI(x)=\frac{I(x')(1-\alpha(x'))\cos\theta'\cos\theta dS'}{\pi d_{xx'}^2}$$

$\cos\theta$ is the solid angle according to which dS is seen by the incoming flux.

$I(x')$ is the surface density of incident power on dS' , only the fraction $I(x')(1-\alpha(x'))$ of which is re-emitted.

In order to simplify the formula, we have grouped the geometrical terms within the same coefficient, that we can call the influence coefficient $K(x,x')$.

$$K(x,x')=\frac{\cos\theta\cos\theta'}{\pi d_{xx'}^2}$$

thus,

$$dI(x)=I(x')(1-\alpha(x'))K(x,x')dS'$$

The surface density of incident power on dS induced by the surfaces considered (ground, buildings, etc.) is therefore

$$I(x) = \int_S K(x, x') I(x') (1 - \alpha(x')) dS'$$

This expression would not be complete if we did not take into account the intensity of the source received directly by dS . This intensity is represented by $I_{d,x}$. The surface component dS has an angle θ_d between its normal and the source. The direct intensity is expressed by:

$$I_{d,x} = \frac{W \cdot Q_s(\theta_d) \cos \theta_d}{4\pi d_{sx}^2}$$

where d_{sx} represents the distance separating the source from the element centred on x , and $Q_s(\theta_d)$ the directivity coefficient of the source.

Therefore we obtain:

$$I(x) = \int_S K(x, x') I(x') (1 - \alpha(x')) dS' + I_{d,x}$$

In order to overcome the integral and allow the equation to be solved numerically, the walls have to be discretised. Therefore the walls have to be broken down into N surface samples by considering that:

- the absorption coefficient α is constant for a same sample
- the surface power density is constant on all the surface S_i of the sample
- each surface sample will be identified by its centroid.

Thus, for a receiving sample S_i , the surface power density is expressed by:

$$I_i = \frac{1}{S_i} \int_{S_i} \int_S I(x') K(x, x') (1 - \alpha(x')) dS' dS_i + I_{di}$$

where $I_{di} = \frac{W Q_s(\theta_{di}) \cos(\theta_{di})}{4\pi d_{si}^2}$ is the power density coming directly from the source and received by sample i at moment t ,

where θ_{si} is the angle between the normal on the surface of sample i and the source,

and d_{si} the distance separating the source from sample i .

Similarly, all the emitting surfaces are discretised as surface samples S_j of absorption coefficient α_j and surface power density I_j .

The equation then becomes:

$$I_i = \sum_{j=1}^N I_j (1 - \alpha_j) K_{ij} + I_{di}$$

where e_{ij} is the distance between the centroids of samples i and j , and with $K_{ij} = \frac{1}{S_i} \int_{S_i} \int_{S_j} K(x, x') dS_i dS_j$, which we can approximate as:

$$K_{ij} = \frac{\cos\theta_{ij} \cos\theta_{ji} S_j}{\pi d_{ij}^2}$$

The above equation can be written as:

$$I_i - \sum_{j=1}^N I_j (1 - \alpha_j) K_{ij} = I_d$$

Let us define a square matrix A of dimension (NxN), N being the number of surface samples with coefficient a_{ij} such that:

$$\begin{cases} a_{ii} = 1 \\ a_{ij} = K_{ij} (1 - \alpha_j) \end{cases} \quad \begin{array}{l} i = \text{line index} \\ j = \text{column index} \end{array}$$

This equation can be written in matrix form: $IA = Id$

where I is the column vector for the power surface densities of dimension (Nx1) and I_d the column vector for the intensities received directly from the dimension source (Nx1).

Vector I is determined by simple solving of this matrix equation by inverting the matrix A.

$$I = A^{-1} Id$$

Knowing the values of vector I, we are able to determine the acoustic intensity received at any point. We will spare the reader the other stages similar to those which we have just described and pass directly to the results which are:

$$I_R = \frac{W}{4\pi d_{SR}^2} + \sum_{i=1}^N \frac{I_i (1 - \alpha_i) \cos\theta_{ri} S_i}{\pi d_{ri}^2}$$

The pressure level is obtained by:

$$L_p = 10 \log \left(\frac{I_R}{10^{-12}} \right)$$

Weather characteristics

In the context of a wind turbine impact study, we seek to calculate the noise levels far from the sources. Any changes in the characteristics of the atmosphere will have an influence on the result. Two phenomena are to be taken into account:

- The change of sound velocity with altitude leading to the refraction of the sound waves
- The absorption of sound by the atmosphere

This latter point is included in our model, as proposed by standard ISO 96-13 Part1. Thus we will not expand on it further here and will examine the refraction phenomenon.

The celerity of sound is written $c = \sqrt{\frac{\gamma RT}{M}}$ where:

- γ is the relationship between the specific heat at constant pressure (C_p) and the specific heat at constant volume (C_v), i.e. $\gamma = \frac{C_p}{C_v}$,
- R is the constant of perfect gases equal to $8314.16 JK^{-1}mol^{-1}$,
- T is the temperature in °K,
- M is the molar mass in $g.mol^{-1}$.

We notice that the celerity of sound depends on the temperature. The wind can also be taken into account in the formula for the speed of sound by using an effective celerity $\vec{c}_{eff} = \vec{c} + \vec{v}$ where \vec{c} and \vec{v} are respectively the celerity of sound and the wind speed.

The parameters γ and M are related to the moisture content of the air. It can be seen that changes to moisture content with altitude lead to variations of celerity that are negligible compare to those induced by the temperature variation. [8].

Thus we will concentrate on assessing the variations in temperature and the wind speed with altitude.

The equation for movement is written as follows (non turbulent atmosphere):

$$\frac{d\vec{V}}{dt} = \vec{g} - \frac{1}{\rho} \vec{\nabla}P - 2\vec{\Omega} \wedge \vec{V} + \vec{F}_v$$

where:

- \vec{g} is the force of gravity,
- $\frac{1}{\rho} \vec{\nabla}P$ is the pressure force,
- $2\vec{\Omega} \wedge \vec{V}$ is the Coriolis effect due to the rotation of the earth,
- \vec{F}_v is the friction force.

Close to the ground (in the layer next to the surface), it may be considered that the pressure force and the Coriolis effect are negligible relative to the friction forces. Therefore, we can show ([3],[15]) that the speed of wind at altitude z is:

$$\vec{u}(z) = \frac{u^*}{k} \ln\left(\frac{z}{z_0}\right) \text{ where:}$$

- u^* is the friction speed which depends on the surface and the meteorological conditions (sunshine, etc.),
- k is Karman's constant, equal to 0.4 in the atmosphere,
- z_0 is the roughness length, corresponding to approximately 10% of the height of obstacles.

It is also shown [15] that the temperature in the layer next to the surface at altitude z can be evaluated as follows:

$$T(z)=T_h+\frac{T_*Pt}{k}Ln(\frac{z}{h}) \text{ where:}$$

- T_h is a reference temperature at altitude h ,
- $T_* = \frac{-Q_s}{U_*}$ (7) where U_* is the friction speed in $m.s^{-1}$,
- $Q_s = \frac{-H_s}{\rho C_p}$ where H_s is the sensible heat flux in $W.m^{-2}$,

Comments: Pt is a constant of 0.74. Sensible heat is the heat emitted or absorbed by the earth leading to a temperature increase or decrease (for example nighttime temperature inversion).

The refraction influence

The variation in the temperature and the wind speed with altitude induces a celerity change with altitude which leads to refraction of the sound waves propagated in the atmosphere. This well-known phenomenon leads to curvature of the sound waves. There are complex models for solving the parabolic approximation of the Helmholtz equation which translates acoustic wave propagation (FFP [27], PE [27], GF-PE [27], Split-step Padé [20, 4], LE and Lagrangien Model [31]) exist. They are expensive in calculation time and cannot be easily adapted to operational applications such as ours. This is part of the geometrical acoustic approximation. In our case, it consists in determining¹ the trajectory of the "ray" of sound. This results from the integration of the following equation:

$$\frac{dz}{dx} = \frac{c(z) \cos i(z)}{c(z) \sin i(z) + U(z)}$$

where $c(z)$ is defined by $c(z) = \sqrt{\frac{\gamma RT(z)}{M}} + u(z) * \cos \beta$ and the terms used are as follows:

- $u(z) = \frac{u_*}{k} \ln(\frac{z}{z_0})$, is the wind;
- $T_1(z) = T_h + \frac{T_*Pt}{k} Ln(\frac{z}{h})$, is the temperature;

The trajectory is curved and the curvature is oriented towards the ground or towards the sky. In the latter case, from a certain distance there would no longer be any acoustic energy coming from the source (shadow zone, see opposite). However, experience has shown the existence of energy in this zone. Several factors explain this

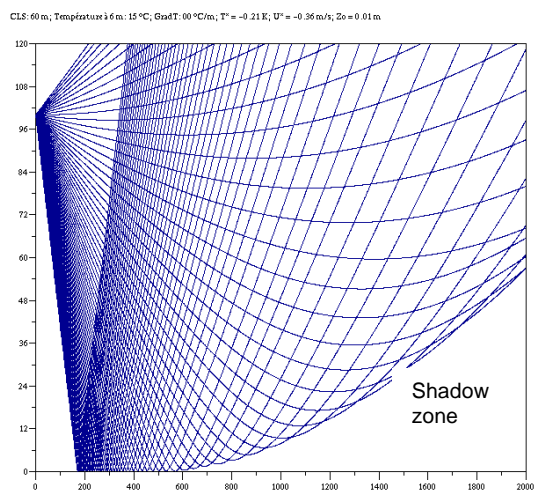


Figure 3 – a few plotted trajectories on flat ground

¹ And use of this trajectory in the model presented in part one

acoustic irrigation of the shadow zone (presence of turbulence in the atmosphere which diffuses the sound energy, diffraction of sound waves by the ground, etc.)

At present, our model takes into account this shadow zone irrigation phenomenon by the diffraction of the sound wave on the ground and by diffusion of the sound energy striking the ground.

Comparison of the calculated results with measured results

In this paper, we present the results obtained on three different wind farm sites. An impact study type of approach has been used to measure the noise level. The purpose of this approach is not to detail its thoroughness² (note that a summary is provided in the Appendix). These results are meant to be representative of the noise level generated by the wind turbines alone (i.e. corrected for background noise).

Site 1

This is a rural site with bush and tree vegetation.

There are six wind turbines on this site (80 m hub height). The ground is to be modelled in the form of a plane (maximum level difference of about 30 m at a distance of 500m). The image below schematises the position of the wind turbines (red points) and the reception points at which the measurements were made:

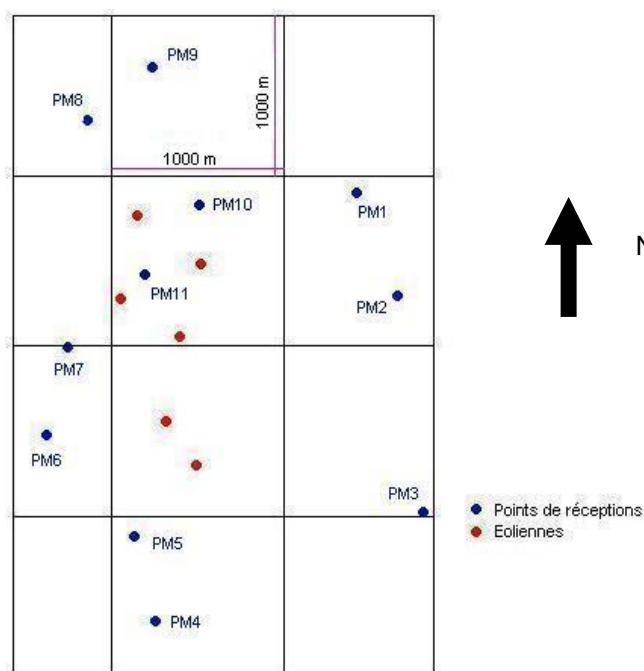


Figure 4 – Site 1

The results of the measurements (which will be compared with the computed results) correspond to a period of nighttime operation with a south-westerly wind and

² The difficulty of measuring the impact of a wind farm is associated with the fact that the noise generated by the wind turbines is often drowned in the background (caused by the wind). The measurement procedures used in France are becoming standardized. A draft standard is currently being prepared. The procedures used for taking the measurements as described in this paper are in line with this draft standard.

a mean wind speed of 2.7s at 10 m above the ground. The average temperature during this period is 9°C.

The results are presented in the table below.

	Dste S-	Direct°	Laeq,cor'ted
	In m	Prop	
PM1	1000	downwind	25
PM2	1070	Slightly downwind.	32 to 39
PM3	1220	crosswind	26
PM4	840	upwind	38 to 46
PM5	560	upwind	27
PM6	710	Slightly upwind.	28.5
PM7	400	crosswind	29
PM8	530	Slightly downwind	25
PM9	800	Slightly downwind	28 to 38
PM1	300	downwind	33.5
PM1	300	downwind	38

Table 1 – Results of measurements on site 1

The shaded boxes in this table correspond to configurations at which the noise level generated by the wind turbines alone is drowned by the background noise observed. For information, these boxes indicate Leq1mn values between which the background noise fluctuated.

The parameters used in the calculation to characterize the wind and temperature, and corresponding to the measurements made, are: $u^*=0.69$, $z_0=0.2$, $T^*=0.32$, $Th=9^\circ\text{C}$, $h=10\text{m}$. The acoustic powers of the sources were measured on the site (in accordance with the stipulations of standard IEC 61400-11).

The following table gives the computed results obtained compared with the measured results.

	Dste S-R	Direct° /	Leq db(A)	Leq dB(A)
	in m	Propa	Meas.	Calcul
PM1	1000	downwind	25	25.1
PM2	1070	Slightly downwind.	32 to 39	24.3
PM3	1220	crosswind	26	22.5
PM4	840	upwind	39 to 46	21.7
PM5	560	upwind	27	26.9
PM6	710	Slightly upwind.	28.5	26.3
PM7	400	crosswind	29	30.4
PM8	530	Slightly downwind	25	29.4
PM9	800	Slightly downwind	28 to 38	26.7
PM10	300	downwind	33.5	35.3
PM11	300	downwind	38	38.5

Table 2 – Computed results for site 1

A comparison of the measured results and the computed results shows good concurrence.

Site 2

This is a rural site with bush vegetation.

There are eight wind turbines on this site (40 m hub height). The turbines are situated on a crest and the relief is broken. The specific characteristic of this analysis is that the measurements which we made always showed that at distance greater than 900 m from the wind turbine line the noise generated by the wind turbines is drowned in the background noise. However, one point concerning the validation of this calculation model appears interesting to us. The image below schematises the wind turbines (red points) and this point of reception:

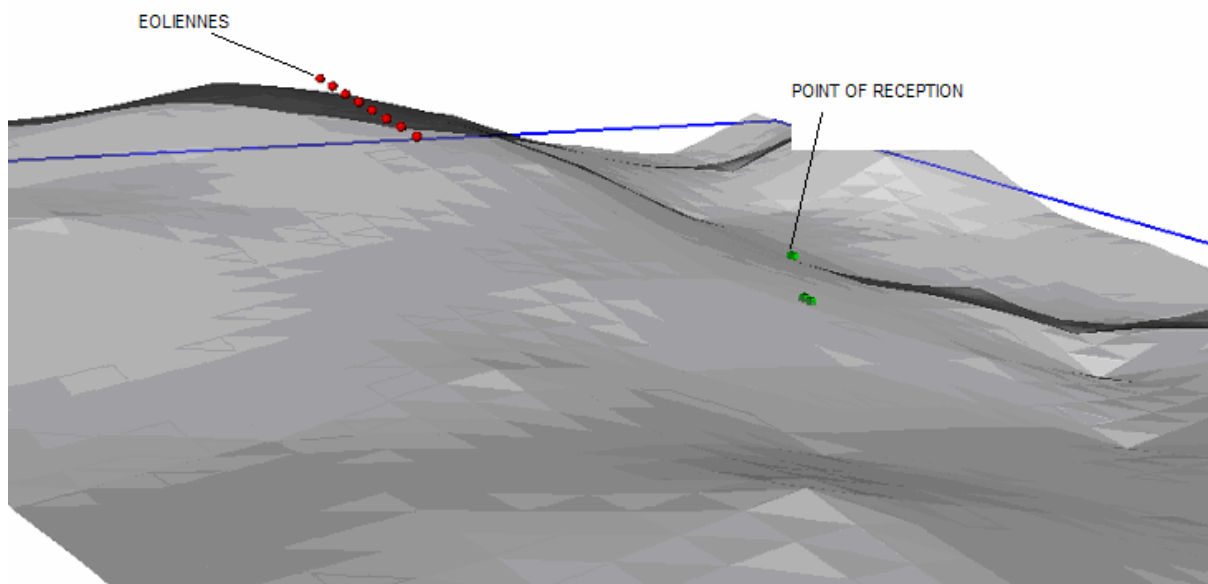


Figure 5 – Site 2

This point is interesting in that it is critical with regard to the combined influence of the topography and refraction. It is located at a lower level (approximately 250 m lower), and a distance ranging between 1000 and 1500 m from the wind turbines. The wind turbine line is not directly visible from this point. However, the noise generated by the wind turbines is slightly audible, whereas the noise level in dB(A) is not impacted by the operation of the wind turbines. This means that the noise of the wind turbines alone is less by several dB(A) than the measured noise level, but the audibility means that the difference between the wind turbine noise alone and the measured noise is less than 10 dB(A). A calculation which does not take into account the influence of refraction but takes account of masking by the topography gives a noise level 20 dB(A) less than the measured noise level at this point. Therefore refraction obviously has an impact at this point.

The measurement results with which we compare the computed results cover a nighttime period with a west-north-west wind at a mean wind speed of 6 m/s 10 m above the ground. The average temperature during this period is 18°C.

The noise level in these conditions is slightly above 30 dB(A), whether the wind turbines are operating or not.

The parameters used in the calculation to characterize the wind and temperature and the corresponding measurements made are: $u^* = 0.52$, $z_0 = 0.1$, $T^* = 0.32$, $T_h = 18^\circ\text{C}$, $h = 10\text{m}$. The acoustic powers of the sources are those communicated by the manufacturer.

The noise level obtained by calculation is 28 dB(A), which is what was expected.

Site 3

This is a rural site with bush and tree vegetation.

There are 21 wind turbines on this site (40 m hub height). As with site 2, they are on a crest and the relief is broken. The level difference between the highest wind turbine and the lowest point of reception is approximately 200m.

The image below represents the position of the wind turbines (red points) and the points of reception at which the measurements were made.

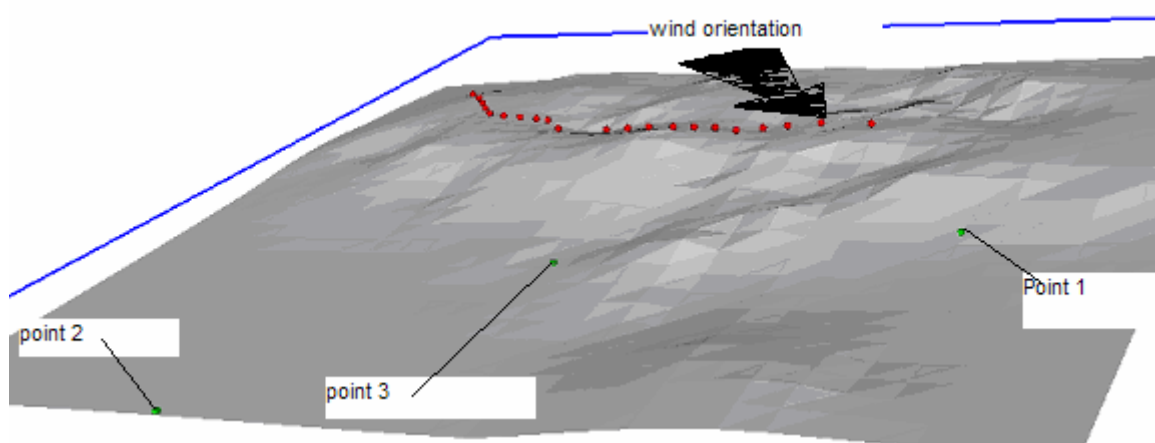


Figure 6 – Site 3

The distance between point 1 and the wind turbines is between 600 and 2100 m, 1600 and 2100 m between point 2 and the wind turbines, and 700 and 1500 m between point 3 and the wind turbines. There is a pine forest close to point 1 which masks the wind turbines from this point.

The measurements compared with the computation results correspond to nighttime operation with a north-east wind at an average wind speed of 6m/s 10 m above the ground. The mean temperature during this period is 10°C.

The table below gives these results.

Points	Leq dB(A)
1	29
2	33.5
3	39

Table 3 – Results of measurements on site 3

The parameters used in the calculation to characterize the wind and temperature, and corresponding to the measurements made are: $u^*=0.61$, $z_0=0.2$, $T^*=0.32$, $T_h=10^\circ\text{C}$, $h=10\text{m}$. The acoustic powers of the sources are those communicated by the manufacturer.

The following table shows the computed results obtained compared with the measured results.

Points	measured dB(A)	Calculated dB(A)
1	29	36
2	33.5	35
3	39	41

Table 4 – Computation results for site 3

At present, our model does not take into account the influence of an attenuation due to crossing a forest. This is most probably the cause of the difference between the calculations and measurements at point 1. It is an improvement to be made. At the two other points, the comparison of the measured results with the calculated results show relatively good concordance.

CONCLUSION

The model that we have presented in this paper can be used to assess the noise impact of wind turbine farms by accurate calculations which match the accuracy of measurements and take account of the main factors that influence sound propagation over long distances. These factors are atmospheric absorption, refraction, diffusion and diffraction on the ground, and topography.

This model is sufficiently operational to allow dimensioning of scenarios in the context of wind turbine impact studies, and to plot useful sound maps for communication to residents living close to wind turbine farms.

Appendix: measuring of a wind farm acoustic impact over long distances

This consists in simultaneously measuring:

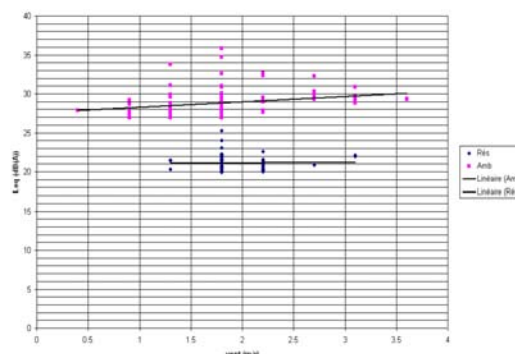
- the noise level in dB(A) at a certain number of points
- the wind speed and the temperature at a height corresponding to a point of reception

Measurements are carried out during operation of the wind turbines, but also during one or more of its shutdown periods.

The equipment consists of an accurate storage integrator sound level meter (class 1 within the meaning of standard NF S 31-009 and NFS 31-109).

The measured Leq levels are integrated for a period of 1 second. From these results we have removed the results which it is felt represent a particular sound event (such as the passage of a vehicle). The Leq 1s are integrated per periods of 1 minute (Leq1mn).

This indicates the evolution of these Leq1mn in relation to the wind at each reception point (see curves opposite). Two groups of results are identified: those with the wind turbine operating (amb: ambient) and those with the wind turbines shut down (res: residual). A trend curve is evaluated for each group of points (by regression). From these curves we deduce a value for the sound level that is considered representative



of a wind speed. The sound level which represents the impact of the wind farm is obtained by correcting the ambient level (amb) using the residual level (res).

REFERENCES

[1] Vol 90 (2004) – PP 24-37, Reinhard Blumrich, Dietrich Heimann, Numerical estimation of atmospheric approximation effects in outdoor sound propagation modelling.

[2] M. C.Berengier, B.Gauvreau, Ph.Blanc-Benon, D.Juve, « Outdoor Sound Propagation: A Short Review on Analytical and Numerical Approaches », Acta Acustica, Vol. 89 (2003) 980-991

[3] A linearize Eulerian sound propagation model for studies of complex meteorological effects, Reinhard Blumrich, Dietrich Heimann, JASA 112, PP 446-455, August 2002.

[4] Simulations météorologiques sur site rural a topographie non plane par emboîtement de domaines avec le modèle SUBMESO, Thèse soutenue le 20 juin 2002, Ecole Centrale de Nantes.

[5] Vol 86 (2000) – PP 260-268, Ostashev, Wilson: Relative contributions from temperature and wind velocity fluctuations to the statistical Moments of a sound field in a turbulent atmosphere;

[6] Comprehensive outdoor sound propagation model. Part 2 : propagation in an atmosphere with refraction, DELTA Acoustics&Vibration Report, Birger Plovsing, jorgen Kragh, Nord 2000;

[7] Contribution à la modélisation de la pollution atmosphérique dans les villes, Stéphane Glockner, Thèse soutenue le 14 décembre 2000, Université de Bordeaux;

[8] Etude de la propagation du son dans l'atmosphère : Application au bruit des avions en phase d'approche et de décollage, Cora Cremezi, Thèse soutenue le 12 mai 2000, Académie de Nantes ;

[9] G. Flemming, J.Burstein et al; « Ground effects in FAA'S integrated noise model », Noise Control Eng. J. 48 (1), 2000 Jan-Feb.

[10] Approximation of a Non linear sound speed profil by an equivalent linear profil, Acoustics&Vibration Report, décembre 1999.

[11] Influence des conditions micrométéorologiques sur la propagation acoustique, modélisation numérique, Benoit Gavreau, Michel Bérenghier, mai – juin 1999 – Réf. 4248 – PP. 55-68;

[12] Bulletin des Laboratoires des Ponts et Chaussées – 221 – Mai-Juin 1999 – Réf 4248 – PP. 55-68 ;

[13] Météorologie générale, météo France, ENAC, 1999 ;

[14] Effets des conditions météorologiques sur la propagation du bruit. Prise en compte pratique; méthode d'essai n°51 - Réf. LCPC, ME51, Vadim Zouboff, Jean-Claude Laporte, Yves Brunet, 1998;

[15] Vol 84 (1998) – PP 870-883, D.Kühner, Excess attenuation due to meteorological influence and ground impedance;

[16] Etude expérimentale et théorique de la couche limite atmosphérique en agglomération parisienne, laurent Menut, Thèse soutenue le 15 décembre 1997 ;

[17] Bulletin des Laboratoires des Ponts et Chaussées - 210 –Juillet – Août 1997 – Réf. 4138 – PP. 105-119 ; Prise en compte des conditions météorologiques dans la propagation du bruit – Approche pratique.

[18] PICAUT J., SIMON L., POLACK J-D. : « A mathematical model of diffuse sound field based on a diffusion equation ». *Acoustica* Vol. 83 (1997) 614-621.

[19] Tony F. W. Embleton, «Tutorial on sound propagation outdoors » *J. Acoust. Soc. Am.* Vol. 100, No. 1, July 1996

[20] Bulletin des Laboratoires des Ponts et Chaussées – 198 – Juillet – Août 1995 – Réf 3908 – Application des méthodes factorielles à la caractérisation des effets météorologiques sur la propagation du bruit à grande distance.

[21] Downwind propagation of sound in an atmosphere with a realistic sound-speed profile: a semianalytical ray model, Erik M. Salomons, *JASA* 95, PP 2425-2436, may 1994;

[22] Simulation numérique des effets de la turbulence sur la propagation du son dans l'atmosphère, Patrick Chevret, Thèse soutenue le 24 mars 1994

[23] SENAT C. : « Prise en compte de l'encombrement, au sein d'un modèle de prévision des niveaux de pression, reposant sur l'hypothèse de réflexion diffuse sur les parois ». Thèse de Doctorat spécialité acoustique de l'Université Paul Sabatier – Toulouse (1992).

[24] An introduction to a boundary layer, Stull, 1988;

[25] MALCOURT C. : « Simulations informatiques pour prédire les critères de qualification acoustique des salles. Comparaison des valeurs mesurées et calculées dans une salle à acoustique variable ». Thèse de 3^e cycle spécialité acoustique. Université Paul Sabatier – Toulouse (1986).

[26] ZULIANI P. : « Elaboration d'un modèle prévisionnel fondé sur l'hypothèse de réflexion diffuse en paroi ». Rapport de DEA Acoustique. Université Paul Sabatier – Toulouse (1986).

[27] Contribution à l'étude des effets du vent et d'un gradient de température sur l'efficacité des écrans acoustique, Michel Rosen ; Thèse soutenue le 23 octobre 1986 ;

[28] Tony.F, W. Embleton, J.E. Piercy, G.A. Daigle, Effective flow resistivity of ground surfaces determined by acoustical measurements, *J. Acoust. Soc. Am.* 74 (4), 1239 1244, 1983.

[29] K.Attenborough, S.I Hayek, J.M Lawther, « Propagation of sound above a porous half-space, *J Acoust. Soc. Am.* 68(5), Nov 1980.

[30] C.I. Chessell, Propagation of noise along a finite impedance boundary, *J. Acoust. Soc. Am.* 62 (4),825-834, 1977.

[31] Three-dimensional acoustic ray tracing in an inhomogeneous anisotropic atmosphere using hamilton's equations, Chessell, *JASA* 53, (1), PP 83-87, 1973;

[32] I. Rudnick, « Propagation of an acoustic wave along a boudary »; *J. Acoust. Soc. Am.* Vol. 19, No. 2 March 1947.

[33] ISO 9613-1&2: 1996-Acoustics-Attenuation of sound during propagation outdoors

**First International Meeting
On
Wind Turbine Noise: Perspectives for Control
Berlin 17th and 18th October 2005**

Noise of Wind Power Turbine V80 in a Farm Operation

Maria GOLEC*, Zdzisław GOLEC*, Czesław CEMPEL*

*Poznań University of Technology, Institute of Applied Mechanics
Piotrowo 3 Street, 60-965 Poznań, Poland

Maria.Golec@put.poznan.pl , [Zdzisław.Golec@put.poznan.pl](mailto:Zdzislaw.Golec@put.poznan.pl) ,
[Czesław.Cempel@put.poznan.pl](mailto:Czeslaw.Cempel@put.poznan.pl)

Summary

The paper presents the results of noise investigation of a V80 wind turbine of 2MW power. The examination was carried out at the Zagórze wind farm, the biggest such a system of the Vestas Company, located near the Zagórze village, to South-East from the Wolin Island. The V80 turbine noise was measured in a single measurement session. The farm is composed of 15 V80 turbines, each of 2MW capacity. Some technical reasons caused that on the measurement day 80 per cent of the turbines were operative. No consent was given for operation of only a single turbine. The noise was analyzed for a turbine located at the farm border at the windward side. Wind velocity during the investigation approached the most probable value for the location, and the turbine power amounted about to 0.6 MW. Results of the noise investigation provide an approximate outlook on the noise emitted by a single turbine located in open air. Consideration of all the turbines cooperating in the farm enables determining distribution of the acoustic field in the surrounding of the Zagórze wind power plant.

Introduction

The interest in renewable energy sources (RES), e.g. the energy of water, sun, wind, biomass, geothermal sources, observed in many countries, is a result of exhaustion of resources of fossil fuels and, on the other hand, is aimed at protecting the natural environment of a man. Development of power plants using renewable power sources, inclusive of wind energy, is one of important tasks for a highly developed community. The European Parliament has adopted in 2001 a Resolution No 2001/77/EU related to promotion of the electric power produced from renewable energy sources (Official Journal EU L 283 of October 27, 2001). Since May 3, 2005, the Law of March 4, 2005, is in force in Poland, that modified the Energetic Law and the Law of Environment Protection (The Journal of Laws of 2005, No 62, Clause 552), regulating implementation of the Resolution No 2001/77/EU. According to the resolution the power generated based on the RES in the countries of European Union is to increase by 2010 by 22 per cent.

The most common source of renewable energy in the world is wind. Electric power of this origin is generated by turbines of wind power plants. Taking into

consideration many years' research carried out in the Institute of Meteorology and Water Management in Warsaw [1] it was found that the conditions suitable for development and location of wind farms occur at 2/3 of the territory of Poland. Yearly average wind velocity observed at the area amounts to 4m/s. Most of wind turbines may operate with the wind velocity in the range of (4÷25) m/s. A map depicting the wind conditions in Poland (Fig. 1 from [1]) shows that the most windy regions are located in the North – at the Baltic shore. The yearly average wind velocity at the height above 50 m amounts there to (5.5÷7.5) m/s.

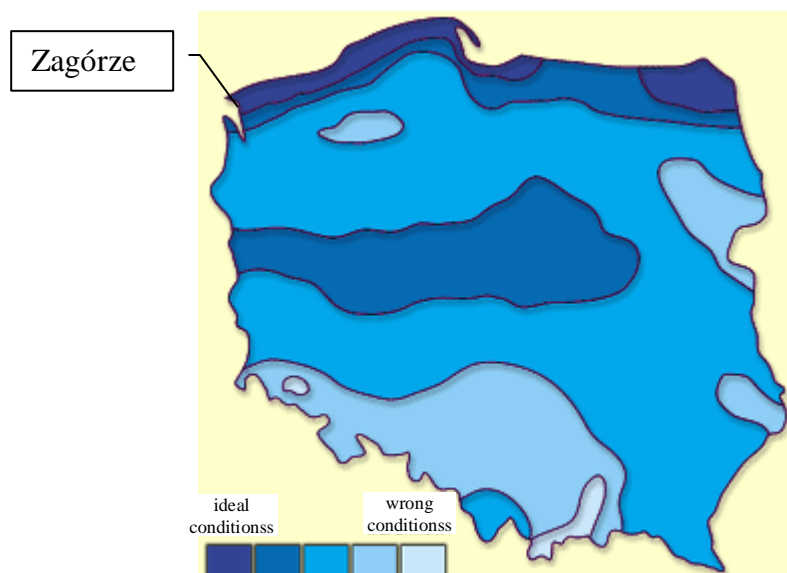


Fig. 1. The map of wind conditions in Poland [1]

In spite of the fact that Poland is considered as a country of average resources of wind energy, the development of the power plants is still rather slow. In January 2003 the biggest wind power plant in Poland, located in Zagórze near Wolin, was put into exploitation. The wind farm includes 15 turbines VESTAS V80, each of the power of 2 MW. Late in 2003 total capacity of wind power plants in Poland [2] amounted to 63 MW, remaining unchanged in 2004.

Introduction of wind farm to the environment, occupying significant area often reaching up to several hectares, brings some harmful consequences. The most important among them are the noise and direct death risk for the birds in case of collision with rotating turbine blades. The noise is mainly due to the rotating blades and, to less degree, to the generator rotor and gear.

Minimization of the wind turbine noise – directions of the action

A wide range of research & development work devoted to the wind turbines, carried out by the National Renewable Energy Laboratory (NREL) [3] includes, among others, the studies aimed at minimizing the noise of operating turbines. The problem, that is not as yet solved, includes minimization of aerodynamic noise generated by the rotating blades. Reduction of burdensome noise accompanying exploitation of the turbines is possible by intervention into the source of the acoustic disturbance or at the sound propagation path. In the first case the acoustic properties of the turbine might be improved by optimization of aerodynamic solutions of the

design of turbine subassemblies, e.g. geometry of the rotor blades or, finally, by the change in rotational speed of the rotors. The acoustic power is proportional to the fifth

power of relative linear velocity of the blade [4,5]: $N \sim \left(\frac{v_r}{v_w}\right)^5$ where v_r is a linear

speed of the blade end and v_w is the wind velocity. A critical value is the turbine power obtained for the given wind velocity, as smaller speed v_r gives more silent operation but, at the same time, smaller turbine power.

Burdensome character of the noise may be reduced at the sound propagation path, among others, by:

- appropriate location of the wind farm with respect to the object potentially affected by the noise, e.g. in the distance of 500-600m from housing estates, considering average yearly distribution of wind direction and velocity;
- proper relative location of the wind turbine sets;
- consideration of the properties of the sound generated by the devices.

In order to verify the numerical models of acoustic power and reasonably assess the noise emitted by the turbines and their parts, the noise studies are carried out during operation of the wind power plants. Results of the studies are used for proper choice of protection zones and for purposes of further design work. Standard requirements [6,7] define the conditions of the investigations to be carried out on the noise emitted by the wind turbines, e.g. the number of measuring points, the number of simultaneously recorded acoustic and non-acoustic values, required values of the non-acoustic values. This determines duration of the investigation and the number of measurement sessions.

The work presents selected results of the noise carried out in a single measurement session in the biggest wind farm in Poland – in Zagórze, during its exploitation. Numerical simulation allowed to assess the noise of a single turbine located in the plant and, considering operation of all the turbines, to assess distribution of the acoustic field in the proximity of the wind power plant.

Characteristics of the Zagórze Wind farm

The Zagórze wind farm of the VESTAS Company was found in the Zagórze village, located south-east of the Wolin Island [8] (Fig. 2).

Such a location was chosen based on the studies of wind velocities [9] (Fig. 3), taking into account such conditions like field obstacles, lacking contraindications related to environment protection, neighbourhood of the Szczecin Bay from the west, good soil quality, and field roughness amounting to 0.05 m.



Fig. 2. Zagórze – location of the wind farm [8]

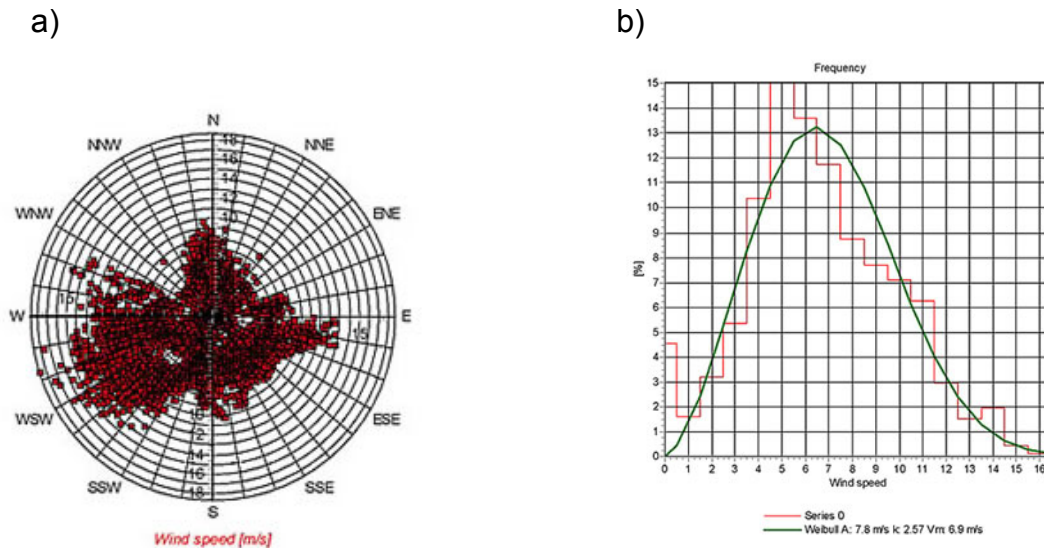


Fig. 3. Results of wind Speer At the area of the Zagórze Wind Farm [9];
 a) the wind rose, b) numerical distribution of wind velocity

The distance between a housing estate and the nearest turbine (at the farm border in the North-East direction) amounts about to 800 m. Location of the farm in the direction opposite to the most frequent wind direction reduces probability of the noise risk at this area. Hence, the condition of appropriate location of the power plant with regard to potentially affected objects (Fig. 2) is met, taking into account the average yearly distribution of wind direction and speed (Fig. 3a).

The wind farm is composed of 15 turbines VESTAS V80, each of 2 MW Power. The view of some of them is presented in Figure 4.



Fig. 4. The view of the Zagórze Wind Farm near Wolin

The turbine VESTAS V80 is a three-blade model, with a rotor of 80 m diameter, provided with the blades of variable inclination angle [10]. Selected additional information related to the V80 turbines are specified in Table 1.

Table1. Basic specification of the V80 turbine [10]

rotor diameter	80 m
Surface area of the blades	5.027 m ²
rotational speed of the rotor	(9.0 – 19.0) r.p.m.
Number of the blades	3
tower height	78 m
initial speed of the wind	4 m/s
rated speed of the wind	15 m/s
critical speed of the wind	25 m/s
mass of the wind power plant	265 T
mass of the tower	170 T
mass of the nacelle	61 T
mass of the rotor	34 T

The wind farm is located at a plane open forming area, characterized by the field roughness amounting to 0.05 m. No filed obstacles are present in proximity of the power plant. The turbines are about 240 m each other apart.

Conditions of Noise Investigation

The noise of the VESTAS V80 Turbine was measured in a single measurement session during in a farm operation. Noise measurement for a single turbine operating (according to the Standard [7]) was not possible, as no consent was given for

stopping the power plant. For technological reasons during the studies 80 percent of the turbines were operative. In order to minimize the effect of their operation on the noise measurement results the turbine located at the border of the farm from the windward side was selected for purposes of the study.

On the measurement day the weather conditions were as follows: air temperature 15°C, atmospheric pressure 1013 hPa, wind direction – north-east, wind speed varying from 5 to 7.3 m/s (according to [7] the reference wind speed assumed for computation of acoustic power level of a single turbine amounts to 8m/s). The speed of wind corresponded to the most probable value in the area (cf. Fig. 3b). The wind aimed at approximating housing (i.e. the Zagórze village), that rarely occurs in this area (cf the wind rose – Fig. 3a). During the noise measurement the turbine power amounted about to 0.6 MW.

For purposes of studying of the noise and acquisition of the acoustic data (tertiary spectra of the noise level in middle frequency bands (1.6-10000Hz) the Sound and Vibration Analyzer SVAN 912AE was used, with the microphone ½” SVO2-C4 provided with a wind shield, and the KA10 Calibrator. In order to minimize the effect of the soil type the microphone was located at a sound-reflecting plate. Measurement points were located at the distance $R_0 \approx 100$ m from the middle of the turbine ($R_0 = H + 0.5 D$, where H – the height of the tower, D – rotor diameter). Arrangement of the points for purposes of acoustic pressure measurement is shown in Fig. 5.

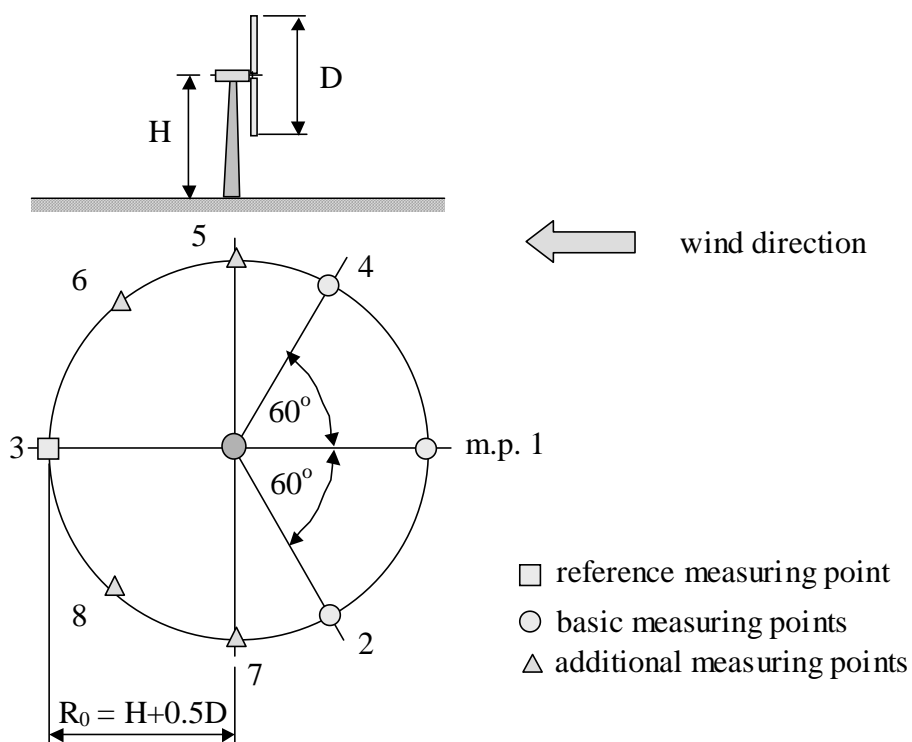


Fig. 5. Distribution of measurement points during the noise investigation

The noise was measured in two series. In order to estimate acoustic power of the turbine and directional properties of the source five values of the acoustic pressure were measured for each of operating locations of the microphone (windward positions – the measuring points 1, 2, 4) and in the reference location – the point 3 (leeward location of the microphone). Another series included additional

five measurements of the acoustic pressure levels in the points 5, 6, 7, and 8, with a view to assessing of noise propagation in the acoustic field.

Discussion of the study noise results

Energetically averaged tertiary spectra of the sound pressure levels for each of the four microphone positions (Fig. 6) depict the frequency-distribution of the noise in the proximity of the turbine.

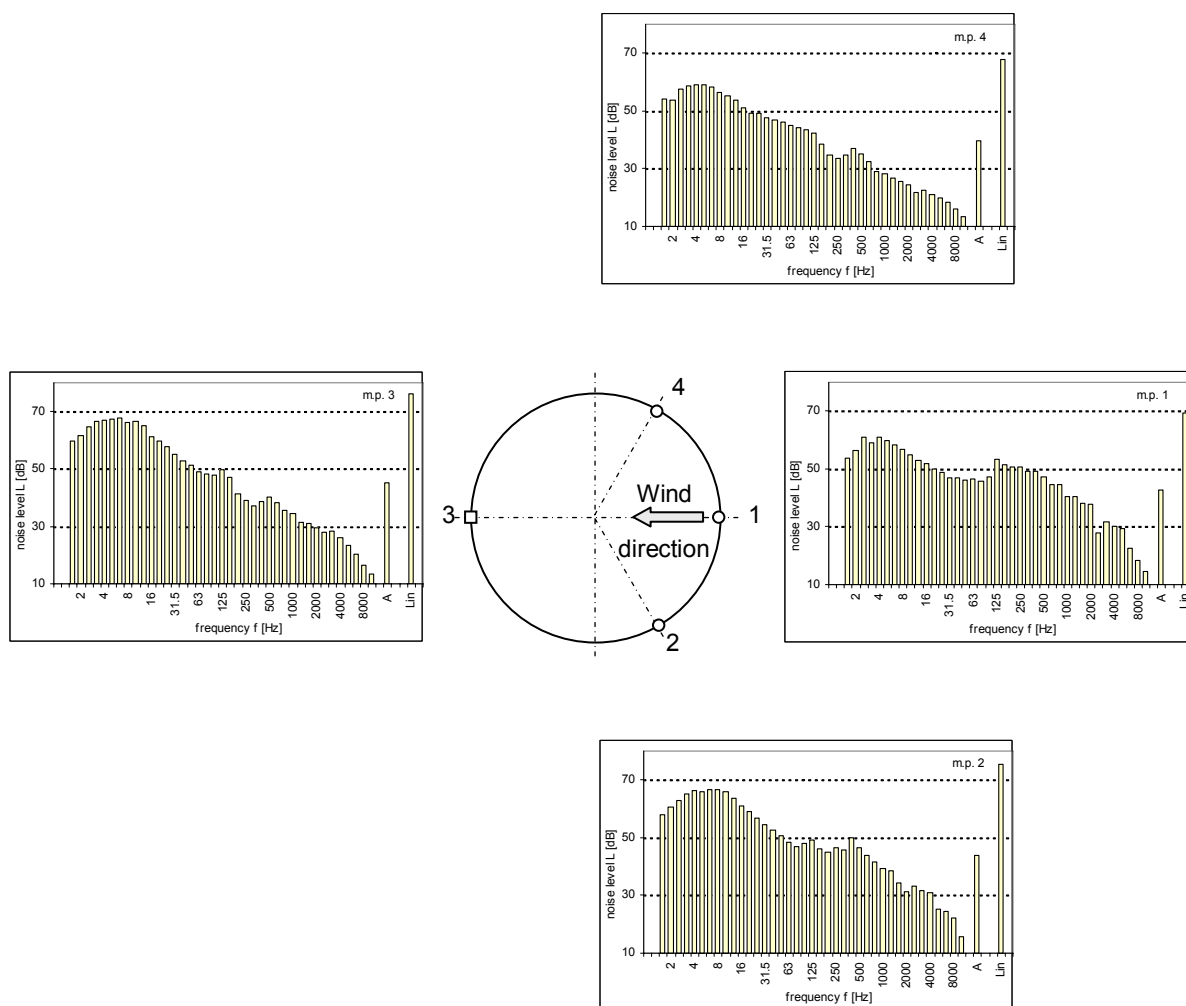


Fig. 6. Averaged 1/3 octave noise spectra of the VESTAS V80 Turbine

The noise spectra presented above may be divided into two frequency sub-ranges characterized by various linear values of sound pressure. In the first frequency band (1.6÷100) Hz, including the low-frequency infrasound noise, lower noise level is observed (particularly in two measuring points – the points 2 and 3) than in the other frequency band (125÷10000) Hz, including the range of hearing. In the second frequency band a significant noise level is observed in the measuring points 1, 2, and 3.

The A-sound level in particular measuring points is not much differentiated, that results from the frequency-characteristics of the A-Filter.

Analysis of the measurement data shown in Fig. 6. clearly indicates that a predominant noise source, both in low-frequency and in the band of hearing, is the passage of the rotor blade near the turbine mast. This fact finds its confirmation in Fig. 7, showing directional characteristics of the sound source of the turbine, defined as a difference between averaged A-sound levels in predetermined measurement locations and an averaged A-sound level in a reference location (the measurement point No 3). The observed increase in the directional characteristics in the measurement points 2 and 1 is a result of air whirls behind the moving rotor blade.

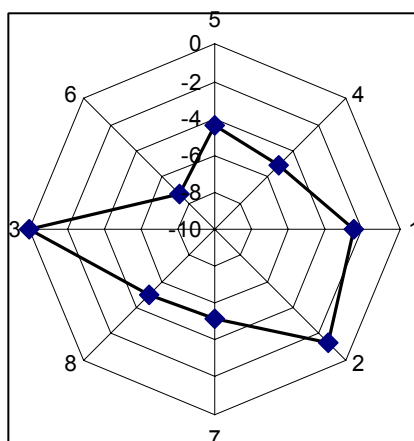


Fig. 7. Directional characteristics of the sound source of the turbine VESTAS V80 in Zagórze

Based on the energetically averaged level of sound pressure in the reference point No 3 the acoustic power of the turbine VESTAS V80 and acoustic efficiency of the turbine for the A-sound were determined, the last value being defined as the ratio of acoustic to instantaneous power of the turbine during the measurement process. The data and results of the acoustic power of the turbine [4,5] are specified in Table 2.

Table 2. Calculation results of acoustic power of the turbine VESTAS V80 in Zagórze

sound level in the measurement point No 3	L_{Lin} [dB]	76.5
acoustic power level	$L_{N,Lin}$ [dB]	127.5
acoustic power	N_{Lin} [W]	5.61
A-sound level in the measurement point No 3	L_A [dB]	45.1
acoustic power level	$L_{N,A}$ [dB]	96.1
acoustic power	N_A [W]	0.0041
turbine power during the measurement	N_t [MW]	0.6
acoustic efficiency of the turbine	$\eta_A = N_A/N_t$	$6.8 \cdot 10^{-9}$

The values obtained this way comply with experimental data of acoustic power of the turbine VESTAS V80 provided by [9], showing that the acoustic power level L_{NA} is included in the range 97dB to 106.5 dB for wind velocity (5÷8) m/s.

The acoustic power so determined served as a basis for simulation computation of noise propagation around the turbine up to the distance of 800 m, i.e. to the

nearest housing area (for linear and A-sound levels). Results of the simulation shown in Fig. 8 indicate that at the distance of the nearest houses the noise emitted by a single turbine would amount to $L_{Lin\ 800} \leq 55$ dB, $L_{A\ 800} \leq 25$ dB, respectively, in considered weather conditions.

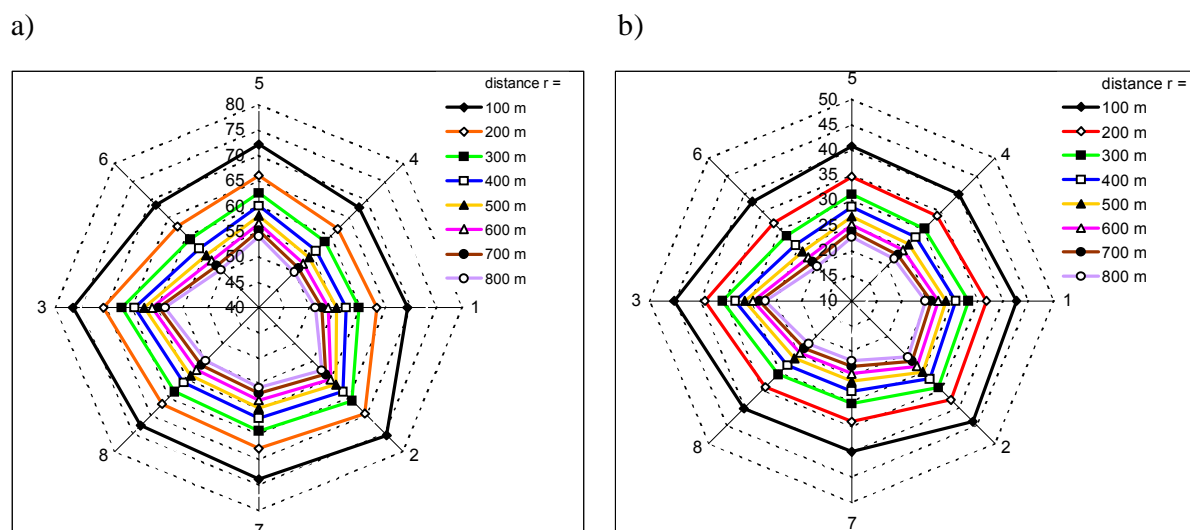


Fig. 8. Distribution of noise levels around the wind turbine in Zagórze subject to the study, of instantaneous power 0.6MW

a) linear sound levels; b) A-sound levels

Taking into account the computation of the acoustic power level for a single turbine a simulation of distribution of A-sound in the area around the wind farm was carried out for the case of operation of all the turbines. For this purpose it was assumed that every turbine is a point-source of a sound of the acoustic power $L_{N,A}=96.1$ dB, located at the height $H=78$ m, corresponding to the height of a turbine tower. Neither the effect of wind direction on the sound level distribution nor acoustic background level were taken into consideration for the computation purposes.

The results of noise simulation around the farm are presented in Fig. 9, showing:

- location of the wind farm in the area – a map of the proximity of the farm;
- the lines of equal A-sound levels during operation of all the turbines.

Analysis of noise propagation around the wind power plant in Zagórze (c.f. Fig. 9) carried out under above mentioned weather conditions show that the noise emitted by the turbines in this case is not burdensome for the environment (for the housing area located 800 m from the turbine).



Fig. 9. Distribution of A-sound levels around the wind farm in Zagórze during operation of all the turbines

Conclusions

The above described noise research makes a case study for the turbine noise in predetermined weather conditions and turbine power resulting there from (below its rated power). Nevertheless, the results enable assessment of acoustic field distribution around the designed wind farms. The research allow to state that the wind turbines in Zagórze gave no rise to noise threat for the environment under above mentioned weather conditions, as the A-sound level amounting to 40 dB as admissible for night-time was not exceeded.

References

- [1] www.elektrownie-wiatrowe.org.pl (April 2005).
- [2] www.gigawat.net.pl (June 2005).
- [3] Turbine noise and the environment; Bruel&Kjaer magazine Nr 2, 2003, pp. 24-25, (in polish).
- [4] Cempel C., Applied vibroacoustics, PWN, Warsaw 1989, pp. 72-76, (in polish).
- [5] Engel Z., Protection of the environment against vibration and noise, PWN, Warsaw 2001, pp. 84-86, (in polish).
- [6] Norma IEC61400 Wind Turbine Generator Systems.
- [7] Norma PN – EN 61400 – 11: 2001, Wind Turbine Generator Systems, (in polish)
- [8] www.mapapolski.pl (May 2005).
- [9] http://elektrownie-wiatrowe.org.pl/zagorze/i_wietrzosc.htm (May 2005).
- [10] General Specification V80-2MW offshore OptiSpeed™ – Wind Turbine Item no.: 944407.R6.

**First International Meeting
on
Wind Turbine Noise: Perspectives for Control
Berlin 17th and 18th October 2005**

Understanding the acoustical behaviour of a wind turbine by means of acoustic imaging.

K. Haddad (karim.haddad@acb-engineering.fr),
V. Benoit (vincent.benoit@acb-engineering.fr) – ACB Engineering (Paris, France)

Summary

Although, wind turbines tend to become quieter years after years they are placed closer to urban areas because of the increasing lack of place in more remote areas and also due to the high development rate of the wind industry.

Moreover, it is not only one wind turbine which is usually installed but wind farms comprising tens of them and noise problems in the neighbourhood due wind farms most of the time finds a solution resulting in reducing the overall output capacity of the farm to fulfil the noise regulations.

Such a solution has a high impact on the efficiency of the wind electricity cost production and directly impacts the return on the investment of the wind farm (facts which are not often mentioned in the current literature on cost and production rates...).

Therefore it becomes increasingly important to understand in details the acoustic behaviour of the wind turbine in order to make them quieter and to avoid jeopardizing the wind farm investments near urban areas.

This article presents how time domain acoustic imaging can be applied (and has been applied) in order to thoroughly understand the noise behaviour of a wind turbine under operation. The investigation can be done with non stationary conditions of wind speed, directions, etc., and clearly quantifies and localizes where the real noise sources are acting on the turbine. Moreover, the data extracted from the analysis can also be used to generate more accurate and reliable noise impact analysis which gives more credibility to the wind farm investments.

Introduction

The development of wind farms induces a higher proximity with urban areas, involving an increasing sensibility of the people to the wind turbine noise. Whereas there is a demand for this renewable energy, one of the factors which can slow down the progression is the noise. First there is a limit to the geographical expansion of

wind farms, because of the proximity to cities. Secondly, sometimes the production is reduced to fulfil the noise regulations.

These reasons justify the necessity to understand where the sources are and how they generate the sound field.

The constructors, users or associations can evaluate the noise level of a wind turbine thanks to the IEC 61400-11 standard [1]. It provides a power level, a 1/3 octave spectrum and the tonality. Optionally, it provides an evaluation of the directivity: the measurements are made at four points around the studied wind turbine.

These measurements indicate if the noise regulation is satisfied or not. When the limit values imposed by noise regulations are exceeded, in general the IEC 61400-11 does not provide enough data to establish what part(s) of the wind turbine is (are) more important in the global noise. To quantify the contributions to the global noise of each part of the wind turbine, it is necessary to pass to other methods of measurement.

Among those methods, the acoustical imaging is probably the most practical tool and the most general-purpose.

The most practical tool, because it is 'enough' to have a microphone array at a relatively important distance of the wind turbine. After processing, it provides quick results on site. The most general-purpose, because the technique allows localizing both aero-acoustic and vibro-acoustic sources (which are often on different frequency bands).

In the first part of this paper, we describe the basic principles of the acoustical imaging method. We also analyse the useful parameters to obtain reliable results in the context of wind turbines.

In a second part, we interest in practical problems relatively to the deployment of the microphone array, and to the solutions that we developed.

Finally, we show the types of results obtained from this acoustical imaging technique, and how they can be used.

The acoustical imaging method

The acoustical imaging methods are based on the acquisition from a microphone array, also called an antenna. The method used in this paper is the beamforming technique [2]. As indicated by this word, the processing consists in forming narrow beams to 'hear' a local point in the space. The most robust method to form a beam is the delay & sum technique. As shown below (Figure 1), each signal from the microphones is first delayed and then all the contributions are summed. The delays are calculated to compensate the difference of time propagation between the hearing point and the microphones. Applying these delays for all the microphones makes the wavefront is lined up with the antenna.

The output is a time signal, representative of the original signal from the source. The time domain version of the beamforming (it exists also a frequency domain version) allows dealing with non-stationary sources. For example, it allows tracking aeroacoustic sources on blades. It is possible to obtain an acoustic image every 1ms.

The time domain also brings more flexibility in low frequencies, since it is not necessary to have one period of signal to localize a source. To obtain an acoustic image, one just have to change the delays to scan a surface (called an 'acoustic image' below).

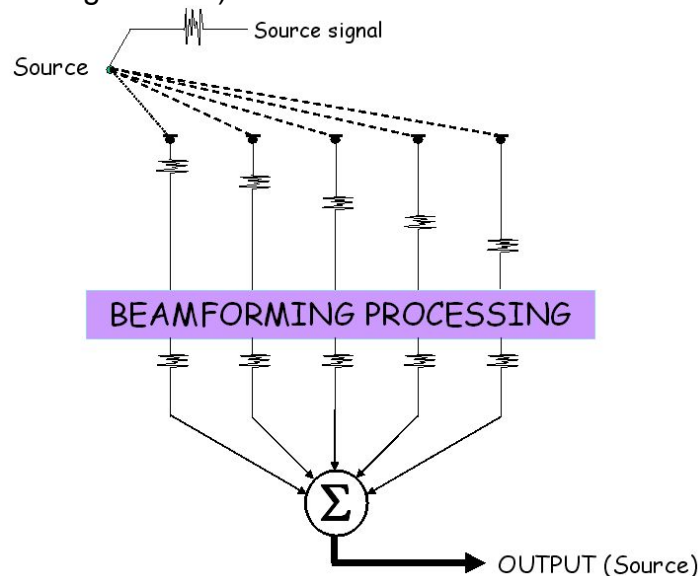


Figure 1: the 'delay & sum' processing

The parameters of the beamforming technique

The discrete nature and the finite dimensions of the microphone array make that it captures only a fraction of the sound field emitted by the sources. These elements contribute not to have a perfect image of the sound field. Practically, the sources are localized with a certain resolution, and ghost sources, without physical existence, appear on the acoustic image.

Actually, these limitations are similar to those of the Discrete Fourier Transform (DFT), especially if the repartition of the microphones is regular. For this type of antenna, the parameters are the dimensions of the antenna along the X and Y axis, and the constant space between microphones d .

For that case, it appears two kind of false sources: side lobes and grating lobes. Grating lobes appear because of the non respect of the Shannon's theorem. To avoid grating lobes (high level ghost sources), d must be lower than the half-wavelength. Thus, higher is the frequency of the sound field, smaller must be the space between microphones.

Side lobes are relatively low level ghost sources and, are mainly related to the repartition of microphones. For a rectangular antenna with a constant step, the higher level of the side lobes is about 13 dB below the level of the main real source.

The resolution is mainly governed by the dimensions and the frequency of the sources. The resolution is improved as the dimension of the antenna is increased. Also, the resolution is increasing with the frequencies. Practically the resolution is roughly related to the ratio λ / L , where λ is the wavelength of the sound field, and L is a dimension of the microphone array.

Thus for low frequency sources, it is interesting to use a big antenna. This concerns directly measurements of wind turbines, since the radiated noise is in important part in low frequencies.

The resolutions are given in degrees and it expresses the capabilities of the system to separate two close sources at two angular positions (Figure 2).

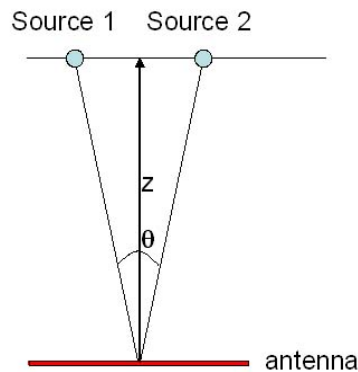


Figure 2: the resolution of a microphone array

If we translate the resolution in term of a linear dimension, we obtain (see Figure 2):

$$\Delta x = 2 \cdot z \cdot \tan(\theta/2)$$

Where θ is the angular resolution, z the distance from the antenna to the plane of the sources and Δx the linear resolution, which gives the minimum distance to separate the sources 1 and 2 of the Figure 2.

This relationship shows that the distance z between the antenna and the sources should be small as possible to improve the linear resolution (but not too small to avoid near-field effects).

To summarize, the study of wind turbines on a broad frequency band requires a big dimension antenna, but at the same time the space between microphones should be lower than the shortest half wavelength. For example, the localization of sources on the band 100 – 1000 Hz can be done with an antenna of 8 x 8 meters. The Shannon's theorem requires that the space between sensors is lower than 17 cm (half wavelength of 1 kHz): at least the antenna must be composed of 24 x 24 microphones. This high number of microphones makes the measurement system expensive.

Another possibility consists in using a non regular repartition of microphones to reduce the number of sensors. But the repartition must be carefully optimised to avoid high ghost sources. The main parameter to improve is the dynamic; it means the difference of levels between the source level and the highest level of lobes. This is the way we choose and we developed two antennas with an optimised geometry of respectively 96 (8 x 8 meters) and 121 microphones (9 x 9 meters), dedicated to studies of wind turbine noises.

For a given antenna size, it is also important to have a sufficient density of microphones. First it limits the influence of ghost sources, but it also improves the robustness of the processing against background noise, providing a noise reduction of the acoustic image.

Improving the resolution (with the dimension of the antenna) and the dynamic (the arrangement of microphones) makes a better separation of sources and a reduction of ghost sources: the spots are smaller and well identified.

Thus all these parameters, resolution, dynamic and robustness, contribute to the precision of the processing in the localization of sources.

The acoustical imaging system

The complete system is composed of the microphone array, the acquisition system and a computer.

The antenna of 9 m x 9 m and with 121 microphones is shown below (Figure 3). With this arrangement, the bandwidth of the system is 80 – 2000 Hz.

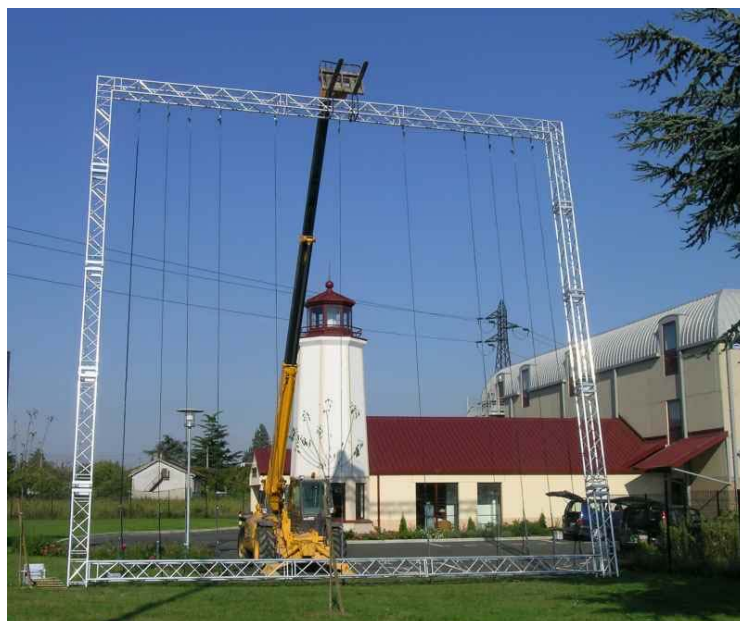


Figure 3: antenna of 9 x 9 meters, 121 microphones

If we want to study acoustic sources on the whole wind turbine, the microphone array is not posed on the ground vertically, but with a certain angle, so that the aperture of the antenna covers the full length of the wind turbine (see Figure 4). In this case, the angle between the antenna plane and the wind turbine is taken into account in the processing. However a too important angle introduces a decrease of the resolution for off-axis sources: it should be compensated by an increase of the antenna size. This configuration imposes the minimum distance between the wind turbine and the microphone array.

But if we study only a partial area of the wind turbine, it is interesting to be as close as possible to improve the resolution. As previously, the microphone array can be set up on the ground in a position allowing the coverage of the interested area by the antenna aperture, or if it is possible, the microphone array can be elevated in front of the studied zone: in that case we can be very close.

Because of the dimensions of the antennas, the practical deployment was studied carefully to simplify the set-up. The 9 x 9 m antenna is built from a structure which

defines the framework (see Figure 3). The framework can be folded in 5 parts. To unfold the antenna, we use a fork-lift truck (Figures 3 and 5). Since the garlands of microphones can stay on the framework during the folding and the unfolding, it is possible to make the measurements in two positions of antenna in one day. For a greater autonomy, the folded antenna can reach the site of measurements on a truck having its own lifting system.

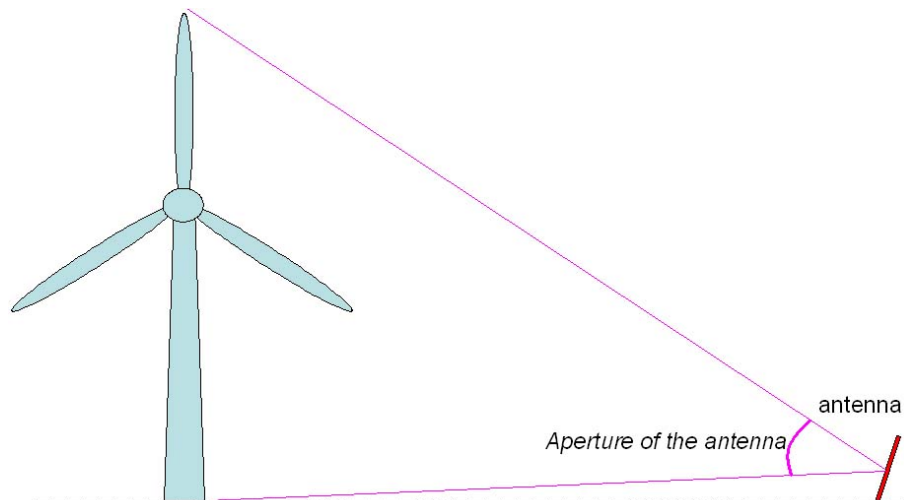


Figure 4: Position of the antenna relative to the wind turbine



Figure 5: The folded antenna and the fork-lift truck to unfold the structure

The acquisition system is shown below (Figure 6).



Figure 6: The acquisition system

The repartition of microphones was optimized in regard of acoustic performances, but also in term of deployment. The chosen geometry makes that microphones are arranged by columns. We built garlands carrying the microphones and thus they are easily transported and unfolded. This construction also allows a reliable and fast setting in position of the microphones on the framework.

In addition, a special coating along garlands supporting the microphones gives a protection against wind and (moderate) rain.

The acquisition system records the time signal of each microphone. The complete system is autonomous in energy (it is powered by a 12 Volts power supply). The hardware is made to record signals with no limit in time, except that related to the hard-disk size of the computer. Thus the acquisition can last several hours or more.

In the context of outdoor measurements, and especially in the case of wind turbines, it is important to acquire climatic parameters. The system also allows recording at the same time these data: the speed and the direction of the wind, the ambient pressure, the temperature and the humidity.

Also, a channel is dedicated to the tachometric signal coming from the wind turbine.

Before the measurements, it is necessary to carry out the calibration of the antenna to make sure that the sources will be correctly localized and that the measured levels will be accurate. We developed a simple and fast procedure for the calibration.

The wind may influence the time propagation of sound between the sources and the sensors. Based on a given wind speed profile, it is possible to use a ray method to calculate the effective time propagation between sources and microphones.

What kind of results can provide the system?

The technique provides acoustic images showing the localization of sources with their levels in regard of the frequency band and the time moment. Since the processing is done in time domain, it is also possible to play a movie illustrating the evolution of the sources, or still to listen a specific source.

When the microphone array stands on the ground, the localized sources are related to the main parts of the wind turbine: the tower, the blades and the rotor. As examples, we show below sources relative to these parts (Figure 7).

These images are reproductions, but correspond to experimental acoustic images. The first image localizes acoustic sources on the tower. The acoustic radiation is probably related to a vibration mode of the tower. The second image shows a source on the rotor. And the third indicates a source on a blade. All of the three images correspond to different frequency bands (lower than 800 Hz).

Studying higher frequencies makes an improvement in the resolution. We can find these high frequency aeroacoustic sources along the blades. To illustrate that point, we show below (Figure 8) a simulation of the localization of sources with the 9 x 9 meters antenna, at 153 meters away from the wind turbine.

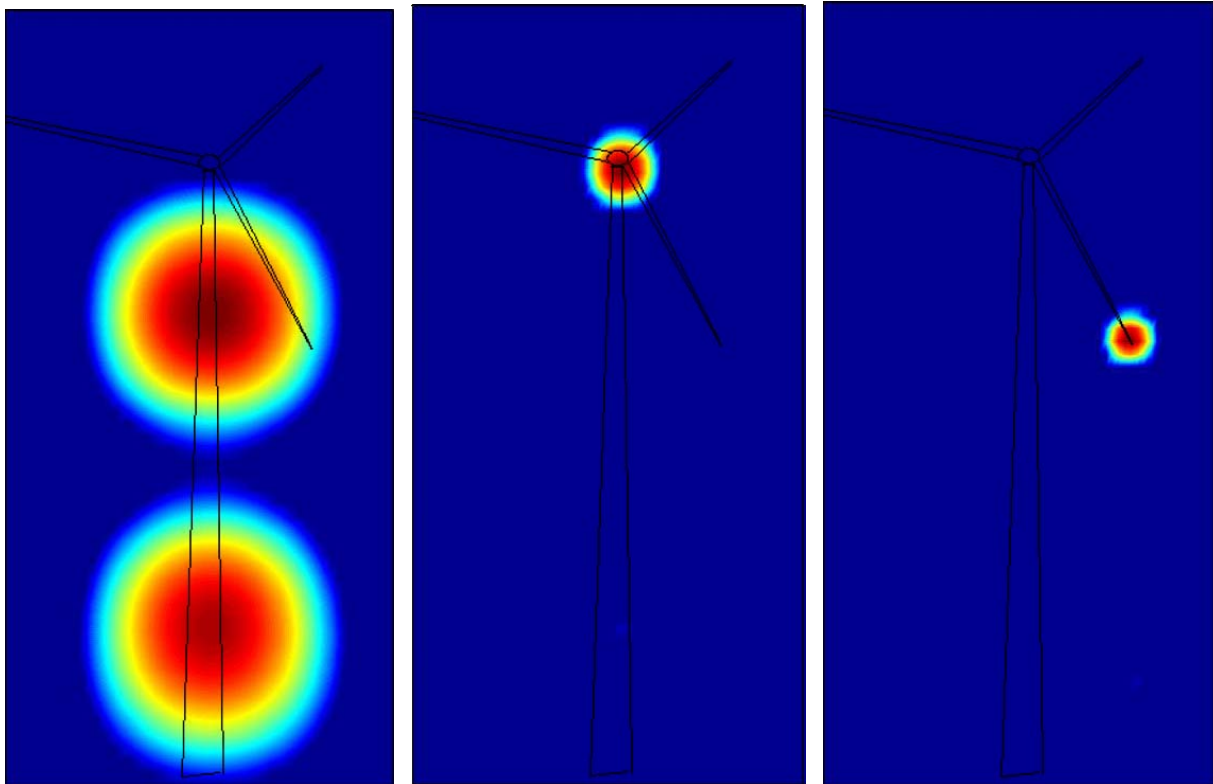


Figure 7: Localization of sources with the 9 x 9 meters antenna

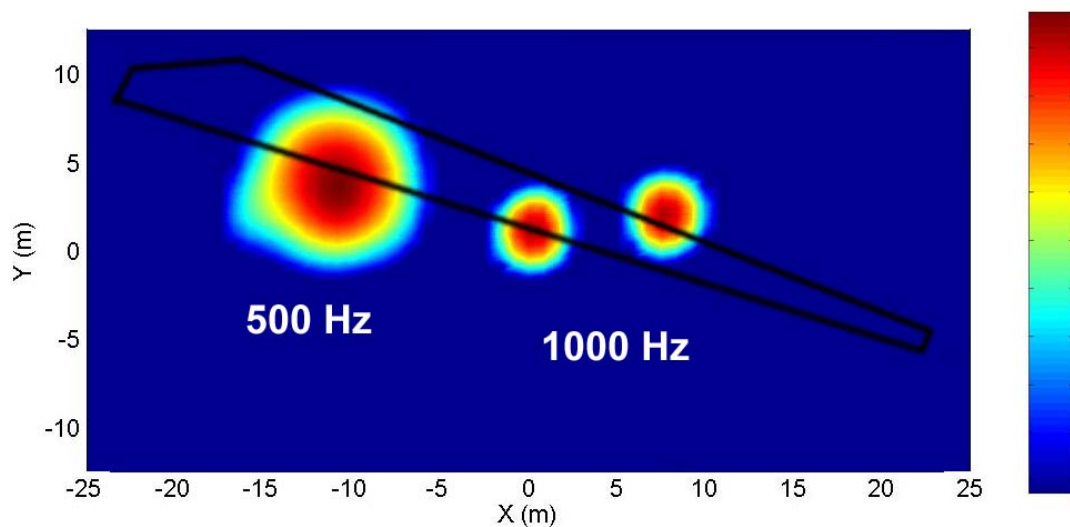


Figure 8: Simulation of the localization of sources along a blade with the 9 x 9 meters antenna, at 153 meters away from the wind turbine

This image indicates a good possibility to separate sources along the blade at relatively high frequencies, even if the distance between the antenna and the wind turbine is important. But practically, the levels of sources along the blade are relatively low in comparison with other sources, and thus they may be not detected by the system.

One solution to detect these sources consists in approaching the microphone array, in such a way to focus on the acoustic radiation from the blades (Figure 9).

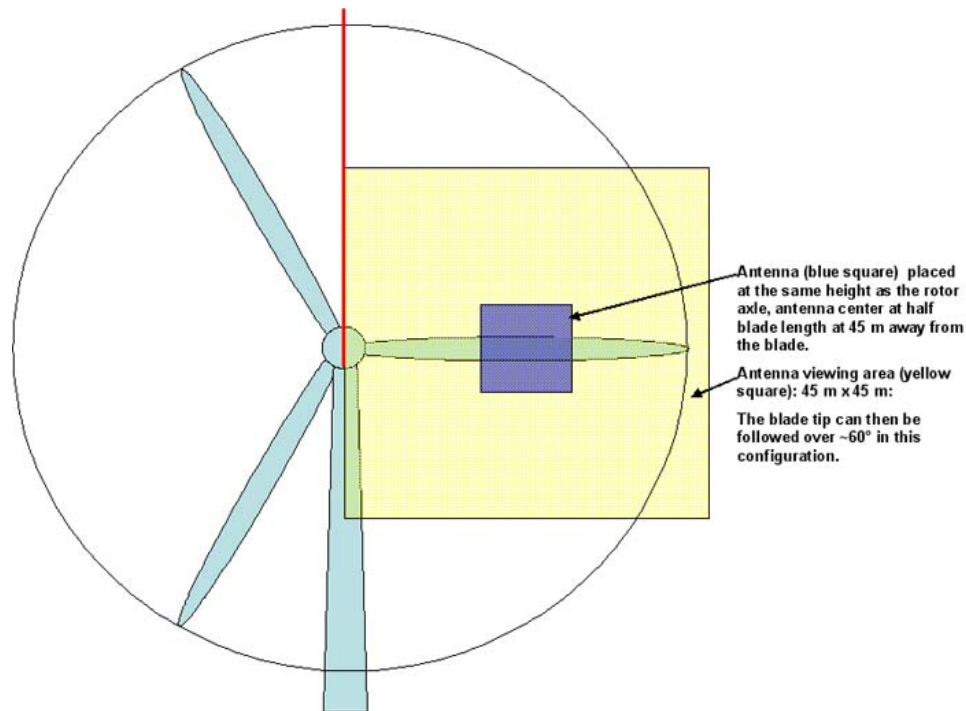


Figure 9: Localisation of sources along the blade

For this case, the localization of the same sources as given by the Figure 8, are shown on the figure 10 for the distance antenna – wind turbine of 45 meters. As expected, the Figure 10 shows a better separation of sources.

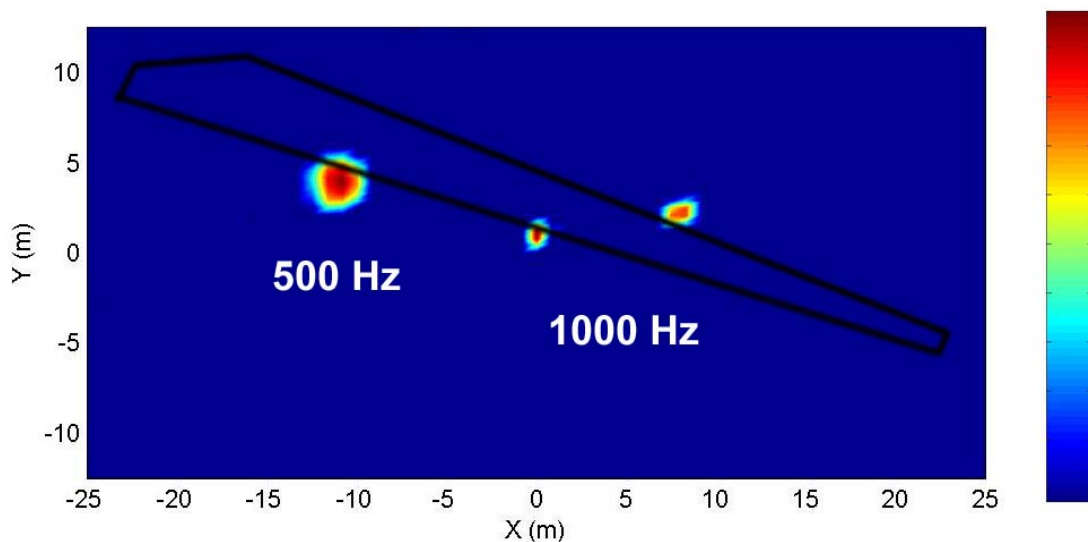


Figure 10: Simulation of the localization of sources along a blade with the 9 x 9 meters antenna, at 45 meters away from the wind turbine

Thus the same antenna can be used for long and for short distance studies (actually these distances depends on the size of the wind turbine as shown on the Figure 4).

For long distances, the microphone array localizes the most important sources on the tower, the blades and the rotor. In general, the antenna stands on the ground,

simplifying the deployment of the system. To localize the different sources, the images are made for different frequency bands. Since the signals are sampled, we can use digital narrowband filters.

This configuration is very helpful in complement of the IEC 61400-11 measurements. Indeed the application of this international standard does not inform in general where the sources are, and thus why the levels are too high relatively to regulations. But it provides a 1/3 octave spectrum and the tonality and then the frequency bands for which there is a problem. These frequency bands can be applied to the acoustic images to localize sources which are responsible of the non-respect of the regulations. The hardware (described before) and software system makes possible to carry out measurements based on the IEC 61400-11 (channels are dedicated to climatic data) and measurements for the acoustical imaging.

Using the system for short distances makes possible to obtain a better description of the sources along a specific part of the wind turbine. The implementation is practically more difficult: for example the configuration of the Figure 4 requires a crane jib. But also, it is necessary to take into account other parameters: stability of the antenna, possible influence of the antenna on the acoustic radiation from blades.... Thus this kind of tests needs a time of preparation and is delicate to set-up. But it provides more information. This configuration is thus made for in-depth studies.

Conclusions

In this paper, we introduced a new measurement technique in the field of the wind turbine noise. This technique, based on the acoustical imaging method called beamforming, allows obtaining images showing the localization of acoustic sources. The beamforming method is a robust technique and thus well adapted for outdoor measurements.

The acoustical imaging systems are tools for the investigation of the sound sources. We developed a complete and autonomous system dedicated to the study of wind turbines, providing acoustic images for a better understanding of the real acoustic sources. The system that we developed is also a very helpful tool in complement of the IEC 61400-11 standard. The hardware and software system allows carrying out acoustic, tachometric and climatic measurements at the same time, and thus IEC 61400-11 calculations can be made on the same system. This configuration allows localizing spatially, in time and in frequency what part of the wind turbine contributes to the non-respect of the regulation.

References

- [1] International Standard IEC 61400-11: 'Wind turbine generator systems - Acoustic noise measurement techniques', 2002-12.
- [2] K. Haddad, V. Benoit – "Localization of aeroacoustic sources all along a vehicle by means of the acoustical imaging system ANT64 in the semi-anechoic wind-tunnel Pininfarina", Euronoise 2003.

**First International Meeting
on
Wind Turbine Noise: Perspectives for Control
Berlin 17th and 18th October 2005**

Analysis of the sound characteristics of large stall-controlled wind power plants in inland locations

Harders, H.; Albrecht, Dr. H. J.;
Landesumweltamt Brandenburg (Brandenburg State Office for Environment);
D-14467 Potsdam - Germany;
e-mail: hermann.harders@lua.brandenburg.de

Summary

Stall wind turbines show an increasing sound power level above the measured interval according to DIN/IEC 61400-11. Also an increasing background noise usually covers this phenomenon in smaller wind energy converters. Plants with hub heights of 100 m or more together with a layout for inland locations show decoupled wind speeds at v_{95} at hub height and near ground level. Thus there is no masking of the stall noise. Based on differentiated probabilities of exceeding v_{95} criteria are proposed that would avoid the shut down and severe disturbing effects to the vicinity.

1. Introduction

The sound power level of wind energy converters (WEC) is established in accordance with DIN/IEC 61400-11 (1), (3) which determines standardized wind velocities of 6 m/s, 7 m/s, 8 m/s, 9 m/s and 10 m/s up to a maximum of 95% of the rated power (P_{95} at v_{95}). The standardized wind velocity v_{std} is calculated using a standard wind profile based on the hub wind speed v_H which is derived from the electrical power (P_{el}). Above P_{95} there is no distinct connection between P_{el} and v_H . These procedures make it easy to record the noise characteristics of pitch controlled WECs. The maximum noise level of stall-controlled WECs, however, exceeds the wind velocity v_{95} . For this reason, the standard procedure is not sufficient for this model to meet the regular requirements of environmental allowances (2), (5). In a case put before the appellate administrative court of the state of Northrhine-Westfalia in the city of Muenster, it was decided that all applicants and government agencies must ensure that there will be no detrimental effects to the immediate vicinity before receiving permission to erect a stall-controlled wind energy converter (4). In case of doubt, the WEC will have to be shut down if wind exceeds v_{95} . In the following, an alternative system is presented, requiring significantly higher standards to be met by the applicant, the acoustic expert as well as the government authorities.

2. A short overview of aerodynamic causes

The stall in wind energy converters is achieved passively through speed controlled generators or actively by the rotation of the rotor blades. After the aerodynamically optimal wind speed

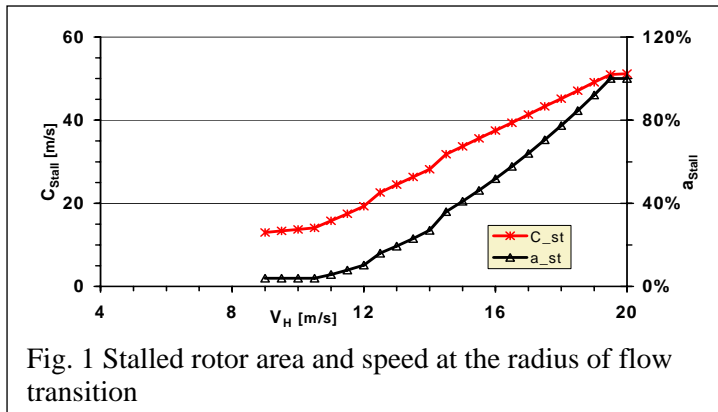


Fig. 1 Stalled rotor area and speed at the radius of flow transition

associated velocity of flow increase with the wind speed (Fig. 1).

- Local lift coefficient (c_l) and the velocity of flow increase at the rotor tip, the tip vortex and edge flow are intensified (Fig. 2).

3. Probability of Wind Velocity and Operating Conditions

The decisive period for the assessment of immissions is during the night. The wind conditions at hub height at this particular time must be known in order to arrive at an indication of the frequency of certain operating conditions of a plant and the associated acoustic emissions. The determinant is the wind velocity using

$$(1) \quad v_H > v_{95}$$

The wind velocity is calculated by using the Weibull's distribution function $F(v)$. This equation represents the probability of exceeding the wind speed (v).

$$(2) \quad F(v) = \exp \left[- \left(\frac{v}{a} \right)^k \right]$$

If the scale and shape parameters (a , k) of the function are known, equation (2) can be used to calculate the probability of exceeding the wind speed v .

The applicants are aware of the parameters for location and hub height. They are the essential requirements for operating efficiency studies.

has been surpassed, the angle of attack of the rotor blades rises. In the inner radius, the critical angle, at which the flow stalls is then reached. This point moves on while the v_H continues to rise to the rotor blade tip (see Fig. 1). Two factors can contribute to the increase in the sound power level:

- The portion of the rotor area with turbulent flow and the

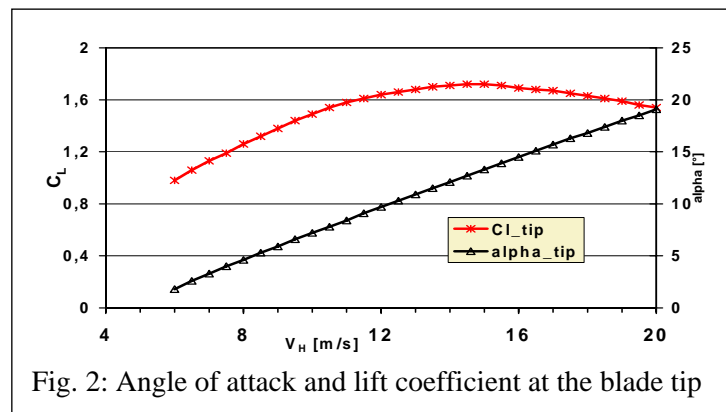


Fig. 2: Angle of attack and lift coefficient at the blade tip

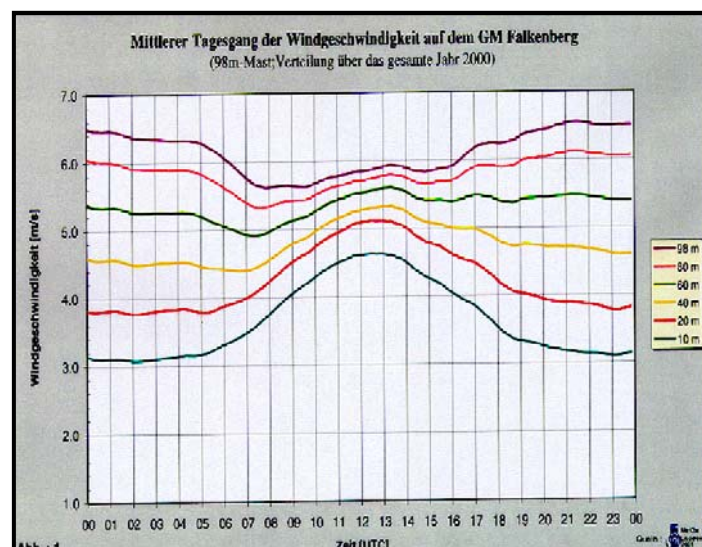


Fig. 3 : Mean diurnal variation; Heights 10m, 20m, 40m, 60m, 80m, 98m; DWD Observatory Lindenberg, year 2000

4. The Influence of Stratification

The standard procedure for calculating wind velocity distribution (the European Wind Atlas) uses neutral stratification. It occurs mainly in the transition period between night (stable period) and day (unstable period). During the unstable period, there is a distinct vertical impulse exchange and a minor vertical gradient in wind velocity. During the stable period, there is a weaker impulse exchange and greater vertical gradients. Therefore, during the stable period, with identical v_H , the velocity is less at ground level than during neutral or unstable stratification periods. This is proved by measurements on the 100m mast of the Lindenberg Meteorological Observatory (Fig. 3) (6). The inverse diurnal variation at ground level and above 80m can be easily seen. Ground level wind velocity reaches the daily maximum at midday and the minimum during the night. Above 80 m the opposite occurs. The European Wind Atlas (7) can take the effects of the negative nightly thermal radiation on the vertical wind profile into account. The necessary input values in order to determine the scale and shape parameters for the different heights of a stable nightly layer were determined for the state of Brandenburg (8), (9).

Using this as a basis, the Deutsche Wetterdienst (DWD) (German Meteorological Service) calculated the parameters a and k for eight meteorological stations in stable conditions during the night as well as with the standard procedure (10). In addition to this, the average wind velocity at a height of 10m during the day, the night, as well as the combined day and night speed were determined for the period 1992 – 2001.

Meteorological Observatory	$v(10)_{m,T+N}$ in m/s	$v(10)_{m,T}$ in m/s	$v(10)_{m,N}$ in m/s
Seehausen	4,2	4,9	3,6
Kyritz	4,3	5,0	3,7
Angermünde	4,2		3,6
Manschnow	4,0	5,4	3,5
Berlin Schönefeld	4,3	5,0	3,7
Lindenberg	4,2	4,5	4,0
Doberlug Kirchhain	4,0	4,6	3,6
Cottbus	3,9		3,3

Table 1: Mean wind speed of that DWD-observatories that the a and k parameters were calculated (1992 - 2001)

5. Development trends for Wind Energy Converters and the Relevant Technical Parameters of Stall-controlled Converters

Up to now, three development trends have been pursued:

- higher masts (up to 120m) in order to make use of stronger and more constant wind conditions
- converters on inland sites with reduced specific output (W/m^2) or v_{95} respectively
- larger, specifically (dB (A) / kW) quieter rotor blades

WEC-Model	P_{95} [kW]	Hub Height z_N [m]	v_{95} [m/s]
1	950	50, 60, 70	13,6
2	1235	60, 80, 90	13,7
3	2185	60, 80, >80	12,9
4	1900	60, 80, 90	13,0
5a	1568	94, 109	11,8
5b	1425	94, 109	10,9

Table 2: Important characteristic data for wind turbines

An obligatory requirement for the study is the knowledge of the v_{95} for the proposed wind energy converter. This is determined by the output curve (P_{el} over v_H) and is exemplified in Fig. 4 which shows the curves for three turbines. The unsecured correlation between P_{el} and v_H above v_{95} is visible. Lines 5a and 5b are two different layouts of the same turbine. Important data for six different plants are shown in Table 2. This compilation is not an exhaustive one. The v_{95} values in particular can vary greatly even in the same model and hub height when using different layouts(see turbines 5a and 5b).

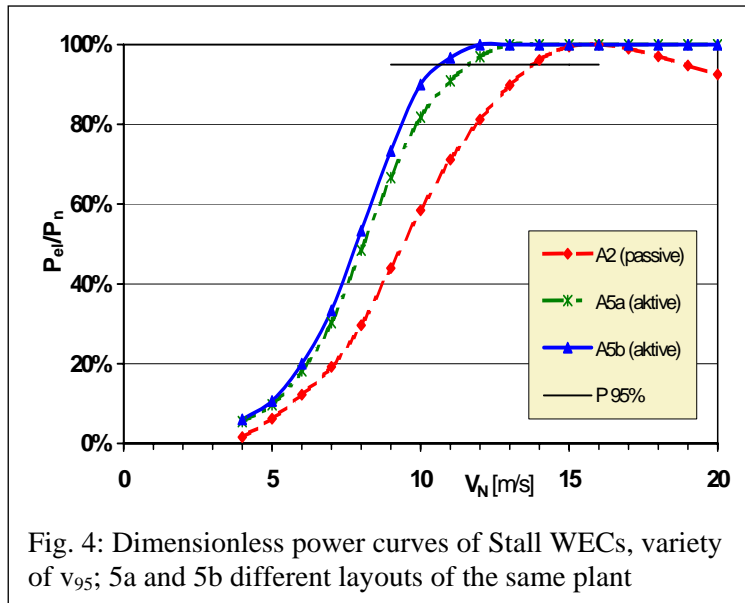


Fig. 4: Dimensionless power curves of Stall WECs, variety of v_{95} ; 5a and 5b different layouts of the same plant

6. Probability of Exceeding Wind Velocity v_{95}

6.1 Stable Stratification during nighttime period

For all eight DWD sites (Table 2) the distribution density function $f(v)$ and the distribution function $F(v)$ were calculated irrespective of the wind direction for heights of 50m, 100m and 200m with a roughness length of $z_0 = 0.03m$. Subsequently, the frequency of exceeding the v_{95} for the six turbines was determined. The differences, although minor in all cases, are highest at the

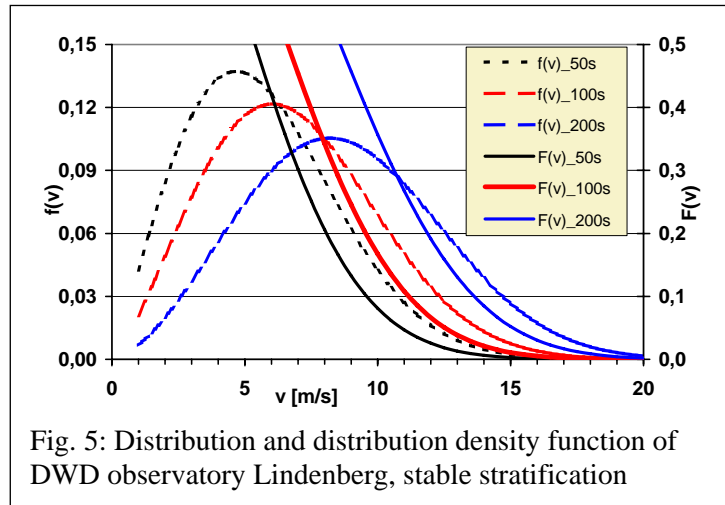


Fig. 5: Distribution and distribution density function of DWD observatory Lindenberg, stable stratification

WEC-Model	v_{95} [m/s]	$F(v_{95})_{50m}$ in %	$F(v_{95})_{100m}$ in %	$F(v_{95})_{200m}$ in %
1	13,6	0,9	2,7	10,1
2	13,7	0,8	2,5	9,7
3	12,9	1,4	4,1	13,6
4	13,0	1,3	3,8	13,1
5a	11,8	2,9	7,3	20,5
5b	10,9	4,9	11,3	27,6

Tab. 3: Probability of exceeding v_{95} ($F(v_{95})$) of different WECs, stable stratification, nighttime heights 50 m, 100 m, 200 m

Lindenberg station. For this reason, this station is used as the measuring unit (Fig. 4). This figure shows how the frequency maximum of wind velocity shifts towards higher speeds with increased height. While the maximum at a height of 50m is found at approx. 4.5 m/s, at a height of 200m it is located at approx. 8 m/s. The probability of exceeding a given velocity

clearly increases at lower wind speeds and greater heights. For example, $v = 11$ m/s at a

height of 50m will be exceeded at a probability of $F(v) = 0.047$ (4.7%) and at 100m with $F(v) = 0.108$ (10.8%). This representation was used to determine the probability of exceeding of v_{95} for the particular converter models. The survey can be found in Table 3 which also shows the precise influence of the plant layout on the frequency of exceeding the velocity for v_{95} . The reduction from 13 m/s (turbine 4) to 10.9 m/s (turbine 5b) signifies that at a height of 100m, the risk of exceeding the v_{95} will be three times as high.

6.2 Neutral Stratification

Most feasibility studies are based on the stability independent method used by the European Wind Atlas (7).

Both methods are compared for the Lindenberg location (Fig. 5). At heights of up to 50m, marginal differences are measured in the area under 11 m/s. With increasing height and decreasing wind speed, the differences between the two calculation methods grow. As anticipated, the values are greater during the stable (night) stratification. Nevertheless, the differences in the current hub heights of approx. 100m and v_{95} speeds of approx. 10 m/s to 14 m/s are comparatively small. The results for precise wind energy converters are compiled in Table 4. The comparison with Table 3 shows that there are little deviations in the probability of exceeding in WECs up to a height of 100m examined here

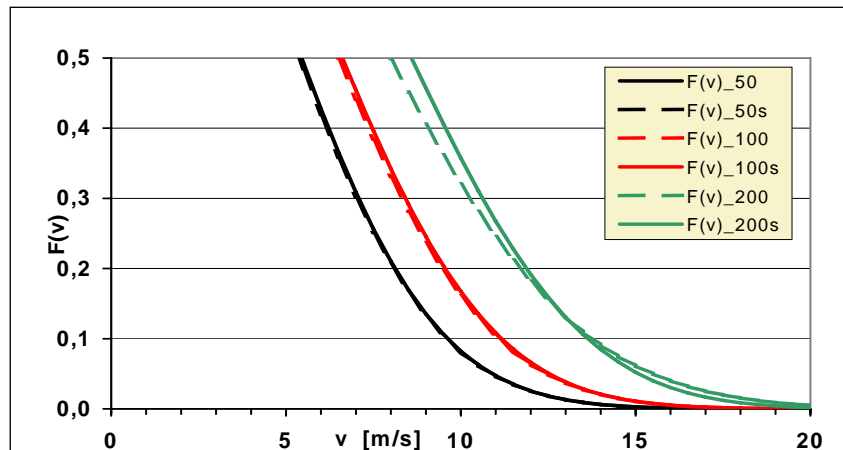


Fig. 6: Comparison of distribution functions based on nighttime stable [$F(v)_{zs}$] and neutral stratification [$F(v)_z$]; heights $z = 50$ m, 100 m and 200 m; $z_0 = 0,03$ m; observatory Lindenberg (1992 - 2001)

WEC-Model	v_{95} [m/s]	$F(v_N)_{50m}$ in %	$F(v_N)_{100m}$ in %	$F(v_N)_{200m}$ in %
1	13,6	0,8	2,6	10,6
2	13,7	0,8	2,4	10,2
3	12,9	1,4	3,9	13,6
4	13,0	1,3	3,7	13,1
5a	11,8	2,9	7,1	19,4
5b	10,9	5,0	10,9	25,2

Table 4: Probability of exceeding v_{95} ($F(v_{95})$) of different WECs neutral stratification, heights 50 m, 100 m, 200 m

7. Masking of WEC noise through wind-induced background noise

7.1 Wind-induced background noise

The ground level wind speed ($z = 10$ m) at $v_H > v_{95}$ must be known to evaluate the masking of the turbine noise through wind-induced background noise. It can be calculated by using the v_{95} under the assumption of stable stratification and the corresponding wind profile. Alternatively, it can be ascertained through the measured data of the 100m mast of the Meteorological Observatory Lindenberg (11) for the $v_H > v_{95}$ cases.

Subsequently, the second method will be applied. However, it can only be generalized with regard to inevitable restrictions. Only the limited data set for 2001 was at our disposal. The correlations precisely apply only for the given roughness and stability conditions. The mast is situated in a sparsely structured farming area. The heights for which the Weibull parameters a and k were calculated are not exactly concurrent with the mast measurement heights. The measurement height of 60m was allocated to the calculated height of 50m and the measurement height of 98m to the calculated height of 100m. Despite these modifications, tentative conclusions about expected ground level wind speeds can still be reached. Either the minimal, the median or the wind speed of the 90% lower confidence limit, which is exceeded in 90% of the cases $v_H > v_{95}$, can be used as the basis for estimating the dimension of wind-induced background noise.

In (12) the relationship between wind speed at a height of 10m and wind-induced noise in five and fifteen-year-old housing areas is shown. The wind-induced noise in the older housing area is at a lower level during the winter, approximately at the summer level gauged during the summer in the five-year-old housing areas (12). Therefore, these two cases provide the basis for the calculation of the level of background noise.

$$(3) \quad \begin{aligned} L_{bg} &= 4,83 \times v(10) + 8,7 \text{ dB(A)} \\ R^2 &= 0,92 \\ s_R &= 1,85 \text{ dB} \end{aligned}$$

7.2 Assessment Levels

The results for $L_{bg,m}$ and $L_{bg,lc190}$ for hub heights of 50m and 100m are presented in the following Figure 7 and in Table 5.

At identical wind speed v_H , the wind-induced background noise levels are lower at a hub height of 100m than at one of only 50m. Based on the limited data at our disposal, the minimal background noise $L_{bg,min}$ does not exceed 52 dB(A), despite an increase in wind speed at a height of 50m from 12.5 m/s to 14 m/s. It would, therefore, appear that this does not represent a stable reliable value. At the same wind speed and hub height, the median level $L_{bg,m}$ is approximately 10 dB to 15 dB greater than the minimal. The results of $L_{bg,lc190}$ are approximately 3 to 8 dB higher (Table 5).

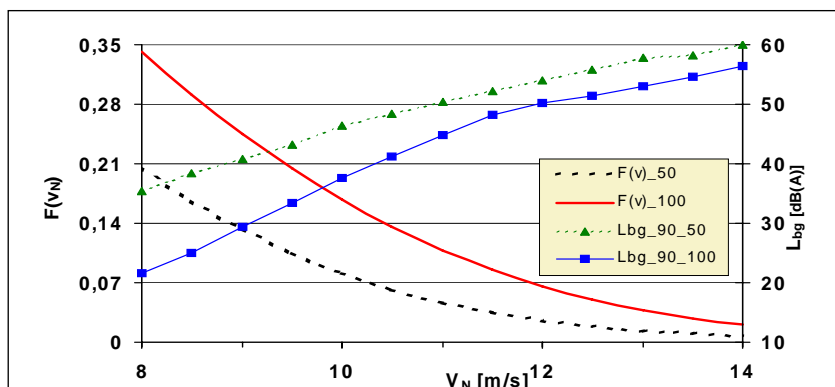


Fig. 7: Wind-induced background noise levels $L_{bg,m,xx}$ and $L_{bg,90,xx}$ together with the probability of occurrence $F(v_N)$ depending on wind speed at hub height 50m and 100m, nighttime stable stratification

WEC-Model	v_{95} [m/s]	$L_{bg,min}$		$L_{bg,m}$		$L_{bg,UVG90}$	
		50m	100m	50m	100m	50m	100m
1	13,6	52	51	64	61	58	55
2	13,7	52	51	64	61	58	55
3	12,9	52	46	63	60	58	53
4	13,0	52	46	63	60	58	53
5a	11,8	50	44	60	57	54	50
5b	10,9	46	38	57	53	51	45

Table 5: Possible levels of background noise in case of $v_N > v_{95}$

In practice, this value is exceeded in 90% of all cases. Hence, the determination of the level L_{bg_lc190} would be recommended. It would provide more protection for the potentially affected residents than would the use of the median background noise level. In 10% of all cases, levels in the range of $L_{bg_min} \leq L_{bg} \leq L_{bg_lc190}$ are to be expected.

Table 5 illustrates a summary of the possible background noises for different turbine models. In conclusion, it should again be pointed out that these observations do not apply for immission locations in mountainous regions or in the lee of larger obstacles.

8. Conclusions

- (1) Detailed individual examinations are necessary to avoid nightly overall shutdowns of wind energy converters upon reaching 95% of the rated power.
- (2) The probability of exceeding the wind speed at which 95% of the rated power is reached increases with increased hub height and decreased wind speed v_{95} .
- (3) For the practical licensing procedure a relevance criteria for the immission protection assessment of the frequency of certain occurrences is necessary. The threshold point should be approximately 3%. Occurrences or operating conditions with a cumulative percentage of less than 3% would therefore be regarded as irrelevant.
- (4) At hub heights of up to 100m, the differences between the probability of exceeding the wind speed v_{95} , which are calculated either by using the Wind Atlas method or by taking the nightly stable stratification as a basis, are negligible. In the State of Brandenburg, the probability of exceeding the wind speed v_{95} can also be calculated with the Weibull parameter, as used by the applicants in their economic feasibility calculations.
- (5) Wind-induced background noise becomes less with increased hub height z_H and decreased wind velocity v_{95} .
- (6) A reliable masking of the WEC noise produced by wind-induced ambient noise for all turbine types and hub heights is no longer guaranteed due to the present trend towards greater hub heights and the ability to achieve the rated output at lower wind velocity.
- (7) The observations regarding wind-induced background noise apply only for horizontal, flat and non-structured locations. The immission site cannot be in the lee of other buildings.
- (8) For WECs with a hub height of approx. 50m, the WEC noise can be masked in 90% of all cases through wind-induced ambient noise with $v_{95} > 12$ m/s and at hub heights of approx. 100 m with $v_{95} > 13.5$ m/s.
- (9) In 10% of the cases under analysis, a background noise situation in compliance with $L_{bg_min} \leq L_{bg} < L_{bg_lc190}$ is to be expected.
- (10) The studies presented here will enable the licensing agency to deduce the following: if an application for a WEC with a hub height of 90m is filed with the agency, it can be assumed that wind speed at hub height at which 95% of the rated power is achieved averages $v_{95} = 13,7$ m/s. Figure 5 shows the probability of exceeding the wind speed $F(v)$ to equal 0.028 or 2.8%. This means that during 10.2 nights per annum operating conditions above 95% of the rated power are to be expected. In other words, during 10 nights p.a. higher noise immission rate than that calculated can occur. At the same time, Figure 7 shows that it is to be expected that during nine of these ten nights, the wind-induced noise value (L_{bg_lc190}) of 55 dB(A) will be reached and during one night, a wind-induced noise level of between 51 and 55 dB(A) is probable (see Fig. 7 and Tab.5). In order to mask the WEC noise through wind-induced background noise, a level of at least 10 dB is necessary under the precondition that the WEC noise contains neither tonality nor pulsating noise(13).

- (11) In Model 5b wind energy converters, the likelihood that the wind speed v_{95} will be exceeded is at almost 11% or 38 nights (Tables 3 and 4). Simultaneously, the expected wind-induced background noise level is such that a masking of the WEC noise cannot be expected. Due to these conditions, it will be necessary to shut down the turbine upon reaching 95% of the rated power in order to prevent considerable inconvenience.
- (12) In Model 3 wind energy converters, the likelihood that wind speed v_{95} will be exceeded at hub heights of up to 80m is less than 3% with an expected wind-induced background noise level of approximately 55 dB(A). At hub heights of 90m, a nightly shutdown could become necessary due to local conditions. The probability of exceeding the level exceeds the relevance criterion (Table 4) at 3.7% and the expected wind-induced background noise level is at 53 dB(A). Should the immission guideline value of 45 dB(A) be barely maintained, masking is no longer probable and, upon reaching 95% of the rated power, the WEC must be shut down. If the immission guideline value of 40 dB(A) is maintained, the level difference is large enough and a shutdown can be avoided.
- (13) These studies illustrate the importance and necessity of appropriate on-site inspections to determine the exact conditions at the immission locations and also that they should be made when preparing the noise predictions.
- (14) When checking the WEC after start-up, it will not suffice to merely determine and analyze the emissions themselves. In stall converters, it will be necessary to determine and assess the immission conditions and locations as well. The evaluation of the WEC noise at the immission location can be calculated.

Indexes and Sources

- (1) Standard DIN/IEC 61400-11 Ed. 2 Wind turbine generator systems – Part 11: Acoustic noise measurement techniques (2003)
- (2) Technische Anleitung zum Schutz gegen Lärm (TA Lärm) vom 26. August 1998: GMBI Nr. 26 1998 S. 503 - 515
- (3) Fördergesellschaft Windenergie: Technische Richtlinien für Windenergie, Teil 1: Bestimmung der Schallemissionswerte; Revision 15, Stand 01.01.2004
- (4) Oberverwaltungsgericht für das Land Nordrhein-Westfalen vom 19. 03. 2004; 10 B 2690/03; 2 L 1909/03 Münster
- (5) Gesetz zum Schutz vor schädlichen Umwelteinwirkungen durch Luftverunreinigungen, Geräusche, Erschütterungen und ähnliche Vorgänge (Bundes-Immissionsschutzgesetz – BImSchG) i .d. F. der Bek. Vom 26. 09.2002 (BGBl. I S. 1578)
- (6) Adam, W.: Windmessung am großen Mast auf dem GM des MOL in Falkenberg. Deutscher Wetterdienst, Meteorologisches Observatorium Lindenberg (2001)
- (7) Europäischer Wind Atlas: Riso Nat. Laboratory, Roskilde, Dänemark
- (8) Giebel, G.; Gryning, S.-E.: Prediction of local wind in the Brandenburg region with WAsP during atmospheric stable conditions; Riso National Laboratory, Roskilde Denmark (2002)
- (9) Giebel, G.; Gryning, S.-E.: On the stability treatment in WasP; Poster Ausstellung Nizza 2003
- (10) Wichura, B.: Scale- und Shape-Parameter der Weibullverteilung für ausgewählte Stationen im Land Brandenburg; Deutscher Wetterdienst: Potsdam (2004)
- (11) Deutscher Wetterdienst: Messergebnisse des Meteorologischen Observatoriums Lindenberg vom 100 m-Mast für das Jahr 2001
- (12) Jakobsen, J.; Andersen, B.: Wind noise. Danish Acoustical Institute, Report Nr. 108 (1983)

- (13) Piorr, D.: Schallemissionen und –immissionen von Windkraftanlagen, Fortschritte der Akustik, DAGA ' 91
- (14) Albrecht, H. J.: Untersuchung von Möglichkeiten zur Berücksichtigung der akustischen Besonderheiten von Windenergieanlagen mit Stall-Regelung, Fachbeiträge des Landesumweltamtes Brandenburg; Nr. 91

Abbreviations

a	scale parameter of the Weibull distribution function
a_{st}	stalled portion of rotor area
c_{st}	flow speed at the radius of flow transition to stall
$f(v)_{-z}$	distribution density function of wind speed v due to Weibull for the height z at neutral stratification
$F(v)_{-z}$	distribution function of wind speed due to Weibull for the height z at neutral stratification. The form used here means the probability of exceeding the wind speed v
$f(v)_{-zs}$	distribution density function of wind speed v due to Weibull for the height z at stable (s) stratification
$F(v)_{-zs}$	distribution function of wind speed due to Weibull for the height z at stable (s) stratification.
k	shape parameter of the Weibull function
L_{bg}	background noise level
$L_{bg,min,z}$	minimal background noise level evaluated on the base of wind speed at height z
$L_{bg,lcl90,z}$	lower confidence limit of background noise level evaluated on the base of wind speed at height z exceeded in 90% of cases
OVG	appellative administrative court
P_{el}	electric power of WEC
P_n	rated power of WEC
P_{95}	95% of rated power
R^2	coefficient of determination
s_R	remaining scattering
v	wind speed
$v(z)$	undisturbed vertical wind speed profile
v_{std}	standardized wind speed
v_H	wind speed at hub height
v_{95}	wind speed at 95% rated power at hub height
$v(10)$	wind speed at 10 m height
$v(10)_{m,T+N}$	day and night average wind speed at 10 m height in the period 1992 - 2001
$v(10)_{m,T}$	average wind speed at 10 m height in the period 1992 - 2001 during the day
$v(10)_{m,N}$	average wind speed at 10 m height in the period 1992 - 2001 during the night
WEC	wind energy converter
z	height (in general)
z_0	roughness length
z_H	hub height

First International Meeting
on
Wind Turbine Noise: Perspectives for Control
Berlin 17th and 18th October 2005

**Development of noise reduction technology for a 500 kW
prototype wind turbine**

By Geoff Henderson, Chief Executive Officer, Windflow Technology Limited,
P.O. Box 13 952, Christchurch, New Zealand. geoff@windflow.co.nz

Summary

In July 2003 the prototype of New Zealand's first indigenous grid connected wind turbine was officially opened at Gebbies Pass, Christchurch. The Windflow 500 differs from traditional windmills in several important ways, with its two bladed teetering system and torque-limiting gearbox giving it the ability to run a synchronised synchronous generator directly online.

Operation of the prototype generated a low gearbox tone, and measurements showed that sound emissions exceeded the Resource Consent condition. After several unsuccessful attempts to dampen the gearbox vibrations causing the tone, Windflow researched and developed technology that eliminated the vibration and consequently eliminated the tone and reduced total sound power from 107.7 dBA to 100.7 dBA. As a result, the assessed sound level dropped from 36 dBA to 24 dBA at the critical location for the Resource Consent.

Introduction

New Zealand is situated in the southern part of the Pacific Ocean and lies directly across the path of the well-named "Roaring Forties" winds. These strong winds provide a consistent resource for wind power.

However the abundance of relatively inexpensive water, geothermal steam, natural gas and coal resources has allowed them to meet the steadily increasing demand for electricity until recently. This and the country's unsubsidised manufacturing economy has inhibited the development of a wind power industry.

Recent events have encouraged the country's major electricity generators to look to wind power as a means of increasing supply: the country's Resource Management Act (1991) has made it increasingly difficult for generating companies to further exploit major water sources; geothermal and gas supplies are dwindling; and there is strong public debate over the acceptability of coal-fired generation.

Since 1990 the author has had a vision of designing and manufacturing wind turbines in New Zealand for the country's high wind and unsubsidised conditions. This has required the development of technologies to provide a turbine light enough to be manufactured commercially in New Zealand and yet resilient enough to withstand the

high and often turbulent wind conditions experienced in the better wind resource areas of the country.

Certain that the combination of a two bladed teetering system and a torque-limiting gearbox would provide a resilient and commercially viable wind turbine, the author established the company Windflow Technology in 2000. The company raised funds in 2001 for the design and manufacture of the full-scale prototype of the “Windflow 500”, a 500 kW wind turbine.

The Company – Windflow Technology

The company’s mission statement is “to be a global leader in wind turbine technology innovation”. We now have over 700 shareholders and are listed on the NZAX share market. We specialise in the design, development and manufacture of utility size wind turbines, which are manufactured and installed with over 90% New Zealand content.

We have 14 staff, mainly professional engineers, and two subsidiary companies, Wind Blades Ltd, which manufactures our wind turbine blades, and NZ Windfarms Ltd which we will be floating off later this year to develop our first wind farm project.

The Wind Turbine - Windflow 500

Our turbine has a 33 m rotor and a rating of 500 kW. It combines two proven technologies based on the author’s experience in Britain in the 1980’s:

- two bladed teetering with pitch-teeter coupling
- a patented torque-limiting gearbox driving a standard synchronous generator, which runs synchronised with the grid, ie at constant 1500 rpm.

The 16 m blades are made of laminated wood-epoxy and fibreglass. The wood species is pinus radiata (New Zealand’s main commercial species). The structure is based on a stressed shell concept, similar to that used by Vestas’ 40 m blades from their factory on the Isle of Wight, England. The blades are made in Auckland by Wind Blades Ltd.

The gearbox is made in Auckland by AH Gears Ltd. It is a 4 stage design with an overall ratio 30.94 and rated power 548 kW (mechanical). Starting from the low speed end the stages are planetary – planetary - parallel - epicyclic with patented torque limiting on the fourth stage. The torque limiting gearbox (TLG) system was developed by the author in the late 1980’s to solving the wind turbine gearbox torque control problem, which it does by including a differential stage and a simple hydrostatic torque control circuit. The TLG system is patented in several countries including the USA.

Input speed varies from 48.5 to 51 rpm while the output speed is constant at 1500 rpm.

The parallel stage is helical and the three epicyclic stages use straight cut spur gears. Flexible spindles (as patented by Ray Hicks in 1964) carry all planets, enabling a multitude of planets and a compact design. The first planetary stage has eight planets, the second has four and the fourth stage has six planets. The gearbox has an integral low speed shaft (LSS) so that the main bearings in the gearbox carry the loads from the wind turbine rotor.

Lubrication is based on a dry sump draining to a de-aeration tank and being injected via an external filtered cooling circuit. The casing is SG iron and total weight of the gearbox is 2.6 tonnes including the LSS extension.

The turbine operates in wind speeds from 5.5 to 30 m/s and uses a synchronised, synchronous generator. The design is light-weight throughout, using approximately 50% less steel and concrete than comparable 3-bladed turbines.

Background to the Noise Problem

Prior to installing the prototype, we consulted with the local neighbours from a standpoint that measurable sound levels should conform to community-set standards (40 dBA being the local council's requirement) and if possible go even better. Normally wind farms do much better, and we agreed to a particularly low sound level (30 dBA including any tonal penalty at the house of the nearest objecting neighbour) as part of our resource consent. Why did we do this when we did not have to? There were three main reasons:

- a) the nearest objector lived 1.4 km away and we believed we would easily meet that standard
- b) the neighbour is question experienced very low background sound levels in a sheltered valley (sometimes as low as 20 dBA or lower) and expressed the strong value that she placed on that sound quality
- c) the turbine was a prototype. Therefore we accepted the need to “go the extra mile” for the local community. We also knew that if the sound levels exceeded 30 dBA at that distance, we would have a serious marketing problem with the turbine.

The Noise Problem

After commissioning, the prototype generated noise complaints from the neighbour in question. It was difficult to obtain the right conditions to determine the offending sound level but eventually we obtained an evening measurement showing a level of 31.2 dBA at that residence against a background of about 23.4 dBA (see Figure 1).

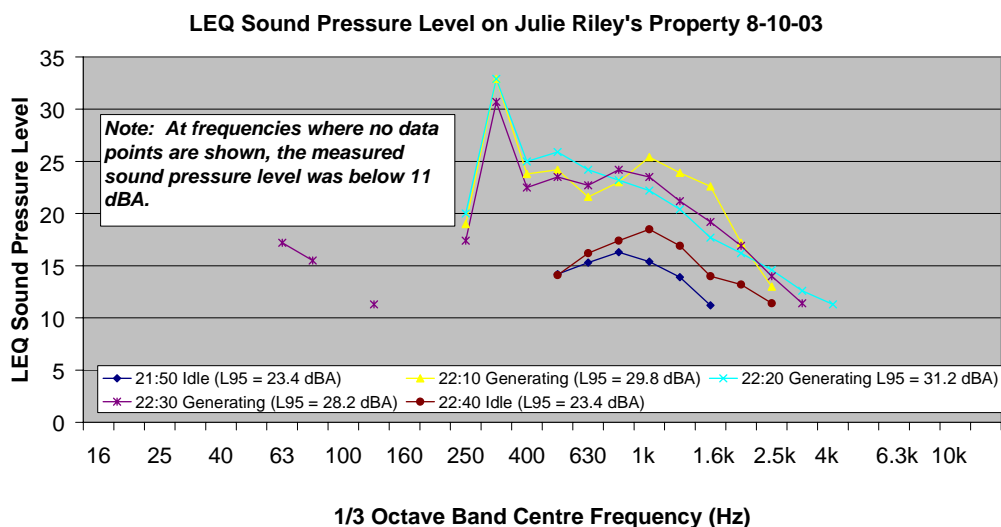


Figure 1 – Evening measurements at affected residence, generating and idle.

From the outset there was a clear tonal component at around 315 Hz (as shown in Figure 1 and even more clearly in narrow-band vibrations measurements like Figure 2).

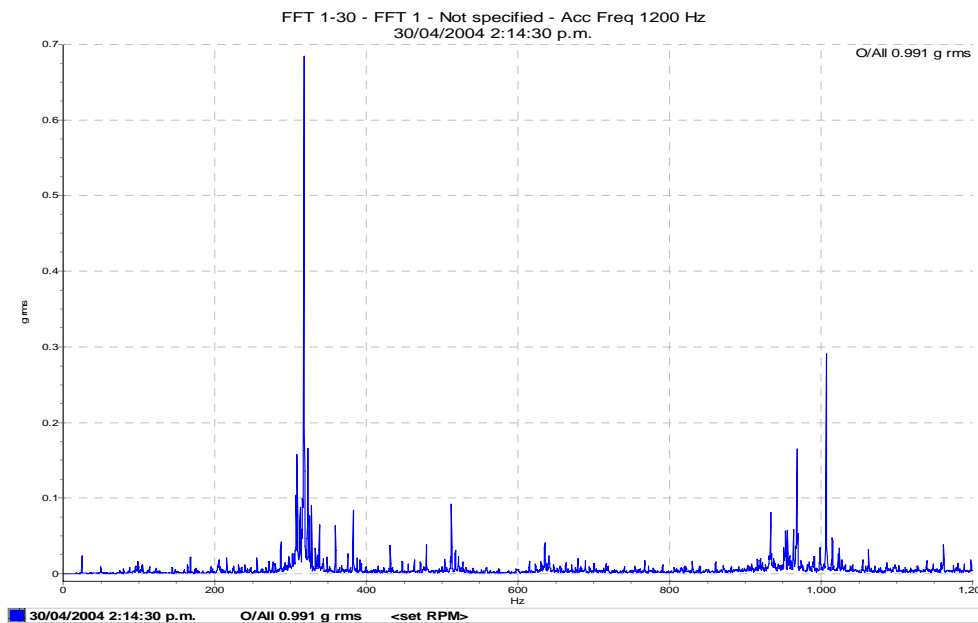


Figure 2 – Gearcase vibration measurements showing 311 Hz peak.

This added another 5 dBA to make the assessed level 36 dBA. Therefore we voluntarily restricted operation to daylight hours, five days a week. After three months of trying various remedial measures, in November 2003 we shut down the turbine completely in accordance with our resource consent and took the time to get it right.

Identifying the Root Cause

Tower

While the tone was clearly coming from the gearbox, and closely coinciding with the Stage 2 gearmesh frequency, initially our attention focussed on the tower. Why? Because there was obviously some resonance occurring in the tower. Sound levels in the nacelle right beside the gearbox did not seem excessive, whereas sound levels at the base of the tower were unusually high. Not only were measured sound levels there close to 100 dBA, the experience was like being inside a bell, with the vibration being able to be felt in one's body.

Therefore we examined the prospect of stiffening the tower panels with steel ribs. However finite analysis of a range of different rib configurations showed that there were simply too many modes in the range 300-320 Hz. Addition of stiffening ribs would simply shift the modes, not eliminate them.

Damping therefore seemed an attractive option. After considering various options, we decided to pursue rubber matting, glued to the interior of the tower. Laboratory testing showed that two layers of 25 mm rubber were considerably more effective than one at damping vibration in the range 200-500 Hz. Some tuned absorption was taking place with two layers, so we decided to proceed. The product was a type of matting made from recycled rubber, commonly used as a playground surface.

Lining about 20% of the tower interior with 50 mm of this product produced a major reduction in tower base sound levels, which came down about 8 dBA. A success of sorts!

However sound levels at a distance were unaffected. The tower was not the main problem after all.

Nacelle Cladding

Similar efforts were made to improve the sound reduction properties of the nacelle cladding. However nothing made any measureable difference to sound levels inside or outside the cladding.

Sound intensity measurements were made at this stage. Even with the measurement problems of using a stationary sound intensity meter on top of the nacelle aimed at the rotating blades, it became clear that 92% of the sound power was coming from the blades, with the balance coming from the tower and nacelle cladding.

Therefore attention shifted to the blades and the mechanism by which Stage 2 gearmesh vibration was being amplified.

In Search of the Hidden Resonance

By this time we had a large team of advisers working on the problem, drawing on the best acoustic advice available to us in Christchurch. The strength of the peak in the sound and vibration measurements indicated a structural resonance somewhere in the system. Based on the experience with the tower we realised that the blades themselves were probably not the root cause, but simply providing panel vibration or broad-spectrum resonance to propagate the vibration.

We tried to identify a component that would be more clearly resonant at about 311 Hz. In retrospect the answer was obvious, but we came to it in a roundabout way. We examined the gearbox/pallet sub-system, using both FE analysis and bump tests. A local company, Commtest Instruments Ltd, provided their "VB" vibration analyser initially on a loan basis. (We have since bought two VB units from them.)

However none of the initial bump tests on the gear case and pallet showed a clear natural frequency in the suspect range. Similarly the FE analysis showed a range of minor modes rather than a strong single mode at those frequencies.

But we felt we were on the right track so we commissioned the government-owned research company, Industrial Research Ltd (IRL), to investigate natural frequencies by doing bump tests on the gearbox/pallet system.

Low Speed Shaft

Finally it became apparent why our early bump tests had not uncovered the real "culprit". All those tests had been on the external components which were easily accessible.

In situ access to the low speed shaft (LSS) was difficult, and made somewhat more difficult by the teetering hub. On a fixed-hub wind turbine, bump tests on the hub would provide good information about any LSS modes. However in our case the teeter bearings were isolating the hub from the LSS. Bump tests on the hub showed only a hint of a resonance but we were able to get direct access by removing hub inspection covers and positioning the accelerometer directly on the LSS.

Figure 3 shows the result. A significant bending mode of the LSS was apparent at about 290 Hz.

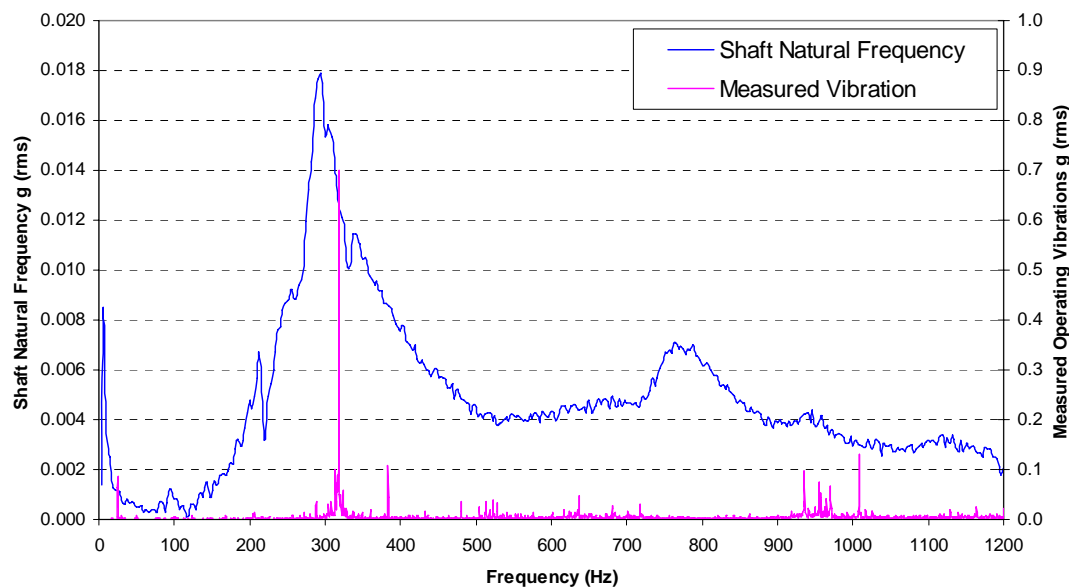


Figure 3 – LSS bump test result compared to measured gearbox vibration

Finally the noise problem made sense. The Stage 2 sun gear rides directly on bearings on the LSS, which in turn is mounted on the main gearbox bearings. The turbine rotor is mounted on the cantilevered section of the LSS. The front LSS bearing is a spherical roller bearing, which is self-aligning. Any forcing from the Stage 2 gearmesh was thus able to bend the LSS between its main bearings, giving rise to deflections of the cantilevered section out the front. The turbine rotor was being shaken at 311 Hz as it rotated!

This became our “tuned music system” model to explain the problem:

- the Stage 2 gearmesh was the “CD player”
- the LSS resonance was the “amplifier”
- the blades (being large hollow wooden items) acted as “speakers”.

The “music” being propagated into the neighbourhood was a very boring single note, about E flat above middle C (311 Hz).

Developing and Implementing the Solution

Having identified that the root cause was deep inside the gearbox, we decided in March 2004 to remove the gearbox and return it to the AH Gears factory in Auckland. Using a full-load test rig, we carried out baseline sound and vibration tests at full and part load while working on a programme of retrofits to modify the gearing.

Our approach was to (as far as possible) “turn off the CD player”. In addition we changed the Stage 2 gearmesh frequency away from 290 or 311 Hz, increasing it to 375 Hz by changing the gear module. However by this time our researches had produced an innovative approach to the problem, so that the shift in frequency became something of a precaution, rather than a key part of the solution. Indeed we

did not want to rely on simply shifting frequencies (forcing or natural) because we had already experienced how difficult it can be to eliminate resonances altogether.

Rebuilding a gearbox is an expensive business and we did not want to start a process of trial and error looking for the quietest part of the spectrum in a complex system response!

Our key innovation in gearbox design is the subject of a current patent application so we are unable to reveal the full details. It is a unique combination of technologies which came together for the first time in our gearbox. Our researches showed that there was a theoretical possibility of substantially eliminating the gearmesh forced vibration in any planetary stage, and we decided to pursue this.

However it was not at all certain that theory would translate into practice. The gearbox manufacturer in particular did not want to rely on it and advised us to try other approaches as well.

Accordingly we planned a series of three main retrofits to the gearing, which would progressively establish whether the new theory, or more traditional approaches such as tip relief modification, would be more effective. These three retrofits were carried out and tested between April and June, 2004.

Retrofit 3 involved full implementation of the new theory throughout the gearbox, not just for Stage 2 but Stages 1 and 4 also. Testing confirmed this gave the best results, as shown in figure 4.

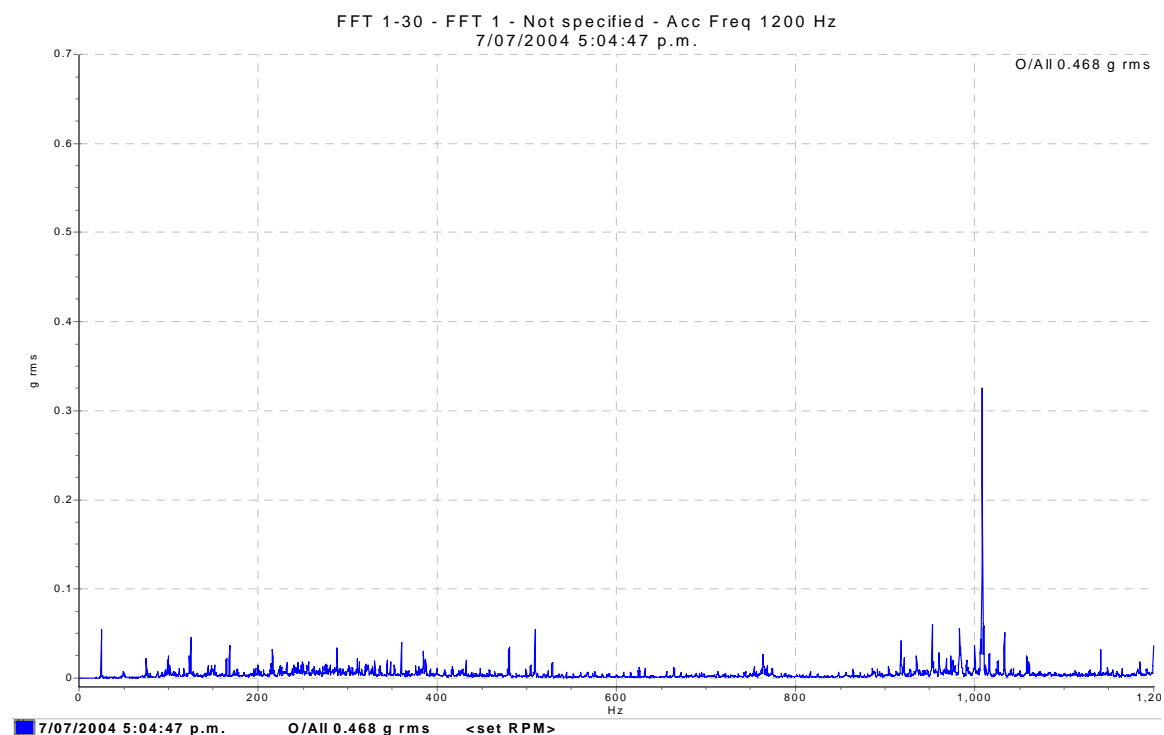


Figure 4 – Gearcase vibration measurements after Retrofit 3

Comparison of Figures 2 and 4 shows that we have substantially eliminated the 311 Hz vibration at the heart of our noise problem. The only significant vibration peak is at Stage 3 gearmesh frequency (1008 Hz) which is the only parallel stage in the gearbox. All the vibrations at planetary gearmesh frequencies have been substantially eliminated, as predicted by the new theory. Retrofits 1 and 2 showed

only partial elimination. Again this served to confirm the new theory and its superiority over conventional methods of gear vibration reduction.

Following retrofit 3, the gearbox was returned to Christchurch and refitted to the prototype windmill in July 2004.

The Result

Compliance testing carried out for the Banks Peninsula District Council indicates that sound levels at the affected residence have reduced to about 24 dBA. This compared to our original assessment of 36 dBA (31 dBA measured plus 5 dBA tonal penalty). Near field measurements to determine sound power (Figures 5 and 6) also show about a 7 dB reduction plus elimination of the tonal component.

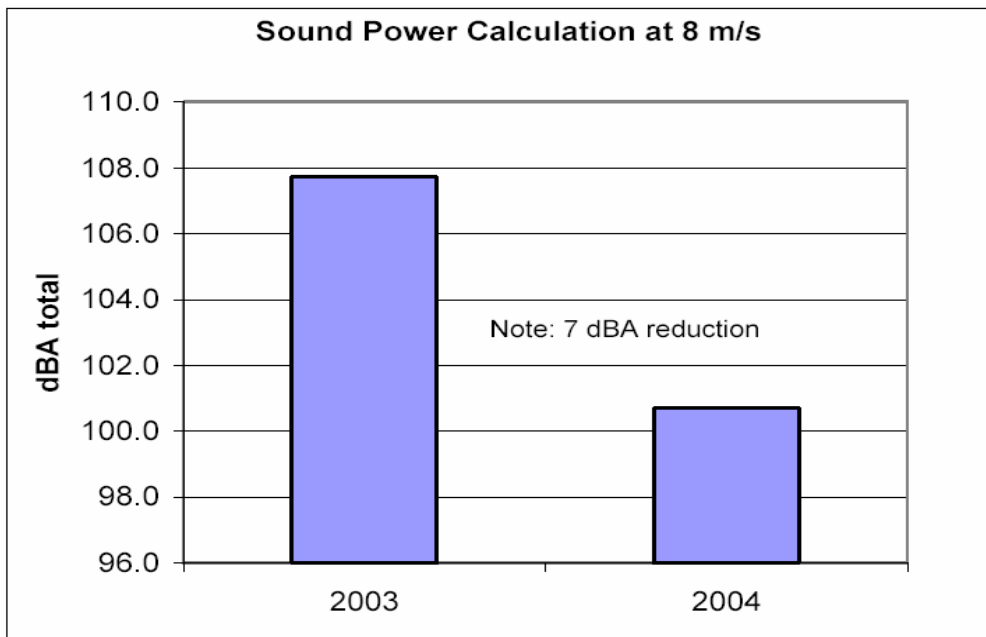


Figure 5 – Overall sound power levels before and after.

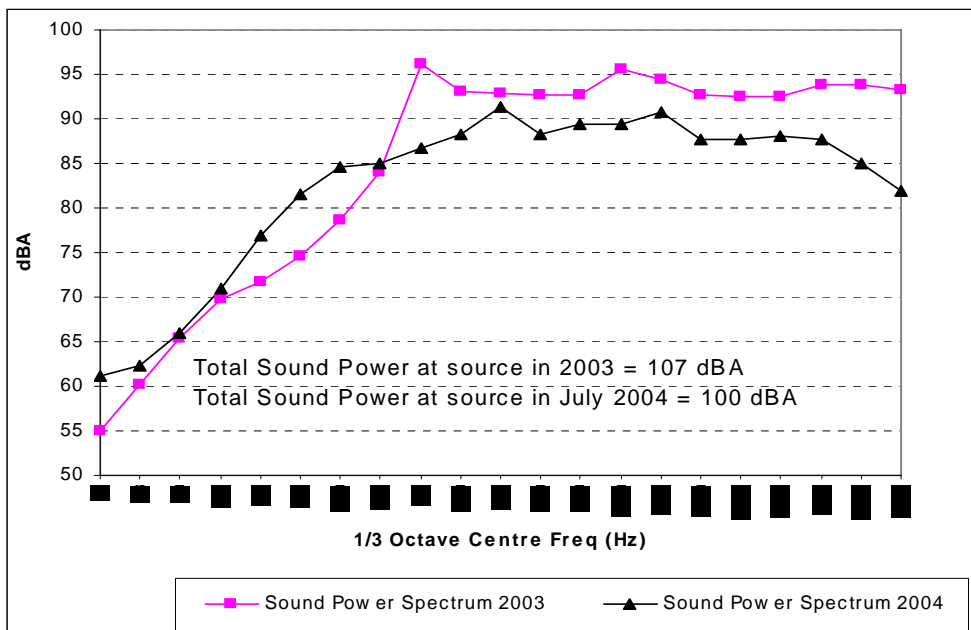


Figure 6 – Sound power spectra before and after.

The Future

Windflow Technology Ltd is currently working on its first batch of five production machines, to be completed in early 2006. It will be developing a wind farm near Palmerston North for NZ Windfarms Ltd over the next 2-3 years. This is a 97 turbine project of 48.5 MW, for which the company has obtained resource consent from the local council and a contract for carbon credits from the New Zealand government.

It will be New Zealand's first "made-in-NZ" wind farm.

Conclusions

Windflow Technology has encountered and overcome a classic wind turbine noise problem. Like many such problems:

- a) gear noise has been central to the problem and thus difficult to rectify
- b) residents in a sheltered valley nearby have been affected, and focussed attention on it
- c) a resonance was involved, though this was not easy to pinpoint
- d) the blades and tower were providing panel vibration to propagate the sound.

We have achieved a dramatic 12 dBA reduction in assessed sound level, due to the combination of:

- the LSS resonance being a big part of the problem
- the theoretical breakthrough in planetary gear vibration which we invented and validated in the course of our researches.

**First International Meeting
On
Wind Turbine Noise: Perspectives for Control
Berlin 17th and 18th October 2005**

**Low frequency underwater noise from offshore wind turbines:
Detection ranges and potential implications for marine mammals**

Oluf Damsgaard Henriksen¹
Uffe Degn²
Jakob Tougaard^{3,4}
Lee Miller⁴

1)
DDH-Consulting AS
Ringstedvej 20
DK-4000 Roskilde
Denmark
oda@hedeselskabet.dk

2)
Ødegaard & Danneskiold-Samsøe AS
Titangade 15
DK-2200 Copenhagen N
Denmark

3)
National Environmental Research Institute
Frederiksborgvej 399
DK-4000 Roskilde
Denmark

4)
University of Southern Denmark
Campusvej 55
DK-5230 Odense M
Denmark

This paper is a summary of a paper submitted to the Journal of Acoustical Society of America (JASA).

Summary:

Several large offshore wind farms are under construction in coastal waters in Northern Europe and The United States. Offshore wind farms are often placed high-density areas for small marine mammals, such as harbour seals (*Phoca vitulina*) and harbour porpoises (*Phocoena phocoena*).

In this study, broadband underwater noise from three different wind turbines in normal operation was recorded, analysed and compared with the auditory capabilities of harbour seals and harbour porpoises. The calculated source levels, measured as 1/3-octave spectrum levels, were converted into noise levels that are directly comparable with audiograms of harbour seals and harbour porpoises, so-called critical band levels. The maximum critical band level is 9 -18 dB above the assumed hearing threshold of harbour porpoises, corresponding to a detection range of 8 - 63 meters (assuming shallow water cylindrical spreading). These very limited detection ranges taken into

consideration, harbour porpoise are most likely not affected by the low frequency wind turbine noise.

The maximum critical band level is 34-40 dB above the assumed hearing threshold of harbour seals, corresponding to a detection range of 2.500 - 10.000 meters. This relatively high perceived noise level can potentially have some masking effects on harbour seal communications and affect harbour seals in general.

Introduction:

General background:

Noise levels in the oceans have continuously increased since engine powered shipping was introduced in the late 18th century.

In a now classic comparative study Ross (1986) found a 15 dB increase in the low frequency ocean ambient noise level between 1950 and 1975. A more recent study shows that the noise level at the continental shelf off the coast of California has increased by 3-10 dB in the frequency range from 20-300 Hz from the mid sixties to the turn of the century (Andrew et al. 2002). Both studies conclude that the major source is increased shipping activity.

Seen in the light of the general noise impact on the marine environment from human activity, noise emitted from operational wind farms might seem negligible. But where most human offshore noise sources such as shipping, sonars and seismic activity are transient in nature, the lifetime of an offshore wind farm is expected to be at least 20-30 years and associated noise emissions will be almost permanent on a year round basis. Thus noise from offshore wind farms could potentially present barriers to marine mammals that have not been seen from transient human noise sources.

Noise sources in relation to construction, operation and decommissioning of offshore wind farms are many and of highly various nature. Noise sources consist of low frequency, low intensity humming from the gearbox and generators in active wind turbines, airborne noise from turbine blades and activities of construction and maintenance crafts, and high impact noise pulses from pile driving of steel mono pile foundations. This study focuses exclusively on the nearly continuous noise from fully operational wind turbines at various wind speeds.

Noise related impacts on marine mammals have been under investigation for years, but as the methodology is not standardized it is often difficult to compare studies. Four "zones of influence" on marine mammal behavior and hearing are typically considered; "the zone of audibility", "the zone of responsiveness", "the zone of masking" and "the zone of hearing loss, discomfort and injury". These zones are thoroughly described by Richardson et al. (1995). Even though the establishment of these four zones for different species and noise sources is not standardized, they have resulted in better and more uniform noise related impact assessments. The extension of the four zones are in their nature very different as they describes different aspects of the noise related influences, from the faintest sound that are just perceivable by the animal to immediately lethal underwater sounds and pressure waves. The spatial extension of the zones furthermore differs from species to species, from individual to individual and sometimes even for the same individual depending on the physical and behavioral status of the animal.

As a first cautionary approximation, the zone of audibility is often used as a measure of the potential impact on marine mammals from a noise source, even though being able to detect a noise source tells little about the true impact.

As this study is to be considered as a theoretical risk assessment, only the zone of audibility, or plainly the detection distance, is considered further in this paper.

Hearing and noise perception:

In order to compare broad band noise to an audiogram the noise level must be stated in “critical band levels”, describing sound power pr. critical bandwidth (as done by e.g. Erbe 2000) instead of using the standard expression of sound power pr. 1 Hz bands. If spectrum levels at a given frequency, say 200 Hz as the center frequency, are converted into critical band levels the spectrum level must be converted from dB re 1 $\mu\text{Pa}^2/\text{Hz}$ into dB re 1 $\mu\text{Pa}^2/46 \text{ Hz}$, where 46 Hz 1/3-octave bandwidth with a center frequency of 200 Hz

If critical bandwidths are not taken into account when comparing broad band noise measurements with hearing thresholds, large errors in the perceived noise levels, i.e. the numerical difference between the noise level and the hearing threshold, will occur. Varying critical bandwidths obviously affects the calculated zone of audibility and zone of masking. A narrow critical bandwidth, which is an adaptation to high-resolution frequency discrimination (Au 1993), will result in poor ability to detect broadband noise whereas wide critical bands enhance the sensitivity to broadband sounds.

Each time the critical bandwidth is halved the critical band level, and as such the perceived noise level, is lowered by 3 dB.

Although tested once for harbour seals (Terhune & Turnbull 1995), it is assumed in this study that the critical bandwidths for harbour seals and harbour porpoises are similar to those of related species (Terhune & Turnbull 1995, Terhune & Ronald 1995, Moore & Schustermann 1987, Johnson 1968, Au & Moore 1990, Johnson et al. 1989, Thomas et al. 1990). Harbour seal critical bandwidths are considered to be between 1/6 and 2/3 octaves wide, whereas harbour porpoise critical bandwidths are assumed to be between 1/12 and 2/3 octaves wide. In the following all calculations are based on 1/3-octave wide critical bandwidths, and as such all spectrum density levels are converted into Third Octave Levels (TOLs), dB re 1 $\mu\text{Pa}^2/(1/3\text{-octave})$, making the noise recordings directly comparable with the presented audiograms.

Methods:

Low frequency underwater noise (10Hz – 22 kHz) from 3 offshore wind turbines was recorded using standard digital DAT equipment. All recordings were analyzed as spectrum density levels (dB re 1 $\mu\text{Pa}^2/\text{Hz}$) on a Hewlett Packard 35670A spectrum analyzer and presented as TOL's. Subsequently noise levels were converted into source levels assuming cylindrical spreading, i.e. 3dB attenuation pr. doubling of distance.

Results:

Underwater noise source levels (TOLs) from the three offshore wind turbines are presented in figure 1, together with background noise levels and audiograms for harbour porpoises (Kastelein et al. 2002) and harbour seals (Kastak & Schustermann 1998). The audiograms below 250 Hz and 80 Hz are extrapolated data for harbour porpoises and

harbour seals respectively, as the hearing sensitivity for the two species has not been tested below these frequencies. Common to most marine and terrestrial mammals, is that the low frequency decline in hearing sensitivity is approximately 35 dB/decade (Stebbins 1983, Au 1993), why the harbour seal and harbour porpoise audiograms have been extrapolated according to these values.

The maximum perceived noise level for both species are found in figure 1C, indicated by hatched bars. The maximum perceived noise level for harbour seals is 37 dB, and 15 dB for harbour porpoises. Assuming cylindrical spreading these values corresponds to detection distances from the wind turbine of 5000 and 32 meters respectively.

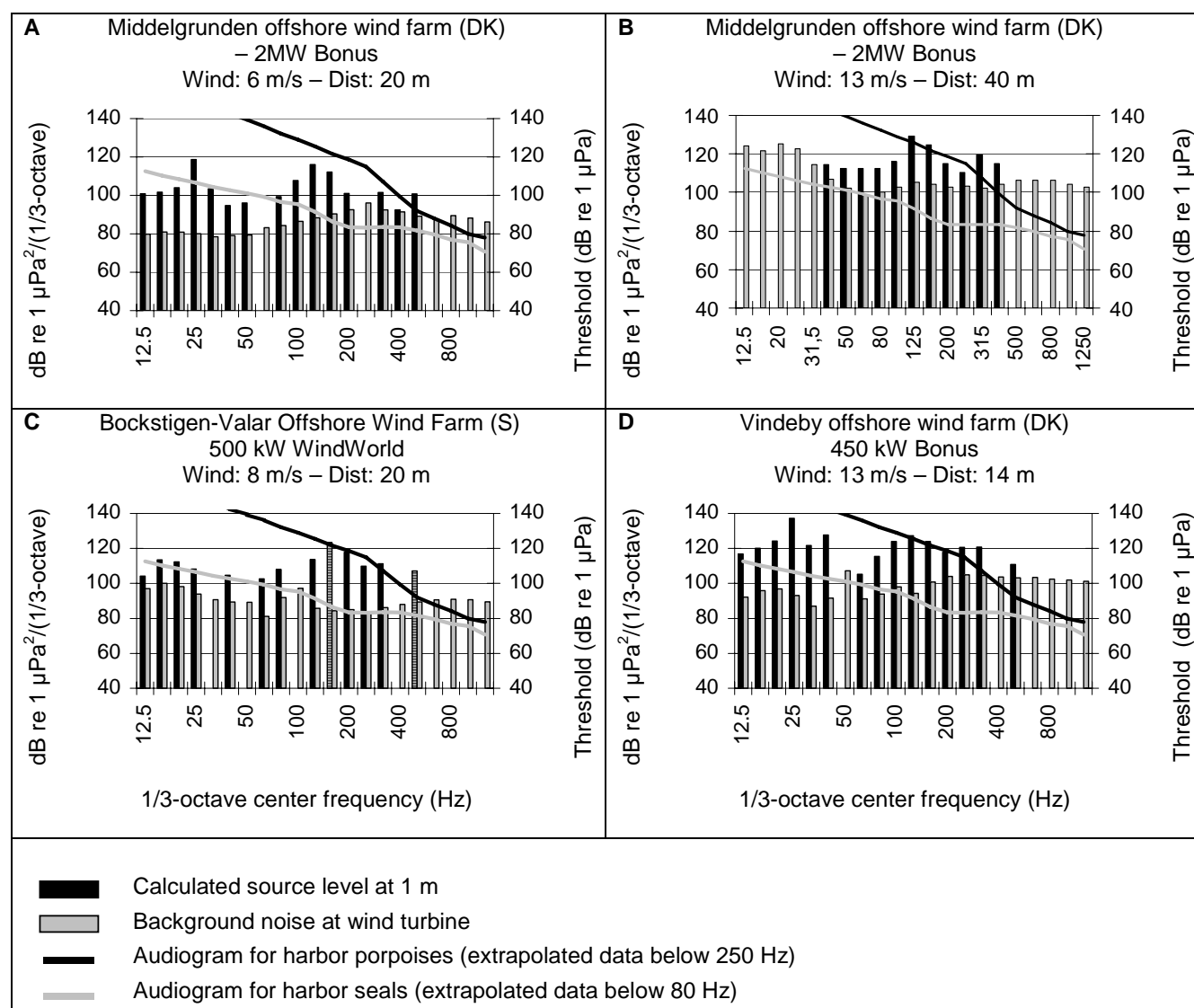


Figure 1 – audiograms for harbour seals and harbour porpoises shown together with underwater noise recordings from three different wind turbines.

The maximum perceived noise levels assuming different critical bandwidths are shown in Table 1 together with the corresponding detection distances.

Critical bandwidth	Zone of audibility				1/3 octave center frequency
	1/12 octave	1/6-octave	1/3-octave	2/3-octave	
Harbor seals	-	34 dB \cong 2500 meters	37 dB \cong 5000 meters	40 dB \cong 10000 meters	160 Hz *
Harbor porpoises	9 dB \cong 8 meters	12 dB \cong 16 meters	15 dB \cong 32 meters	18 dB \cong 63 meters	500 Hz

* the zone of audibility is limited by background noise rather than hearing threshold

Table 1 – perceived noise levels and detections distances related to different critical bandwidths.

Conclusively harbour seals will be able to detect the wind turbine noise above the background ocean noise at distances between 2.5 to 10 kilometers from the wind turbines, depending on the critical bandwidths in this frequency range, whereas harbour porpoises will be able to detect the noise on distances between 8-63 meters.

Conclusion:

Harbour porpoises are predicted to be able to detect underwater wind turbine noise within a radius between 8 and 63 meters from the wind turbine foundation. Due to the short detection range and the low perceived noise level, the wind turbine noise is not expected to have any direct negative effects on harbour porpoises.

Harbour seals, on the other hand, are predicted to be able to hear the wind turbine noise within a range of roughly 2,5 to 10 kilometres from a wind turbine, and the low frequency wind turbine noise has the potential to mask the seal's use of sound for foraging and communication and as such have much greater effects on harbour seals than on harbour porpoises. Common to both species, and any other marine mammal, is that wind turbine noise will most likely not induce any kind of temporary or permanent hearing damage.

References:

- Andrew,R.K., Howe,B.M. & Mercer,J.A. (2002) Ocean ambient sound: Comparing the 1960s with the 1960s for a reciever off the California cost. *ARLO*, **3**, 65-70.
- Au,W.W.L. (1993) *The sonar of dolphins*. Springer.
- Au,W.W.L. & Moore,P.W.B. (1990) Critical Ratio and Critical Bandwidth for the Atlantic Bottle-Nosed-Dolphin. *J.Acoust.Soc.Am*, **88**, 1635-1638.
- Erbe,C. & Farmer,D.M. (2000) A software model to estimate zones of impact on marine mammals around anthropogenic noise. *J.Acoust.Soc.Am*, **108**, 1327-1331.
- Johnson,C.S. (1968) Masked tonal tresholds in the bottlenosed porpoise. *J.Acoust.Soc.Am*, **44**, 965-967.

- Johnson,C.S., McManus,M.W. & Skaar,D. (1989) Masked tonal hearing thresholds in the beluga whale. *J.Acoust.Soc.Am*, **85**, 2651-2654.
- Kastak,D. & Schusterman,R.J. (1998) Low-frequency amphibious hearing in pinnipeds: Methods, measurements, noise, and ecology. *J.Acoust.Soc.Am*, **103**, 2216-2228.
- Kastelein,R.A., Bunskoek,P., Hagedoorn,M., Au,W.W.L. & de Haan,D. (2002) Audiogram of a harbor porpoise (*Phocoena phocoena*) measured with narrow-band frequency-modulated signals. *J.Acoust.Soc.Am*, **112**, 334-344.
- Moore,P.W.B. & Schusterman,R.J. (1987) Audiometric assessment of northern fur seals, *Callorhinus ursinus*. *Marine mammal science*, **3**, 31-53.
- Richardson,W.J., Greene,C.R., Malme,C.I. & Thomson,D.H. (1995) *Marine Mammals and Noise*. Academic Press.
- Ross,D. (1993) On ocean underwater ambient noise. *ARLO*, **18**, 5-8.
- Stebbins,W. (1983) *The acoustic sense of animals*. Harvard University Press.
- Terhune,J.M. & Ronald,A. (1975) Masked hearing thresholds of ringed seals. *J.Acoust.Soc.Am*, **58**, 515-516.
- Terhune,J.M. & Turnbull,S. (1995) Variation in the psychometric functions and hearing thresholds of a harbour seal. *Sensory systems of aquatic mammals* (eds R. Kastelein, J. A. Thomas & P. E. Nachtigal), De Spil Publishers.
- Thomas,J.A., Pawlovski,J.L. & Au,W.W.L. (1990) Masked hearing abilities in a false killer whale (*Pseudorca crassidens*). *Sensory abilities in cetaceans/Laboratory and field evidence* (eds J. A. Thomas & R. A. Kastelein), pp. 395-404. Plenum.

**First International Meeting
on
Wind Turbine Noise: Perspectives for Control
Berlin 17th and 18th October 2005**

***Trailing-Edge Noise Measurements
of Wind Turbine Airfoils
in Open and Closed Test Section Wind Tunnels***

A. Herrig, W. Würz, Th. Lutz, K. Braun and E. Krämer
*Institute of Aerodynamics and Gas Dynamics, University of Stuttgart,
Pfaffenwaldring 21, D-70550 Stuttgart, Germany
{herrig,wuerz, lutz, braun, kraemer}@iag.uni-stuttgart.de*

and

S. Oerlemans
*National Aerospace Laboratory NLR, Department of Helicopters and Aeroacoustics,
P.O. Box 153, 8300 AD Emmeloord, The Netherlands.
stefan@nlr.nl*

Summary

This paper describes two-dimensional trailing edge noise measurements in open and closed test section wind tunnels. The investigations are related to the EU-funded project SIROCCO, which aims to find quiet airfoils for wind turbines without a decrease in aerodynamic performance. Trailing edge noise measurements were performed in the open jet of the Aeroacoustic Wind Tunnel Braunschweig (AWB) using a phased microphone array. In addition, the trailing edge noise of the same models was measured in the closed section of the Laminar Wind Tunnel Stuttgart (LWT), using the new Coherent Particle Velocity (CPV) method. This method is based on the cross correlation of two hot-wire signals. The experimental results obtained in the two wind tunnels could be quantitatively compared after application of appropriate wind tunnel corrections. The sound pressure frequency spectra are basically parallel in the range of sufficient measurement accuracy. The total sound pressure levels vs. lift coefficient show a more or less constant offset of about 2 dB between AWB and LWT. Given the totally different measurement principles this can be regarded as a very good agreement.

1 Introduction

Turbulent Boundary-Layer Trailing-Edge (TBL-TE) interaction noise is the dominant far-field noise radiated from wind turbines for typical inflow conditions. Wind park acceptance and growingly strict regulations concerning noise emissions require a reduction of this noise. The aim of the EU-funded project SIROCCO is therefore to find new optimized airfoil contours, which provide a reduction of total sound pressure levels, but must not suffer from decreased aerodynamic performance. An overview of SIROCCO is given in [1].

Before application of the airfoils on wind turbines the aerodynamic and aeroacoustic characteristics have to be verified in two-dimensional wind tunnel tests.

Typically, acoustic measurements are performed in open test section wind tunnels with a surrounding anechoic room. Acoustic damping measures can be applied to nearly achieve free-field conditions without disturbing reflections of sound waves. Phased microphone array systems [2] are the established method, because the processing technique provides the possibility to locate noise sources and suppress background noise. Furthermore, a gain in signal-to-noise ratio (SNR) can be achieved by the large number of sensors. Microphone arrays have been successfully used in previous wind energy related projects DRAW [3] and DATA [4] for example. Therefore, array measurements were also chosen for the acoustic verification of the airfoils in SIROCCO.

Open-jet wind tunnels are not optimally suited for aerodynamic measurements, on the other hand. Measurements for the verification of aerodynamic performance must be performed in low turbulence closed test section wind tunnels. So a drawback of the combined aero-acoustic verification is that two wind tunnel campaigns are necessary and models have to suit two wind tunnels. The comparison of the obtained data is also complicated by the different aerodynamic boundary conditions.

Therefore, it is desirable to develop methods for acoustic measurements in closed test section wind tunnels. This can increase the consistency of the data. At the Institute of Aerodynamics and Gas Dynamics (IAG) of the University of Stuttgart a new hot-wire based method for the in-flow measurement of TE noise has been developed [5]. The method was used for supporting the enhancement of the aeroacoustic prediction code in SIROCCO.

In this paper trailing edge noise results from open jet and closed section wind tunnel tests will be compared. In Section 2 the experimental set-up in both wind tunnels is described, followed by some aerodynamic aspects of the measurements. In Section 3 the acoustic results for both wind tunnels are discussed and compared to each other. Example results are used of the work done for Gamesa Eólica from Spain. Two different airfoils are considered: the existing reference airfoil ('GAM') and a newly designed and aeroacoustically optimized new airfoil ('TL132').

2 Measurement techniques and experimental setups

2.1 Laminar Wind Tunnel

2.1.1 Aerodynamic measurements

The Laminar Wind Tunnel [6] of the Institute of Aerodynamics and Gas Dynamics (IAG) is of Eiffel type and has a closed test section of 0.73×2.73 m² and a maximum velocity of 90 m/s (Fig. 1). Its very low turbulence level of $Tu=0.02\%$ ($f=20$ -5000 Hz, 30 m/s) makes it ideal for laminar boundary layer measurements and investigations of sailplane airfoils. The models span the short distance of the test section vertically and the gaps to the walls are sealed (Fig. 2).

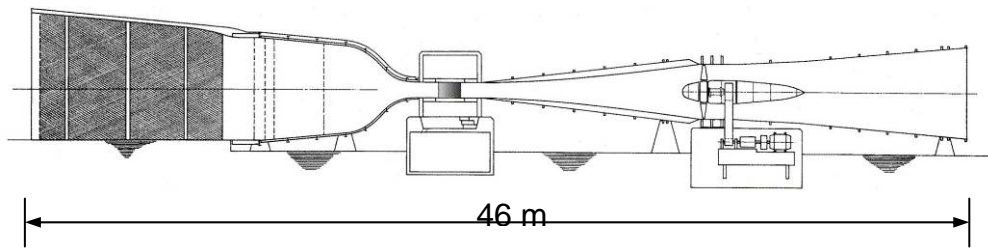


Fig. 1: Cross-section view of Laminar Wind Tunnel (LWT).



Fig. 2: The test section of the Laminar Wind Tunnel. The wake rake is located downstream of the model.

The aerodynamic verification measurements were carried out in the LWT. To be able to use the same wind tunnel models in the AWB, the SIROCCO models have a chord length of 400 mm and a span of 800 mm and a trailing edge thickness of 0.3 mm. The Reynolds number was fixed at $Re = 1.6 \times 10^6$. Lift is measured by experimental integration of the pressure distribution on the wind tunnel walls and drag is determined using an integrating wake rake. From the lift curves c_l - α and drag polars c_l - c_d lift coefficients and corresponding reference angles of attack which are used for the following detailed acoustic investigations were selected. Measurements of the transition position were performed using a stethoscope. The main focus of the measurements was not on the 'clean' configuration but the practically more important 'rough' case. For all tripped measurements 2D turbulator strips at $x/c=0.05$ were used. Several oil flow visualizations on the suction side of the airfoil sections were performed to visualize the extent of turbulent separation at the trailing edge.

Severe geometric and aerodynamic constraints were prescribed by the manufacturers to enable the implementation of the airfoils in existing turbine blades [19]. The aerodynamic verifications showed that the new airfoils fulfil these constraints and for tripped boundary layer even show better performance.

Despite the LWT is very well suited for aerodynamic measurements, it is a worst case scenario for acoustic measurements. The fan is located 12 m downstream in the diffuser and in straight line to the test section. No acoustic damping measures are applied. Due to the area relation between the location of the fan and the test section of 5.7:2 the total sound pressure in the test section is rather high. An overall sound pressure level of $L_p = 94$ dB(A) at 60 m/s was measured in-flow using a 1/2" B&K microphone with a nose cone (Fig. 3). The background noise has broadband character and most of the energy is concentrated in the low frequency range (Fig. 4). Special methods are required to measure airfoil trailing edge noise under such conditions, because it must be separated from the high background noise.

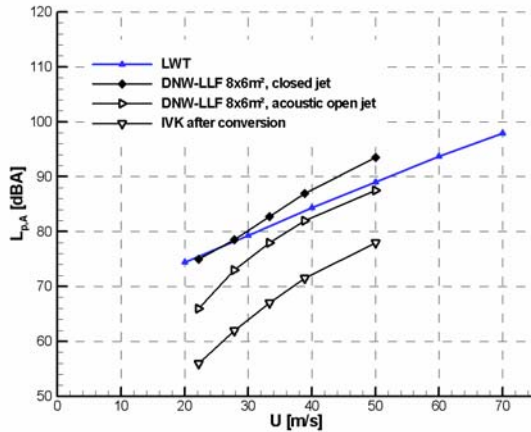


Fig. 3: A-weighted total background noise level of LWT compared to other European wind tunnels (data from [7]).

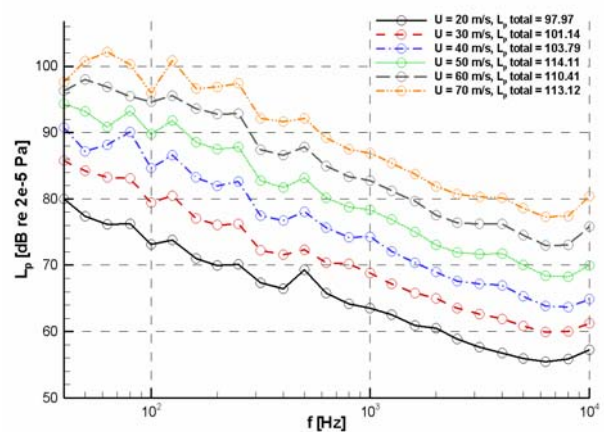


Fig. 4: Unweighted 3rd-octave sound pressure spectra of LWT background noise for different velocities.

2.1.2 Previous approaches for acoustic measurements

The development of acoustic measurement methods at the IAG was started by Guidati [8] in 1998. One of the first approaches for in-flow measurements was a wall-mounted array with random distribution of 72 microphones (Fig. 5). Standard algorithms for processing of the signals were applied (compare [9]). It turned out that measurements of airfoil trailing edge noise were not possible. The signal-to-noise ratio was poor because of the large source-sensor distances and turbulent boundary layer flow over the microphones. A special non-planar in-flow microphone array was finally developed solving these problems (Fig. 6). A total of 88 microphones are mounted in the stagnation point of the mounting struts and can be brought close to the source. The signals are sampled at 48 kHz using Σ - Δ -converters with 18 bit resolution. First measurements were performed on a symmetric NACA 0012 airfoil (Fig. 7). The comparison of the measurement results for the tripped and free transition case proves, that the measured noise is indeed radiated from the test model. But in the application on cambered sections problems arose, e.g. from the non-symmetric potential velocity field. The convection of sound waves causes propagation times deviating from the monopole source model (more refined Green functions have not been implemented up to now). The mismatch of the delayed signals reduces array spatial resolution and signal-to-noise ratio.

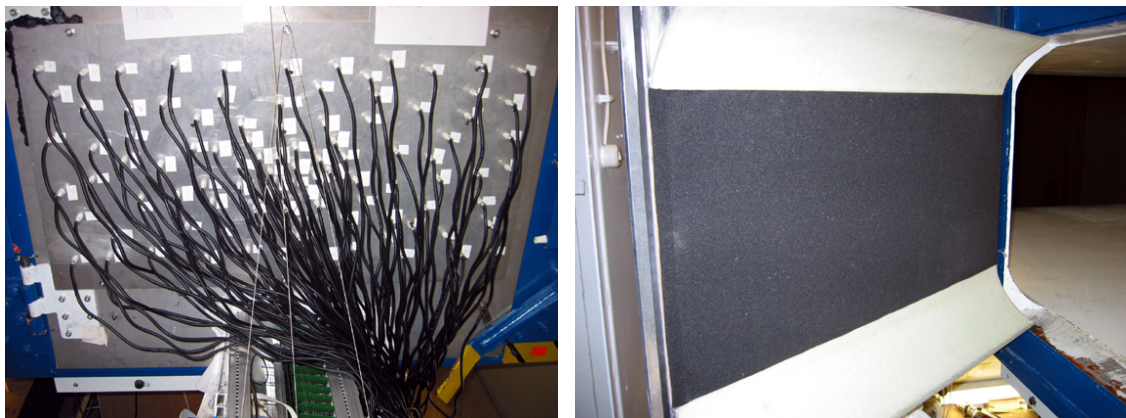


Fig. 5: Microphones of a wall array mounted in the LWT test section door seen from outside (left). The microphones were covered with open cell foam (right).

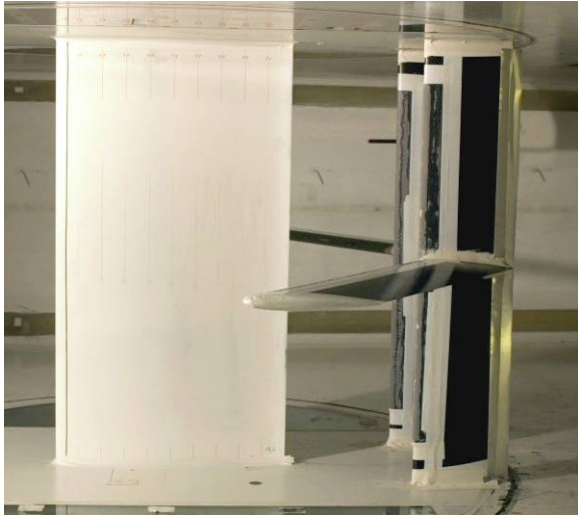


Fig. 6: In-flow array mounted downstream the GAM airfoil in the LWT.

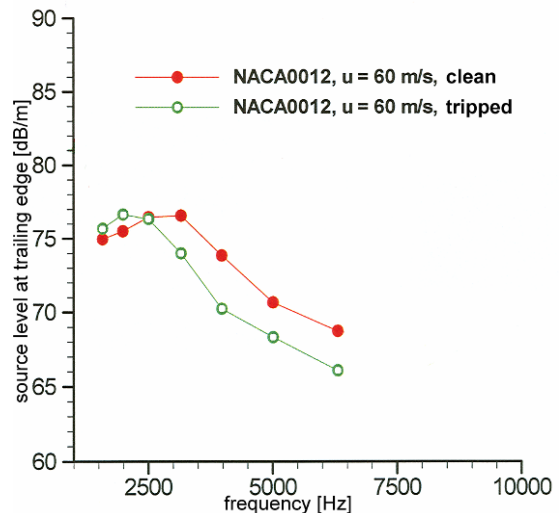


Fig. 7: Spectra of NACA 0012 measured with the in-flow array, $\alpha=0^\circ$ (from [8]).

2.1.3 Coherent Particle Velocity method

The aforementioned problems with the use of wall-mounted and inflow array systems gave motivation to develop an alternative method for in-flow acoustic measurements of trailing edge noise. Furthermore it was desired to extend the measurement range to low frequencies. The current solution is an experimental setup similar to the one chosen by Hutcheson and Brooks [10], who placed two microphones on both sides of the airfoil and calculated the cross-spectrum of sound pressure. With the new method the Coherent Particle Velocity (CPV) of the sound waves is measured directly, instead of the sound pressure.

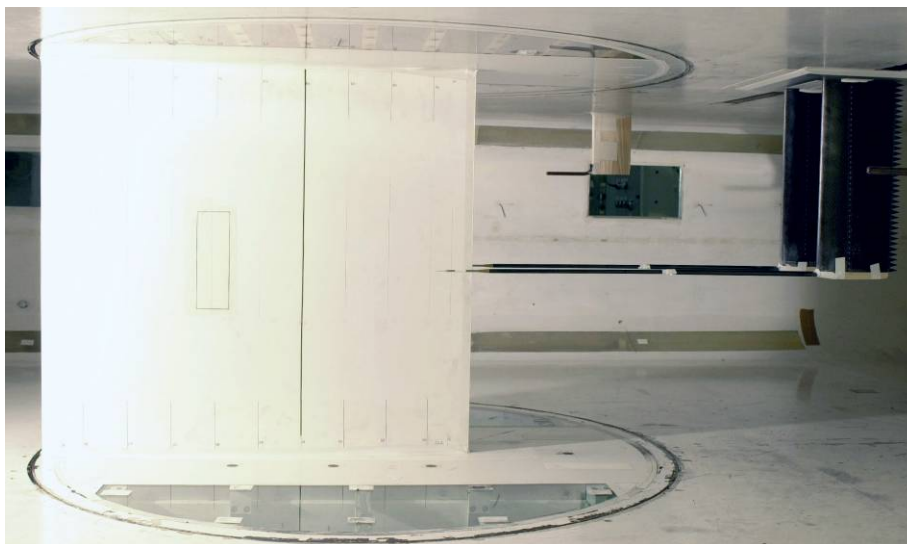


Fig. 8: The CPV-system mounted in the LWT downstream a wind tunnel model of 0.8 m chord.

Two 45 degree slanted hot-wires (Dantec P12) are placed in one plane vertical to the trailing edge and at a distance of $y = \pm 75\text{mm}$ (Fig. 8). The wires are mounted in front of carbon tubes with 0.7 m length, which are fixed to two streamlined struts. The wake of the model can pass between the struts. To improve the signal-to-noise ratio (SNR) $2.5\mu\text{m}$ wires are used instead of standard $5\mu\text{m}$ wires. The AC-signals of the Dantec 55M10 CTA-bridges are amplified by AMI-321A low-noise amplifiers ($1\text{nV}/\text{Hz}^{1/2}$ eqv. input noise) with rates of 1,000. A 200 Hz high-pass filter was used to improve the

dynamic range. Final AD-conversion is done by a 24 bit audio-system (RME Multiface DSP) at a sampling rate of 44.1 kHz per channel. The Σ - Δ converters with 64 times over-sampling provide excellent anti-aliasing filtering at half the data rate. Typically continuous time traces of 10min are recorded and then processed by 4096 point Fast Fourier Transforms yielding a frequency resolution of 10.78 Hz. The cross correlation spectrum is calculated from the Fourier coefficients of the two simultaneous streams A, B and averaged over the whole record length of $n \approx 6500$ blocks:

$$\bar{G}_{AB}(f) = \frac{1}{n} \sum_{k=1}^n [\bar{X}_{Ak}^*(f) \bar{X}_{Bk}(f)]. \quad (1)$$

The phase difference $\varphi_{AB}(f) = \arctan[\text{Im}(G_{AB})/\text{Re}(G_{AB})]$ is obtained from the cross spectrum. It is known, that the sound pressure (and particle velocity) radiated from the trailing edge have opposite signs on opposite airfoil sides. So the phase relation delivers the desired information in which frequency range airfoil noise is higher than background noise and can therefore be measured. With a symmetric setup exactly 180° phase shift are expected.

The strongly anisotropic directional sensitivity of the hot-wires is exploited to improve the SNR of the measurements. This is a very important difference to using microphones, because in this way a large part of background noise and possible corner noise from the model are suppressed. Tests had failed to reproduce the measurements using B&K microphones with nose cone in the same setup. The phase shows irregular behaviour indicating that other noise sources mask the TE noise.

Calibration of the hot-wires is done in-situ by variation of the tunnel speed U and approximation of $\partial U/\partial E$ from the hot-wire mean voltage changes ΔE recorded simultaneously. The derivatives are evaluated from the fitted polynomials of second order. Fig. 9 shows an example. This procedure improved the accuracy in $\partial U/\partial E$ to about 0.1 dB. The airfoil potential velocity at the hot-wire position is obtained from a panel code and taken into account.

To obtain quantitative values of sound pressure the TE line source is simulated by incoherent monopoles (Fig. 10). This means the conversion from particle velocity v to sound pressure p is given by the radial impedance

$$p = Z_R v = \rho_0 c_0 / (1 - \frac{ic_0}{\omega r}) v. \quad (2)$$

The convection of the sound waves causes a retardation of the effective hot-wire position, which is also taken into account. The results are finally given as the sound pressure level L_P (dB re 20 μ Pa) produced by a trailing edge of $L=1$ m at a distance of $r=1$ m and an observer placed at an angle of 90° to the airfoil chord. Anisotropic directivity of the TE noise might introduce uncertainties in the obtained levels. In the limit of $\omega \rightarrow 0$ the directivity of a compact dipole source is expected and for $\omega \rightarrow \infty$ the directivity should approach a cardioid [11]. From refined theory [12] frequency dependend 'finger-like' directivity functions with multiple lobes are expected due to multiple scattering for the frequency range in between. First experiments had indicated that the directivity of L_P measured on a flat plate like airfoil with $c=0.5$ m corresponds to the isotropic monopole directivity quite well [5], therefore detailed corrections for the source directivity are currently not performed.

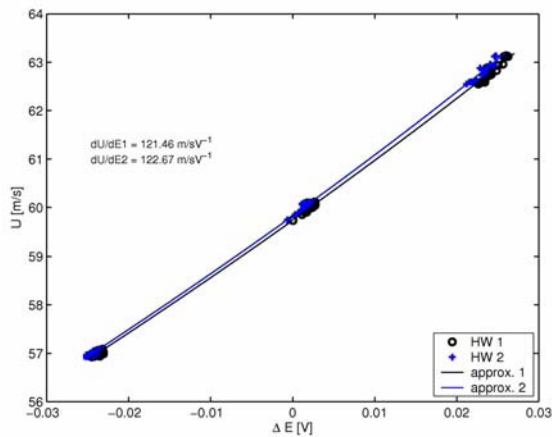


Fig. 9: Variation of hot-wire voltage with mean velocity. The derivatives are evaluated from the fitted polynomials of second order.

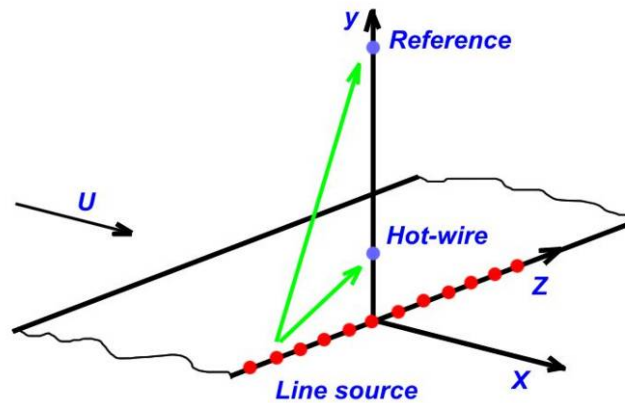


Fig. 10: Conversion of the measured sound pressure to the reference position by simulation of a line source.

2.2 Aeroacoustic Wind Tunnel Braunschweig

Acoustic verification measurements of the SIROCCO airfoils were performed in the Aeroacoustic Wind Tunnel Braunschweig (AWB). The maximum flow velocity is about 60 m/s, the turbulence level is significantly higher than in the LWT and not exactly specified. In contrast to the LWT the AWB is a closed return open-jet tunnel with a rectangular nozzle of 1.20x0.80 m² and a surrounding anechoic test chamber. Besides the low background noise level this makes it possible to achieve nearly free-field conditions without disturbing reflections of sound waves.

The wind tunnel models are mounted horizontally between two endplates coated with open cell foam for reducing acoustic reflections. Fig. 11 shows the nozzle of the AWB and the GAMESA airfoil mounted in the test section with the acoustic array of the NLR below the model. Note that the results in the present paper were obtained with the array above the test section (on the suction side of the airfoil). The 1 m diameter array consisted of 96 microphones in an open metal grid. The phased array processing was similar to Ref. 13, and resulted in 1/3-octave band spectra of the trailing edge noise radiated from the central 0.2 m of the model span. Special measures were taken to physically reduce extraneous noise sources at the model-endplate junctions. In some cases, extraneous noise from these junctions influenced the measured TE noise levels. Therefore, a routine was used which automatically determines the importance of these 'corner sources' and which, in case the influence of the corner sources on the trailing edge noise level is more than 0.5 dB, calculates an upper limit for the actual 2D trailing edge noise level.

Prior to the array measurements a lift balance was used for the determination of lift curves and subsequently of the reference angles of attack. With the balance installed a gap was remaining between the endplates and the model. To achieve reproducible conditions, these gaps were sealed with soft adhesive tape. Transition location checks and oil flow visualizations were performed similar to the investigations at the LWT.

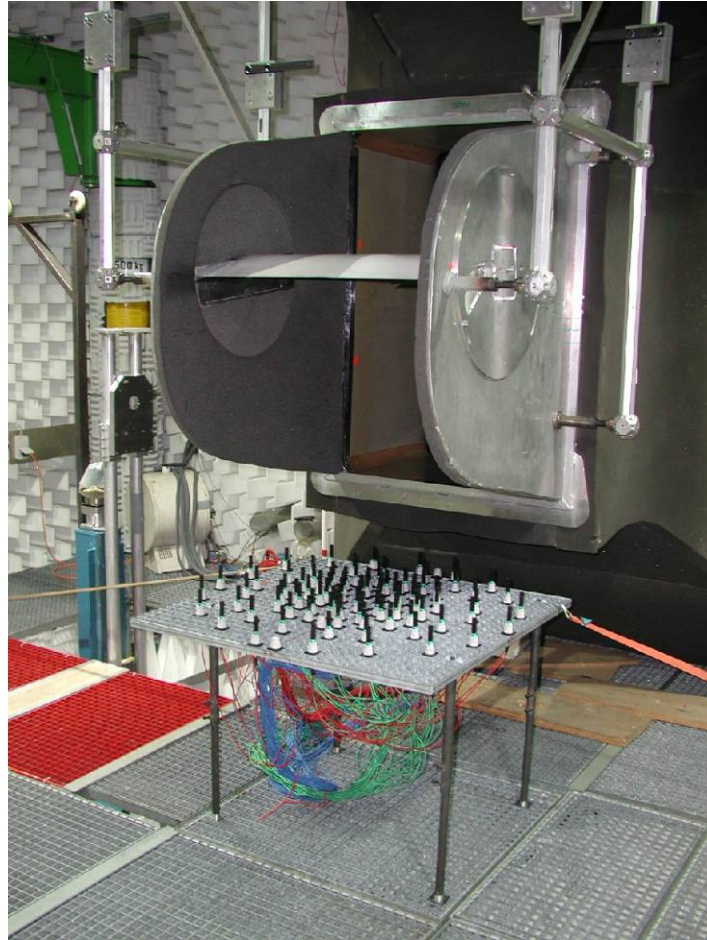


Fig. 11: The GAMESA reference airfoil mounted in the test section of the Acoustic Wind Tunnel Braunschweig. The lift balance is removed and the acoustic array is installed below the model.

2.3 Wind tunnel corrections

It is commonly accepted that comparisons of airfoil TE noise spectra should be performed on the basis of equal lift coefficients to be representative. In the LWT the aerodynamic coefficients are by default corrected for streamline curvature (SC) and solid blockage to represent values that would be obtained in an infinite flow field (IFF). The corrections are in the order of 1-2%. For open-jet wind tunnels much larger SC corrections are necessary, because the air stream is deflected by the airfoil and therefore the effective airfoil shape changes quite significantly. Depending on the ratio of chord length and jet dimensions, the same lift coefficient $c_{l,t}$ as in the IFF is reached at a much higher geometric angle-of-attack (AOA) α_t . Typically, correction terms are applied only to α_t to obtain the AOA of equivalent lift α [14]. But in order to achieve exact equivalence of the c_p pressure distributions between the open-jet and IFF quite large deviations in the airfoil contour itself would be required (compare [15]).

Fig. 13 shows lift curves of the Gamesa airfoil measured in LWT and AWB (symbols). It is apparent, that the slope is reduced to half the IFF value in the AWB. It was also found that for equal lift coefficient, the transition location in the AWB was more upstream than in the LWT. The influence of the higher turbulence level is assumed to be relatively small, because close to $c_L=0$ the transition locations are quite similar. Therefore for higher lift coefficients this means that the pressure distributions must be very different. For equal transition locations, the lift coefficient is lower in the AWB than in the LWT (Fig. 15). For the higher AOA's for some airfoils

more trip strips had to be applied on the lower surface than in the LWT in order to achieve boundary layer transition. Both this and the fact that separation was occurring significantly more forward on the upper surface (Fig. 14) also gave rise to the presumption, that wind tunnel corrections need to be applied which also act on the lift coefficient (in contrast to [14]).

In order to obtain a good comparison between two wind tunnels, the c_p pressure distributions should match as close as possible, because the aerodynamic as well as aeroacoustic behaviour is strongly influenced by even small details in this distribution. Therefore the influence of the open jet was investigated in more detail using MSES [16]. MSES solves the coupled Euler and boundary layer equations by a Newton scheme. Constant pressure along the upper and lower grid boundaries can be forced to represent a free jet. The transverse grid dimensions were chosen as in the experiment. The resulting lift curve (Fig. 13, orange) corresponds to the AWB already quite good, but there is still a too steep lift slope. The reason is the induction of a downwash at the airfoil position due to the wake circulation developing downstream of the endplates is not considered in MSES. This changes the effective angle of attack and reduces the lift. An equation for the lift slope of a ‘clipped’ horseshoe vortex (Fig. 12) was derived based on the principle of Pistoiesi [17]. It is assumed, that the shear between the jet and the surrounding air corresponds to vortices having the same circulation as the bounded vortex at quarter chord and that they start at the endplates. Using this approximation, the corrected lift curve matches the experiments (Fig. 13, red line).

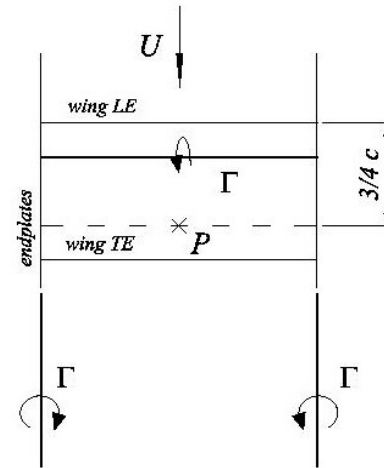


Fig. 12: Vortex system for calculation of lift slope. The wake vortices begin downstream the endplates

When comparing the MSES calculated pressure distributions of open-jet and IFF it is found that complete equivalence cannot be achieved with the same airfoil contour, even for only one angle of attack. But the slopes $\partial c_p / \partial x$ agree fairly well for a c_L reduction of about $\Delta c_L / c_L = 0.17$. That is also the amount the calculated open-jet transition curves are scaled down compared to the IFF curves. Additionally correcting this for the downwash, the agreement with the larger relative downshift of $\Delta c_L / c_L = 0.25$ observed in the measurements (Fig. 15) is very good.

Thus to summarize, when the trailing edge noise results from the AWB are compared to those from the LWT, lower lift coefficients have to be used for the AWB, to account for the open jet effect on the pressure distribution. Using a correct reduction, the pressure gradients are nearly the same and the transition locations are similar in both tunnels. This results in boundary layer states at the trailing edge, which correspond to each other reasonably.

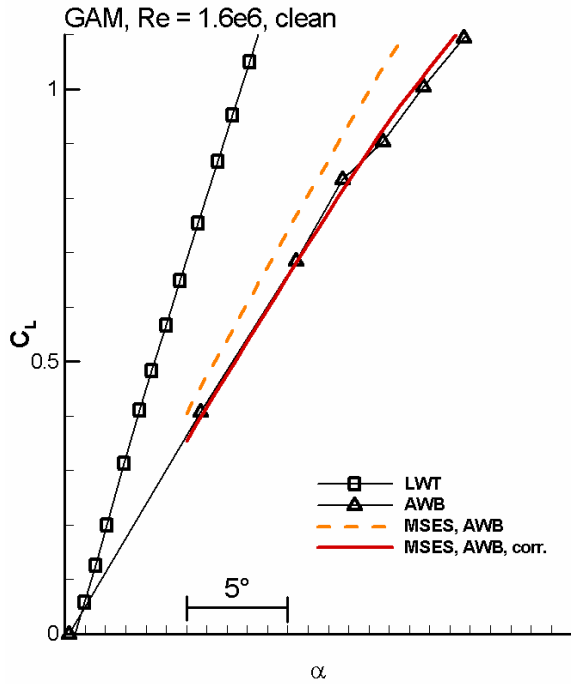


Fig. 13: Comparison of lift curves measured in LWT (IFF) and AWB (open jet) as well as MSES calculations.

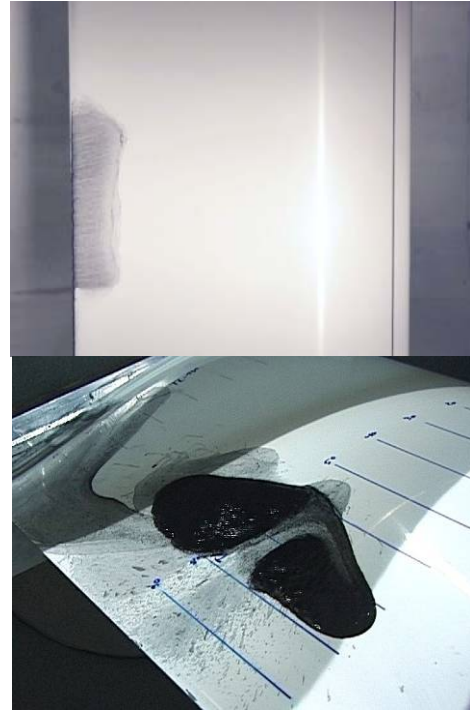


Fig. 14: For the same lift coefficient ($c_L \approx 0.9c_{L,max}$), the airfoil shows negligible turbulent separation in the LWT (above), but significant recirculation in the AWB (below). $U \leftarrow$

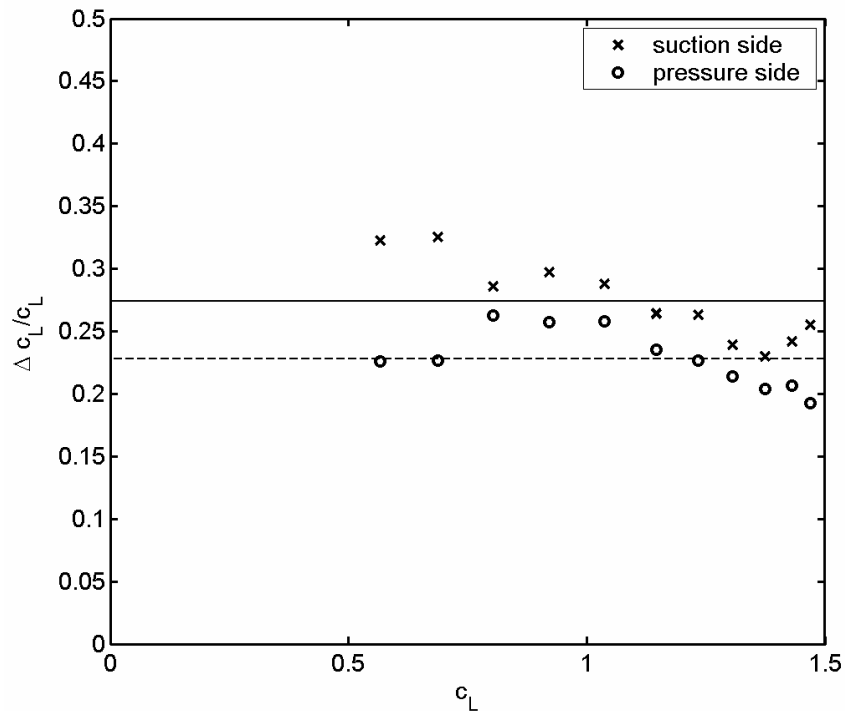


Fig. 15: The normalized shift in the transition curve (measured data) shows nearly constant values. The lines indicate the mean values for suction and pressure side.

3 Analysis and discussion of results

In this section the acoustic results of the AWB and LWT measurements are first discussed separately (Sections 3.1 and 3.2 respectively), followed by a comparison between the two (Section 3.3).

3.1 AWB results

Typical examples of acoustic source plots showing trailing edge noise are given in Fig. 16. These plots clearly show broadband noise radiation from the trailing edge. The resolution increases with frequency due to the decreasing acoustic wavelength. The acoustic source plots were further processed to trailing edge noise spectra. The trailing edge noise spectra for the clean and tripped GAMESA baseline airfoil at several lift coefficients are given in Fig. 17. In these graphs an open marker indicates an upper limit for the actual trailing edge noise (see Section 2.2). The tripped results show smooth broadband trailing edge noise spectra. For increasing angle-of-attack, the levels increase at low frequencies and decrease at higher frequencies. This shift to lower frequencies can be understood from the increased boundary layer thickness on the suction side. The results for the clean condition are less regular, due to the fact that the location of the boundary layer transition is not fixed. Tones do not occur for any airfoil or angle-of-attack, and generally the clean airfoils are quieter than the tripped ones.

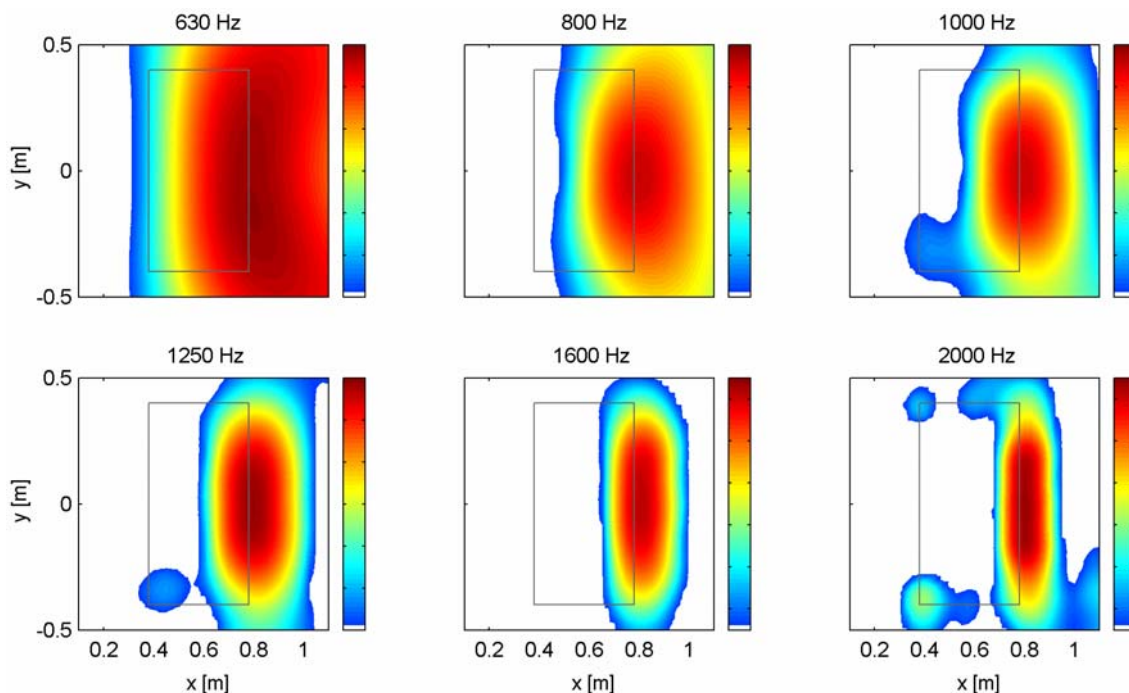


Fig. 16: Typical example of acoustic source plot showing trailing edge noise. The airfoil contour is indicated by the grey line, flow goes from left to right. The range of the color scale is 12 dB.

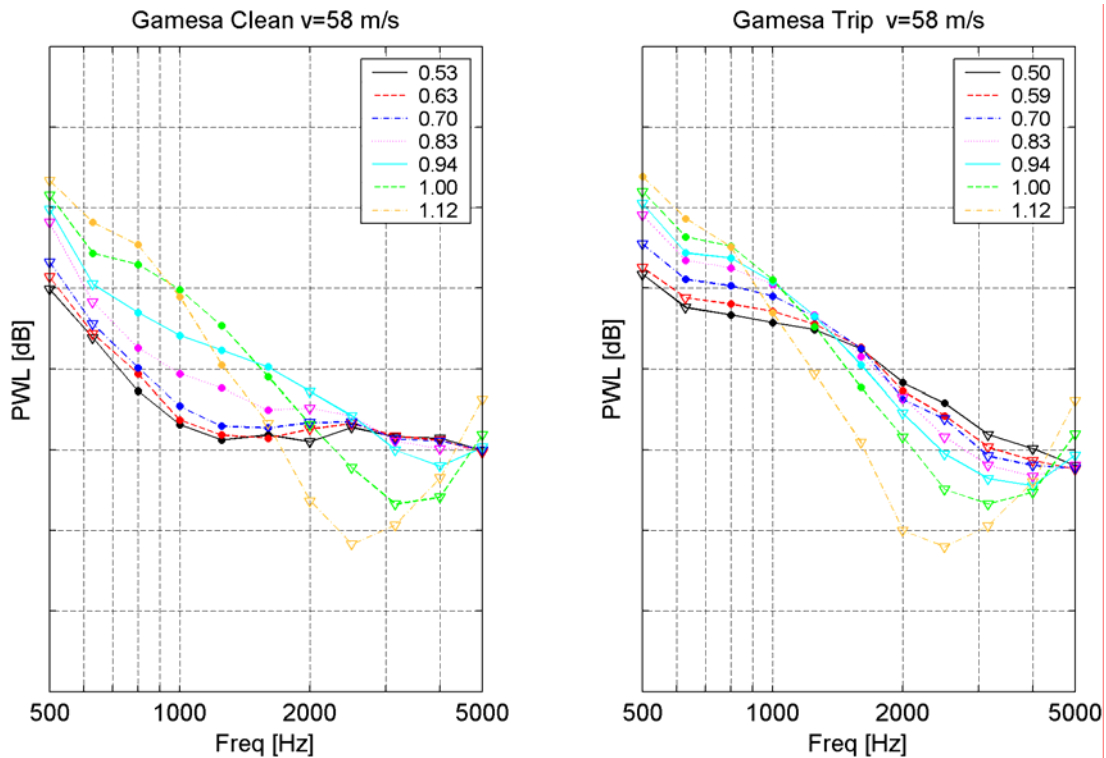


Fig. 17: Trailing edge noise spectra for the GAMESA airfoil. The values of the lift coefficient are given in the caption. The range of the y-axis is 40 dB (5 dB/division).

3.2 LWT results

All airfoils show smooth spectra similar to the tripped Gamesa airfoil at a lift coefficient of 1.0 shown in Fig. 18 (upper plot). Tonal BTE noise and laminar boundary-layer vortex-shedding noise are not found. The few peaks in the CPV spectra seem to result from vibrations of the hot-wires. Depending on the welding points and temperature they sometimes occurred. With reduction of frequency the levels rise strongly and the airfoil noise gets masked by the background noise from the tunnel. At high frequencies there is an increase of electronic noise because of hot-wire thermal noise amplified by the bridge amplifier. The signals are getting more incoherent here, which can be seen from the level difference between the single spectra (G_1 , G_2) and the cross spectrum G_{12} , as well as the random phase.

Completely incoherent noise is reduced by averaging proportional to $1/\sqrt{n}$, with n the number of averages (typically 6500). Assuming that all noise is incoherent, a signal-to-noise ratio can be approximated according to $SNR = 10 \cdot \lg(\gamma\sqrt{n})$ with $\gamma^2 = G_{12}^2 / G_1 G_2$ being the coherence squared (lower plot in Fig. 18). In the plot of the phase difference between the two sensor signals four ranges can be identified:

- a) Up to about 300 Hz the phase tends to zero. Coherent background noise from downstream dominates.
- b) From 300 to 600 Hz tunnel background noise seems to be higher than the airfoil noise. The phase shows some fluctuations, but the SNR is high as indicated in Fig. 18. Reflected sound waves and/or boundary layer vortices seem to cause this behaviour and the reason is not fully understood, yet.
- c) Above 600 Hz, the TE noise dominates the signals and can be measured reliably. The phase shows the expected 180° behaviour, the slope to higher frequencies is caused by a time shift of noise due to a slight asymmetry of the setup and a stronger

convection on the suction side.

d) The upper bound of the useful measurement range is given by the loss of SNR at about 3 kHz. It is possible to increase this upper bound by longer averaging. In contrast the lower bound does not change then, it depends on the setup and the coherent background noise of the tunnel.

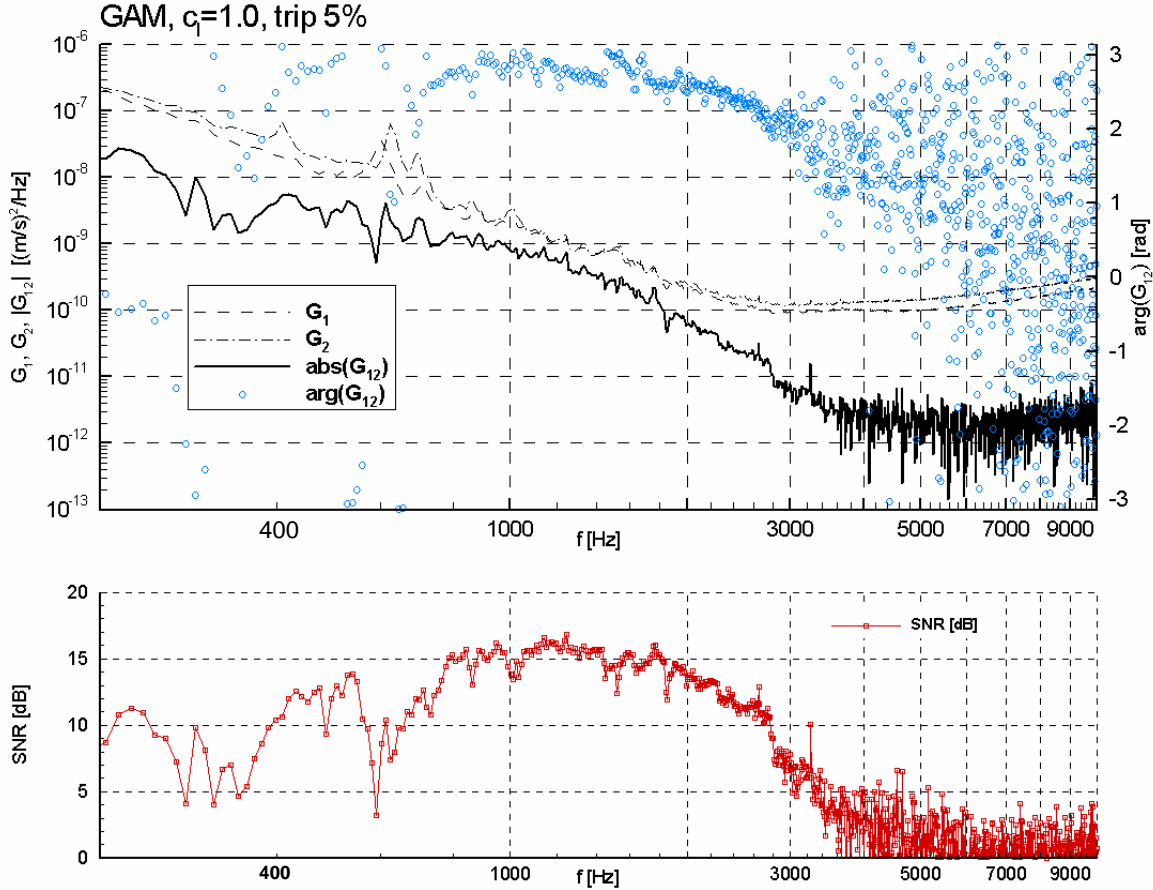


Fig. 18: Single and cross-spectra of particle velocity (above). The signal-to-noise-ratio (below) together with the phase information indicates the region of reliable values (600-3000 Hz).

From the narrow-band cross spectra third-octave spectra of sound pressure level are calculated by energetic summation. Based on the phase distribution a criterion was established to ensure that only valid data points are accepted.

3.3 Comparison of LWT and AWB measurements

For comparison of the results of both tunnels, the AWB values are converted to LWT results for convenience. As the AWB results are given as sound power levels PWL (equals the monopole sound pressure level in a distance of $1/\sqrt{4\pi}$ m) for a trailing edge segment of 0.2 m length, the re-scaling is as follows:

$$L_p = PWL - 20 \cdot \lg \frac{r_2}{r_1} + 10 \cdot \lg \frac{l_2}{l_1} + 50 \cdot \lg \frac{U_2}{U_1} = PWL - 3.26 \text{ dB} \quad (3)$$

The TBL-TE noise is incoherent, therefore $L_p \sim \sqrt{l}$. The last term is to correct the small difference in tunnel velocity (in the AWB the velocity was 58 m/s, in the LWT 60 m/s). From theory [18] a Ma^5 dependence is expected for the non-compact frequency range, but as the boundary layer properties depend on the Reynolds

number, lower values are often found in practice. For the AWB tests, 5 turned out to be a very good value for the exponent that matches the spectra of 50 and 58 m/s.

When comparing the third-octave spectra obtained in both wind tunnels (Fig. 19), lower test lift coefficients for the AWB have been used, to account for the open-jet effect on the pressure distribution and the wake influence (see section 2.3). The general similarity of the spectra is surprisingly good. In the high-frequency region where the measurement certainty is good, only small differences exist. In the low frequency region the values differ a bit more, which is probably due to effects of the measurement techniques. The CPV values tend to lower values when an additional coherent signal with opposed phase exists (mainly the fan noise).

The total sound pressure levels of the two airfoils obtained in AWB and LWT are compared in Fig. 20. The values are obtained by summation in the measurable frequency range. The minimum frequency for summation is indicated at the data points. As the peak frequency depends strongly on the angle of attack, the integration must be started at the appropriate lower frequencies for every lift coefficient. When calculating total levels, the inclusion of the third-octave band where the maximum level occurs is very important to get meaningful values (this is illustrated in [19]). Lower frequency bands where the SPL is decreasing again have only small further effects. For the CPV-method, missing third-octave band levels were linearly interpolated in the dB scale.

With the new TL132 airfoil a reduction of 1-1.5 dB is obtained for tripped boundary layer in both wind tunnels. Larger reductions only seem possible without the strong geometric and aerodynamic constraints that were prescribed by the manufacturer.

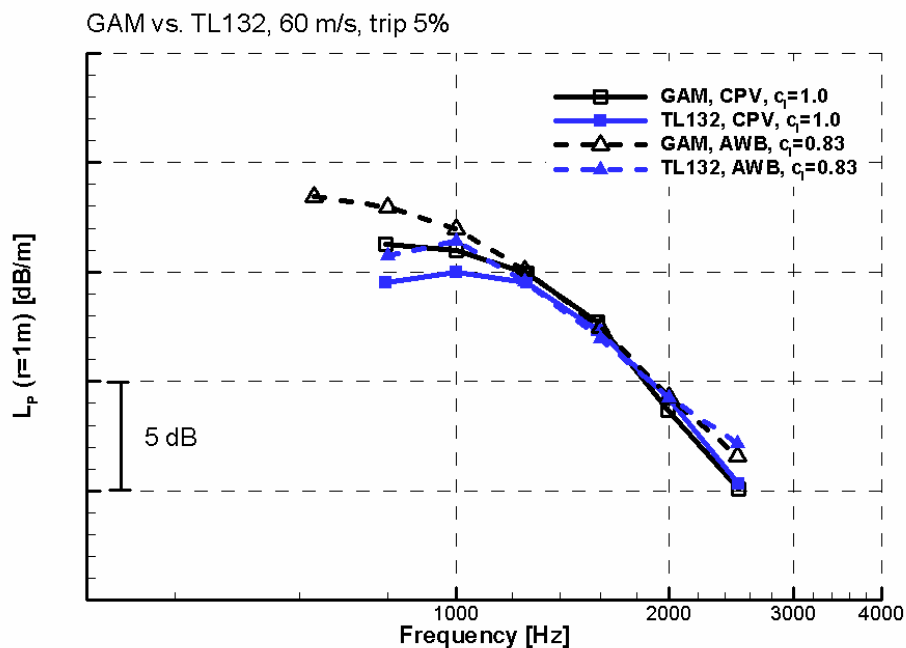


Fig. 19: Comparison of third-octave sound pressure spectra obtained in LWT and AWB for the GAM and TL132 airfoils.

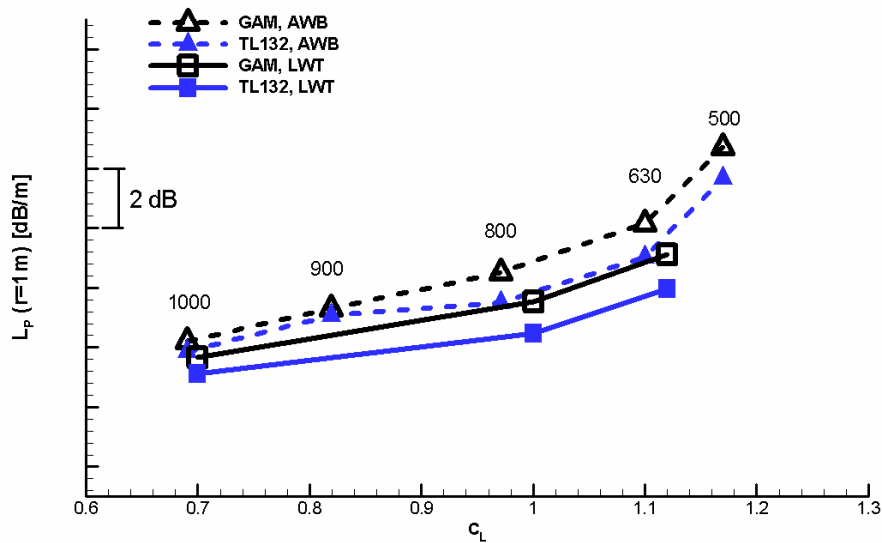


Fig. 20: Total SPL polars for the tripped GAM and TL132 airfoils. The lower frequency bound for starting the integration is denoted at the labels. The AWB c_L 's have been scaled down to represent IFF values.

4 Conclusions and Outlook

Two-dimensional trailing edge noise measurements were carried out in open and closed test section wind tunnels. The measurements were performed in the frame of the EU-funded project SIROCCO, which aims to find quiet airfoils for wind turbines without a decrease in aerodynamic performance.

In the open-jet AWB wind tunnel a phased microphone array was used, while in the closed test section of the LWT wind tunnel the new Coherent Particle Velocity method was applied. The 1/3-octave SPL spectra obtained with both methods are similar in the frequency range of 800-2000 Hz. The absolute total SPL's agree very well, when appropriate open-jet wind-tunnel corrections for lift coefficient and angle of attack are applied. The noise reduction achieved with the new TL132 airfoil is in the order of 1-1.5 dB(A) for tripped boundary layer state. A higher reduction was not possible for this particular airfoil because of the severe geometric and aerodynamic constraints and the already good aeroacoustic behaviour of the reference airfoil.

Given the good agreement of the results, the CPV-method will be used in the near future for the verification of optimized airfoils for GE Wind Energy. Besides a reduction of the costs this allows an increase of the consistency of the data, because only one wind tunnel campaign is necessary. Furthermore, measurements at a higher Reynolds number being closer to operational conditions are considered.

5 Acknowledgements

This research project is supported by the European Commission's Fifth Framework Programme, project reference: ENK5-CT-2002-00702 SIROCCO, Silent Rotors by Acoustic Optimisation. The authors would also like to thank Gamesa Eólica for the permission to publish selected results.

References

- [1] Schepers, J.G. et al.: *SIROCCO: Silent Rotors by Acoustic Optimisation*, First International Meeting on Wind Turbine Noise: Perspectives for Control", Berlin, 17-18 October 2005
- [2] Mueller, T.J.: *Aeroacoustic Measurements*, Springer-Verlag Berlin, 2002
- [3] DRAW: Development and Testing of design tools for reduced aerodynamic noise wind turbines, European Commission, JOUL III, JOR3-CT95-0083
- [4] DATA, Design and Testing of Acoustically Optimized Airfoils for Wind Turbines, Non-Nuclear Energy Program, European Commission, JOR3-CT98-0248
- [5] WÜRZ, W.; GUIDATI, S.; HERRIG, A.; LUTZ, T.; WAGNER, S.: Measurement of Trailing Edge Noise by a Coherent Particle Velocimetry Method. ICMAR Novosibirsk, 28.06.-02.07. 2004
- [6] WORTMANN, F. X.; ALTHAUS, D.: Der Laminarwindkanal des Instituts für Aero- und Gasdynamik an der Technischen Hochschule Stuttgart. In: *Zeitschrift für Flugwissenschaften* 12 (1964), April, Nr. 4, S. 129–134
- [7] R. Küstner, J. Potthoff, U. Essers: The Aero-Acoustic Wind Tunnel of Stuttgart University, SAE Tech. Paper 950625, Int. Congress and Exp. Detroit, 1995.
- [8] S. Guidati: "Entwicklung eines akustischen Messsystems für aerodynamisch optimierte Windkanäle", Ph.D. Thesis, University of Stuttgart, 2004.
- [9] D.H. Johnson, D.E. Dudgeon: "Array Signal Processing – Concepts and Techniques", Prentice-Hall, NJ, 1993
- [10] HUTCHESON, F.V., BROOKS, T.F.: Measurement of Trailing Edge Noise Using Directional Array and Coherent Power Methods. In: *Proceedings of 8th AIAA/CEAS Aeroacoustics Conference*, 2002 (AIAA paper 2002-2472)
- [11] W. K. Blake: *Mechanics of Flow-Induced Sound and Vibration*, Volume II, Complex Flow-Structure Interactions, Applied Mathematics and Mechanics Volume 17-II
- [12] M. S. Howe: "Edge-Source Acoustic Green's Function for an Airfoil of Arbitrary Chord, with Application to Trailing-Edge Noise", *Quarterly Journal of Mechanics and Applied Mathematics* 54 (1) pp. 139-155, Feb. 2001.
- [13] S. Oerlemans and P. Migliore: "Aeroacoustic Wind Tunnel Tests of Wind Turbine Airfoils", AIAA paper 2004-3042, 2004.
- [14] M. Gaunaa, P. Fuglsang, C. Bak and I. Antoniou: "Open-Jet Wind Tunnel Validation Using a NACA 0012 Airfoil", in "The Science of Making Torque from Wind", pp. 37-48, Delft University of Technology, The Netherlands, April 2004.
- [15] Thomas F. Brooks, Michael A. Marcolini and Dennis S. Pope: "Airfoil Trailing-Edge Flow Measurements", *AIAA Journal* 24 (8) pp. 1245-1251 (1986).
- [16] DRELA, M.: *Newton Solution of Coupled Viscous/Inviscid Multielement Airfoil Flows*. AIAA 21st Fluid Dynamics, Plasma Dynamics, and Lasers Conference. 1990. – AIAA 90-1470
- [17] E. Pistolesi: "Betrachtungen über die gegenseitige Beeinflussung von Tragflügelssystemen", Hauptversammlung der Lilienthal-Gesellschaft, Berlin, 1937
- [18] J.E. Ffowcs Williams and L.H. Hall: "Aerodynamic Sound Generation by Turbulent Flow in the Vicinity of a Scattering Half Plane", *Journal of Fluid Mechanics* 40 pp. 657-670 (1970).
- [19] T. Lutz; A. Herrig; W. Würz, K. Braun, E. Krämer: Constrained Aerodynamic & Aeroacoustic Design of Wind-Rotor Airfoils, First International Meeting on Wind Turbine Noise: Perspectives for Control", Berlin, 17-18 October 2005

**First International Meeting
on
Wind Turbine Noise: Perspectives for Control
Berlin 17th and 18th October 2005**

A Review of Wind Turbine Noise

Helmut Klug, DEWI
Deutsches Windenergie-Institut GmbH Ebertstr. 96
D-26382 Wilhelmshaven – Germany

h.klug@dewi.de

1 INTRODUCTION

In many countries the noise radiation is still the major limitation in the tremendous development of wind energy over the last years. New designs resulted in considerable noise reductions of both aerodynamic noise from the blades and machinery noise. The sound power levels of variable speed machines can be adjusted even after they have been put into operation and after the sound pressure levels at the nearest dwellings have been verified.

Some national codes work with absolute noise limits, while in some other countries the limits are based on the ambient noise. The nature of the wind turbine noise and the wind induced background noise are very important for defining masking criteria.

The national codes for noise regulations have to be consistent with the international standards of measuring the wind turbine noise including the assessment of tonality and the standards for noise propagation.

The IEC standard 61400-11 Wind Turbines – Part 11 ‚Acoustic Noise Measurement Techniques‘ was revised recently in order to present a procedure expected to provide accurate results that can be replicated by others. Immission measurements are not within the scope of this IEC standard. The different measurement procedures of noise immission from wind turbines at noise receptor locations are described in an IEA Recommendation.

In this general review the history and the state of the art of wind turbine noise is given with special emphasis on:

- Noise sources
- Propagation effects
- Standards and Recommendations
- Noise reduction
- Measurement procedures at high wind speeds
- Noise characteristics (e.g. tonality)
- Declaration and verification of sound levels

2 NOISE SOURCES

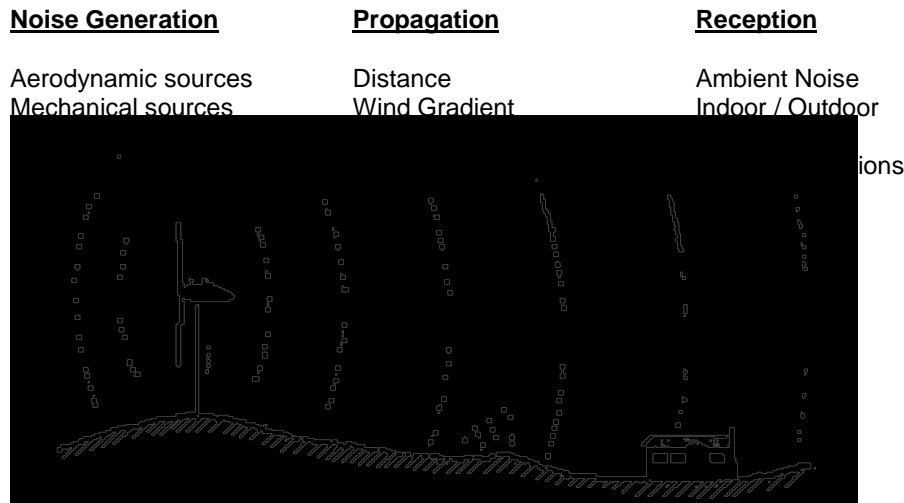


Fig. 1: Wind Turbine Noise Assessment Factors

Source: Sheperd, K. P.; Grosveld, F. W.; Stephens, D. G.: *Evaluation of Human Exposure to the Noise from Large Wind Turbines Generators*. *Noise Control Engineering Journal*, Vol. 21, No. 1 pp. 30-37, July-August 1983

In order to assess the noise at the receptor locations (nearest dwellings) we have to distinguish between noise generation (noise sources) noise propagation (propagation conditions, prediction standards) and sound pressure levels at the receptor location. The noise sources can be split up into the aerodynamic noise [1] sources and the machinery noise. The aerodynamic noise sources are inflow turbulence noise (leading edge of the blade), turbulent boundary layer noise (interaction with the trailing edge of the rotor blade) and tip noise (see. Fig. 2)

Machinery noise (mainly (gearbox noise, generator noise) has been reduced significantly so that it is mostly not contributing to the overall sound power level. On the other hand there are still some turbines radiating an audible tone which is assessed according to IEC 61400-11 ed.2. In some countries national codes penalties are given depending on the audibility of the tone.

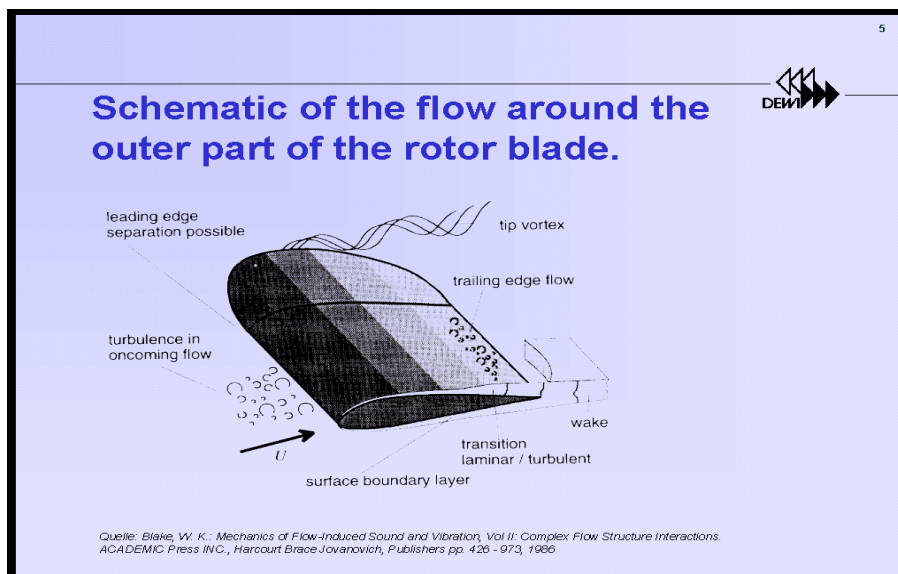


Fig 2: Tip Noise

Fig. 3 shows the sound power levels of 49 different types of wind turbines in the range of 80kW to 2500kW (see also [2]). These are published data in a catalogue issued annually by the German Wind Energy Association BWE (Market Survey 1997-2005)

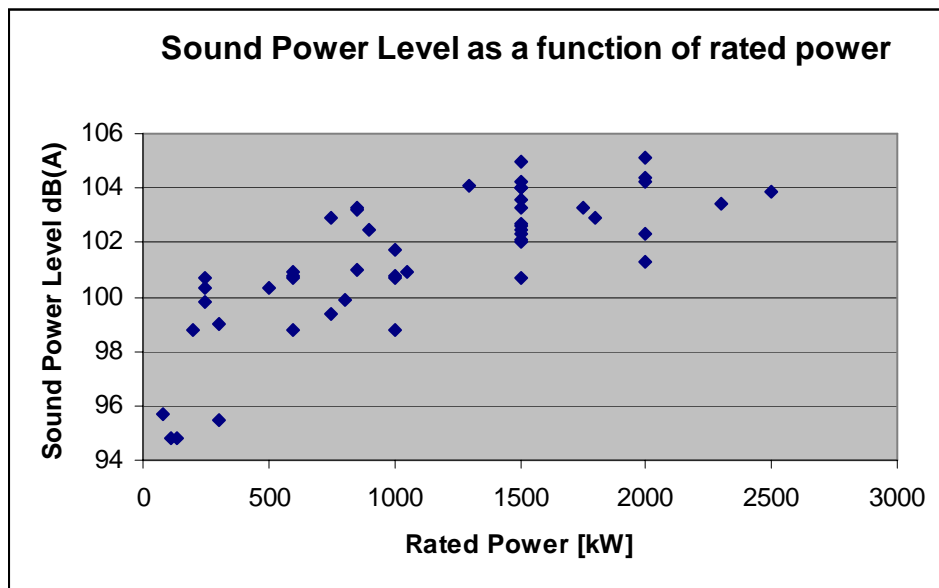


Fig 3: Sound Power Level vs. Rated Power

When looking at the wind speed dependency of the sound power level we have to distinguish between stall-regulated turbines and pitch regulated turbines. The power control by the stall-effect causes an increase of sound power level also at high wind speeds, while pitch regulated turbines not only keep the power constant at high wind speed but also the sound power level. Due to the pitching at rated power the sound power level may even decrease at high wind speeds (see table I).

V[m/s] at 10 m height	6	7	8	9	10
Sound Power Level	98.6	99.6	100.8	102.4	104.1
Stall-regulated turbine 1300 kW					
Sound Power Level	98.8	100.0	101.1	101.5	101.0
Pitch-regulated turbine 850 kW					

Tab. 1: Sound Power Level vs. Wind speed. Examples for a stall and a pitch-regulated turbine

3 PROPAGATION

Meteorological conditions, mainly wind and temperature profiles in the boundary layer affect outdoor sound propagation [3]. Wind speed and temperature are functions of height. They are interrelated and can be described by the Monin-Obukhov similarity theory. The Monin-Obukhov length L is a stability parameter for the turbulent boundary layer. The largest sound speed gradients causing the highest sound pressure levels at large distances occur for downwind conditions at night-time. The most pronounced stable atmospheric stratification can be expected during clear nights and low wind speeds. For that reason a lot of national codes require measurements at low wind speeds at night-time (often referred to as 'downwind condition'). As the wind turbines have the highest sound power levels at high wind speeds these national codes for noise regulations have to be made consistent with the international standards of measuring the wind turbine noise at wind speeds from 6 to 10 m/s at 10 m height.

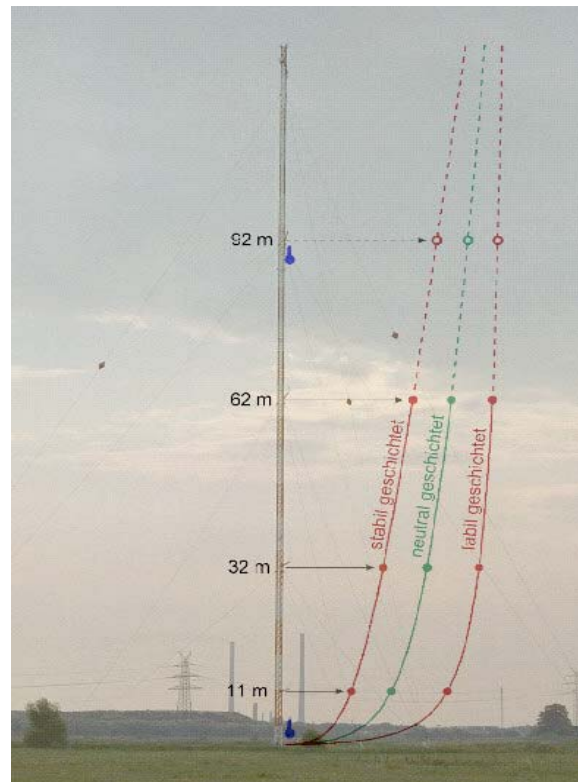


Fig. 4: Wind Profiles for stable, neutral and unstable atmospheric conditions. Measured at the DEWI's 130m-mast.

4 STANDARDS AND RECOMMENDATIONS

4.1 IEC Standard 61400-11

The IEC standard 61400-11 ed. 2 Wind Turbines – Part 11 ‘Acoustic Noise Measurement Techniques’ provides a uniform methodology that will ensure consistency and accuracy in the measurement and analysis of acoustical emissions by wind turbine generator systems (WTGS). The sound power level is determined for wind speeds from 6 to 10 m/s at 10 m height.

There is a preferred method described (mandatory for declaration and certification measurements) using the electrical power output of the turbine (in combination with the power curve of the machine) as a measure for the wind speed instead of a 10 m met mast. This is the only method to get **reproducible sound power levels** of a wind turbine independent on the instantaneous wind profile during the measurement period (see also chapter 3) which also means independent of the time of the day. In other words: the propagation conditions for large distance propagation change significantly with the boundary layer stabilities (see chapter 3) but **not** sound power level of the sound source measured by the 61400-11 standard (if the preferred method is used). The sound power levels are determined for **standardised wind speeds at 10 m height**. The wind speed at hub height is determined by the electrical power through the power curve of the turbine. The related wind speed at 10 m is determined by a standardised wind profile given in the IEC –11 standard.

The IEC group on the –11 standard right now works on an amendment in order to define a procedure to measure reproducible sound power levels at high wind speeds as well. If the standardised wind speed corresponding to 95% of rated power is below 10 m/s, one of the following two methods shall be used to determine the wind speed for data above 95% of rated power:

Nacelle anemometer method:

A linear regression using the nacelle wind speed V_n and corrected hub height wind speed determined from electrical power measurements V_H shall be determined. The corrected wind speed above 95% of rated power shall be determined applying the resulting linear regression to the nacelle wind speed V_n .

κ -factor method

For all data points with power levels below 95% of rated power the ratio of standardised wind speed and measured wind speed, κ , shall be derived. This ratio shall then be applied to the measured wind speed of the data points with power levels above 95% of rated power to estimate the standardised wind speed.

The nacelle anemometer method is the preferred method as the correlation between nacelle wind speed and the electrical power output typically is better than for the wind speed measured below hub height.

The presence of tones in the noise at different wind speeds shall be determined on the basis of a narrow band frequency analysis as follows (see also [4]):

- The sound pressure level L_{pt} of the tone shall be determined
- The sound pressure level of the masking noise L_{pn} in a critical band around the tone shall be determined
- The tonality ΔL_{tn} , the difference between the sound pressure level of the tone and the masking noise level shall be found

The tonal analysis shall cover the same wind speed range as the sound power level measurement. For each wind speed bin, the two one-minute periods with wind speeds closest to the integer wind speed value shall be analysed.

The narrow band frequency spectrum for the whole two-minutes period shall be determined. Then the two one-minute recordings shall be divided into twelve ten-second periods, from which twelve narrow band frequency spectra are obtained. From these twelve spectra all lines representing tones shall be identified.

Every spectral line is classified as a) 'tone', b) 'masking', or c) 'neither tone nor masking' as illustrated in the figure below.

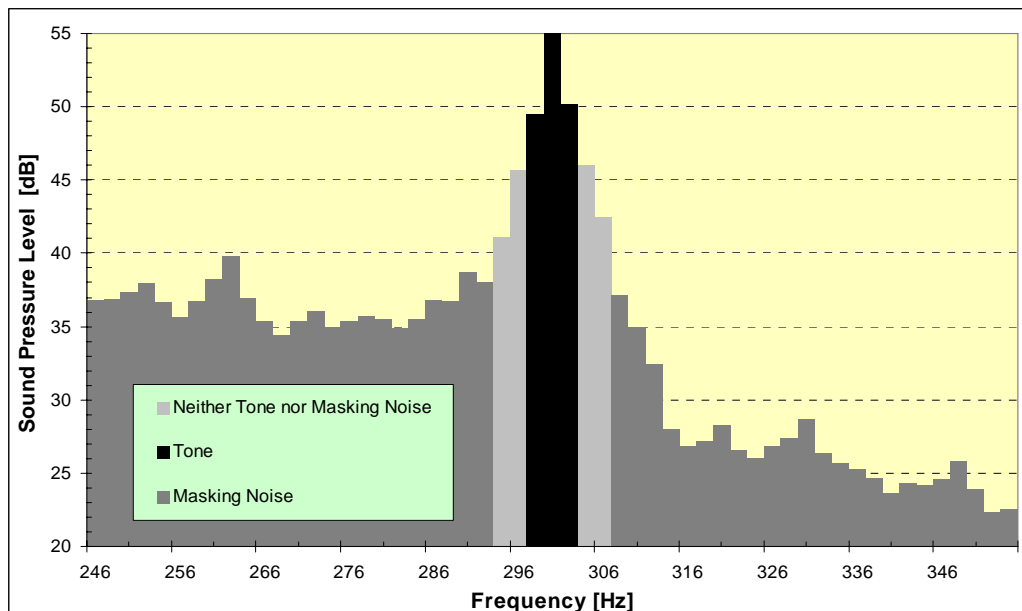


Fig. 5: Illustration of classifying all spectral lines

Determination of the tone levels $L_{pt,i}$

The sound pressure level of the tone, $L_{pt,i}$ is determined by energy summing all the spectral lines identified as tones from each 12 ten-second spectrum

Determination of the masking noise levels $L_{pn,i}$

The 12 sound pressure levels of the masking noise, $L_{pn,i}$, are defined as follows:

$$L_{pn} = L_{pn,avg} + 10 \lg \left[\frac{\text{critical bandwidth}}{\text{effective noise bandwidth}} \right]$$

Where $L_{pn,avg,i}$ is the energy average of the spectral lines identified as 'masking'.

Determination of the tonality ΔL_{tn}

The tonality $\Delta L_{tn,i}$ is the difference between the sound pressure level $L_{pt,i}$ and the level $L_{pn,i}$. The 12 $\Delta L_{tn,i}$ are then energy averaged to one ΔL_{tn} .

4.2 IEC Technical Specification 61400-14: Declaration of Sound Power Level and Tonality Values of Wind Turbines

Information on the sound power level and tonality of wind turbines is needed by planners, manufacturers and authorities. At present wind turbine noise specifications tend to be based on measurement results from a single turbine of a particular make and model and these are then taken to be representative of these turbines as a whole. Clearly this is unlikely to be the case, as there will be individual variation between different turbines. The intention of this document is to determine declared noise emission values from a sample of turbines of the same type. The declaration will increase the reliability of wind farm planning and shall facilitate the comparison of sound power levels and tonality values of different types of wind turbines.

The document IEC TS61400-14 gives guidelines for declaring the apparent sound power level and tonality of a batch of wind turbines (see also [4]).

For the declaration procedure the influence of turbine characteristics on the acoustical performance is of great importance:

- Hub height : The sound power level is correlated to the acoustic reference wind speed and not to the wind speed at hub height. An increase of hub height will increase the sound power level and might have an unpredictable effect on tonality.
- Tip speed: the sound power level is very sensitive to the tip speed ($L_w \sim 50 \dots 60 \log V_{tip}$). An increase in tip speed will cause an increase in sound power level, and may have an influence on aerodynamic tones.
- Pitch setting: Pitch settings affect the fundamental aero-acoustic processes on the blades, which may significantly change the overall sound power level and the tonality.
- Gear box: A major source of mechanical tones is the gear box. Small changes in the design (like ratio's, tooth shape, casing thickness) can have a significant effect on the frequency and level of the tones
- Blades: Changes to the blade geometry such as trailing edge thickness, tip shape, blade surface finish , internal structure, twist distribution, may all cause significant changes to the acoustical performance.
- In addition to the above mentioned items, there are a number of other items, generator, tower type, yaw motors, cooling fans, hydraulic pumps, etc., which may influence the acoustical performance.

4.3 Measurement of Noise Immission from Wind Turbines at Noise Receptor Locations

The IEA recommendation **Measurement of Noise Immission from Wind Turbines at Noise Receptor Locations [5]** recommends measurement techniques and methods which will enable a characterisation of the noise immission from wind turbines at a noise reception location. In several countries standards or guidelines from industrial sources have been implemented. However, it is not possible to apply these procedures to wind turbine acoustic measurements since they must be carried out in windy conditions outside the scope of the standards dealing with noise from industrial plants.

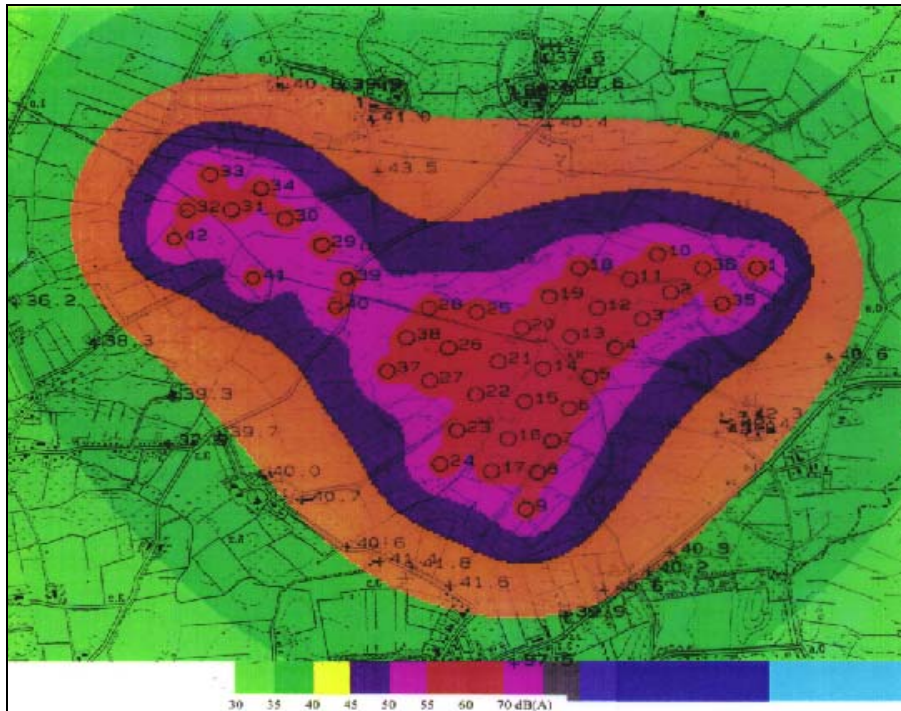


Fig. 6: Sound Pressure Levels around a Wind Farm

A major problem when measuring noise immission from wind turbines is the influence of background noise generated by, for instance

- the wind at the microphone
- the wind acting on adjacent trees, shrubs and structures
- traffic on nearby roads and rail tracks
- aircraft and industries
- animal and human activities
- streams or waves on shorelines.

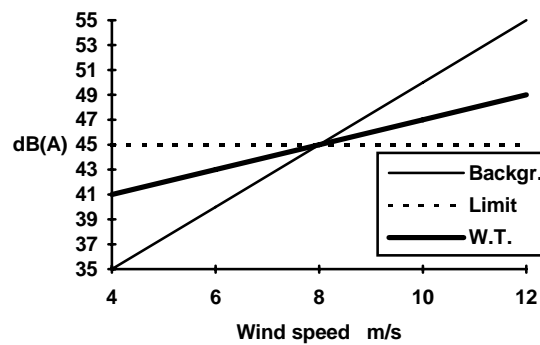


Fig. 7: Example: Wind turbine Noise and Background Noise as a function of wind speed at 10 m height.

In many measurement situations, the sound level of a wind farm is of the same order of magnitude as the background noise level (see fig. 7). This implies that a very important task is to correct the measured levels for the influence of background noise. For the same wind speed range immission measurements have to be performed for

- turbines operating
- turbines parked.

Measurements at high wind speeds performed only when the turbines are operating are useless in most cases.

The IEA recommendation gives guidance how to increase the signal-to-noise-ratio for immission measurements like

- use of a secondary wind screen
- small boards on a building facade
- large free standing vertical boards

Some national codes work with absolute noise limits, while in some other countries the limits are based on the ambient noise. The nature of the wind turbine noise and the wind induced background noise are very important for defining masking criteria.

The measurement of the background noise at the nearest dwellings should be performed

- for a defined wind speed range (e.g. 4-8 m/s at 10 m height)
- at night time in order to reduce noise from traffic and human activities
- for relevant wind directions
- with a secondary wind screen
- at noise relevant conditions (like without leaves on the trees)

The evaluation of the background noise should include L_{eq} , but also statistical values like L_{50} , L_{90} , and L_{95} in order to be able to define masking criteria or noise limits.

5 INFRASOUND

Wind turbines are radiating sound at extremely low levels in the infrasound range (below 20 Hz). This sound is far below the detection threshold and thus far below levels which can cause any diseases. Measurements at a turbine in the megawatt class at the DEWI Test Site showed levels of 58 dB at a distance of 100 m to the turbine in the one-third octave band level at 10 Hz, which means more than 30 dB below the hearing threshold at this frequency. (Source: Measurement Report ITAP: Messung der Infraschall-Abstrahlung einer WEA des Typs Vestas – 1,65 MW; ITAP-Institut für technische und angewandte Physik GmbH, Oldenburg, 26.06.2000)

6 NOISE REDUCTION PROCEDURES

Considerable noise reductions have been reached by modifications of the trailing edge (sharp or serrated trailing edge) and new tip designs (avoiding tip vortex-trailing edge interaction by 'trailing edge cutting'). The tip noise experiments on commercial wind turbines have confirmed the results obtained in the wind tunnel. Tip designs generating strong tip vortices (e.g. extreme curvature at the leading edge) interacting with the TE (trailing edge longer than the leading edge) cause additional noise in the high frequency range (a second maximum in the 2kHz frequency range of the sound power spectra is an indication of tip noise). Reductions of the overall sound power level up to 4 dB(A) have been reached by designs avoiding these effects [6],[7].

The choice of a wind turbine's blade pitch setting and its rotational speed is a compromise between noise radiation and energy production. The advantage of wind turbines with changed operational conditions (rotational speed/pitch setting) in noise-sensitive conditions (e.g. for specific wind directions or at night-time) are obvious: The acoustically affected area is smaller so that more wind turbines can be erected in a wind farm. The proposed noise-reduction-tool can also be used for subsequent noise reduction in cases of complaints.

As changes in the operating conditions of the wind turbines will influence their power curves, any resulting loss in energy production can be calculated, so that the cost effectiveness of the measures can be evaluated.

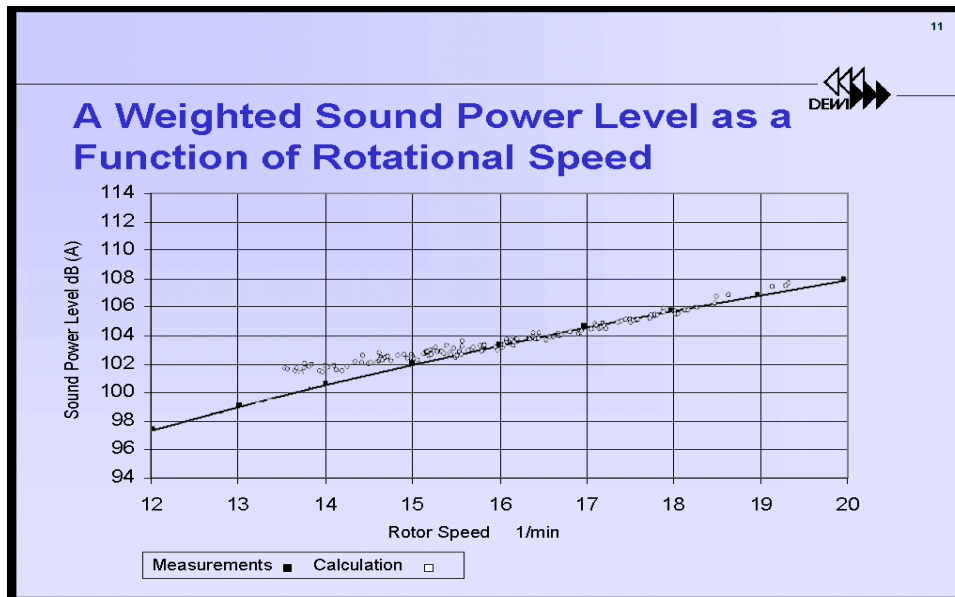


Fig. 8: Sound Power Level of a 3 MW Turbine as a Function of Rotational Speed:

Some manufacturers offer the same type of turbine with different sound power levels. They differ due to different control settings (e.g. rotational speed as a function of electrical power). The Technical Guideline TR 1 (Rev. 16) about noise measurement from wind turbines in Germany as well as the MEASNET measurement procedure for that reason requires the recording of the rotational speed during the noise measurement as a function of the normalised wind speed (defined in 61400-11) so that the control setting during the noise measurement can be clearly identified. The authorities can also determine from the track record of the turbines data acquisition system (time series of power and rotational speed) if a noise reduced control version was active for certain periods (e.g. at night time).

The MEASNET procedure requires the following: Relevant wind turbine control parameters such as rotor speed shall be measured and reported. These data may be obtained by online data acquisition of signals from the wind turbine controller. In that case the data have to be verified for example by using optical or acoustical counting of the blade passages during the measurements. These parameters shall be reported as a function of active power and standardised wind speed.

7 REFERENCES:

- [1] Howe, M.S., 'A Review of the Theory of Trailing edge noise', J. Sound Vib. 61, 3, 437-465 (1978).
- [2] Klug, Helmut; Osten, Tjado; Gabriel, Joachim: Noise from wind turbines or how many Megawatts can you get for a 100 dB(A). ? Proceedings of the EWEC1997 in Dublin, Ireland, 6th to 9th October, 124-127.,1997
- [3] Helmut Klug, Sound Speed profiles determined from outdoor sound propagation measurements, 475-481; J.Acoust. Soc. Am. 90 (1), July 1991.
- [4] Klug, 'Noise from Wind Turbines -Standards and Noise Reduction Procedures-', Forum Acusticum 2002, Seville
- [5] Recommended Practices for Wind Turbine Testing, 10. Acoustics - Measurement of Noise Immission from Wind Turbines at noise Receptor Locations, 1. edition, 1997 International Energy Agency. Edited by Sten Ljunggren, Sweden.
- [6] Klug, Osten, Lawson, Jakobsen, Andersen, van der Borg, Vink, Betke, Schultz-von Glahn, Larsen, 'Aerodynamic Noise from Wind Turbines and Rotor Blade Modification', Final Report DEWI V-95 0006 (EU-Projekt JOU2-CT92-0233), Wilhelmshaven, 1995.
- [7] H. Klug, 'Aerodynamic Noise from Wind Turbines and Rotor Blade Modification - Experimental Results', Forum Acusticum 1996, Acta Acustica, S.81.

First International Meeting on Wind Turbine Noise: Perspectives for Control Berlin 17th and 18th October 2005

Prediction of Wind Turbine Noise Propagation over Complex Terrain in All Kinds of Weather with Nord2000

Jørgen Kragh, Birger Plovsing
DELTA Danish Electronics, Light & Acoustics www.delta.dk
Venlighedsvej 4, DK-2970 Hørsholm, Denmark
jk@delta.dk, bp@delta.dk

Bo Søndergaard
DELTA Danish Electronics, Light & Acoustics www.delta.dk
Kongsvang Allé 33, DK-8000 Aarhus, Denmark
bsg@delta.dk

1. Summary

Mapping of noise from wind turbines today is normally made by means of a prediction method assuming downwind sound propagation. This is a worst case consideration since the wind cannot at any time blow in all directions from every wind turbine.

The new Nordic Nord2000 model directly takes the actual weather conditions into account, and DELTA has applied Nord2000 for predicting wind turbine noise propagating in a variety of directions relatively to the wind direction. Such more nuanced assessment made by means of more sensitive prediction tools than has been used hitherto may result in significant improvements, environmentally as well as economically. Some wind turbines might be operated with fewer restrictions leading to significant increase in power production, or more wind turbines might be located in the same area. Especially in hilly terrain significant differences have been found between results of calculations made with the old methods and results of computations applying the new model.

A phase of software development and testing as well as method validation is foreseen before environment authorities, wind farm developers as well as wind farm neighbours can use the new tool with confidence in real life.

2. Introduction

When considering a potential site for wind turbines / wind farms, the noise from the future wind turbines is mapped. Nowadays this mapping is normally based on a prediction method assuming downwind sound propagation. The wind cannot at any time blow in all directions from every wind turbine, so this way of determining the noise levels is a worst case consideration.

The reasons for basing wind turbine noise mapping on such a worst case consideration may be:

- a) an environmental policy aiming at preventing noise levels from exceeding given noise limits at any time and/or

- b) that prediction methods for downwind were the only methods available at the time of deciding on the present environment policy.

Recently, significant progress has been made in the field of engineering methods for predicting environmental noise. The new Nordic method Nord2000 was published at the change of the century. Since then it has been tested and adjusted, and many of its features have been incorporated into the “Harmonoise” method, the European method coming into being for predicting road and rail traffic noise. The “Harmonoise” method has not yet been thoroughly tested in practical engineering applications although some validation was made within the Harmonoise project.

DELTA has applied Nord2000 for predicting wind turbine noise propagating in a variety of directions relatively to the wind direction, and in particular in complex terrain such as mountainous areas predicted noise levels may deviate essentially from those predicted at the same distance in a flat terrain.

More nuanced assessment made by means of more sensitive prediction tools than has been used hitherto may result in significant improvements, environmentally as well as economically.

3. Nord2000 Properties

Nord2000 is a new generation propagation model intended for predicting various types of environmental noise. Its development was financed by the Nordic Council of Ministers and by the Nordic environment and traffic authorities. It was developed by DELTA Acoustics & Vibration, by SINTEF Telecom & Informatics, and by SP Swedish National Testing and Research Institute.

Physical Model

The Nord2000 sound propagation model based on geometrical ray theory and on diffraction theory was developed for calculating one-third octave band attenuation in a homogeneous atmosphere. The new propagation model involves direct application of theory algorithms in frequency band calculations. Such direct application of algorithms from theory is a novelty. In the present and past Nordic prediction methods, only approximate or empirical solutions have been used because theoretical solutions were too time-consuming or too complicated for “manual” calculation. With the availability of personal computers and the rapid growth in their calculation speed, there seems to be no need for avoiding calculation according to theory.

The combined effect of ground and single or multiple noise barriers are dealt with in Nord2000 as well as the effect of rough ground surfaces, non-flat terrain, and terrain consisting of combinations of different types of ground. Also, the effect of reflection from obstacles and scattering by objects such as buildings or vegetation can be calculated.

The model has been extended to include the effect of various weather conditions by curving the sound paths. Downwind of the source the sound is refracted downwards, and upwind of the source the sound is refracted upwards giving rise to a sound shadow zone, cf. Figure 1.

Nord2000 is valid for any terrain profile consisting of any combination of ground surface types (acoustic impedance), and there is no longer a need for having skilled users interpret the terrain and decide how to represent it in the calculation. Instead, with a computer program the predictions can be made solely based on digital elevation data and information on the type of surface and the weather conditions.

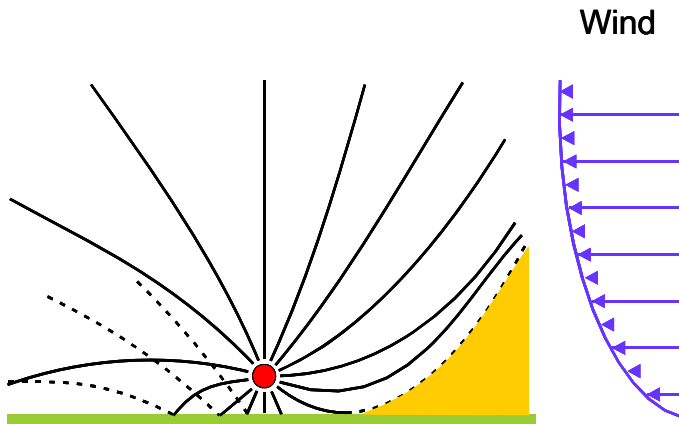


Figure 1
*Illustration of wind influence on sound propagation:
 Upwind of the source a shadow zone (hatched) occurs.*

The range of frequencies in Nord2000 is 25 Hz - 10 kHz, and the ambition has been to cover distances up to 1000 m with “good” accuracy, and distances 1000 m to 3000 m with “acceptable” accuracy while the project did not deal with propagation over larger distances.

Numerical methods like the Parabolic Equations (PE) method and the Boundary Element Method (BEM) are not useful in practical prediction methods due to the excessive calculation times. However, numerical methods are useful and have been used to develop and validate Nord2000.

Short-Term Noise Levels

The Nord2000 model allows calculation of one-third octave band sound pressure levels for specified weather conditions including rapid turbulent motions of the atmosphere. Therefore, the model applies to calculation of short-term noise levels for time periods shorter than a few hours.

Long-Term Noise Levels

Long-term noise levels including the effect of slowly varying large-scale motions of the atmosphere (synoptic scales) can be computed by combining the calculated short-term noise levels with meteorological statistics. In practice, short-term level calculations are made for a limited set of meteorological classes, and the long-term level is the weighted average of these results. This approach makes it possible to calculate long-term levels such as the yearly average L_{den} and L_{night} specified as noise indicators in the EU Directive on environmental noise, maximum noise levels for longer periods, or even complete statistical distributions of noise levels.

Air Absorption

The method described in [1] has been decided upon in Nord2000. The third-octave band attenuation is calculated based on ISO 9613-1 [2] pure-tone attenuation at the centre frequency, corrected to obtain the band attenuation. The band attenuation is smaller than the attenuation at the centre frequency, and the difference increases with increasing attenuation. The difference between the centre frequency attenuation and the band attenuation is insignificant when the air absorption is less than 10 dB while there is substantial difference at high attenuation.

Ground Effect

Geometrical ray theory deals with the interference between sound waves transmitted directly from source to receiver and sound waves reflected from the ground between source and receiver. The important parameters are the difference in travel time of the direct and the reflected ray, the angle of reflection from the ground, and the ground surface impedance.

A major improvement in the new model compared with the present Nordic prediction methods is that the ground surface impedance is used in the calculations, cf. Table 1. In existing methods distinction is made only between “hard” and “porous” ground. In Nord2000 a classification has been introduced for typical ground surfaces.

Ground Class	Ground type σ [Nsm⁻⁴]	Description
A	12,500	Very soft (snow or moss-like)
B	31,500	Soft forest floor (short, dense heather-like or thick moss)
C	80,000	Uncompacted, loose ground (turf, grass, loose soil)
D	200,000	Normal uncompacted ground (forest floor, pasture field)
E	500,000	Compacted field and gravel (compacted lawn, park area)
F	2,000,000	Compacted, dense ground (gravel road, parking lot)
G	20,000,000	Hard surface (dense asphalt, concrete, water)

Table 1

Classification of ground type in Nord2000 with corresponding values of the ground flow resistivity σ [3].

Other major improvements are that Nord2000 can deal with ground surfaces consisting of a mixture of different types of ground, based on Hothersall et al. [4], and with terrain profiles consisting of many plane surface segments.

Examples of Model Behaviour

Figure 2 shows the effect of the type of ground on the noise level from road traffic in a slightly downwind situation [5]. The sources are low and the reflected wave incidents on the ground surface at a grazing angle. At 100 m the noise level is 12 dB higher if the ground is hard (asphalt, concrete, or water) than if the ground is grass. The ground impedances used in Figure 2 are from [6].

Figure 3 shows the corresponding difference for a high source such as a wind turbine in a downwind of 8 m/s. Note the significantly larger range of distances in Figure 3 than in Figure 2. The angle of incidence as well as the travel time difference of direct and reflected wave is larger in Figure 3 than in Figure 2. With the high source the difference between hard and porous ground becomes independent of the distance from the turbine, and the noise level above hard ground (Class G) is in the order of 2 - 2.5 dB higher than the noise level above very soft ground (Class A).

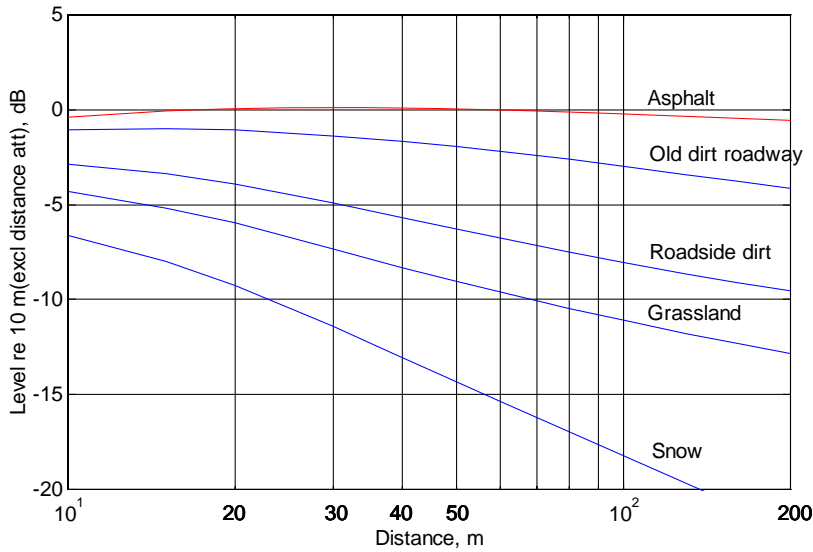


Figure 2

Effect of various types of ground surface. Ground effect on the A-weighted noise level from road traffic (noise level relatively to free-field + 6 dB).

$h_s = 0.0 - 0.2$ m, $h_r = 2$ m, $v = 50$ km/h, $p = 10\%$ heavy vehicles [5].

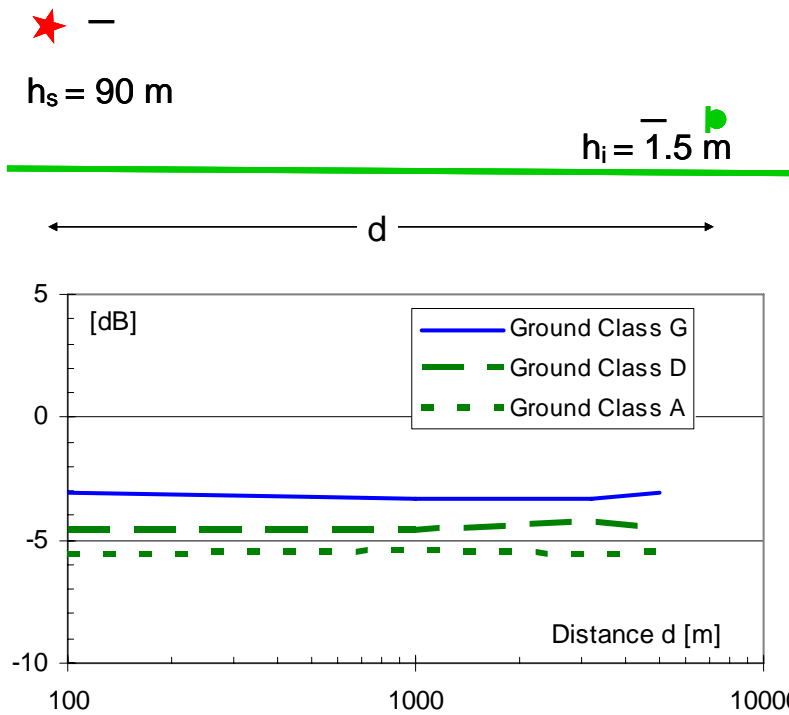


Figure 3

Effect of the ground type on the noise level [dB] downwind from a wind turbine (noise level relatively to free field + 6 dB).

Screening

A diffraction model by Hadden and Pierce has been selected for Nord2000 [7]. The effect of multiple screens is calculated according to [8] by combining diffraction coefficients for each screen into an overall diffraction coefficient. The effect of reflection from the ground on the

source side and receiver side of the screen is combined with the screening effect according to the so-called “image method” [9].

Comprehensive Model for Non-Flat Terrain

An essential achievement of Nord2000 is that it gives meaningful answers in many situations not covered by existing methods, which mainly deal with flat ground and thin, vertical screens. The comprehensive model is documented in [10] and [11]. The real terrain profile shall be approximated by a number of straight-line segments, and the comprehensive model consists of three parts [10]:

Flat terrain includes undulating terrain which does not deviate significantly from flat ground. An equivalent flat terrain is determined using the least-squares fit (linear regression) to the actual terrain, and predictions are made using the model for flat terrain.

Valley-shaped terrain is terrain that is non-flat and at the same time does not provide significant screening. A new method has been developed based on predictions made by the flat terrain model for each ground segment separately. These contributions are then added according to a Fresnel-zone interpolation principle.

Hill-shaped terrain includes cases with significant screening. Each terrain profile segment not being part of a screen is a reflecting impedance surface. A calculation is made for every combination of screen and terrain surface segment, and the calculation results are combined according to a Fresnel-zone interpolation principle.

Transitions. Discontinuity in prediction results has been avoided in Nord2000 wherever possible. Transition principles have been elaborated to obtain a smooth transition between the flat terrain, valley, and hill model. An example is the transition between “screened” and “un-screened” case, using a parameter expressing the “efficiency” of the screen based on a combination of path length difference and screen height relatively to the wavelength and to the effective width of the sound field at the screen.

Weather Effects

Geometrical ray theory is valid for a sound field without atmospheric refraction generated by wind speed or temperature gradients. In Nord2000 the theory has been extended to be valid also in the presence of refraction. Modified interference between direct and reflected sound is taken into account as a consequence of sound ray curvature caused by refraction, and reflection and diffraction angles are modified to account for the ray curvature.

Linear gradient. The model presupposes that the sound speed varies linearly with the height above the ground, so the sound path is part of a circle. The non-linear sound speed profiles occurring in a real atmosphere must be approximated in a way that ensures good calculation results. A principle for doing so has been developed [11].

Fluctuating gradient. When contributions from different rays are added coherently, the interference patterns in calculation results are stronger than observed in outdoor measurement results, among other things because of fluctuations in the sound speed gradient. This is taken into account by introducing coherence coefficients [11].

Multiple rays or shadow. In strong downward refraction a larger number of rays may reach the receiver than in the non-refraction case. This has been taken into account in Nord2000 by a model adding incoherent sound energy depending on the number of extra rays. In upward refraction shadow zones may occur into which no ray can enter, cf. Figure 1. A model for calculating the sound level in shadow zones has been developed considering the shadow zone as being screened by a wedge of terrain.

Turbulent scattering. Atmospheric turbulence scatters sound energy into the shadow zone behind a screen. A model has been developed for adding incoherent scattered energy to the sound behind screens.

Examples of Model Behaviour

The upper part of Figure 4 shows an example of a terrain profile in a mountainous area with grass-covered ground (Class D). A wind turbine with 90 m hub height is situated at the left side and a receiver at 1.5 m above the ground to the right. The middle part of Figure 4 shows the terrain profile near the receiver in more detail and reveals a terrain edge screening the sound from the turbine.

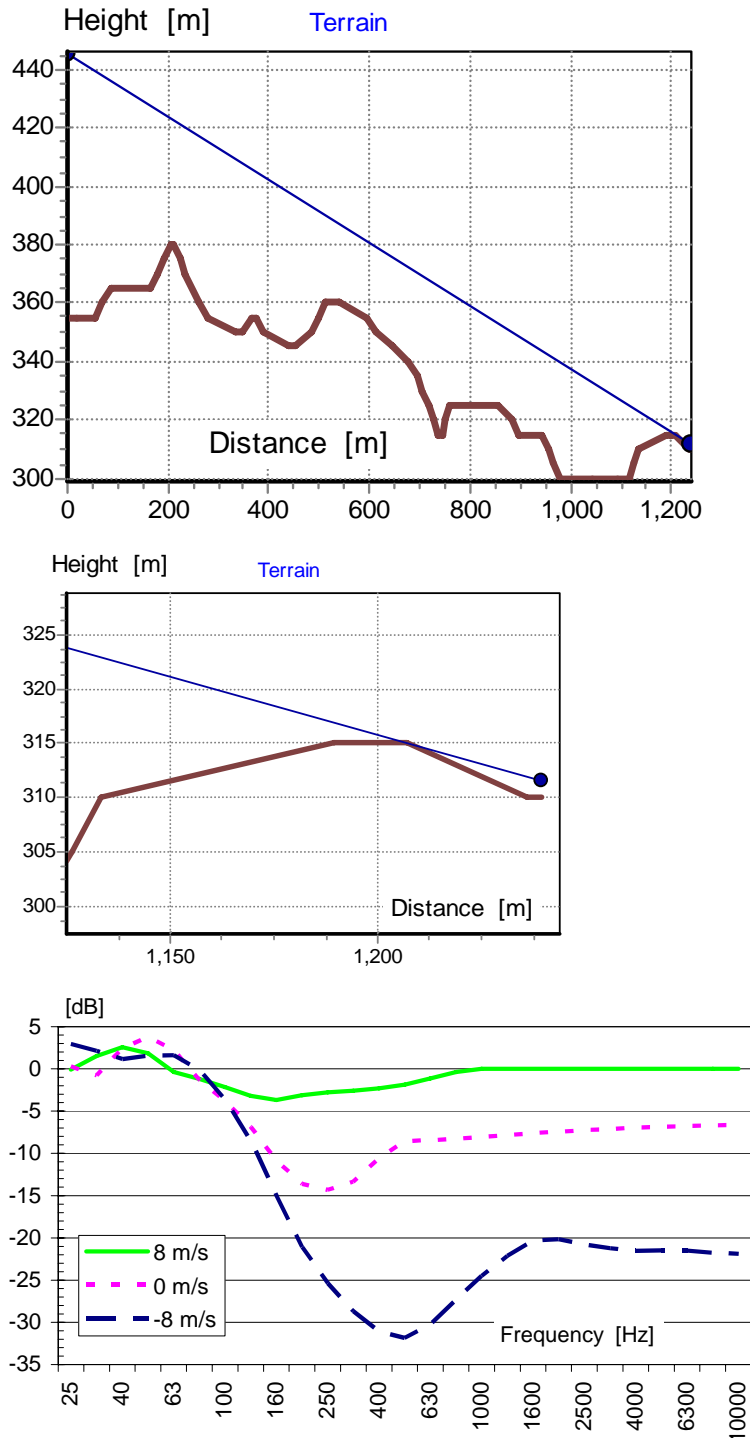


Figure 4

Vertical section through source and receiver (top), a zoom-in near the receiver (middle), and the combined ground and screening effect [dB] (bottom) calculated for 8 m/s downwind, zero-wind, and 8 m/s upwind, respectively.

The bottom part of Figure 4 shows the calculated effect of ground and screening per one-third octave in the frequency range from 25 Hz to 10 kHz. The full line shows the result with 8 m/s downwind (wind from turbine to receiver), the dotted line for zero-wind (crosswind) and the dashed line for 8 m/s upwind (wind from receiver to turbine). The attenuation of the noise depends strongly on the weather with much lower noise levels during crosswind and upwind than during downwind. This is due to screening and shadow zone formation.

The upper part of Figure 5 shows another terrain profile: a wind turbine with 90 m hub height is situated on flat ground with a receiver at the same horizontal distance of 1240 m as in Figure 4. The bottom part of Figure 5 shows the calculated ground effect under the same wind speed conditions as in Figure 4. There is less difference between downwind and crosswind ground effect in Figure 5 than in Figure 4. Lower noise levels upwind due to shadow zone formation are seen in Figure 5 as well as in Figure 4, but less pronounced in Figure 5. The effect of the flat ground in Figure 5 differs significantly from that of the undulating ground in Figure 4.

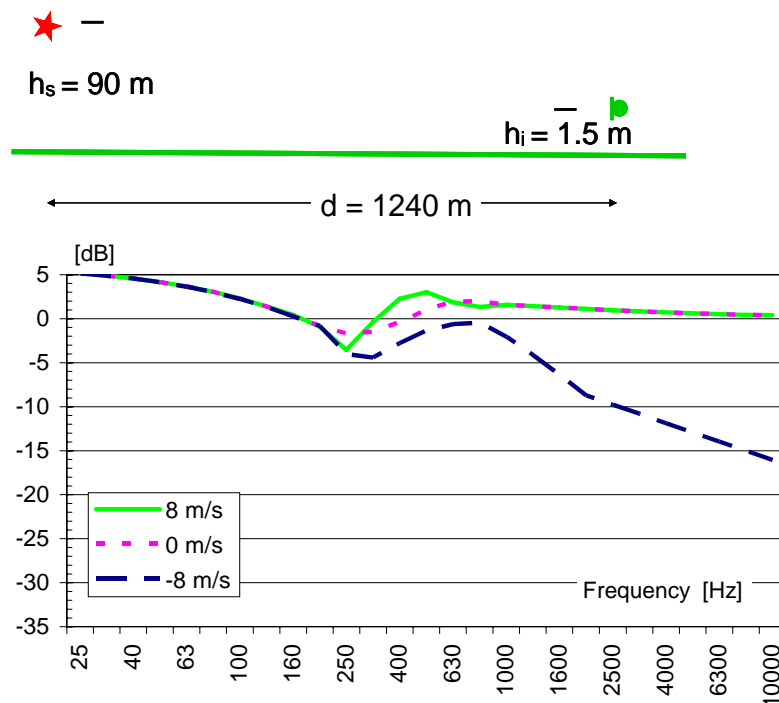


Figure 5

Ground effect [dB] calculated for 8 m/s downwind, for zero-wind, and for 8 m/s upwind, respectively, as a function of frequency for the source-receiver situation shown at the top.

Figure 6 compares the combined Nord2000 propagation effect of ground and air absorption on the overall A-weighted noise level due to a modern 2MW wind turbine on flat grassland (Class D). The difference between 8 m/s downwind and crosswind ground effect is within 1 dB with the highest noise level during downwind. Upwind the ground effect is within 1 dB from the crosswind ground effect up to 1000 m or so. At larger distances noise levels are significantly lower due to shadow zone formation. Similar results are shown in Figure 13 for sound propagating above water from an offshore wind turbine.

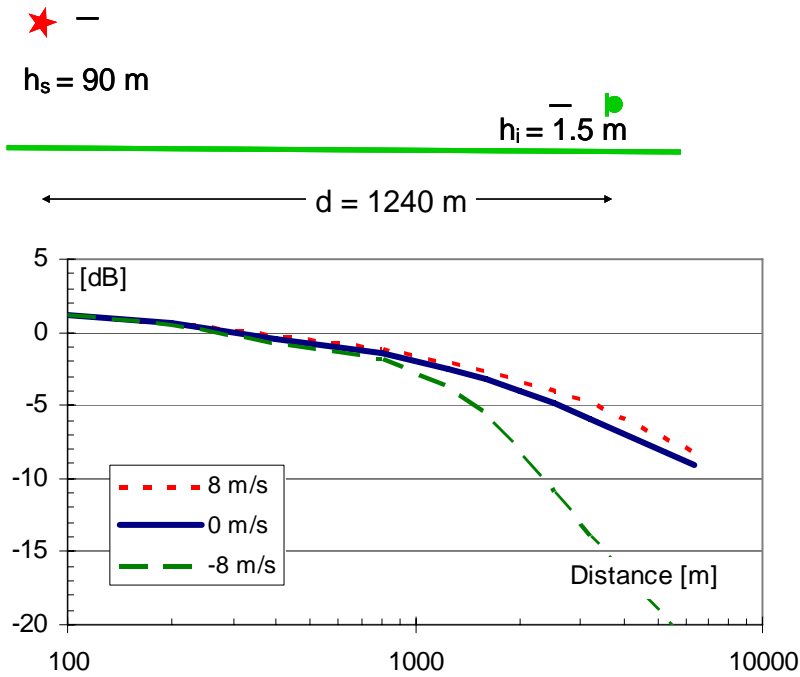


Figure 6
 Combined propagation effect of air absorption and ground [dB] on the total A-weighted noise level from a wind turbine as a function of source-receiver distance calculated for 8 m/s downwind, crosswind, and 8 m/s upwind propagation, respectively.

4. Examples of Application

A comparison of measurement and calculation is shown in Figure 7. The upper part of the figure shows the geometry: a loudspeaker 22 m above a grassy airfield (representing an “old-fashioned” wind turbine) and a receiver 1.5 m above the ground at 400 m distance [12].

The lower part of Figure 7 shows the one-third octave band ground effect as a function of the frequency. The points show the average measured ground effect, and the small horizontal lines show this average plus and minus the sample standard deviation of the measurement results. Below these intervals the number of good measurements is shown for each one-third octave band. The measurement results have been corrected for the effect of air absorption, so only the effect of the ground is displayed in the figure.

The full line shows the calculation according to Nord2000. The agreement between measured and calculated ground effect is excellent. The calculations were made for a downwind speed of 6.5 m/s corresponding to the average wind speed during the measurements and for a ground flow resistivity $\sigma = 125,000 \text{ Nsm}^{-4}$, which in short-range measurements were found to represent the airfield ground surface [12].

Figure 8 and Figure 9 illustrate measurements of road traffic noise in a suburban detached housing area behind a 6 m high earthwork along a 6-lane motorway [13]. The noise was measured before and after the road was repaved, under similar weather conditions. Measured and calculated results agree within the measurement uncertainty. The calculated noise level is 25 dB higher when a fresh breeze blows from the road than when it blows in the opposite direction. The measurement results fit well with the calculated noise level.

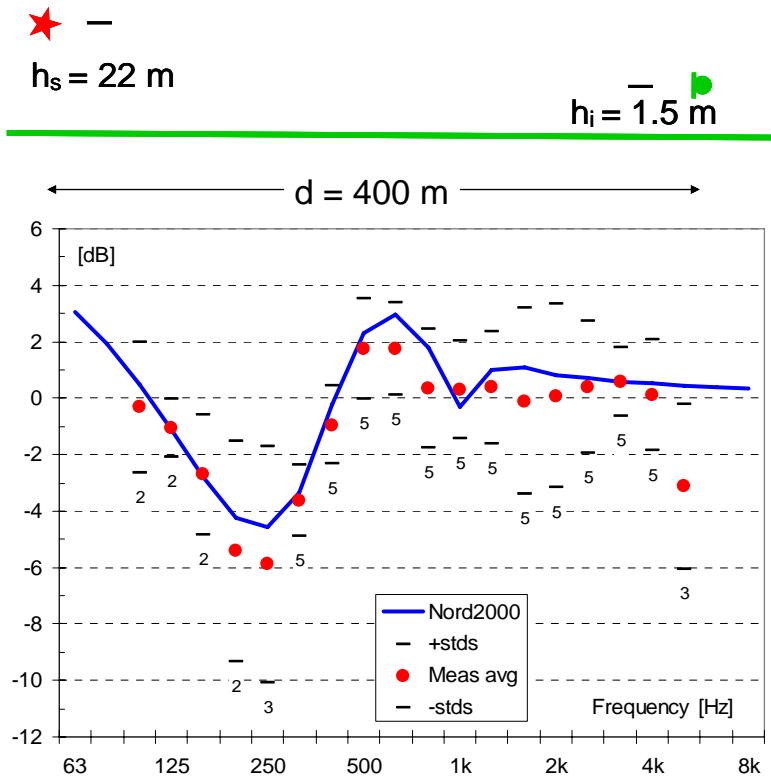


Figure 7

Measured and calculated ground effect [dB] for the source-receiver terrain shown in the upper part of the figure.

Figure 10 compares the calculated overall A-weighted noise level from a wind turbine with 90 m hub height as a function of the wind speed for the source-receiver situation in undulating terrain shown in Figure 4 and for a flat site. The results have been calculated presupposing constant source noise emission whatever the wind speed, and they have been shown relatively to the noise level at 8 m/s downwind at the flat site. The results show the variation due to weather dependent sound propagation attenuation. As already illustrated in Figure 4 and Figure 5, the ground affects the noise level much more in the undulating terrain – with a range of 8 dB between 15 m/s downwind and 15 m/s upwind – than at the flat site where the corresponding range is 4 dB. At the flat site the noise levels are higher than at the site with undulating terrain, with the largest difference in upwind and crosswind.

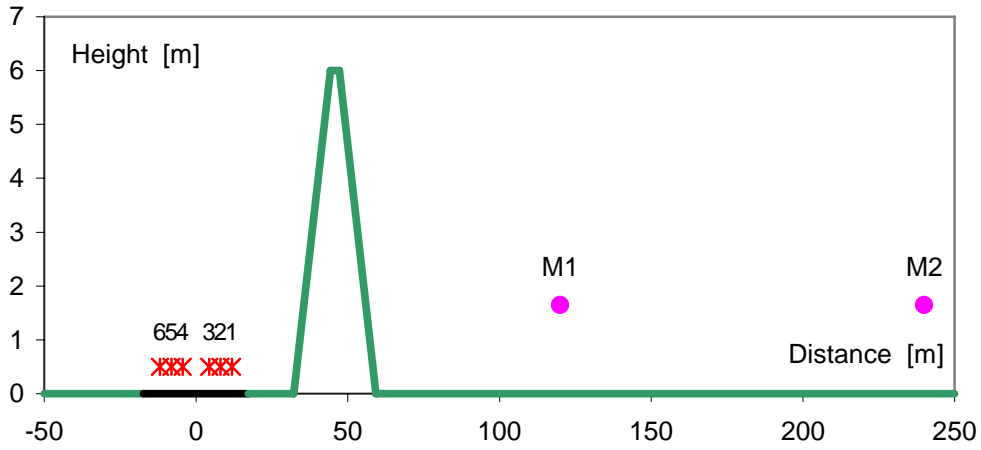


Figure 8
Cross section through the 6-lane motorway and the measurement positions.

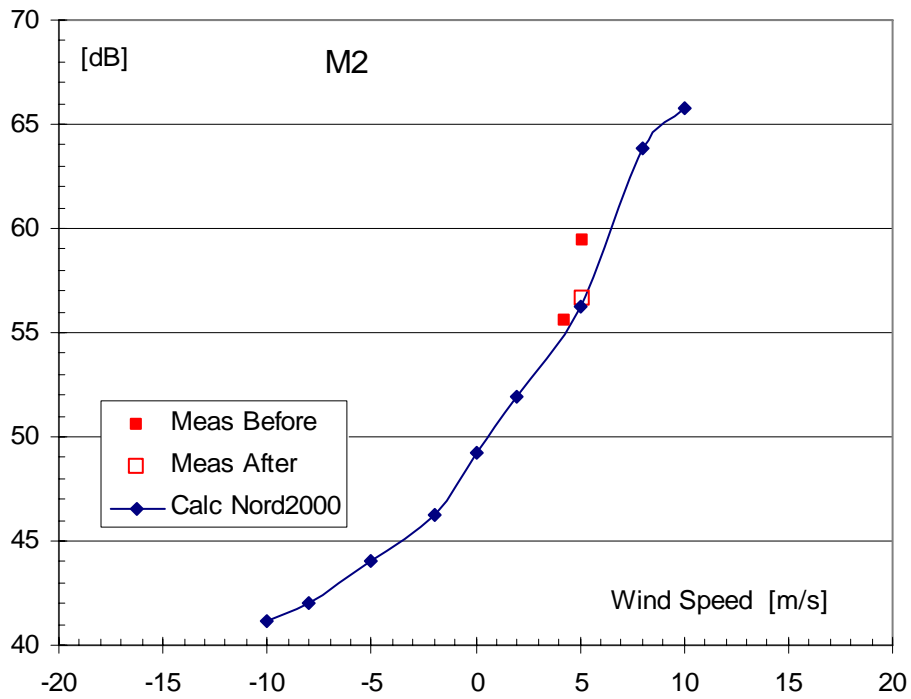


Figure 9
Calculated noise level [dB] from road traffic in position M2 (Figure 8) as a function of the wind speed, and noise levels measured before and after repaving the road.

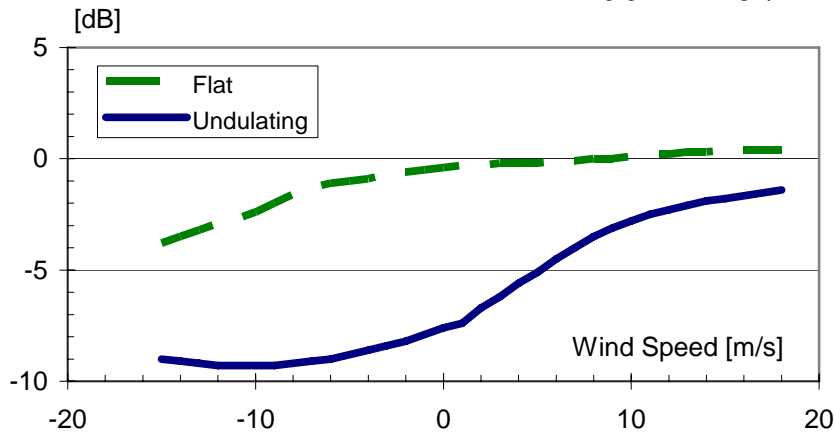


Figure 10

Calculated overall A-weighted noise level [dB] at 1240 m from a wind turbine with 90 m hub height as a function of the wind speed for the source-receiver situation shown in Figure 4 (undulating ground – full line) and in the upper part of Figure 5 (flat ground – dashed line). The source emission has been kept constant and the results are presented relatively to the noise level (0 dB) at 8 m/s.

Figure 11 compares the flat ground noise levels found with Nord2000 in Figure 10 with the results of calculations according to ISO 9613-2 [14] assuming hard and porous ground, respectively. The figure illustrates the range of 4 dB between the noise level according to Nord2000 downwind and upwind of the wind turbine with a wind speed of 15 m/s. ISO 9613-2 was developed to predict noise levels at 2-3 m/s downwind while Nord2000 has the wind speed as a primary parameter. ISO 9613-2 in the present case predicts lower values than Nord2000 when assuming porous ground and higher values than Nord2000 when assuming hard ground, the difference being 2-4 dB.

Figure 12 shows the variation in wind turbine noise source strength as a function of the wind speed in the top of the figure while the bottom of the figure shows the corresponding overall A-weighted noise levels according to Nord2000 at 1240 m distance at a flat site as a function of the wind speed. This figure includes both source strength variation and weather-induced variation in transmission path attenuation. Nord2000 gives lower noise levels at all wind speeds than ISO 9613-2 for hard ground and lower noise levels for porous ground.

Figure 13 shows the ground effect calculated with Nord2000 on the sound propagating over water from a wind turbine with a hub height of 100 m at distances from 100 to 10,000 m assuming the source spectrum of a modern 2MW wind turbine at a wind speed of 8 m/s at 10 m height [15]. The ground effect has been defined as the difference between the A-weighted sound pressure level and the A-weighted free-field sound pressure level. When calculating the sound pressure levels, the air absorption corresponding to an ISO-atmosphere (15° C and 70% RH) has been used. A flow resistivity of $\sigma = 20,000,000 \text{ Nsm}^{-4}$ corresponding to a hard surface has been assumed.

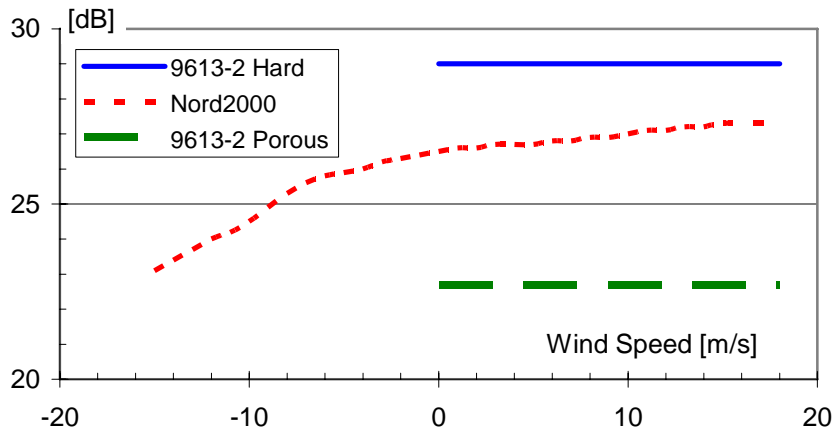


Figure 11

Calculated overall A-weighted noise level [dB] at 1240 m from a wind turbine with hub height 90 m as a function of the wind speed – for the source-receiver situation in Figure 5. The source emission has been kept constant.

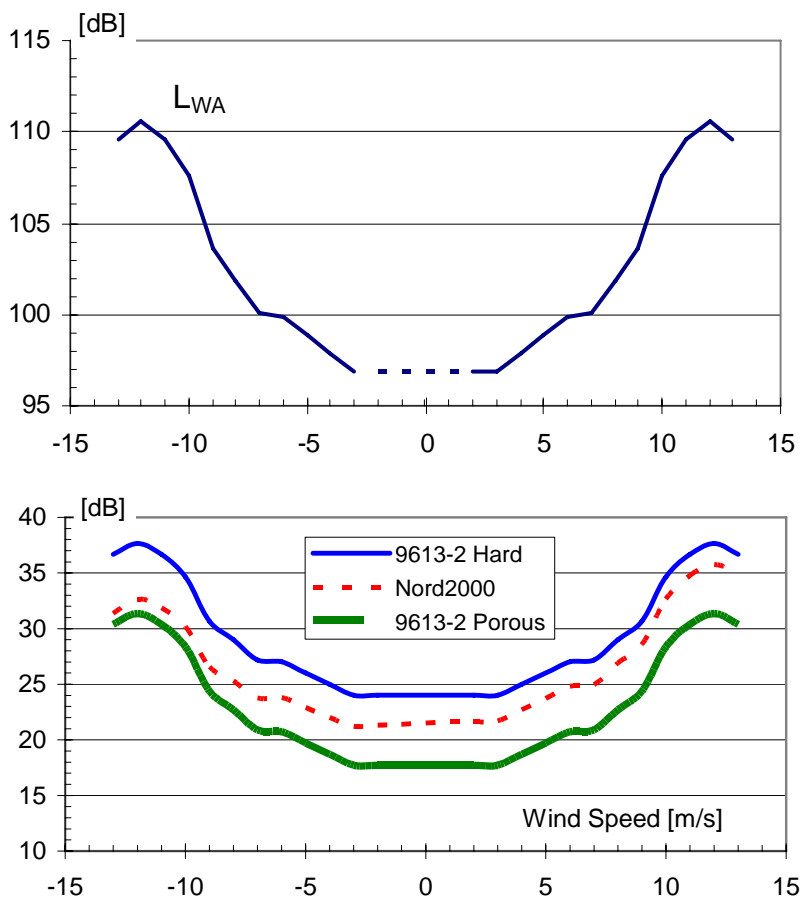


Figure 12

Source strength L_{WA} [dB] (top) and calculated noise level [dB] (bottom) from a wind turbine as a function of the wind speed – for the source-receiver situation in Figure 5, cf. text.

Figure 13 shows that the crosswind ground effect does not deviate much from the downwind ground effect. The figure shows that the ground effect may be slightly higher (higher noise levels) during crosswind than during downwind at large distances. This is because the path length difference of the direct wave from source to receiver and the wave reflected from the ground is smaller in a homogeneous atmosphere than in a downward refracting atmosphere (meaning that the reflection from the ground is more likely to approach a +6 dB effect in the former case at large distances). The same effect can be seen for upwind at distances just below the distance where the shadow zone occurs. In upwind large attenuations are observed above a given distance due to a meteorological shadow zone. Below this distance the ground effect by and large corresponds to the situation for the other wind directions.

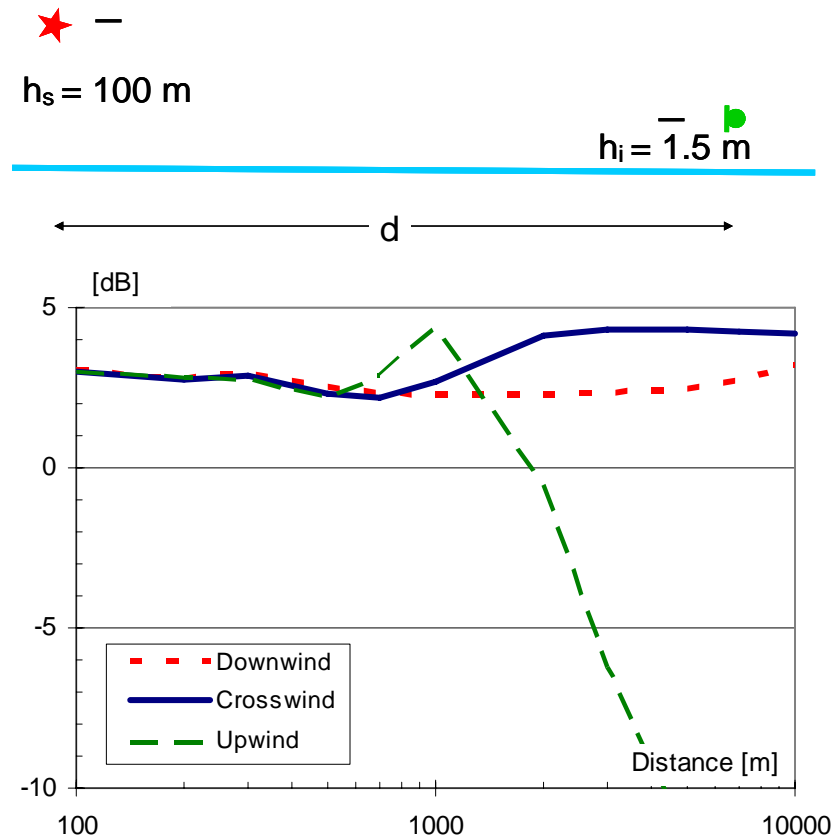


Figure 13

Calculated ground effect [dB] on sound propagating over water from a wind turbine with a hub height of 100 m at distances from 100 to 10,000 m [15].

5. Discussion

The Nord2000 sound propagation model is based on physics more than former prediction methods. Its major improvements are the ability to predict the influence of complex terrain and to include the weather as a primary parameter. The new model deals with terrain with varying surface properties (asphalt, grass, water etc.) as well as with terrain with varying topography (hills, valleys, mountains etc.).

The method has been validated for a range of situations, primarily for low source positions representing road traffic noise, and there is reason to expect it to work equally well for high sources such as modern wind turbines. An example of excellent agreement between results of measurement and computation at a flat site is given in Figure 7. Validation using data from measurements at real wind turbines in undulating terrain is important, but so far we have been unable to obtain extensive data from such measurements.

With these features Nord2000 seems to have significant potential as a tool for computing wind turbine noise levels for which noise generation and propagation depend on the wind speed and the wind direction. The main benefits seem to be: 1) more nuanced description of the environmental noise around wind turbines; e.g. the lower noise levels upwind than downwind of a wind turbine can be computed, 2) calculations can be made for more complex situations than has been possible till now, and 3) reliable and nuanced results will enable wind farm planners to work with a higher degree of confidence in the predictions.

The new ability of nuanced noise level prediction (e.g. upwind/downwind) could facilitate optimum control strategies for operating wind farms. When the wind blows towards a noise sensitive area some of the wind turbines may have to be operated at a low noise mode, which reduces the amount of power produced. On the other hand, when the wind blows away from the noise sensitive area, the wind turbines can be operated at normal mode giving full power production. The presently applied prediction methods were developed to yield the noise levels as they occur during moderate downwind (2-3 m/s) and are not useful for the design of optimum wind farm operation.

Further improvement could be obtained by combining the nuanced noise computations of Nord2000 with the ability of a wind flow model – such as the Wind Atlas Program (WAsP) developed by Risø (www.wasp.dk), which many people today consider the industry standard in wind turbine and wind farm production estimation – for computing the wind velocity distribution so that noise levels could be computed based on the actual wind speed at each of the wind turbines. Such nuanced computation instead of assuming worst case conditions for each individual wind turbine implies a potential for higher wind farm power production, particularly at sites with undulating terrain.

6. Conclusions

The Nord2000 propagation model is more generally valid than the methods applied until now for predicting wind turbine noise. Nord2000 has facilities for taking the actual weather conditions into account as well as the details of the terrain profile between the wind turbine and the receiver. This opens for more nuanced description of the environmental noise levels from wind turbines / wind farms and thereby for running wind farms with fewer restrictions than may be the case today when environmental noise levels are assessed assuming downwind from every wind turbine in every direction at the same time. Such nuance in assessment may at the same time lead to more power production and less neighbour conflict.

A phase of software development and model validation is foreseen in order for environmental protection officers, wind farm neighbours, and wind farm planners to gain confidence in the new model. This phase should include combining the noise propagation modelling with wind flow modelling (e.g. in WAsP) to allow mapping of noise levels using actual wind speeds at each individual wind turbine in the farm.

7. References

- [1] P. D. Joppa et al.
Representative Frequency Approach to the Effect of Band-pass Filters on Evaluation of Sound Attenuation by the Atmosphere
Noise Control Eng. J. 44, pp. 261-273, 1996
- [2] ISO 9613-1
Acoustics – Attenuation of sound during propagation outdoors - Part 1: Calculation of the absorption of sound by the atmosphere
- [3] M. E. Delaney and E. N. Bazley
Acoustical Properties of Absorbent Materials
Appl. Acoust. 3, p. 105-116, 1970
- [4] D. C. Hothersall et al.
Approximate Models for Sound Propagation above Multi-Impedance Plane Boundaries
J. Acoust. Soc. Am. 97, pp. 918-926, 1995
- [5] H. G. Jonasson
The Propagation and Screening of Wheel/Rail Noise
SP Swedish National Testing and Research Institute, Acoustics, SP Report 1996:43, Borås 1996
- [6] T. Embleton
Effective Flow Resistivity of Ground Surfaces Determined by Acoustical Measurements
Noise Control Engineering, Jan.-Feb. 1982
- [7] W. J. Hadden et al.
Sound Diffraction around Screens and Wedges for Arbitrary Point Source Locations
J. Acoust. Soc. Am. 69(5), pp. 1266-1276, 1981
- [8] E. M. Salomons
Sound Propagation in Complex Outdoor Situations with a Non-Refracting Atmosphere: Model based on Analytical Solutions for Diffraction and Reflection
Acta Acoustica 83(3), pp. 436-454, 1997
- [9] H.G. Jonasson
The Propagation of Sound over Ground with and without Acoustic Barriers
Report No. 18, Division of Building Technology, Lund 1971
- [10] B. Plovsing, J. Kragh
Nord2000. Comprehensive Outdoor Sound Propagation Model, Part 1: Propagation in an Atmosphere without Significant Refraction
DELTA Acoustics & Vibration, Report AV 1849/00 Kgs. Lyngby 2000.
- [11] B. Plovsing, J. Kragh
Nord2000. Comprehensive Outdoor Sound Propagation Model, Part 2: Propagation in an Atmosphere with Refraction
DELTA Acoustics & Vibration, Report AV 1851/00, Kgs. Lyngby 2000
- [12] J. Kragh et al.
Propagation of Wind Turbine Noise. Outline of a Prediction Method
DELTA Acoustics & Vibration, Report AV 320/95, Kgs. Lyngby 1995
- [13] Results of measurements made by DELTA for the Danish Road Directorate
To be published
- [14] ISO 9613-2
Acoustics – Attenuation of sound during propagation outdoors - Part 2: A general method of calculation
- [15] *Noise Emission Measurements and Sound Propagation from Offshore Wind Turbines*
Working Report by DELTA for the Danish Environmental Protection Agency, Copenhagen 2004

**First International Meeting
on
Wind Turbine Noise: Perspectives for Control
Berlin 17th and 18th October 2005**

How the "mythology" of infrasound and low frequency noise related to wind turbines might have developed

Geoff Leventhall
Noise Consultant 150 Craddocks Avenue
Ashted Surrey KT21 1NL UK
geoff@activenoise.co.uk

Summary Objections based on infrasound and low frequency noise, often raised against wind farm developments, arise largely from a misunderstanding of these topics by the general public, for whom the problem has developed through media and related exaggerations. There was a period, about 30 years ago, when each time infrasound and low frequency noise were given publicity, more and more of the "facts" were lost in a cloud of increasing embellishment.

This paper traces some of the history of interest in infrasound and low frequency noise, showing how the misunderstandings have arisen, how they have been used in the past to cause confusion in international politics and are used currently by objectors to wind turbine developments.

Introduction Infrasound and low frequency noise are often raised in objections to the development of wind farms. It is necessary to understand how the concerns might have arisen, so that objectors can be shown that their anxieties are likely to be without foundation. In the UK there has been misrepresentation of the facts of infrasound and low frequency noise, both by objectors and also by some of the noise consultants who support the objectors. It is necessary to re-educate the public in order to remove the misconceptions which have developed.

In the definitions of infrasound and low frequency noise, infrasound is often considered as sound at frequencies below 20 Hz. However, from the subjective point of view, there is no reason for terminating a continuous process of hearing at this arbitrary frequency, so that from about 10Hz to 100Hz could be taken as the low frequency range. It may also be argued that there is no reason for terminating at 100 Hz, and the range is sometimes extended to about 200Hz. But we have to stop somewhere.

Atmospheric infrasound This is a well established discipline, studying frequencies from about one cycle in 1000 seconds up to, say, 2Hz. (Bedard and George, 2000) These infrasounds are caused by weather variations, meteorites, distant explosions, waves on the seashore, practically any occurrence which puts energy into the atmosphere over a relatively short period of time and any process with a low repetition rate, including pressure pulses from wind turbines. The attenuation with distance is very low. Monitoring of atmospheric infrasound is an essential part of ensuring the success of the Nuclear Test Ban Treaty.

Of course, it is important to realise that our evolution has been in the presence of naturally occurring atmospheric infrasound.

The American Space Programme Early work on low frequency noise and its subjective effects was stimulated by the American space programme. It was known that very large launch vehicles produce their maximum noise energy in the low frequency region. Furthermore, as the vehicle accelerates, the crew compartment is subjected to boundary layer turbulence noise for about two minutes after lift off. Experiments were carried out in low frequency noise chambers on short term subjective tolerance to bands of noise at levels of 140dB to 150dB in the range up to 100Hz (Mohr et al., 1965). It was concluded that subjects who were experienced in noise exposure, and who were wearing ear protection, could tolerate both broadband and discrete frequency noise in the range 1Hz to 100Hz at sound pressure levels up to 150dB. Later work suggests that, for 24 hour exposure, levels of 120-130dB are tolerable below 20Hz (von Gierke, 1973; von Gierke and Nixon, 1976). These limits were set to prevent direct physiological damage. It was not suggested that the

exposure is pleasant, or even subjectively acceptable for anybody except those whose work requires them to be exposed to the noise.

Work was also in progress in the UK (Hood and Leventhall, 1971; Yeowart et al., 1969) and France (Gavreau, 1968; Gavreau et al., 1966) from the 1960's and in Japan and Scandinavia from the 1970's (Møller, 1980; Yamada, 1980). Japan and Scandinavia are now the main centres for work on infrasound and low frequency noise. A review of studies of low frequency noise has been given by Leventhall (Leventhall et al., 2003)

Origins of the Mythology The early American work was published in the middle 1960's and did not attract attention from the public, but a few years later *infrasound* entered upon its mythological phase, echoes of which still occur, currently in relation to wind turbines. The main name associated with the early phase is that of Gavreau from CNRS Marseille, whose work was in progress at the same time as that of the American space programme. (Gavreau, 1968; Gavreau et al., 1966). Infrasound from a defective industrial fan led to investigations of infrasonic problems and the design of high intensity low frequency sound sources. Gavreau made some misleading statements, which led to confusion of harmful effects of very high levels at higher frequencies with the effects of infrasound. (Note: According to the definition above, most of the sources developed by Gavreau and his colleagues were not infrasonic.) For example from the 1968 paper on "Infrasound", which was published in a "popular science" journal:

Infrasounds are not difficult to study but they are potentially harmful. For example one of my colleagues, R Levavasseur, who designed a powerful emitter known as the 'Levavasseur whistle' is now a victim of his own inventiveness. One of his larger whistles emitting at 2600Hz had an acoustic power of 1kW.....This proved sufficient to make him a life-long invalid.

Of course, 2600Hz is not infrasound, but the misleading implication is that infrasound caused injury to Levavasseur. A point source of sound power 1kW will produce a sound level of about 140dB at 1m, which is a very undesirable exposure at 2600Hz.

Gavreau's progress Gavreau initially energised his sources in a laboratory, exposing himself and his co-workers to very high levels of noise at relatively high frequencies. For example at 196Hz from a pneumatic "whistle" and 37Hz from a larger whistle. Exposure to the 196Hz source at a level of 160dB¹ led to irritation of internal organs, so that Gavreau and his colleague felt ill for some time following a five minute exposure, which is not surprising. Again from the 1968 paper:

...after the test we became aware of a painful 'resonance' within our bodies – everything inside us seemed to vibrate when we spoke or moved. What had happened was that this sound at 160 decibels..... acting directly on the body produced intense friction between internal organs, resulting in severe irritation of the nerve endings. Presumably if the test had lasted longer than five minutes, internal haemorrhage would have occurred.

196 Hz is not infrasound, but the unpleasant effects are described in a paper which is described as on "Infrasound". Internal haemorrhage is often quoted as an effect of exposure to any infrasound.

The 37Hz whistle was run at a low level, but sufficient to cause the lightweight walls of the laboratory to vibrate. (Some of Gavreau's earlier work had been in the development of pneumatic high intensity ultrasonic sources, so that he merely had to scale up the size).

Gavreau generated 7Hz with a tube of length 24m, driven by either a loudspeaker or a motor- driven piston. He suggested that 7Hz was particularly "dangerous" because the frequency coincided with alpha rhythms of the brain. He also used a tube to generate 3.5Hz, but further details were not given.

However, from the 1968 paper:

The effects of low frequency sound and infrasound are noxious. However, we found one exception: the intense vibration of the nasal cavities produced by our

¹ 160dB is about 2000Pa, or 1/50 of an atmosphere, which is in the non-linear region.

whistle (340Hz, 155 decibels) had favourable effects! In one case, a subject recovered a sense of smell which he had lost some years back and was able to breathe more easily.

Infrasound and the public By present standards, Gavreau's work was irresponsible, both in the manner in which it was carried out and in the manner in which it was described. Today, the experiments on people could lead to prosecution for negligence. Much of the paper with title of 'Infrasound' is not about infrasound. However, the work was picked up by the media and embellished further, including a statement that 7Hz was fatal. There was manipulation, sometimes willing manipulation, of scientists by the media, which was happy to describe all the sources developed by Gavreau as infrasound sources and to attribute all the adverse effects to infrasound, although they were actually due to high levels at frequencies above the infrasonic range.

The misunderstanding between infrasound and low frequency noise continues to the present day. A recent newspaper article on low frequency noise from wind turbines (Miller, 24 January 2004), opens with:

Onshore wind farms are a health hazard to people living near them because of the low-frequency noise that they emit, according to new medical studies.

A French translation of this article for use by objectors' groups opens with

De nouvelles études médicales indiquent que les éoliennes terrestres représentent un risque pour la santé des gens habitant à proximité, à cause de l'émission d'infrasons.

The translation of *low frequency noise* into *infrasons* continues through the article.

This is not a trivial misrepresentation because, following on from Gavreau, infrasound has been connected with many misfortunes, being blamed for problems for which some other explanation had not yet been found (e.g., brain tumours, cot deaths of

babies, road accidents). A selection of some UK press headlines from the early years is:

The Silent Sound Menaces Drivers - Daily Mirror, 19th October 1969

Does Infrasound Make Drivers Drunk? - New Scientist, 16th March 1972

Brain Tumours 'caused by noise' - The Times, 29th September 1973

Crowd Control by Light and Sound - The Guardian, 3rd October 1973

Danger in Unheard Car Sounds - The Observer, 21st April 1974

The Silent Killer All Around Us - Evening News, 25th May 1974

Noise is the Invisible Danger - Care on the Road (ROSPA) August 1974

Absurd statements were made in the book 'Supernature' by Lyall Watson, first published in 1973 as 'A Natural History of the Supernatural' and which has, unfortunately, had a number of reprints and large sales. This book includes an extreme instance of the incredible nonsense which has been published about infrasound. It states that the technician who gave the first trial blast of Gavreau's whistle "fell down dead on the spot". A post mortem showed that "all his internal organs had been mashed into an amorphous jelly by the vibrations". It continues that, in a controlled experiment, all the windows were broken within a half mile of the test site and further, that two infrasonic generators "focused on a point even five miles away produce a resonance that can knock a building down as effectively as a major earthquake".

One can detect a transition from Gavreau and his colleague feeling ill after exposure to the high level of 196Hz to "fell down dead on the spot" and a further transition from laboratory walls vibrating to "can knock a building down", transitions which resulted from repeated media exaggerations over a period of five or six years.

Perhaps the singer David Bowie had read "Supernature". On the 20th September 1977, the London Evening News published an interview with him, giving his views on life, including the following:

"He also expresses fears about America's new Neutron Bomb. 'It was developed along the lines of the French sound bomb which is capable of

destroying an area 25 miles around by low frequency vibration'. According to Bowie, plans for such a bomb are readily available in France and any minor power can get their hands on a copy. Low frequency sounds can be very dangerous. The 'sensurround' effect that accompanied the film 'Earthquake' was achieved by a noise level of nine cycles per second. Three cycles per second lower is stomach bleeding level. Any lower than that and you explode".

We cannot blame the public for their anxiety about infrasound and low frequency noise when they have been exposed to statements like these. Public concern over infrasound was one of the stimuli for a growth in complaints about low frequency noise during the 1970's and 1980's and has continuing effects. It appears that concerns over infrasound and low frequency noise have found a place deep in the national psyche of a number of countries and lie waiting for a trigger to bring them to the surface. Earlier triggers have been gas pipelines and government establishments. A current trigger is wind turbines.

Infrasonic weapons The media follow-up of Gavreau's work led to interest in infrasonic weapons, although these have not been produced, as it is not possible to generate directional infrasound of high enough level to be effective at a distance. For example, to produce 150dB ($1000\text{W}/\text{m}^2$) at 100m distance requires a point source power of about 60MW. At 20Hz, which has a wavelength of about 17m, an efficient directional reflector, which must have dimensions of several wavelengths, is not feasible. However, during the cold war, the Conference of the Committee on Disarmament (see: www.unog.ch), which commenced its work in Geneva in about 1960, and is believed to be still sitting, was presented with a paper from the Hungarian Peoples' Republic (Anon, 1978) which discussed infrasonic weapons and concluded:

".....infrasound can become the basis of one of the dangerous types of new weapons of mass destruction....."

All this leads to the unequivocal conclusion that the scope of the agreement on the prohibition of the development and manufacture of new types of weapons of mass destruction must also be extended to the military use of infrasound weapons of mass destruction....."

An example of an infrasonic weapon was given as a jet engine attached to a long tube – reminiscent of Gavreau's 24m tube, as shown in Fig 1. Of course, the physics is at fault, because the rapid flow of the exhaust gas from the engine will prevent the development of resonance (Leventhall, 1998).

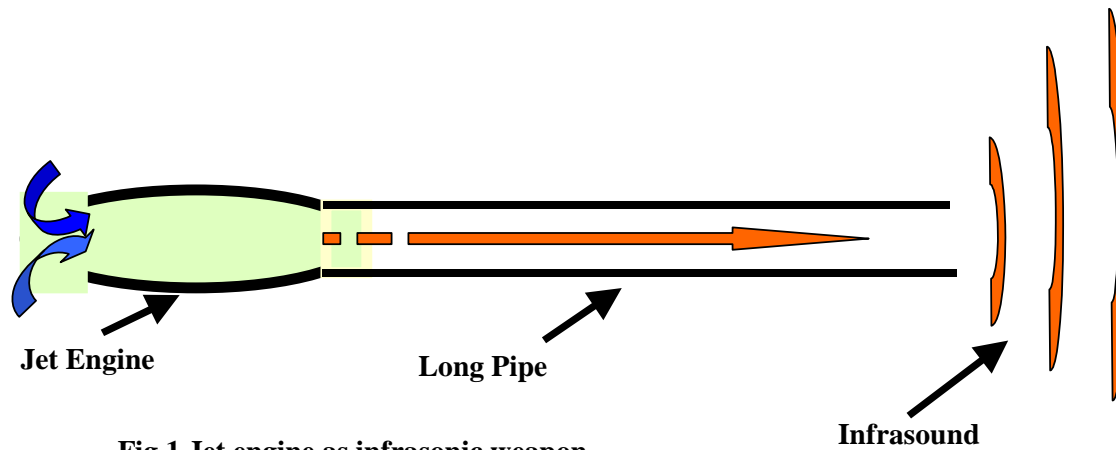
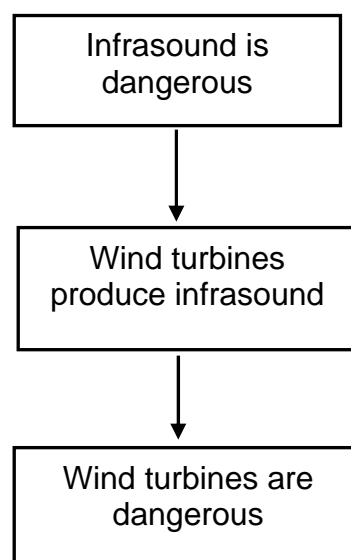


Fig 1 Jet engine as infrasonic weapon

However, after taking advice, the Western powers concluded that infrasonic weapons were a political distraction from the main points of the disarmament negotiations.

In relation to wind turbines, the concept that "infrasound is dangerous" has been absorbed into the minds of objectors, who take a one dimensional view of infrasound. That is, they consider only that it may be present from wind turbines and ignore the very low levels. So we have the relation:



Which objections are pleased to believe and which they make use of in planning applications.

A recent example is from the leaflet from an objectors' group which stated:

"wind turbines still create noise pollution, notably 'infra sound' - inaudible frequencies which nevertheless cause stress-related illness ..."

The wind farm developers referred this statement, and others, to the UK Advertising Standards Authority, which ruled that it was misleading.

What infrasound do we hear? The audibility of infrasound for subjects exposed in infrasonic chambers, has been measured reliably down to 4Hz, Fig 2, is based on work by Watanabe and Møller from 4Hz and on ISO 226 from 20Hz (ISO:226, 2003; Watanabe and Møller, 1990b). The median threshold at 4Hz is 107dB, at 10Hz is 97dB and at 20Hz is 79dB. The standard deviation of the threshold measurements is about 6dB, so that a very small number of people may have 12dB or more greater sensitivity than the median.

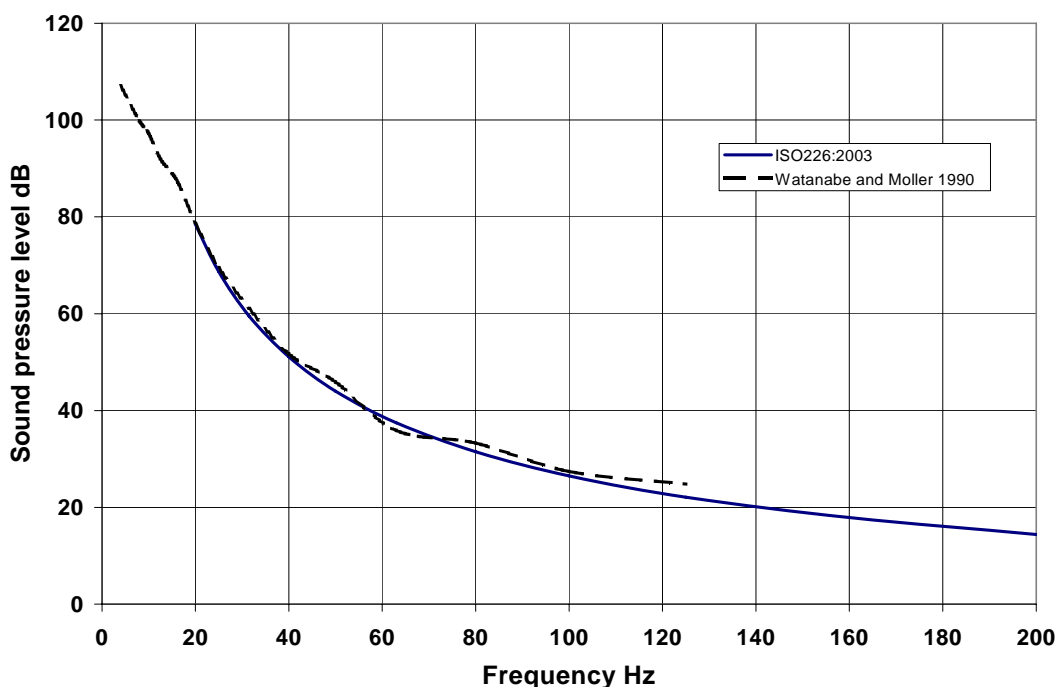


Fig 2. Low frequency threshold

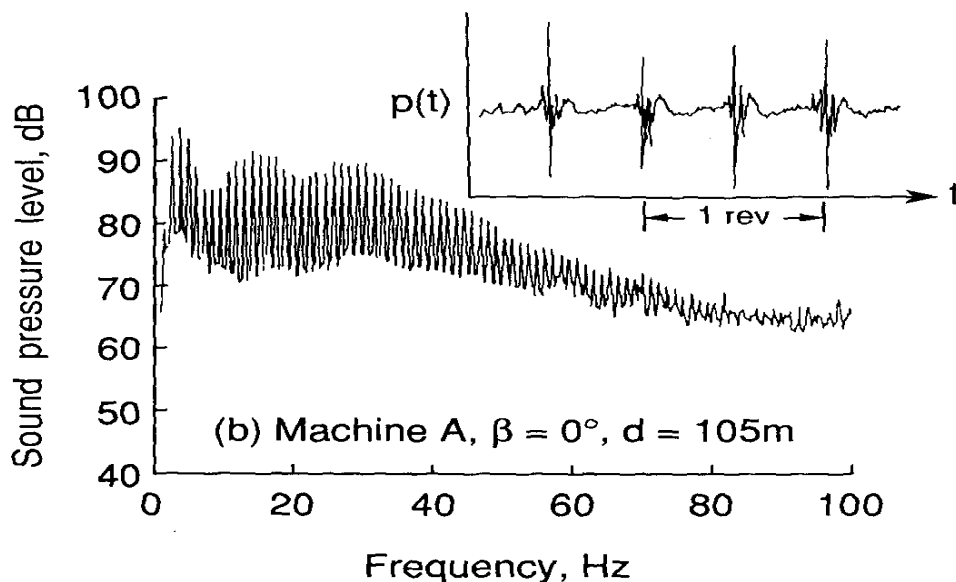
Part of the mythology is that infrasound can be felt but not heard. However, the ear is the most sensitive receptor in the body, as has been shown by threshold measurements on both normal hearing subjects and profoundly deaf subjects, which were carried out down to 8Hz (Yamada et al., 1983). If you can't hear it you can't feel it.

Gavreau (1968) used loud music to show that 7Hz infrasound could be masked by higher frequencies. Initially the sound was throbbing unpleasantly, but

'This musical experiment proved that this infrasound acted through the ears and not directly on the body. Furthermore, any kind of strong audible sound, by reducing the sensitivity of the ear, rendered this infrasound perfectly harmless.'

Gavreau did not give the level of the 7Hz, but it is likely to have been at least 110 - 120dB.

Infrasound and wind turbines As is well known, earlier downwind turbines produced pulses at levels which caused vibration effects in light-weight buildings,



MOD-1 Downwind 1.5MW to 2MW 61m diameter rotor BPF ~ 1Hz

Fig 3 Infrasound from early downwind turbine

occurring twice a revolution from a two bladed turbine, as shown in Fig 3. (Shepherd and Hubbard, 1991)

Any slow train of pulses will analyse as infrasound. For example, pulses occurring once a second, as in Fig 3, will analyse as infrasound with a harmonic series at 1Hz intervals. But it was actually the peak pressure from the pulses which caused transient effects in the buildings, such as rattling of loose components, not the emission of a continuous infrasonic wave. These effects were heard as separate events.

Modern up-wind turbines produce pulses which also analyse as infrasound, but at low levels, typically 50 to 70dB, well below the hearing threshold. Infrasound can be neglected in the assessment of the noise of modern wind turbines (Jakobsen, 2004)

Low frequency noise

There is an easy transition from infrasound to low frequency noise and much of the publicity about infrasound applies equally to low frequency noise. Sometimes the terms are used interchangeably. However, audible low frequency noise does have annoying characteristics which are not shown in conventional environmental noise measures, such as the A-weighting. This has been recognised by the World Health Organisation, which makes a number of references to low frequency noise in its publication on Community Noise (Berglund et al., 2000) with statements such as:

It should be noted that low frequency noise, for example, from ventilation systems can disturb rest and sleep even at low sound levels

For noise with a large proportion of low frequency sounds a still lower guideline (than 30dBA) is recommended

When prominent low frequency components are present, noise measures based on A-weighting are inappropriate

Since A-weighting underestimates the sound pressure level of noise with low frequency components, a better assessment of health effects would be to use C-weighting

It should be noted that a large proportion of low frequency components in a noise may increase considerably the adverse effects on health

The evidence on low frequency noise is sufficiently strong to warrant immediate concern

An example of the difference between responses to low frequency noise/infrasound and other noises is in the growth of annoyance, illustrated in Fig. 4.

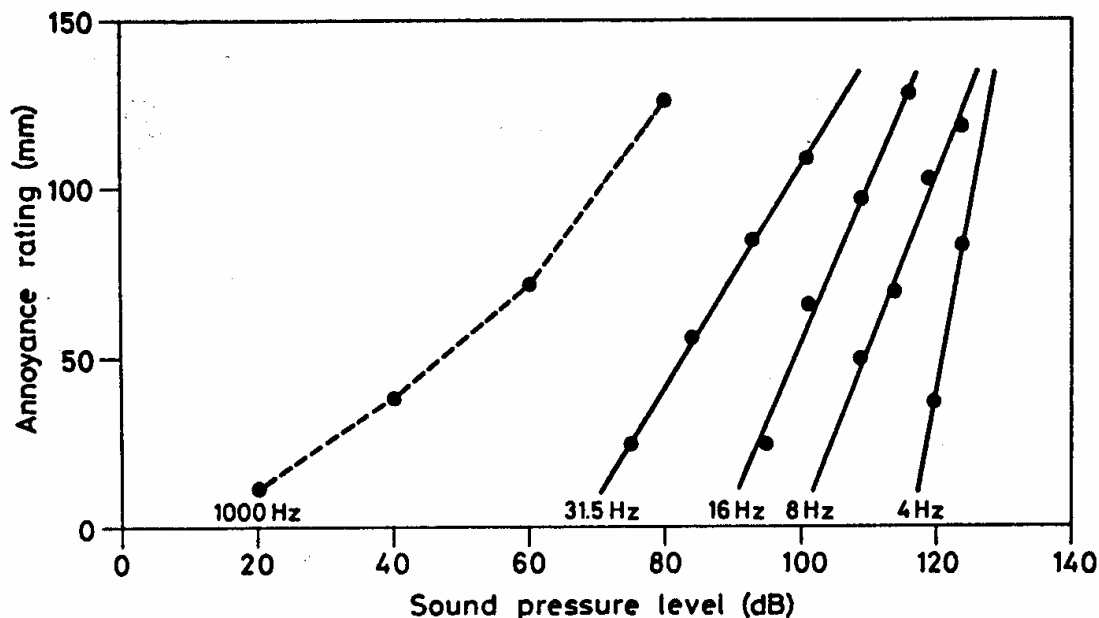
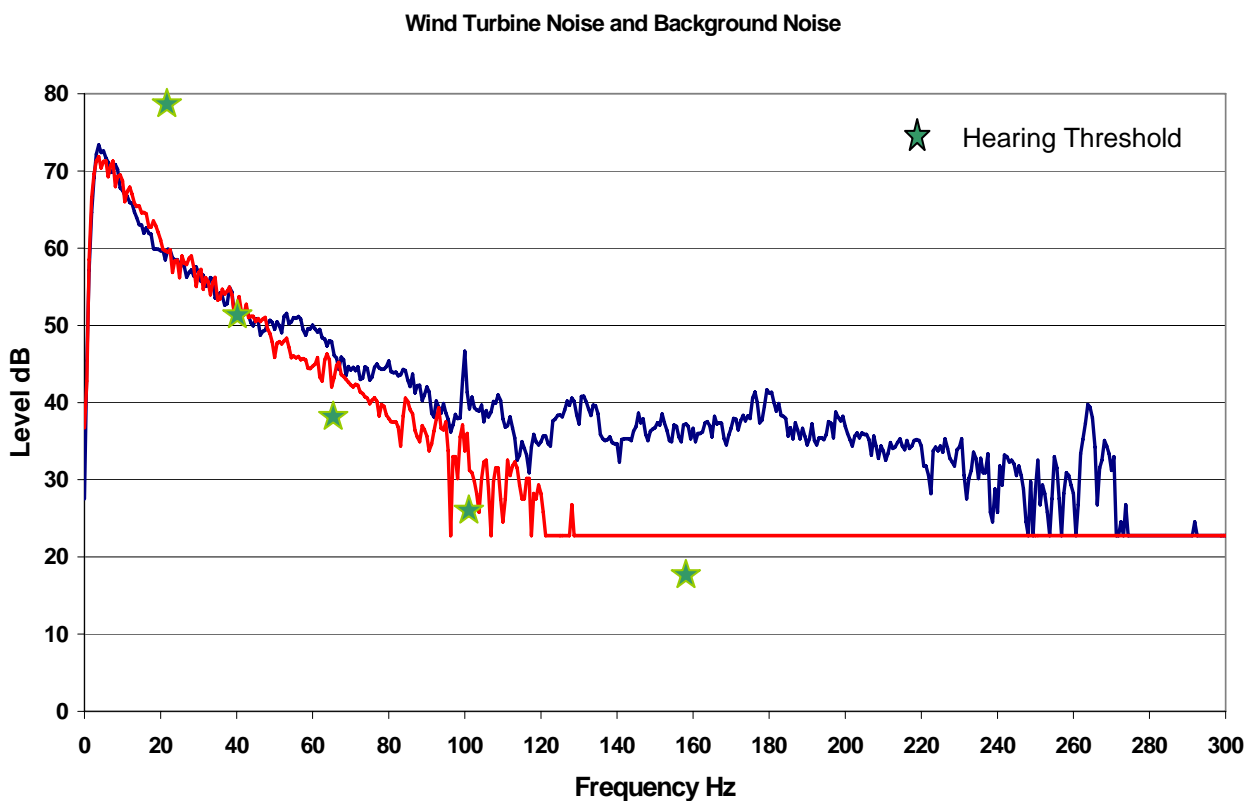


Fig 4 Growth of annoyance at low frequencies

Although low frequency tones require a higher level for the on-set of perception, their annoyance rating increases more rapidly with level. At 4Hz the range of annoyance is covered in a rise of about 10dB, compared with about 50dB at 1000Hz. Annoyance does not normally commence until the tone is 5 to 10dB above its threshold.

The concerns of the WHO on low frequency noise require us to look carefully at low frequency noise from wind turbines. In general, there is not a problem, although the mythology is that wind turbine noise has a substantial low frequency component.

This may be a misunderstanding of the "swish – swish - swish", at about once a second, which is typical of wind turbines. However, the swish is a modulation of a higher frequency, typically in the 500Hz to 1000Hz range, and does not contain low frequencies or infrasound. An analogy is with an amplitude modulated radio wave, which contains only the carrier and side bands, not the modulation frequency.



**Fig 5 Wind turbine noise — and background noise —
65m distance. wind speed at hub ~ 15m/s**

All wind turbines produce low frequencies, mainly mechanical noise, which has been reduced to low levels in modern turbines, but there are also circumstances in which turbines produce increased levels of low frequency noise. This is mainly when the

inflow air to the turbine is very turbulent and there are interactions between the blade and the turbulence.

Fig 5 shows the infrasonic and low frequency noise at 65m from a 1.5MW wind turbine on a windy day. The following should be noted.

- The fall off below about 5Hz is an instrument effect. The background noise actually increases down to the frequencies of atmospheric pressure variations .
- Frequencies below 40Hz cannot be distinguished from background noise due to wind.
- The wind turbine noise and background noise separate above about 40Hz and both rise above the median hearing threshold.
- The measurements were taken at 65m. Levels are likely to be about 15dB lower at normal separation distances

On the occasions, such as turbulent inflow conditions, when low frequency noise is produced by wind turbines, it may not be perceived as a noise, but rather as an unidentified adverse component in the environment, which disappears if the turbines stop, or if the inflow conditions change. This is because we are not accustomed to listening to low levels of broad band low frequency noise and, initially, do not always recognise it as a "noise", but more as a "disturbance" in the environment.

Conclusions. Specialists in noise from wind turbines have work to do in educating the public on infrasound and low frequency noise. Specifically,

- Infrasound is not a problem,
- Low frequency noise may be audible under certain conditions,
- The regular 'swish' is not low frequency noise.

Advice to objector groups in this connection could be that, by dissipating their energy on objections to infrasound and low frequency noise, they are losing credibility and, perhaps, not giving sufficient attention to other factors.

References

- Anon (1978): Conference of the Committee on Disarmament. *Paper CCD/575 14 August 1978*.
- Bedard, A. J., and George, T. M. (2000): Atmospheric Infrasound. *Physics Today* **53** (3), 32 - 37.
- Berglund, B., Lindvall, T., Schwela, D., and Goh, K.-T. (2000): Guidelines for Community Noise. *World Health Organisation*.
- Gavreau, V. (1968): Infrasound. *Science Journal* **Vol 4**, 33-37.
- Gavreau, V., Condat, R., and Saul, H. (1966): Infra-sons: generateur, detecteurs, proprietes physique, effets biologiques. *Acustica* **17**, 1-10.
- Hood, R. A., and Leventhall, H. G. (1971): Field measurement of infrasonic noise. *Acustica* **25**, 10-13.
- ISO:226 (2003): Acoustics - Normal equal-loudness contours.
- Jakobsen, J. (2004): Infrasound emission from wind turbines. *Proc 11th International Meeting on Low Frequency Noise and Vibration and its Control, Maastricht August 2004*, 147 to 156.
- Leventhall, H. G. (1998): The infrasonic weapon revisited. *Noise and Vibration WorldWide*, 22 - 26.
- Leventhall, H. G., Benton, S., and Pelmear, P. (2003): A review of published research on low frequency noise and its effects. *Prepared for Defra* <http://www.defra.gov.uk/environment/noise/research/lowfrequency/index.htm>.
- Miller, C. (24 January 2004): Wind farms 'make people sick who live up to a mile away'. *Sunday Telegraph*.
- Mohr, G. C., Cole, J. N., Guild, E., and Gierke, H. E. v. (1965): Effects of low frequency and infrasonic noise on man. *Aerospace Medicine* **36**, 817-824.
- Møller, H. (1980): The influence of infrasound on task performance. *Proc Conference on low frequency noise and hearing. Aalborg, 1980*.
- Shepherd, K. P., and Hubbard, H. H. (1991): Physical characteristics and perception of low frequency noise from wind turbines. *Noise Control Eng* **36**, 5 -15.
- von Gierke, H. E. (1973): Effects of infrasound on man. *Proc. Colloquium on Infrasound. CNRS, Paris, 1973*, 417 - 435.
- von Gierke, H. E., and Nixon, C. (1976): Effects of intense infrasound on man. In: *Infrasound and Low Frequency Vibration*. Editor: W Tempest. Academic Press.
- Watanabe, T., and Møller, H. (1990b): Low frequency hearing thresholds in pressure field and free field. *Jnl Low Freq Noise Vibn* **9**, 106-115.
- Yamada, S. (1980): Hearing of low frequency sound and influence on the body. *Conference on Low Frequency Noise and Hearing, Aalborg, Denmark*, 95-102, (Editors: H Møller and P Rubak).
- Yamada, S., Ikuji, M., Fujikata, S., Watanabe, T., and Kosaka, T. (1983): Body sensations of low frequency noise of ordinary persons and profoundly deaf persons. *Jnl Low Freq Noise Vibn* **2**, 32-36.
- Yeowart, N. S., Bryan, M. E., and Tempest, W. (1969): Low frequency noise thresholds. *J Sound Vibration* **9**, 447-453.

**First International Meeting
on
Wind Turbine Noise: Perspectives for Control
Berlin 17th and 18th October 2005**

***Constrained Aerodynamic & Aeroacoustic Design
of Wind-Rotor Airfoils***

Th. Lutz, A. Herrig, W. Würz, K. Braun, E. Krämer
Institute of Aerodynamics and Gas Dynamics (IAG),
University of Stuttgart, Pfaffenwaldring 21, D-70550 Stuttgart
{lutz, herrig, wuerz, braun, kraemer}@iag.uni-stuttgart.de

Summary

The EU-funded research project SIROCCO aims on the reduction of the blade trailing-edge noise which represents the dominant noise source of modern wind turbines. This objective is followed by the design of new silent airfoils for the outer part of the blade. The present paper describes the staggered design procedure applied which involves parametric investigations, constrained numerical optimizations and a manual fine-tuning using a mixed-inverse design procedure. To enable a consistent noise prediction the aerodynamic calculation procedure had to be extended in order to better account for boundary-layer history and anisotropy effects and to improve the prediction of the relevant turbulence length scale. The enhanced method was validated and applied in the design of two airfoils which were wind-tunnel tested and showed the predicted acoustic gain and the intended aerodynamic performance.

1. Introduction

Even though the implementation of wind parks is steadily growing, the noise emission is one of the major obstacles for a further spread of onshore wind turbines and significantly limits public acceptance. Tightened noise regulations force the wind turbine manufacturers to make serious efforts in noise reduction by design of silent blades.

Wind turbines possess different sources of noise emission. While mechanical noise, e.g., generated by the gear box, can efficiently be reduced by well-established engineering approaches, the flow-induced noise is more complex to comprehend and eliminate, and, therefore, represents the current focus for further noise reduction. Different flow-induced noise sources can be distinguished, e.g. tip noise, inflow-turbulence noise, blunt trailing-edge noise or turbulent boundary-layer trailing-edge interaction noise, subsequently denoted trailing-edge noise. These particular noise sources were investigated in the frame of previous EU-funded research projects

(STENO, DRAW, DATA). Furthermore, noise prediction schemes for airfoils and 3D rotating blades were developed. The investigations showed that, as long as the blade tips are adequately shaped and the freestream turbulence level is moderate enough that inflow noise is not pronounced, the trailing-edge noise remains the most dominant noise source of modern wind turbines. This broadband noise stems from an interaction of turbulent eddies, i.e. unsteady events within the boundary-layer, and the trailing edge of the blade. The turbulence properties in the vicinity of the trailing edge are dependent on the boundary-layer development which is determined by the onset flow conditions and the pressure distribution along the blade sections. Therefore, the noise emission can be influenced and finally reduced by adequate shaping of the blade airfoil sections. This was demonstrated in the DATA project for clean airfoils with extended laminar flow regions [5].

During most of the operation time the leading edges of the blades, however, are contaminated by dirt, insects or erosion which yields premature laminar to turbulent transition. As a consequent next step the noise reduction potential for “rough” blades is currently investigated in the EU-funded SIROCCO project (Silent ROTors by aCoustic Optimization), see [17]. The partners involved at the beginning of the project were two manufacturers, namely GAMESA and NOI, along with CTC, ECN, NLR and the IAG (University of Stuttgart). After the insolvency of NOI, GE Wind Energy joined the project.

The main objective of this project is to design new airfoil shapes for the outer part of the blades that show reduced total sound pressure level without loss in aerodynamic performance. Since the performance of the new airfoils shall be demonstrated in field tests on two full-scale wind-turbines [15], [17], all relevant aerodynamic and geometric constraints were to be considered during the airfoil design. Beside the enhancement of the prediction methods, the challenge of this task was to consider all these constraints in a combined aerodynamic and aeroacoustic airfoil design. For this purpose, a multi-stage design and optimization process was accomplished. In a first step, systematic variations of the reference airfoils were analysed in order to obtain experience about the main design drivers for the acoustic airfoil design. In a next phase, constrained numerical optimizations were performed with the objective to minimize the total sound pressure level while keeping all geometric and aerodynamic requirements as prescribed by the industry partners. For this purpose the optimization environment POEM, developed at the IAG, was extended and applied. Finally, a manual modification phase using inverse and mixed-inverse design procedures was initiated to account for critical airfoil characteristics that are hard to predict, like stall- and post-stall behaviour.

In the present paper the main features of the optimization tool, the noise prediction method along with enhancements achieved during the SIROCCO project, will be outlined. Two new airfoil designs will be discussed and recent acoustic validations will be given which quantify the gain compared to existing airfoils and approve the consistency of the enhanced prediction method.

2. Numerical Optimization Environment POEM

With direct numerical optimization (DNO) an automated, computer-based, search for an optimal solution w.r.t. a given scalar objective function is performed. The objective function may be the drag - or in case of the SIROCCO project the noise level - at a certain design point or a weighted mean for a complete design range. The optimization is accomplished by means of a more or less systematic variation of the design variables which parameterize the shape to be optimized.

At the IAG the modular optimization environment POEM is being developed [10], [11], [13], [14], [18] which enables the constrained aerodynamic optimization of 2D or 3D configurations, compare Fig. 1. As optimization algorithm, first of all, an evolution strategy with derandomized covariance matrix adaption (CMA-ES) is implemented [6]. Furthermore, the commercial optimization software EPOGY [20] can be utilized. The latter involves various strategies including genetic algorithms, downhill simplex and gradient methods. Currently this software is replaced by the process integration and optimization tool iSIGHT which contains, among others, the same hybrid optimizer kernel as EPOGY.

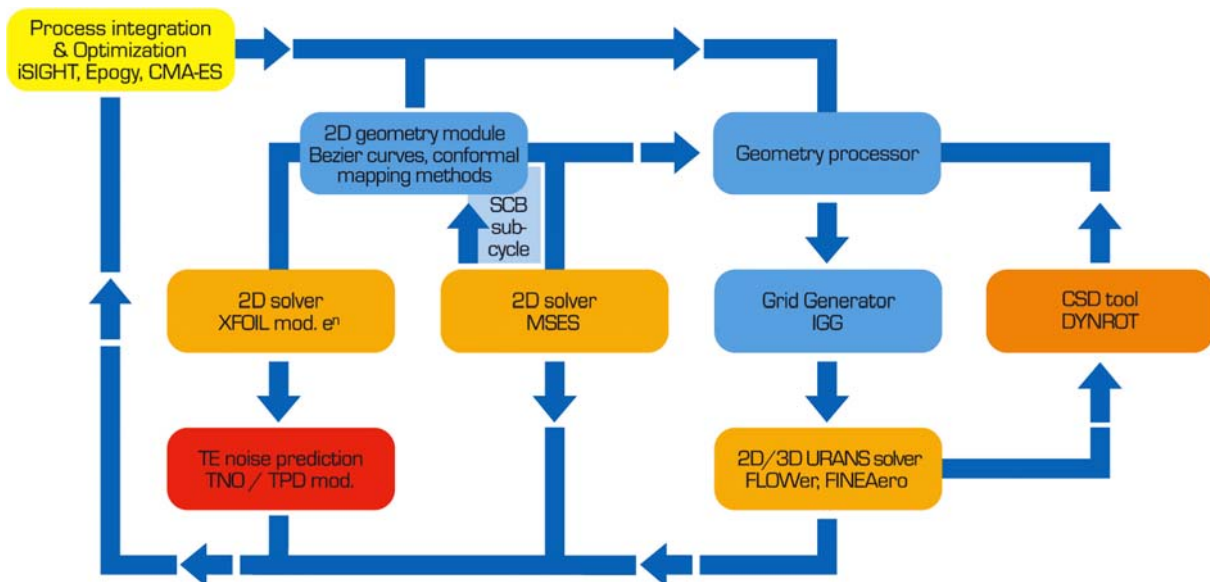


Fig. 1: Optimization environment POEM.

The 2D geometry module contains various direct and indirect parameterization techniques. To generate the contour of airfoil-like shapes, BEZIER-curves and different conformal mapping methods are implemented. For the present investigations a BEZIER representation of complete airfoils or certain parts of it was chosen with the ordinate values of the corresponding control polygon being used as design variables. To analyse the aerodynamic quality of subsonic airfoils the highly efficient coupled panel boundary-layer code XFOIL [4] was included in the optimization tool. To determine the laminar to turbulent transition location, an e^n data-base method was linked to the XFOIL code with the data-base being derived from extensive parametric linear stability analyses [12].

For transonic airfoil optimizations the coupled EULER boundary-layer code MSES [3] and the structured RANS code FLOWer [9] were implemented. The latter flow solver

can also be applied for 3D aerodynamic optimizations [10]. Recently, the POEM tool was extended to account for aeroelastic effects during the analysis and optimization of elastic wings and aircraft. [11].

To consider all geometric and aerodynamic requirements as requested by the industry partners, the available set of optional constraints was extended during the SI-ROCCO project. Among others, it is enabled to constrain the drag, moment or lift coefficient, the lift curve, the transition or separation locations and several geometrical limitations by adding a penalty function to the objective function value.

3. Aerodynamic and Noise Prediction Scheme

To enable aeroacoustic airfoil optimizations, a module for the trailing-edge noise prediction was implemented and linked to the XFOIL airfoil analysis code used for the present airfoil designs. Following a theory proposed by Chandirami [2] and Blake [1], the basic noise prediction scheme chosen was developed by TNO-TPD within the EU project DRAW [16]. According to this method the spectrum of the trailing-edge far-field noise can be determined once the mean velocity profile and the relevant turbulence properties in the vicinity of the trailing edge are known. More precisely, the distributions of the rms-value of the auto-correlation of the turbulent vertical velocity fluctuations $\overline{v'^2}$, the turbulence energy k_T and the vertical integral length scale Λ_2 are required.

If the noise prediction is based on the results of the integral boundary-layer procedure implemented in the XFOIL code, first of all, the boundary-layer profile has to be approximated from the calculated integral parameters like displacement thickness δ_1 , momentum thickness δ_2 or skin friction coefficient c_f . In the present implementation, the mean velocity profile can be approximated by either a COLES Law of the Wall combined with the Law of the Wake representation or an approach proposed by Swafford [19]. The parameters of these analytical profile families are iterated until the corresponding integral boundary-layer parameters match the values resulting from the XFOIL analysis. Once the mean velocity profile is known, the required turbulence properties are estimated by means of a mixing-length approach following the TNO-TPD prediction scheme [16].

This prediction scheme represents an elegant and very efficient approach that has turned out to yield rather reasonable results at least for “usual” types of airfoil pressure distributions. The approach was successfully applied for the aeroacoustic design of less noisy natural laminar flow (NLF) airfoils during the DATA project [5]. However, one should be aware that with the method described above the turbulence properties, which have a decisive impact on the predicted noise spectrum, are derived by means of a mixing-length approach. This approach is based on an evaluation of the *local, approximated* mean velocity profile. The streamwise development of the turbulent fluctuations and the growth of the turbulent eddies are not calculated *directly*, i.e. turbulence history effects are not considered explicitly. Moreover, this history effect also affects the anisotropy of the turbulence, i.e. the differences of the amplitudes of the turbulent fluctuations in streamwise, crosswise and wall-normal direction. The anisotropy, however, is only considered by a constant empirical anisotropy factor. For these reasons it was expected that the range of applicability is more or less limited to

equilibrium boundary layers but inaccuracies may show up for “unusual” types of pressure distributions with regions of strong flow deceleration or acceleration. Actually, this problem led to a first set of airfoil designs that did not achieve the predicted acoustic gain in the acoustic wind-tunnel tests [17]. Comparisons to detailed boundary-layer experiments and aeroacoustic measurements performed later on confirmed this tendency. Therefore, the methodical developments within the SIROCCO project aimed at the improvement in the prediction of the relevant turbulence properties that are required for the noise prediction and to enhance the link between aerodynamic and aeroacoustic prediction based on detailed experiments [8] in the Laminar Wind Tunnel (LWT) of the IAG [22].

In practical airfoil analysis both, history and anisotropy effects can be considered by means of a REYNOLDS-averaged NAVIER-STOKES solver (RANS) or a Finite-Difference (FD) boundary-layer procedure in combination with a nonlinear non-algebraic turbulence model or a complete REYNOLDS-stress turbulence model. Because RANS-solvers usually require too much computation time for the purpose of high-degree-of-freedom optimizations, the more efficient FD-code EDDYBL, developed by Wilcox [21], was coupled to the present prediction scheme. EDDYBL offers a great variety of different turbulence models. For the present investigations the most promising candidate, namely the Wilcox stress- ω turbulence model has been chosen that provides the complete REYNOLDS-stress tensor [21]. This means anisotropy effects are considered and the $\overline{v'^2}$ distribution as required for the noise prediction is calculated directly. With FD-codes the boundary-layer and the turbulence equations are solved on a computational grid with discretisation in streamwise and in wall normal direction. As a result, these methods provide the distribution of the mean velocity and also the distributions of some turbulence properties at each streamwise station. The initial and the boundary conditions along the boundary-layer edge have to be specified. These properties are determined by a preceding XFOIL analysis that takes the boundary-layer displacement effect into account by a simultaneous solution of the coupled potential flow and integral boundary-layer equations.

A second quantity which has a decisive impact on the predicted noise spectrum is the vertical integral length scale Λ_2 [1] which is defined as the integral of the normalized spatial two-point correlation of the vertical fluctuations. Λ_2 is related to the vertical extend of the turbulent eddies. This quantity, however, is not provided by any established turbulence model or boundary-layer procedure. Rather, a scalar quantity is determined that somehow characterizes the size of the energy-bearing eddies. The definition of this turbulence length scale L differs from turbulence model to turbulence model and is physically not explicitly related to the required length scale Λ_2 . To overcome this problem, commonly, the calculated value of L is multiplied by an empirical constant in such a way that the predicted noise spectrum finally fits to experimental results.

Within the present investigations such an “aeroacoustic” scaling and adaptation was avoided. Instead, a direct scaling based on measured Λ_2 distributions was derived. For this purpose detailed boundary-layer measurements for different airfoil sections at several onset flow conditions were conducted in the LWT [7], [8]. Using two miniature split-film probes, distributions of the two-point correlation of the vertical fluctuations were measured and integrated to obtain the Λ_2 distribution across the boundary layer. When comparing the predicted distributions for the turbulence length scale L to

the measured Λ_2 values it became obvious that a constant scaling factor is not sufficient to obtain good agreement for all test cases examined. In general, for “heavily” loaded boundary layers (e.g. fully turbulent flow along the suction side of an airfoil at high lift) Λ_2 is underpredicted with a constant average scaling factor, whereas the tendency is vice versa for “lightly” loaded boundary layers. An improvement could be achieved by relating the Λ_2 distribution to the predicted turbulence energy k_T and the dissipation ε rather to scale the length scale L . To minimize the deviations, the experimental data base was used to derive an empirical scaling law that takes the boundary-layer development into account. Scaling laws were correlated for the extended approach based on the FD boundary-layer analysis as well as for the simplified scheme based on an integral boundary-layer procedure.

4. Validation Examples

Both, the basic prediction method available at the beginning of the SIROCCO project and the enhanced method (Sec. 3) were validated w.r.t. the determination of turbulence properties being relevant for the noise prediction. For this purpose a special wind-tunnel model with variable shape in the rear part was designed [7]. The shape variant with a concave type of main pressure recovery, denoted VTE KAV, shows a strong and steep pressure recovery on the suction side with the turbulent boundary layer being not far from separation. This represents a very challenging test case for any prediction method. Detailed boundary-layer experiments were conducted using single wire and x- hot wire probes and compared to the predictions. As an example, Fig. 2 shows a comparison for the suction side of the VTE KAV airfoil in the vicinity of the trailing edge. The transition was fixed to 5% chord. The dashed lines give the results obtained from an evaluation of the integral boundary-layer properties (Coles profile) predicted by the original XFOIL code. The solid lines, on the other side, represent the results achieved by a subsequent EDDYBL analysis applying the stress- ω turbulence model. Even though small deviations result for the mean velocity profile, the extended method gives an excellent agreement to the measured distribution of the turbulent streamwise fluctuations $\overline{u'^2}$ and thus adequately captures the anisotropy.

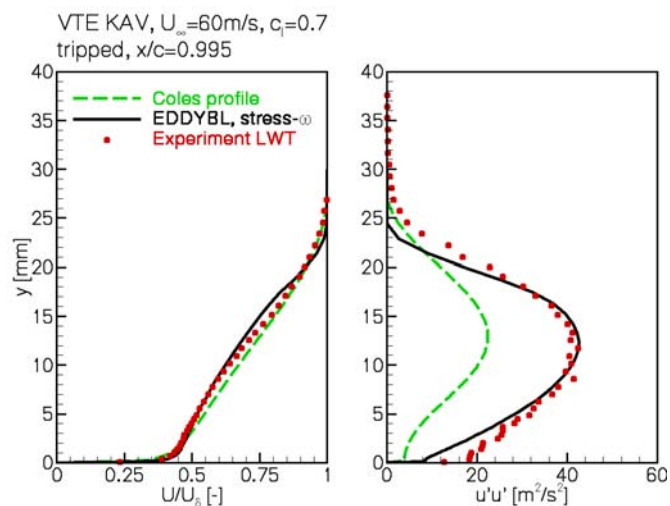


Fig. 2: Predicted and measured boundary-layer properties for the tripped VTE KAV airfoil ($x_{tr}/c=0.05$).

Detailed boundary-layer experiments were conducted using single wire and x- hot wire probes and compared to the predictions. As an example, Fig. 2 shows a comparison for the suction side of the VTE KAV airfoil in the vicinity of the trailing edge. The transition was fixed to 5% chord. The dashed lines give the results obtained from an evaluation of the integral boundary-layer properties (Coles profile) predicted by the original XFOIL code. The solid lines, on the other side, represent the results achieved by a subsequent EDDYBL analysis applying the stress- ω turbulence model. Even though small deviations result for the mean velocity profile, the extended method gives an excellent agreement to the measured distribution of the turbulent streamwise fluctuations $\overline{u'^2}$ and thus adequately captures the anisotropy.

In a next step the predicted noise spectra were verified. For this purpose a set of different airfoils considered in the SIROCCO project and within previous investigations were examined in the LWT applying the new CPV method [23]. As an exemplary re-

sult the predicted and measured spectra for an airfoil with natural transition and tripped boundary layer respectively are compared in Fig. 3. It should be mentioned that the shift in the absolute noise level between the experiments and the predictions stems from different distance laws that were used to map the noise spectrum to a fictive standard observer position. It can be seen that the extended method gives rather good results for the relative differences between the spectra for the clean and the tripped case as well as for the shapes of the spectra, and the crossing points do also match. The results obtained with the simplified approach are less consistent. Altogether, the validation showed that the extended method is much more consistent compared to the former noise prediction based on calculated integral boundary-layer parameters. In particular, the new method was able to reproduce the relative differences in the noise spectra for the complete set of airfoils considered in the acoustic LWT tests so far, see also Sec. 5. This is an important requirement for the use within an acoustic airfoil design.

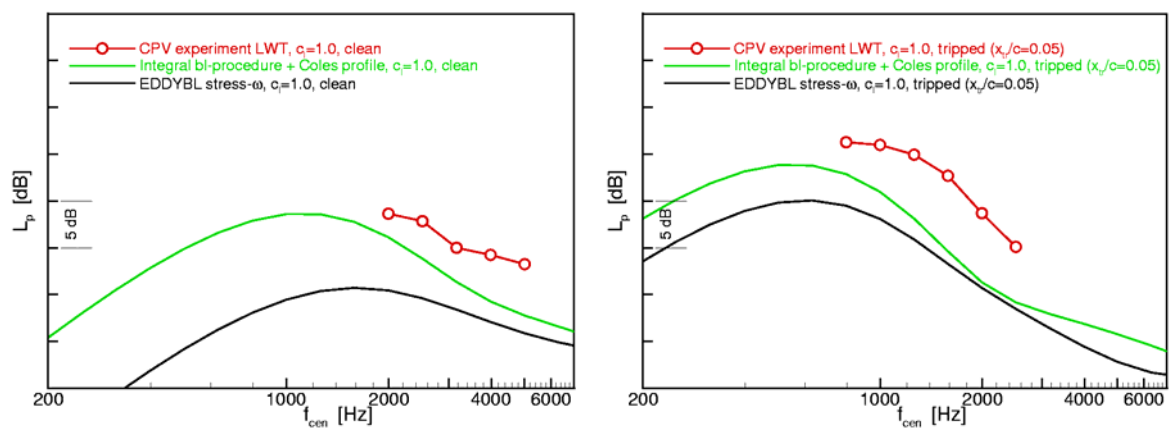


Fig. 3: Predicted and measured noise spectra of a clean and a tripped airfoil at $U_\infty=60\text{m/s}$, $c=0.4\text{m}$, $c_l=1.0$.

5. Airfoil Design and Verification

As a starting point for the new airfoil designs, the industry partners defined a reference section of the selected baseline turbines along with detailed aerodynamic and aeroacoustic design objectives. Since in the frame of the SIROCCO project existing blades shall be modified by implementing more silent airfoils in the outer part of the blades, severe geometric and aerodynamic constraints had to be considered in the design process. To minimize the costs for the fabrication of the new full-scale blades, use of existing blade moulds or beams should be made as much as possible. This put severe constraints on the geometric freedom of the airfoil design and, for example, on the acceptable shift of the lift curve compared to the reference airfoils. For obvious reasons, this limits the achievable gain.

The main design objective was to minimize the A-weighted total sound pressure level (SPL) for fully turbulent flow while constraining the drag level to avoid a loss in performance compared to the reference airfoils. Each industry partner specified an individual set of design points. The focus of the present project was not on an improvement for clean conditions, i.e. for natural laminar to turbulent transition, but during the

design it was ensured that at least the aerodynamic performance of the reference airfoils was achieved for clean conditions as well. For fully turbulent flow and because the main design lift coefficients were rather high, the value of the total SPL is dominated by the noise contribution of the thick suction side boundary layer which yields a peak in the spectrum in the low frequency domain (below 1 kHz), compare Fig. 5. Therefore, in order to minimize the *total* SPL, the noise level had to be reduced particularly in the low frequency range. Preliminary investigations showed that this could only be achieved at the expense of a slightly increased noise level at medium to high frequencies, compare results in Fig. 5. To enable a sound assessment and wind-tunnel verification of the new airfoil designs it was therefore important to check the measurable lower frequency bound and to improve the accuracy of the acoustic test methods for the lower frequency domain at an early stage of the project. The importance of this can be seen from Fig. 4 where the resulting gain of one new airfoil compared to the reference section is plotted vs. the lower cut-off frequency used during the evaluation of the experimental CPV results obtained in the LWT.

After the capability to measure down to the expected peak frequency was assured, a parametric design study was conducted to examine the impact of relevant geometric airfoil parameters and the shape of the main pressure recovery on the SPL. Thereafter, numerical optimization runs applying the POEM tool (Sec. 2) were performed considering all the geometric and aerodynamic constraints specified by the industry partners. Because an evolution strategy was used for the present high-degree-of-freedom optimizations a huge amount of airfoils had to be generated and analyzed which typically ranges in the order of 20000 designs for each optimization run. Supplementary optimization runs with eased restrictions gave insight into the impact of individual constraints on the achievable noise reduction and the resulting airfoil characteristics.

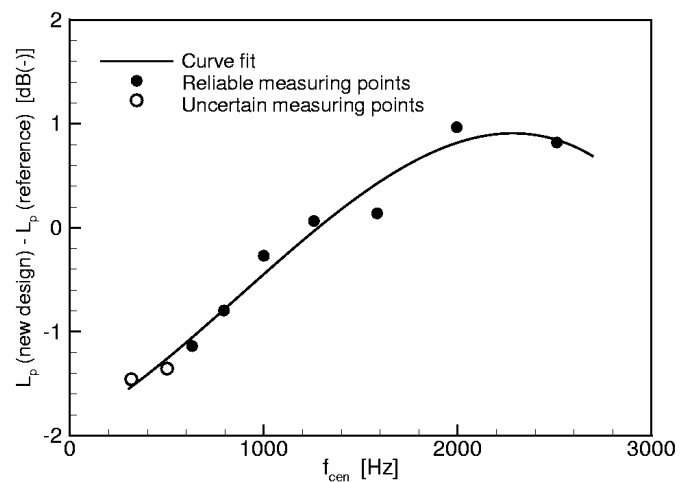


Fig. 4: Difference in total sound pressure level between one new design and the reference airfoil in dependency of the lower cut-off frequency for the noise measurement.

It is not reasonable to consider all intended design objectives especially w.r.t. off-design behaviour, e.g. stall- and post-stall characteristics in the numerical optimization process. This would increase the number of imposed constraints to an irrational amount and strongly increase the computational effort. Moreover, the optimization result may very much depend on the capability of the analysis method to accurately predict the aerodynamic characteristics near maximum lift where the flow is dominated by massive separation. Available prediction methods, however, require profound experience in the interpretation and assessment of the results for this region. These aspects are better considered in a subsequent manual “fine-tuning” phase. Therefore, the numerical optimization results were revised to consider the off-design behaviour and the performance for clean conditions making use of XFOIL’s mixed-

inverse design capability. Moreover, RANS simulations were performed to give additional information about the predicted boundary-layer characteristics in the main design region.

Two complete airfoil design cycles were performed for each baseline turbine. During the first design round the basic prediction method was applied while the enhanced approach (Sec. 3) was available for the second design round. Design round 1 failed in a sense that noise reductions as predicted with the simplified method could not be realized in the acoustic wind-tunnel tests. The resulting designs along with the related aerodynamic and aeroacoustic tests, however, gave valuable insights in the acoustic airfoil design and the mechanism of the noise generation and justified the effort spent to develop the extended calculation method. With the enhanced method the characteristics of the design round 1 airfoils could accurately be reproduced.

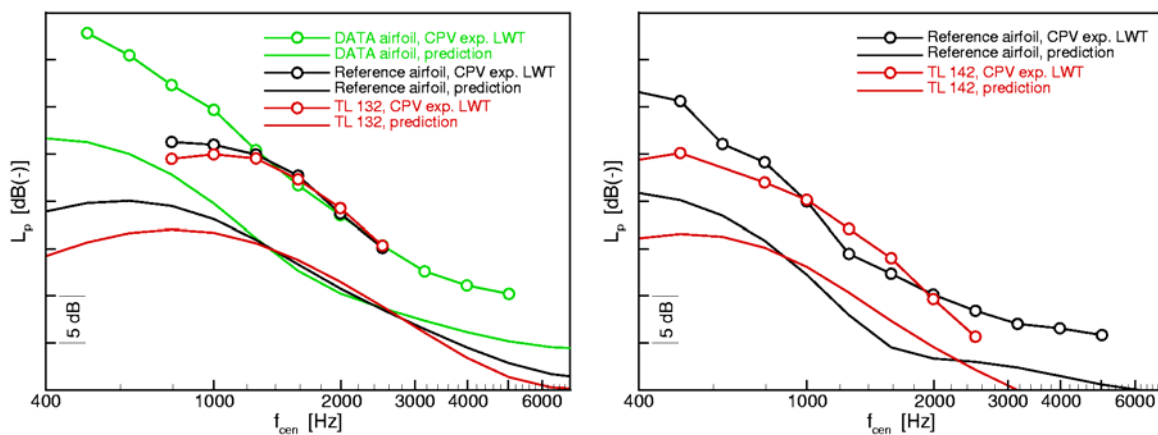


Fig. 5: Predicted and measured noise spectra of the new airfoil designs compared to their reference sections, $U_\infty=60\text{m/s}$, $c=0.4\text{m}$, $c_t=1.0$, tripped conditions ($x_{tr}/c=0.05$).

Applying the new method in round 2 both airfoils designed so far, showed the predicted acoustic gain which is, for tripped conditions, in the order of 1~1.5dB for one airfoil and about 2.5dB for the other design. Fig. 5 gives a comparison of the predicted spectra and the CPV measurements obtained in the LWT for both airfoils and their respective reference sections. It is obvious that the calculations quite accurately reproduce the shapes of the spectra and the relative differences between the airfoils. Amazingly, even details like the upper and lower crossing frequency and the overlapping of the compared spectra are exactly predicted. The aerodynamic wind-tunnel tests, which shall be not discussed in the present paper, moreover proved that the new less noisy airfoils show at least the high performance of the reference sections and that all aerodynamic constraints could be realized. On the left hand diagram of Fig. 5 the spectrum of one airfoil examined in the DATA project is added. This airfoil was designed to feature reduced noise for *clean* conditions. Two conclusions can be drawn from a comparison of the spectra. Firstly, the acoustic airfoil design has to be performed specifically for the respective onset flow conditions and, secondly, the reference airfoil depicted in the left diagram already shows excellent behaviour for fully turbulent flow which reduces the achievable gain.

6. Conclusion

Detailed boundary-layer experiments and acoustic measurements in the LWT approved the importance of an accurate calculation of the relevant turbulence properties required for a consistent prediction of the airfoil trailing-edge noise. The conclusion drawn from the comparison of measurements and predictions was that the calculation of the boundary-layer properties required as input for the noise prediction should consider history, non-equilibrium and anisotropy effects. Moreover, a correct scaling of the calculated turbulence length scale to the vertical integral length Λ_2 as needed for the present noise prediction, turned out to be most important and confirmed the need for the derivation of a new scaling law. Based on recent experiments, a semi-empirical approach was developed. The available theoretical model was extended to account for the mentioned aspects without significant loss in efficiency. The enhanced tool was applied in the design of new less noisy airfoils taking severe aerodynamic and geometric constraints into account to enable the implementation in the outer part of existing wind turbine blades. Detailed wind-tunnel tests verified the predicted gain and demonstrated the accuracy and consistency of the new method.

Acknowledgement

This work was supported by the European Commission in the frame of the SIROCCO project [ENK5-CT-2002-00702]. The authors would like to acknowledge the EU for the funding of this research and the project partners for the good and fruitful cooperation.

References

- [1] W. Blake: *Mechanics of Flow-Induced Sound and Vibration Vol. I and II*. Academic Press, 1986.
- [2] K. Chandiramani: *Diffraction of evanescent wave with application to aerodynamically scattered sound and radiation from un baffled plates*. J. Acoust. Soc. Amer., Vol. 55, 1974.
- [3] M. Drela, M. Gilles: *ISES: A Two-Dimensional Viscous Aerodynamic Design and Analysis Code*. 25th AIAA Aerospace Science Meeting, January 12-15, 1987, Reno, Nevada, USA.
- [4] M. Drela: *XFOIL: An Analysis and Design System for Low Reynolds Number Airfoils*. Proc. Low Reynolds Number Aerodynamics, June 1989, University of Notre Dame, USA.
- [5] G. Guidati, K.A. Braun, S. Wagner: *Lärmreduktion an Windkraftanlagen durch Profilloptimierung und gezackte Hinterkanten*. Proc. DEWEK 2000.
- [6] N. Hansen, A. Ostermeier: *Adapting Arbitrary Normal Mutation Distributions in Evolution Strategies: The Covariance Matrix Adaption*. Proc. of the 1996 IEEE International Conference on Evolutionary Computation, May 20-22, 1996, Nagoya, Japan.

- [7] A. Herrig: *Grenzschichtmessungen und aeroakustische Untersuchungen an einem Profil mit variabler Kontur*. Diploma thesis, University of Stuttgart, 2003.
- [8] A. Herrig: SIROCCO. *Trailing edge noise measurements of wind turbine aerofoils in open and closed test section wind tunnels*. Wind Turbine Noise: Perspectives for Control, Berlin, Germany, October 17-18, 2005.
- [9] N. Kroll, C.C. Rossow, D. Schwamborn, K. Becker, G. Heller: *MEGAFLOW a Numerical Flow Simulation Tool for Transport Aircraft Design*. Proc. 23rd ICAS Congress, 2002, Toronto.
- [10] M. Kutzbach, Th. Lutz, S. Wagner: *RANS-basierte direkte numerische Optimierung adaptiver Flügel*. Proc. Deutscher Luft- und Raumfahrtkongress, September 20-23, 2004, Dresden.
- [11] B. König, M. Kutzbach, Th. Lutz: *Extensions of the Optimization Environment POEM with Respect to Aeroelastic Effects*. 14th DGLR-Symposium of STAB, 25th anniversary of STAB, Bremen, November 16-18, 2004.
- [12] Th. Lutz, S. Wagner: *Numerical Shape Optimization of Subsonic Airfoil Sections*. Proceedings ECCOMAS 2000: European Congress on Computational Methods in Applied Sciences and Engineering, Barcelona, Spain, September 11-14, 2000.
- [13] Th. Lutz, A. Sommerer, S. Wagner: *Parallel Numerical Optimisation of Adaptive Transonic Airfoils*. IUTAM Symposium Transsonicum IV, Fluid mechanics and its applications, Volume 73, Kluwer Academic Publishers, ISBN 1-4020-1608-5, 2003.
- [14] Th. Lutz, W. Würz; A. Herrig; K. Braun, S. Wagner: *Numerical Optimization of Silent Airfoil Sections*. DEWEK 2004, 7th German wind energy conference, Wilhelmshaven, October 20-21, 2004.
- [15] S. Oerlemans, B. Mendez: *Localisation and Quantification of Noise Sources on a Wind Turbine*. Wind Turbine Noise: Perspectives for Control, Berlin, Germany, October 17-18, 2005.
- [16] R. Parchen: Progress report DRAW: *A prediction scheme for trailing-edge noise based on detailed boundary-layer characteristics*. TNO Report HAG-RPT-980023, TNO Institute of Applied Physics, The Netherlands, 1998.
- [17] J. G. Schepers, A.P.W.M. Curvers, S. Oerlemans, K. Braun, T. Lutz, A. Herrig, W. Würz, B. Mendez Lopez: *SIROCCO: Silent Rotors by Acoustic Optimisation*. Wind Turbine Noise: Perspectives for Control, Berlin, Germany, October 17-18, 2005.
- [18] A. Sommerer, Th. Lutz, S. Wagner: *Numerical Optimisation of Adaptive Transonic Airfoils with Variable Camber*. Proc. 22nd ICAS Congress, Harrogate, UK, 2000.

- [19] T.W. Swafford: *Analytical Approximation of Two-Dimensional Separated Turbulent Boundary-Layer Profiles*. AIAA Journal, Vol. 21, No. 6, 1983.
- [20] SYNAPS: *EPOGY 2003 – User’s Guide*. © Synaps Inc., www.Synaps-Inc.com.
- [21] D.C. Wilcox: *Turbulence Modeling for CFD*. DCW Industries Inc., 2nd edition, ISBN 0-9636051-5-1, 1998.
- [22] F.X. Wortmann, A. Althaus: *Der Laminarwindkanal des Instituts für Aero- und Gasdynamik*. TH Stuttgart. ZFW 12, Heft 4, 1964.
- [23] W. Würz, S. Guidati, A. Herrig, Th. Lutz, S. Wagner: *Measurement of trailing edge noise by a coherent particle velocity method*. Proc. ICMAR 2004, Novosibirsk, June 28 –July, 2004.

**First International Meeting
on
Wind Turbine Noise: Perspectives for Control
Berlin 17th and 18th October 2005**

**LOCALISATION AND QUANTIFICATION OF NOISE
SOURCES ON A WIND TURBINE**

Stefan Oerlemans

National Aerospace Laboratory NLR, Emmeloord, The Netherlands (stefan@nlr.nl)
Department of Helicopters and Aeroacoustics, P.O. Box 153, 8300 AD Emmeloord

Beatriz Méndez López

Gamesa Eólica, Madrid, Spain (bmendez@eolica.gamesa.es)
Cañada real de las merinas 7, Edificio 3, Planta 4, Madrid 28042

Summary

Acoustic array measurements were performed on a three-bladed GAMESA G58 wind turbine with a rotor diameter of 58 m and a tower height of 53.5 m. The goal was to characterize the noise sources on this turbine, and to verify whether aerodynamic noise from the blades is dominant. In order to assess the effect of blade roughness, one blade was cleaned, one blade was tripped, and one blade was left untreated. The acoustic array consisted of 152 microphones mounted on a horizontal wooden platform (15 by 18 m²), which was positioned about 58 m upwind from the rotor. In parallel to the acoustic measurements, a number of turbine parameters were monitored, such as wind speed, power, turbine orientation, RPM, and blade pitch angle. In total more than 100 measurements were taken at wind speeds between 6 and 10 m/s. Two array processing methods were used to characterise the noise from the turbine. First, the noise sources in the rotor plane were localised using conventional beamforming. These results clearly show that, besides a minor source at the rotor hub, practically all noise (radiated to the ground) is produced during the downward movement of the blades. The noise is produced by the outer part of the blades (but not by the very tip), and blade noise levels scale with the 5th power of the local flow speed. The second processing method employed rotating scan planes to localise the noise sources on the individual blades. It turns out that the tripped blade is significantly noisier than the clean and untreated blades, which is a strong indication of trailing edge noise (rather than inflow turbulence noise). The similar noise levels for the clean and untreated blades suggest that the untreated blade was aerodynamically clean.

1 Introduction

Wind turbine noise is one of the major hindrances for the widespread use of wind energy. For modern large turbines, the dominant noise source is considered to be aerodynamic noise from the blades. Therefore, the subject of the European SIROCCO project ('Silent Rotors by Acoustic Optimisation') is the design, testing,

and full-scale validation of quiet wind turbine blades. The objective is to obtain a noise reduction of 3-6 dB with respect to the current state-of-the-art, without a reduction in power performance. As a first step in the project, acoustic array measurements were performed on an existing baseline wind turbine. The goal was to characterize the noise sources on this turbine, and to verify whether indeed aerodynamic (in particular trailing edge) noise from the blades is dominant. The SIROCCO project can be regarded as the continuation of the previous DATA project, where quiet wind turbine blades were tested on a model scale rotor in a wind tunnel¹.

The measurements were carried out in December 2003, on a three bladed GAMESA G58 wind turbine (rotor diameter 58 m) which was located on a wind farm in northern Spain. In order to assess the effect of blade roughness due to e.g. dirt or insects, prior to the acoustic tests one blade was cleaned, one blade was tripped, and one blade was left untreated. The acoustic array consisted of 152 microphones mounted on a horizontal wooden platform (15x18 m²), which was positioned about one rotor diameter upwind from the rotor. In parallel to the acoustic measurements, a number of turbine parameters were monitored, such as wind speed, power, turbine orientation, RPM, and blade pitch angle. In total more than 100 acoustic measurements were taken at wind speeds between 6 and 10 m/s (at the standard a height of 10 m). The 35 measurements with the most stable conditions were selected for further processing. Two different acoustic processing methods were applied to characterise the noise from the turbine. With the first method the noise sources in the rotor plane were localised, thus showing the integrated effect of the three blades. The second method was used to localise and quantify the noise sources on the individual blades.

The organisation of this paper is as follows. The experimental method is described in detail in Section 2. The experimental results for both processing methods are discussed in Section 3. The conclusions are summarised in Section 4.

2 Experimental Method

2.1 Test Set-up

The measurements were carried out on a pitch-controlled, three-bladed GAMESA G58 wind turbine, which has a rotor diameter of 58 m and a tower height of 53.5 m (Figure 1). The turbine was located on the wind farm 'Los Monteros' in Pedrola (northern Spain). In order to obtain a 'clean' inflow, a turbine on the upwind edge of the farm was chosen. About one week before the acoustic tests, one blade was

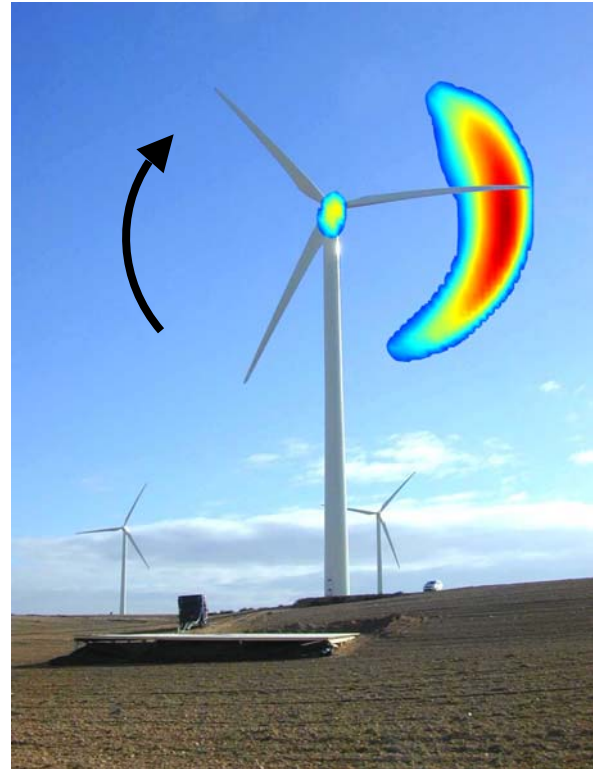


Figure 1: Test set-up with G58 turbine and microphone array platform. The noise sources in the rotor plane (averaged over several rotations) are projected on the picture.

cleaned, the second blade was first cleaned and then tripped, and the third blade was left untreated. Tripping was done using zigzag tape of 0.4 mm thickness over the complete span, at 5% chord on the suction and pressure sides of the blade. In addition to the trip, a sticker was attached to the tripped blade, in order to enable visual identification of the blades.

The acoustic array consisted of 152 Panasonic WM-61 microphones, mounted on a horizontal wooden platform of $15 \times 18 \text{ m}^2$, which was positioned about 58 m upwind from the turbine (Figure 2). As a reference, two calibrated B&K microphones were mounted on the platform as well. All microphones were mounted flush to the surface of the platform, with the membrane parallel to the platform, and without wind screens.

The microphone array had an elliptic shape to obtain approximately the same array resolution in the horizontal and vertical direction, despite the 'view angle' of about 45° (Figure 2). The ellipsis was 'pointed' to the right-hand side of the rotor plane, to obtain maximum resolution on the side where the blades move downward and where maximum noise radiation was expected. The array had a high microphone density in the center to ensure good array performance at high frequencies, and a low-density outer part to obtain a good resolution at low frequencies.

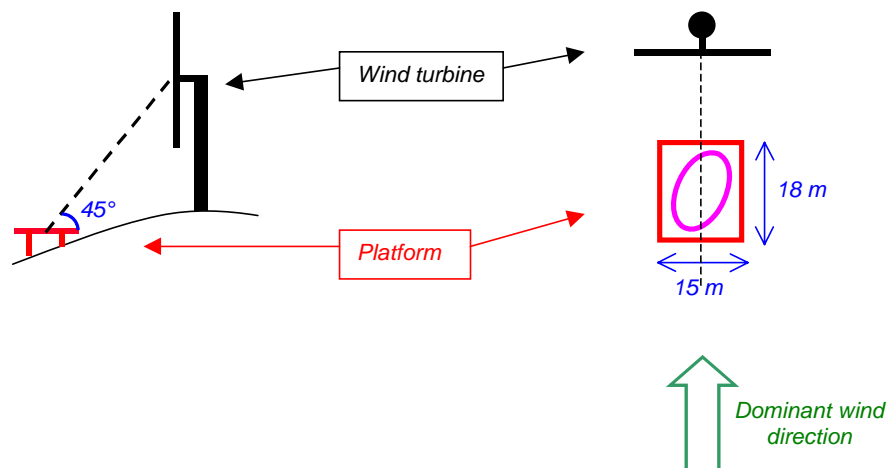


Figure 2: Side view (left) and top view (right) of test set-up. The microphones were mounted on the platform in an elliptic shape.

2.2 Data Acquisition

Acoustic data from the array microphones were synchronously measured at a sample frequency of 51.2 kHz and a measurement time of 30 s. The acoustic data were processed using a block size of 2048 with a Hanning window and an overlap of 50%, yielding 1500 averages and a narrowband frequency resolution of 25 Hz. A 500 Hz high-pass filter was used to suppress high-amplitude pressure fluctuations at low frequencies, and thus extend the dynamic range to low pressure amplitudes at high frequencies. The sound levels in this paper are corrected for the filter response. Before the measurements, the sensitivity at 1 kHz was determined for all array microphones using a calibrated pistonphone. The frequency response of the Panasonic microphones was taken from previous calibration measurements. No corrections were applied for microphone directivity, since calibration measurements showed that these effects amounted to less than 2 dB up to 20 kHz, for angles smaller than 75° with respect to the microphone axis. Moreover, this effect is the

same for all measurements. Phase matching of the microphones was checked before the measurements using a calibration source at known positions.

In parallel to the acoustic measurements, the following turbine parameters were acquired (sample rate 3 Hz): wind speed, power production, turbine orientation, RPM, blade pitch angle, and temperature. The turbine data were synchronised with the acoustic measurements. The measured wind speed (at the hub) was normalised to the wind speed at 10 m height using the standard wind profile from Ref. 2. For the present tests this means that the wind speed at 10 m height was taken to be the measured wind speed at hub height multiplied by 0.760.

2.3 Phased Array Processing

The array data were processed using two different methods. With the first method, noise sources in the rotor plane were localised using conventional beamforming³. Thus, noise from the rotor hub can be separated from blade noise, and it can be seen where in the rotor plane the blade noise is produced (see e.g. Figure 1). This method shows the integrated effect of the three blades, averaged over the complete measurement time of 30 s (i.e. several rotations). The first step of this processing involves the calculation of an averaged cross-power matrix which contains the cross-powers of all microphone pairs in the array. To improve the resolution and suppress background noise (e.g. wind-induced pressure fluctuations on the microphones), the main diagonal of the cross-power matrix (i.e. the autopowers) was discarded. A frequency-dependent spatial window was applied to the microphone signals, in order to improve the resolution and suppress coherence loss effects (due to propagation of the sound through the atmospheric boundary layer). The scan plane, with a resolution of 1 m in both directions, was placed in the rotor plane of the wind turbine, and was rotated in accordance with the orientation of the turbine (depending on wind direction). The 6° angle between the rotor axis and the horizontal plane was also accounted for. The effect of sound convection in the atmospheric boundary layer was taken into account by assuming a constant wind speed between the scan location and the microphones. This constant wind speed was calculated as the average wind speed between the rotor hub and the array center, using the standard wind profile in Ref. 2. Thus, for the present test the average wind speed was taken to be the measured wind speed at hub height multiplied by 0.866. The narrowband acoustic source plots were summed to 1/3-octave bands, and the scan levels were normalized to a distance of 0.282 m $[(4\pi)^{-1/2}]$, so that for a monopole source the peak level in the source plot corresponds to the Sound Power Level. The noise sources in the rotor plane were quantified using a power integration method⁴. By defining an integration contour around the whole rotor plane and one only around the hub, noise levels from the hub and the blades were determined.

The second processing method employed three rotating scan planes to localise the (de-dopplerised) noise sources on the three individual blades⁵. This enabled a comparison of the noise from the clean, tripped, and untreated blade. The start position of the scan planes was determined using a 1P tacho signal from the turbine, that was recorded synchronously with the acoustic data. The scan resolution was 0.5 m in both directions, and the scan plane was placed in the rotor plane. Similar to the first processing method, the narrowband acoustic source plots were summed to 1/3-octave bands, and the scan levels were normalized to a distance of 0.282 m $[(4\pi)^{-1/2}]$. Since the source plots of the complete rotor plane indicated that practically all measured noise was produced during the downward movement of the blades (Figure 1), and since the array resolution was highest on this side of the rotor plane,

the blades were only scanned during their downward movement (from 0° to 180° , with 0° the upper vertical blade position). In order to limit processing time, only the first two rotations after the start of each acoustic measurement were processed (one at a time). In the discussion of results (Section 3.2) it will be shown that, despite the use of only one rotation, the signal-to-noise ratio and repeatability (correspondence between the results for the first and second rotation) are very good. The noise from the blades was quantified using an integration method for moving sound sources⁶. An integration contour was defined which surrounds the noise from the blade but excludes the noise from the rotor hub.

2.4 Test Program

During the test campaign, that lasted from 8-15 December 2003, a total number of 110 acoustic measurements was done, so that the target of at least 30 valid measurements (taken from Ref. 2) could be easily met. Therefore, a selection was made of the measurements with the most constant conditions during the measurement time of 30 s. Using the following criteria, 35 measurements were selected for further processing:

- 1) Variation of wind speed within 15% (and within 1.5 m/s) of average;
- 2) Misalignment angle smaller than 12° , variation within 2° of average;
- 3) Variation in rotor RPM within 8% of average;
- 4) Variation in blade pitch angle within 3° of average;
- 5) Overloads in acoustic data (e.g. due to wind gusts) less than 1%.

The 'misalignment angle' is the angle between the turbine axis (depending on wind direction) and the line from turbine to array (Figure 4). The distribution of the 35 selected measurements over the different wind speed intervals is given in the table below. It can be seen that all wind speed intervals are well represented. The rotor RPM typically varied between 22 and 26.

wind speed at 10 m	6 m/s	7 m/s	8 m/s	9 m/s	10 m/s
# measurements	6	6	12	5	6

3 Results and Discussion

In this section the results of the acoustic measurements are presented and analysed. Section 3.1 describes the location and quantification of the noise sources in the rotor plane: the noise level from the rotor hub is compared to the blade noise levels, and trends in source locations are shown. Furthermore, the speed dependence of the blade noise levels is investigated. In Section 3.2 the noise sources on the individual rotating blades are analysed: the noise sources are localised and the levels from the clean, tripped, and untreated blade are compared.

3.1 Noise Sources in the Rotor Plane

Typical noise source distributions in the rotor plane are shown in Figure 3. Note that these plots show the integrated effect of the three blades, averaged over the complete measurement time of 30 s (i.e. several rotations). A number of observations can be made from these plots. The most striking phenomenon is that practically all downward radiated blade noise (as measured by the array) is produced during the downward movement of the blades. Since the range of the color scale is 12 dB, this means that the (downward radiated) noise produced during the upward movement is at least 12 dB less than during the downward movement. This effect was observed

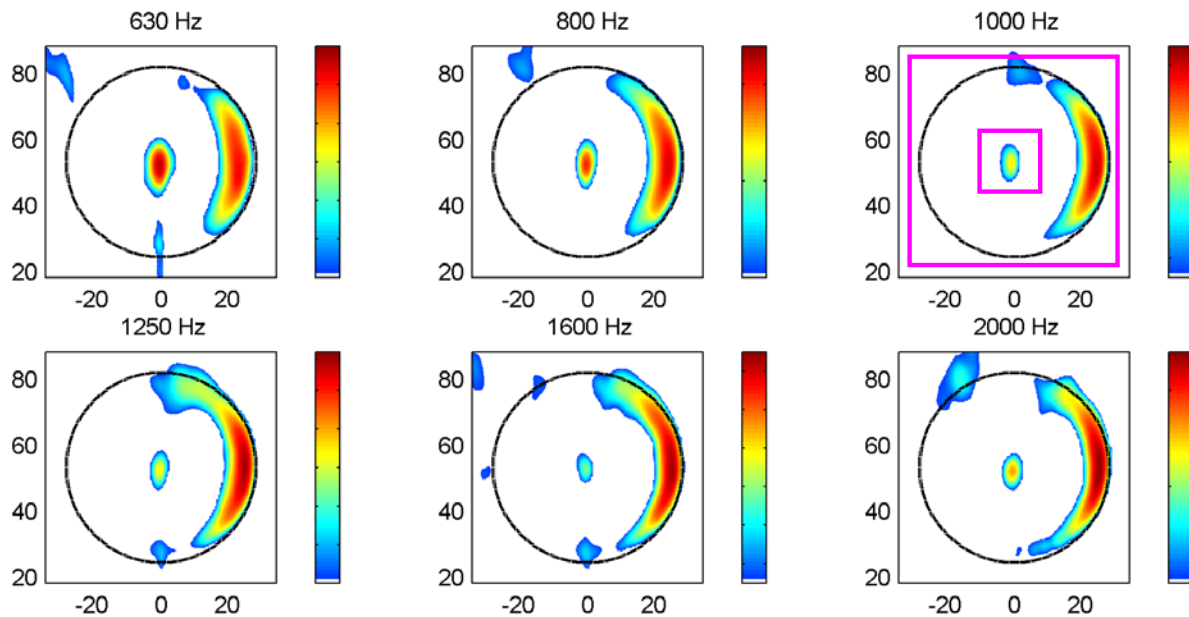


Figure 3: Typical example of noise source locations in the rotor plane, as a function of frequency. The trajectory of the blade tips is indicated by the black circle. The range of the color scale is 12 dB. The pink lines (1 kHz) indicate the integration contours for the quantification of blade and hub noise.

for basically all measurements and all frequencies, and is very similar to results obtained earlier on a model scale wind turbine, where it was attributed to a combination of convective amplification and directivity of trailing edge noise. It should be noted that for a different observer location the pattern may be different. A second important observation is that the noise from the blades clearly dominates the noise from the rotor hub. Furthermore, it can be seen that the blade noise is produced by the outer part of the blades, but not the very tip. The sources move outward for increasing frequency, which can be explained by the higher flow speeds and the smaller chord, resulting in a thinner boundary layer at the trailing edge (assuming that trailing edge noise is the responsible mechanism).

Comparison of measurements with different rotor orientation shows that the location of the source region shifts upward or downward when the right- or left-hand side of the rotor plane is turned towards the array respectively (Figure 4). This effect was also observed in Ref. 1, and can be attributed to the change in the component of

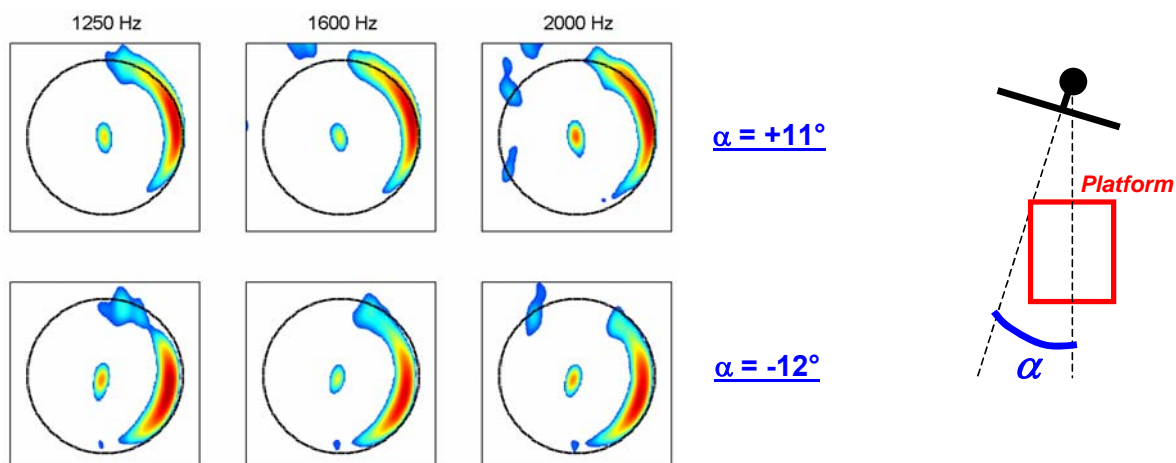


Figure 4: Shift of blade noise location due to difference in misalignment angle α .

the blade velocity in the direction of the array, which results in a change in convective amplification.

The noise from the blades and the rotor hub was quantified using the power integration method mentioned in Section 2.3. The integration contours are shown in Figure 3: the small box was used for quantification of hub noise, while blade noise was defined as the difference between the large and small box. The spectra in Figure 5 (averaged over all selected measurements) confirm the observation in the source plots, that the blade noise is significantly higher than the noise from the hub. The hub noise shows a peak at 630 Hz, which is probably due to the gear box. The blade noise is broadband in nature, as would be expected for trailing edge noise. The highest A-weighted levels occur around 800 Hz. Interestingly, the blade noise spectrum seems to consist of two broad 'humps': a low-frequency hump centered at 800 Hz, and a high-frequency hump starting at 2 kHz. These two humps may be caused by trailing edge noise from the suction- and pressure-side boundary layers respectively. The difference between the overall sound pressure levels from hub and blades was found to increase with wind speed, from about 8 dB(A) at 6 m/s to about 11 dB(A) at 10 m/s. Apparently, blade noise increases faster than hub noise for increasing wind speed. In conclusion, blade noise is clearly dominant for this wind turbine.

The blade noise spectra for the individual measurements are shown in Figure 6a. The speed dependence of the noise levels was investigated by plotting normalised levels as a function of Strouhal number $St=f \cdot L/U$, where f is frequency and L a typical length scale. For trailing edge noise, L is normally taken to be the boundary layer

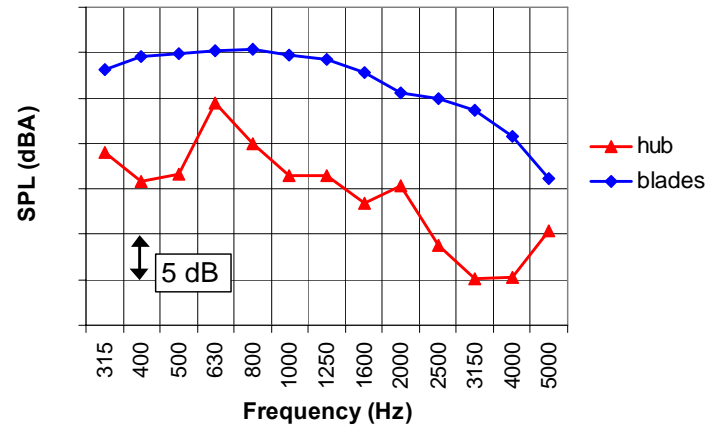


Figure 5: Average spectra of hub noise and blade noise.

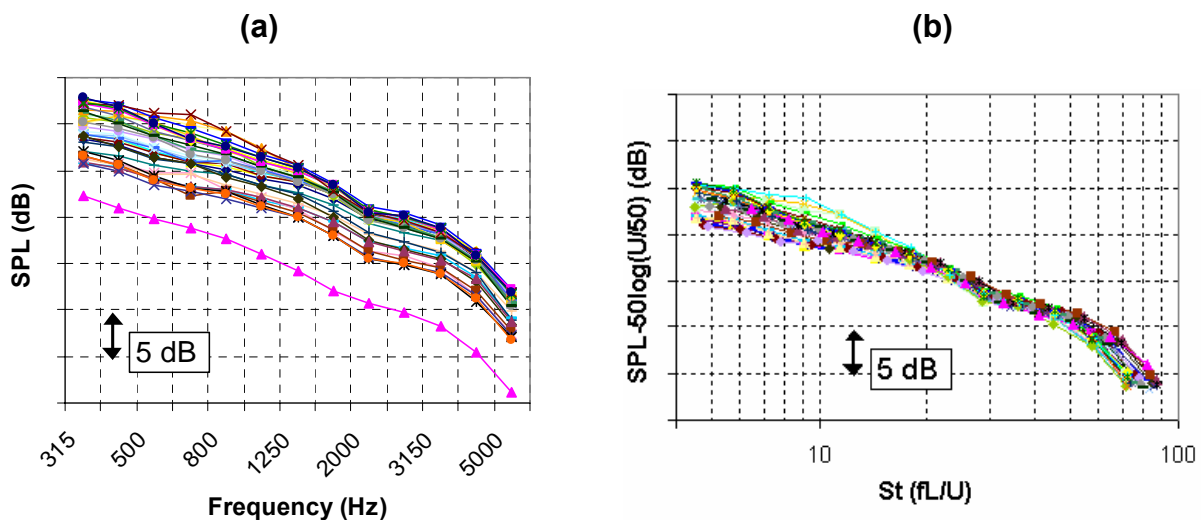


Figure 6: Measured (a) and normalised (b) blade noise spectra for all selected measurements.

thickness at the trailing edge, but since this information was not measured a constant value of 1 m was chosen here. For this normalisation the undisturbed flow speed as perceived by the blade (U) was used, which is the vector sum of the wind speed and the rotational speed (the induced velocity is neglected). The rotational speed was calculated for a radius of 25 m, which is the location where we typically observed blade noise (Figure 3). The noise levels were normalised as $SPL_{norm} = SPL - 10 \cdot x \cdot \log(U_{blade}/U_{ref})$, with SPL and SPL_{norm} the measured and normalised noise levels respectively. U_{ref} is a constant reference speed, for which here a value of 50 m/s was chosen. The variable x indicates the dependence of the blade noise on the flow speed: the acoustic energy is assumed to be proportional to the flow speed to the power of x ($p^2 \sim U^x$).

The normalised blade noise spectra are shown in Figure 6b. The normalisation was done using a value of 5 for x , which seemed to give the best data collapse. This is indicative of trailing edge noise, since normally the value of x is around 5 for trailing edge noise, and around 6 for inflow turbulence noise^{7,8}. It can be seen that without normalisation the scatter in data is 5-10 dB, even when the quietest measurement is neglected. After normalisation the scatter is only 2-5 dB, including the quietest measurement. The remaining scatter in the normalised spectra is probably due to differences in turbine and weather parameters. It was investigated whether this scatter (after correcting for the speed effect) correlated with turbine orientation (i.e. misalignment angle) or blade pitch angle, but no clear relation was found.

3.2 Noise Sources on the Rotating Blades

The noise source distributions on the three rotating blades, averaged over all selected measurements, are shown in Figure 7 for three frequency bands. Note that the signal-to-noise ratio is very good (i.e. 'clean' source plots), despite the fact that only half a rotation was used (see Section 2.3). These plots confirm the observations that were already made from the source plots of the rotor plane: the blades are noisier than the hub and the relative importance of the hub is largest at 630 Hz (compare to Figure 3). Most of the noise is produced by the outer blades and the sources move outward with increasing frequency. In addition, Figure 7 seems to

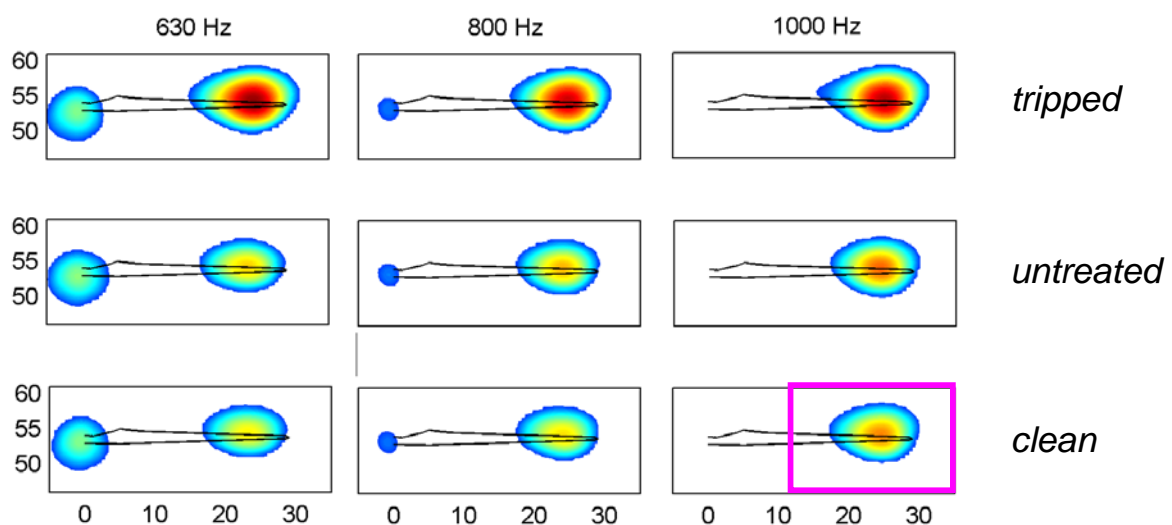


Figure 7: Averaged acoustic source plots showing the noise sources on the individual blades. The black line indicates the blade contour (leading edge on lower side). The range of the color scale is 12 dB and the color scale is the same for the three blades. The pink line (1 kHz) indicates the integration contour used for the quantification of the blade noise.

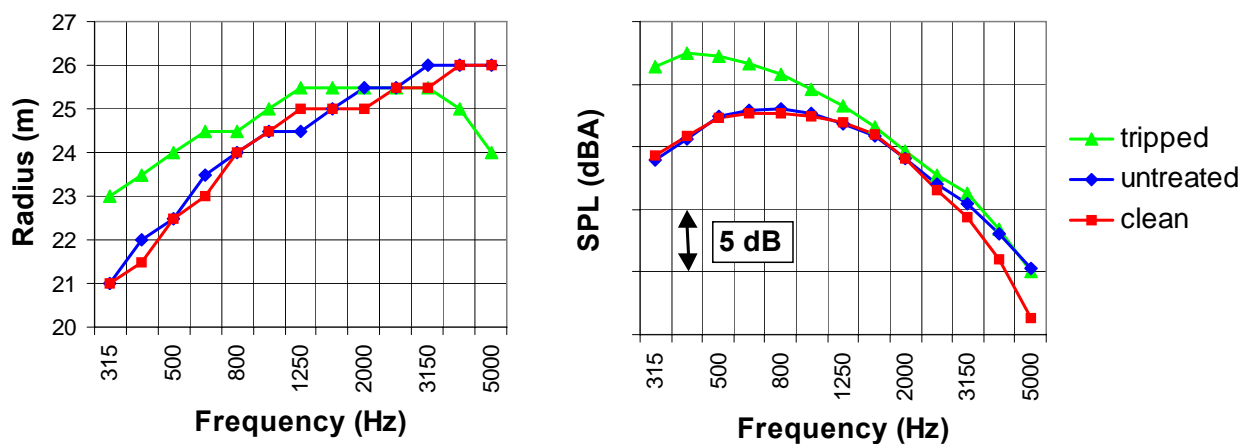


Figure 8: Average source location (left) and noise spectra (right) for the three blades.

indicate that the sources for the tripped blade are located at a slightly higher radius than for the clean and untreated blade. To visualize these observations regarding the source locations more clearly, the source radius was plotted as a function of frequency for the three blades (Figure 8, left plot). Here the source radius is defined as the radius at which in the averaged source plots (Figure 7) the maximum source level occurs. It can be seen that, for the important frequency range up to 2.5 kHz, the sources move outward with increasing frequency, and that the source radius is largest for the tripped blade. These trends can be understood from the decrease in boundary layer thickness with increasing radius, and from the thicker boundary layer for the tripped blade.

The resolution of the source plots in Figure 7 does not seem to be sufficient to determine whether the noise is radiated from the leading or trailing edge of the blade. However, the plots clearly indicate that the tripped blade is significantly noisier than the other two. This observation is a strong indication of trailing edge noise, since earlier studies have indicated that tripping has no influence on inflow turbulence (leading edge) noise.

The noise from the individual blades was quantified using the method mentioned in Section 2.3. The integration contour used to quantify the blade noise is shown in Figure 7. The resulting averaged de-dopplerized spectra for the three blades are shown in Figure 8 (right plot). This figure clearly shows that the tripped blade is noisier than the other two for low frequencies, and that the tripped and untreated blades are slightly noisier than the clean blade at higher frequencies. The tripped spectrum peaks at 400 Hz, while the other two peak at 800 Hz. The lower peak frequency for the tripped blade can be explained by the increased boundary layer thickness at the trailing edge. As explained in Section 2.3, the spectra in Figure 8 were obtained using the acoustic data for the downward part (180°) of one rotation. To check the repeatability of the blade noise spectra, the spectra were also calculated using only the data for the *second* rotation (not shown). It turns out that the differences in *averaged* blade noise levels between the first and second rotation are smaller than 0.3 dB for all frequencies, which indicates the good repeatability. For the individual measurements the differences were generally smaller than 1 dB.

Figure 8 shows differences between the blades up to 7 dB at low frequencies, while at high frequencies differences up to 4 dB occur. The differences at low

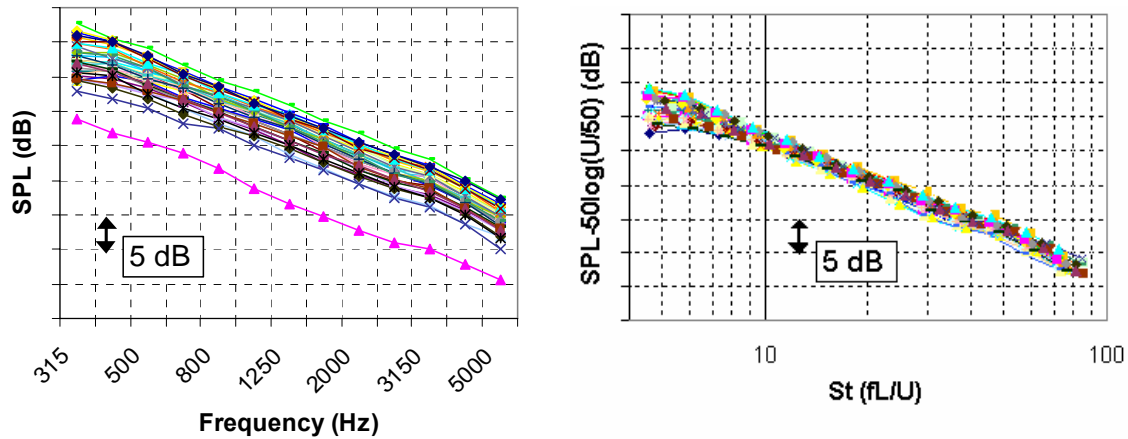


Figure 9: Measured (left) and normalised (right) noise spectra for the tripped blade (for all selected measurements).

frequencies are most important for the overall, A-weighted noise levels: the overall levels of the clean and untreated blades are practically identical, while on the average the tripped levels are 3.6 dB(A) higher. This level difference between the tripped and the other two blades was practically independent of wind speed.

Similar to Section 3.1, the speed dependence of the blade noise was further investigated by plotting normalised blade noise spectra as a function of Strouhal number. Again, the levels and frequencies were normalised using the flow speed at a radius of 25 m. As an example, the measured and normalised spectra for the tripped blade are shown in Figure 9. These plots confirm that a good data collapse is obtained for $x=5$, which is indicative of trailing edge noise (compare to Figure 6). Similar to the results in Section 3.1, the remaining scatter in the normalised spectra is probably due to differences in turbine and weather parameters.

Since the blade noise spectra are in 1/3-octave bands and summed over the whole blade radius (except the hub), possible blunt-trailing-edge tones could be obscured. Therefore, narrowband source spectra were produced for individual radial positions. Analysis of these spectra for all measurements did not show any significant narrowband tones, which strongly suggests that blunt-trailing-edge noise is not an issue for the present turbine.

The acoustic results can also provide information about the flow state on the untreated blade, which is representative for a turbine blade during normal operation. The similarity between the noise levels of the clean and untreated blade suggests that the untreated blade was aerodynamically clean (i.e. no boundary layer transition close to the leading edge). However, an alternative explanation could be that both the 'clean' and 'untreated' blades were in fact dirty (i.e. transition close to the leading edge), because there was about one week between the cleaning of the blade and the acoustic measurements. The higher levels for the tripped blade could then be explained by the relatively large trip thickness (0.4 mm), which may have caused overtripping. The flow state on the blade (clean vs. tripped vs. overtripped) may also depend on the radius, as a result of the different flow conditions at different radii.

To get more insight in the different possibilities, acoustic wind tunnel tests were performed in which the trailing edge noise levels of the GAMESA airfoil were measured for several types of tripping⁹. These measurements showed that the noise levels for the GAMESA airfoil with a 0.4 mm zigzag tape (as in the field

measurements) were practically identical to those for a 2D turbulator strip with a thickness of 0.18 mm. This means that in the wind tunnel the zigzag tape did not cause overtripping. Moreover, the spectra for the tripped airfoil showed a low-frequency noise increase with respect to the clean airfoil, similar to the low-frequency increase observed in Figure 8. Thus, it seems that the untreated blade was in fact aerodynamically clean during the field tests.

The above argumentation applies to the low frequencies, which are considered to be produced by the (thick) suction side boundary layer around a radius of 24 m. A possible explanation for the small difference in high-frequency noise between the clean and untreated blade, could be that only the pressure side of the untreated blade was contaminated, causing increased levels at high frequencies. However, insect impact calculations¹⁰ indicate that *if* contamination occurs, it will occur on both suction and pressure side. Another possibility could be that the untreated blade was dirty close to the tip, where it is easier to trip the boundary layer and where high frequencies are produced. However, since no information is available on the flow state on the blades, this hypothesis cannot be verified.

4 Conclusion

Acoustic array measurements were performed on a GAMESA G58 wind turbine, to characterize the noise sources and to verify whether aerodynamic noise from the blades is dominant. In order to assess the effect of blade roughness, one blade was cleaned, one blade was tripped, and one blade was left untreated. Two array processing methods were used to localise and quantify the noise sources in the rotor plane and on the individual blades. The main conclusions can be summarised as follows:

- Broadband aerodynamic noise from the blades is the dominant noise source for this turbine;
- Practically all noise (emitted to the ground) is produced during the downward movement of the blades;
- The blade noise is produced by the outer part of the blades, but not by the very tip;
- Blade noise levels scale with the 5th power of the local flow speed;
- The tripped blade is significantly noisier than the clean and untreated blade;
- The acoustic results suggest that the untreated blade was aerodynamically clean.

In principle, there are two mechanisms which may be responsible for the aerodynamic noise from the blades¹¹. The first is inflow-turbulence noise (IT noise), which is radiated from the leading edge of the blade, and which is caused by upstream atmospheric turbulence. The second mechanism, trailing edge noise (TE noise), is caused by an interaction of boundary layer turbulence with the blade trailing edge. The present test results strongly suggest that TE noise is the responsible mechanism for the present turbine. The most important evidence for TE noise are the increased levels for the tripped blade, since it has been shown before that tripping has no influence on IT noise levels. Furthermore, the 5th power speed dependence and the noise source distribution in the rotor plane are indicative of TE noise.

The next step in the project consists of acoustic field measurements on the same GAMESA turbine with a newly designed blade (planned for late 2005). This blade is optimized for low TE noise emissions, while keeping the aerodynamic performance the same. The turbine rotor will consist of one optimized blade and two baseline blades, so that the noise levels can be compared for identical inflow conditions. Besides the new blade design, reduction concepts such as trailing edge serrations may be tested as well.

Acknowledgments

The authors would like to thank the colleagues from the University of Stuttgart and from the Netherlands Energy Research Foundation (ECN) for their valuable contributions to the definition of the tests and the interpretation of the results. Financial support for this research was given in part by the European Commission's Fifth Framework Programme, project reference: SIROCCO, Silent Rotors by Acoustic Optimisation (ENK5-CT-2002-00702). Financial support was also given by the Netherlands Organisation for Energy and the Environment (NOVEM).

References

1. Oerlemans, S., Schepers, J.G., Guidati, G., and Wagner, S., "Experimental Demonstration of Wind Turbine Noise Reduction through Optimized Airfoil Shape and Trailing-Edge Serrations", presented at the European Wind Energy Conference, Copenhagen (2001).
2. IEC norm 61400-11, "Wind turbine generator systems – Acoustic noise measurement techniques" (2002).
3. Johnson, D.H., and Dudgeon, D.E., "Array Signal Processing", Prentice Hall (1993).
4. Oerlemans, S., and Sijtsma, P., "Acoustic Array Measurements of a 1:10.6 Scaled Airbus A340 Model", AIAA paper 2004-2924 (2004).
5. Sijtsma, P., Oerlemans, S., and Holthusen, H., "Location of rotating sources by phased array measurements", AIAA paper 2001-2167 (2001).
6. Sijtsma, P., and Stoker, R.W., "Determination of Absolute Contributions of Aircraft Noise Components using Fly-Over Array Measurements", AIAA paper 2004-2958 (2004).
7. Oerlemans, S., and Migliore, P., "Aeroacoustic wind tunnel tests of wind turbine airfoils", AIAA paper 2004-3042 (2004).
8. Brooks, T.F., Pope, D.S., and Marcolini, M.A., "Airfoil Self-Noise and Prediction", NASA Reference Publication 1218 (1989).
9. Oerlemans, S., "Acoustic Wind Tunnel Measurements on GAMESA Baseline and Optimised Airfoils", SIROCCO Deliverable D13a (January 2005).
10. Würz, W., "Insect impact calculations for the Gamesa G58-R27 airfoil section", SIROCCO memorandum (March 2005).
11. Wagner, S., Bareiss, R., and Guidati, G., "Wind Turbine Noise", Springer Verlag (1996).

**First International Meeting
on
Wind Turbine Noise: Perspectives for Control
Berlin 17th and 18th October 2005**

Human response to wind turbine noise – annoyance and moderating factors

Eja Pedersen and Kerstin Persson Waye
Department of Environmental Medicine, Göteborg University,
Box 414, SE-504 30 Göteborg, Sweden
eja.pedersen@set.hh.se, kerstin.persson-waye@envmed.gu.se

Summary

Wind turbines are regarded as industrial sources of noise and as such, guidelines based on knowledge originate from situations rather different from those normally connected to wind turbines are used. A rural setting, constantly moving rotor blades, unpredictable incidences of noise, and easily perceived sound properties are examples of factors that indicate the need for new regulation. In an ongoing project on human responses to wind turbines, the relationship between A-weighted sound pressure level (SPL) and self-reported annoyance with wind turbine noise is studied together with moderating factors. In an initial cross-sectional field study among people living in a rural area with several wind turbines close by, a dose-response relationship between A-weighted SPL and noise annoyance was found ($r_s=0.40$; $n=341$; $p<0.001$). When comparing the findings with dose-response relationships for other stationary noise sources, the proportion annoyed by wind turbine noise increased more rapidly with exposure. Of the possible moderating factors measured in the study, the attitude to wind turbines' visual impact on the landscape scenery seemed to be most important. To deepen the understanding of why the noise sometimes causes severe reactions and explore the influence of non-audible factors, a qualitative study was completed. In-depth interviews with people ($n=15$) living in the vicinity of wind turbines were analyzed according to Grounded Theory. The wind turbine noise was by some of the informants perceived as intruding into private domain, physically into the garden and the home, but also as intruder into themselves. The informants' conception of the countryside as either a place of peace and quietness or a place for development and economic growth seemed to influence the adverse effect of the noise, together with feelings induced by the experience of lacking control, being subjected to injustice, lacking influence, and/or not being believed.

1. Introduction

Wind turbines are regarded as industrial sources of noise and as such, guidelines based on knowledge originate from situations rather different from those normally connected to wind turbines are used. A rural setting, constantly moving rotor blades, unpredictable incidences of noise, and easily perceived sound properties are examples of factors that may require a new base for regulation. A dose-response relationship between A-weighted sound pressure levels (SPLs) of wind turbine noise at the dwellings of people in wind turbine areas and responses as proportion annoyed by the noise should be established. Such relationships have been established for other types of community noises, e.g. transportation noise [Miedema and Voss 1998], and recently for stationary (industrial) sources [Miedema and Voss 2004] although that study did not include wind turbines.

In developing dose-response relationship for wind turbines moderating factors known from studies of other community noise sources (road traffic, railways, aircraft, and industries) should be taken into account. Two factors that more consistently has been found to be of importance for noise response are noise sensitivity and attitude to the noise source. In a review of factors influencing the relationship between community noise exposure and reaction, research from ten different countries and nine different types of noise sources were examined [Job1988]. The mean correlation between reaction and noise sensitivity was 0.30 and between reaction and attitude 0.41. The correlation between the noise exposure and noise sensitivity was low ($r=-0.01$), and between noise exposure and reaction 0.15. Job suggests that there is a cause-effect relation between sensitivity and reaction even if the direction of causality is not established. The influence of attitude to the source is somewhat more complicated; it seems to be in part, a genuine factor of reaction, and in part, a result of the reaction itself. The results were supported by a meta-analysis of 136 community noise surveys with the objective to evaluate 22 personal and situational variables hypothesised to influence noise annoyance [Fields 1993]. In this study, none of the nine demographical variables (age, sex, social status etc.) could be associated to noise annoyance. Noise annoyance was related to five factors; general noise sensitivity, fear of danger from the noise source, noise prevention beliefs, beliefs about the importance of the noise source, and annoyance with non-noise impacts of the noise source (e.g. air quality). Of special interest for the case of wind turbines was the findings that noise annoyance was not affected to an important extend by ambient noise levels. It should though be noted that only a few studies on community noise annoyance have been carried out in areas with ambient noise levels as low as 40 dB (L_{Aeq}). Interesting was also that even at low noise levels (in Fields meta-analysis defined as below DNL 55), a small percentage of the respondents were highly annoyed and that the extent of annoyance was related to noise exposure. This indicates that a dose-response relationship between noise and reaction could be found even for sources producing low level noise.

Other moderating factors not so frequently studied could also be of interest when exploring the effects of wind turbine noise. Visual interference of relationships between noise exposure and noise annoyance has been found in experimental studies of traffic noise [e.g. Kastka and Hangartner 1986, Viollon *et al.* 2002], findings highly relevant for large, tall objects as wind turbines. The visual variables were though in these studies not the actual noise sources. Wind turbines are not only visual objects, but sources of visual stimuli in addition to noise. Flashing shadows occur if the sun is shining behind the wind turbine in relation to a dwelling and the rotor

blades are directed perpendicular to the sun rays. When the sun rays are cut off by the rotor blades, a strobe-like light can be perceived at the dwelling. The number of events and the lasting of the events could be calculated out of astronomical data and expressed as hours per year. The value is dependent of the distance between the wind turbine and the receiver as the noise exposure, but it also depends on the geographical direction, hence the two types of exposures are only to a part correlated. The effect of both visual and audible stimuli from the same source could be hypothesised to influence the response.

As wind turbines are new sources of noise and visual annoyance it is important also to study the occurrence of hitherto unknown moderating factors.

The most relevant previous study on human responses to wind turbine noise when exploring dose-response relationships, to our knowledge, was performed in Denmark, the Netherlands, and Germany in the early 1990's. [Wolsink *et al.* 1993]. The main aims of that study were to explore the correlation between noise exposure from wind turbines and noise annoyance among residents and to find other variables of importance for the annoyance. The sampling of study subjects were done so that the average A-weighted SPL due to wind turbines that subjects were exposed to was approximately 35 dB with a standard deviation of 5 dB from an almost normal distribution. Of the 574 residents who responded to a questionnaire, 93.6% answered that they were not at all annoyed by wind turbine noise; remaining 6.4% (n=37) reported some degree of annoyance. Most of the noise was experienced outdoors and between 16.00 pm and midnight. Only a weak correlation between A-weighted SPL and noise annoyance was found (Kendall's coefficient for correlation rank order variables $t=0.09$; $p<0.05$). Variables reported to be related to noise annoyance were stress caused by wind turbine noise, daily hassles, perceived effects of wind turbines in the landscape (visual intrusion), and the age of the turbine site (the longer it had been operating, the less annoyance).

An attempt to find more of the knowledge needed was done within an ongoing project on human responses to wind turbines. In an initial cross-sectional field study, Study I, the aims were

- to evaluate the prevalence of annoyance due to wind turbine noise
- to study dose-response relationships between calculated A-weighted SPL and noise annoyance
- to describe interrelationships between noise annoyance and individual factors such as noise sensitivity and attitude to the source

To further describe the response and reveal new factors influencing the dose-response relationship, people whom experienced audio and visual exposures from wind turbines in their homes were interviewed and their reports analysed qualitatively in Study II.

Study I has previous been presented in Pedersen and Persson Waye [2004]. A summary of the main result and some new aspects of the data analysis will be presented here. The results of Study II have not yet been published.

2. Method

Study I was carried out in the south of Sweden in the summer 2000 and comprised respondents exposed to different SPLs from wind turbines. In the study areas, 16 wind turbines (14 of nominal power 600 kW) were situated. The study population consisted of one randomly selected subject between the ages of 18 and 75 in each household living in the vicinity of at least one wind turbine (n=518). Subjective responses were obtained through a questionnaire, which purpose was masked. Among questions of living conditions in the countryside, questions directly related to wind turbines were included. Annoyance perceived outdoors was rated on five categories verbal scales ranging from "do not notice" to "very annoyed". The term "annoyed" in this paper refers to respondents that rated themselves "rather annoyed" or "very annoyed". Noise sensitivity was measured with four categories from "not sensitive at all" to "very sensitive". Attitude questions comprised of five categories from "very positive" to "very negative". A total of 356 respondents were included (response rate 69%). For each respondent outdoor A-weighted SPL (free field) from nearby wind turbines were calculated based on wind conditions of 8 m/s with the wind direction towards the respondent according to [The Swedish Environmental Protection Agency 2001]. The calculations are summarised in Pedersen and Persson Waye [2004]. The value represents an equivalent SPL for a period of 5-10 minutes under the described conditions. It is not known how often these sound pressure levels occur and therefore the equivalent SPL for 24 hours is not possible to estimate. The respondents were divided into 6 SPL-intervals; <30dB (n=15), 30.0-32.5 (n=71), 32.5-35.0 (n=137), 35.0-37.5 (n=63), 37.5-40.0 (n=40), >40.0 (n=25). Note that there were few respondents in the lowest and in the highest intervals and hence results from these intervals should be treated with care. All significance tests presented in this paper were two-sided and $p < 0.05$ was considered statistically significant.

In Study II, data were collected through 15 interviews that was taped and transcribed verbatim. Subjects were first chosen strategically among those who in the questionnaires of Study I stated that they were willing to be contacted for further questioning and gave their telephone numbers. The objective of the strategic sampling was to obtain a heterogeneous group by regarding self-rated noise annoyance of wind turbine noise in relation to calculated SPLs from wind turbines as well as gender. As a model emerged the sampling became more theoretical, seeking variance within the identified categories. Subjects were at this stage also chosen from among those who had complained to local authorities concerning various aspects of wind turbines. The interviews were analysed according to the constant comparative method for discovering Grounded Theory [Glaser and Strauss 1967]. The transcribed interviews were coded line-by-line using the subject's own words or immediate expression. The codes were associated with each other to form clusters, categories were identified, and relationships between categories established. Constant comparison among and between transcribed interviews, memos, and categories led to reflections, confirmations, and adjustments in formulating the emerged model.

The results from Study I and Study II will here be presented thematically, but with references to which study they originate from.

3. Results

3.1. Perception

Most informants interviewed in Study II described noise as the dominating *not chosen stimulus* of wind turbines, adding blinking shadows, shadows sweeping over the garden, or the constant movement of the rotor blades as a second source of annoyance. The noise was often described as a swishing sound, but throbbing (dunkande), resounding (rungande), rattling (skramlande), and howling (tjutande) were also used as descriptors. Incidents that accidentally increased the noise were remembered (e.g. loose parts) and seemed to increase the negative affection even after they were taken care of. The noise was perceived as constant, not just passing by as a car on the road:

”Well, it’s this that it is never really quiet. It sort of swishes all the time.” (IP9, p.2).

The informants' descriptions of their feelings when exposed to wind turbine noise, as well as shadows and the rotating movement of the rotor blades, were in the analysis interpreted as an *intrusion into private domain*. The noise was physically perceived in the living environment, e.g. in the garden, in spite of bushes and fences put up to keep out invaders, and was to those who could not mentally shut it out, an obstacle to pleasant experiences decreasing the joy of daily life at home. For some of the informants the intrusion went further into the most private domain, themselves, creating a feeling of violation that was expressed as anger, uneasiness, and tiredness.

Noise was also the most noticed exposure from wind turbines when measured in Study I and related to the dose. The proportion of respondents who noticed noise from wind turbines outdoors increased with increasing A-weighted SPLs (Figure 1). At SPLs exceeding 35.0 dBA, 85% or more reported that they could hear the noise.

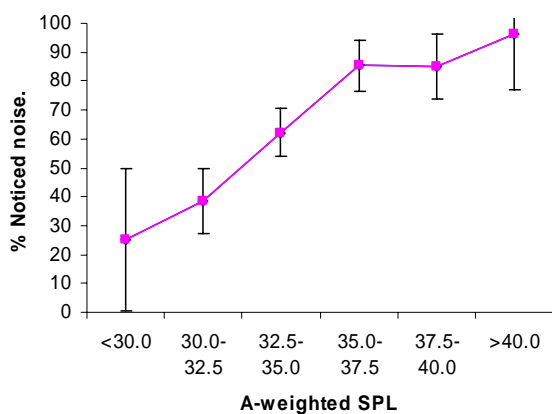


Figure 1. The proportion of respondents who noticed noise from wind turbines related to A-weighted SPLs with 95% confidence intervals.

Of those respondents who noticed the sound, 54% (n=103) stated that the noise was more noticeable at downwind conditions (when the wind was blowing from the wind turbine towards their dwelling), 39% (n=68) at strong wind, and 26% (n=44) at warm summer nights. There was

though a variation; some respondents stated that the noise was less noticeable at strong wind and downwind conditions as seen in Figure 2.

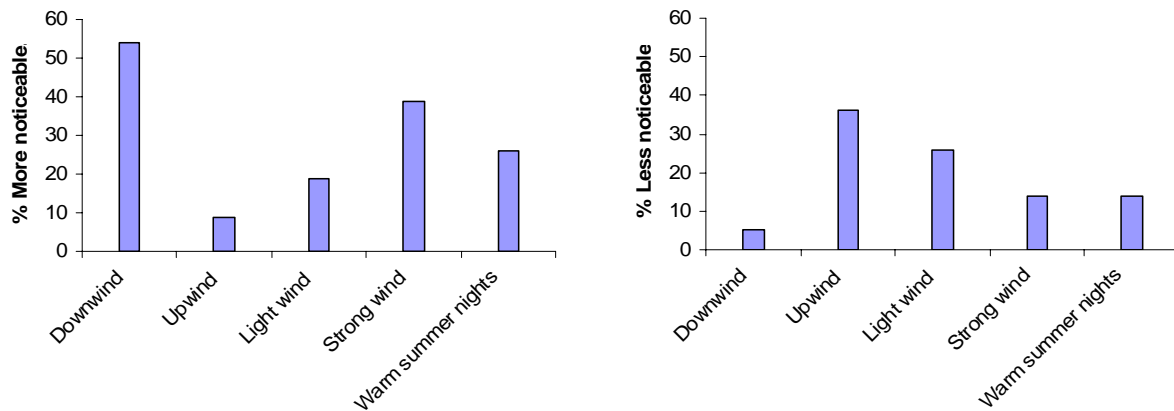


Figure 2. Proportion of respondents who noticed the wind turbine noise more or less in different situations.

3.2. Dose-response

Study I showed that the proportions of outdoor annoyance (rather and very annoyed) due to wind turbine noise increased with increasing A-weighted SPL at SPLs exceeding 35.0 dB (Figure 3). No respondent stated them selves annoyed at A-weighted SPLs below 32.5 dB. At A-weighted SPL of 37.5-40.0 dB the proportion annoyed was 28% (n=11; 95%CI: 14 - 41%) and above 40 dB it was 40% (n=11; 95%CI: 19 - 57%).

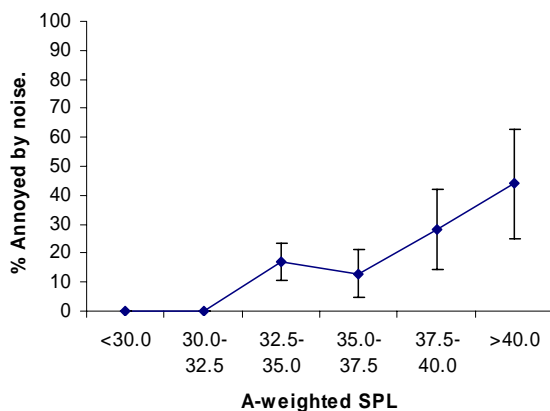


Figure 3. Proportion of respondents annoyed by wind turbine noise related to A-weighted SPLs with 95% confidence intervals.

To compare the dose-response relationship for wind turbine noise and response with that for other stationary sources (excluding shunting and seasonal industry) presented by Miedema and Voss [2004], noise exposure metrics day-evening-night levels (DENL) were calculated out of the hypothetical assumption that the SPLs presented above represented the noise exposure $L_{Aeq24hours}$.

A polynomial approximation of the dose-response relationship (eq.1) was plotted together with the annoyance curve for other stationary sources (eq. 2) in Figure 4.

$$\text{Wind turbine noise: \%A} = 224.77 - 13.625 \text{ DENL} + 0.2057 \text{ DENL}^2 \quad (\text{eq. 1})$$

$$\text{Other stationary sources: \%A} = 36.854 - 2.121 \text{ DENL} + 0.03270 \text{ DENL}^2 \quad (\text{eq. 2})$$

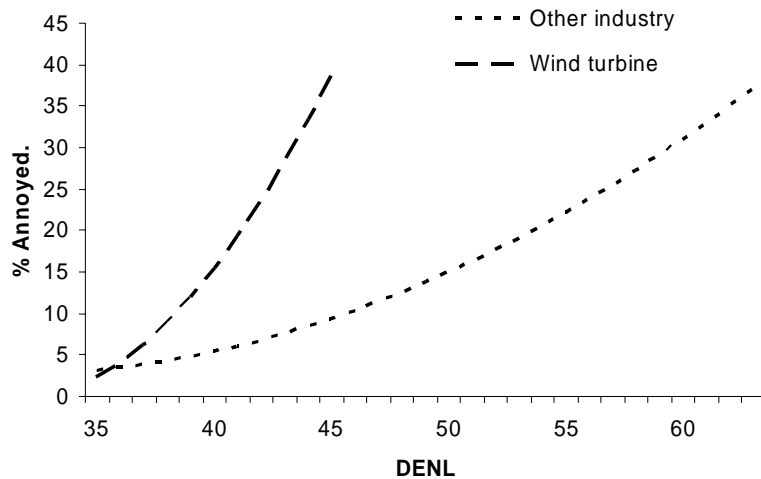


Figure 4. *The proportion annoyed persons as a function of DENL for noise from wind turbines and for noise from other industry (not shunting or seasonal industry).*

Figure 4 shows that the proportions of annoyed respondents were comparable between wind turbines and other industries at the starting point of 35 DENL. At higher SPLs the proportion annoyed by wind turbine noise increased more rapidly with exposure than the proportion annoyed by noise from other stationary sources.

3.3. Noise sensitivity

Of the respondents in Study I, 50% (n=169), stated that they were "rather sensitive" or "very sensitive" to noise. No association between noise sensitivity and A-weighted SPL was found ($r_s=0.07$; $p=0.204$); the proportion of noise sensitive varied some what between the six SPL-intervals, but no trend towards a higher proportion of noise sensitive at higher SPL was seen. Noise sensitivity was statistically significantly related to noise annoyance ($r_s=0.20$; $p<0.001$). Noise sensitivity seemed to influence the dose-response relationship especially at higher SPLs (Figure 5).

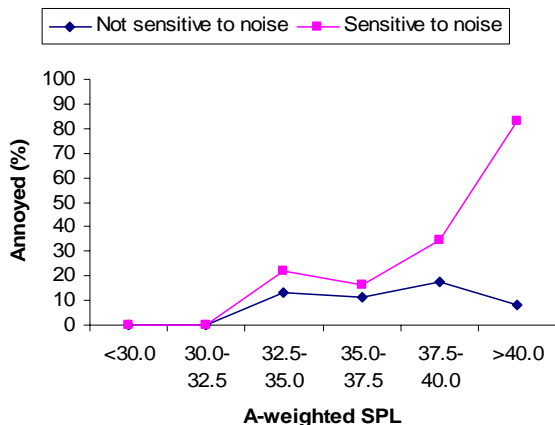


Figure 5. Proportion of respondents annoyed by wind turbine noise related to A-weighted SPLs comparing respondents not sensitive to noise (not sensitive at all, slightly sensitive) and respondents sensitive to noise (rather sensitive, very sensitive).

Some of the interviewed informants in Study II spontaneously stated that they did not want to get used to the exposure, even though they did not relate this behaviour to being noise sensitive.

“I never wanted to get used to it. We have bought far too expensive cars just so that they would be quiet. [...] No, I am not unusually sensitive. I have been at construction sites all my life [...] But I have been better at using hearing protectors than most people. So I have. [...] We totally agree, me and my wife. We value silence. We seek it.” (IP12, p.9)

3.4. Attitude to source

Of the respondents in Study I, 13% stated that they were "rather negative" or "very negative" to wind turbines. Attitude to wind turbines was positively correlated to noise annoyance ($r_s=0.33$; $p<0.001$) and seemed to influence the dose-response relationship (Figure 6). It could not though be excluded that the noise exposure caused part of the annoyance response. No statistically significant association between attitude to wind turbines and A-weighted SPL was found ($r_s=0.07$; $p=0.170$), but the proportion negative to wind turbines were somewhat higher at higher SPLs. Of the respondents living in areas with SPLs > 35 dBA, 16% were negative to wind turbines compared to 11% among those living at lower SPLs.

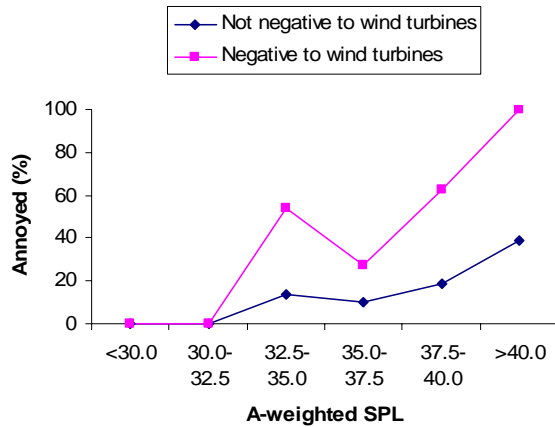


Figure 6. Proportion of respondents annoyed by wind turbine noise related to A-weighted SPLs comparing respondents not negative to wind turbines (very positive, positive, neither positive nor negative) and respondents negative to wind turbines (negative, very negative).

Attitude was also measured in a question regarding the respondent's attitude to wind turbines' impact on the landscape scenery. This factor was related both to SPL ($r_s=0.15$; $p<0.01$) and to noise annoyance ($r_s=0.51$; $p<0.001$); hence attitude to the wind turbines' impact on the landscape scenery could explain the variation in noise annoyance (Figure 7) or it could be that being annoyed by the noise caused a negative attitude to the wind turbines' visual impact. When modelling the dose-response and the influence of attitude in a logistic regression, the noise exposure was still a statistically significant variable for predicting noise annoyance ($\text{Exp}(b)=1.74$; 95% CI:1.29-2.34), even though the attitude to wind turbines' visual impact influenced the prediction highly ($\text{Exp}(b)=5.05$; 95% CI:3.22-7.92).

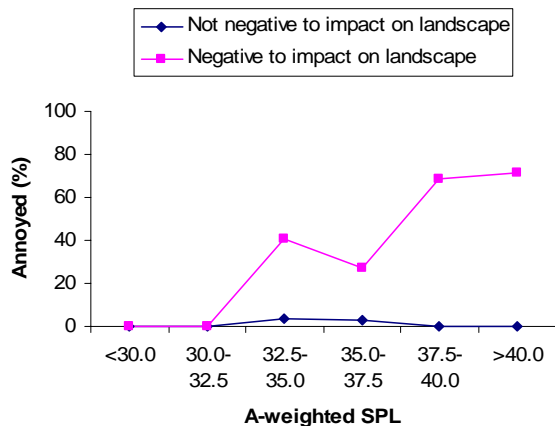


Figure 7. Proportion of respondents annoyed by wind turbine noise related to A-weighted SPLs comparing respondents not negative to wind turbines' impact on the landscape scenery (very positive, positive, neither positive nor negative) and respondents negative to wind turbines' impact on the landscape scenery (negative, very negative).

3.5. Visual exposure

Some of the respondents in Study I were exposed to shadows as well as noise from wind turbines. There was a correlation between shadow exposure (hour/year) and A-weighted SPL ($r_s=0.62$; $p<0.001$), but among the respondents exposed to higher A-weighted SPLs the intensity of shadow exposure varied. Of those respondents exposed to wind turbine noise > 35 dBA ($n=128$), 41% were exposed to shadows more than 10 hours/year and hence 59% were exposed to less than 10 hours/year. Among those exposed to lower A-weighted SPLs ($n=217$), almost no one (3%) were exposed to shadows more than 10 hours/year. The shadow exposure did not seem to influence the dose-response relationship between A-weighted SPL and noise annoyance (Figure 8). Noise annoyance and shadow annoyance were correlated ($r_s=0.50$; $p<0.001$).

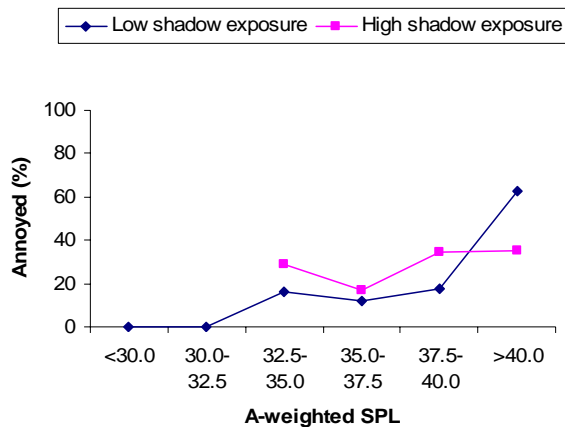


Figure 8. Proportion of respondents annoyed by wind turbine noise related to A-weighted SPLs comparing respondents subjected to low shadow exposure (< 10 h/year) and respondents subjected to high shadow exposure (> 10 h/year).

Several of the interviewed informants in Study II were annoyed by the movement of the rotor blades; a factor not thought about when designing Study I. They described the movement as something that involuntarily attracted the eye. The rotor blades were almost always rotating, leaving no rest from the stimulus to the receivers.

“Every time you walk in the garden or look at that direction, it is spinning. It just spins and spins. It gets you irritated. [...] If you are walking around looking down on the ground, you sort of have it in front of you so that you see it whisk around.” (IP3, p.2)

3.6. The rural setting

Some of the interviewed informants in Study II expressed that wind turbines were foreign objects that did not belong in the landscape and that one should be able to expect peace and quietness in the countryside.

”It is quiet and peaceful in the countryside in spite of tractors and the rail way. I mean, these are occasional sounds. A tractor passes and you know what it sounds like. And a train passes and that sounds too. The neighbours have the hay fans operating, but that is certain weeks and you have to accept that, as they of course need to dry the hay. There

are sounds in the countryside, but some sounds are natural and some are not. It is novel this with wind turbines, that is to say the sound.” (IP13, p.9)

Other informants thought of their living environment as a place for technical achievements and economical growth, and did not perceive the wind turbine noise as obstruct for a good quality of life. The informants hence had different *conception of the living environment*; a factor that might influence the response to wind turbine noise. Some of the informants stated that they had actively chosen to live in the countryside, seeking a place for recovery, even though they were brought up or had temporary lived in a city.

“Where you live is where you should feel well and regain strength in the breaks. We have moved to the countryside because it suits us, you know. Down-to-earth and all that.” (IP9, p11)

Reanalysing the data of Study I, some indications of the importance of the concepts of the living environment could be found. The respondents were asked were they lived before moving to their present residence. About 30% (n=102) had lived in a city before moving to the countryside and the remaining 70% had either lived at the same address as now, in another place in the countryside or in a small town. Former city-residents were slightly more annoyed by wind turbine noise (Figure 9), but the difference was not statistically significant. The main difference in attitude between the two groups was found regarding the attitude to wind turbines impact on the landscape scenery. Of the former city-residents 55% (n=56) had a negative view compared to 33% (n=80) among the others. The difference was statistically significant (Mann Whitney U: $Z_{MU}=-3.746$, $p<0.001$).

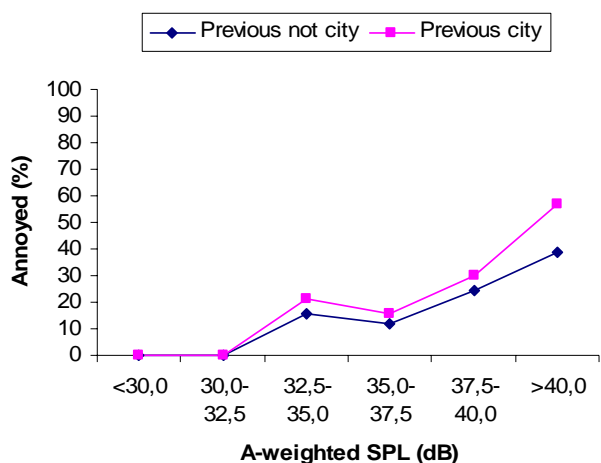


Figure 9. Proportion of respondents annoyed by wind turbine noise related to A-weighted SPLs comparing respondents that had not previously lived in a city and respondents that had previously lived in a city.

The respondents in the two groups also described the wind turbines slightly different. The respondents were asked to agree or not agree on 14 adjectives as descriptors of the phenomenon wind turbines. Both group rated "Environmentally friendly" the highest, but then the former city-

residents chose "Ugly" (48%) and "Unnaturally" (38%), while the other group rated "Necessary" (39%) and "Effective" (33%) as second and third.

3.7. Other variables formed out of experiences

The extent of intrusion by stimuli from wind turbines felt by the interviewed informants in Study II seemed to in part be determined by the informants' experiences of the situation. The experiences formed four categories, all comprising feelings of inferiority and all somewhat related. Feeling *lack of control* when the wind turbines were built, not being aware of the development plans or the impact the wind turbines would make on the living environment was common. Also the unpredictable occurrences of noise exposure and the impossibility to stop the wind turbines when reacting to audible and visual stimuli, created a feeling of no control of the situation. When trying to take control of the situation by contacting local authorities, a feeling of *lack of influence* sometimes occurred. Most of the informants did not believe that they had any say in the planning of new wind turbines or that complains about the noise would be treated seriously. They felt that they were *being subjected to injustice*, not only by the authorities, but also by the owners of the wind turbines that sometimes lived in other areas, not exposed to audible and visual stimuli themselves. For some informants, the feeling of *not being believed* was the most frustrating; friends and authorities had no understanding for the implication of living close to a wind turbine and the strong reactions the low levels of noise raised.

4. Concluding comments

A dose response-relationship between A-weighted SPL and noise annoyance was found. The results suggest that the proportion annoyed increases more rapidly with increasing SPL than for other stationary sources. The influence of hypothesised moderating factors showed high consistency with previous studies on community noise [Job 1988]; both noise sensitivity and attitude were associated with noise annoyance, especially when attitude was expressed as attitude to the wind turbines' impact on the landscape scenery. The latter indicates that the rapid increase of annoyance could be due to interference of visual factors on the audio perception. Visual aspects could be merely esthetical but the feelings of intrusion found in Study II point towards a complex influence of the wind turbines with a possibility of multi modal and/or interacting effects between audio and visual exposure. The visual stimuli of the rotor blades' constant movement might be a factor that enhances adverse effects. The rapid growth of noise annoyance could also be explained by an appraised incongruence between wind turbine noise and the respondent's conception of his or her living environment in a rural surrounding; the latter a factor probably firmly rooted within a personality and therefore difficult to change. Negative feelings induced by contacts with local authorities and owners of wind turbines also seem to be of importance for the reaction to wind turbine noise, but should be feasible to avoid with proper regulation and appropriate planning process.

In the next phase of the ongoing project on human responses to wind turbines, more data will be collected to achieve a larger base for evaluating dose-response relationships between wind turbine noise and noise annoyance. It would be of great interest if similar studies would be carried out in other countries to enlarge the data base, but also to study possible cultural differences. To evaluate sound propagation algorithms used to calculate the dose, measurements

of sound and meteorological data should also be carried out. The effect of simultaneous audible and visual exposures from the same source is of special interest for future research on responses to wind turbines.

References

- Fields, J.M. (1993). Effect of personal and situational variables on noise annoyance in residential areas. *Journal of Acoustical Society of America*, **93**, (5), 2753-2763.
- Glaser, B. G., & Strauss, A. L. (1967). *The discovery of grounded theory: strategies for qualitative research*. Chicago: Aldine.
- Job, R.F.S. (1988). Community responses to noise: A review of factors influencing the relationship between noise exposure and reaction. *Journal of Acoustical Society of America*, **83**, (3), 991-1001.
- Kastka, J. and Hangartner, M. (1986). Machen hässliche Strassen den Verkehrslärm lästiger? *Arcus*, **1**, 23-29
- Miedema, H. and Vos, H. (1998). Exposure-response relationships for transportation noise. *Journal of Acoustical Society of America*, **104**, (6), 3432-3445.
- Miedema, H. and Vos, H. (2004). Noise annoyance from stationary sources: Relationships with exposure metric day-evening-night level (DENL) and their confidence intervals. *Journal of Acoustical Society of America*, **116**, (1), 334-343.
- Pedersen, E., and Persson Waye, K. (2004). Perception and annoyance due to wind turbine noise – a dose-response relationship. *Journal of Acoustical Society of America*, **116** (6), 3460-3470.
- Swedish Environmental Protection Agency (2001). *Ljud från vindkraftverk*. (Sound from wind turbines). Report no. 6241. Stockholm, Sweden.
- Viollon, S., Lavandier, C., and Drake, C. (2002). Influence of visual setting on sound ratings in an urban environment. *Applied Acoustics*, **63**, 493-511,
- Wolsink, M., Sprengers, M., Keuper, A., Pedersen T.H. Westra, C.A. (1993). Annoyance from wind turbine noise on sixteen sites in three countries. In: *European community wind energy conference 8-12 March*, Lübeck, Travemünde, 273-276.

**First International Meeting
on
Wind Turbine Noise: Perspectives for Control
Berlin 17th and 18th October 2005**

SIROCCO: Silent ROTors by aCoustic Optimisation

**J. G. Schepers, A.P.W.M. Curvers¹
S. Oerlemans²
K. Braun, T. Lutz, A. Herrig, W. Wuerz³
B. Méndez López⁴**

¹Energy Research Centre of the Netherlands, ECN, The Netherlands
P.O. Box 1
1755 ZG Petten, The Netherlands
schepers@ecn.nl, curvers@ecn.nl

²National Aerospace Laboratory NLR, The Netherlands
P.O. Box 153, 8300 AD Emmeloord, The Netherlands
stefan@nlr.nl

³University of Stuttgart, Germany
Pfaffenwaldring 27
70569 Stuttgart, Germany
braun@ica.uni-stuttgart.de, Thorsten.Lutz@iag.uni-stuttgart.de,
Andreas.Herrig@iag.uni-stuttgart.de, wuerz@ica.uni-stuttgart.de

⁴Gamesa Eólica, Spain
Cañada real de las merinas 7
Edificio 3, Planta 4
28042 Madrid, Spain
bmendez@eolica.gamesa.es

Summary

In this paper the status and the main results from the European 5th Framework project 'SIROCCO' are described. The project started in January 2003 and will end in February 2007. The participants in this project are the Energy Research

Centre of the Netherlands (ECN) and the National Aerospace Laboratory (NLR), both from the Netherlands, the University of Stuttgart (USTUTT) from Germany and Gamesa Eólica from Spain. GE Wind Energy joined the project in May 2005. The main aim of the SIROCCO project is to reduce wind-turbine aerodynamic noise significantly while maintaining the aerodynamic performance. This will be achieved by designing new acoustically and aerodynamically optimised airfoils for the outer part of the blade. The main focus of the project is on the reduction of trailing edge noise, which is broadly believed to be the dominant noise mechanism of modern wind turbines.

1. Introduction

Wind turbine noise is still one of the major obstacles for the widespread use of wind energy in Europe. For this reason the European 5th Framework project SIROCCO is performed. The principal objective of the SIROCCO project is to obtain a significant noise reduction on full-scale wind turbines, without negative effects on the aerodynamic performance. The main focus of the project is on the reduction of trailing edge noise, which is broadly believed to be the dominant noise mechanism of modern wind turbines. Thereto the existing airfoils at the outer part of the blade are replaced by airfoils with an improved aerodynamic flow at the trailing edge. Only the outer part of the blade needs to be considered, because this part is exposed to the maximum flow velocities and consequently produces the highest aero-acoustic noise levels. The project can be seen as the natural successor of the past EU project with acronym DATA ('Design and Testing of Acoustically Optimised Airfoils for Wind Turbines') where similar activities led to a noise reduction on a model wind turbine, placed in the large German Dutch Wind Tunnel DNW.

The SIROCCO project started in January 2003 with 6 participants: the Energy Research Centre of the Netherlands (ECN), the National Aerospace Laboratory (NLR) and Composite Technology Center (CTC) from the Netherlands, the University of Stuttgart (USTUTT) and NOI Rotortechnik from Germany and Gamesa Eólica from Spain. Since then the project consortium has undergone some changes: In 2004 NOI and CTC withdrew and in 2005 GE Wind Energy joined the project. The project is scheduled to end in February 2007.

The activities in the SIROCCO project are carried out on two reference turbines: One of these turbines is a three bladed Gamesa 850 kW turbine, the other turbine is a 2.3 MW turbine from GE Wind Energy. Since GE Wind Energy joined the project very recently, it is only the results on the Gamesa turbine, which will be discussed in this paper.

The project started with acoustic field measurements to characterise the noise sources on the existing Gamesa wind turbine. Thereto a new acoustic array measurement technique, developed in the DATA project has been extended and utilised to localise and quantify noise sources on the rotating blades. The aim of

this task was to verify that trailing edge noise is the dominant noise source for the baseline turbine indeed. This would make it worthwhile to continue the project and spend further effort on the reduction of this noise source. These activities were mainly carried out by NLR and Gamesa, where as a spin off activity ECN compared the measurements with calculations.

Parallel to the field measurements, a combined aero-acoustic design methodology that was developed in DATA has been extended and improved to design low-noise airfoils for the outer part of the rotor blade taking into account the constraints imposed by Gamesa.

This activity was mainly carried out by the University of Stuttgart with support from Gamesa.

Subsequently the new airfoils were tested in two-dimensional acoustic and aerodynamic wind tunnel tests. This activity was mainly carried out by the University of Stuttgart in their Laminar Wind Tunnel. The acoustic wind tunnel measurements were performed by NLR in the AWB anechoic tunnel from DLR. After the design of the acoustic airfoils and the validation of their behaviour in the 2D wind tunnel environment, the airfoils are implemented into full-scale blades by Gamesa. Thereafter ECN and NLR assess their acoustic and aerodynamic behaviour by means of extensive field measurements of the noise, the power and the loads at different operational conditions. At the time of writing the paper, the design and manufacturing of the blades is underway.

The present paper aims to give a global overview of the Sirocco project and therefore it will address only the main results from the above mentioned tasks. For a more detailed description of the acoustic field measurements, reference is made to [1], the airfoil design is reported in detail in [2] and the wind tunnel measurements are described in [3].

2. Acoustic field measurements

Acoustic measurements on the GAMESA baseline turbine took place in December 2003, on a site close to Zaragoza (Spain). The aim of these experiments was to verify whether trailing edge noise is the dominant noise source. In order to assess the effect of blade roughness (e.g. due to dirt) on the noise, one blade was cleaned, one blade was cleaned and tripped (0.4 mm zig-zag tape at 5% chord on upper and lower surface), and the third blade was left untreated.

The acoustic measurements were done using a 150-microphone acoustic array, which was placed upstream of the turbine in the prevailing wind direction. The measurement time for each data point was 30 s. Synchronously with the acoustic measurements, several turbine parameters and meteorological conditions were stored using a GAMESA turbine monitoring program and an adjacent meteo mast. In total, more than 100 data points were taken for the desired wind direction and speed range, where most of the analysis took place on the 35 'best'

data points (i.e. data points with small variations in wind speed, yaw angle, small misalignment between array position and wind direction, etc.)

The array signals were processed to obtain the noise source distribution in the rotor plane. A typical example of such an acoustic 'source plot' is given in figure 1. It shows that the blade noise (i.e. the aerodynamic noise) is dominant where mechanical noise coming from the nacelle plays a minor role. It furthermore shows that practically all the noise is produced by the outer part of the blades, although, opposite to the expectations, it is not the very tip of the blade which dominates, but roughly speaking the part of the blade which is between 75 and 95% span.



Figure 1: Picture of test set-up for acoustic measurements on the GAMESA baseline turbine. The distribution of noise sources in the rotor plane is projected onto the picture. The rotor rotates clockwise

Most of the noise is produced when the blades are moving down. This effect was observed for all measurements and all frequencies, and it is very similar to results obtained earlier on the model scale wind turbine in the DATA project, where it was attributed to a combination of convective amplification and directivity of trailing edge noise. It should be noted however that for a different observer location, the pattern may be different.

Using a power integration method, the acoustic source plots were translated to absolute sound levels. The results indicated that the noise produced by the

blades is proportional to the 5th power of the wind speed at the blades, which is an indication that the responsible mechanism is trailing edge noise. Another aerodynamic noise source, i.e. inflow-turbulence noise, typically shows a U^6 speed dependence.

In a next processing step, an alternative method was used (ROSI – ROTating Source Identifier) which allowed locating the noise sources on the *rotating* blades, so that the noise from the three blades can be distinguished. These measurements showed the tripped blade to be much noisier than the other two blades. This observation is again an indication that trailing edge noise is the dominant mechanism (if inflow-turbulence noise were dominant, then tripping would have no effect on the noise levels).

Although the resolution of the source localization method does not seem to be sufficient to determine whether the noise comes from the leading- or trailing edge of the blades, the above-mentioned observations indicate that trailing edge noise is the most likely source mechanism.

For a more detailed description of the results obtained in this task, reference is made to [1].

3. Validation of aero-acoustic wind turbine code SILANT with acoustic array measurements

As a spin-off to the investigations described in the previous chapter, the NLR-measurements have been used to validate the aero-acoustic wind turbine code SILANT. This code was developed in 1996 by a Dutch consortium which consisted of Stork Product Engineering (SPE), the Dutch Aerospace Laboratory (NLR) and TNO. For a detailed description of the code reference is made to [4]. The SILANT code calculates the sound power level of the wind turbine blades and sums it to the overall wind turbine sound power level. The input for the code consists mainly of geometrical and aerodynamic data, operational conditions and external conditions.

Basically SILANT calculates the noise level according to the following lines:

- The wind turbine blades are divided in a number of elements (usually the number of elements is in the order of 10 to 20);
- For every blade element two noise sources are calculated:
 - Inflow noise: This noise source is calculated from the model of Amiet and Lawson [6]
 - Trailing edge noise: This noise source is calculated from the model of Brooks, Pope and Marcolini [5].

The noise sources are ('acoustically') summed over the elements in order to obtain the total blade and turbine sound power level.

The above mentioned models from Amiet and Lawson and the model from Brooks, Pope and Marcolini require the following data, which need to be provided per blade element:

- The Reynolds number;
- The displacement thicknesses of the boundary layer at the trailing edge of the blade element for both the pressure and the suction side.

The displacement thicknesses are found from a database, which was created a-priori and delivered along with the SILANT program. These displacement thicknesses were calculated with the XFOIL airfoil design and analysis code [7] for a limited number of angles of attacks, Reynolds numbers and airfoils. Within the present project, ECN extended and improved the SILANT database. Among others, the displacement thicknesses are calculated with the RFOIL code [8]. RFOIL is an extension of XFOIL, developed by ECN, NLR and DUT and it takes into account rotational effects.

Furthermore it was assured that all the necessary Reynolds numbers, angles of attack and airfoils for the present calculations are covered in the database.

Then the only missing data are still the Reynolds number and the angle of attack at every blade element. These data are found from an aerodynamic wind turbine model, based on the blade element momentum theory.

Figure 2 shows the comparison between the SILANT calculated and measured overall sound power level. The results are presented as function of power (measured: electrical power; calculated: aerodynamic power) instead of the more common presentation where noise is plotted versus wind speed. This is due to the fact that the wind speed measurements were suspected to suffer from large uncertainties. The figure shows an excellent agreement at below rated conditions. The results indicate a very slight under prediction of noise level but if the unknown power losses (which are typically in the order of 5%) could be included, an even better agreement is expected. Near rated conditions, the results show an over predicted noise level. It is noted that no results can be presented for above rated conditions due to the fact that the noise-power curve becomes multi-valued at constant rated power.

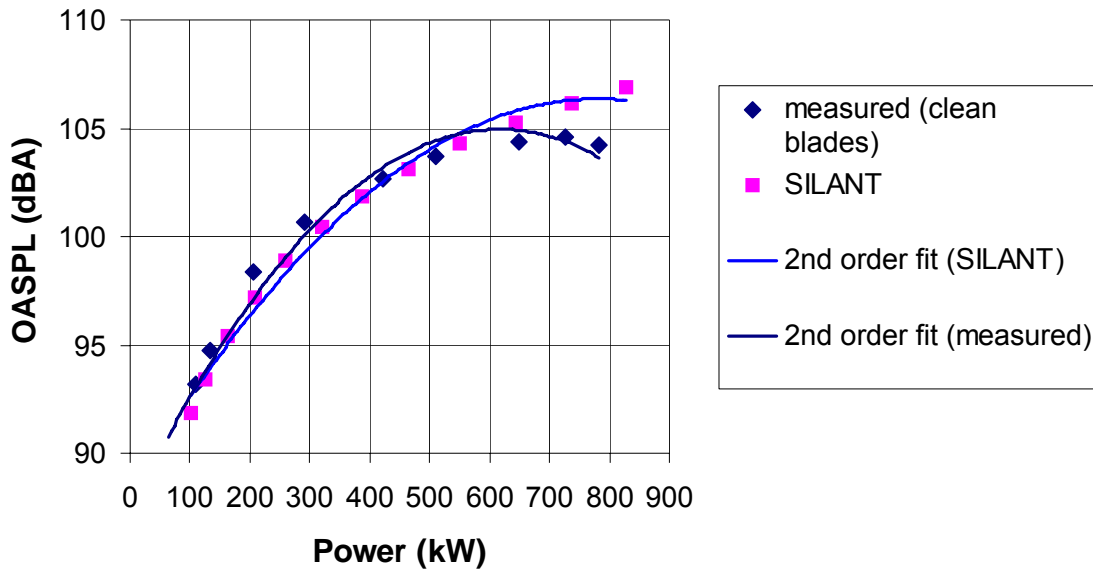


Figure 2: Calculated and measured noise production as function of power

The results from figure 2 gave sufficient confidence into the SILANT code to use it for an additional investigation on the question whether trailing edge noise is the dominant noise source. Thereto the contribution of trailing edge noise in relation to the inflow turbulence noise and the total noise is determined at two wind speeds (6.34 m/s and 10.15 m/s) The turbulence intensity at the site is determined using a roughness height of 0.2 m (as a matter of fact the results turned out to be very insensitive to this roughness height). The results for the inflow noise, trailing edge noise and the total noise (per blade) are given in table 1:

V_w [m/s]	Inflow [dB(A)]	Trailing edge [dB(A)]	Total [dB(A)]
6.34	82.30	91.27	91.79
10.15	94.04	101.19	101.96

Table 1: SILANT calculations: Inflow noise, trailing edge noise and total noise (per blade)

According to these calculations the trailing edge noise level is much higher than the inflow noise level. This is a further indication that trailing edge noise is dominant.

4. Aero-acoustic design methodology

The main aim of the SIROCCO project is to design low noise blades. Thereto the airfoils at the noisiest outer part of the blade are replaced by acoustically optimised airfoils with the same aerodynamic performance.

The low noise airfoils were designed with a combined (2D) aerodynamic/aero-acoustic model, which was implemented into a numerical optimisation tool, see also [14].

The basic philosophy in the design of low noise airfoils relies on the idea to modify the boundary layer state at the trailing edge. This is accomplished by adjusting the main pressure recovery at the rear part of the airfoil. For this purpose an aero-acoustic design methodology, which is capable of modelling the boundary layer around an airfoil and the resulting noise levels was required. During the previous project DATA, acoustic airfoils have been designed with the noise prediction scheme developed by TNO-TPD in the EU project DRAW [9]. This TNO-TPD model is based on the theory proposed by Chandiramini [10] and Blake [11]. It essentially calculates the spectrum of the trailing edge noise from several boundary layer properties, one of which is the mean velocity profile $u(y)$ at the trailing edge. This profile is approximated from an integral boundary layer procedure based on integral parameters like displacement thickness, momentum thickness or skin friction, where the boundary layer profiles were assumed to behave according to the Coles law of the wall profile in combination with the law of the wake.

The integral boundary layer parameters were calculated by the airfoil design and analysis code XFOIL [7].

Apart from the mean boundary layer profile $u(y)$, the TNO-TPD model requires a number of turbulence quantities across the boundary layer at the trailing edge, more precisely the distributions of the rms-value of the vertical velocity fluctuations $\overline{v'^2}$ and the integral length scale Λ_2 of the vertical velocity fluctuations in the boundary layer. The length scale Λ_2 is a measure for the vertical extent of the turbulent eddies and it is defined as:

$$\Lambda_2 = \int_0^{\infty} R_{22}(\xi, t) d\xi$$

With R_{22} the normalised spatial two point correlation coefficient of the vertical velocity fluctuations. In the TNO-TPD scheme the required turbulent quantities are found from a mixing length approach where Λ_2 is derived from a specific calculated turbulence length scale, by multiplying it with an empirical constant.

The combined aero-acoustic models have been implemented into the numerical optimisation environment POEM. This makes it possible to generate airfoil shapes with a minimal noise production in an automatic way. Thereto the 2D airfoil geometry is parametrised through Bezier curves with the ordinate values of the control polygon as design variable and the minimal noise production as objective function. The inclusion of the constraints imposed by the manufacturer

played an important role. This holds among others for aerodynamic and geometric requirements. One can think of constraints on $c_{l,max}$, α_0 , c_l/c_d , parts of the airfoil geometry which should remain unchanged etc.

It should be emphasized that these constraints are a result of the fact that the present project aims to modify existing blades. It is only the outer part of the blade that will be equipped with new airfoils and in order to fit the outer and inner part, constraints should be imposed on the aerodynamic behaviour of the new airfoils. If low noise blades were designed from 'scratch', many constraints could be released, which, by definition, yields better performance.

The acoustic airfoil has been designed in two rounds. The first round airfoil was based on the methodology as described above, which relies on the integral boundary layer procedure. Unfortunately, the experimental verification (see section 5) showed that the required design goals (a noise reduction at the same aerodynamic performance) were not met. This then led to critical review of the assumptions in the methodology. An extensive experimental program in the Laminar Wind Tunnel from the University of Stuttgart supported this assessment. In particular boundary layer measurements on an airfoil with a variable trailing edge (and consequent pressure recovery) led to important insights, see section 5.1:

- The optimised airfoils, which are designed in the present project, have flow regions with significant acceleration and deceleration. For such airfoils the Coles velocity profile (or alternatively the Swafford boundary layer velocity profile) show considerable deviations to the measured profile;
- The mixing length approach to determine the $\overline{v'^2}$ from the mean boundary layer profile $u(y)$ works reasonably well for 'conventional' airfoils. It is however a local approach, which assumes the boundary layer to be in equilibrium, where 'history' effects, i.e. the stream wise development of the turbulence properties in the boundary layer are not explicitly taken into account. For the optimised airfoils however, having flow regions with significant acceleration or deceleration, 'history' effects are much more important. Moreover these history effects may alter the anisotropy of the turbulence where the anisotropy was modelled through the commonly used empirical constants;
- A similar observation was found in the measurements of the vertical integral length scale Λ_2 . In the original method, a constant scaling factor was used to calculate the Λ_2 from a given turbulence length scale. The experiments indicated that this assumption is only valid for equilibrium boundary layers.

These results showed the necessity to account for history and anisotropy effects along with the importance of a good scaling law. Therefore the aero-acoustic design method was changed. Although the acoustic part remained essentially the same, the boundary layer was represented with the finite-difference EDDYBL procedure in combination with a stress- ω turbulence model [12]. In this way the

boundary layer and the turbulence equations are solved on a computational grid with discretisation in streamwise and wall normal direction. The stress- ω turbulence model provides a direct estimate of $\overline{v'^2}$ at the grid points, in which the anisotropy and history effects of the boundary layer are taken into account. XFOIL provides the initial and boundary conditions along the boundary layer edge.

The stress- ω turbulence model also calculates a turbulence length scale, which is then used to derive the Λ_2 scale. The relation between the 'stress- ω turbulence length scale' and the Λ_2 is determined semi-empirically from the experimental database. Opposite to the previously used scaling factors it takes into account the boundary layer development. In this way the scaling factor has become variable instead of constant.

The design methodology, as described in this way, has been used to produce the second round airfoil designs. This yielded a noise reduction, not only in the theoretical results (which is obvious from the optimisation), but also in the wind tunnel measurements (see section 5.2 and 5.3). Furthermore it was shown that the noise spectra and the boundary layer properties, which are relevant for the noise generation are predicted much better with the new method.

For more detailed information on the design methodology, reference is made to [2] and [14].

5. 2D Wind tunnel measurements

In the previous section, it was already pointed out that 2D wind tunnel measurements have been carried out which supported and validated the theoretical design efforts. Several types of wind tunnel measurements have been performed. Roughly speaking they can be distinguished into the following categories:

1. Measurements on an airfoil with a variable trailing edge (VTE). These measurements aimed to understand the effect of different pressure recoveries on the trailing edge boundary layer properties;
2. Measurements of aerodynamic polars c_l , c_d (α) etc. on the reference airfoils and the optimised airfoils. These measurements aimed to verify the aerodynamic performance of the optimised airfoils in comparison with the performance of the reference airfoil;
3. Acoustic measurements on the reference airfoils and the optimised airfoils. These measurements aimed to verify the acoustic behaviour of the optimised airfoils in comparison with the behaviour of the reference airfoils.

The first and second types of measurements have been performed in the Laminar Wind Tunnel (LWT) of the Institute of Aerodynamics and Gas Dynamics, University of Stuttgart. The LWT is an open return tunnel with a closed test section.

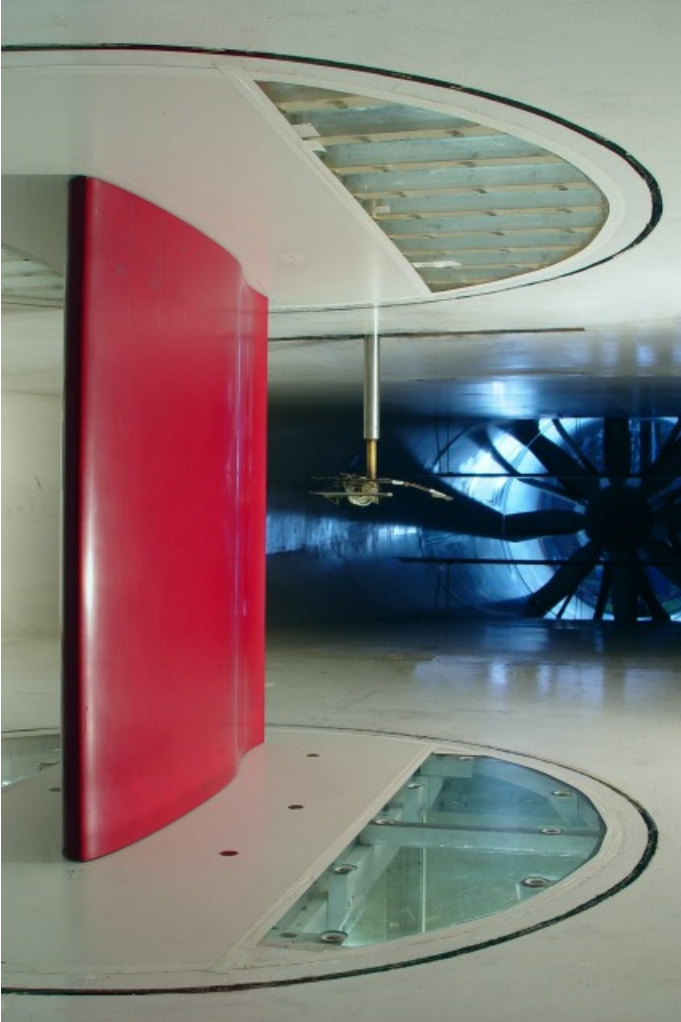


Figure 3: Test section of LWT wind tunnel

The rectangular test section measures $0.73 \times 2.73\text{m}^2$ and is 3.15m long, see figure 3. Typical turbulence intensities are only 0.02%. The lift is determined by experimental integration of the pressure distribution along the opposite two tunnel walls. The drag is determined by a wake rake. Although originally not planned in the project, USTUTT also performed acoustic measurements using the new Coherent Particle Velocimetry Method (CPV) technique [13]. These acoustic measurements could be done in parallel to the aerodynamic measurements.

Originally it was planned to perform acoustic tests in DLR's Aeroacoustic Wind Tunnel AWB only, which is located in Braunschweig. These measurements were carried out under supervision of NLR.

The AWB is an open jet wind tunnel with a rectangular nozzle of 1.20 m height and 0.80 m width, see figure 4. An anechoic chamber surrounds the test section, downstream of the nozzle. Two vertical endplates are mounted to the sides of the nozzle, providing a semi-open test section for 2D airfoil noise measurements. Trailing edge noise emissions were quantified on both suction and pressure side

of the model using an acoustic microphone array. Balance measurements were performed to obtain the aerodynamic forces on the airfoils, which then could be compared to USTUTT's aerodynamic measurements.



Figure 4: Test set-up in AWB. The (white) model is mounted horizontally between two endplates which are mounted to the nozzle. The microphone array is mounted above the test section.

5.1 Measurements on VTE airfoil.

The measurements were performed on an airfoil with a variable trailing edge (the so-called VTE airfoil). The VTE airfoil was designed at the Institute of Aerodynamics and Gas Dynamics (IAG) of the University of Stuttgart. The basic geometry should represent the properties of the airfoil sections, which are used by the manufacturers in the present project. The upper airfoil shape has been made variable between $x/c = 0.4$ and $x/c = 1.0$, see figure 5, leading to different pressure recoveries at the rear part of the suction side. The figure shows airfoil shapes, which yield a convex (VTE_vex) and a concave pressure recovery (VTE_kav). The reference situation giving a linear pressure recovery is also represented.

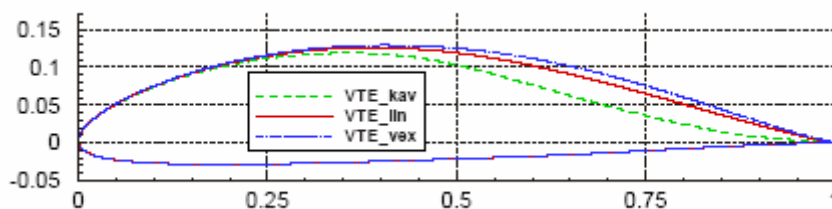


Figure 5: Design contours of the VTE model

The VTE-kav and VTE_vex geometries shown in the figure represent the limiting

airfoil shapes, but the contour was adjustable to a wide variety of shapes between these two extremes. The different pressure recoveries, reached in this way, yield different trailing edge boundary layer parameters and as such a different trailing edge noise production. Most of the experimental data gained in the present project were obtained on the VTE-lin airfoil and the VTE-kav airfoil at a Reynolds number of $3 \cdot 10^6$ with natural and fixed transition (fixed at $x/c=0.05$ at upper and lower surface). The following measurements have been performed:

- Measurements of c_l , c_d and x_{tr} as function of the angle of attack.
- Measurements of pressure distributions. In figure 6, a typical result is shown for the VTE_lin and VTE_kav airfoil geometry at $c_l=0.7$, where the measured pressure distribution is compared with the XFOIL pressure distribution (a comparison with MSES is also presented in the figure, but this code will not be discussed in this paper).

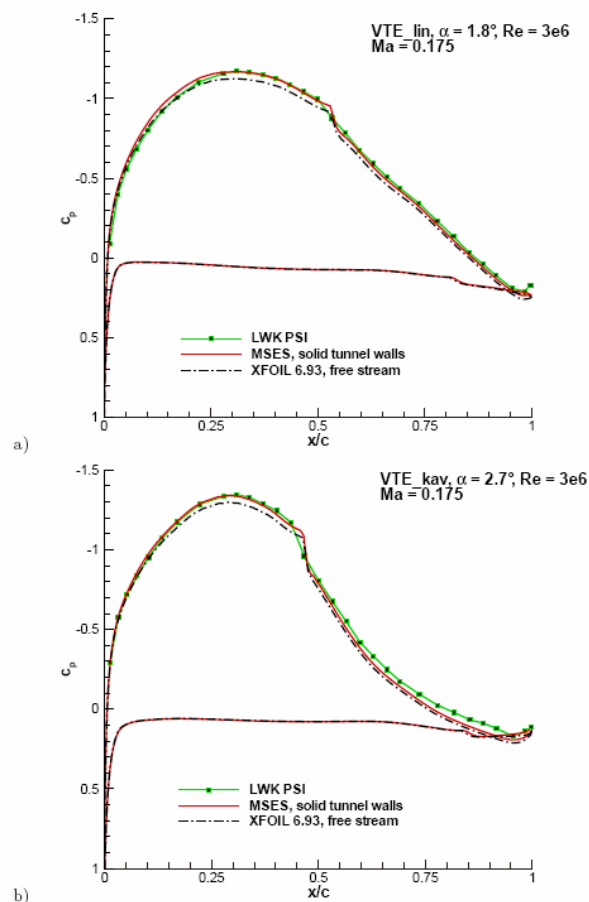


Figure 6: Comparison of measured pressure distribution with XFOIL (and MSES) calculations for $c_l = 0.7$, $Re = 3 \times 10^6$, $Ma = 0.175$, clean.

The influence of the geometry on the pressure recovery is clearly visible. Furthermore it can be seen that the effects from the different airfoil geometries are predicted well by XFOIL. This is very important information in view of the fact that the design method which models the effect of the airfoil geometry changes, relies among others on XFOIL.

- Boundary layer measurements of the velocity (fluctuations) in x and y-direction using hot-wire probes. As already pointed out in section 4, the measured boundary layer profiles and the fluctuations u' and v' were used for the selection of adequate turbulence models for the noise prediction codes. Figure 7 shows a very good agreement between the measured results and the EDDYBL stress- ω model, even for the VTE-kav airfoil, which can be considered as an extreme test case. Furthermore, measurements of the vertical correlation length Λ_2 have been performed using split-film probes. These measurements supported the determination of a reliable correlation between the turbulence length scale from the stress- ω model and the actual value of Λ_2 .

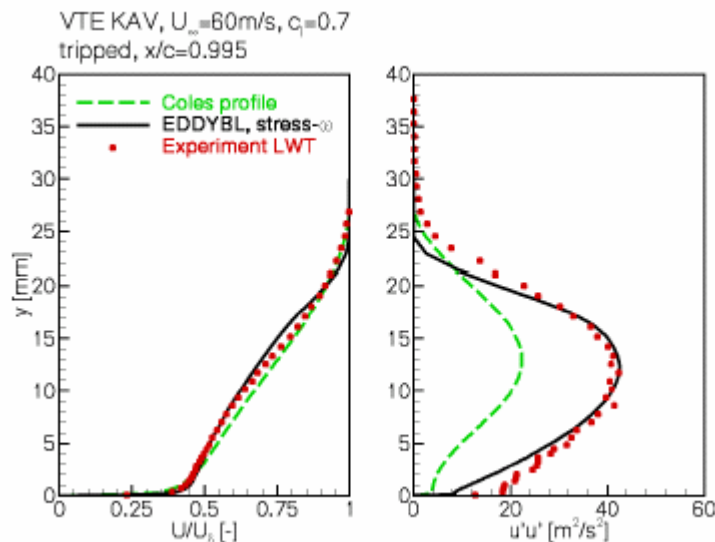


Figure 7: Predicted and measured boundary layer properties for the tripped VTE-KAV airfoil ($x_{tr}/c=0.05$)

- Additional acoustic tests, using the Coherent Particle Velocimetry Method (CPV) developed at the LWT have been performed on the VTE model to support the noise prediction

5.2 Aerodynamic verification of optimised airfoils in LWT wind tunnel:

As mentioned in section 4, the acoustically optimised airfoils have been generated with an optimiser in which a number of constraints were included. The manufacturer imposed these constraints. The constraints mainly result from the fact that the new airfoils should be implemented on the outer part of an existing blade, where the inner part of the blade remains the same. This limits the 'design freedom' considerably and generally speaking the optimised airfoils were only allowed to differ slightly from the reference airfoils in terms of α_0 , C_{dmin} , $C_{l,max}$, C_l/C_d and airfoil thicknesses,

In order to check whether the theoretical constraints are met, the aerodynamic performance of the airfoils has been measured in the LWT. The measurements were done at Reynolds numbers of $1.6 \cdot 10^6$ with natural and fixed transition

($x_{tr}/c=0.05$). More detailed information on these measurements is given in [3] but the most important conclusion is that the aerodynamic constraints are met.

5.3 Acoustic verification of optimised airfoils in AWB wind tunnel

In order to validate the noise reduction, which was expected from the combined aerodynamic/aero-acoustic design method, wind tunnel measurement were performed of the noise production of the optimised airfoils and the reference airfoils. The measurements were mostly done at a Reynolds number of $1.5 \cdot 10^6$ with natural and fixed transition ($x_{tr}/c=0.05$). A detailed discussion of the results is outside the scope of this paper, but the main result is a noise reduction which is between 1.0 and 1.5 dB(A) where the noise reduction is larger for clean conditions than for tripped conditions. It was also found that for other airfoils than the one applied by Gamesa, a larger noise reduction is possible (in the order of 2.5 dB(A)). The measurements confirmed that the design method based on the EDDYBL/stress- ω model performs much better than the method based on an integral boundary layer procedure.

In addition to the acoustic array measurements in the AWB tunnel the noise reduction has also been measured in the LWT tunnel using the CPV technique. Generally speaking the results are consistent although some differences appeared which could be explained by the open-jet effect in the AWB. After taking into account the open-jet effects, the differences were relatively small. More detailed information on these measurements is given in [3]. The future validation of the airfoils, which will be developed for GE, will be done solely in the LWT. This leads to an increase of the consistency of the data, because aerodynamic and aero-acoustic measurements can be performed in the same facility.

6. Future activities in the SIROCCO project

At the time of writing the paper, Gamesa is incorporating the new airfoils at the outer 25% of the blade. This task is far from trivial in view of the 3D aspects in the blade design and the fact that the aerodynamic behaviour of the outer airfoils has undergone some slight changes, where the inner part of the blade remains unchanged.

Subsequently the full-scale optimised blades will be manufactured. The acoustic and aerodynamic performances of the optimised blades will be measured by ECN and NLR for several operational conditions and compared to the baseline blades. The acoustic array technique will be used to quantify the noise reduction, while the aerodynamic performance is assessed through extensive meteorological, power and flatwise moment measurements. Special attention is paid to the comparison procedure in view of the difficulty of interpreting field measurements under instationary and uncontrollable weather conditions. For this

reason it is planned to perform measurements on a 'hybrid rotor' with one acoustically optimised blade and two baseline blades insuring identical conditions on the blades.

7. Conclusions

- Detailed acoustic field measurements have been performed on the Gamesa G58 baseline turbine. The measurements indicated that trailing edge noise was the dominant noise source. This observation was confirmed by calculations using a wind turbine aero-acoustic model;
- An acoustic airfoil has been designed for the outer part of the Gamesa turbine. The airfoil was designed in two rounds:
 - The first round used an aerodynamic/aero-acoustic design method, based on an integral boundary layer procedure. The expected theoretical noise reduction did not appear in the wind tunnel experiments. This was explained by the fact that the boundary layer procedure and the evaluation to obtain the input data for the noise prediction, is essentially a local method, which does not take into account 'history' effects of the boundary layer development.
 - The second round airfoil has been designed with a finite difference boundary layer method, including a stress- ω turbulence model and a new semi-empirical scaling law for the vertical correlation length scale. This yielded a noise reduction, not only in the theoretical results, but also in the experimental wind tunnel measurements. Furthermore it was shown that the noise spectra and the boundary layer properties, which are relevant for the noise generation are predicted much better with the new method.
- The potential noise reduction is obviously limited by the constraints, which result from the fact that existing blades and airfoils are modified. An unconstrained optimisation 'from scratch' is expected to yield a higher noise reduction.

Acknowledgement

'Financial support for this research was given in part by the European Commission's Fifth Framework Programme. Project Reference: ENK5-CT-2002-00702 Sirocco: Silent ROTors by Acoustic Optimisation. ECN and NLR received additional funding from SenterNovem under project number 400003700

References

- [1] S. Oerlemans, B. Méndez López: *Localisation and quantification of noise sources on a wind turbine*, First International Meeting on Wind Turbine Noise: Perspectives for Control", Berlin, 17-18 October 2005
- [2] Th. Lutz, A. Herrig, W. Würz, K. Braun, E. Krämer: *Constrained Aerodynamic & Aeroacoustic Design of Wind-Rotor Airfoils*, First International Meeting on Wind Turbine Noise: Perspectives for Control", Berlin, 17-18 October 2005
- [3] A. Herrig, W. Würz, Th. Lutz, K. Braun and E. Krämer, S. Oerlemans: *Trailing-Edge Noise Measurements of Wind Turbine Airfoils in Open and Closed Test Section Wind Tunnel* First International Meeting on Wind Turbine Noise: Perspectives for Control", Berlin, 17-18 October 2005
- [4] F. Hagg: *User's documents SILANT* (in Dutch), Stork Product Engineering, Amsterdam December 1996
- [5] T.F. Brooks, D.S. Pope and M.A. Marcolini *Airfoil Self Noise and prediction* NASA, Reference publication 1218, 1989
- [6] R.K Amiet, *Acoustic radiation for an airfoil in a turbulent stream*, Journal Sound Vib, Volume 41, number 4, 1985, page 407
- [7] M. Drela, *XFOIL: An analysis and design system for low Reynolds number airfoils*, Low Reynolds number aerodynamics, T. J. Mueller, Ed., University of Notre Dame, Paris, 1989
- [8] B. Montgomerie, A. Brand, J. Bosschers, R. van Rooij Three-dimensional effects in stall, ECN-C--96-079, The Energy Research Center of the Netherlands, ECN, 1997
- [9] R. Parchen: *Progress report DRAW: A prediction scheme for trailing edge noise based on detailed boundary layer characteristics*. TNO-Report HAG-RPT-980023, TNO Institute of Applied Physics The Netherlands, 1998
- [10] K. Chandiramani: *Diffraction of evanescent wave with application to aerodynamically scattered sound and radiation from un baffled plates*, J. Acoust. Soc. Amer. Vol. 55, 1974
- [11] W. Blake: *Mechanics of Flow Induced Sound and Vibration Vol I and II*, Acad. Press, 1986
- [12] D.C. Wilcox: *Turbulence modelling for CFD*. DCW Industries Inc., 2nd edition, ISBN 0-9636051-5-1, 1998
- [13] Würz, W.; Guiditati, S.; Herrig, A.; Lutz, T.; Wagner, S.: *Measurement of Trailing Edge Noise by a Coherent Particle Velocimetry Method*. ICMAR Novosibirsk, 28.06.-02.07. 2004
- [14] Th. Lutz, W. Würz; A. Herrig; K. Braun, S. Wagner: *Numerical Optimization of Silent Airfoil Sections*, DEWEK 2004, 7th German wind energy conference, Wilhelmshaven, October 20/21, 2004

**First International Meeting
on
Wind Turbine Noise: Perspectives for Control
Berlin 17th and 18th October 2005**

**Modelling of noise from wind farms
and evaluation of the noise annoyance**

Erik Sloth

Vestas Wind Systems
Alsvej 21,
8900 Randers
Denmark

erslo@vestas.com

1. Summary

The present paper focuses on potential errors in using sound power levels obtained by the IEC 61400-11 standard as the basis for noise modelling. Focus is also on the need for modelling sound pressure level around wind farms as a function of the actual wind speed.

A discussion will furthermore be made of the methodology in using background noise measurements as a means to determine the potential noise annoyance from a planned wind farm.

Finally, the paper includes a discussion of the uncertainties inherent in calculated sound pressure levels from wind farms that sum up emitted sound power level, transmission path, and the number of turbines in a farm.

2. Introduction

Traditionally, modelling of noise from wind farms is based directly on sound power measurement results obtained according to IEC 61400-11.

This is, however, not necessarily the correct basis for the modelling as the noise emission may come to depend on factors which have been standardized during the measurements. In order to correct for this, the parameters needed for the correction must be identified. After determining the immission corrected sound power level of the turbine, this paper claims that wind speed dependant comparison of the calculated sound pressure imission with the existing background noise level is a far better descriptor for the noise annoyance from wind turbines than a simple comparison with fixed noise limits. Finally, a method for calculating a confidence interval for the imission noise level is introduced and thus a complete procedure for modelling of noise annoyance and ensuring accuracy of the calculations is outlined.

3. Standardized sound power levels as basis for sound predictions

3.1 What is measured in an IEC 61400-11 measurement

Noise measurements throughout the world are carried out according to the IEC 61400-11 standard.

According to this, the emitted sound power levels from wind turbines are determined for the standardized conditions stated in IEC 61400-11 at integer wind speeds 10 meters above ground from 6 to 10 m/s. Strict compliance with the standard provides no information at all at wind speeds outside this range.

Furthermore, standardized values for 1/1 octave or 1/3 octave values, a measure for any potential audible tones in a reference distance behind the turbine, and any directivity of the sound emission can be documented.

All emitted sound power is expected to be radiated as an acoustic point source placed in the centre of the rotor.

As a consequence, the standard possesses a proper basis for the preparation of contracts between turbine manufacturers and buyers, but problems occur when the values are used directly as a basis for modelling of sound in the areas surrounding the wind turbine or farm.

3.2 Standardized conditions for measurements

At measurements according to the latest version of IEC 61400-11, usually described as the 2002 version or ed2, all values are calculated during standardized conditions.

The standardisation parameters stated directly in the standard are: Air temperature of 15° Celsius, an atmospheric pressure of 101,3 kPa, and an upwind terrain roughness of 0.05 m.

In addition to this, a power curve “preferably measured according to IEC 61400-12 and preferably for the same turbine or, otherwise, for the same type of wind turbine with the same components and adjustments”, is used during the measurements.

During the measurements, the wind speed at 10 m height must be measured directly using an anemometer placed 2 to 4 rotor diameters upwind from the turbine. It is directly specified that the anemometer must not be placed in the wake of other turbines, and that the wake from other turbines shall be considered to extend 10 rotor diameters downwind of this other turbine.

At first view, these limitations seem logical as they provide proper reproducible measurement results, but at the same time, the limitations impose several restrictions on where measurements can be performed and what results can be used for without corrections.

First of all, since a power curve is used during the measurements it indirectly limits the terrain at which measurements can be performed to the terrain at which the power curve is valid. For instance, if the turbine is placed on a ridge or on the “edge of a valley” as often seen in real life, the actual power curve may depend on the wind direction – is the wind blowing along the ridge or across the ridge – and it is very rare that the flat low inclined terrain upwind to the turbine, as described in IEC 61400-12 standard, can be found at all.

Secondly, due to the “no wake demand”, the measurement results obtained will definitely not represent the noise emission from a turbine situated inside a wind farm, which may be operating in a wake field for many wind sectors.

Thirdly, during the measurements, the wind speed is determined on the basis of power production and power curve, and then recalculated to a 10 m wind speed using the standardized terrain roughness. If the actual site roughness differs from the standardized, the result will be a different relation between the hub height wind speed and the standardized 10 m wind speed, thus also a difference in noise emission at a given 10 m height wind speed. As a consequence, the site wind shear must be taken into account.

The demands regarding standardized air temperature and pressure can also create deviations due to different control strategies of the turbines.

The best example of this could be an active stall[®] regulated turbine. If such a turbine is placed in very “thin” air, it will need to power regulate at a much higher wind speed than if placed in standard air density. By this it will operate at more positive pitch angles, emitting significantly lower sound power levels than at the same wind speed in standard air density.

3.3 Correction of data to immission relevant values

It is very often seen that the values used directly in the modelling are the measured values instead of immission corrected values.

Since verification of noise emission is based on the noise measurement standard, any control measurements of the emitted sound power level will show compliance with the documented noise emission from the turbine, but at the same time, there may be deviations – positive or negative – if measurements are made at the immission points.

The correct way to resolve this issue is to rectify the measured sound power values according to the site specific data before using them for modelling purposes. Alternatively, a wide margin from calculated noise immission to allowable limit must be introduced.

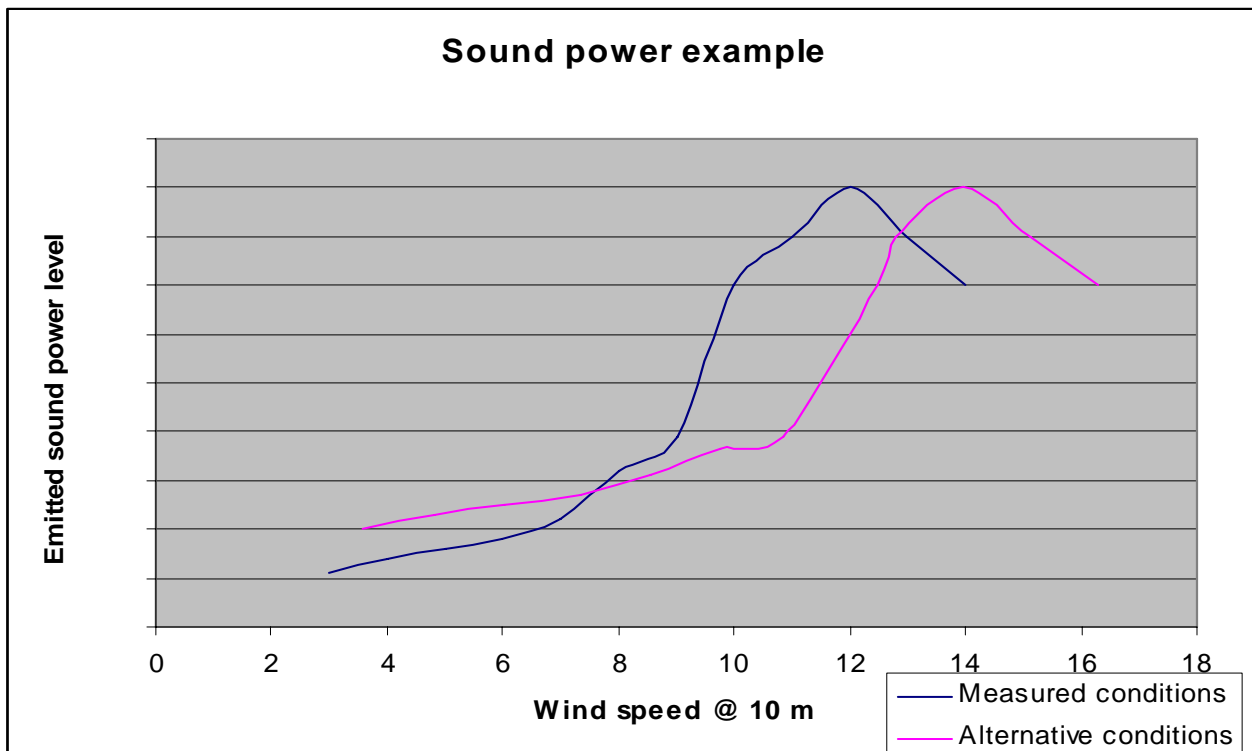
Using one set of values for guarantees and a corrected set of data for modelling purposes will, of course, complicate wind farm approval but, at the same time, it will maximize the number of turbines that can be erected within a given area, and it will minimize noise immission at the neighbouring positions.

The calculated example below shows the differences between guaranteed sound power level, according to IEC 61400-11, and the sound power level that should form the basis for calculations..

In this example, the site is imagined as a site in a hilly terrain, at a high elevation above sea. The yearly average values for the site as compared to the standardized measurement results are:

	Standardized values	Alternative site values
Hub height	60	80
Wind shear	0,16	0,1
Air density:	1,225	1,12
Turbulence intensity	16%	22%
Inflow angle	2 deg	6 deg

Based on this data, the immission relevant data as compared to the standardized values is shown below.



As evident from the figure, the sound power level at the site with alternative conditions must be expected to be above the standardized values at low wind speeds, and below the standardized values at higher wind speeds. Consequently, using the standardized values will result in an underestimation of the noise contribution from the wind turbine at low wind speeds, and an overestimation of the noise contribution at higher wind speeds.

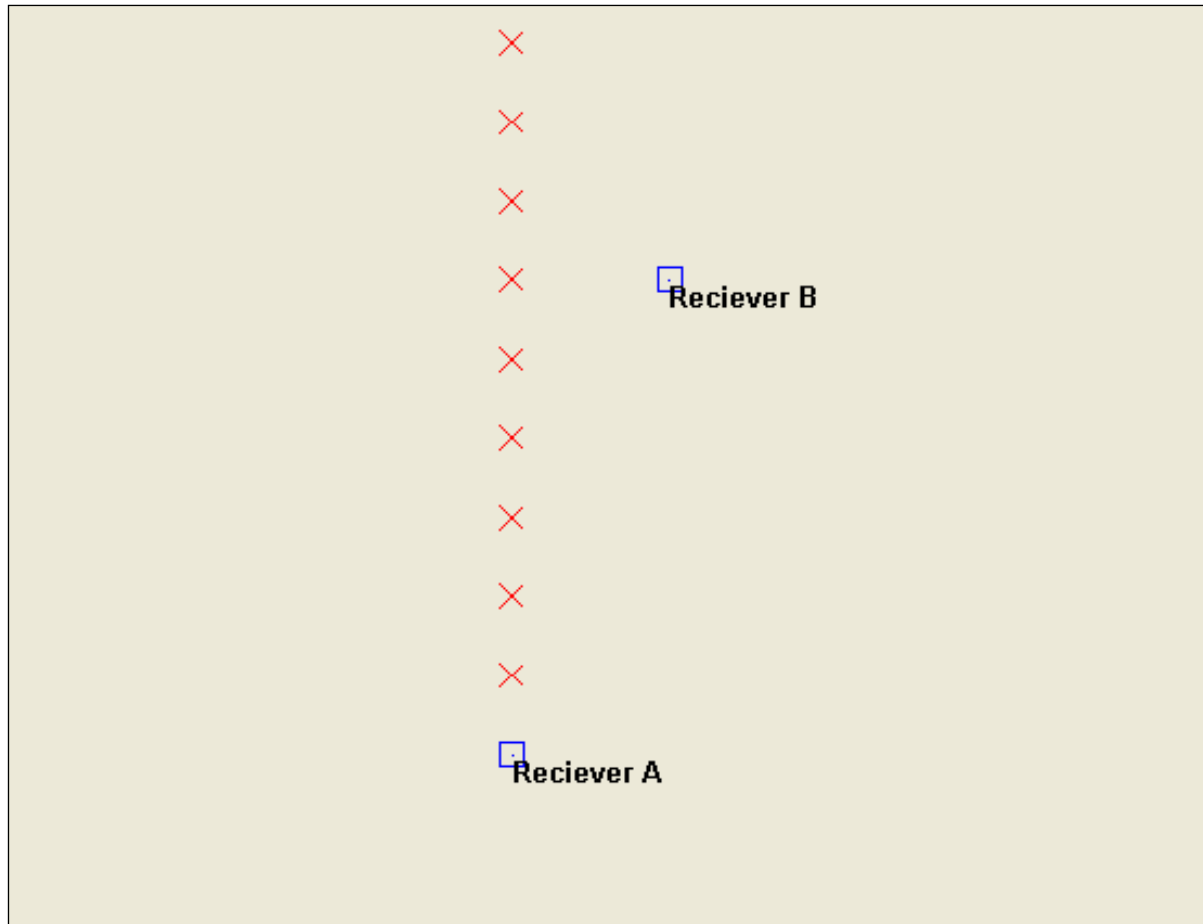
3.5 Modelling methods normally used

When using the immission relevant data for the modelling, several methods are used throughout the world. The most commonly used methods are:

- ISO 9613-2
- VDI 2714
- Concawe
- BS 5228
- General prediction method (Danish)
- Danish EPA guidelines
- Netherlands guidelines 1999
- Swedish method (different methods for land and sea)

A common characteristic in most of these methods is that measurement results are only accurate if the noise transmission from the noise source to the receiving point is directly downwind, or within a narrow sector downwind. Depending on the wind farm layout and

the positioning of the neighbours, this can result in different validity of the calculated results.



Example of wind farm layout relative to receiver positions

From the example layout above it is clear that when the wind comes from north, Receiver A is directly downwind to all turbines and, at the same time, Receiver B is not at all downwind to all the turbines. As a consequence, the calculated immission at position A has a good validity for this wind direction, and the calculated immission at position B has a poor validity for this wind direction.

If the wind comes from east, Receiver A is not at all downwind to any of the turbines and Receiver B is more or less downwind to the nearest 3 turbines, which are the turbines that will give the highest contribution to the immission level at this position. Hence, the validity of the calculated immission values for easterly winds is poor for Receiver A, and acceptable for Receiver B.

The example clearly shows the importance of evaluating the validity of the calculated results at the same time as comparing these with the allowable limits.

3.6 Sound limit strategies

The next natural step in performing noise modelling is to determine the level of annoyance of the imission noise level.

The strategy for determination of noise annoyance is basically divided into two different methods.

- Fixed noise limits as used, for instance, in Germany

The advantage of using fixed noise limits is that it is very simple to determine whether a limit is exceeded or not. It is a simple comparison of the limit value with the calculated imission values at maximum noise emission from the turbine and thus nearly independent of the actual wind speeds. The allowable limit value depends on the area type of the imission point where, for example, higher levels are allowed in industrial areas than in residential areas.

The major disadvantage of the method is that most neighbours around wind farms will base judgement of their annoyance level on whether they are able to hear the turbines or not, instead of making an assessment of whether they only can hear the turbine at less than a given sound pressure level. Therefore, the fixed limits method does not at all represent the nature of the annoyance or the nature of the noise emission from the turbine, where the highest noise emission normally occurs at higher wind speeds.

In addition, nature often creates a masking noise in the surrounding vegetation at higher wind speeds. This noise will mask the turbine noise, and this is not taken into account by the fixed limit method..

Finally, if the existing background noise level is high, for instance if the turbines are placed near a motorway, this noise will mask the turbine noise and it may be impossible both to hear the turbines and to perform verification of the calculated imission values.

- Noise limits that depend on existing background noise levels as used, for instance, in most English- speaking areas.

Using background noise dependent limits is more complicated at the planning stage as it requires that a background noise study be carried out at the receiver positions before erection of the turbines.

The advantage of this method is that it takes into account both the nature of the noise emission from the turbine and the nature of noise generation in nature. In this way, it represents both the noise annoyance, as described above and the nature of noise emission from the turbine. Furthermore, it is relatively easy to verify the noise imission,

since the nature of the background noise already is taken into account in the definition of the allowable noise limits.

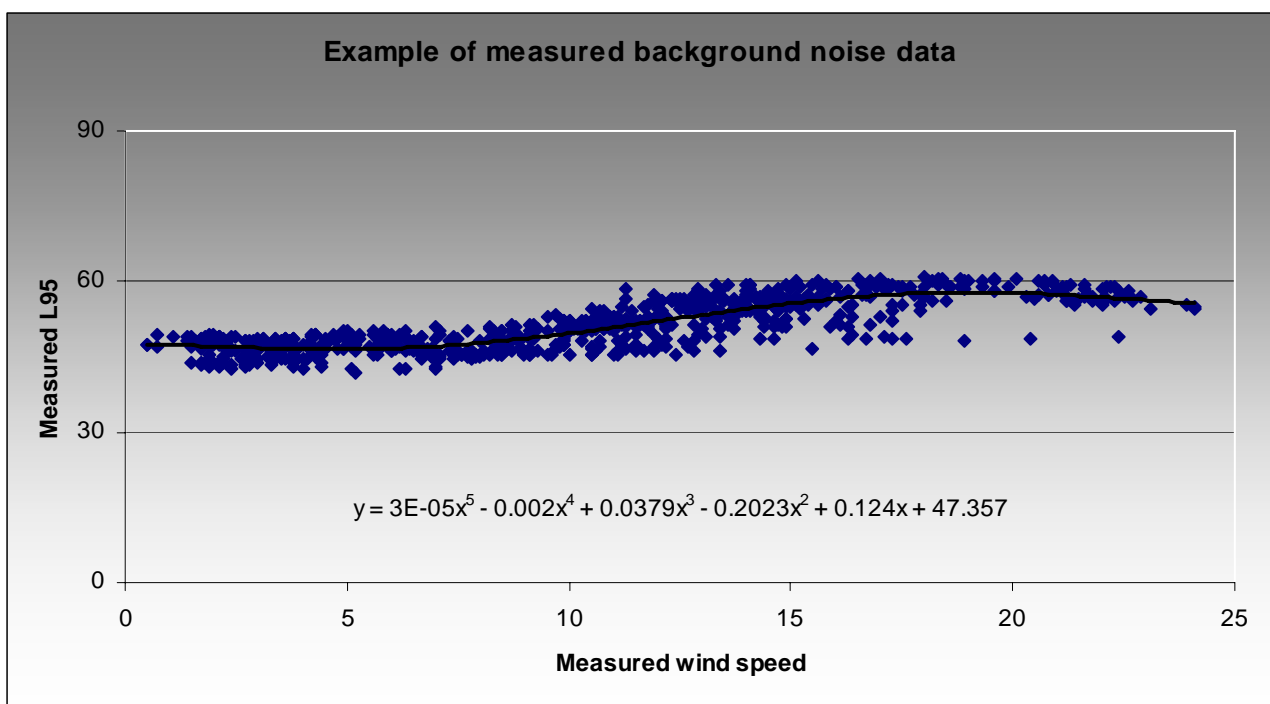
The disadvantage of this method is that if the masking noise from e.g. a forest changes due to happenings beyond the control of either neighbours or turbine owners (e.g. wind fall, or fire), an increased annoyance may suddenly occur. How to solve this situation is not discussed in this paper.

4 Methodology in background noise measurements

The normal procedure for determination of background noise level is described in ETSU-R-97. The basic idea in the method is that the background noise level is logged at the receiver position during a period that will represent all wind speeds and directions. In parallel with the noise logging, wind logging is performed at a position that is representative of the wind speed that the turbines will be exposed to.

Normally, the measurement campaign will last for at least three weeks, and it must at least cover a wide range of wind speeds, typically 3 to 14 m/s. 10 min average values for adjacent noise levels and wind speeds are logged. In order to exclude noise phenomena occurring very close to the microphone, the statistical L95 sound pressure level is often used. Values logged during rain or other abnormal weather conditions are disregarded.

Finally, the values are analysed using regression analysis where the best fit regression order is determined by visual inspection of the measurement values and the regression line. An example of this procedure is shown below:



After having determined these polynomial estimates of the background noise level as a function of the wind speed, it is possible to compare the calculated immission values, including the estimated validity of the values, with the existing background noise levels. The comparison must be made at all wind speeds – typically at all integer values. The result could look like the table below, where the noise limit is defined as 41 dB or the background noise level, whichever is the highest:

Wind Speed	3	4	5	6	7	8	9	10	11	12
Background	40	40	41	41	42	42	43	44	45	46
Noise Limit	41	41	41	41	42	42	43	44	45	46
Predicted	33,0	33,0	38,0	41,6	42,8	44,7	46,3	46,9	46,8	45,9
Excess				0,6	0,8	2,7	3,3	2,9	1,8	

From this example it can be seen that at 3 to 5 m/s the expected sound immission value is less than both the background noise level and the allowable sound pressure level, so no annoyance is expected at these wind speeds. At wind speeds from 6 to 11 m/s the expected sound immission value exceeds both the background noise level, and the allowable noise level. At these wind speeds annoyance must be expected due to the excess of the background noise level. Note that if the nature of the noise limit had been a fixed noise limit at e.g. 45 dB as often seen in reality, this would not have been exceeded.

5 Inclusion of uncertainties in calculations

When comparing calculated immission values with allowable limits, as described above, it is, of course, of great importance to focus on the uncertainty of the calculated value. For example, nobody would find it very advantageous to find a statement that the allowable sound pressure level is 34 dB, and that the calculation has shown that the wind farm will yield a sound pressure level of 33.9 +/- 5 dB. Likewise, if the calculated sound pressure level is 34.1 +/- 2 dB, it would probably not be regarded as an acceptable value by any authority.

The proper way to handle this is to include the uncertainty in all levels of the calculation. The first step is to remember that there is a difference between the standard deviation given by IEC 61400-11 and the probability value that is normally used in any comparison.

Remembering this, the probability can be included using normal statistical methods in the calculations.

Note that since both sound power level, the standard deviation on the sound power level, and the standard deviation on the calculation method all vary with the wind speed, it is necessary to perform this calculation individually for each wind speed bin.

By multiplication of the resulting standard deviation with the factor relating it to the local probability demands (e.g. 1.65 for a 95% probability), the probability interval for the calculated value is found.

It is now possible to compare the calculated immission level with the allowable levels, and by this achieve both an estimate of how annoying the noise is expected to be at the emission point, and an estimate on how certain we are that the calculated value is within the allowable limits.

The rules to be used are, when assuming a 95% probability for excess, as in many European countries:

1. If the predicted values minus the confidence level exceed the noise limit then it is more than 95% probable that the noise limit is exceeded.
2. If the predicted values plus the confidence level are less than the noise limit there is more than 95% probability of compliance with the noise limit.
3. If the predicted values minus the confidence level exceed the background noise level, then it is more than 95% probable that neighbours will hear the turbines, and by this may feel annoyed.

Adding these clauses to the result scheme presented in chapter 4, the following is obtained:

Wind Speed	3	4	5	6	7	8	9	10	11	12
Background	41	41	41	41	42	42	43	44	45	46
Noise Limit	44	44	44	44	45	45	46	47	48	49
Predicted	33,0	33,0	38,0	44,6	46,8	47,3	48,3	48,9	49,1	50,4
95% probability	1,9	1,8	1,9	2,1	2,1	2	1,9	2	2	2
Limit excess >95%	no	no	no	no	yes	yes	yes	no	no	no
Limit compliance > 95%	yes	yes	yes	no	no	no	no	no	no	no
Background excess >95%	no	no	no							
Background excess >95%	anoy	anoy	anoy							

From this it can be seen that at 3 to 5 m/s there is still no expectation of any annoyance or exceeding of the allowable noise level.

At 6 m/s and from 10 to 12 m/s, there is compliance with the allowable noise limits, but annoyance may be expected, and from 7 to 9 m/s both exceeding of the noise limit and annoyance is seen.

6 Conclusions

The discussions in the present paper show that the normal procedure of basing noise modelling of wind farms on the standardized sound power levels of the turbines is not necessarily sufficient if the goal is to maximize the number of turbines in a given area, and at the same time minimize the neighbours noise annoyance.

Principles to correct the emitted sound power level to immission relevant values are outlined, and methods on how to include the uncertainty in the calculations are introduced.

Finally, a potential method for extended evaluation of the calculated results that will result in reduced noise annoyance is shown.

**First International Meeting
on
Wind Turbine Noise: Perspectives for Control
Berlin 17th and 18th October 2005**

Noise measurements according to IEC 61400-11. How to use the results

Bo Søndergaard

M.Sc (Physics)

DELTA Danish Electronics Light & Acoustics www.delta.dk

Kongsvang Allé 30, DK 8000 Aarhus Denmark

bsg@delta.dk

Abstract

The noise from wind turbines are usually measured according to IEC 61400-11 and the results are used for declaration purposes, comparison between wind turbines, noise calculations etc. Noise measurements made for declaration purposes and noise assessment are usually made on ideal test sites where the performance of the turbines regarding noise and power production are expected to be at its best. Are these data applicable when the wind turbines are erected in a non ideal terrain? The presentation will discuss some of the problems.

Introduction

The noise measurement standard IEC 61400 -11 [1] was originally published in a first version in 1998 and in a revised version in December 2002. In this version especially the tonality assessment was improved for better reproducibility. An amendment [2] to the standard is expected to be published in spring 2006. The amendment will amongst other things give access to using the nacelle anemometer for wind speed measurements above 95 % of rated power for the wind turbine and for background noise measurements.

IEC 61400-11:2002 prescribes how to measure the noise from wind turbine generator systems to be able to achieve reproducible results. A method to estimate the measurement uncertainty is included. In IEC 61400-14 [3] is described a principle for declaring the sound power level and tonality of a batch of wind turbines.

The idea behind [1] is given in the introduction as:

The standard has been prepared with the anticipation that it would be applied by:

- *the wind turbine manufacturer striving to meet well defined acoustic emission performance requirements and/or a possible declaration system;*
- *the wind turbine purchaser in specifying such performance requirements;*
- *the wind turbine operator who may be required to verify that stated, or required, acoustic performance specifications are met for new or refurbished units;*

- *the wind turbine planner or regulator who must be able to accurately and fairly define acoustical emission characteristics of a wind turbine in response to environmental regulations or permit requirements for new or modified installations.*

This means that the standard is intended for use in a variety of situations under different circumstances like different terrain and meteorology conditions.

As the results of measurements according to the standard are often used for comparison with noise limits or verification of declared or specified values on tenth of decibels even minor flaws in the method can prove to be significant.

The measurement method

The principles behind the measurement method are illustrated in Figure 1. The noise is measured on a plate on the ground. This reduces the wind induced noise in the microphone and simplifies the ground effect to a + 6 dB contribution at all frequencies. The board is circular with a diameter of at least 1 m. [4]

Noise Measurements (IEC 61400-11:2002)

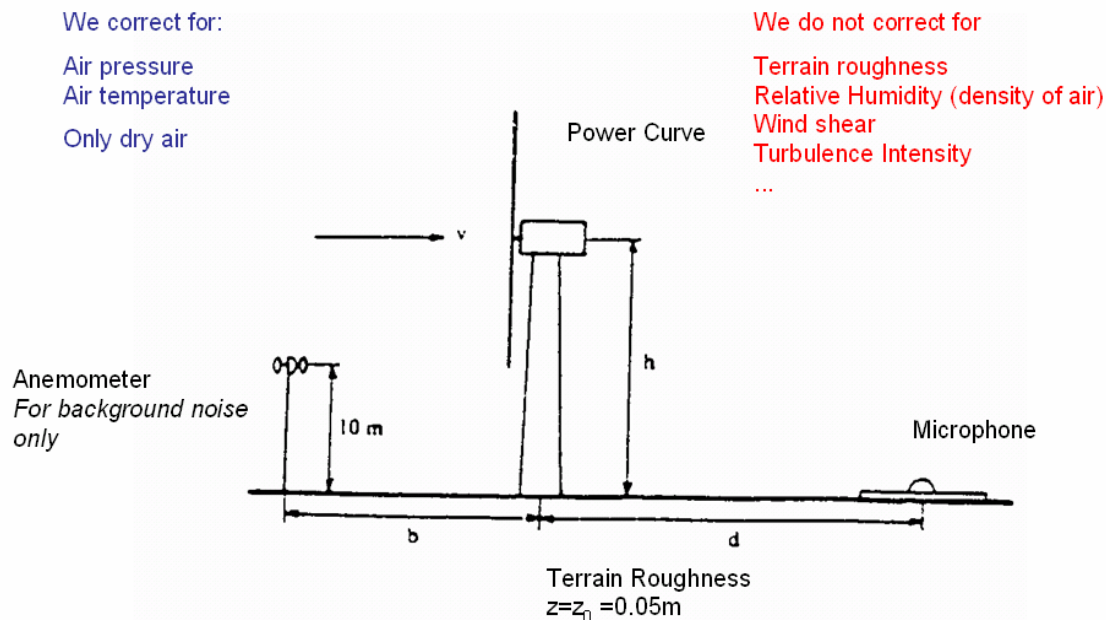


Figure 1 Noise measurements according to IEC 61400-11:2002

The measurement distance is given as the hub height + half the rotor diameter.

The wind speed at 10 m is obtained from the produced power through a power curve and a logarithmic wind speed profile given in Equation 1.

$$V_s = V_z \cdot \frac{\ln\left(\frac{z_{\text{ref}}}{z_{0\text{ref}}}\right)}{\ln\left(\frac{z}{z_0}\right)}$$

Equation 1

Where,

$z_{0\text{ref}}$	= reference roughness length of 0.05 m
V_z	= Wind speed at height z above ground level
z	= The height for which we know the wind velocity (hub height)
z_0	= Roughness length in the current wind direction ($z_0=z_{0\text{ref}}=0.05$ m)
z_{ref}	= The height for which we want to know the wind velocity (10 m)

The power curve should be measured according to [5] which are pretty restrictive about the test site. This means that most power curves are determined under for ideal conditions (roughness length, Turbulence Intensity....).

In Figure 1 some of the parameters that the method includes and some of the parameters the method does not include are mentioned.

The Sound Power Level is reported at integer wind speeds from 6 – 10 m/s through a second order regression line. [2] allows for regression orders up to 4.

A method for assessing the tonality at individual wind speeds is included in the standard.

Examples of results are shown in Figure 2 - Figure 4.

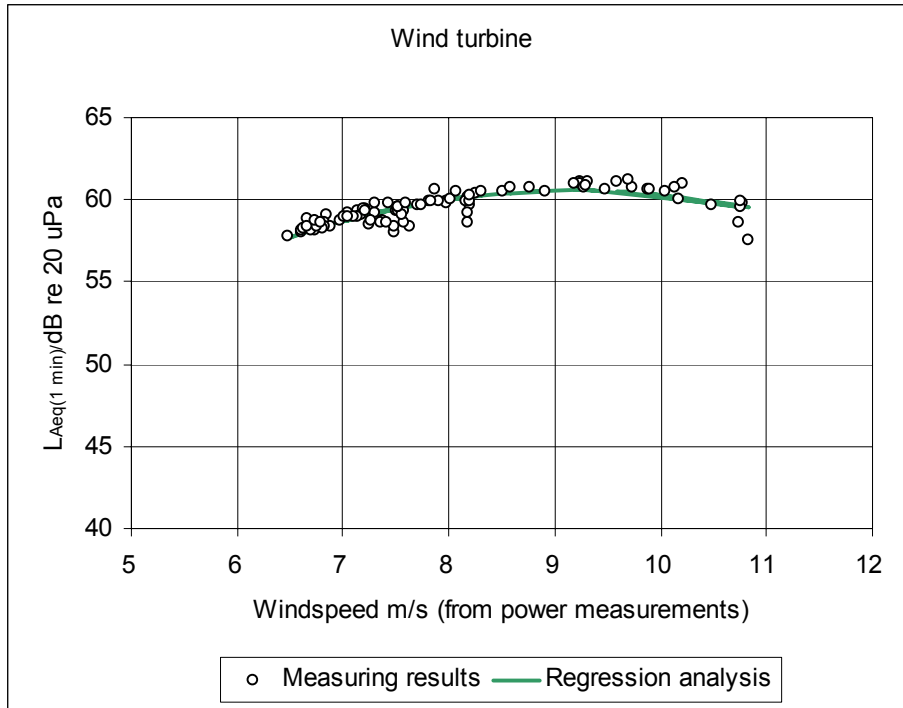


Figure 2

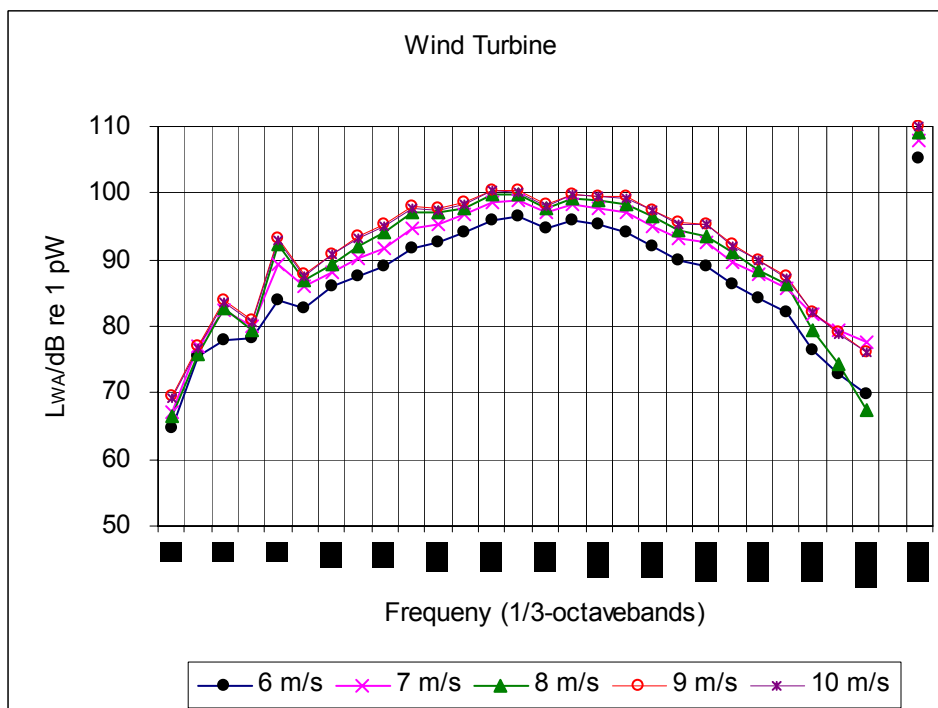


Figure 3

Linespacing (analysis bandwidth)	Wind Turbine												Avg
	Wind speed: 8 m/s												
Spectrum no	1	2	3	4	5	6	7	8	9	10	11	12	
Frequency/Hz	1082.0	1080.0	1082.0	1082.0	1082.0	1080.0	1082.0	1082.0	1082.0	1082.0	1082.0	1082.0	
Lp, tone/dB re 20 uPa	33.8	36.4	36.7	35.4	35.3	34.3	37.8	37.8	34.2	34.7	36.3	36.8	
Critical bandwidth/dB re 20 uPa	171.5	171.3	171.5	171.5	171.5	171.3	171.5	171.5	171.5	171.5	171.5	171.5	
Lower frequency/dB re 20 uPa	996	994	996	996	996	994	996	996	996	996	996	996	
Upper frequency/dB re 20 uPa	1168	1166	1168	1168	1168	1166	1168	1168	1168	1168	1168	1168	
Lp, noise, avg/dB re 20 uPa	23.1	21.6	21.0	21.8	22.7	21.8	21.3	21.0	20.9	22.8	22.1	22.4	
10*log(Critical bandwidth/Analysis bandwidth)	17.6	17.6	17.6	17.6	17.6	17.6	17.6	17.6	17.6	17.6	17.6	17.6	
Lp, critical band/dB re 20 uPa	40.7	39.1	38.6	39.4	40.2	39.3	38.8	38.6	38.5	40.4	39.7	40.0	
ΔL_{tn}	-6.9	-2.8	-1.9	-4.0	-4.9	-5.0	-1.0	-0.8	-4.3	-5.6	-3.3	-3.2	-3.3
ΔL_a	-4.0	0.1	1.0	-1.1	-2.0	-2.1	1.9	2.1	-1.4	-2.8	-0.5	-0.3	-0.4

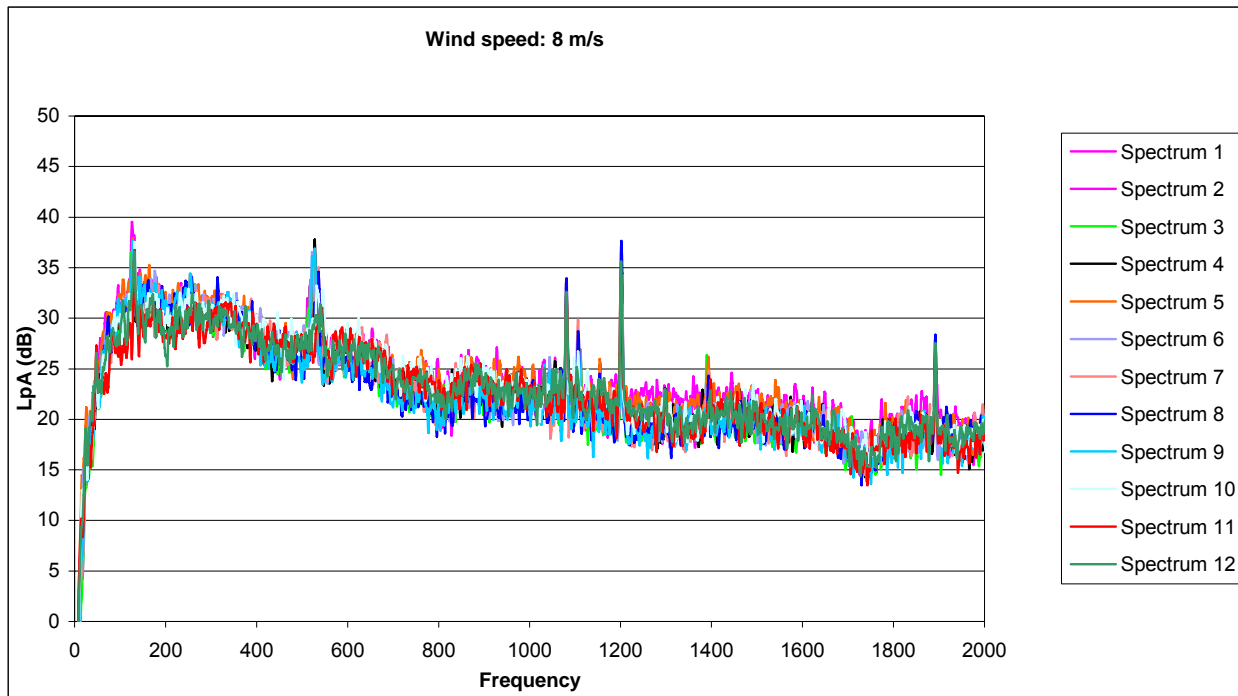


Figure 4 Tonality analysis for a wind turbine

Use of results from IEC 61400-11

The measurements results are intended for declaration, verification and noise prediction i.e. siting and noise assessment.

Declaration

The measurement results can be used for declaration according to [3]. The declared values are the Sound Power Level including the uncertainty given as a single sided 95% confidence interval. This makes comparison between different types and makes easy and reliable as most often the measurements used for declaration is made under ideal or close to ideal conditions.

Verification

Wind turbines are purchased including a noise guarantee. This guarantee is usually taken directly from measurements according to [1] from a single measurement or as declared values according to [3]. As seen in Figure 5 actual sites can be different from the measurement situation in Figure 1 and measurement on an actual site can not be expected to yield the same results as from an ideal site.

At an ideal site the roughness length can be as small as 0.01m, the standard value is 0.05m and at some sites with steep slopes, trees etc. the roughness length could be even larger. In Table 1 the effect of variations in roughness length is illustrated for a hub height of 80 m.

Use of measurement results

For noise control measurements

For noise level calculations

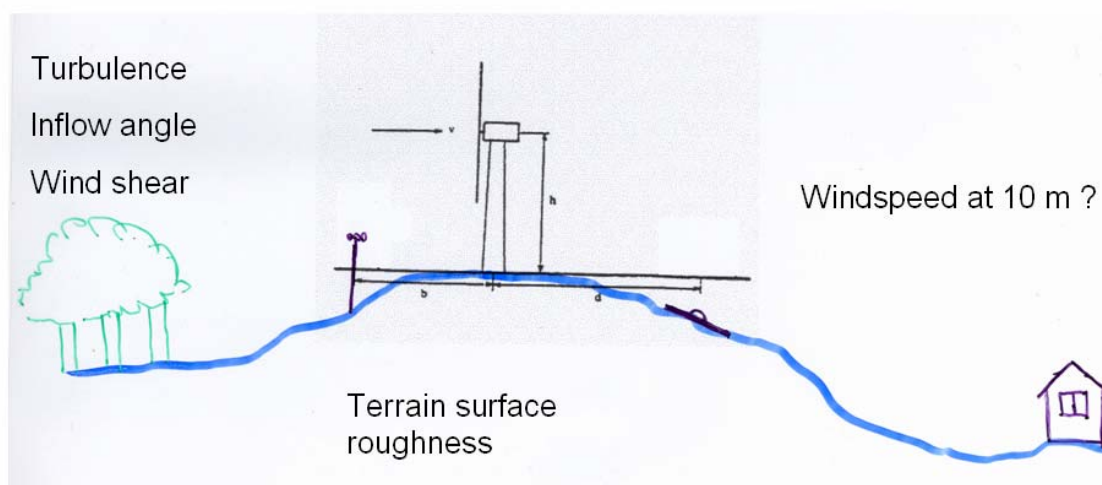


Figure 5

Roughness length	Conversion from hub height to 10 m	Wind speed at hub height	Wind speed at 10 m
0.05 m	0.72	11.1 m/s	8.0 m/s
0.01 m	0.77	11.1 m/s	8.5 m/s
0.10 m	0.69	11.1 m/s	7.7 m/s

Table 1

As a consequence the results can be shifted up to 0.5 m/s. This can mean as much as 0.5 to 1 dB on the sound power level at some wind speeds and even more for stall regulated wind turbines at full production. When verifying measurement results from actual sites against results from ideal sites, there can be a bias of 0.5 to 1 dB from the measurement method. This effect will increase with increasing hub height.

In complex terrain the variation of the wind speed over the rotor is larger than for an ideal site. As the control mechanism (rotor speed, pitch angle) is based on an average wind speed at hub height the noise generation can be different in this situation. Also non-perpendicular inflow for wind turbines near the edge of a hill can increase the noise production. If the power curve used, is not modified to the actual site conditions this will influence the results as well.

Comparison between measurement results from actual sites and declared values should be followed by an evaluation on which parameters may have influenced the results before a conclusion on whether the results are consistent with the declared values.

Siting and Assessment

When calculating the noise from a wind farm or a single wind turbine the noise data is subject to the same considerations as given above regarding the reliability. This means it is necessary to evaluate if the noise data are representative for the site in question. It is not unusual that the results of the calculations are compared to noise limits to a tenth of a dB even though the inaccuracy is of the order of dB.

The inaccuracy is determined from the standard deviation of the measurement result(s) as described in [1] and [3]. The inaccuracy is a statistical parameter describing the probability that a result is within a certain range. Usually a 95% single sided confidence interval is applied.

It is possible to evaluate a measurement result in the following way.

- If the noise level plus the inaccuracy is below or equal to the noise criterion the noise is with 95% probability below the noise criterion.
- If the noise level minus the inaccuracy is above or equal to the noise criterion the noise is with 95% probability above the noise criterion.

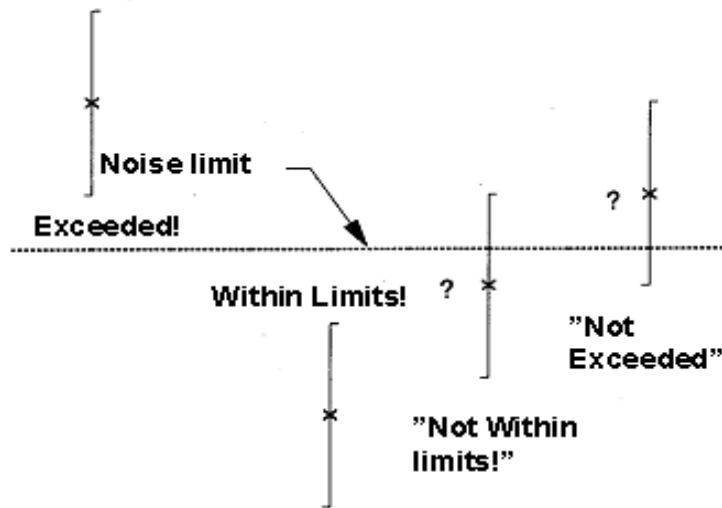


Figure 6

This leaves an interval where it is not possible to state whether the noise is above or below the noise criterion, see Figure 6. It is a common practice in most countries not to react if the noise criterion is not with 95 % probability exceeded.

The inaccuracy is dependent on the number of measurements used. The inaccuracy based on a single measurement of the sound power level normally results in an uncertainty of app. 0.9 dB and an inaccuracy of app. 1.6 dB. These values should be reevaluated according to the site characteristics. More measurements may result in a reduced inaccuracy depending on the spread of the measurement results. From experience the inaccuracy does not decrease significantly after 3-5 measurements.

When calculating the noise from a wind turbine park the total noise level at a receptor position can be treated as the sum of the noise from a number of independent noise sources [8]. The standard deviation of the calculated noise level can be given as Equation 2:

$$\sigma_{calc} = \frac{\sqrt{\sum (\sigma_i \cdot 10^{L_i/10})^2}}{\sum 10^{L_i/10}}$$

Equation 2

σ_i is the standard deviation for the noise level from wind turbine no. i and L_i is the noise contribution from wind turbine no. i. All input values should be given in dB.

The total standard deviation of the noise level at a receptor position is given as the sum of the standard deviation from the sound power measurements and the calculations:

$$\sigma_{res} = \sqrt{\sigma_{calc}^2 + \sigma_{source}^2}$$

Equation 3

σ_{calc} is the standard deviation of the calculations [dB] and

σ_{source} is the standard deviation of the sound power measurements [dB].

The result of using this method is a reduced inaccuracy on the calculated immission noise level, but still it will not reduce or eliminate the basic problems on finding the correct sound power level, and evaluation of the annoyance of the noise.

It is now possible to include meteorological parameters such as wind speed, wind direction and temperature gradients as well as complex terrain in the calculations [7].

Other Aspects

Research indicates that one of the most important parameters when erecting wind turbines is the visual impact [9]. However most complaints are about noise, e.g. too much noise, low frequency noise, tones in the noise etc. How can this be handled?

As described above, the measurement method gives an A-weighted sound power level at wind speed range from 6 – 10 m/s that can be extended to higher and lower wind speeds. Further a tonality analysis is given. A range of parameters are not quantified in the method e.g. low frequency noise, impulsivity, modulation...

This means that the data representing the noise from a wind turbine at a neighbour position is based solely on the A-weighted noise level (wind speed dependent) and the corresponding tonality. This can be an appropriate description, but community reactions indicate that a wider range of parameters might be relevant

- low frequency noise
- modulation
- traditional descriptors such as sharpness, roughness,
- masking (background noise from nature, roads, factories etc.)
-

If these effects are to be clarified further research is needed including:

- Psychoacoustic experiments
- Listener test
- Measurements at low frequencies
- Analysis for other characteristics
-

References

- [1] IEC 61400-11:2002 *Wind turbine generator systems – Part 11: Acoustic noise measurement techniques*
- [2] Amendment 1 to IEC 61400-11:2002 to be published
- [3] IEC 61400-14 Wind Turbine generators - Declaration of sound power level and tonality values.
- [4] Nii Yoshinori: "Sound level distributions on a circular ground board for wind turbine noise measurements". *Noise Control Eng. J.* 50 (3) , 2002 May-June
- [5] IEC 61400-12:1998 *Wind turbine generator systems – Part 12: Wind turbine power performance testing*
- [6] Sloth Erik et al, AWEA 2004: "Problems related to the use of the existing noise measurement standards when predicting the noise from wind turbines and wind farms"
- [7] Kragh Jørgen, Plovsing Birger, Søndergaard Bo, First International Meeting on Wind Turbine Noise 2005: "Prediction of Wind Turbine Noise Propagation over Complex Terrain in All Kinds of Weather with Nord2000"
- [8] Sperling Henrik, Inter-Noise 95:"Calculation of uncertainty of noise generated by several sound sources"
- [9] Holm Pedersen Torben, Report no. 150, 1994, "Annoyance from wind turbines" (in Danish) DELTA.

**First International Meeting
on
Wind Turbine Noise: Perspectives for Control
Berlin 17th and 18th October 2005**

**A Detailed Study of the Propagation and Modelling of the Effects of Low
Frequency Seismic Vibration and Infrasound from Wind Turbines**

Peter Styles¹, Richard England¹, Ian G. Stimpson¹, Sam Toon¹, David Bowers², Malcolm Hayes³

- 1 Applied and Environmental Geophysics Group, School of Physical and Geographical Sciences, Keele University, Keele, Staffs ST5 5BG, UK, (p.styles@keele.ac.uk)*
- 2 Division of Forensic Seismology, AWE Blacknest, Brimpton, Reading, Berks RG7 4RS, UK, (bowers@blacknest.gov.uk)*
- 3 Hayes McKenzie Partnership, Lodge Park, Tre'r-ddol, Machynlleth, Powys SY20 8PL, UK, (Malcolm@hayesMckenzie.co.uk)*

Summary

In order to meet, and in fact exceed, Kyoto targets, the UK government has set the challenge of reducing the UK's carbon dioxide emissions by 60% by 2050. The development of renewable energy, especially wind power, will be an important contributor to the outcome of that policy with a target of 10% of UK energy from renewable sources by 2010. The Scottish Executive has decided that Scotland should aspire to generate 40% of its energy from renewable sources by 2020.

The Southern Uplands of Scotland offer a prime wind resource because of a large region of high topography, appropriate wind conditions, the proximity to the large urban centres of Glasgow and Edinburgh and the main national grid connections between Scotland and England. In excess of 1 Gigawatt of onshore wind generation capacity is planned for the Southern Uplands.

However, the United Kingdom international seismic monitoring site which constitutes its component of the Comprehensive Test Ban Treaty (CTBT) compliance for nuclear testing is situated at Eskdalemuir near Langholm in the Scottish Borders. This is a very low noise vibration site located in the centre of this wind resource region. Concern was expressed by statutory consultees that vibration from wind farm developments might prejudice the detection capability of this facility. The Ministry of Defence (MoD) therefore placed a precautionary blanket objection to any wind farm developments within 80 km of Eskdalemuir in case this compromised UK capability to detect distant nuclear test and breached the UK's agreement under the CTBT. This effectively

removed at least 40% of the UK renewable wind resource identified by the Department of Trade and Industry (DTI).

This led to the commissioning of a detailed study funded by MoD, the DTI and the British Wind Energy Association (BWEA) into the levels of vibration and infrasonic noise which might be generated by fixed and variable speed turbine wind farms. A 10 station broadband seismic network and a 4 station infrasound network were established for a 6 month period at distances out to more than 20 km from a 26 turbine (Vestas V47) wind farm at Dun Law. This wind farm is situated on very similar geology and topography to Eskdalemuir and the planned wind farm developments in the Southern Uplands. The study permitted the identification of the principal propagation mode for ground vibrations from wind turbines and enabled their characterisation.

This has allowed the development of a predictive model for the aggregate vibration contribution from any planned distribution of wind turbines for comparison with ambient vibration levels as presently experienced at Eskdalemuir. As a result of this study, planning guidance has been given to the Scottish Executive, the MoD and local planning officers to protect the functionality of this important facility whilst optimising wind energy resource exploitation in the Southern Uplands of Scotland. By carefully considering the present ambient background experienced at the monitoring site it has been possible to set a noise budget which is permissible at Eskdalemuir without compromising its detection capabilities, and we have demonstrated that at least 1.6 GW of planned capacity can be installed and have developed software tools which allow the MoD and planners to assess what further capacity can be developed against criteria established by this study.

Introduction

The Eskdalemuir Seismic Array (EKA)

The Eskdalemuir seismic array (**EKA**), operated by the Atomic Weapons Establishment (AWE) Blacknest, is part of the auxiliary seismic network of the International Monitoring System (IMS) being set up to help verify compliance with the CTBT which bans nuclear-test explosions. So far the CTBT has been signed by 175 states, and ratified by 121. The UK and France were the first nuclear-weapons states to ratify the treaty. The facility at Eskdalemuir is to be upgraded to be an alternate primary IMS seismic station. The treaty requires that States Parties shall not interfere with the verification system, of which Eskdalemuir is an element.

EKA became operational on the 19 May 1962 and comprises a recording laboratory, a seismological vault and an array of vertical Willmore MK2 short period seismometers. The array has two arms, each of ten seismometers, with each line having eleven pits (of which only ten on each line are used) approximately 1000 yards apart (Figure 1). The lines run roughly from SSW to NNE and from WNW to ESE and intersect off centre, forming an unequal cross. The pits have been excavated through an overburden of superficial soil (peat in some instances) or thickness up to 1 m into shales of the Llandovery Series (Silurian age). These were folded during late Silurian times, and as a result of the lateral pressures exerted are highly cleaved.

The array has recorded signals associated with about 400 nuclear explosions (up to 15,000 km away from EKA). The sensitivity arises because it occupies a seismically very quiet site, one of only three ever considered in the UK (Bache *et al.*, 1986), and it approaches the low noise model of Petersen (1993). EKA is the longest operating steerable array in the world, detecting events over 42 years, and is well calibrated. It has a low explosion detection threshold, for example recording signals from the detonation of c 100 tonnes of conventional explosive in Kazakhstan.

A study of the background noise at Eskdalemuir was undertaken in 1997/8 as an AWE report (Trodd 1998). The winter and summer root-mean-squared (RMS) averages of the unfiltered summed channels of the array were found to be 8.96 and 1.65 nanometres respectively. This, together with years of historical data, makes EKA an unparalleled resource for forensic seismology.

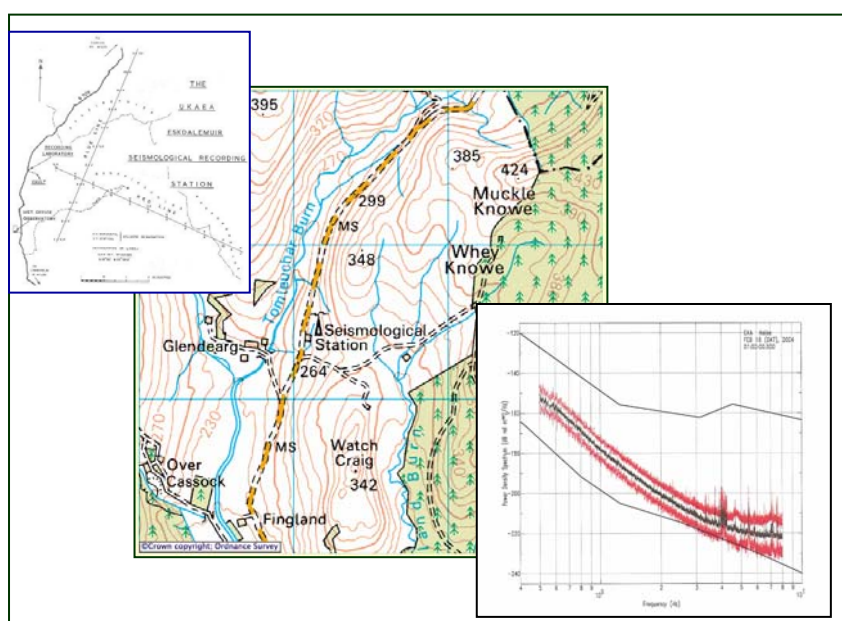


Figure 1 The Location of the EKA seismological array, the detailed layout of the arms of the array and the noise spectrum at the array which closely approaches the Low Noise Model of Petersen (1993).

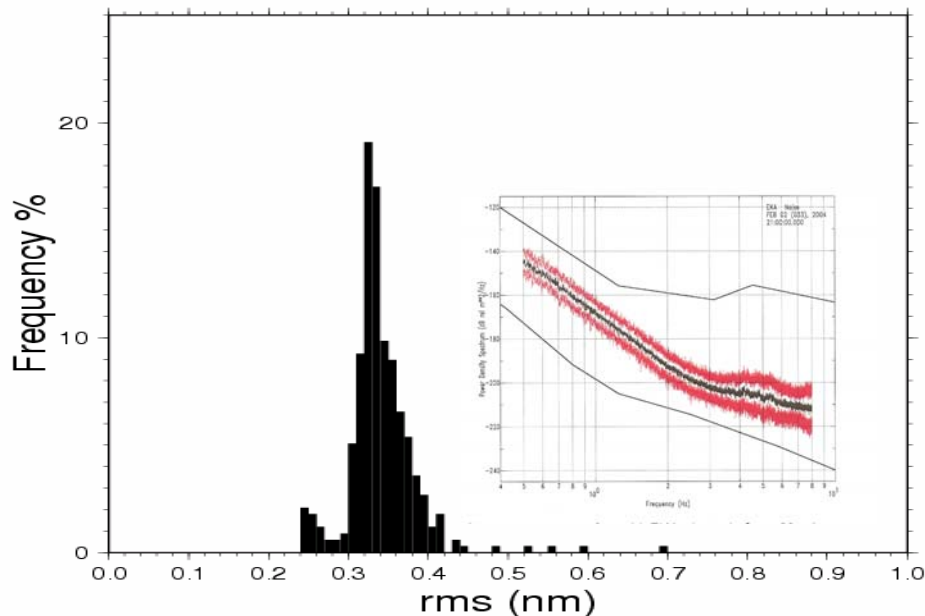


Figure 2 Statistics of the seismic background noise levels at Eskdalemuir for 330 half-hour data sets. Inset shows the power spectrum of the mean at 20 EKA channels for one of the 30 minute samples at high wind speeds (25 knots) compared to the noise models of Petersen (1994), from Bowers (2004)

Renewable Energy in the Southern Uplands of Scotland and its implications for Seismic Verification

The hills of the English Lake District and Scottish Borders constitute a major wind resource and some existing wind farms have been operating for many years and many new facilities are planned. As part of the UK renewable energy targets set in order to meet the Kyoto protocol, in excess of 1 GW of wind energy capacity are planned for the Southern Uplands of Scotland, a valuable wind resource area.

Wind turbines are large vibrating cylindrical towers, strongly coupled to the ground with massive concrete foundation, through which vibrations are transmitted to the surroundings and with rotating turbine blades generating low-frequency acoustic signals which may couple acoustically into the ground. This may occur in several ways:

1. As a cantilever carrying the nacelle/blade mass, with frequencies typically less than 1Hz, depending on height of tower.
2. As a torsional oscillator at low frequencies.
3. As a complex distributed system at higher frequencies

Additionally, the blade tower interaction is a source of pulses at a low repetition rate, which contain components in the infrasound region. The local and surrounding geology especially layering may play an important part in determining vibration transmission. Energy may propagate via complex paths including directly through the ground or principally through the air and then coupling locally into the ground

In late December 2003 AWE/MoD recognised that many wind farm developments were planned in the vicinity of the Eskdalemuir International Monitoring Site and the discrimination capabilities of EKA might be affected by vibration from wind turbines. Because of uncertainty at that time as to the actual levels of seismic vibration generated by wind turbines, the MoD placed holding objections on wind farm development within a radius of 30 km from Eskdalemuir and those up to 80 km radius would be re-examined.

Previous Work

Very few studies of the microseismic vibrations from wind farms have been carried out previously. The only UK studies were carried out by the Microseismology Research Group at the University of Liverpool (led by Dr Peter Styles).

The Department of Earth Sciences at the University of Liverpool operated a single three-component seismic station at the Powys Observatory, Knighton, Powys, Wales for several years to monitor the seismicity of the Welsh Borders after the large ($M_L 5.1$) Bishop's Castle earthquake of 2 April 1990. When plans were submitted for a wind farm development a few kilometres away on an adjacent farm it raised concerns that this might produce vibrations which would interfere with the detection of seismic events. Preliminary experiments were carried out near existing Mid-Wales wind farms followed by a significant study at St Breock Downs, Cornwall, England funded by POWERGEN and ETSU (Styles P., 1996) and reported by Snow (1997), Manley and Styles (1995) and Legerton *et al.* (1996).

St. Breock Downs wind farm was commissioned in July 1994 and comprises 11 Bonus 450kW Wind Turbines. Two sets of three-component seismometers were in buried pits from 18 March until 30 March 1996 in order to record data from a wide range of wind speed and directions. Measurements were made at distances of 100 metres, 50 metres and 25 metres for Turbine 1. A portable, compact three-component instrument with a bandwidth from 0.2 Hz to 64 Hz was used for measuring the variation in the low-frequency signal from different turbines and at a range of distances. Acoustic noise level variation with azimuth was measured with a microphone and frequency analyser and accelerometers were mounted on the base of Turbine 1 to measure the tower vibration.

This study showed clear harmonic components at multiples of the 1.5 Hz blade-passing frequency with particular spectral peaks at 0.5, 3.0, 4.5, 6.0, 7.5 Hz and higher frequencies at levels of up to 250 nanometres s^{-1} (0.25 microns s^{-1}) and general levels of 50 to 80 nanometres s^{-1} (Figure 3). The presence of so many harmonics which are multiples of the blade passing frequency and the clear attenuation of signal amplitude with distance especially for the 7.5 Hz component is a *prima facie* argument that the signals are being generated from the wind turbines and although the levels are small they can easily be detected on appropriate sensors. The 1.5 Hz component (blade-passing frequency) was not the strongest harmonic as might have been suspected.

Frequencies above 3.0 Hz were seen to attenuate with distance with higher frequencies decaying faster as expected. During a sequential shutdown, these frequencies were

observed over a distance of some 500 to 700 metres and significant attenuation noted with the exception of the very lowest frequencies. The 0.5 Hz signals were detected at a distance of c 1 kilometre from St Breock Downs.

Measurements were made over a range of wind speeds from c 7 ms⁻¹ to 14 ms⁻¹ at a constant direction. The amplitude of the harmonics generally increase with increasing wind speed. This was particularly marked for the 0.5, 3, and 7.5 Hz harmonics. However, and rather surprisingly, the amplitude of the 6 Hz signal decreases with increasing wind speed. It seems that the partition of energy between the 6 and 7.5 Hz harmonics in particular is strongly dependent on wind speed. Notwithstanding the reservations expressed concerning the nature of the ultra-low vibrations, the increase in amplitude of the 0.5 Hz component with wind speed suggests that it does have a source which is related to the wind farm.

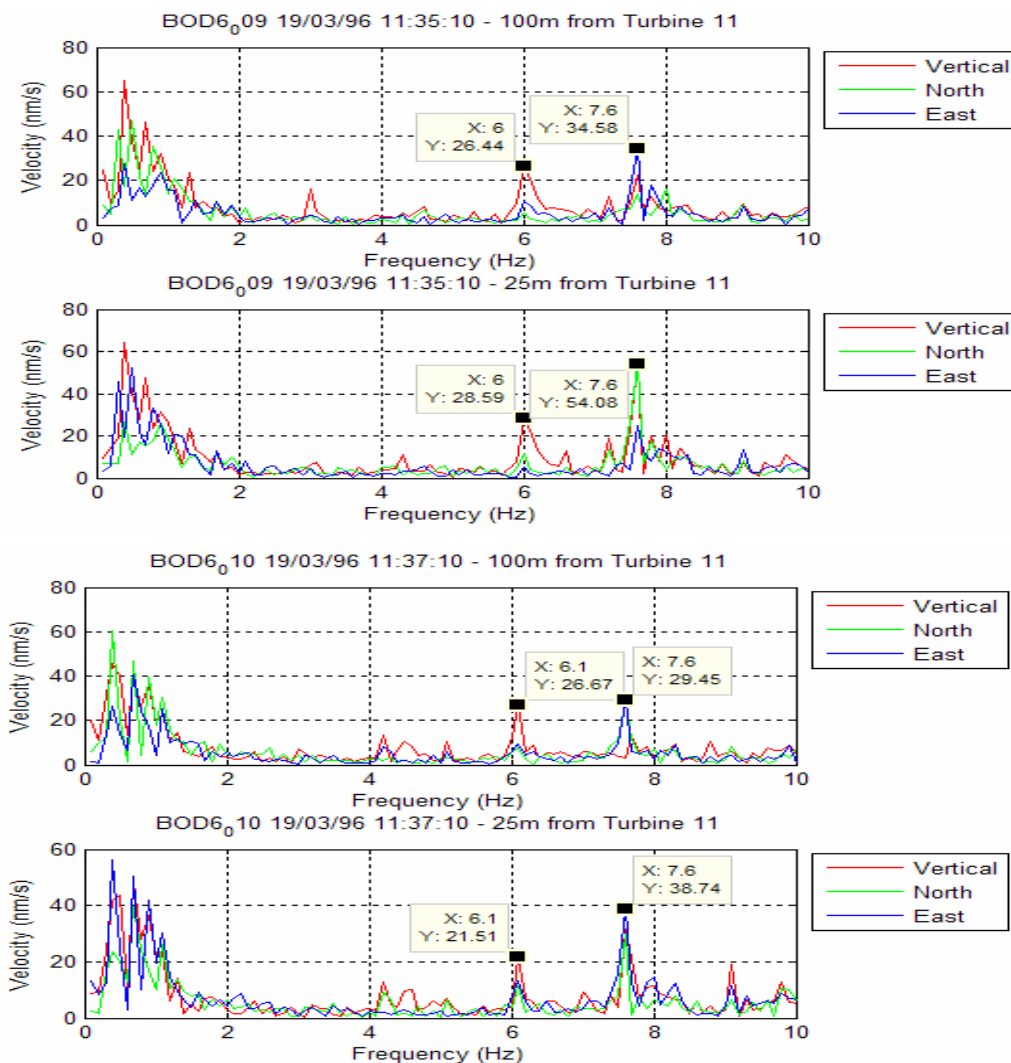


Figure 3 Selected spectra during the sequential shut-down at St Breock Downs

Measurements were made over a range of wind directions from c 120° to c 310° at a constant wind speed of 10 ms⁻¹. Clear variations in amplitude were observed with levels varying by about a factor two. The variation had the same spatial pattern for most

frequencies and this pattern correlated with acoustic measurements made at closer angular increments within the limitations of the data.

The levels of vibration fell in a manner which was consistent with their origin being from the wind farm. The lowest frequencies persisted even when the whole turbine field was shut-down which indicates that their source may be external to the site or that some complex interference is happening between the multiple vibration sources such as the resonance of the tower structure itself under wind loading.

Accelerometers mounted on the base of Turbine 1 clearly showed tonal components which correspond with the frequencies observed on seismometers. The 4.5 and 7.5 Hz components seen on the microseismic records were particularly pronounced within the infrasonic band (below 20 Hz) as are other harmonics of 1.5 Hz.

Figure 4 shows the variation in amplitude of the best detected 6 and 7.5 Hz harmonics, against distance from the turbine during the switch-off experiment. These and their averages have then been compared with different models for the attenuation of the amplitude with distance. There is considerable variation but the data fit a $r^{-(1/2)}$ model much better than a r^{-1} model.

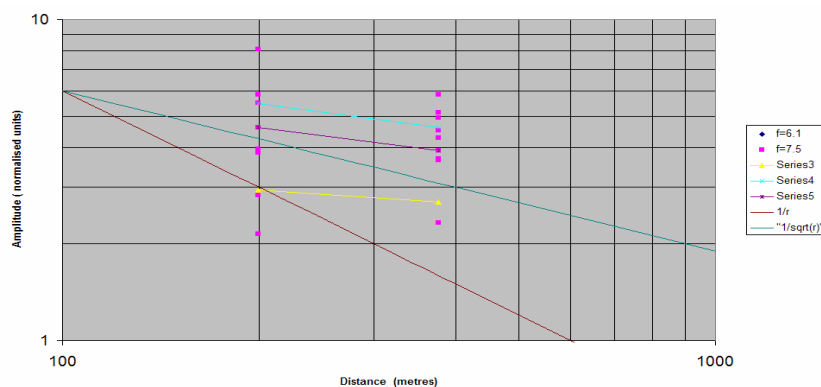


Figure 4 Variation of amplitude of well-detected frequencies with distance and a comparison with various attenuation models.

US Results from the Stateline Survey Schofield (2001)

The Maiden wind farm development of 150 MW capacity was planned c 20 km away from the Laser Interferometry Gravitational Observatory (LIGO) at Hanford in Washington State. This will try to detect gravitational waves from black holes and supernovae to test the predictions of Einstein's General Theory of Relativity. Schofield (2001) carried out an appraisal of vibrations for the operational Stateline wind farm (also in Washington State) which comprises 399 Vestas V47 Turbines and confirmed Styles' (1996) and Snow's (1997) conclusions that harmonic seismic signals were generated from wind farms and could be detected to considerable distances. Signals above LIGO ambient seismic background were detected out to 18.3 km which has significant implications for Eskdalemuir, particularly as estimates of seismic background noise level at EKA are well below the noise levels measured at Stateline and at the LIGO site. Schofield considered that, from the decay of signal amplitude with distance, the

signals propagated as infrasound through the air and coupled into the ground to generate seismic vibrational signals in a manner which was not completely understood.

Microseismic and infrasound monitoring of wind farms in southern Scotland

This study was designed to answer the question of whether seismic signals generated by wind turbines would significantly affect the operational performance of EKA. A site was chosen at Dun Law (Soutra Hill) in the Lammermuir Hills where 26 Vestas V47 turbines of the same type as monitored by Schofield (2001) are situated. The site has very much the same geology (cleaved Silurian shales and mudstones) as Eskdalemuir and the site is a grouse moor with very little ambient seismic noise.

Ten Guralp CMG-6TD three-component seismometers were deployed at increasing distances away from Dun Law wind farm to monitor the ground vibration levels and infrasound signals generated by modern wind farms as a function of distance out to c 17.5 km which operated almost continuously from July to December 2004. Four DASE MB2000 microbarometer infrasound stations were co-located with seismic stations at specific distance from Dun Law to ascertain whether the signals detected propagate as infrasound or as seismic surface waves and hence determine the characteristics and mode of propagation and attenuation rates of these signals. Figure 5 shows the location of seismic and infrasound stations deployed around Dun Law. Accelerometers were installed on fixed speed (Dun Law) and variable speed (Ardrossan) wind turbine towers and strong motion detectors placed in their immediate vicinity to ascertain how the mechanical vibrations of the towers compare to ground vibrations.

The results were then compared with current ambient seismic levels at the Eskdalemuir site and used to develop a model for the propagation of seismic signals from wind farms. This is then used to assess the potential impact of planned capacity on the detection capability of Eskdalemuir.

On-Tower Measurements at Dun Law

At the Vestas V47 rotation rate of 28.5 rpm the blade passing frequency is 1.425 Hz and vibrations would be expected at this frequency and its associated harmonics. In order to establish the spectra of the excitation from the turbine towers an experiment was carried out using accelerometers mounted within one of the turbine towers, T22. The wind farm was then sequentially switched off and then back on. Figure 6 shows the vibration record recorded on one of the accelerometers clearly showing the drop and rise in amplitude during the switch-off.

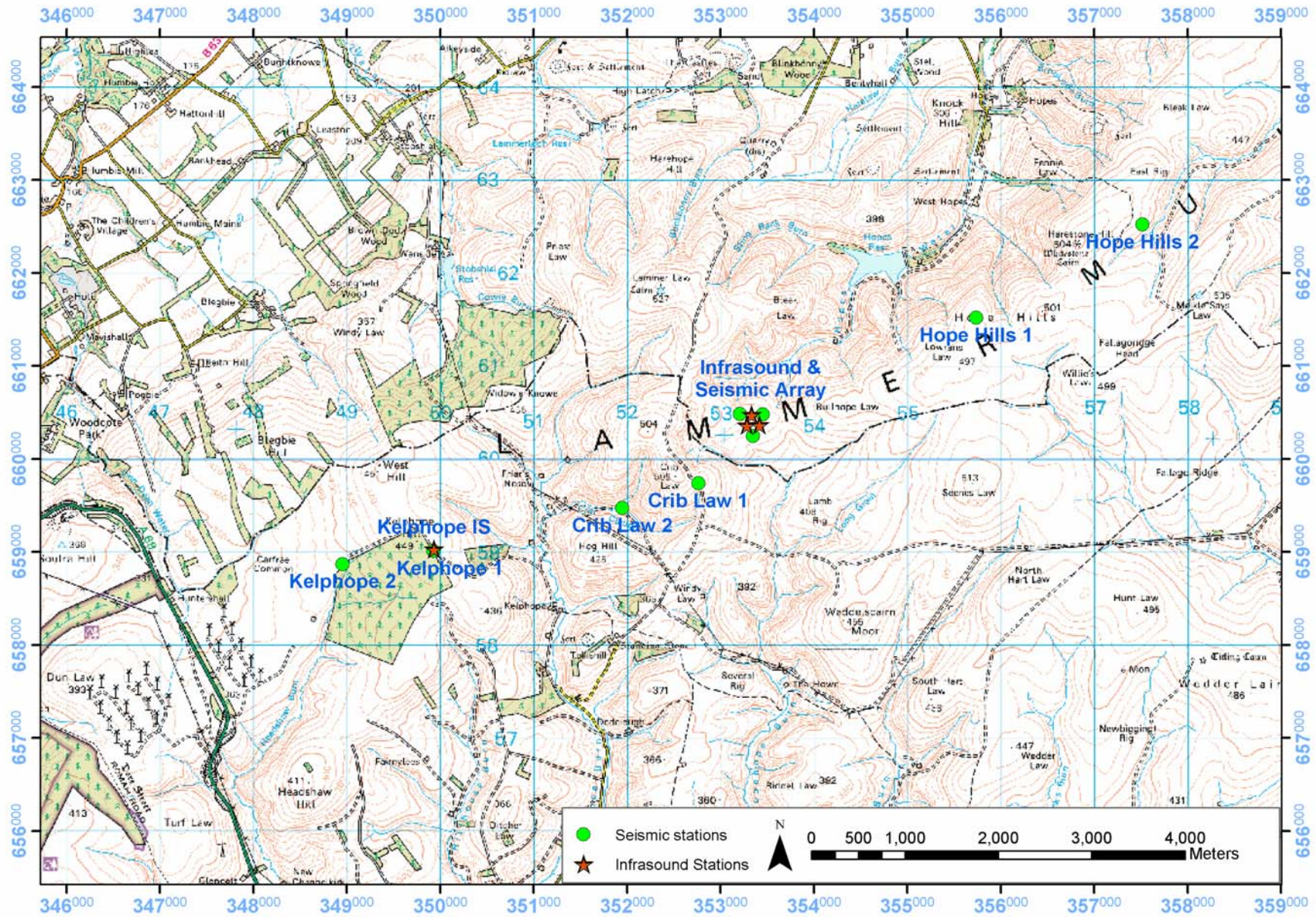


Figure 5 Map showing the location of infrasound and seismic monitoring stations around Dun Law windfarm.

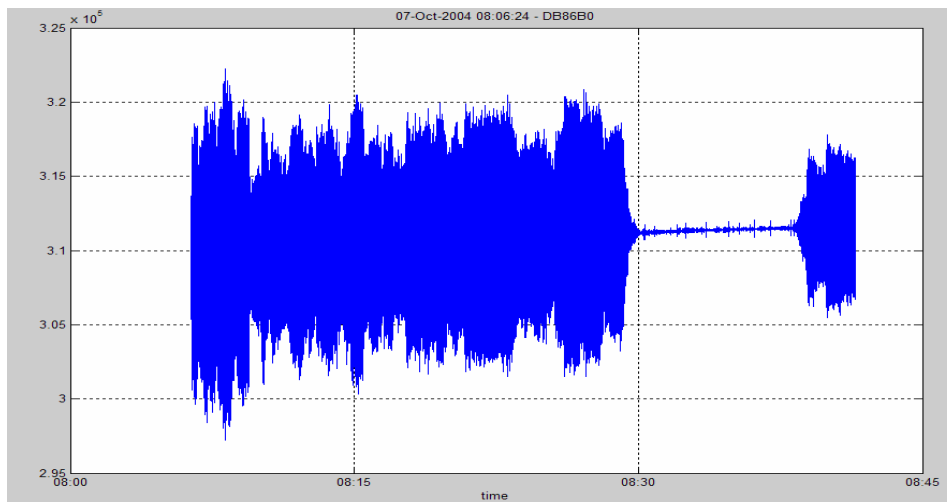


Figure 6 Accelerometer record of DB86A0 on Turbine T22 during switch off and back on 7 October 2004

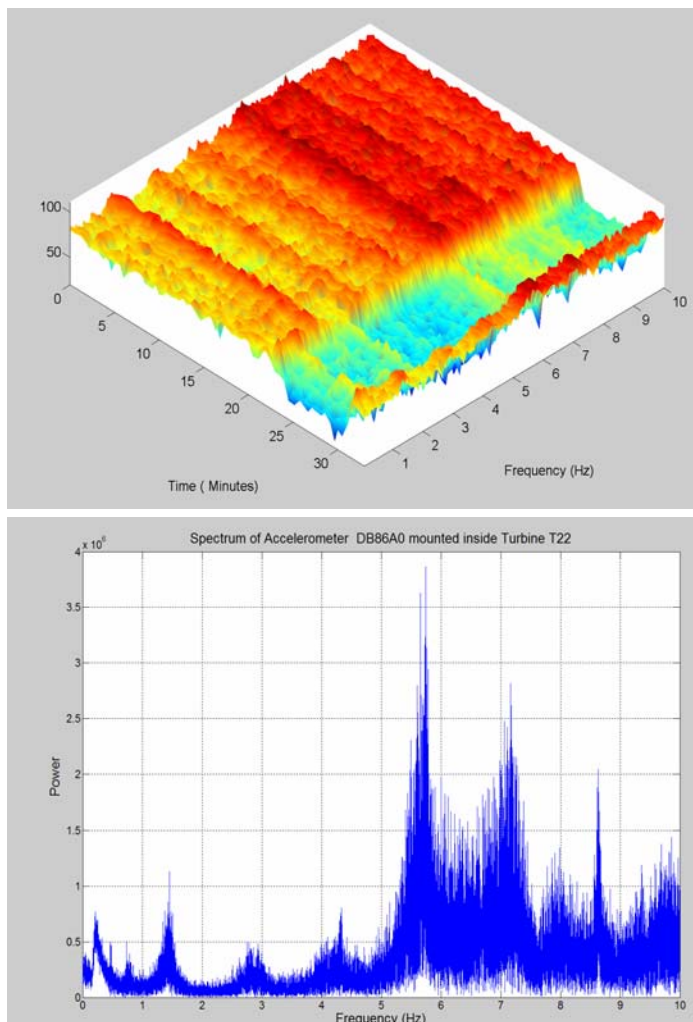


Figure 7 Spectrogram of accelerometer on turbine during Turbine T22 switch off and a spectrum showing Blade-passing (1.43Hz and Harmonics) and structural resonances of Turbine T22

Figure 7 shows a spectrogram of the signal during this period. It is clear that frequencies are occurring close to those predicted and that they cease during the switch-off and then re-appear at switch-on. However, there are low amplitude frequency components which appear to continue across the switch-off and indeed some that appear to be only present then. It seems probable that these are related to structural modes of the turbine powers which are excited when the blades are braked and energy has to be dissipated in the tower itself. There is a low frequency peak at c 0.75 Hz which may correspond to the 0.67 Hz peak observed by Schofield.

Figure 7 also shows a composite spectrum throughout the interval and significant components at 1.4, 2.8, 4.3, 5.7 Hz and higher can be clearly seen. The broadening of the peaks is due to the complex sequence of events which are composited into this spectrum. Consequently, if peaks at these frequencies are observed on more distant seismometer records, there is some confidence that they have their origin in vibrations generated from Dun Law wind farm.

Analysis of seismic records from the Lammermuir array

Notwithstanding the search for a quiet site away from ambient background noise, and the Lammermuir Hills is an exceptional site, the background noise is still some 20dB greater than Eskdalemuir, confirming how quiet a site EKA really is.

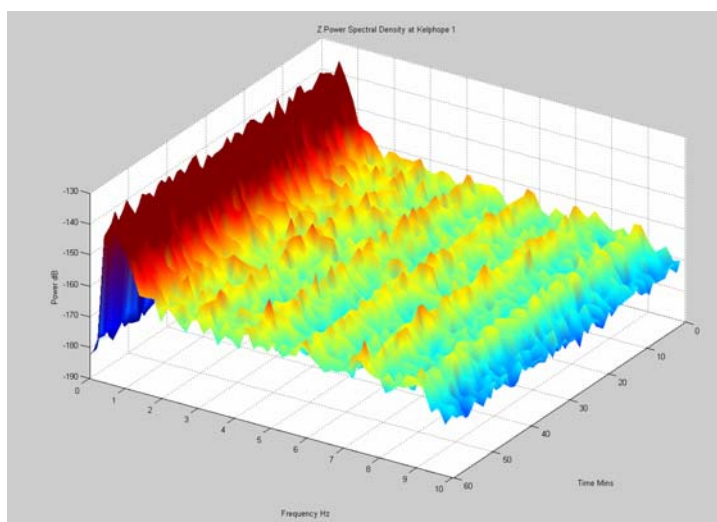
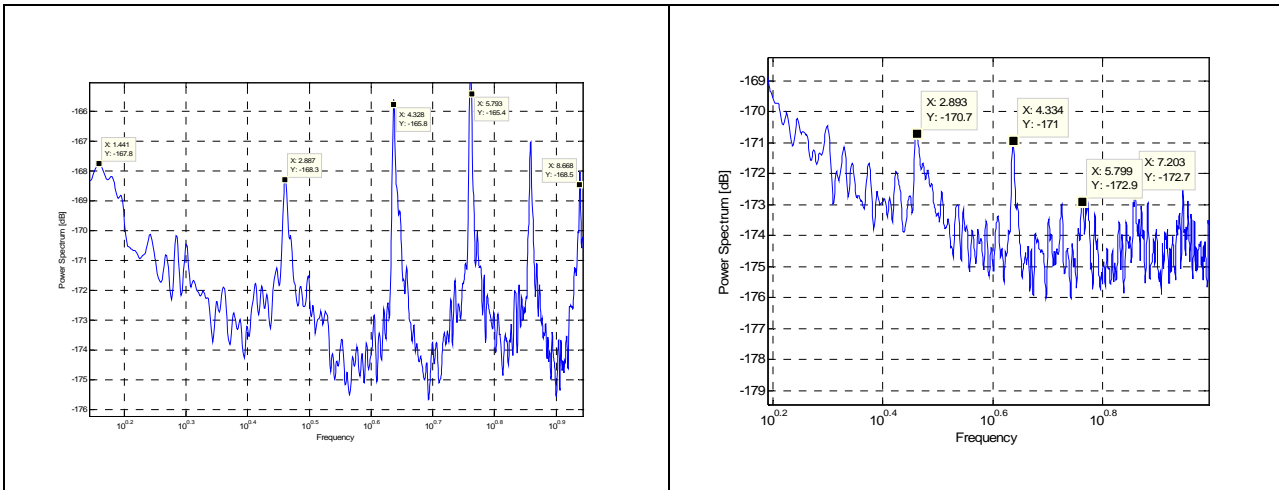


Figure 8 Spectrogram at Kelpheope 1 on 19 September 2004 between 00:00 and 01:00

Figure 8 is an example of a spectrogram of seismic data for 19 September 2004 between midnight and 01:00 am GMT from the Kelpheope 1 site, some 2.4 km away from the nearest point of the Dun Law wind farm and shows the prominent presence of the principal harmonics of 2.8, 4.3, 5.7, 7.1, 8.5 Hz as predicted and as observed in the on-tower measurements. The fundamental blade-passing frequency is not readily apparent but is masked by the rising background noise which climbs sharply below 2 Hz and the averaging process which is employed to give robust estimates of the power spectral density for the spectrograms. However, a narrow-band analysis (Figure 9) of part of the data shows that a 1.4 Hz component is present and also demonstrates even more clearly the principal harmonics.



Figures 9 and 10 Narrow-band spectral analysis of part of the seismic data from 19 September at Kelphope 1 showing the 1.4 Hz and higher harmonics of the blade-passing frequency and from 19 September at Crib Law 2 (5.2 km) showing the 2.8 Hz and higher harmonics of the blade-passing frequency

Figure 10 shows a similar narrow-band spectrum from the Crib Law 2 site some 5.2 km away from Dun Law during the same interval. Figure 11 shows the spectrogram recorded at the Array 3 site, some 6 km away from Dun Law and again the 5.7, 7.1 and 8.5 Hz components can all be clearly seen throughout the whole duration of the record. The data have been rotated into principal components with the X-component parallel to the direction towards Dun Law, the Y-component perpendicular and the Z-component vertical. After this rotation, the energy is largely confined to the X and Z-components suggesting that that it is propagating as vertically polarised Rayleigh waves.

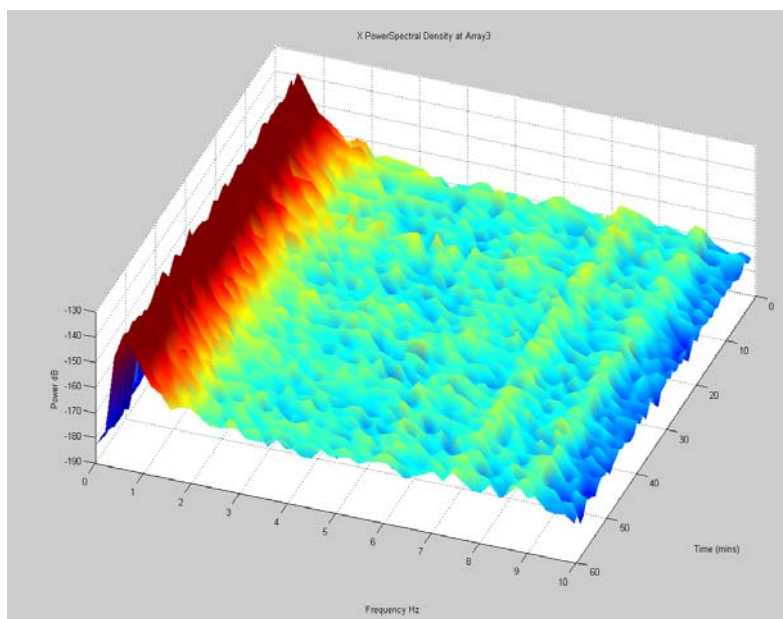


Figure 11 Seismic spectrogram at Array 3 (6 km) on 19 September 2004 between 00:00 and 01:00

These examples from a very large data set demonstrate clearly the presence of harmonic components which we associate with the Dun Law wind farm and which can be identified on many of the seismometers throughout the 6 month monitoring period. This confirms the previous work of Styles (1996) and Schofield (2001) that wind farms do produce discernible harmonic signals which can be detected over considerable distances.

While it becomes more difficult to discern the individual harmonic components with greater distance because of the ambient background noise, it should not be considered that they then become unimportant as they are contributing to the overall level of ambient noise in the region between 1 and 10 Hz which is the critical discrimination band for forensic seismology and that is why they may lead to degradation of the discrimination capabilities of EKA at Eskdalemuir. It is therefore critically important to establish the mode of propagation and therefore attenuation characteristics of the microseismic noise. The polarisation is a very strong indication that we are dealing with Rayleigh waves (commonly known as 'ground-roll') rather than coupled infrasound. Figures 12 to 14 show a sequence of spectra and spectrograms obtained from Kelphope 1, c 2.4 km from Dun Law over a range of wind conditions on 1st and 2nd of October 2004.

Low wind speed, low production: Date: 01.10.2004

Time:	06:00 to 07:00	Average wind speed:	4.58ms ⁻¹
Average wind direction:	221.33°	Average production:	1826.8 kW

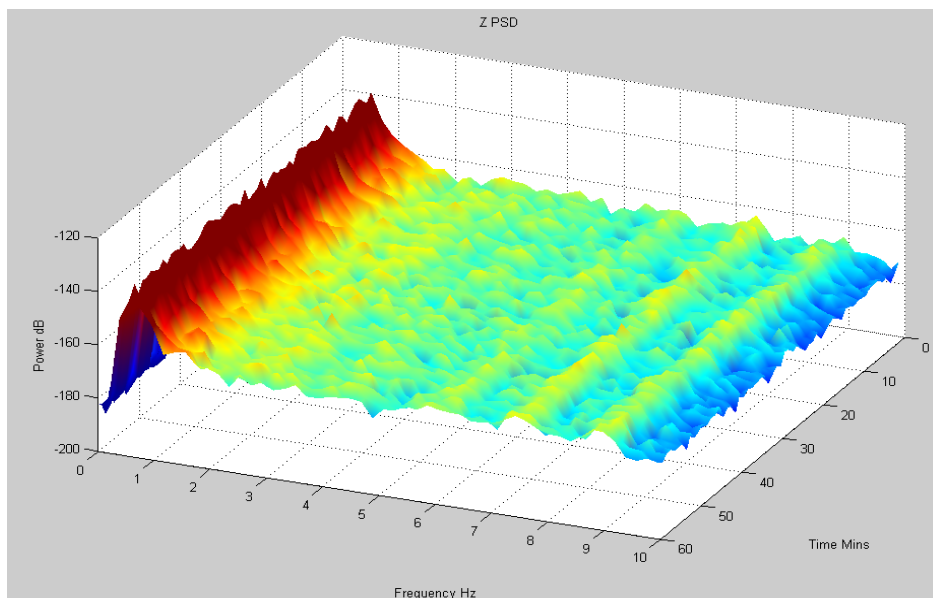


Figure 12 Kelphope 1 on 1/10/2004, 06:00 to 07:00, low wind speed

When the wind farm starts to generate at low wind speeds, considerable microseismic signals can be detected. Clear harmonic components can be seen including the fundamental at 1.4 Hz but there appears to be considerable side bands to the

frequencies. It may be that these are due to the turbine slewing and intermittently operating in the low wind conditions prevailing at this time.

Moderate wind speed, moderate production: Date: 02.10.2004

Time:	00:00 to 01:00	Average wind speed:	7.29 ms ⁻¹
Average wind direction:	245.67°	Average production:	9100.9 kW

When the wind speed and production rise, clear harmonic signals stabilize and are present for the full period. Although some other frequencies can be seen on the narrow-band spectra they are not obvious on the more robust power spectral density spectrograms probably because of the averaging of spectra which takes place to achieve stability of spectral estimates.

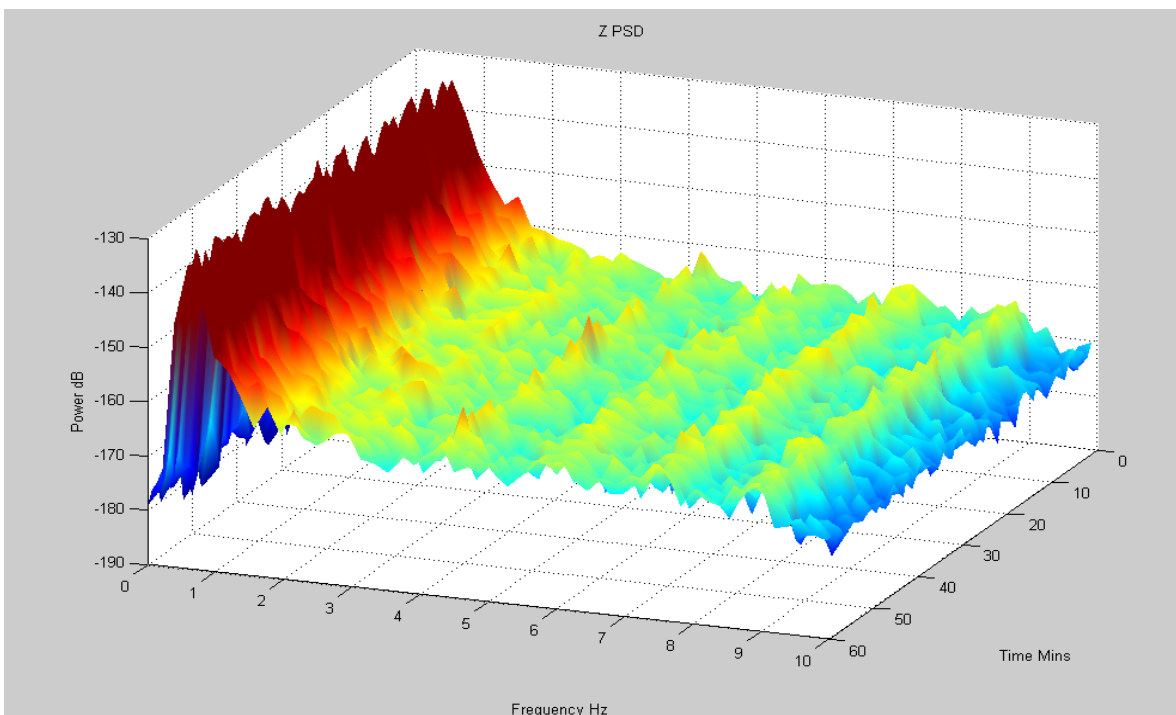


Figure 13 Kelphope 1 on 2/10/2004, 00:00 to 01:00, moderate wind speed

High wind speed, full production: Date: 02.10.2004

Time:	11:00 to 12:00	Average wind speed:	11.189ms ⁻¹
Average wind direction:	254.67°	Average production:	16920.8 kW

In the regime of high wind speed and production very well developed harmonic components are seen with far fewer sidebands. It is clear from this sequence (and further shown in later work) that power in the harmonic components increases as wind speed and associated production increase which is what would be expected for seismically generated and propagating signals.

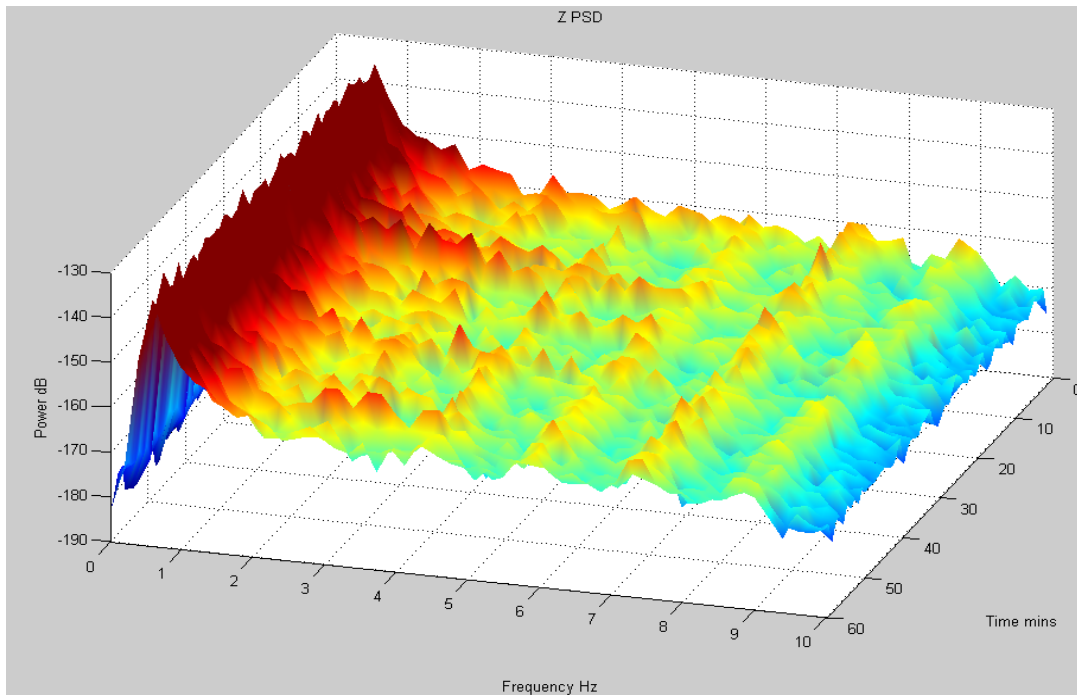


Figure 14 Kelphope 1 on 2/10/2004, 11:00 to 12:00, high wind speed

Infrasound Measurements

The infrasound equipment was more difficult to maintain than the seismic systems due to the very high power drain and the poor weather which made the solar panels less effective than planned and data coverage is patchy. However, the most optimal infrasound records during a range of wind speeds were recorded over 3 of the 4 stations from 01/10/2004 to 03/10/2004 and they show some very important aspects of the study. The operational stations were: Kelphope Infrasound, IS Array 1 and IS Array 2. The results are shown in the following sequence of spectrograms (Figures 15 to 17) recorded over the same range of variable wind conditions as the microseismic records analysed and discussed previously.

Low wind speed, and production:

Date: 01.10.2004

Time: 06:00 to 07:00
 Average wind direction: 221.33°

Average wind speed: 4.58ms⁻¹
 Average production: 3041.8 kW

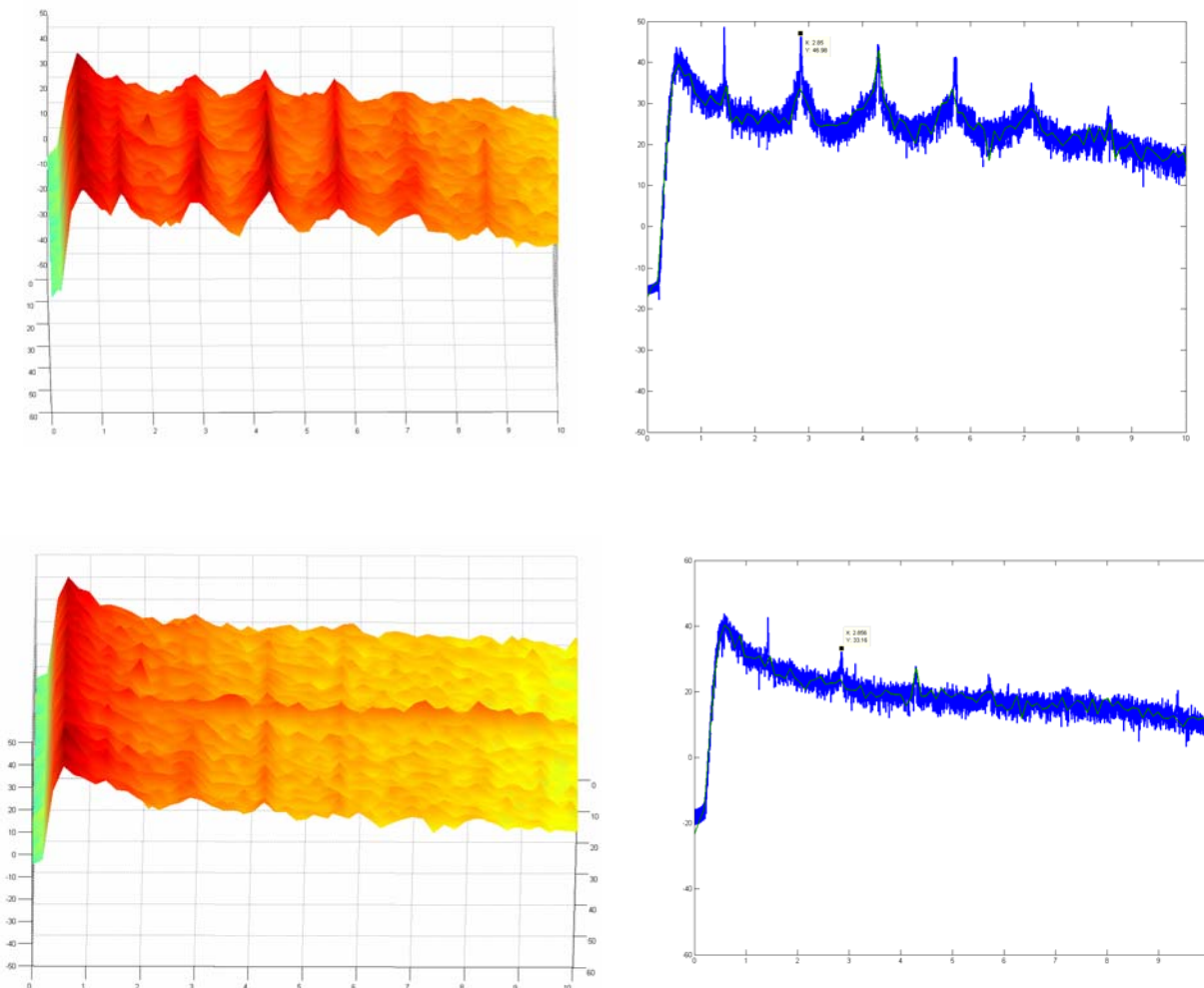


Figure 15. Infrasound spectra at Kelphope 1 (2.4 km) top and Array 2 (6.2) Bottom , Low Wind Speed

When the wind farm starts to generate at low wind speeds, considerable infrasound signals can be detected at all stations out to c 10 km. Clear harmonics of 1.4 Hz can be seen although interestingly, and somewhat enigmatically, the blade-passing frequency itself is not so strongly detected

Moderate Wind Speed and Production Date: 02.10.2004

Time:	00:00 to 01:00	Average wind speed:	7.29ms ⁻¹
Average wind direction:	245.67°	Average production:	9100.9 kW

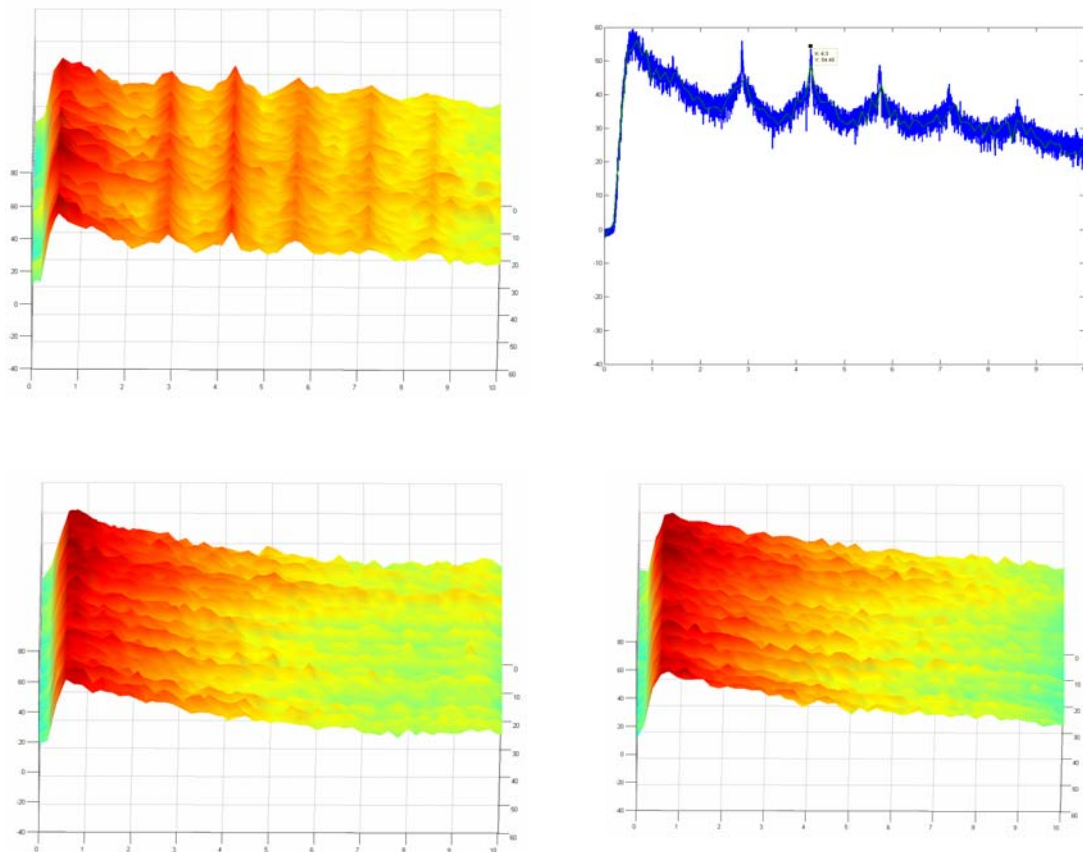


Figure 16. Infrasound spectra at Kelphope 1, Array 1 and Array 2 Moderate Wind Speed

When the wind speed and production rise clear signals can be seen on Kelphope 1 at c 2 km but the signals are not so well detected at the more distant arrays.

High wind speed, full production: Date: 02.10.2004

Time:	11:00 to 12:00	Average wind speed:	11.189ms ⁻¹
Average wind direction:	254.67°	Average production:	16920.8 kW

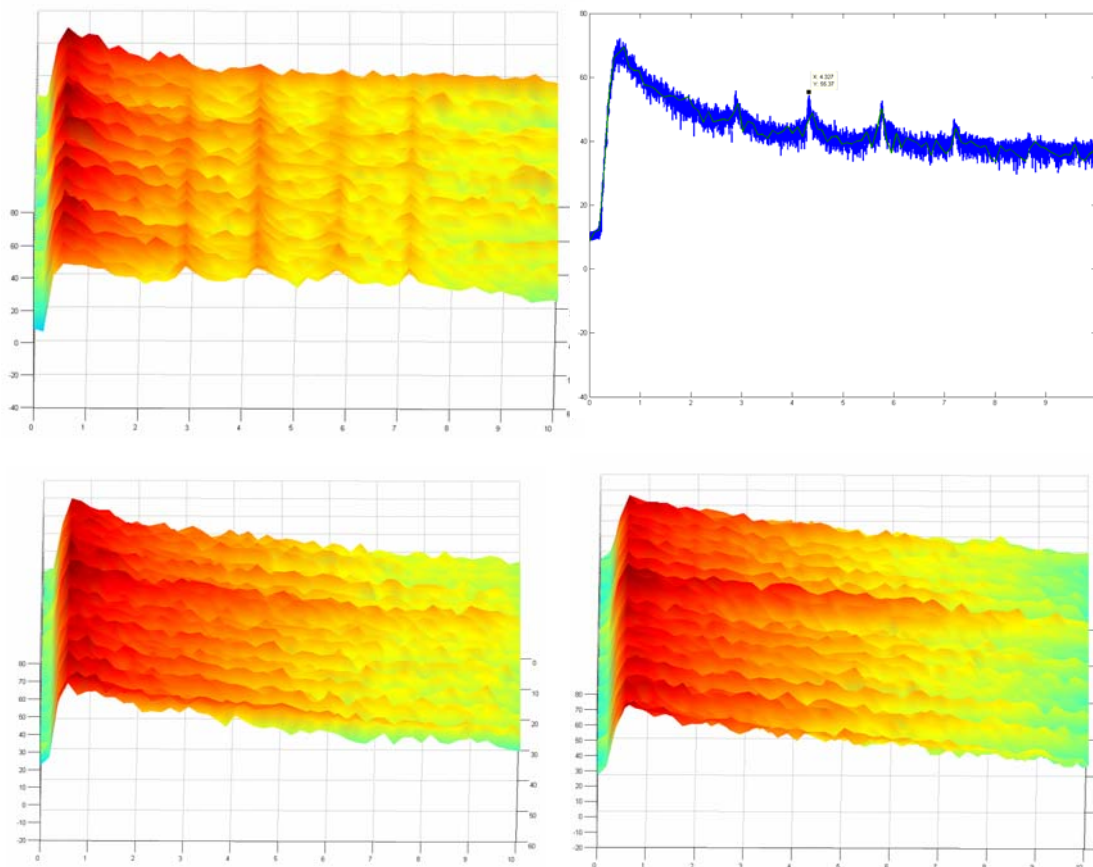


Figure 17. Infrasound spectra at Kelphepe 1, Array 1 and Array 2 High Wind Speed

When the wind speed and production rise then while it is possible to just see the blade-passing frequency harmonics at Kelphepe they are not detectable at all on the more distant array at 6 km. This is a very significant and indicates that infrasound signals from wind farms only appear to propagate efficiently during relatively calm conditions when turbulence associated with high wind velocities is not present.

This is in marked contrast to the microseismic signals observed during exactly the same period which grow in amplitude and power as the wind speed and energy production increase. While it is apparent that infrasound signals can clearly be detected at considerable distances away from a wind farm in the right conditions and may have an importance in this regard, they cannot be the primary source for the ground vibrations measured on buried seismometers. There is an opposing relationship with wind speed and weather conditions for the two phenomena and, therefore, they cannot be causally related.

This confirms that the vibrations experienced on seismometers situated at considerable distances from wind farms propagate through the ground as high frequency Rayleigh

waves and not through the air, and as such must obey the propagation modes and attenuation and absorption laws for geological materials and not air.

Relevance for Eskdalemuir Seismic Array and other vibration sensitive structures

Generation of vibrations by wind farms

It has been clearly shown that wind turbines generate low frequency vibrations which are multiples of blade passing frequencies and which can be detected on seismometers buried in the ground at significant distances away from wind farms even in the presence of significant levels of background seismic noise (many kilometres). Some of these frequencies are non-stationary at very low wind speeds and clear variation is seen in frequency over long and short timescales. It can be postulated that these are generated by the interaction between the blades and the towers. There are other frequencies which are stationary and it can be postulated that these are caused by normal modes of vibration of the towers.

It has also been clearly shown that wind turbines generate low frequency sound (infrasound) and acoustic signals which can be detected at considerable distances (many kilometres) from wind farms on infrasound detectors and also on low-frequency microphones (Hayes *pers. comm.*)

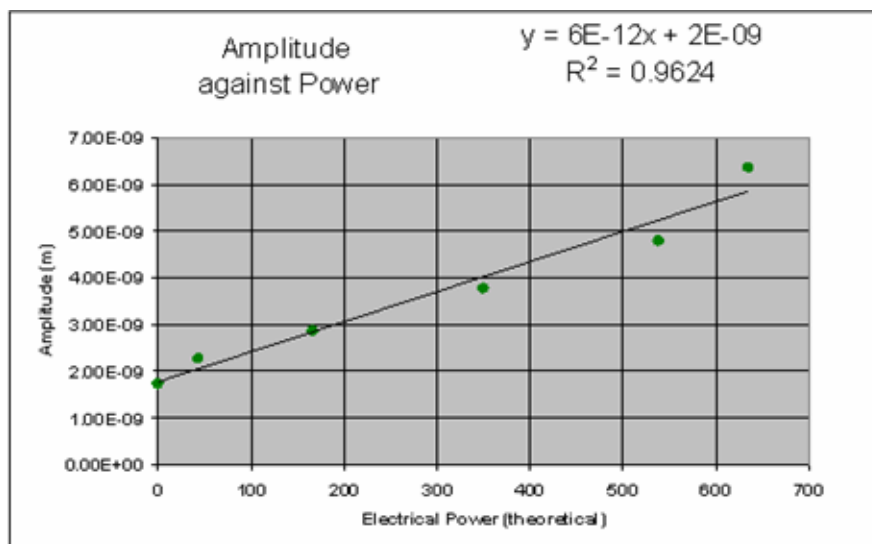
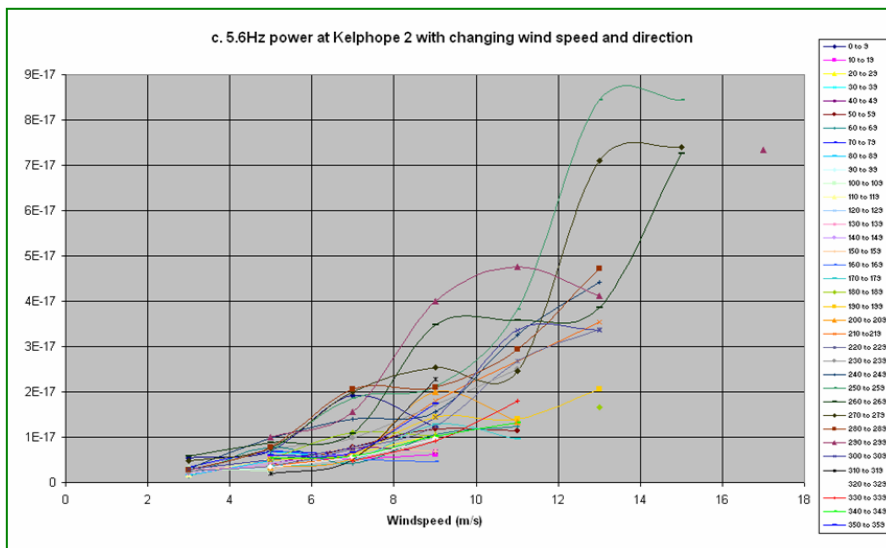
Attenuation of seismic signals

Since it is evident that energy from wind turbines travels to the seismometers as seismic surface waves (Rayleigh) which exhibit cylindrical spreading, their amplitude will be inversely proportional to the square-root of distance.

It is also clear that low-frequency acoustic waves can be detected at considerable distances away from a wind farm under the right atmospheric conditions. At greater distances where the atmosphere acts as a waveguide infrasound may also have a cylindrical dependency on distance.

Interaction of multiple turbines and wind farms

Styles *et al.* (2005) show that seismic amplitude varies as the square root of the number of turbines and this is to be expected because the turbines are not all in phase and neither are they operating at exactly the same frequency because of the slight possible variations in rotation speed and also wind conditions across the farm. There is also a possible 10% variation in speed due to the turbine's Optislip mechanism which will cause broadening of the spectral peaks. They are quasi-random sources and therefore add as the square-root of the turbine number. With similar reasoning, individual wind farms will not be in phase with each other and so they will add in quadrature such that the total is the square-root of the sum of the squares of the individual contributions.



Variation of Seismic amplitude with wind farm power output

Figure 18 Variation of vibration with wind speed and direction for the 5.6 Hz component at Kelphope 2 and variation of seismic amplitude against Electrical Power at Kelphope 2 (1.4 km)

The upper graph in Figure 18 shows the variation of seismic power with wind speed and direction for the 5.6 Hz component at Kelphope 2. Although there is some variation with wind direction there is a clear increase with wind speed within the operational region (up to c 15ms^{-1}) with seismic power proportional to the square of wind speed. Therefore we conclude that seismic amplitude is approximately proportional to wind speed. Electrical power is very nearly proportional to wind speed in the operational band (5 to 15ms^{-1}) and so seismic amplitude is approximately proportional to electrical power as can be seen from the lower graph in Figure 18.

Setting acceptable thresholds for permitted vibration at Eskdalemuir and their affect on detection capability

In order to assess the effect of wind farm vibration on the detection capability we have selected the 4 to 5 Hz band which is very quiet at Eskdalemuir and therefore ideal for discrimination of nuclear events. This is also a frequency band which is very efficiently generated by the wind turbines we have observed in this experiment and previously (St Breock Downs) and also by Schofield (2001) and therefore liable to interfere with the operation of the array.

Even though the strictest possible interpretation of the CTBT agreement would mean no increase in threshold is acceptable the view has been taken that an increase equal to the present observed ambient displacement in this band is acceptable without seriously compromising the detection capability of the array.

We have introduced the concept of a noise budget which is the total additional noise which all wind farms in the southern uplands of Scotland will be allowed to generate in addition to the present noise at Eskdalemuir. The noise budget for wind farms in the Southern Uplands of Scotland should be equal to the windy day RMS median noise level as measured at Eskdalemuir. Initial short-term estimates by Bowers (2004) suggested that the median level was 0.25 nm, but re-analysis of data from Eskdalemuir over a much longer time period for noisy conditions has given the following histogram. The median level of the noise is 0.336 nm (Figure 2) and this has been taken as the noise budget which will be permitted for aggregate wind-farm noise for the region centred on Eskdalemuir.

If the average band-limited noise power of the (20) seismometers comprising EKA is σ_n^2 , then we can define the allowable power (σ_w^2) of seismic signals generated by wind turbine as:

$$\sigma_w^2 = x\sigma_n^2 \quad \text{where } x \text{ is a constant multiplier which we wish to set.}$$

We can assume that σ_w^2 can be considered random because in general the wind turbine seismic signals will be generated by a range of wind farms of varying design and rotation speed, operating under different local wind conditions and at a variety of azimuths and distances from EKA. A question has been posed as to what difference azimuth makes to the sensitivity of Eskdalemuir to wind farm vibration but except for a few specific directions at a few specific frequencies this effect can be ignored.

The RMS noise level, D , after beam forming, can be considered a measure of the detection threshold of the array. If the noise power σ_n^2 is random then

$$D_o = \sqrt{\frac{\sigma_n^2}{N}}$$

In the presence of seismic power from wind farms the RMS noise level becomes

$$D_1 = \sqrt{\frac{\sigma_n^2 + \sigma_w^2}{N}}$$

and the ratio of the degradation of the EKA detection threshold due to wind turbine signals therefore becomes

$$\frac{D_1}{D_0} = \sqrt{1+x}$$

The preliminary recommendation of Styles (2004) considered the value of x to be ≤ 1 (i.e. equal ambient and wind farm noise), giving $D_1/D_0 \leq \sqrt{2}$ (≈ 1.4).

This can be transformed into an estimate of the degradation of the detection threshold in terms of seismic yield, W in kilotonnes, using a standard magnitude-yield relationship such as

$$m_b = b + a \log_{10} W$$

Where typically $a=0.75$ and $b=4.45$ for East Kazakhstan. Therefore,

$$\frac{W_1}{W_0} = (1+x)^{1/2a}$$

At present EKA can detect 100 Tonnes of conventional explosive detonated in Kazakhstan (Equivalent to a magnitude 3.8 m_b earthquake). The suggestion that $x=1$, i.e. equal ambient and wind turbine power, will mean that 160 Tonnes will be the minimum detectable at times when the noise rises to the permitted level of equal power from ambient noise and wind farms

Statistical analysis of the percentage utilisation of wind for Scottish wind farms (Styles *et al.* 2005) shows that wind farm electrical power production exceeds 60% of rated capacity only 20% of the time over a year. If it is acceptable that for 20% of the time averaged over a year, seismic amplitude levels may exceed the permitted threshold set at Eskdalemuir of 0.336 nm (which will also correspond to days on which the Eskdalemuir Array is less effective because of microseismic noise) the predicted seismic amplitude levels which are calculated on rated capacity, can be scaled by 60%.

Mathematical Model of Wind Farm Noise Propagation

There is now sufficient information from the monitoring and analysis of microseismic, infrasound and on-tower data to develop a solution to the problem of what level of vibration is permissible at Eskdalemuir, to know how wind farm vibration propagates and attenuates and to decide what the permissible number and distribution of wind farms and turbines in the Southern Uplands is.

In order to evaluate the nature and properties of noise propagation from wind farms the following mathematical model is postulated following Bowers(2004)

The seismic displacement amplitude spectrum, $U(\omega, r)$ at angular frequency ω , of a single wind turbine operating at distance r , from the recording station is given by the following convolutional mathematical model:

$$U(\omega, r) = S(\omega)G(r)B(\omega, r)P(r) \quad \text{where:}$$

$S(\omega)$ represents the source spectrum, $P(r)$ is a frequency-dependent receiver-site effect, $G(r)$ represents geometrical spreading and $G(r) = r^\eta$, $B(\omega, r)$ is the attenuation.

$$B(\omega, r) = \left(\exp\left(\frac{-\omega r}{2Q(\omega)v}\right) \right) \quad \text{where } v \text{ is seismic velocity.}$$

For Cylindrical Spreading (seismic surface waves) $\eta = -0.5$

Therefore, the amplitude of the signal from a single turbine at a distant location, A_{far} , is related to the amplitude at a location closer to the turbine, A_{near} , by the following equation,

$$A_{far} = A_{near} \sqrt{\frac{R_{near}}{R_{far}}} e^{-\frac{\pi f (R_{near} - R_{far})}{Qv}} \quad \text{where:}$$

R_{near} and R_{far} are the distances from the source to the near and far locations, respectively, Q is a factor giving the non-geometrical attenuation of the wave with distance travelled (i.e. absorption of energy within the rock as the seismic wave does work to vibrate the particles of the material), and f is the frequency of the signal ($\omega = 2\pi f$).

This formula is applicable to surface waves radiating out from the source uniformly. Localised inhomogeneties may cause some focussing of the energy but this is not predictable in a generalised model and is unlikely to significantly affect the conclusions.

Prediction of the levels of vibrations which may be generated by single and multiple wind farms around Eskdalemuir

This mathematical model based on the theoretical attenuation model proposed for the seismic sources and the propagation of vibrations from individual and multiple wind farms can now be used to calculate the predicted vibration levels. These can then be compared individually and in aggregate to the noise budget of 0.336 nm RMS at Eskdalemuir. The wind farms which have been included in this calculation are those which have been given consent or are already in planning as recognised by the MoD Safeguarding Department.

The parameters which are used in the model are as follows and represent best estimates of the appropriate values.

- F=4.5 Hz (mid-point of the pass band)
- Q=50 (determined by MacBeth and Burton, 1986, 1987 for southern Scotland and Bowers *pers. comm.* for Eskdalemuir)
- Velocity=2000 ms⁻¹ (from Eskdalemuir)
- Noise Budget=0.336 nm (median noisy day value for Eskdalemuir)
- Utilisation which is only exceeded 20% of the time = 60%
- The displacement at r=1 km is calculated at 24 nm RMS equivalent for the Stateline Wind farm of 399 Vestas, 0.66 MW, V47 turbines which is calibrated against vibration levels measured throughout this experiment of 5.5 nm at Kelphope 2 (1.3 km) and 2.6 nm at Kelphope 1 (3.1 km) at Dun Law (26 Vestas, 0.66 MW, V47 turbines) and levels of 30nm at 720 meters for Stateline (Schofield 2001).

Table 1 shows the individual levels and the total generating capacity and aggregate seismic noise which we predict will be generated by wind farms in planning or having obtained consent. With the planned capacity of 1.6 GW, the aggregate vibration is 0.307 nm, within the threshold set at 0.336 and with some small headroom for further development.

Attenuation of Displacement in the 4.5 Hz Band as a Function of Number of Turbines, Power and Distance												Noise threshold in 1.5 to 4.5 Hz Band	0.336	24	Noise Power(nm2)
TOTAL GENERATING CAPACITY				1657.1				TOTAL NOISE							
Windfarm	N (Number of Turbines)	Power (per Turbine)	r (km)	Total Power (MW)	Attenuation with Distance	N-Ratio	P_Ratio	Total Scaling Factor	Amplitude (nm)	Scaled by 60% to reflect Utilisation	EXCEEDS <20% of time (ie 60% power)				
Stateline (Ref)	399	0.66	0.71	263.34	1.23645	1.000	1.000	1.23644823	29.6748	17.8049	ref				
KELPHOPE2	26	0.66	1.3	17.16	0.84064	0.255	1.000	0.214589995	5.1502	3.0901	ref				
KELPHOPE1	26	0.66	3.1	17.16	0.42207	0.255	1.000	0.107742194	2.5858	1.5515	ref				
Stateline (Ref)	399	0.66	18	263.34	0.02131	1.000	1.000	0.021311589	0.5115	0.3069	ref				
EWE HILL	22	2.30	18.9	50.6	0.01831	0.235	3.485	0.014985552	0.3597	0.2158				4.66E-02	
CLYDE	173	3.00	30.04	519	0.00301	0.658	4.545	0.008998851	0.2160	0.1296				1.68E-02	
HARESTANES	71	3.00	27.38	213	0.00459	0.422	4.545	0.008797356	0.2111	0.1267				1.60E-02	
MINSCA	17	2.50	24.97	42.5	0.00675	0.206	3.788	0.005278918	0.1267	0.0760				5.78E-03	
CARLESGHILL	5	1.75	19.63	8.75	0.01621	0.112	2.652	0.004811735	0.1155	0.0693				4.80E-03	
MINNYGAP	15	2.00	25.32	30	0.00639	0.194	3.030	0.003752921	0.0901	0.0540				2.92E-03	
DALSWINTON	16	3.00	35.31	48	0.00132	0.200	4.545	0.001197797	0.0287	0.0172				2.98E-04	
MINCH MOOR	12	2.00	38	24	0.00087	0.173	3.030	0.000456049	0.0109	0.0066				4.31E-05	
MIDDLE HILL	12	2.00	28.7	24	0.00372	0.173	3.030	0.001954133	0.0469	0.0281				7.92E-04	
HALKBURN	20	2.00	42.97	40	0.00040	0.224	3.030	0.000274094	0.0066	0.0039				1.56E-05	
SELL MOOR	19	2.00	45.44	38	0.00028	0.218	3.030	0.000183203	0.0044	0.0026				6.96E-06	
TODDLE BURN	26	2.31	48.9	60	0.00016	0.255	3.497	0.00014616	0.0035	0.0021				4.43E-06	
FALAHILL	15	1.75	51.72	26.25	0.00011	0.194	2.652	5.49815E-05	0.0013	0.0008				6.27E-07	
BLACK LAW	62	2.30	60.94	142.6	0.00003	0.394	3.485	3.67534E-05	0.0009	0.0005				2.80E-07	
AFTON RESERVOIR	41	2.76	63.21	113	0.00002	0.321	4.176	2.54967E-05	0.0006	0.0004				1.35E-07	
FALLAGO RIDGE	67	2.00	63.04	134	0.00002	0.410	3.030	2.42814E-05	0.0006	0.0003				1.22E-07	
BROADMEADOWS	25	1.40	58.73	35	0.00004	0.250	2.121	1.97834E-05	0.0005	0.0003				8.12E-08	
CRYSTAL RIG PHAS	40	2.50	74.81	100	0.00000	0.317	3.788	4.074E-06	0.0001	0.0001				3.44E-09	
TORRS HILL	2	2.50	75.21	5	0.00000	0.071	3.788	8.58584E-07	0.0000	0.0000				1.53E-10	
SITE 9	4	0.85	79.27	3.4	0.00000	0.100	1.288	2.26631E-07	0.0000	0.0000				1.07E-11	
														0.3067	

Table 1 Predicted total noise aggregate for all wind farms currently consented or in planning. The total generating capacity of 1.6 GW has a total aggregate noise level below the limit of 0.336 nm.

Conclusions and Recommendations

Wind turbines generate low frequency vibrations which are multiples of blade passing frequencies and can be detected on seismometers buried in the ground many kilometers away from wind farms even in the presence of significant levels of background seismic noise.

Energy from wind turbines travels to the seismometers as seismic surface waves with cylindrical spreading because co-located, coincident seismic records and infrasound records and show that infrasound energy propagation is optimal in quiet wind conditions and decreases as the wind speed (and turbulence) increase and, conversely, seismic amplitude increases with wind speed. Clearly, there cannot be a causal relationship between the seismic amplitude and the infrasound if they have different behaviours with wind speed.

At present there are no current, routinely implemented vibration mitigation technological solutions which can reduce the vibration from wind turbines. Technologies which are helpful in the reduction of vibration from mechanical systems do exist and in the long-term and at some additional cost it should be possible for manufacturers to modify/augment these for application to wind turbines to reduce the levels of vibration transmitted into the ground. However, the following recommendations are based on current turbine designs as built:

- 1 An exclusion zone of 10 km within which no wind farm or turbine development is acceptable as the model shows that this would immediately exceed the threshold.
- 2 In order to optimise total energy generation, it would be inadvisable to permit any additional wind farms of current design to be permitted within 17.5 km of Eskdalemuir as these will effectively sterilise the whole region from generating additional capacity.
- 3 Presently consented and planned wind farms will not exceed the limit of 0.336 nm for approximately 80% of the time. During the remaining 20% of the time where they might exceed the limit, the ambient background noise at Eskdalemuir will also be higher and, as discrimination will be sub-optimal during these periods of higher wind speed, this is acceptable.
- 4 Beyond 50 km, it is not anticipated that any reasonable wind farm development will have an impact on the detection capabilities of Eskdalemuir.
- 5 There is some limited headroom for additional capacity with currently available turbine designs if it is required, up to the aggregate noise level of 0.336 nm, but it is strongly recommended that in order to maximise the energy generation capability this takes place at distances greater than 25 km from Eskdalemuir. The algorithms developed here will permit this to be assessed and optimised.

References

Bache, T. C., Marshall, P. D. and Young, J. B., 1986, High frequency seismic noise characteristics at the four United Kingdom-Type arrays. *Bulletin of the Seismological Society of America*, 76, 601-616.

Bowers D., 2004, Effects of known and foreseeable noise interference on seismic arrays, AWE Report No. 763/04 (M52/2), 1-27

Legerton, M.L., Manley, D.M.J.P, Sargent, J.W, Snow, D.J, Styles, P., 1996 "Low frequency noise & vibration levels at a modern wind farm". *Proceedings of Inter-Noise 96*, 459-462. Liverpool.

MacBeth, C. and Burton, P.W., 1986. Propagation of 0.7-2.5Hz Rayleigh waves in Scotland, *Geophysical Journal of the Royal Astronomical Society*, 84, 101-120.

MacBeth, C. and Burton, P.W., 1987. Single station measurements of high frequency Rayleigh waves in Scotland, *Geophysical Journal of the Royal Astronomical Society*, 89, 757-797.

Manley, D. M. J. P. and Styles, P., 1995. Infrasound generated by large sources, *Proceedings of the Institute of Acoustics*, 17, 239-246

Schofield R., 2001. Seismic Measurements at the Stateline Wind Project, LIGO T020104-00-Z

Snow D.J., 1997. Low frequency noise and vibrations measurements at a modern wind farm, ETSU W/13/00392/REP.

Styles P., 1996. Low-Frequency Wind Turbine Noise and Vibration: ETSU/POWERGEN, Contract Number 503922, 22pp

Styles, P., Stimpson, I. G., Toon, S., England, R., & Wright, M., 2005. Microseismic and Infrasound Monitoring of Low Frequency Noise and Vibrations from Windfarms: Recommendations on the Siting of Windfarms in the Vicinity of Eskdalemuir, Scotland. Report for MoD, DTi & BWEA.

Trodd, H., (1998) Variation in Amplitude of Seismic Noise at Eskdalemuir Array, AWE Internal Technical Note /97/DFS/AG/391 HT052.

**First International Meeting
on
Wind Turbine Noise: Perspectives for Control
Berlin 17th and 18th October 2005**

Wind turbine noise assessment in Australia and comparison of software model predictions for Australian conditions and wind farms

Colin Tickell,
Hatch,
PO Box 1237, North Sydney, NSW 2774, Australia
ctickell@hatch.com.au

Summary

Australia has had a rapid increase in the number of wind farms since 1999. Noise remains a major issue for the community and statutory authorities in considering the approval of new wind farms, yet there is no agreed approach to predicting the likely impact. Each State has its own guidelines for assessment and development of objectives and the approach is based on those for industrial developments. Prediction models used include ENM, as well as theoretical geometric spreading systems and specially developed wind turbine modeling software. Environmental authorities have requested validation of models for Australian conditions be developed, but most compliance assessments to date are based on receiver sound levels being less than objectives. As objectives are designed to be below most ambient sound levels, validation of model predictions has yet to be demonstrated. This paper presents a review of the current assessment and prediction process in Australia, and compares the results of different models for the same conditions. A revised prediction approach for ENM/Concawe type models is included. An alternative approach to assessing validation is recommended. Agreement on prediction and assessment methods are not as developed as they currently appear to be in Europe.

Introduction

Australia has a current installed capacity of wind power of 471 MW, with a further 5734 MW currently proposed [1] and probably more planned but not yet made public. Their development remains dependent to some extent on Government policy, with Commonwealth Government and State Governments requiring fixed percentages of power supplied to consumers to be from renewable sources. Technology development has also helped, and in 2004 a total of approximately 180 MW of wind power was installed. Wind farms are increasingly getting larger, with proposals having from 20 to over 100 wind turbines in some locations. Earlier installed wind farms were smaller, with typically 8 to 15 generators.

New proposals for industrial or community developments require an assessment of the environmental impact to be made to assist the public and decision-makers determine the suitability for the location of the development. This requirement applies to wind

farms and the impacts assessed range from visual and radio -transmission effects to bird strikes and of course, noise.

An earlier paper [2] considered the process for the noise assessment of wind farms in Australia, and presented the difference in predicted results from different prediction software models and approaches. That paper identified a significant difference between the results obtained with commonly used prediction models. The range in predicted sound levels from one wind turbine generator at 1000m was from 22 to 46 dB(A). Apart from the relevance to public confidence in wind farms being able to achieve predicted noise levels, and proponent concerns in achieving the committed or imposed objectives, it also has significance for their future development. For one described project of 38 wtg's, the difference predicted by different models, between the distances to the 35 dB(A) noise contour (commonly used as an objective for residential receivers), was 5km. The accuracy of the prediction scheme can determine the number of wtg's able to be placed in a locality, affecting their financial and environmental viability.

Subsequent to the previous analysis described above, the developer of the software giving the highest sound level has issued a technical note for modification of wind speeds used in the model [3]. This has brought the range of sound levels at 1000m, from the studied models, down by 11 dB – but the difference is still considered to be significant.

In Australia at present, there is also the difficulty of assessment of compliance. The approach to setting objectives seeks to have the contributed sound level below the background or ambient sound level. Compliance is often assessed only by measuring the sound levels at the nearest affected residences – if the wind farm cannot be heard, as would be expected or hoped for, then compliance is assumed. There are yet to be Projects with publicly documented performance measurements at distances where wtg's are still discernible, so that the prediction models used can be validated. There is of course the possibility that these measurements have been done but they are not yet in the public domain.

This paper will briefly describe the two main systems of assessment in Australia, and the types of prediction schemes used in EIS's. The results of different prediction models will be compared, including the modification to wind speed for Concawe based models. Finally, a recommended system for assessment of wind farm noise compliance is discussed. The objective of this is to give everyone – regulators, the community and the developers, a pathway to obtain greater confidence in the noise prediction of wind farms, and remove or reduce noise as an issue for community concern.

Assessment of Wind Farms in Australia

The Commonwealth of Australia is a federation of six States, with each State having regulatory power over environmental planning and setting quality objectives. Whilst there are attempts to have similar environmental quality objectives and approval systems through ministerial councils and National Environment Protection Measures, with noise, amongst others, there is still a difference in the way each State assesses and controls noise from wind farms.

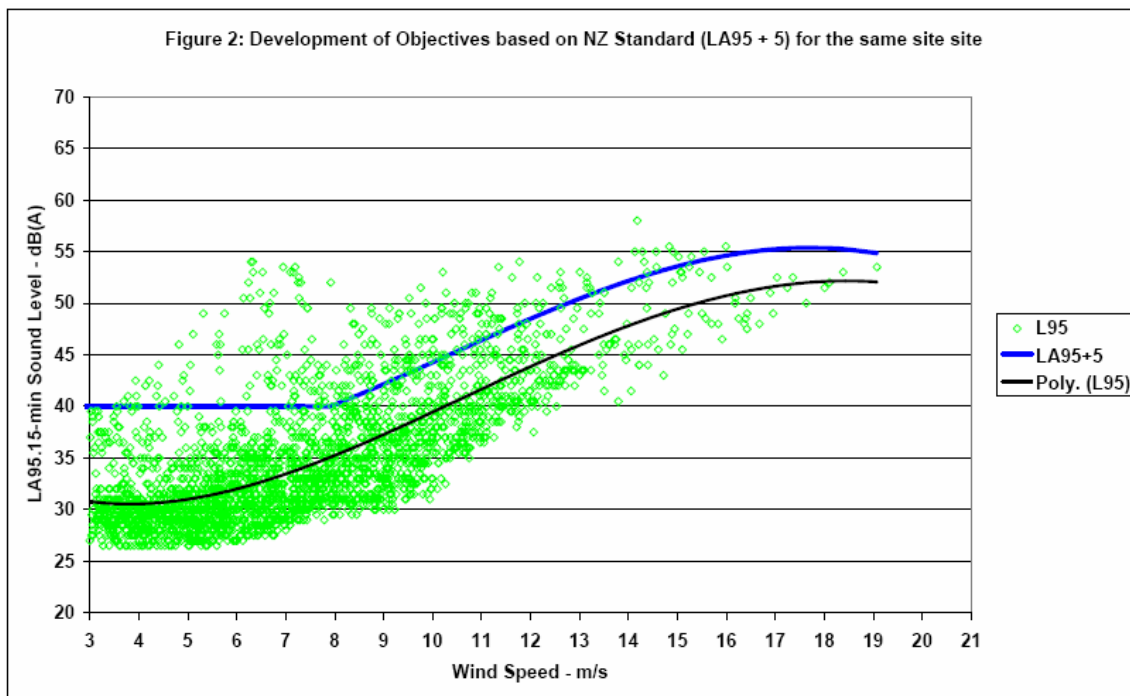
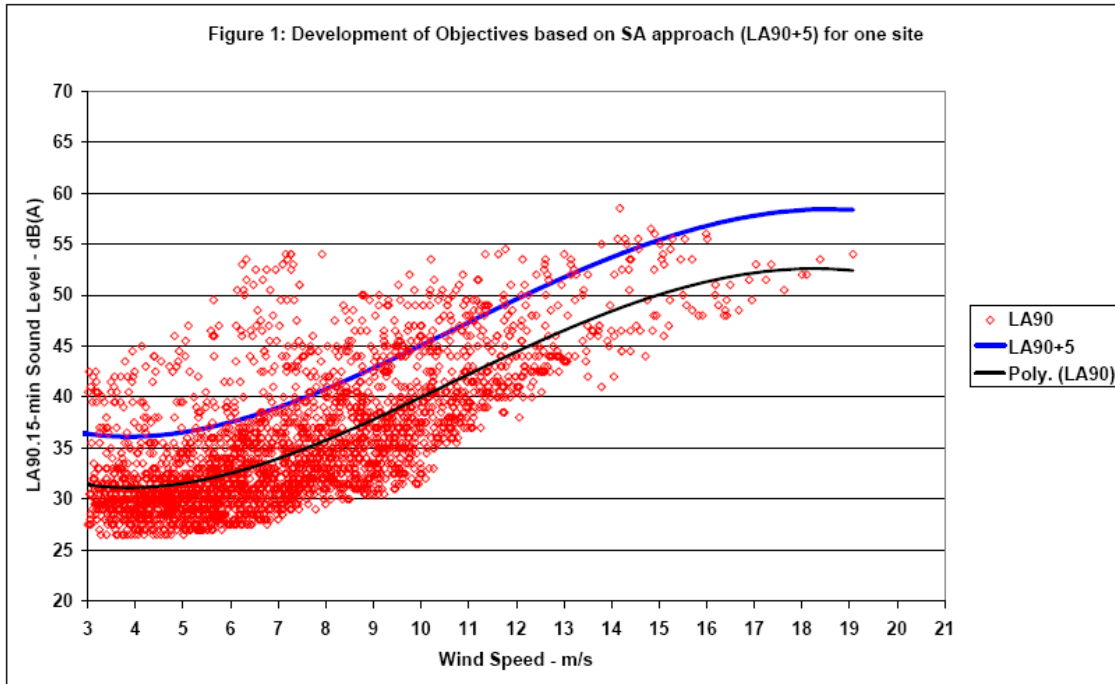
Wind farm locations are often in coastal or elevated rural locations because of both the wind resources and minimal environmental impact. As coastal, and rural living becomes more popular with those seeking a lifestyle alternative to urban life, there are chances that there can be opposition to wind farm development on environmental grounds. The most often discussed objections are visual aesthetics and noise, with others being bird strikes and radio interference.

In assessing new wind farm proposals, the proponent prepares an environmental impact statement (EIS), which is to include predictions of the expected sound level contribution from wind farms. There is no agreed method to determine the prediction; some States require the use of a conservative model while others allow any scheme to be used, with justification to be provided.

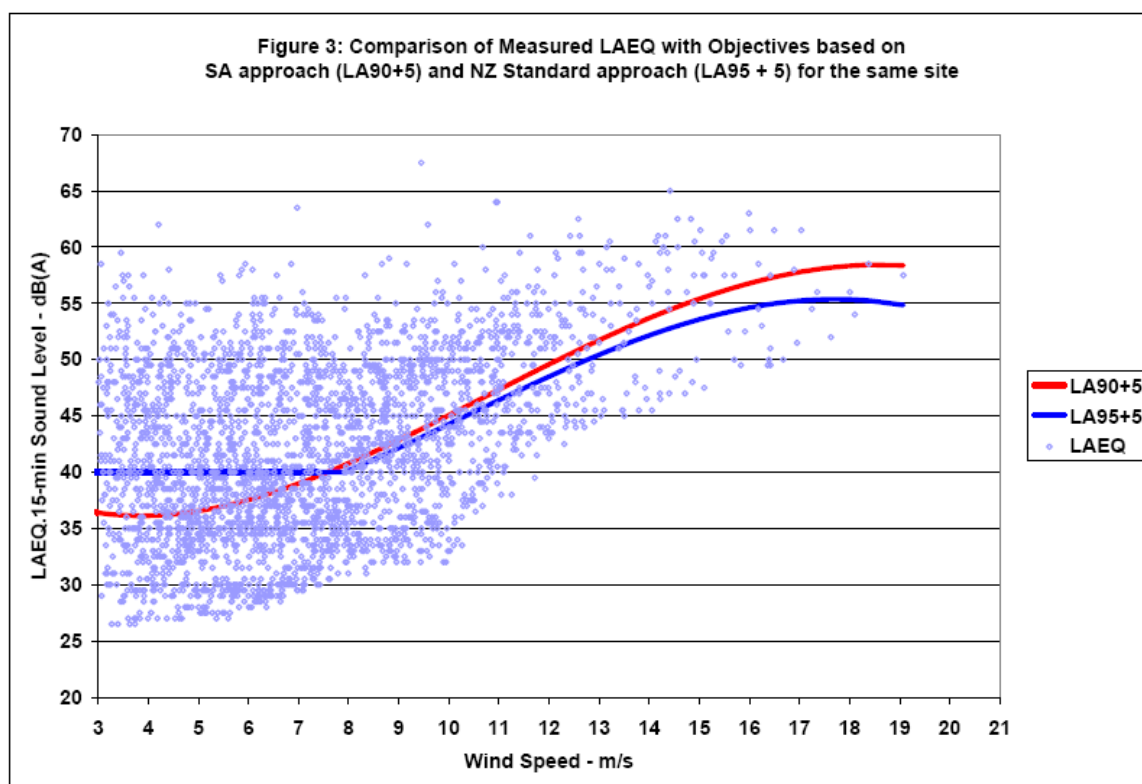
Some States (Victoria and Tasmania) use a system based on the New Zealand Standard NZS 6808 [4]. The prediction method of this Standard is considered by some to be a conservative approach, and considers only the attenuation caused by distance and air absorption. It ignores any additional attenuation from ground absorption or topographic shielding. The objective sound level for contributed noise from a wind farm is the background LA95.10min plus 5 dB at integer wind speeds or 40 dB(A), which ever is greater. In 2004, Tasmania also required assessment of contributed levels down to the 35 dB(A) contour. The LA95.10min is determined from a regression analysis of the sound levels measured at the receiver locations with the wind speeds at the wtg locations. The objective of this approach is to achieve an internal sound level of less than 30 to 35 dB(A). This approach is used in Victoria and Tasmania. One reviewer considers that this approach is no longer conservative because as the turbines have grown in size since 1998, their low frequency noise content is greater and the model under predicts the actual sound level [5]. Anecdotal evidence is that this approach has caused problems for some wind farms in not achieving the general objective of not causing an annoyance.

South Australia (SA) developed their own guidelines in 2003 [6], and these have also been adopted in New South Wales. They have objective sound levels of background LA90.10min plus 5 dB at integer wind speeds or 35 dB(A), which ever is the highest. No noise prediction method is specified and it is up to the proponent to determine what is used and advise on its accuracy. Figure 1 shows the SA 2003 Guidelines method to determine objectives for data from one site. This can be compared with Figure 2, which gives the NZ6808:1998 method used in Victoria, for the same site data.

Figure 3 shows the two objective curves for each system, with the background LAEQ data from the same site. This indicates that there are times when the background LAEQ sound level can be more than 10 dB below the Victorian limit sound levels at low wind speeds. Whilst there is also an exceedance for the SA conditions, it is 5 dB less than the Victorian limit would be.



Standards Australia published a draft Standard in March 2004, which has yet to be issued as a full Standard. Australian Standards in general, do not prescribe limits or prediction methods. They provide a framework to develop a method for measurement, prediction and assessment of noise from wtg's. The Standard appears to have been based on the New Zealand Standard, with some components of the SA guideline.



Environmental regulators around the country have commented on the need for a prediction model validated to Australian conditions. This information has been requested as a part of guidelines for preparation of some EIS's. Operators and industry have also agreed it would be helpful. Yet other than Victoria and Tasmania (using the potentially doubtful accuracy of the New Zealand Standard), none of the regulators are yet to advise on preferred calculation methods or the accuracy that they will allow in their assessments. As noted earlier, in 2004, Tasmania required that compliance assessment include measurements to demonstrate validation of the prediction model used [7].

Prediction Models Used

In recent EIS's for wind farm proposals in Australia, the types of models used have included *ENM*, *Windfarmer*, *Windpro*, the NZ Standard approach, *WiTuProp* and geometric spreading.

The NZ Standard, as does the draft Australian Standard, uses a simple algorithm:

$$L_R = L_w - 10\text{Log}(2\pi R^2) - \Delta L_a$$

Where:

L_R is the sound pressure level at a distance R

L_w is the sound power level (PWL) in dB(A)

ΔL_a is the attenuation caused by atmospheric absorption over distance R

Windfarmer is a proprietary software model which uses the above algorithm, with 2 dB per km as the attenuation rate ΔL_a . *Windpro* is another proprietary model. Geometric spreading is the above formula without the inclusion of the ΔL_a term.

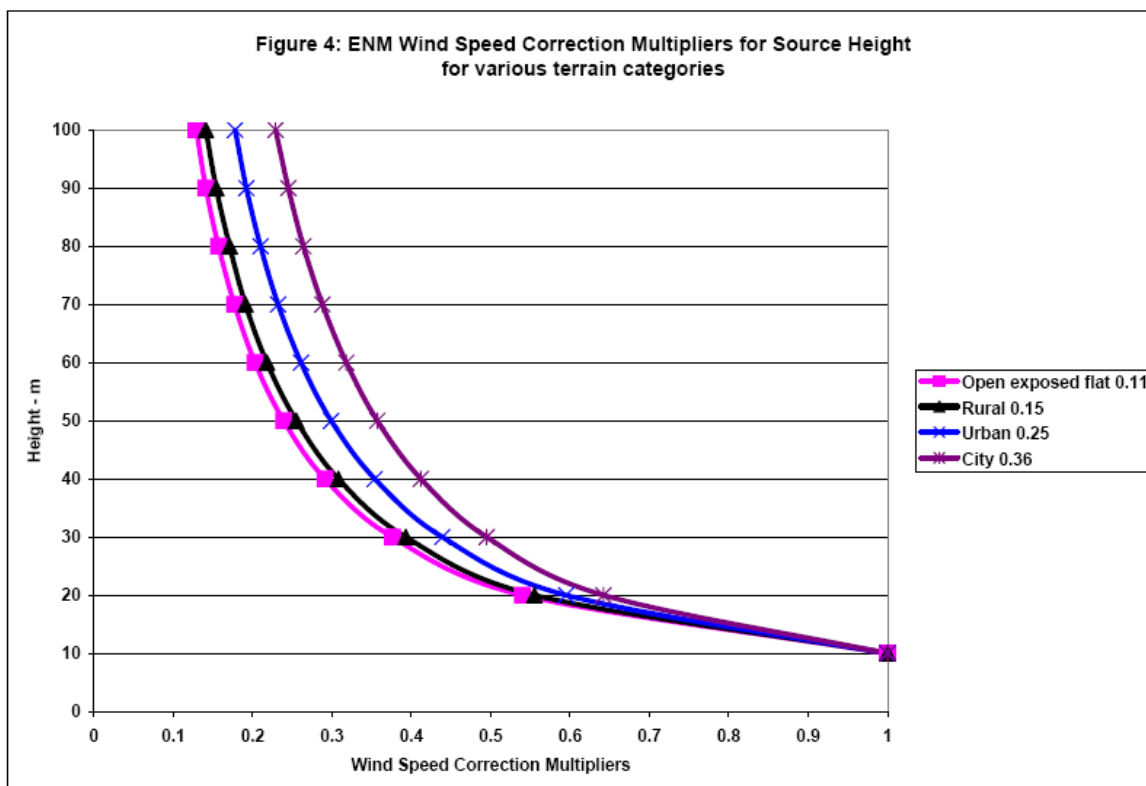
WiTuProp is a heuristic model, based on classical geometrical ray theory for a non-refractive atmosphere, modified for a refractive atmosphere. [8,9,10] (Heuristic models are a method of solving mathematical problems for which no algorithm exists, by narrowing down the field of search for a solution by inductive reasoning from past experience of similar problems). It was developed from a European Commission funded joint project, to investigate turbine measurement methods, the knowledge of noise propagation under different meteorological conditions, measurement of immission at dwellings and the assessment of possible tonal noise from machinery components. [11]. The study was a collaboration between nine European partners in six countries, which commenced in January 1997. The noise propagation model aspects of the study were undertaken by Delta Acoustics & Vibration, of Denmark. One of the outcomes of this project was the development and validation of a noise propagation model for wind turbines, known as *WiTuProp*. This algorithm was used by the author in a recent EIS. The difference between its predictions and those of other methods is one of the reasons for this paper. Australian environmental regulators have requested validation studies be presented for *WiTuProp* in Australian conditions. Data to enable this to be done has yet to be obtained.

ENM (for Environmental Noise Model) is an Australian developed model used for industrial noise sources. It was released in Australia by RTA Software in 1986 and was developed from a research grant by the Australian Environment Council, a joint body of State and Commonwealth Environment Ministers. At its release, it was adopted by all of the environmental regulators in Australia as the preferred model for assessment of industrial noise and has been used extensively by Government and industry. Its accuracy, limitations and assumptions for use are well understood. However its applicability to wind farms is yet to be assessed.

ENM predicts unusually high noise levels for wtg types of noise sources [2]. Because of this difference, RTA Software issued a technical note to recommend and correction to the wind speed used in the model [3]. The note describes how the ENM wind effect algorithm is based on measurements reported by Parkin and Scholes in 1964 and 1965, for a source height of 1.8m and wind speed measured at the standard meteorological height of 10m. As wind effects are related to wind gradient, and wind gradients are significantly lower at the 60 to 120m elevation of wtg noise sources than they are at ground level, it was not surprising that the ENM algorithms did not appropriately address the sound propagation of wtg's. For source heights of greater than 10m, a correction needed to be applied to the wind speed used in the ENM model. For example, for a source height of 100m, a 10m wind speed of 8m/s and an open exposed terrain category, the wind speed correction factor is 0.129, giving a modeling wind speed of 1.032m/s. The technical note explains how the correction factor is derived. Figure 4 shows the variation in wind speed gradients for elevation indicated from the correction to ENM.

The issue of the effects of wind speed gradient variation on prediction modeling and actual sound levels was also described by van den Berg in a study of noise issues for a German wind farm affecting Dutch residences [12]. The situation described in that paper, of relatively flat topography, does not occur for most wind farms in Australia, as they are typically located on the crests of hills or ridges, or on coastal bluffs. However,

inland wind farm locations could experience similar wind gradient variation because of both atmospheric stability in winter, and the land profile. This means that the uncertainties associated with wind speed gradient are likely to have a significant effect on predicted sound levels in Australia also, and need to be further investigated.

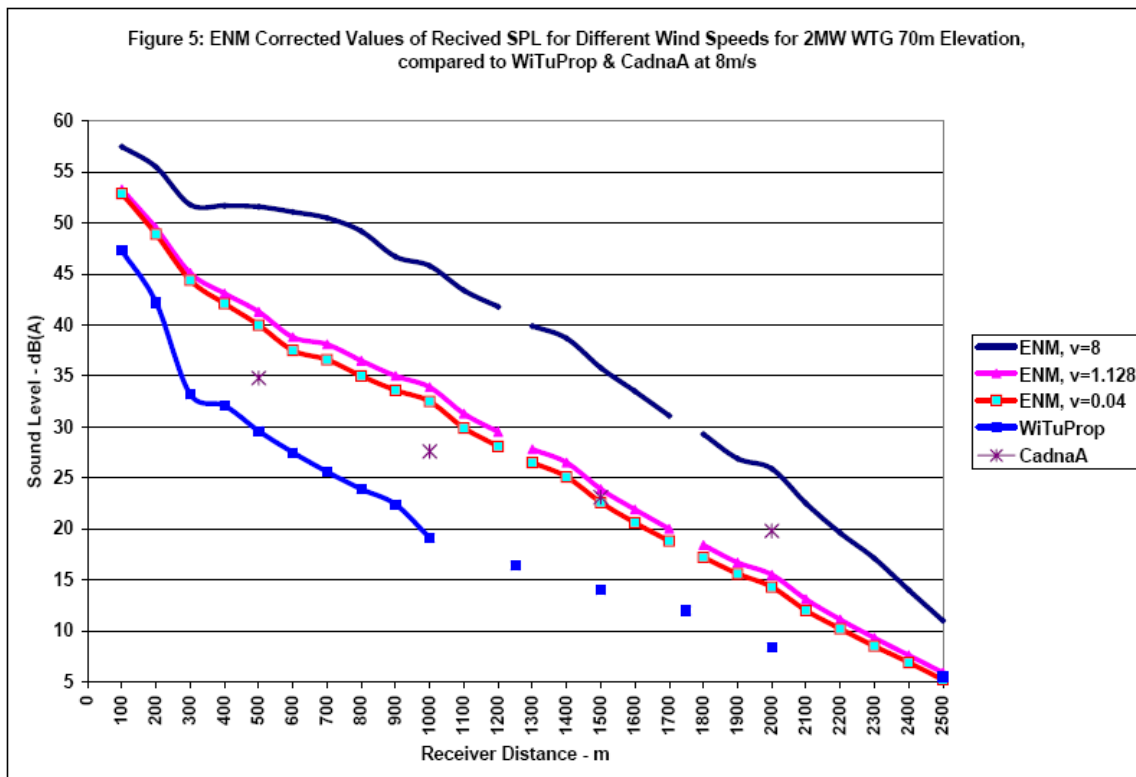


Comparison of Software Predictions with Corrected ENM

A comparison of prediction results for a 2MW turbine with a 70m hub height has already been given [2]. The models used were ENM, WiTuProp, CadnaA, NPL's web page "wind turbine noise model" and the NZ Standard. These results have now also been used to compare with the results using the corrected ENM approach.

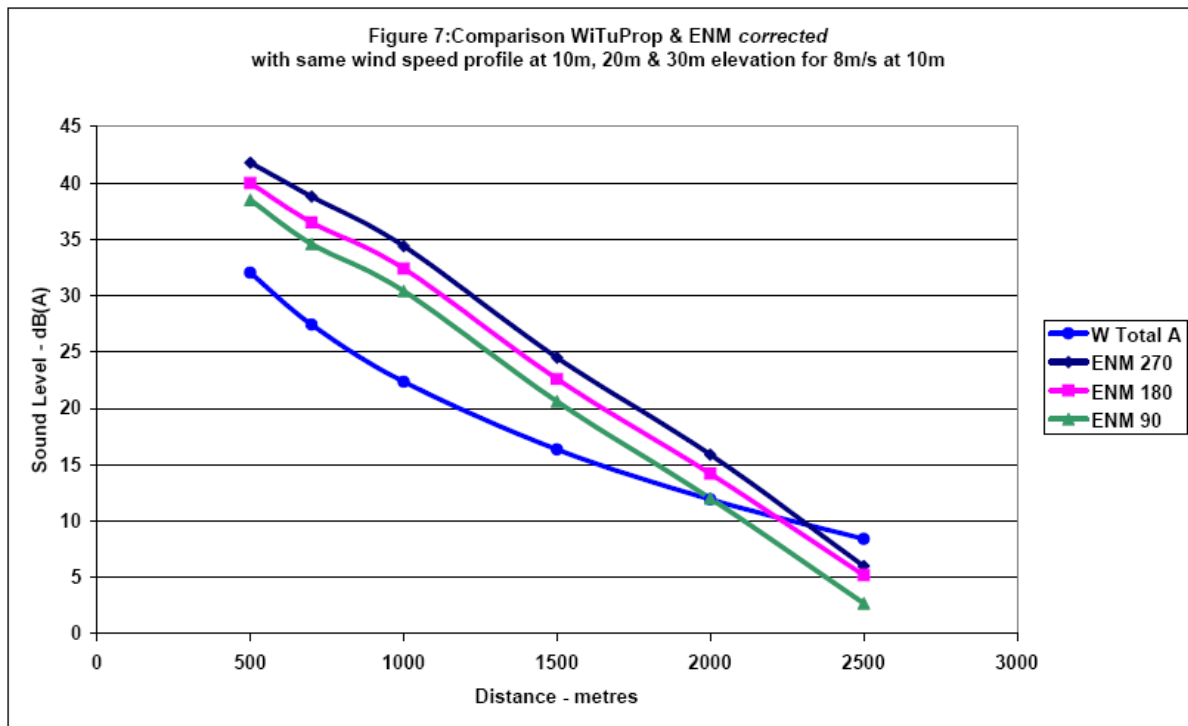
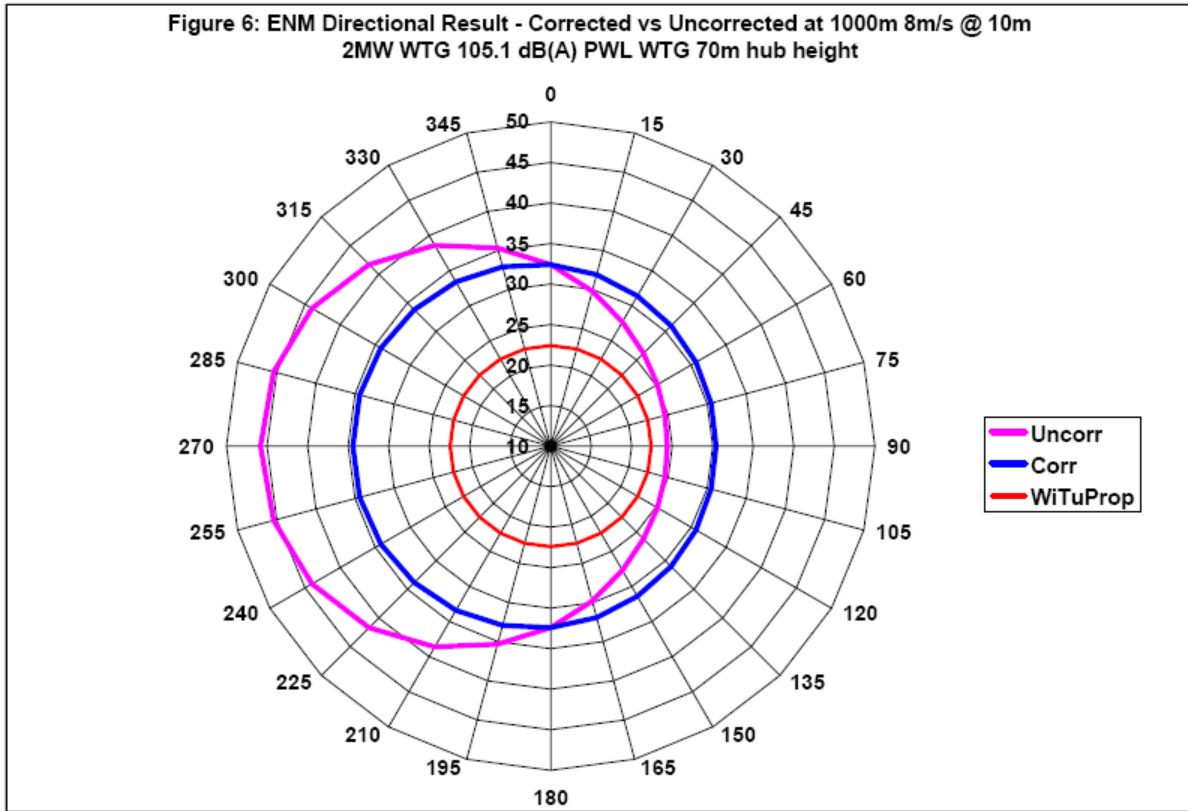
Scenarios used in the modeling are typical for worst case conditions in Australia – a high humidity, cold winter's day, with an air temperature 5° C and relative humidity of 95%. Lapse rate used was for a standard atmosphere, of -0.66 °C per 100m elevation. Whilst it is common to consider atmospheric inversions with positive lapse rates for industrial developments, these tend to only occur with calm or low wind speeds. For a WTG to operate at 8m/s wind speed, there is little chance of there being an inversion. However each model allows consideration of the effects of different lapse rates.

Figure 5 compares the results for receiver sound levels from one wtg of 105 dB PWL at distances from 500m to 2,500m. The height of the hub was set at 70m above ground and the rotor length was 30m. This is typical of a range of larger wtg's of 1 to 2 MW rated power, used in recently proposed and installed wind farms in Australia. Results are shown for ENM, WiTuProp and CadnaA.



The ENM Corrected results are lower than the original model for downwind propagation, have no change for across wind, and are higher for upwind propagation. Figure 6 shows the directional graph comparing ENM, ENM *Corrected*, and WiTuProp results. The comparison with WiTuProp is given because it provides the lowest calculated results of all the models used. The ENM *Corrected* model result is lower than the uncorrected – the 35 dB (A) sound level is achieved at 1000m with the corrected version, compared to 1600m for uncorrected, but it is still 15 dB higher than WiTuProp and 8 dB above the results with CadnaA at 1000m. ENM *Corrected* results become equal with WiTuProp at 2500m and start to become lower than CadnaA at 1500m. The directional graph of Figure 6 shows there is still a directional effect of about 5 dB difference between upwind and downwind propagation for ENM variants, whereas WiTuProp has not effective directional effect calculated.

The difference between the corrected ENM and WiTuProp may be related to wind speed gradient – WiTuProp assumes a linear sound speed gradient with a very small variation. Predictions were made for sound levels with increasing distances for one WTG, using the same meteorological and ground conditions, with the same wind speeds at 10, 20 and 30m elevation in both ENM and WiTuProp. Figure 7 compares the results, showing there is still a significant difference between the two sets of results from each model.



Use of WiTuProp in Australia at present is limited because of the much lower results it provides. Conservative consultants and developers see it as a risk to their proposals until it has been validated.

Assessment of Compliance Procedures

Current compliance assessment requirements are to measure the sound level at the nearest receivers under a typical range of operating conditions for the wind farm. As the design objective is to be less than the ambient sound level in most wind speeds and make the wind farm inaudible, if the predictions are conservative or reasonably accurate, the wind farm will not be discernible. This means compliance will be assessed by being unable to measure wind farm noise - this provides no real assessment of compliance, unless the period of assessment is long enough to encompass the full range of conditions expected. It also provides no real assessment of the accuracy of the predictions made. Measurement also allows the use of normal microphone wind screens, which can add their own noise at microphone wind speeds above 5m/s. Tasmania is the only State requiring compliance assessment reporting to include a validation of the model predictions made in the EIS [11].

A common approach to noise compliance assessment of industrial projects in Australia is to demonstrate it by either measurement or calculation or a combination of the two. Where objectives/limits are to be less than the ambient in most cases, then the calculation part comes from measurement at a shorter distance and calculation at the receiver distance. It is considered that this approach should also apply to wind farms, along with improved performance wind-screens.

Sound levels should be measured at increasing distances from 200m to possibly 1000m, with sound levels correlated to the wind speeds at hub height. The measured sound levels should then be compared with calculated sound levels at the same distances for the same meteorological conditions. One-third octave band spectral analysis should also be included at each location at the same wind speeds to determine if tonality occurs. The measurement data should then be presented in publicly available compliance reports, as is required for other industrial installations. Independent validation of models could then occur.

Conclusions

Assessment of noise immission of proposed wind farms in Australia depends on the approach taken in individual States. Two main methods apply, one questionably conservative and the other allowing any prediction scheme. Assessment of compliance to date has been to measure at receiver locations and there has been no reported validation of prediction models used. This shortcoming is likely to be overcome as more wind farms come on-line and measured data becomes available.

Software models used have a wide variation in predicted results, leading to a greater uncertainty for the public in knowing whether objectives will be achieved, and greater risk for developers for the same reason.

Comparison of the results obtained with ENM, a Concawe based model used extensively in Australia for industrial noise assessment, and other industrial noise and wind turbine noise models shows a variation of up to 14 dB at 500m and 15 dB at 1000m. This difference can affect the number of wtg's that can be placed into a locality with close residences. Until all models can be validated with publicly available information, confidence in using models that provide a low sound level result remains

low, whether or not they are accurate. The uncertainties in this whole approach indicates that Australia still has some way to go to approach Europe in the confidence of wtg predictions.

Validation of model predictions with operating wind farms is a necessary part of improving community confidence wind farm developments. This is starting to occur in some locations, but there is still the likelihood that it won't be done in some jurisdictions because of the added cost and it is not required. Only regulatory requirements forcing validation of prediction is likely to produce sufficient information to allow uncertainties to be identified. Operating measurement data should be publicly available on the public record. Industry may choose to sponsor more validation studies, to improve community confidence in the models used.

References

- 1 Australian Wind Energy Association, "Existing Projects" web page, 29 July 2005, www.auswea.com.au/auswea/projects
- 2 Tickell, C.E., Ellis, J.T., & Bastach, M. "Wind Turbine Generator noise prediction – comparison of computer models", presented at Acoustics 2004, 3-5 November 2004, Gold Coast, Australia.
- 3 RTA Technology Pty Ltd, "ENM wind speed correction for elevated sources", 24 November 2004, www.rtagroup.com.au
- 4 New Zealand Standard Association, New Zealand Standard NZS 6808:1998 Acoustics – The assessment and measurement of sound from wind turbine generators", 1998.
- 5 Fearnside, P., "Wind farm noise in Australia", presented at Auswind 2004.
- 6 Environment Protection Authority – South Australia "Environmental Noise Guidelines – Wind Farms", ISBN 1 876562 43 9, February 2003.
- 7 Environment Division, DPIWE, Tasmania "Wind Energy Projects in Tasmania – Key Issues and Requirements", July 2004.
- 8 Kragh, J., et al, National Engineering Laboratory, "Noise immission from wind turbines", ETSU W/13/00503/REP, 10 February, 1999
- 9 Kragh, J. & Plovsing, B. (Delta Acoustics & Vibration) "Wind Turbine Noise Propagation Model EU Commission DGXII" Report AV 1119/98, Delta Acoustics, 6 March 1998.
- 10 L'Esperance, A. et al, "Heuristic model for outdoor sound propagation based on an extension of the geometrical ray theory in the case of linear sound speed profile" Applied Acoustics, 37, No.2, p. 111 – 139, 1992.
- 11 National Engineering Laboratory for the Energy Technology Support Unit "Noise immission from wind turbines" ETSU W/13/0053/REP, Department of Trade and Industry, 10/2/1999
- 12 Van den Berg, G.P., Effects of the wind profile at night on wind turbine sound", Journal of Sound & Vibration, Vol 277, p955-970, Elsevier

**First International Meeting
on
Wind Turbine Noise: Perspectives for Control
Berlin 17th and 18th October 2005**

CFD-CAA Study Of Generic Savonius Wind Turbine Rotor

Serguei Timouchev

irico@mail.cnt.ru

Laboratory of Numerical Modelling SRCNT MAI

www.lnm.ru

Summary

The acoustic-vortex method developed initially for prediction of pressure pulsations and noise in pumps and ventilators is applied for the problem of noise assessing from a generic wind turbine Savonius rotor. 3D CFD-CAA prediction of the BPF tonal noise is made in a computational domain of $160 \times 160 \times 160$ m size around the rotor.

Introduction

Wind turbines with Savonius rotor are spreading widely due to simplicity of design, reliability and easier installation. Usually the Savonius turbine is applied for small energy consumptions and it is a quieter machine comparing with the common industrial wind turbines with the horizontal-axis rotor. Anyway it will be useful to have a possibility to assess the noise level of a Savonius rotor wind turbine as these machines are built closer to residential areas. The infrasound produced by blade passing can be dangerous for the human health.

Obviously the main source of aerodynamic noise in Savonius rotor is blade-passing perturbations of flow spreading on Blade Passing Frequency (BPF) tones.

$$f_b = 2kf_r,$$

where

f_r – Rotor frequency, Hz;

k – Harmonic number.

The acoustic-vortex method elaborated for pumps and ventilators can be applied in this task as well.

Generally experimental tuning works accompanying by big material expenses resolve the vibration and noise problem of bladed machines.

In the last decade papers are published giving pressure pulsations analysis on the base of solution of unsteady hydrodynamics' equations [1]. Another approach is

proposed in works where the unsteady pressure is defined by integration of Reynolds equations while the non-stationary velocity field is obtained by laser anemometry method. [2, 3]. There are methods proposed comprising solution of Navie-Stocks equations with integral methods of the wave equation solution for the far field noise [4, 5].

The acoustic-vortex method [6-15] of pressure pulsation modelling is developed by a natural transformation of Navier-Stocks equations for the compressible fluid.

Governing acoustic – vortex equation

In development of the Savonius rotor pulsating flow numerical model one have to account the non-linear character of the generation process of oscillations and acoustical nature of its spreading in the ambient air.

Let us make the following assumptions:

- Subsonic flow;
- Isoentropic flow;
- Viscous diffusion is neglected;
- Acoustic oscillations (velocities of acoustic motion due to the fluid compressibility) are small in comparison with the vortex perturbations (velocities of swirl and translation motion of the absolutely incompressible fluid).

In the isentropic flow the following relations take place between enthalpy, pressure and density gradients (a – speed of sound)

$$di = \frac{dP}{\rho}, dP = a^2 d\rho, \quad (1)$$

With relations (1) the main Euler equations can be written as following

$$\frac{\partial \mathbf{V}}{\partial t} + \nabla \frac{V^2}{2} - \nabla \times (\nabla \times \mathbf{V}) = -\nabla i, \quad (2)$$

$$\frac{1}{a^2} \left(\frac{\partial i}{\partial t} + (\nabla i) \mathbf{V} \right) + \nabla \mathbf{V} = 0. \quad (3)$$

For the fluid velocity, splitting the motion on the vortex and acoustic mode one obtains the following expression (φ - acoustic potential, \mathbf{U} – the vortex mode velocity):

$$\mathbf{V} = \mathbf{U} + \nabla \varphi = \mathbf{U} + \mathbf{V}_a. \quad (4)$$

Introducing dimensionless variables using as scaling factors the rotor tip radius R , circumferential tip velocity u and time period of blade passage

$$\tilde{\mathbf{r}} = \frac{\mathbf{r}}{R}; \tilde{\mathbf{U}} = \frac{\mathbf{U}}{u}; \tau = \frac{t}{(\pi R)/(u)}; \tilde{i} = \frac{i}{u^2}, \quad (5)$$

From the main equations (2, 3) of compressible fluid after a set of transformations one obtains the acoustic-vortex equation

$$\Lambda^2 \frac{\partial^2 h}{\partial \tau^2} - \tilde{\Delta} h = -\tilde{\Delta} g \quad (6)$$

The dimensionless similarity criteria of this problem is the ratio of rotor tip radius to the main BPF tone wave length

$$\Lambda = \frac{R}{\lambda} \quad (7)$$

The amplitude of pressure pulsations by an order of magnitude is less than the mean undisturbed pressure; thus one can write for oscillations of specific enthalpy

$$h = \tilde{i} - \tilde{i}_0 \approx \frac{(P - P_0)}{\rho_0 u^2} = \frac{P'}{\rho_0 u^2} \quad (8)$$

Oscillations of pressure in the working fluid equal to the sum of perturbations due to the vortex motion of the incompressible fluid – "pseudo-sound" and acoustic waves.

Here P – pressure in the compressible fluid, i_0 , P_0 , ρ_0 – mean enthalpy, pressure and density. Function g corresponds to the pseudo-sound pressure pulsations ($P_v - P_0$) of the vortex mode

$$g \approx \frac{(P_v - P_0)}{\rho_0 u^2} = \frac{P'_v}{\rho_0 u^2} \quad (9)$$

The right-hand side in the wave equation (6) is determined from the solution of vortex mode equations – equations of the incompressible fluid, which gives

$$-\Delta P_v = \nabla \left[\nabla \left(\frac{U^2}{2} \right) - \nabla \times (\nabla \times \mathbf{U}) \right] \quad (10)$$

Using the local complex specific impedance Z_k , the boundary condition for the acoustic mode can be written by the following relation

$$\frac{\partial (h_k - g_k)}{\partial n} = -\frac{\Lambda k}{Z_k} \frac{\partial (h_k - g_k)}{\partial \tau} \quad (11)$$

where k – BPF harmonic number, n – normal to the boundary surface.

The incompressible liquid flow analysis bases on Navier-Stokes equations

$$\frac{\partial \mathbf{U}}{\partial t} + \nabla(\mathbf{U} \otimes \mathbf{U}) = -\frac{\nabla P_v}{\rho_0} + \frac{1}{\rho_0} \nabla((\mu + \mu_t)(\nabla \mathbf{U} + (\nabla \mathbf{U})^T)) + \mathbf{F} \quad (12)$$

with taking into account the continuity equation for incompressible liquid $\nabla \cdot \mathbf{U} = 0$.

The well-known $K - \varepsilon$ model of turbulence is used to determine the turbulent viscosity

$$\mu_t = 0.09 \cdot \rho \cdot \frac{K^2}{\varepsilon} \quad (13)$$

Initial values of kinetic energy K and dissipation rate ε are calculated automatically during the first iteration.

Numerical procedure

The Savonius rotor is placed near the ground level in the infinite space. It has 1 m radius and 4.03 m height. The blade tip diameter is 1.86 m. The axis diameter is 0.3 m.

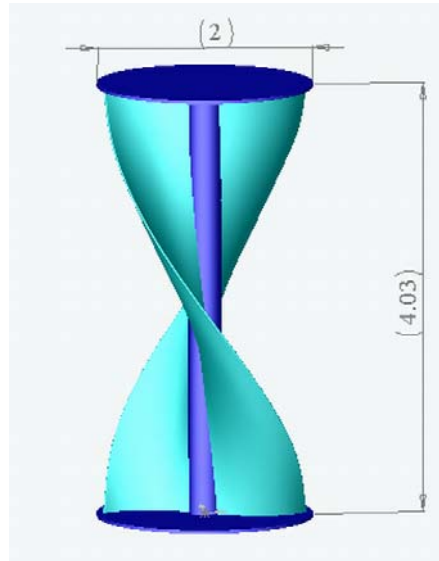


Fig. 1: Savonius rotor dimensions [m]

The computational domain is shown in Fig. 2. The domain is a cub of $160 \times 160 \times 160$ m size. It is divided on two sub-domains. The ambient air sub-domain is bounded by inlet section, where the normal wind velocity of 10 m/s is defined, outlet section, ground level, and side boundaries where the flow-symmetry condition is applied (zero flow gradients) The rotor sub-domain is connected to the ambient air sub-domain through the “sliding-grid” interface. In the rotor sub-domain the computations goes in the relative frame, where in the equations (12) the term \mathbf{F} is non-zero and represents Coriolis and centrifugal inertia forces. The rotation speed is taken by 60 RPM. In solution of the wave equation (6) the combined local impedance boundary condition (11) is applied on the sliding-grid surface. On the ground the impedance equals to infinity. It assumes pseudo-sound perturbations equal zero far from the rotor. On side and top boundaries the specific impedance equals to unity.

On the rotor walls and on the ground, the logarithmic velocity profile is applied as a turbulent flow boundary condition. At the outlet boundary the free-outlet flow condition is applied with linear extrapolation of velocities from the inner nodes.

The numerical procedure is based on the non-staggered Cartesian grid with adaptive local refinement and accurate resolution of curvilinear boundaries, like blade surface, by using polyhedron cells. The initial “parent” rectangular cell intersected by a curvilinear surface is disjoined onto new polyhedron cells formed by the facet of blade surface and the original cell faces.

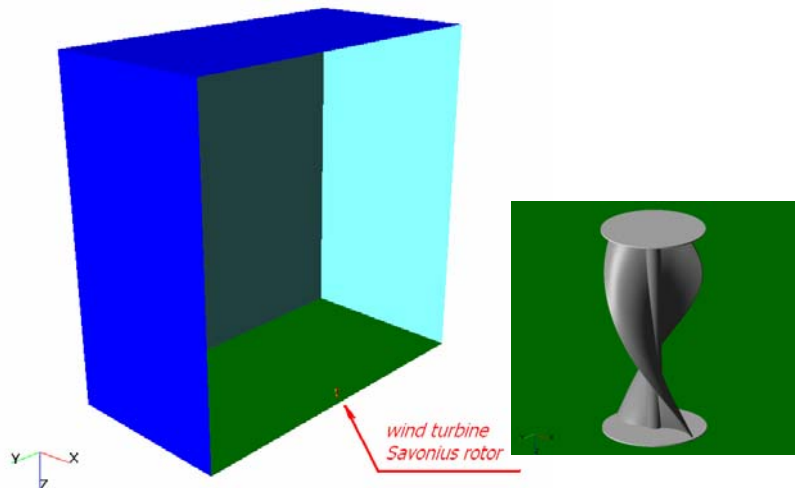


Fig. 2: Computational domain

An adaptive locally refined rectangular grid is introduced in the computational domain. The grid of the first level is an ordinary structured grid. A cell of the grid subdivides (when adaptation occurs) by eight cells of a higher-level grid and these cells subdivide in the next level of adaptation (see Fig. 2). In Fig. 3 a red colour circle marks the sliding surface that is the boundary of the rotor sub-domain. Splitting method with the implicit algorithm and high-order numerical scheme for convective transfer terms solves Navier-Stokes equations. The advantage of the method is that it is possible to reduce processing time by making computation on a rough grid, refining the grid when approaching to the convergent oscillatory solution.

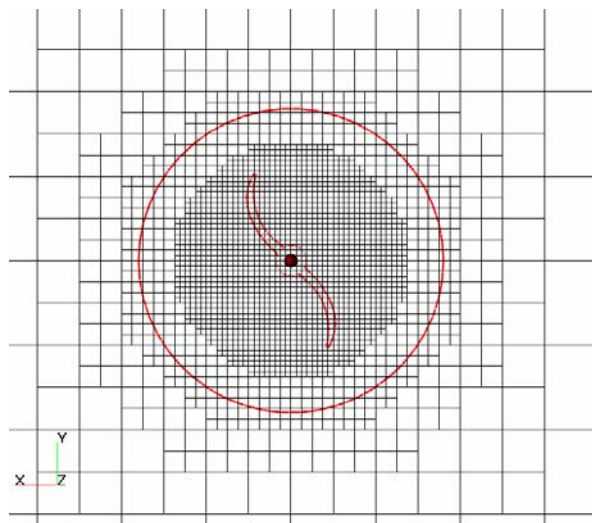


Fig. 3: Computation l grid fragment around the rotor (8^{th} adaptation level)

Iterative procedure goes up to convergence to a periodical solution and subsequent definition of the source function in the wave equation (6). Initial condition of the vortex mode flow is zero pressure and velocity in the entire computational domain.

Finally wave equation is solved in relation to pressure oscillation using an explicit numerical procedure in the ambient air sub-domain. Zero pulsatory pressure is an initial condition for solution of the wave equation.

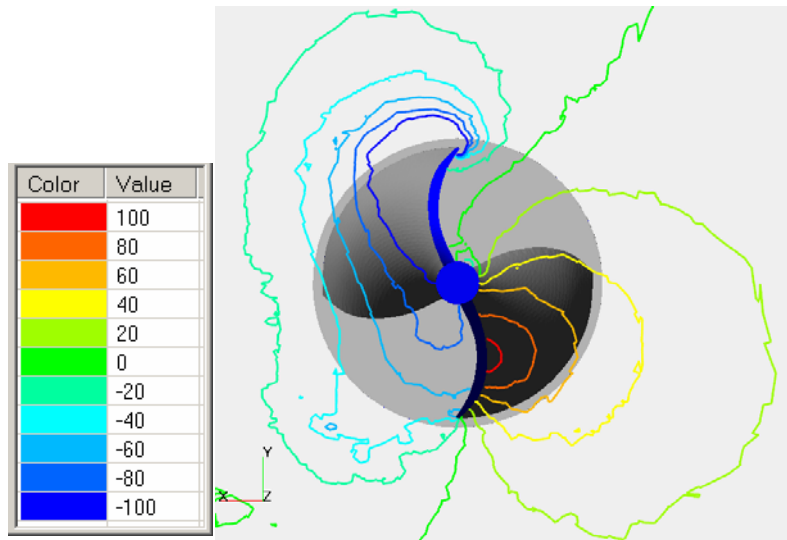


Fig. 4: Instantaneous pressure field [Pa]

Computational Results

In the computational procedure first step the unsteady oscillatory flow parameters are obtained. In Fig. 4 and Fig. 5 are presented instantaneous pressure and velocity fields near the Savonius rotor.

The wind blows in the X-direction, from the right to the left on the pictures. One can see the flow characteristic feature is a stagnation zone on the suction side of the blade going to the upstream direction and higher velocities and lower pressure on the suction side of the blade going to the downstream direction. Besides there is a rise of relative velocity (Fig. 6) on the pressure side of the blade going to the upstream direction that gives an increase of pressure in this zone.

All above-mentioned features of the flow give an unsteady BPF-type behaviour of pressure around the rotor resulting in generation of the acoustic waves.

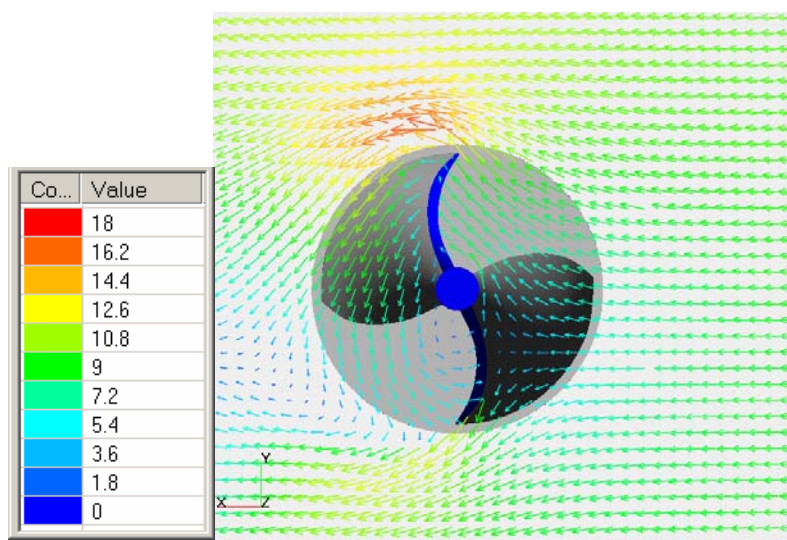


Fig. 5: Instantaneous absolute velocity vectors [m/s]

Unsteady flow parameters are used to calculate the source function of the wave equation (6). During one main BPF period that equals half a second, ten BPF harmonics of source function in the ambient-air sub-domain are written in the disk memory. On the second step of the wave equation solution this data is used to

compute BPF pressure pulsations comprising pseudo-sound and acoustical oscillations.

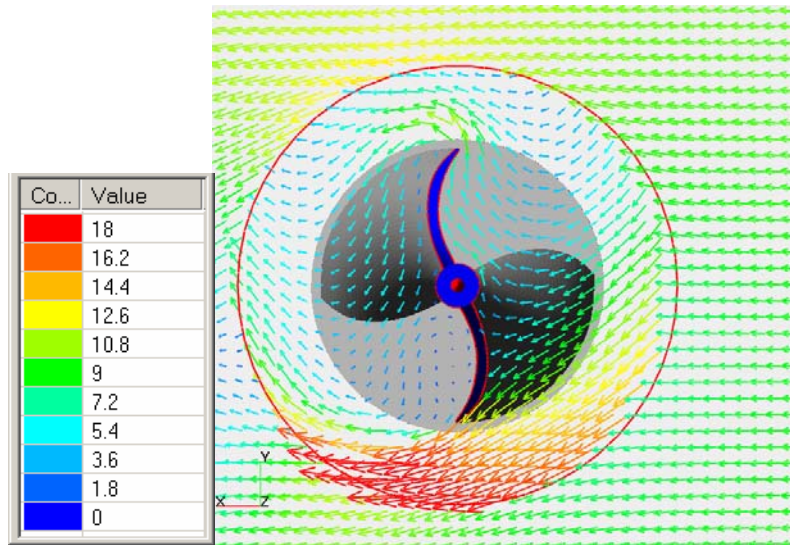


Fig. 6: Instantaneous relative velocity vectors in the rotor sub-domain [m/s]

Instantaneous configuration of the source field is presented in Fig. 7. It is shown by two equiscalar-surfaces $+30 \text{ s}^{-2}$ (red) and -30 s^{-2} (blue). One can imagine that rotation and pulsation (by change of the volume and shape) of this source zone gives the pressure pulsation field.

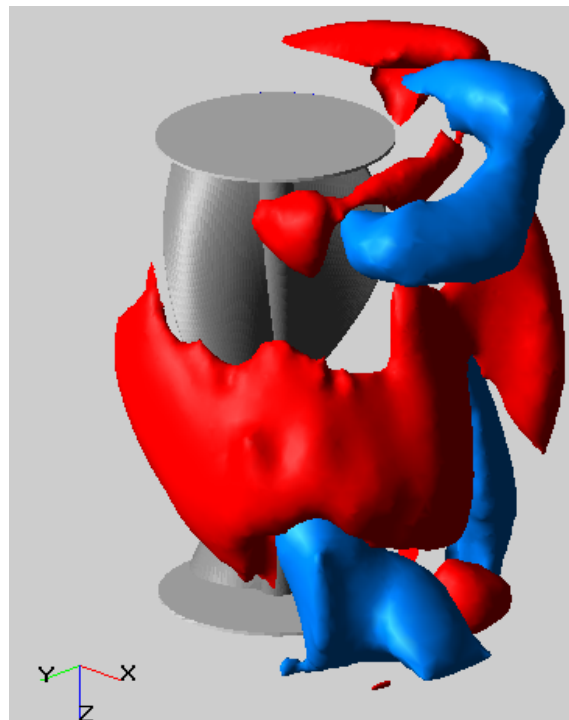


Fig. 7: Instantaneous source function by equiscalar surfaces $\pm 30 [\text{s}^{-2}]$

Configuration of the entire pressure pulsation field is presented by an instantaneous distribution in three planes in Fig. 8. This is the pressure reduced by the factor $\rho(2 \cdot \pi \cdot f_r \cdot R)^2 = 47.77 \text{ Pa}$.

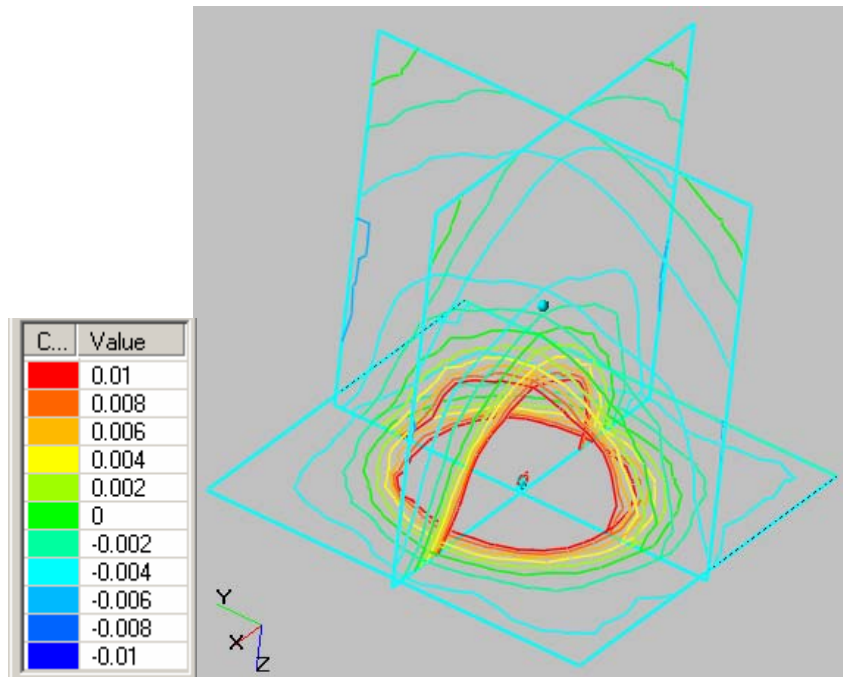


Fig. 8: Configuration of the pressure pulsation field

Spherical shape of the wave - front appears at 25 – 40 m distance from the rotor. The structure of the oscillatory field near the rotor is more complex depending on the pseudo-sound perturbations. In Fig. 9 there is presented the instantaneous distribution of pressure in the distance of 10 m from the rotor.

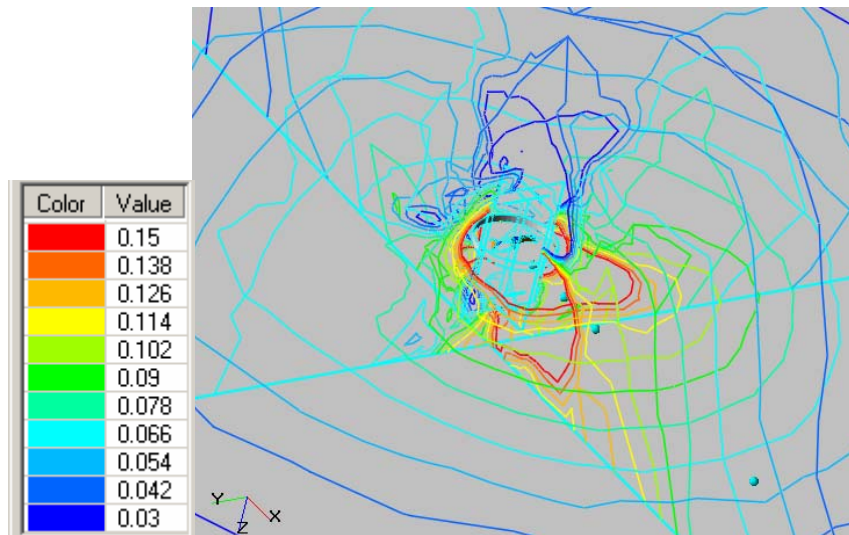


Fig. 9: Configuration of the pressure pulsation field in the 10 m radius

To describe the change of the amplitude of pressure pulsations the plots of the first BPF harmonic amplitude are built along the lines LX and LZ shown in Fig. 10.

Besides the spectrum of pressure pulsation signal is determined in the point P7 (see Fig. 10) located by 25 m from the rotor. The spectrum outlined in Fig. 12 shows the main BPF

tone prevails in the signal by an order of magnitude over higher BPF harmonics. The level of amplitude is 92dB.

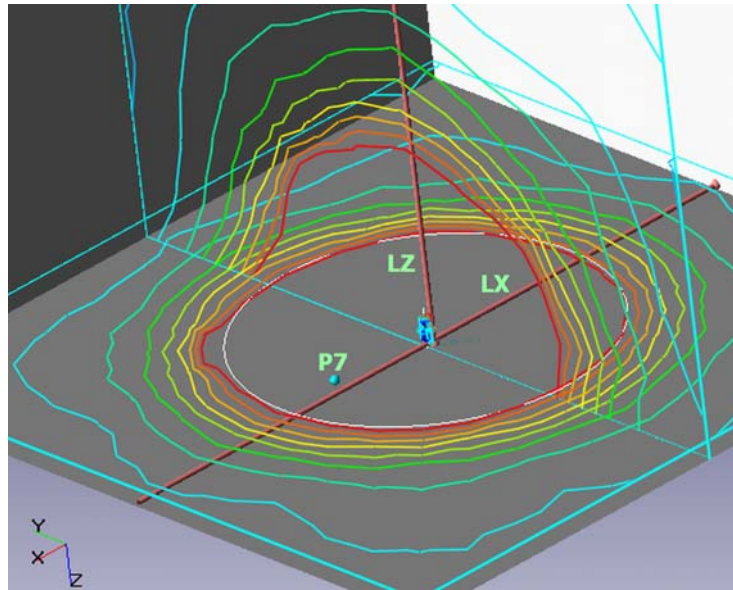


Fig. 10: Location of plot lines and P7-probe point

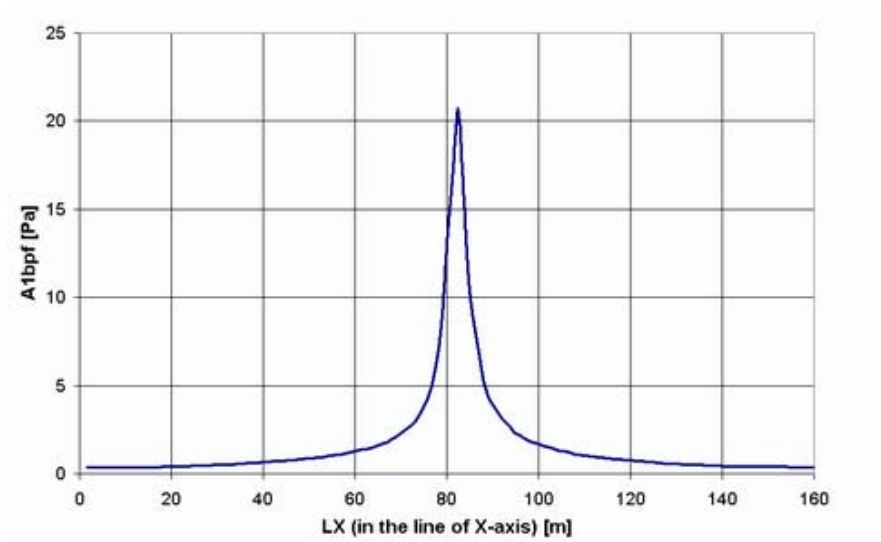


Fig. 11: Distribution of the first BPF harmonic amplitude downwind

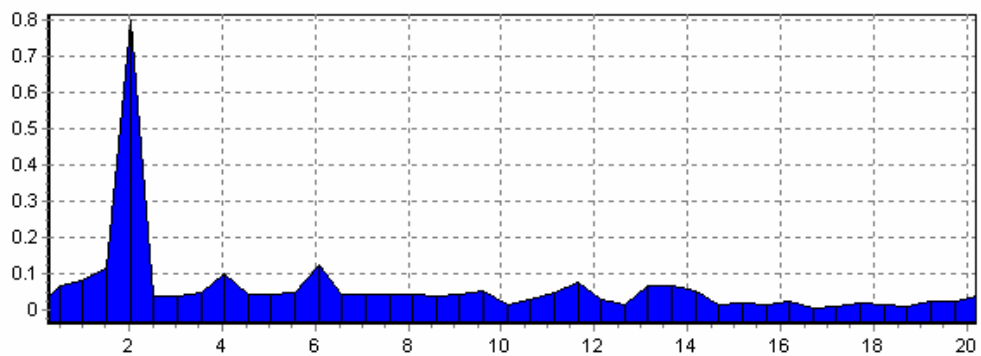


Fig. 12: Spectrum of pressure pulsation in P7 [Pa] Vs [Hz]

One can see in Fig. 11 and Fig. 13 that the amplitude of pressure pulsations attenuates very rapidly in a pseudo-sound zone of about 30 m distance from the rotor.

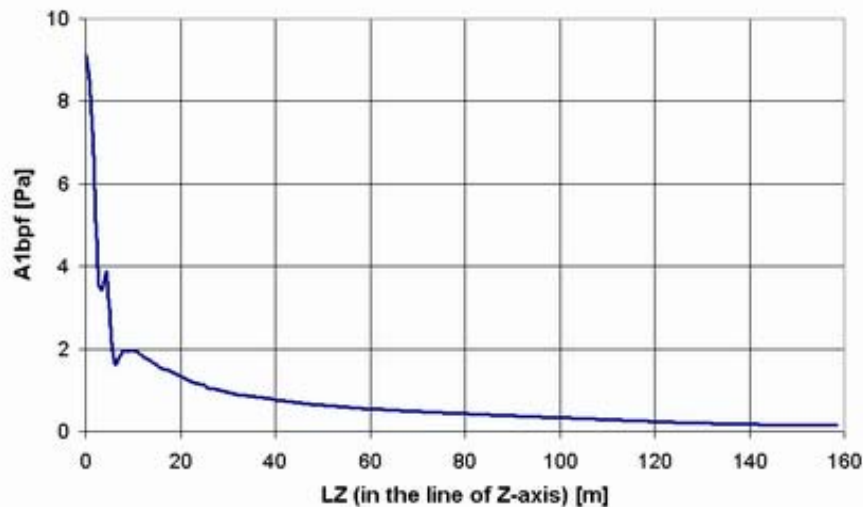


Fig. 13: Distribution of the first BPF harmonic amplitude upward

In a higher distance the amplitude change is close to the L^{-1} -law that corresponds to the acoustical part of the pressure pulsation field.

Conclusions

It is shown that the non-uniformity of flow produced by Savonius turbine blades generates BPF pressure pulsations. The sound near-field configuration comprise two distinct zones – pseudo-sound zone with a rapid attenuation of the BPF amplitude and zone of acoustic wave with L^{-1} -law of the BPF amplitude change. For the Savonius rotor studied, on the boundary between these zones (25 – 30 m from the rotor) the computed main BPF tone level is 92 dB.

References

1. D. Croba, J.L. Kueny. *Unsteady flow computation in a centrifugal pump coupling of the impeller and the volute*. Fan Noise. An International INCE Symposium. Senlis (France). Proceedings, **1992** pp.221 – 228
2. S. Chu, R. Dong, J. Katz. *The effect of blade-tongue interactions on the flow structure, pressure fluctuations and noise within a centrifugal pump*. Pump noise and vibrations. 1st International Symposium, Clamart (France), **1993** pp. 13 – 34
3. M.C. Thompson, K. Hourigan, A.N. Stokes. *Prediction of the noise generation in a centrifugal fan by solution of the acoustic wave equation*. Fan Noise. An International INCE Symposium. Senlis (France). Proceedings, **1992** pp. 197 – 204
4. E. Manoha, S. Redonnet, C. Delahay, P. Segaut, I. Mary, S. Ben Khelil, P. Guillen *Numerical prediction of the unsteady flow and radiated noise from a 3D lifting airfoil*. Colloque: Bruit des Ventilateurs à Basse Vitesse, l'Ecole Centrale de Lyon, 8 et 9 novembre, **2001**, Collection of papers
5. F. Perie, J. Buell *Combined CFD/CAA method for centrifugal fan simulation*. 29th international congress on noise control engineering, InterNoise 2000, Nice (France), Proceedings, **2000**, v. 1, p.641

6. Тимушев С.Ф., Овсянников Б.В. Конечно-разностный метод расчета пульсаций давления на лопаточных частотах в спиральном отводе центробежного насоса. В кн.: Рабочие процессы в узлах и агрегатах двигателей летательных аппаратов./ Сб. трудов МАИ (каф.202), **1987**.
7. Timushev, S.F., Ovsyannikov, B.V. *Pressure Fluctuation Numerical Simulation In A Centrifugal Pump Volute Casing*. Journal de Physique IV, vol. 2. Second French Conference on Acoustics. Arcachon (France), **1992**
8. Timouchev, S.F, Illichov, K.P. *2D Numerical Simulation Of Unsteady Pressure Field In Centrifugal Pumps*. Euro-Noise'95. An International INCE Symposium. Lyon (France). Proceedings, vol. 3, **1995**.
9. S. Timouchev. *Numerical Modeling Of Non-Stationary Hydrodynamic Processes In Centrifugal Pumps And Ventilators*. Harmony, Part I. CETIM, **1998**
10. Serguei Timouchev, Kirill Illichov, Jean Tourret *Prediction Of BPF Pressure Pulsation In Centrifugal Pumps And Ventilators With Taking Into Account The Effect Of Machine Casing On Impeller Flow Parameters*. 164 colloque SHF, Chatou, France, 21-22 November **2000**, Published in: La Houille Blanche, No. 3/4-2001, pp.60-64.
11. S. Timouchev, J. Tourret *Prediction of BPF Pressure Pulsation Field In Centrifugal Pumps And Ventilators*. 4th European Conference on Turbomachinery. Florence, Italy 20-23 Mach, **2001**
12. S. Timouchev, J. Tourret *Harmony Software For Low Noise Design Of Centrifugal Ventilators Of Transport Machines*. 29th international congress on noise control engineering-InterNoise 2000. Nice (France), Proceedings, **2000**, v.6 p.3833
13. Timouchev S., Tourret J. *Numerical Simulation of BPF Pressure Pulsation Field In Centrifugal Pumps*. 19th International Pump Users Symposium, February **2002**, Houston, Texas
14. Michael Bockhoff , Karine Mones, Serguei Timouchev, Kirill Ilhicov, Andrey Aksenov *Numerical and experimental study of 3D unsteady flow in a lawn mower blade for prediction of pressure pulsation and noise*. 2nd International symposium Fan Noise 2003, Senlis (France), 23-25 September **2003**
15. Serguei Timouchev. *Computational study of pressure pulsation in a medium specific speed pump*. Proceedings of FEDSM2005: **2005** ASME Fluids Engineering Division Summer Meeting and Exhibition June 19-23, 2005, Houston, TX, USA

**First International Meeting
on
Wind Turbine Noise: Perspectives for Control
Berlin 17th and 18th October 2005**

Numerical simulations of wind fields over the Baltic Sea with applications to sound propagation

Corresponding author: PhD student Karin Törnblom, University of Uppsala, Department of Earth Sciences, Air and Water Sciences, Villav.16, SE-75236 Uppsala, Sweden.
Phone: +46 (0)18 4717191 Fax: +46 (0)18 551124 Email: karin.tornblom@met.uu.se
Co-author: Dr. Conny Larsson, University of Uppsala, Department of Earth Sciences, Air and Water Sciences, Villav.16, SE-75236 Uppsala, Sweden

Introduction

Sharp changes in temperature and surface roughness between land and sea make coastal areas interesting for studies of winds originating from thermal circulations. These winds may often become supergeostrophic, i.e. stronger than the background wind, and are interesting in several aspects, e.g. transport of pollutions, recreation, wind energy purposes and sound propagation.

It is previously known that the wind field over the Baltic Sea, which is a semi-enclosed sea, is not uniform (Källstrand et al 2000, Grisogono and Tjernström 1996). In this paper a study of the wind field over the Baltic Sea is presented to illustrate how the wind is influenced by various parameters, such as thermal variations between land and sea and changes in the geostrophic wind. The investigation is based on measurements and simulations with the MIUU model.

The sound speed is affected by wind speed and temperature. The speed of sound increases for high temperatures and when the sound is transported in the direction of the wind. For a homogeneous atmosphere, i.e. no dependence on height and horizontal distance, this is not very important. However, in a real atmosphere where wind and temperature changes with height and distance, it is very important for the propagation of sound. Gradients of wind and temperature make the sound waves refract. Depending on if the gradients are positive or negative the sound beams may bend upward or downward, or be trapped in layers. This is very important for what sound level we will hear at the ground. The lower atmosphere in coastal areas shows large complexity in wind pattern and temperature changes, with large gradients, making sound propagation quite delicate and interesting to study. This study is meant to enlighten the atmospheric background information and processes, which is necessary to be able to study sound propagation in further detail.

MIUU-model

The MIUU model used for the model runs in this paper is a three-dimensional hydrostatic mesoscale model. (Enger, 1986) The turbulence is parameterized with a 2.5-level scheme, according to Mellor and Yamada (1974), which implies that the turbulent kinetic energy is calculated by a prognostic equation, whereas the second order moments are obtained by diagnostic expressions described in detail by Andrén (1990). The MIUU model has a terrain following coordinate system (Pielke, 1984). Of the 29 vertical levels used in these simulations, the lowest grid point is at the height z_0 , where z_0 is the roughness length, and the model top is at 10000 m. The model domain is 613 x 675 km and contains 158 x 165 grid points for the simulations over the Baltic Sea. In the horizontal a telescopic grid is used, to achieve a high resolution, i.e. 1 km between the grid points, close to the centre of the domain. In this case that is over the island Gotland (see Figure 1). The grid spacing then gradually expands toward the boundaries until reaching a largest spacing of 9 km. For the simulations over only Gotland the domain is 168 x 236 km, containing 61 x 95 grid points with 2 km spacing in the center of the domain. In the vertical, logarithmic spacing is used near the surface to be able to accurately describe the physics at lower levels. For the upper vertical levels the spacing becomes linear.

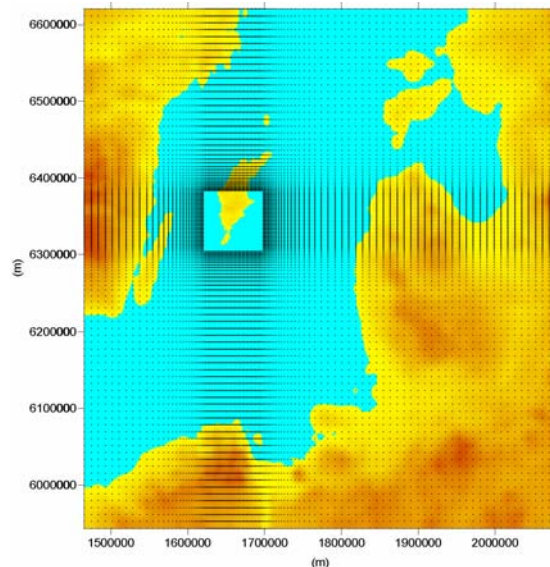


Figure 1 Map showing the model domain and the model grid points. Distances are given in the Swedish geographical coordinate system. In the middle of the model domain (the square) the distance between the grid points is 1 km.

The topography and land use parameters were taken from digitized maps (the U.S. Geological Survey, the University of Nebraska-Lincoln, and the European Commission's Joint Research Centre 1-km resolution global land cover characteristics database, 1999). The model was run for a 30-hour period of time with input data chosen as to simulate a day in May. The background flow in the model is specified as a geostrophic wind. For the simulations in this work, no thermal wind were applied i.e. the geostrophic wind has no shear with height. The model was run with a prescribed and constant temperature for the water surfaces, 12 °C, while the surface temperature over land areas was calculated from an energy balance routine. The cloudiness during the simulations was set to 50%.

Results

Simulations were made for Gotland as an isolated island in a large sea to get a refined picture of what processes take place around the coastline of an island. The scenario is a hypothetical day in May and tests are made with background winds of different strength and direction, as well as for different properties of the ground.

Gotland as an isolated island with light southwesterly winds

As a reference for the simulations made for this paper, a simulation with 2.5 m/s geostrophic wind from southwest was chosen. This is the simulation that gives the largest thermally driven circulation and the physics is well illustrated. Figure 2 shows the time evolution of the wind field at the height of 72 meters. In the morning the sun starts to heat Gotland. This leads to the evolution of a convective layer that grows with time. The turbulence produced by the convective layer and the roughness of the island works as

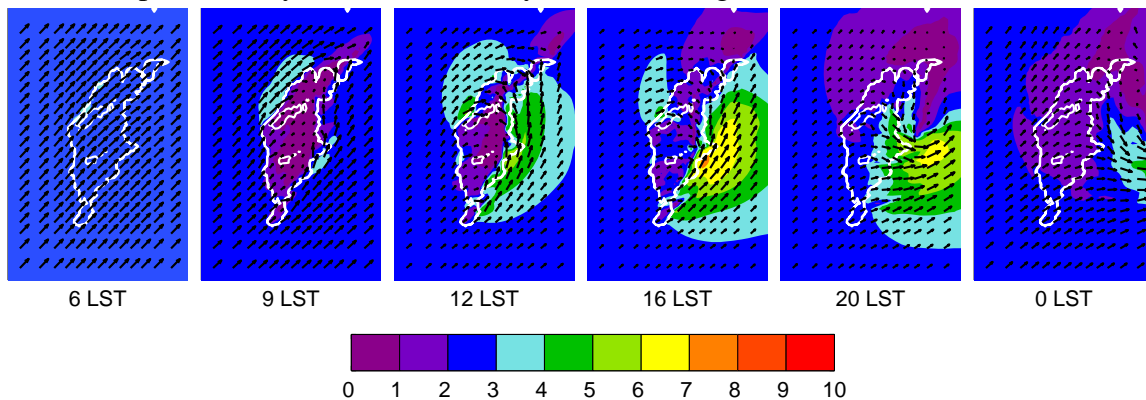


Figure 2 The change of the wind field with time at the height of 72 meters, for 2.5 m/s geostrophic wind from the southwest.

a hinder for the background wind (9 LST), which flows around the island instead, creating two light jets at both sides of the island while there are hardly no wind over the island. As the surface of the island becomes warmer (12 LST), the convective layer increases, building up a thermal low over the island, and the temperature gradient between land and sea increases. This in turn gives rise to a thermally driven circulation at the east coast of Gotland, enhanced by the background flow. The jet at the west coast does not augment since it is opposed by the background flow. At this time the wind around the coastline has also started to veer against the coast of the island, creating a front with low wind speeds in over the island. Further, in the north in the lee of the island, an area with low winds is created. This low wind area works as a cradle for a light sea breeze that evolves during the day and evening. In the evening (20 LST) when the warming of the land ceases, the forcing for the thermally driven circulation disappears and the jet at the east coast weakens. Without the thermal forcing from the island, the remnant of the jet is advected away with the background flow (0 LST).

Comparison with measurements

The same structures seen in the simulations can also be found in measurements. Wind profiles were measured at Gotland in the spring of 2000, using single theodolite tracking

of free flying balloons (Johansson and Bergström, 2005). The profiles were measured at the southern part of Gotland, both at east coast sites, inland sites and west coast sites. From the 110 profiles measured, 65% contained a low level jet (LLJ), i.e. a wind speed maximum below the height of 500 meters, created by mesoscale effects. Out of the 47 profiles from the east coast sites the same figure was 83%. The wind direction during this time was dominantly from the southwest. Figure 3 show the difference in wind speed between the maximum wind speed in the LLJ and the minimum above the jet. The blue and the red curves show, respectively, the mean of all east coast sites and all the inland sites containing low level jets. It can be seen that the wind maximum increases during the day with a maximum around 16 LST, just as in the simulation. The wind in the jet is, as a

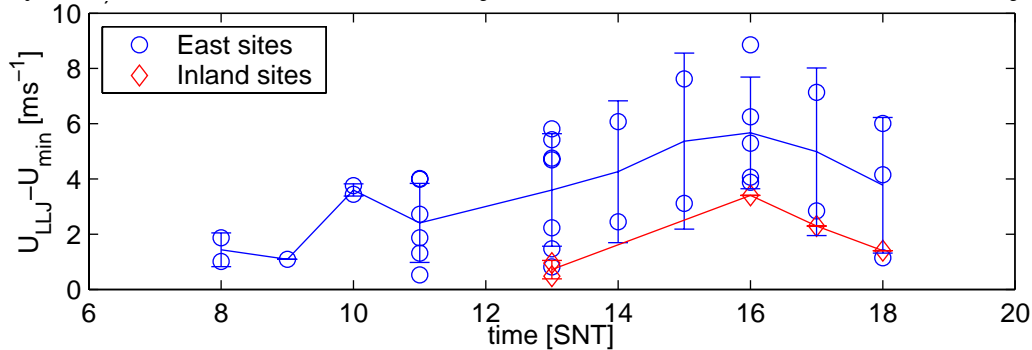


Figure 3 Difference in wind speed between the maximum wind speed in the LLJ and the minimum above the jet for east coast sites and inland sites. The symbols are individual measurements and the lines are average values.

mean of all the east coast profiles, up to 5.5 m/s higher in the jet than in the minimum above. That is in the same order as found in the simulations, and can be seen in Figure 5 later in this paper. Another resemblance that can be seen between measurements and simulations is how the jet spread in over land in the late afternoon. It is clearly seen from the red curve in Figure 3 that the jet exists also over land and evolves in the same manner as over the sea, with the difference that the jet is somewhat lighter over land. In the simulation (Figure 2) the jet also spread in over land in early evening. Also the turning of the wind towards south at the east coast, as seen in Figure 2, is observed in the measurements.

Background wind

Simulations were made with geostrophic winds of different strength and direction in order to isolate the influence of the background forcing. Since southwesterly winds are very common in the area, the simulations were made with westerly, southwesterly, southerly, southeasterly and easterly background winds. The magnitudes of the forcing were set to 2.5 m/s, 5 m/s, 7.5 m/s and 10 m/s. For the simulations with a geostrophic forcing of 2.5 m/s and 5 m/s, large thermally driven circulations were created. For stronger forcing, this feature did not appear, a result that agrees well with earlier studies. (e.g. Arritt, 1993)

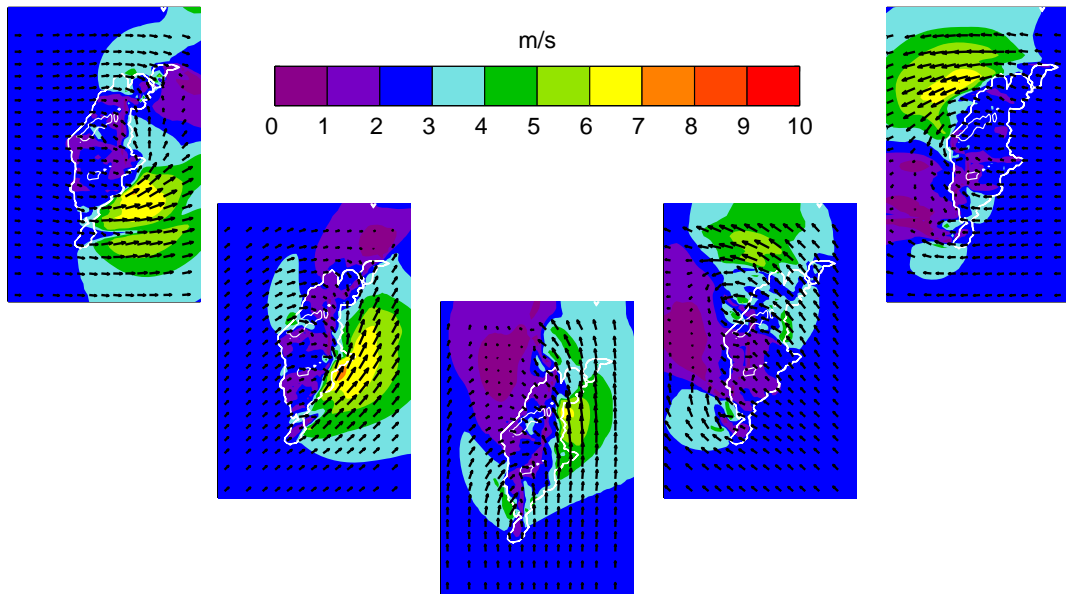


Figure 4 Thermally driven circulations at 16.00 at a height of 72 meters for 2.5 m/s geostrophic forcing coming from west, southwest, south, southeast and east, respectively.

Figure 4 shows the scenario at a height of 72 meters over Gotland at 16.00 LST for 2.5 m/s geostrophic forcing coming from 5 different directions, namely west, southwest, south, southeast and east, respectively. The highest wind speeds are found at this time and height for all five simulations. (Not shown) The presence of the island induces thermally driven circulations for all directions of the forcing, even though this feature seems to be strongest for southwesterly background winds. Most probably this is due to the shape of the island and coastline.

In all five scenarios a high wind zone evolves when the wind come in contact with the right hand side of the island and approaches the leeside. Here the wind speed becomes super-geostrophic (i.e. higher than the background wind) in all cases with a low level jet maximum at a height around 50-100 meters and a veering of the wind towards the coast of the island. Further downstream the jet, on the very leeside of the island, an area with low wind speeds is found for all directions of the background flow, and just as in the reference case above, a sea breeze circulation is started in this area. Figure 5 shows a vertical view of the eastern coast of Gotland at 16.00 LST. It can be seen that above the low wind area, seen in Figure 4, is another jet at around 1000 meters. The explanation to this being continuum reasons. Interesting to see is also that the belt of low wind reaches all the way up to about 2000 meters, quite high above the large thermally driven jet.

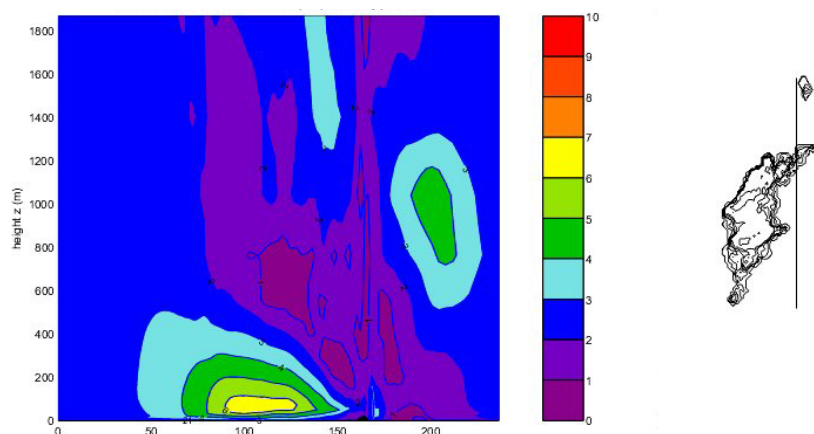


Figure 5 A vertical view (along the south-north line shown on the map to the right) of the wind speed at the eastern coast of Gotland at 16.00 LST

Surface properties

In order to further study the physical reasons for the modification of the wind field the surface properties of the island were changed. Figure 6 shows the wind field at 16.00 LST at the height of 72 meters above the island Gotland for 5 m/s geostrophic forcing and for different surface properties. The first picture, a), shows the reference with a realistic island. In picture b) the island is not heated by the sun, nor cooling in the night. The surface temperature stays the same as the temperature of the surrounding sea. Picture c) shows the scenario with Gotland when the topography is taken away, but the roughness length remains the same as in the reference case. In picture d) the topography and the roughness are taken away, and in the last picture, e), Gotland is completely removed. The pictures easily show that it is the heat and the surface roughness that play the important roles for the modification of the wind field in these simulations. By only removing the topography (figure c) the picture does not change significantly from the reference case. Of course, this does not have to be general, as the topography is quite moderate on Gotland (as most about 50-70 m a.s.l). If the diurnal heat changes are taken away from the island, i.e. setting the temperature to a constant seawater temperature (figure b), but keeping topography and surface roughness intact, the wind does not slow down over the island in the same manner at this height as in the reference case a). However there is still a small (very local in height) wind maximum just north west of

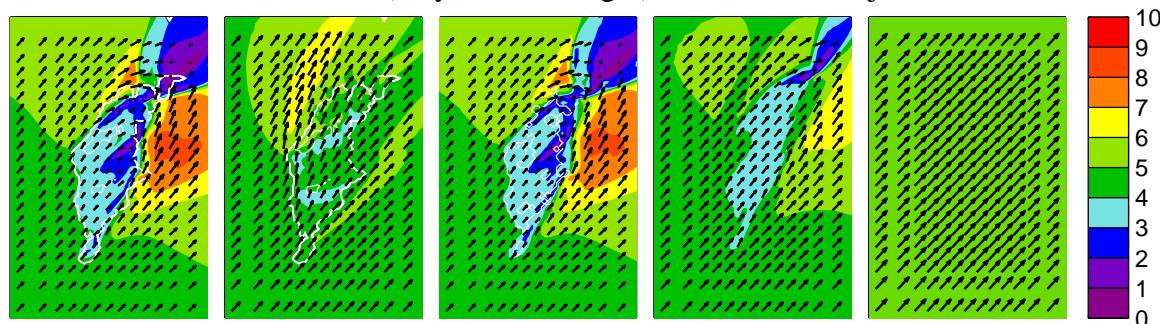


Figure 6 Wind field at 16.00 LST at 72 meters above Gotland for 5 m/s geostrophic forcing and different surface properties a) a realistic Gotland, b) no heating, c) without topography, d) neither topography nor surface roughness, e) no island

the island, most likely because of continuum reasons. When the surface roughness is set to the same value as for water, but the heat is again allowed to change diurnally (figure d), it is seen that the thermally driven circulation is not just thermally driven, since the max is much smaller now than in the reference case. The surface roughness also play a role in the circulation in that it slow down the wind over the island, up to a certain height, depending on the ambient wind. Parts of the wind then take the path around the island instead of over it, producing a maximum at the eastern and western coast of Gotland. The last picture, (figure e), shows that the wind field is undisturbed without the island, and that at this height the undisturbed wind field is equal to the geostrophic forcing.

The Baltic domain

Gotland is situated in the Baltic Sea, and the realistic picture of the wind field is much more complex than for an isolated island in an infinite sea. In Figure 7 the wind field at 16.00 LST at the height of 72 meters is shown, from a simulation with 2.5 m/s geostrophic forcing from the southwest. It is the same scenario as the reference case in this paper, the only difference being a larger simulation domain. It is interesting to see how the thermally driven circulation originating from the Swedish mainland influences the entire Baltic Sea. The structures in the wind field, seen around Gotland earlier in this paper remain. On the east coast the jet is still present, and so is the low winds just north of Gotland. But the ambient wind around Gotland is stronger, especially at the west coast, just opposite the Swedish mainland. For 5 m/s geostrophic forcing, the picture looks similar, but the thermally driven circulations are more spread in the direction of the background wind. (Not shown) For 7.5 m/s forcing, no thermal circulations are seen. Instead the wind speed increases over the entire sea, because of the lower surface roughness, compared to land, and the lack of a convective layer. (Not shown)

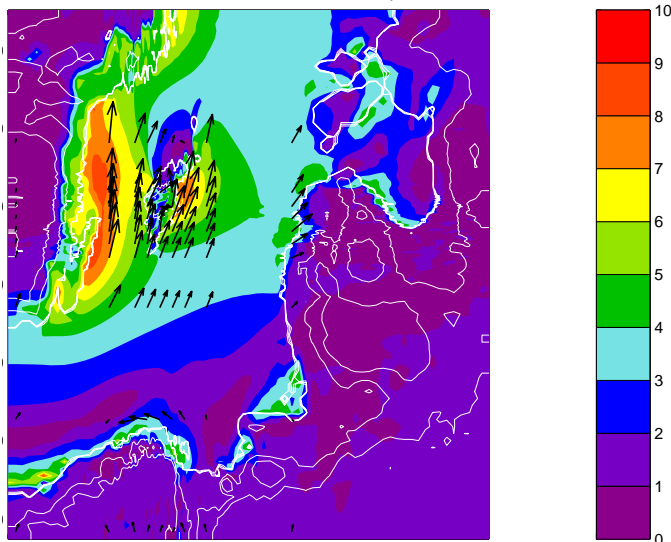


Figure 7 The wind field over the Baltic Sea area at 16.00 LST at the height of 72 meters, for 2.5 m/s geostrophic wind from the southwest. (The same as the reference case but with a larger domain.)

Supergeostrophic winds

In Figure 8 the ratio between mean wind and geostrophic forcing is plotted at 72 meters height at 16.00, for 4 different geostrophic directions for the west coast and east coast of Gotland, respectively. It is easily seen that the wind generally becomes more supergeostrophic for low background winds. The forcing is then less dominant and the effect of thermally driven circulations thus becomes stronger. The strongest winds are found for southwesterly forcing, in this case mostly caused by the chosen sites. If the sites were chosen differently another direction of the forcing would give the largest ratio. For a south westerly forcing of 2.5 m/s the measured wind at the east coast is up to 2.8 times as strong as the geostrophic wind. The wind climate at the east coast is dominated by a large thermally driven circulation that can be seen in Figure 7. It results in a supergeostrophic jet with maximum strength at about 100 meters height, in late afternoon. On the west coast the wind also becomes stronger than the geostrophic forcing in the afternoon. The thermally driven circulation originated over the Swedish mainland is the cause to this.

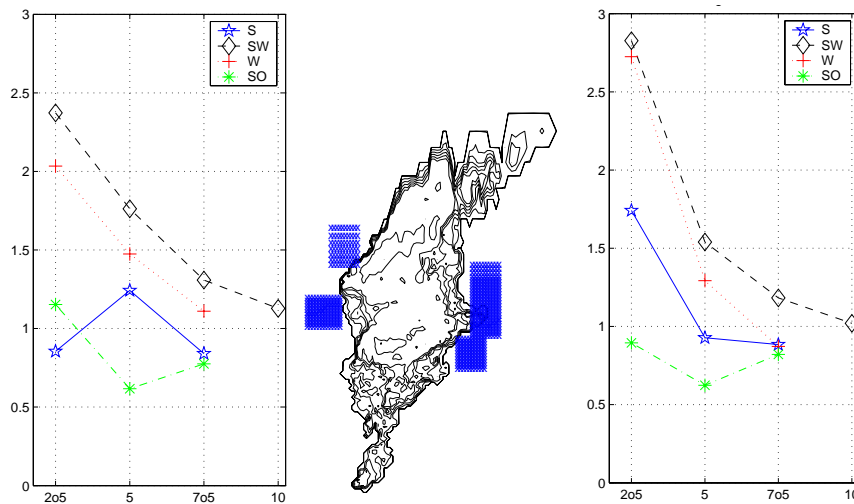


Figure 8 Mean winds divided by geostrophic forcing as a function of geostrophic wind. West coast and east coast respectively, for 4 different directions of the geostrophic forcing.

Measurements indicate that the modeling of thermally driven winds is reasonable. In Figure 10 measured wind is plotted against geostrophic wind for two sites: Östergarnsholm at the east coast of Gotland and Näsudden at the west coast (Figure 9). At both sites the measurements are made on towers at the height of 28.6 m and 75 m,



Figure 9 The location of Näsudden (blue) and Östergarnsholm (cyan)

respectively. The measured wind speed data was collected from the first of June 1995 until the end of December 1998. The geostrophic wind was calculated every sixth hour for the same period, using pressure fields. In Figure 10a and b the collected data is plotted against geostrophic wind every sixth hour for the period. The data is scattered, but it is clear that the measured wind decreases compared to the geostrophic wind for high geostrophic wind speeds. In figure c the mean of the measured wind divided into intervals of 1 m/s is plotted against geostrophic wind. The curve clearly shows that for a geostrophic wind lower than 5 m/s the actual wind is generally higher, depending on mesoscale effects. On the opposite, for stronger geostrophic winds higher than 5 m/s the actual wind is generally lower.

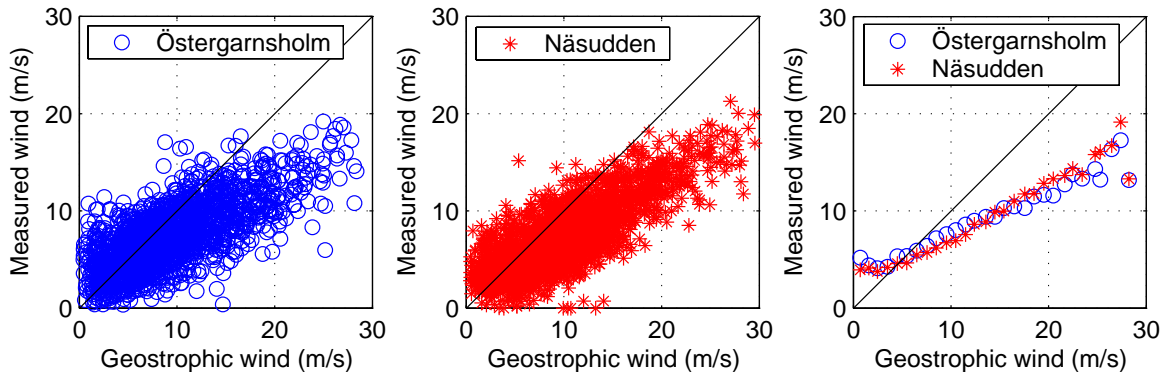


Figure 10 Measured wind speed plotted against geostrophic wind for the years of 1995-1998 for two sites, Östergarnsholm and Näsudden, respectively. The first two plots show all measurements and the last plot shows the means of wind speeds divided into intervals of 1 m/s.

Sound speed profiles

The speed of sound is affected by wind speed and temperature. The sound speed is calculated from the reference wind simulation above (2.5 m/s geostrophic wind from the south west at 16.00 LST), and plotted in Figure 11 at three sites for head wind and tail wind. The blue curve is from an offshore site situated in just east of Gotland where the large jet is located. The black curve (represented as cyan in the map) is over land, just west of the offshore site. The red curve is from the site just north of Gotland, which is dominated by low winds in this case.

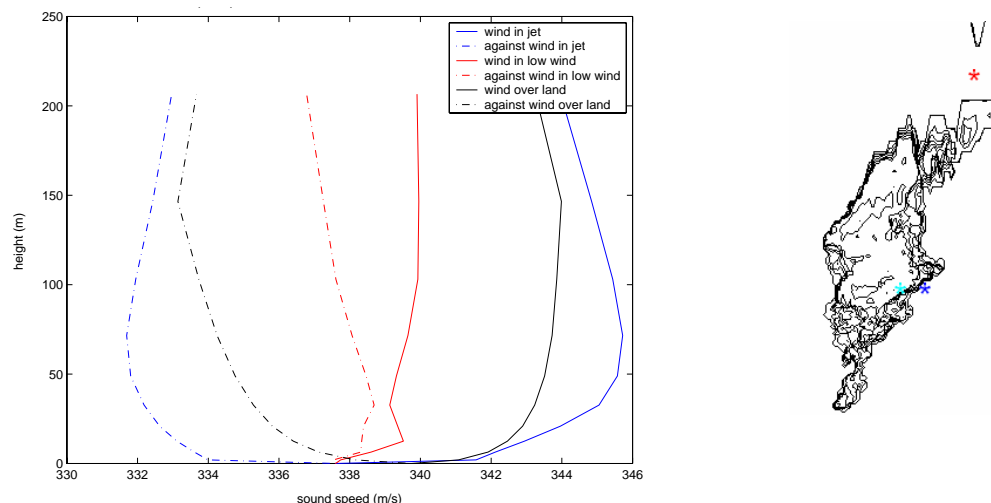


Figure 11 Sound speed profiles at 16.00 LST at three sites around Gotland

In Figure 11 the sound speed changes from the lowest 332 m/s up to 346 m/s inside the jet, depending on whether the propagation is against the wind or with it. Also it can be seen that for the low winds just north of Gotland (red) the speed does not change that much, but since there is a sea breeze the wind veers a lot giving rise to gradients, directly seen in the sound speed profile. An interesting thing to think of when viewing the profiles is that the curves also can be seen as wave fronts. The propagation of sound is always perpendicular to the profile, implying downward refraction up to about 50 meters height for the tailwind profile in the jet above (blue). Comparing the blue tailwind profile over sea with the black one over land, the one over sea show greater downward refraction. This is because the atmospheric stability over sea is higher than over land at this time.

Conclusions

This study, which was made for a day in May, shows that thermally driven circulations affect the wind field and gradients in coastal areas, often giving rise to low level jets, sea breezes and supergeostrophic winds. It is the diurnal heating of the islands together with the surface roughness changes between land and sea that have the greatest effect on the wind climate in the Baltic Sea, where the topography is considered to be moderate.

The sound propagation is highly dependent on atmospheric conditions, such as gradients of wind and temperature. Small variations of these gradients in time and space, e.g. a LLJ changes height with tens of meters, may change the whole sound scenario at a specific place a distance away from the sound source, since the sharp wind gradient may work as a lid for upward or downward propagation, depending on where the source is situated. In a real atmosphere the gradients change even faster and more vividly than they can ever do in a numerical model, which is restricted by the distance between its grid points. Numerical sound models that do not take into account the atmosphere or that simplify it too much therefore miss a lot of physics important for an accurate modelling of sound propagation. It also seems that calculating a mean value for the sound in decibel is not a good way to represent the result. A better way might be to make a statistical distribution on the sound level and when they occur.

References

- Andrén A. 1990, Evaluation of a turbulence closure scheme suitable for air-pollution applications, *J. Appl. Meteorol.* **29**, 224-239
- Arritt, R. W., 1993, Effects of the Large-Scale Flow on Characteristic Features of the Sea Breeze, *J. Appl. Meteorol.*, **32**, 116-125
- Grisogono B., Tjernström M. 1996, Thermal mesoscale circulations on the Baltic coast: 2. Perturbation of surface parameters, *J. Geophys. Res.* **101** p 18999-19012.
- Johansson, C., Bergström, H. 2005, A study of the wind field above Gotland, Wind energy report WE2005:1, Department of Earth Sciences, Uppsala University.
- Källstrand, B., 1998, Low Level Jets in a Marine Boundary Layer During Spring, *Contr. Atmos. Phys.*, p. 359-373
- Källstrand, B., Bergström H., Hojstrup J., Smedman A., 2000, Mesoscale wind field modifications over the Baltic Sea, *Boundary-Layer Meteor.* **95**(2), p 161-188
- Mellor G. and Yamada T. 1974, A hierarchy of turbulence closure models for planetary boundary layer, *J. Atmos. Sci.*, **31**, 1791-1806.
- Pielke, R. A.: 1984, '*Mesoscale Meteorological Modeling*', Academic Press Inc., Orlando, 612 pp.
- U.S. Geological Survey, University of Nebraska-Lincoln and European Commission's Joint Research Centre 1-km resolution global land cover characteristics database, 1999, available at <http://edcdaac.usgs.gov/glcc/glcc.html>

**First International Meeting
on
Wind Turbine Noise: Perspectives for Control
Berlin 17th and 18th October 2005**

Mitigation measures for night-time wind turbine noise

G.P. van den Berg

Science Shop for Physics, University of Groningen, Nijenborgh 4, 9747 AG Groningen,
the Netherlands; g.p.van.den.berg@rug.nl

Summary

Increasing stability of the atmosphere causes the sound power of a wind turbine to increase relative to the ambient sound level. Also, it causes an increase of the fluctuation strength of the sound.

The first effect is only relative: the wind turbine reaction to hub height wind speed is not essentially different from that in an unstable atmosphere (daytime), but the sound is more intrusive in a stable atmosphere (night) because of the lower background level. Manufacturers are already trying to solve this problem by attempting to develop 'silent turbines', either through new designs or with the help of a control system. A proposal for a further development is to control the sound power level relative to the ambient background level.

The second effect, the change in sound character, must be solved in a different way, as this is due to changes the blades encounter within one revolution. New designs may offer several ways to reduce the level of the fluctuations, for example continuous blade pitch control or variable tilt. Furthermore, the turbines in a wind farm can be desynchronized by applying random fluctuations to the blade pitch angle.

1. Introduction

It has been shown in two earlier papers [1, 2] that atmospheric stability has a pronounced effect on the sound wind turbines produce. With increasing stability the sound may become louder when 10m wind speed (= wind speed at 10 meter height) does not change or even decreases [1]. Moreover the sound may become more annoying because blade swish develops into a more distinctive beating sound [2].

Atmospheric stability will occur when the ground cools due to heat loss from skyward infrared radiation at low sun or sundown and a clear or partially clear sky. The radiation temperature of a clear sky is low, especially when the air is very dry, so there is little downward ('reflected') radiation to compensate for heat loss due to outward radiation. Stability occurs more readily when air temperature is relatively high and daytime ground heating has been significant, as this creates a situation in which significant cooling occurs during the subsequent night.

Statistics for this phenomenon in flat land have been given in a separate paper [3]. The effect on wind speed can be thought of as a rotation of the wind speed profile: below a certain

altitude (of several tens of meters) the wind abates, while above it the wind picks up when the atmosphere becomes stable.

In undulating and certainly in mountainous terrain this change in wind profile may be influenced or even overridden by relief related changes. For example: in a valley a downflowing (decelerating) wind may enhance the effect of stability, whereas an upflowing (accelerating) wind may compensate for the effect of stability. Furthermore the wind profile as well as the temperature profile will simultaneously influence the propagation paths of sound.

Combined effects are therefore complex and, though readily understood qualitatively, are not easily predicted in quantitative terms.

2. Meeting noise limits

In a neutral and unstable atmosphere wind turbine sound is the result of induced (and also atmospheric) turbulence on the blades: reduction of this source is the topic of dedicated research, such as the SIROCCO (*Silent ROTors by aCCoustic Optimisation*) program which seeks to improve the design of the wind turbine blade. Sound reduction by reducing blade speed is an option already available in modern turbines.

In this paper we will deal with the ('added') sound produced by a wind turbine due to increasing atmospheric stability. To address this problem two types of mitigation measures can be explored:

1. Reduce the sound level to the pertinent (legal) limit for environmental noise;
2. Reduce the level variations due to blade swish/beating.

The first measure is, of course, a legal obligation in most countries, but the type of limit varies. E.g., in Germany the limit applies to the maximum sound immission level (the level produced at nominal maximum power), regardless of wind speed as such. In many countries the limit is based on the wind speed related background ambient sound level (L_{95} or L_{90}).

In the UK and elsewhere the limit is a constant at low 10m wind speeds and 5 dB above background ambient level ($L_{90} + 5$ dB) at higher 10m wind speeds. In the Netherlands the limit is a reference curve constructed from 1. a constant value for wind speeds at less than 10m height and 2. a variable element dependent on wind speeds at heights greater than 10m (for wind farms over 15 MW other limit values may apply).

Until recently the significance of atmospheric stability has usually been disregarded, and the wind speed at 10m height was erroneously used for all atmospheric conditions. Consequently, these limits are not always met. In stable atmospheric conditions, when hub height wind speed exceeds the cut-in wind speed, this implies that an extra effort to reduce the immission level may be necessary.

The second measure, the reduction of level

Part of an article in *Press and Journal* of Aberdeen. 25 May 2005

NOISE FROM WINDFARM MAKING LIFE A MISERY

A recent settler in Caithness claimed yesterday his life is being blighted by ghostly noises from his new neighbours, the county's first large-scale windfarm. (.....)

"The problem is particularly bad at night when I try to get to sleep and there's a strong wind coming from the direction of the turbines. They just keep on droning on. It's a wooh wooh type of sound, a ghostly sort of noise. It's like torture and would drive anyone mad."



variations due to blade swish/beating, is worth considering when the noise limit incorporates a penalty for a sound having a distinctive (impulsive or fluctuating) character. In that case either the sound immission level should be reduced by a value equal to the penalty (usually 5 dB) or the sound character must change. Many press reports as well as some scientific investigations clearly indicate that the character of wind turbine sound is important in its perception [2, 4] (see also the press article excerpt on the previous page –about a wind farm in a hilly countryside). In spite of this, turbine manufacturers, developers, and some acoustic consultants seem to be reluctant to acknowledge any added annoyance due to the sound character. In the long term this may increase the incidence of avoidable annoyance, feed opposition to wind energy, and thus prove to be counterproductive.

3. Reduction of sound level

When the sound immission level is limited to a value depending on (supposedly 10m wind speed dependent) ambient sound level, the problem is that hub height wind speed is not uniquely related to 10m wind speed and the sound emission as well as immission level can have a range of levels depending on atmospheric stability. The turbine operates at hub height wind speed, but must be controlled by a 10m based wind speed.

A. Wind speed controlled sound emission

As a result of opposition to wind farm proposals in the relatively densely populated central province of Utrecht in the Netherlands all proposals but one were cancelled. The exception is in Houten, where the local authorities wish to stimulate wind energy by allowing the constructing of several 3 MW turbines, but at the same time are anxious to ensure that residents will not suffer noise disturbance. Atmospheric stability has been taken into account by rejecting the usual logarithmic relation between wind speeds at 10m and hub height. The official permission will require that the immission sound level at specified locations must not exceed the background level of all existing ambient sound. Of course, ambient sound level depends on wind speed if the wind is sufficiently strong, but in this area it also depends on wind direction as that determines audibility of distant sources: a motorway to the west, the town to the north-east and relatively quiet agricultural land to the south-east. So the background ambient level, measured as L_{95} , must be measured in a number of conditions: as a function of wind speed (1 m/s classes), wind direction (4 quadrants) and time of day (day, evening, night). These values equal the limit values for the immission level L_{imm} , and from this the maximum allowable sound power level L_{Wmax} per turbine can be calculated for every condition, presuming all (or perhaps a selection of) turbines are operational. It is advisable to determine wind characteristics and turbine performance over a period of at least five minutes, as wind speed variations are relatively strong over shorter periods and weak over periods from 5 minutes up to several hours [5]. On the other hand rapid control is desirable to adapt to changing conditions, so averaging over 5 minutes seems the best choice.

Control will thus be achieved in a number of steps:

- a. Measure wind direction D_{10} and wind speed v_{10} at 10m height in open land over an appropriate period (probably 5 minutes);
- b. Determine the limit value for the sound power level L_{Wmax} from previously established relations $L_{imm}(L_W)$ and $L_{imm,max} = L_{95}(T, v_{10}, D_{10})$;
- c. Determine the actual sound power level $L_{W,5min}$ from wind turbine performance (electric power or speed);
- d. If actual $L_{W,5min}$ exceeds L_{Wmax} (equivalent to $L_{imm,5min} > L_{95}$) the control system must decrease sound power level for the next period; if $L_{W,5min} < L_{Wmax}$ the reverse applies (until maximum speed is attained).

Changing the sound power level can be effected by increasing blade pitch (slowing the blades down).

In favour of this control system we may note that it is straightforward, simple, easy to implement and directly related to existing Dutch noise limits. However, it is based on the assumption that L_{95} depends on three parameters only, namely wind speed, wind direction and diurnal period. In reality the background level will also depend on the hour (*e.g.* nighttime traffic is very quiet at around 4am, and most busy just before 7am), day of the week (weekends, working days), season (vegetation, holidays), atmospheric stability (little or no wind in low vegetation in stable conditions, even when 10m wind speed is several m/s) and other weather conditions such as rain. Also sound propagation from distant sources will differ with weather conditions.

Measurements show that indeed 10m wind speed is not a precise predictor of ambient sound level. These measurements were performed on behalf of the Houten authorities from June 9 through June 20, 2005 at two locations: wind speed was measured at 10m height in open terrain, at least 250m from any obstacles over 1m in height (trees lining the busy and broad Amsterdam-Rhine Canal to the northeast) and over 1000m from obstacles in any other direction; the sound level was measured close to a farm next to the canal (see figure 1). Total measurement time was 220 hours.

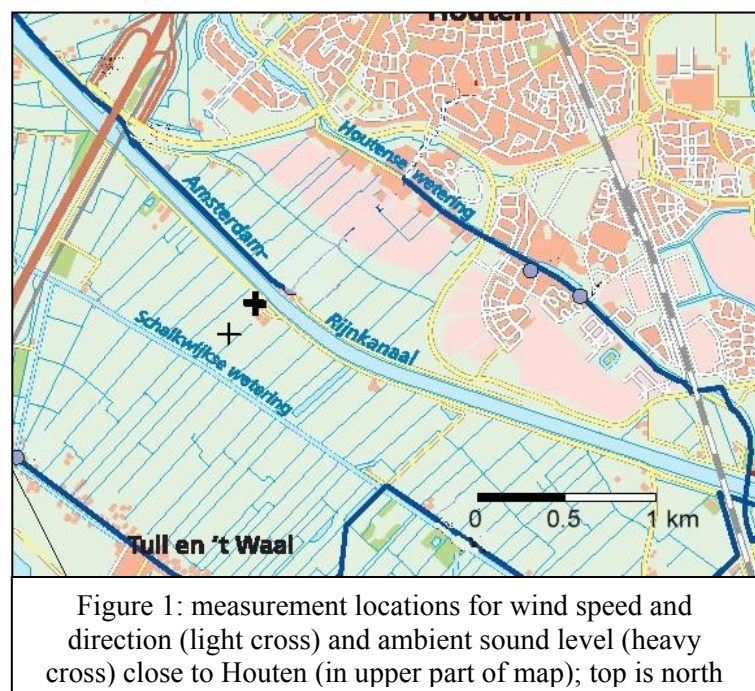
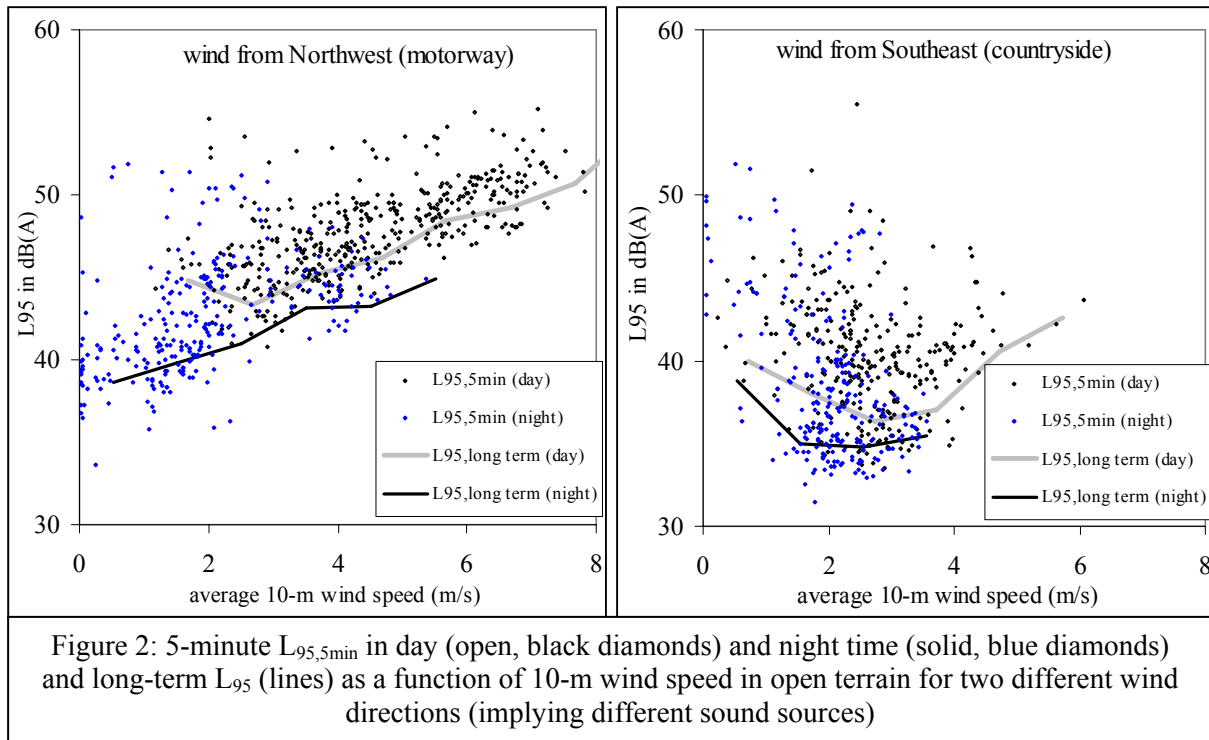


Figure 1: measurement locations for wind speed and direction (light cross) and ambient sound level (heavy cross) close to Houten (in upper part of map); top is north

Some results are plotted in figure 2: L_{95} per 5-minute period as a function of wind speed (averaged per 5 minutes), separately for two wind directions and two periods. The periods are night (11pm – 7am) and day (7am – 7 pm), the wind directions southeast ($90^\circ - 180^\circ$ relative to north) and northwest ($270^\circ - 360^\circ$), where respectively the lowest and highest ambient levels were expected. The northwest data total 675 five-minute periods, or 26% of all measurement time, while the southeast data cover 511 periods or 19% of the measurement time.

The 5-minute L_{95} values are calculated from all (300) 1-second samples within that period. To determine a long-term background level an appropriate selection (wind direction, period) of all measured 1-second sound levels can be aggregated in 1 m/s wind speed classes (0-1 m/s, 1-2 m/s, etc.). In figure 2 these aggregated values (connected by lines to assist visibility) are plotted for day and night separately. It is clear that in many cases the 5-minute period values of L_{95} are higher, and in fewer cases lower than the long-term value. This means that if the immission limit is based on the measured long-term background sound level, then in a significant amount of time the actual background level will not be equal to the previously established long-term level. This is important for 10-m wind speeds as low as 2 m/s, as even then wind at 100m height may be strong enough to drive a turbine at high speed.



B. Ambient sound level controlled sound emission

An alternative to a wind speed controlled emission level is to measure the ambient sound level itself and thus determine the limit value directly. To achieve this the background ambient sound level can be determined by measurement (*e.g.* in 5-minute intervals) and compared to the immission level calculated from actual turbine performance. If the immission level L_{imm} is exactly equal to the ambient background level L_{95} without turbine sound (so $L_{imm} = L_{95} = L_{imm,max}$), then background sound level including turbine sound is $L_{95+wt} = \log.sum(L_{imm,max} + L_{95}) = L_{imm,max} + 3 \text{ dB}$ or $L_{imm,max} = L_{95+wt} - 3 \text{ dB}$. If the calculated immission level is equal to measured ambient L_{95+wt} , turbine sound apparently dominates the background level and the turbine should slow down.

This type of control can also be achieved in several steps. Again assuming 5-minute measurement periods, these are:

- Determine the actual sound power level $L_{W,5min}$ (integrated over 5 minutes) from turbine power production or speed;
- Measure actual background level $L_{95+wt,5min}$ at a location where the limit applies;
- If $L_{W,5min} > L_{W,max}$ (*i.e.* $L_{imm} > L_{95+wt,5min} - 3 \text{ dB}$) then the control system must decrease sound power level for the next 5-minute period, if $L_{W,5min} < L_{W,max}$ the reverse must happen (until maximum speed is attained).

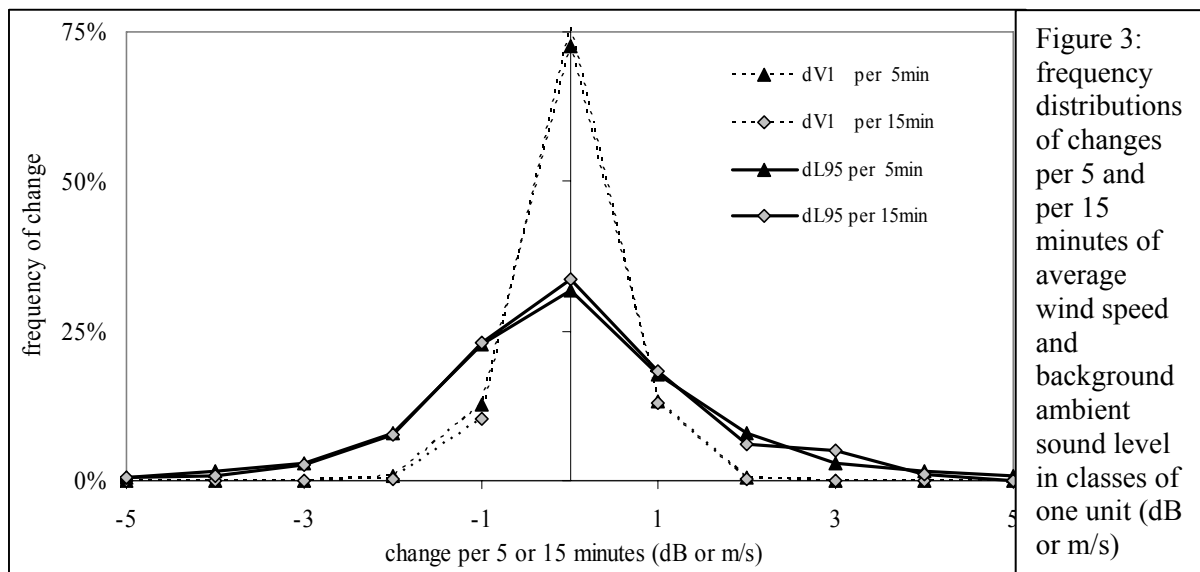
Here it is assumed that the microphone is on a location where the background ambient level L_{95} (without any turbine) equals the limit value. If a measurement location is chosen further away from the turbine(s), the immission sound level will decrease with a factor ΔL_{imm} at constant L_W , whereas L_{95} will not change (assuming that ambient sound does not depend on location). In this case a correction must be applied to the measured L_{95+wt} ($L_{imm,max}$ now being equal to $L_{95+wt} - 10 \cdot \log(10^{-\Delta L_{imm}/10} + 1)$) to determine what sound power level is acceptable. A similar approach may be used if the limit is not L_{95} itself, but $L_{95} + 5 \text{ dB}$. In that case, is it not possible to determine L_{95} from measurements at a location where this limit applies, as the

turbine sound is allowed to be twice as intense as background sound itself. In that case a measurement location may be chosen where ΔL_{imm} is 5 dB.

An apparent drawback of this sound based control method is that measured ambient sound may be contaminated by local sounds, that is: from a source close to the microphone. Also, figure 2 suggests that there are significant variations in $L_{95,5\text{min}}$, which could imply large control imposed power excursions if these variations occur in short time.

The first drawback can be solved by using two or more microphones far enough apart not to be *both* influenced by a local source. The limit value is then either $L_{95,5\text{min}}$ determined from all measured sound levels within the previous 5-minute period, or the lowest value of $L_{95,5\text{min}}$ from each microphone location.

Secondly, large variations in either wind speed or background sound level are rare, as is shown in figure 3 where the difference is plotted between consecutive 5-minute and 15-minute values of L_{95} and average free 10-m wind speed. For 99% of the time the change in wind velocity averaged over consecutive periods of 5 or 15 minutes is less than 1.5 m/s (in 72% less than 0.5 m/s). For 94% of the time the change in background sound level over consecutive periods of 5 minutes is less than 3.5 dB and in 88% of the time the change is less than 2.5 dB (for 15 minute periods the percentages are almost the same: 96% and 89%). So if the adjustment of sound power level is in steps no larger than 3 dB, most changes can be dealt with in a single step.



The frequency of changes between 5-minute periods that are 10 minutes apart (that is: with two 5-minute periods in between) is very similar to the distributions in figure 3. This means that when there is a change of 3 dB for two consecutive periods, it is less likely that a similar change will occur within the next one or two periods.

4. Reduction of fluctuations in sound level

The level variation due to blade swish increases when the atmosphere becomes more stable because the angle of attack on the blade changes. When the blade passes the tower this angle can change from its optimum value (zero) up to 4° or 5° . As a result the turbulent layer at the trailing edge of the blade becomes thicker and produces more sound. In a wind farm the increased level variations from two or more turbines may coincide to produce still higher fluctuations. Both effects may lead to clearly audible level variations of 3 -10 dB as has been shown theoretically as well as in practice [2].

The increase of blade swish, resulting in blade *beating*, may be lessened by adapting the blade pitch angle, the increase due to coincidence (also) by desynchronizing turbines.

A. Pitch angle

When a blade rotates in a vertical plane the optimum blade pitch angle α is determined by the ratio of the wind speed and the rotational speed of the blade. As the rotational speed is a function of radial distance (from the hub), blade pitch changes over the length of the blade and is lowest at the tip. At zero angle of attack, the blade pitch is 10° (0.17 radians) with a typical blade tip speed of 70 m/s, and wind speed of 12 m/s. As wind speed closer to the ground is usually lower, the wind speed at the low tip (where the tip passes the tower) is lower than at the high tip. As a result the angle of attack changes within a rotation if blade pitch is kept constant. For a 100 m hub height and 70 m diameter turbine at 20 rpm this change is about 0.8° at the lower tip in an unstable atmosphere, increasing to almost 3° in a very stable atmosphere [2].

In front of the tower there is a further change in angle of attack due to the fact that the tower is an obstacle slowing down air passing the tower. This change is of the order of 2° [2].

The optimum angle of attack of the incoming air at every position of the rotating blade can be realized by adapting the blade pitch angle to the local wind speed. Pitch must then increase for a blade going upward and decrease on the downward flight. Such a continuous change in blade pitch is common in helicopter technology.

Even if the effect of stability on the wind profile can be compensated for by pitch control, blade swish due to the presence of the tower would still be left. This residual blade swish, which also occurs in daytime, can be reduced further by an additional decrease in blade pitch close to the tower. If the variations in angle of attack can be reduced to 1° or less, blade swish will cause variations less than 2 dB which is not perceived as a (relatively annoying) fluctuating sound.

B. Rotor tilt

If the rotor is tilted backwards, the angle of attack will change while the blade rotates. If the tilt angle changes from zero to θ , the angle of attack at the low tip increases from α to α' , and it follows from geometrical analysis that:

$$\tan(\alpha') = (\tan[\arctan\{\sin(\alpha)/\rho\} + \theta] - \tan(\theta)) \cdot \rho / \cos(\alpha) \quad (1)$$

where $\rho = r/b$ is the ratio of radius r and blade width b (at radius r). For small blade pitch angles and blade slenderness ρ between 10 and 40 the increase of angle of attack with tilt (from 0 to θ) can be approximated with:

$$\Delta\alpha = \alpha' - \alpha = 1.1 \cdot \alpha \cdot \theta^2 \quad (\text{angles in radians}) \quad (2a)$$

In the range $\alpha \leq 20^\circ$, $10 \leq \rho \leq 40$ and $\theta \leq 30^\circ$, the standard deviation of the constant 1.1 is 0.06. With angles expressed in degrees, equation 2 reads:

$$\Delta\alpha = (33 \pm 2) \cdot 10^{-5} \cdot \alpha \cdot \theta^2 \quad (\text{angles in degrees}) \quad (2b)$$

This means that for a tilt angle of 2° , as used in modern turbines and 10° blade pitch (tip rotational speed 70 m/s, wind speed 12 m/s), the change in angle of attack (relative to a vertical rotor with zero tilt) is negligible (0.014°).

Rotor tilt could compensate for a 2° change in angle of attack due to high stability when the tilt angle is 17° . In this case the horizontal distance between the low tip and the turbine tower increases with at least 10 m. This will also lead to a smaller change in angle of attack as at this distance the velocity deficit (due to the presence of the tower) is lower.

C. Desynchronization of turbines

When the atmosphere becomes stable, large scale turbulence becomes weaker and wind speed is more coherent over larger distances. The result is that different turbines in a wind farm are exposed to a wind with fewer variations, and the turbines become more or less synchronized. This synchronization may lead to coincidence of blade beats from two or more turbines for an observer near the wind farm, and thus higher pulse levels. To desynchronize the turbines in this situation, the random variation induced by daytime atmospheric turbulence can be simulated by small and random fluctuations of the blade pitch angle or the electric load of each turbine separately.

In an unstable atmosphere turbulence strength peaks at a non-dimensional frequency $n = fz/U \approx 0.01$, where U is the mean wind speed and z is height (this is according to custom in acoustics; in atmospheric physics traditionally f is non-dimensional and n physical frequency) [6]. At $z = 100$ m and $U = 10$ m/s this corresponds to a physical frequency $f = nU/z = 1$ mHz. At higher frequencies the turbulence spectral power density decreases with $f^{-5/3}$. When atmospheric instability decreases, the maximum shifts to a higher frequency and wind speed fluctuations in the non-dimensional frequency range of 0.01 to 1 tend to vanish. So, to simulate atmospheric turbulence the blade pitch setting of each turbine must be independently fed with a signal corresponding to noise such as pink (f^{-1}) or brown (f^{-2}) noise, in the range of appr. 1 to 100 mHz. The (total) amplitude of this signal must be determined from local conditions, but is of the order of 1° .

References

- 1: G.P. van den Berg: "Effects of the Wind Profile at Night on Wind Turbine Sound", J. Sound Vib. 277 (4-5), 955-970 (2004)
- 2: G.P. van den Berg: "The beat is getting stronger: the effect of atmospheric stability on low frequency modulated sound of wind turbines", Journal of Low Frequency Noise, Vibration And Active Control, Vol. 24 (1), 1-24 (2005)
- 3: G.P. van den Berg: "Wind gradient statistics up to 200 m altitude over flat ground", proceedings First International Meeting on Wind Turbine Noise: Perspectives for Control, Berlin (October 2005)
- 4: E. Pedersen and K. Persson Waye: "Perception and annoyance due to wind turbine noise – a dose-response relationship", J. Acoust. Soc. Am 116 (6), 3460-3470 (2004)
- 5: S. Wagner, R. Bareiss and G. Guidati: "Wind Turbine Noise", Springer, Berlin, 1996.
- 6: J.R. Garrat, "The atmospheric boundary layer", Cambridge University Press (1992)

**First International Meeting
on
Wind Turbine Noise: Perspectives for Control
Berlin 17th and 18th October 2005**

Wind gradient statistics up to 200 m altitude over flat ground

G.P. van den Berg

Science Shop for Physics, University of Groningen, Nijenborgh 4, 9747 AG Groningen,
the Netherlands; g.p.van.den.berg@rug.nl

Summary

The KNMI (Royal Netherlands Meteorological Institute) has an instrumented tower of 200 m height at Cabauw in the western part of the Netherlands. Meteorological data are available as half hour averages over several years. Data of 1987 have been analyzed to assess wind energy potential at several altitudes. Diurnal wind speed variation close to the ground (more wind in daytime, less in night time) is reversed at altitudes over 80 m. As a result ‘small’ wind turbines produce on average more energy in daytime than in at night, but the reverse is true for tall wind turbines. The same is true for the sound produced by wind turbines. Statistics will be presented for the distribution of wind gradients throughout the year and in relation to time of day, atmospheric stability and altitude. Data will be compared to data that have been published from other areas and applied to a modern wind turbine.

1. Introduction

Atmospheric stability has a profound effect on the vertical wind profile and on atmospheric turbulence strength. Stability is determined by the net heat flux to the ground, which is a sum of incoming solar and outgoing thermal radiation, and of latent and sensible heat exchanged with the air and the subsoil. When incoming radiation dominates (clear summer days) air is heated from below and rises. Thus, thermal turbulence implies vertical air movements, preventing large variations in the vertical wind speed gradient (*i.e.* the change in time averaged wind speed with height). When outgoing radiation dominates (clear nights) air is cooled from below; air density will increase closer to the ground, leading to a stable configuration where vertical movements are damped. The ‘decoupling’ of horizontal layers of air allows a higher vertical wind speed gradient.

In the European Wind Atlas model (‘Wind Atlas Analysis and Application Program’ or WAsP) [1] wind energy available at hub height is calculated from wind speeds at lower heights. The Atlas states that “modifications of the logarithmic wind profile are often neglected in connection with wind energy, the justification being the relative unimportance of the low wind speed range. The present model treats stability modifications as small perturbations to a basic neutral state.” [1]. With the growth of wind turbine heights this is now an understatement. In recent years atmospheric stability is receiving gradually more attention as a determinant in wind *energy* potential, as demonstrated by a growing number of articles on stability related wind profiles in different types of environments such as Danish offshore

sites [2], the Baltic Sea [3], a Spanish plateau [4] or the American Midwest [5]. Recently (2003) Archer and Jakobsen showed that wind energy potential at 80 m altitude in the contiguous US ‘may be substantially greater than previously estimated’ because atmospheric stability was not taken into account: on average 80-m wind speeds appear to be 1.3 – 1.7 m/s higher than assumed from 10-m extrapolated wind speeds in a neutral atmosphere [6].

For wind turbine *noise* atmospheric stability has not been taken into account at all, leading to an underestimate of the level as well as the level fluctuations at locations and times when stability does occur. This has been argued theoretically as well as demonstrated in practice for the Rhede wind farm at the Dutch-German border [7,8]. The effect of increasing atmospheric stability is that higher sound levels occur more often than predicted by logarithmic extrapolation from 10 m observations, and that blade swish becomes more pronounced. The conclusion that this may be an important factor in noise annoyance is supported by a Swedish survey [9].

2. Wind profile models

Wind speed at altitude h_2 can be deduced from wind speed at altitude h_1 with a simple power law function:

$$V_{h2}/V_{h1} = (h_2/h_1)^m \quad (1)$$

Equation 1 is an engineering formula used to express the degree of stability in a single number (the shear exponent m), but has no physical basis. A physical model to calculate wind speed V_h at height h is:

$$V_h = (u_*/\kappa) \cdot [\ln(h/z_0) - \Psi] \quad (2)$$

where $\kappa = 0.4$ is von Karman’s constant, z_0 is roughness height and u_* is friction velocity, defined by $u_*^2 = \sqrt{[\langle uw \rangle^2 + \langle vw \rangle^2]} = \tau/\rho$, where τ equals the momentum flux due to turbulent friction across a horizontal plane, ρ is air density and u , v and w are the time-varying components of in-wind, cross-wind and vertical wind speed, with $\langle x \rangle$ the time average of x . The stability function $\Psi = \Psi(\zeta)$ (with $\zeta = h/L$) corrects for atmospheric stability. Monin-Obukhov length L is an important length scale for stability and can be thought of as the height above which thermal turbulence dominates over friction turbulence; at heights below L (if L is a, not very large, positive length) is the stable boundary layer. The following approximations for Ψ , mentioned in many text books on atmospheric physics (*e.g.* [10]), are used:

- ◆ In a stable atmosphere ($L > 0$) $\Psi(\zeta) = -5\zeta < 0$.
- ◆ In a neutral atmosphere ($|L|$ large $\rightarrow 1/L \approx 0$) $\Psi(0) = 0$, and equation 2 reduces to a simple logarithmic expression.
- ◆ In an unstable atmosphere ($L < 0$) $\Psi(\zeta) = 2 \cdot \ln[(1+x)/2] + \ln[(1+x^2)/2] - 2/\tan(x) + \pi/2 > 0$, where $x = (1-16 \cdot \zeta)^{1/4}$.

For $\Psi = 0$ equation 2 reduces to $V_{h,\log} = (u_*/\kappa) \cdot \ln(h/z_0)$, the widely used logarithmic wind profile. With this profile the ratio of wind speeds at two heights can be written as:

$$V_{h2,\log}/V_{h1} = \log(h_2/z_0)/\log(h_1/z_0) \quad (3)$$

For a roughness length of $z_0 = 2$ cm (pasture) and $m = 0,14$, the wind profiles according to equations 1 and 3 coincide within 2% for $h < 100$ m. For a non-neutral atmosphere equation 3

is not valid, though relevant publications (*e.g.* [11]) may suggest otherwise by not mentioning the limited applicability of equation 3.

3. The Cabauw site and available data

To investigate the effect of atmospheric stability on wind, and thence on energy and sound production, data are available from the meteorological research station of the KNMI (Royal Netherlands Meteorological Institute) at Cabauw in the western part of the Netherlands. The site is in open pasture for at least 400 m in all directions. Farther to the west the landscape is open, to the distant east are trees and low houses. More site information is given in [12, 13]. The site is considered representative for the flat western and northern parts of the Netherlands. These in turn are part of the low-lying plain stretching from France to Sweden. Meteorological data are available as half hour averages over several years. In the present paper data of the year 1987 are used. Wind speed and direction are measured at 10, 20, 40, 80, 140 and 200 m altitude. Cabauw data are related to Greenwich Mean Time (GMT); in the Netherlands the highest elevation of the sun is at approximately 12:40 Dutch winter time, which is 20 minutes before 12:00 GMT.

An indirect measure for stability is Pasquill class, derived from cloud cover, wind speed and position of sun (above or below horizon). Classes range from A (very unstable: less than 50% clouding, weak or moderate wind, sun up) to F (moderately to very stable: less than 75% clouding, weak or moderate wind, sun down). Pasquill class values have been estimated routinely at Dutch meteorological stations [14].

4. Reference conditions

To relate the meteorological situation to wind turbine performance, an 80 m hub height wind turbine with three 40 m long blades will be used as reference for a modern 2 to 3 MW, onshore wind turbine. To calculate electrical power and sound power level, specifications of the 78 m tall Vestas V80 – 2MW wind turbine will be used. For this turbine cut-in (hub height) wind speed is 4 m/s, and highest operational wind speed 25 m/s. This turbine has an ‘Optispeed’ sound reduction possibility to reduce sound power level (by blade pitch adjustment). We will present data for the highest (‘105.1dB(A)’) and lowest (‘101.0dB(A)’) sound power curve.

Most data presented here will refer to wind velocity at the usual observation height of 10 m and at 80 m hub height. Wind shear will be presented for this height range as well as the range 40 to 140 m where the rotor is. The meteorological situation is as measured in Cabauw in 1987, where roughness height is 2 cm. The year will be divided in meteorological seasons, with spring, summer, autumn and winter beginning on the first day of April, July, October and January, respectively.

We will consider four classes of wind speed derived from Pasquill classes A to F and shown in table 1: unstable, neutral, stable and very stable. In table 1 this is also given in terms of the shear exponent, but this is tentative as there is no fixed relation between Pasquill classification and shear exponent or stability function Ψ . This classification is in agreement with an earlier paper, though there typical mid-class values of m were given, not values at the boundaries between classes [7]. In our reference situation ‘very stable’ ($m > 0.4$) corresponds to a Monin-Obukhov length $0 < L < 100$ m, ‘stable’ ($0.25 < m < 0.4$) refers to $100 \text{ m} < L < 400$ m, near neutral to $|L| > 400$ m.

This is somewhat different from the Monin-Obukhov length based classification used by Motta *et al* [2] for a coastal/marine environment. Motta *et al* qualified $0 < L < 200$ m as very

stable, $200 \text{ m} < L < 1000 \text{ m}$ as stable and $|L| > 1000 \text{ m}$ as near-neutral, so they considered a wider range of conditions as (very) stable when compared to table 1.

Table 1: stability classes and shear exponent m

Pasquill class	name	shear exponent
A – B	(very – moderately) unstable	$m \leq 0.21$
C	near neutral	$0.21 < m \leq 0.25$
D – E	(slightly – moderately) stable	$0.25 < m \leq 0.4$
F	very stable	$0.4 < m$

5. Results: wind shear and stability

A. Height dependence of wind speed

In figure 1 the average wind velocities at altitudes of 10 m to 200 m are plotted versus time of day. Each hourly average is the average over all appropriate half hours in 1987. As figure 1 shows, the wind velocity at 10 m follows the popular notion that wind picks up after sunrise and abates after sundown. This is obviously a ‘near ground’ notion as the reverse is true at altitudes above 80 m. Figure 1 helps to explain why this is so: after sunrise low altitude winds are coupled to high altitude winds due to the vertical air movements caused by the developing thermal turbulence. As a result low altitude winds are accelerated by high altitude winds that in turn are slowed down. At sunset this process is reversed. In figure 1 also the wind velocity V_{80} is plotted as calculated from the measured wind speed V_{10} with equation 3 ($z_0 = 2 \text{ cm}$, equivalent to equation 1 with $m = 0.14$), as well as the shear exponent m calculated with equation 1 from the measured ratio V_{80}/V_{10} ($m_{h_1,h_2} = \ln(V_{h_2}/V_{h_1})/\ln(h_2/h_1)$). The logarithmically extrapolated V_{80} approximates actual V_{80} in daytime when the shear exponent has values close to 0.14. The prediction is however very poor at night time, when m rises to a value of 0.3, indicating a stable atmosphere. For the hourly progress of wind speeds large deviations from the average wind profile occur. This is illustrated in figure 2 for a week in

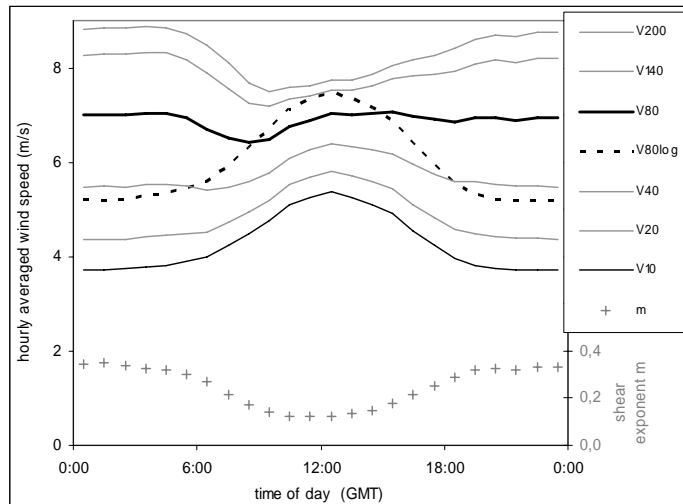


Figure 1: 1987 wind speed per hour GMT at different heights 10 to 200 m (solid lines, bottom to top); logarithmically extrapolated V80 (dotted line); and shear exponent $m_{10,80}$ (+)

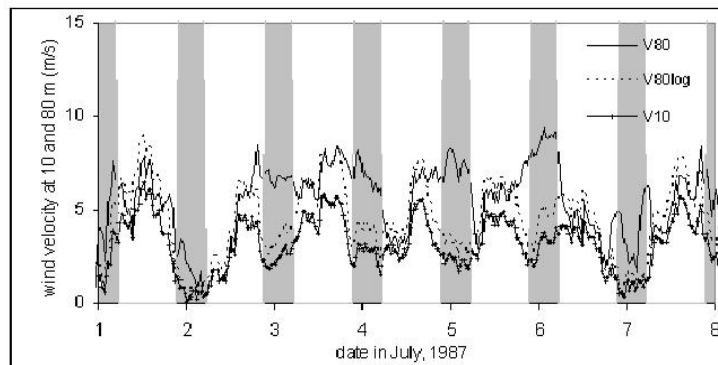
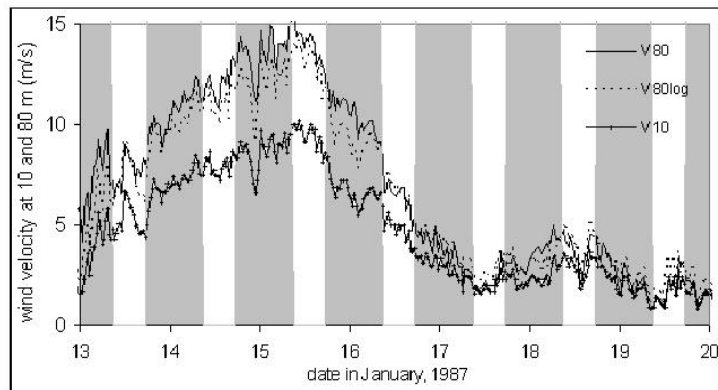
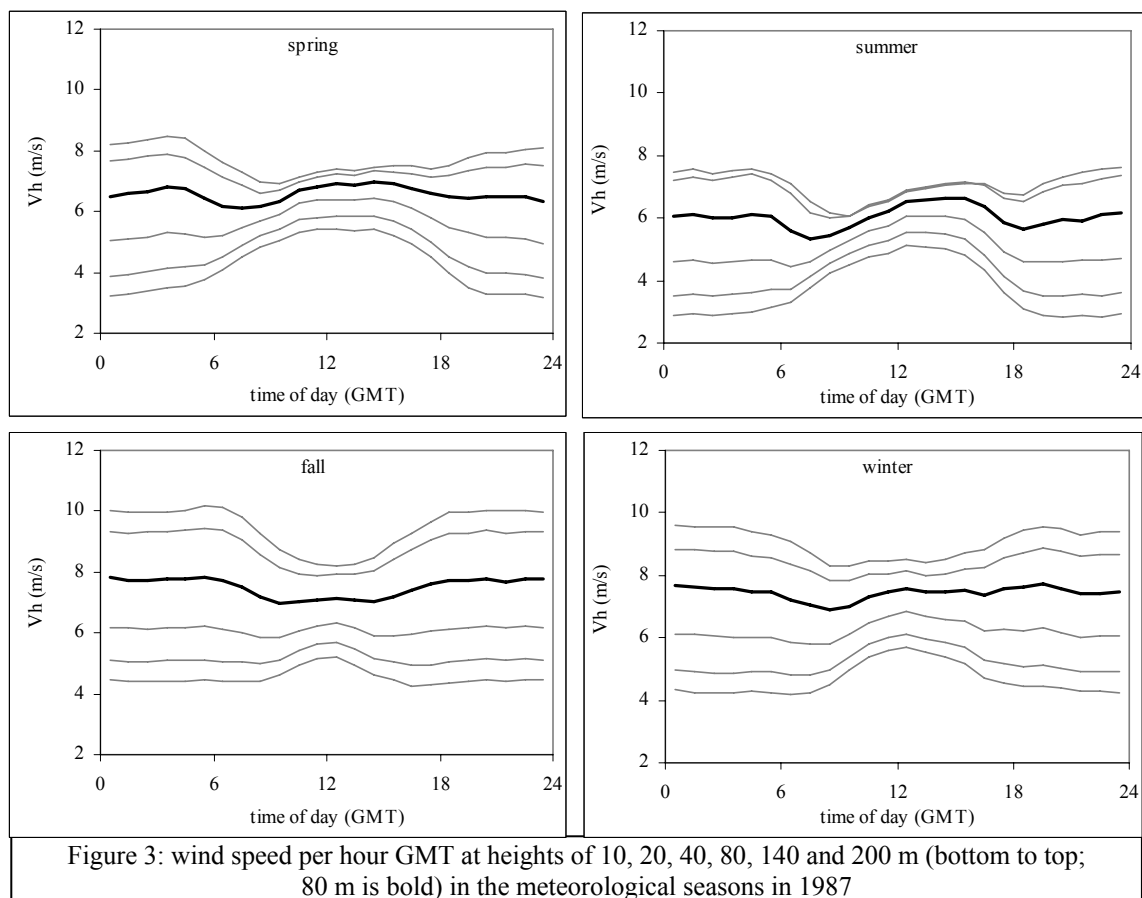


Figure 2: wind speed at 10 and 80 m (solid lines), and logarithmically extrapolated V80 (dotted line) over 7 days in January (top) and July (bottom); grey background: time when sun is down

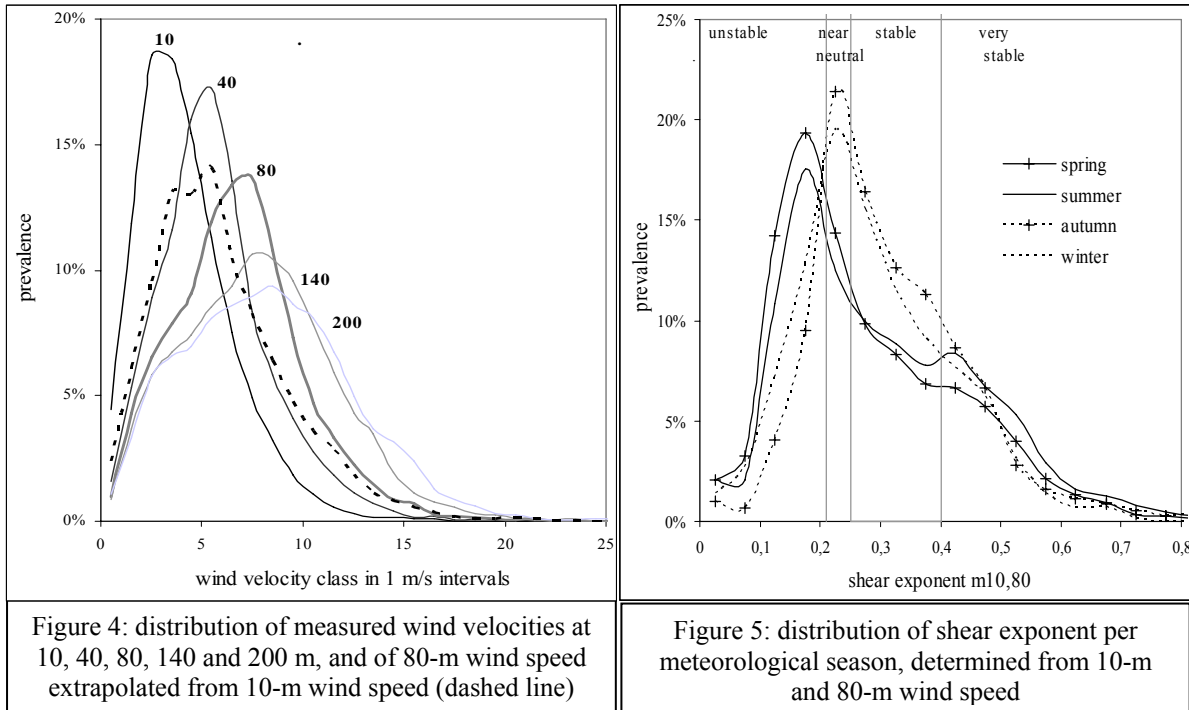
winter and a week in summer with measured V_{10} values and measured as well as logarithmically extrapolated V_{80} values. In the winter week in January 1987 ground and air were cold for a long time (below freezing point) with very little insolation. Temperature varied from night to day (diurnal minimum to maximum) with $7\text{ }^{\circ}\text{C}$ on the first day and $5\text{ }^{\circ}\text{C}$ or less on the next days, and the atmosphere was close to neutral with measured V_{80} more or less equal to the extrapolated V_{80} . In the summer week in July 1987 there was little clouding after the first two days; insolation was strong in daytime, and nights were 10 to $14\text{ }^{\circ}\text{C}$ cooler than days, resulting in a stable to very stable night time atmosphere. Here, night time wind speed was rather higher than predicted with the logarithmic wind profile.

In figure 3 wind velocities per hour are again plotted for different heights, as in figure 1, but now hourly averaged per meteorological season. In spring and summer differences between night and day seem more pronounced than in autumn or winter. In fall and winter, when nights are longer, wind speeds are higher.



In figure 4 the frequency distribution is plotted of the half-hourly wind speeds at five different heights. Also plotted is the distribution of wind speed at 80 m as calculated from the 10-m wind speed with the logarithmic wind profile (equation 3). Wind speed at 80 m has a value of $7 \pm 2\text{ m/s}$ for 50% of the time. For the logarithmically extrapolated wind speed this is $4.5 \pm 2\text{ m/s}$.

In figure 5 the frequency distribution is plotted of the shear exponent in the meteorological seasons, determined from the half-hourly 10-m and 80-m wind speeds. It shows that, relative to autumn and winter, instability occurs more often in spring and summer whereas a neutral or mildly stable atmosphere occurs less often. A very stable atmosphere occurs more often in summer: as summer nights are short this means that a relatively high percentage of night time hours has a stable atmosphere.



B. Shear and ground heat flux

Figure 6 shows how the shear exponent depends on the total heat flow to the ground for two different height ranges: 10 – 80 m in the left panel, 40 – 140 m in the right panel. The heat flow at Cabauw is determined from temperature measurements at different heights, independent of wind speed. Total heat flow is the sum of net radiation, latent and sensible heat flow, and positive when incoming flow dominates. For heat flows above approximately 200 W/m^2 the shear exponent m is between 0 and 0.21, corresponding to an unstable atmosphere, as expected. For low or negative (ground cooling) heat flows the range for m increases, extending from -1 up to +1.7. These values include conditions with very low wind speeds. If low wind speeds at 80 m height ($V_{80} < 4 \text{ m/s}$, occurring for 19.7% of the time) are excluded, with very few exceptions $m_{10,80}$ varies between 0 and 0.6, and $m_{40,140}$ varies between -0.1 and +0.8. A negative exponent means wind speed decreases with height. The data show that below 80 m this occurs in situations with little wind ($V_{80} < 4 \text{ m/s}$), but at

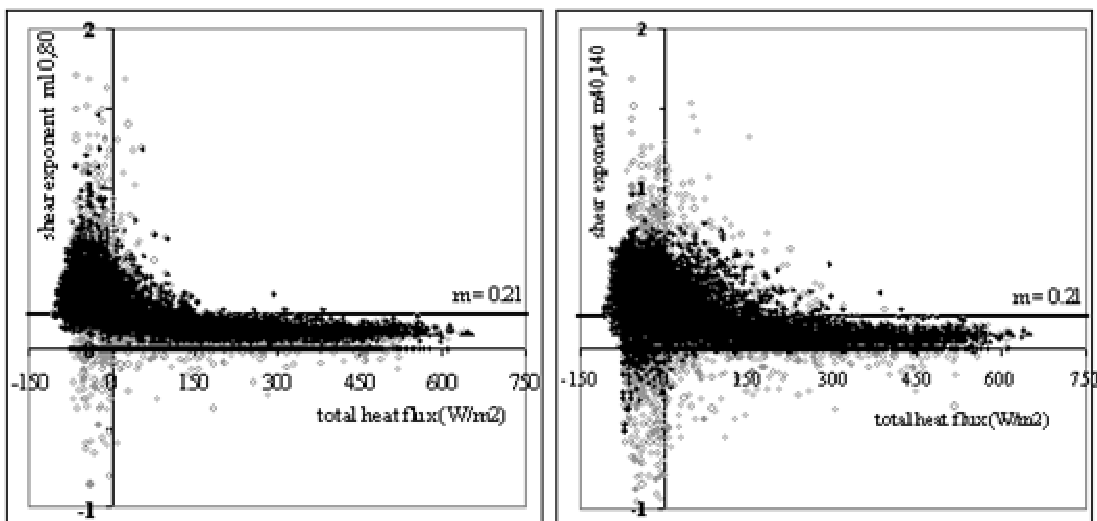


Figure 6: shear exponent m from wind speed gradient between 10 and 80 m (left) and 40 and 140 m (right) vs. total ground heat flux; grey circles: all data, black dots: $V_{80} > 4 \text{ m/s}$

greater heights also at higher wind speeds. In fact, V_{140} was lower than V_{80} for 7.5% of all hours in 1987, of which almost half (3.1%) when V_{80} was over 4 m/s. Such a decrease of wind speed with height occurs at the top of a ‘low level jet’ or nocturnal maximum; it occurs at night when kinetic energy of low altitude air is transferred to higher altitudes.

For $V_{80} > 4$ m/s both shear exponents ($m_{10,80}$ and $m_{40,140}$) are fairly strongly correlated (correlation coefficient 0.85), showing that generally there is no appreciable change between 10 m and 140 m. For low wind speeds ($V_{80} < 4$ m/s) both shear exponents are less highly correlated (c.c. 0.62).

C. Wind direction shear

When stability sets in the decoupling of layers of air also affects wind direction: the higher altitude wind more readily follows geostrophic wind and therefore changes direction while lower altitude winds are still influenced by the surface following the earth’s rotation. In the left panel of figure 7 the change in wind direction at 80 m relative to 10 m is plotted as a function of the shear exponent as a measure of stability. A positive change means a clockwise change (veering wind) at increasing altitude. The left panel shows the wind direction change from 40 to 140 m as a function of the shear exponent determined from the wind velocities at these heights. In both cases the average change from $m=0$ to $m=1$ is 30° (best least squares linear fit), but with a considerable variation (correlation coefficients are 0.44 and 0.29, respectively).

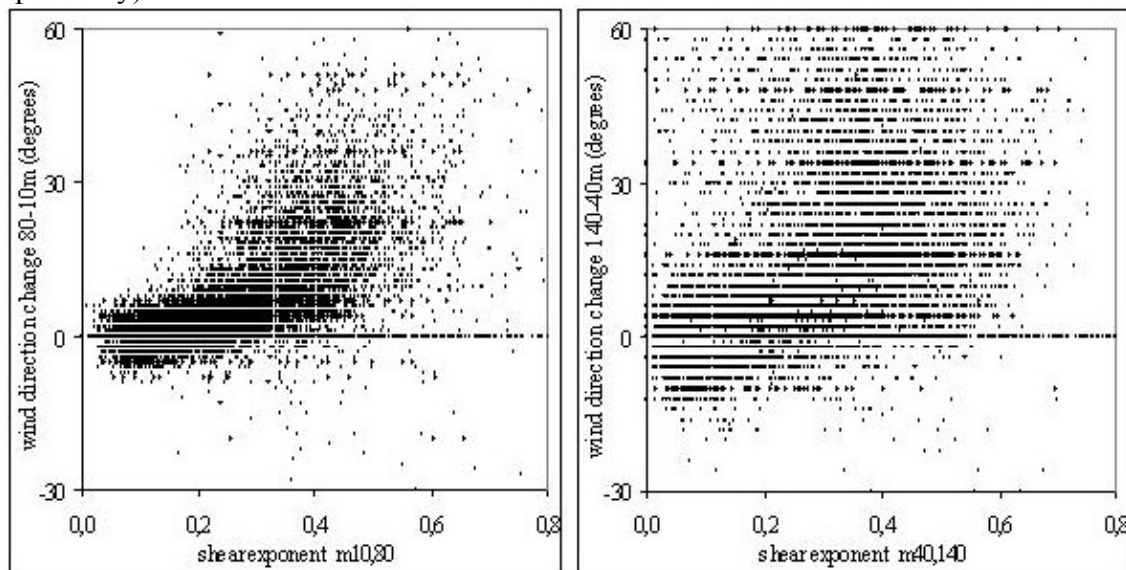


Figure 7: wind direction change between 10 and 80 m (left) and 40 and 140 m (right) vs. shear exponent between same heights

D. Prevalence of stability

In figure 8 the percentages are given that the atmosphere is unstable, neutral, stable or very stable (as defined in table 1) for 1987 as a whole and per meteorological season. Prevalence is given for heights from 10 and 80 m (upper panel figure 6) and for heights from 40 to 140 m (lower panel). The upper panel is in fact a summation over the four ranges of the shear exponent in figure 5. It appears that in autumn the atmosphere is most often stable, and least often unstable. In spring the opposite is true: instability occurs more often than stability. Overall the atmosphere up to 80 m is unstable ($m < 0.21$) for 47% of the time and stable ($m > 0.25$) for 43% of the time. At higher altitudes (40 to 140 m) percentages are almost the same: 44% and 47%, respectively. This means that for most of the daytime hours the atmosphere is

unstable, and for most of the night time hours stable. For the rest of the time, 9 to 10% of the time, the atmosphere is near neutral.

Climatological observations can put the Cabauw data in national perspective. In figure 9 the prevalence of Pasquill classes E and F (corresponding to approximately $m > 0.33$) are given as observed at 12 meteorological stations all over the Netherlands over the period 1940 - 1970 [14], ordered according to yearly prevalence. Three of the four lowest values are from coastal stations: Valkenburg is just behind the dunes on the Northsea coast, Vlissingen is at the Westerschelde estuarium and Den Helder is on a peninsula between the Northsea and the Waddensea. At Den Helder a stable atmosphere occurs for only 8% of the time per year, whereas at both other coastal stations this is 13% to 16% and at the other landward stations 15% to 20% of the time. At Cabauw a value of $m > 0.33$ occurs for 27% of the time, but this is based on measurements, not on Pasquill classification.

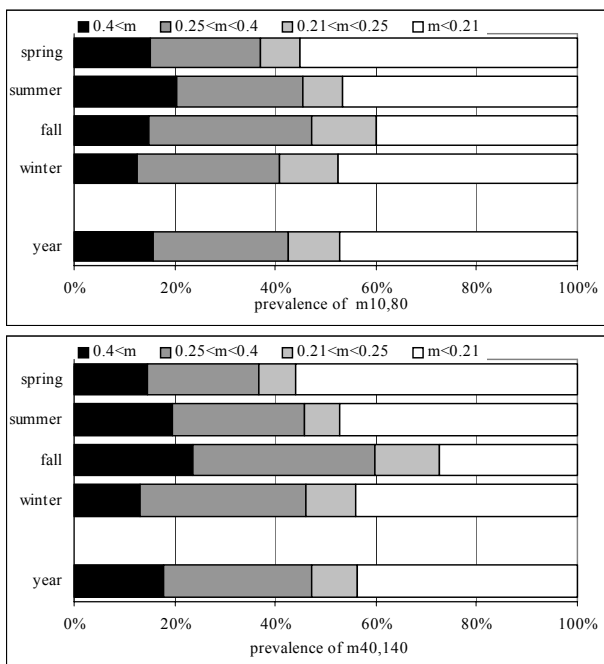


Figure 8: prevalence of shear exponent m between 10 and 80 m (top) and 40 and 140 m (bottom) in four seasons and year of 1987

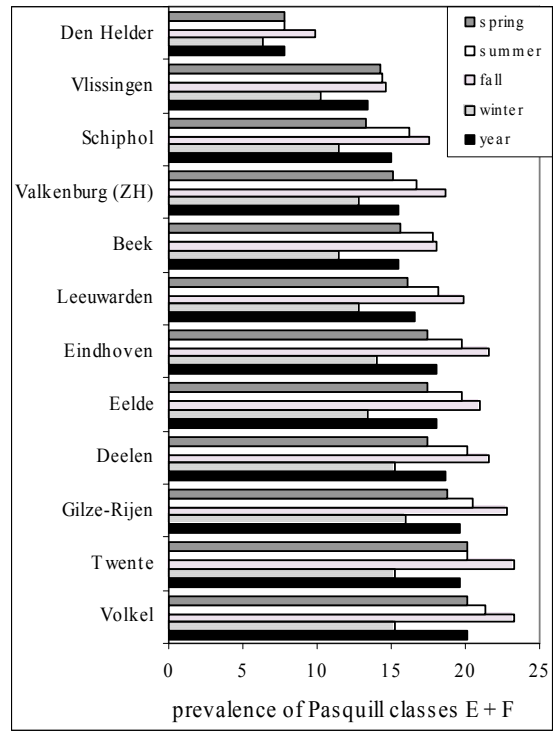


Figure 9: prevalence of observed stability (Pasquill classes E and F) per season and per year at 12 different Dutch stations over 30 years

6. Results: effects on wind turbine performance

A. Effect on power production

The effect of atmospheric stability can be investigated by applying the Cabauw data to a reference wind turbine, the Vestas V80-2MW [15, 16]. To calculate the electric power P_{80} as a function of wind speed V_h at hub height the factory ‘105.1dB(A)’ highest power (‘hp’) curve is approximated with a fourth power polynome:

$$P_{h, hp} = 0.0885 \cdot V_h^4 - 8.352 \cdot V_h^3 + 185.9 \cdot V_h^2 - 1272,5 \cdot V_h + 2897 \text{ kW} \quad (4)$$

which is valid for $4 < V_h < 14.3$ m/s. In figure 10 this fitted curve is plotted as diamonds on top of the manufacturer’s specification [15]. A fourth power relation is convenient to fit to the curvature at 12 m/s where maximum power is approached. For lower wind speeds ($V_h < 11$ m/s) the power curve can be fitted with a third power ($P_h = 1.3 \cdot V_h^3$) in agreement with the physical relation between wind power and wind speed.

For high wind speeds (>14.3 m/s; 2% of time) electric power is constant at 2000 kW, for low wind speeds (< 4 m/s; 20% of time) electric power is set to zero. Electric power can thus be calculated from real wind speeds as measured each half hour at 80 m height, or from 80-m wind speeds logarithmically extrapolated from wind speed at 10 m height. The result is plotted in figure 11 as an average power versus time of day P80,hp (averages are over all hours in 1987 at each clock hour). Actual power production appears to be more constant than estimated with extrapolations from 10-m wind speeds. When using a logarithmic extrapolation, daytime power production is overestimated, while night time power production is underestimated. The all year average is plotted with large symbols at the right side of the graph in figure 11: 598 kW when based on measured wind speed or a 30% annual load factor, 495 kW when based on extrapolated wind speed or a 25% load factor. In figure 11 also the wind power is plotted when the turbine operates in the lowest '101.0dB(A)' power curve (best fit $P_{h,lp} = 0.089 \cdot V_h^4 + 0.265 \cdot V_h^3 + 43.1 \cdot V_h^2 - 326.4 \cdot V_h + 749$ kW). The year average is now 569 kW, corresponding to a 28% annual load factor. The 4 dB lower sound level setting thus means that yearly power production has decreased to a factor 0.94.

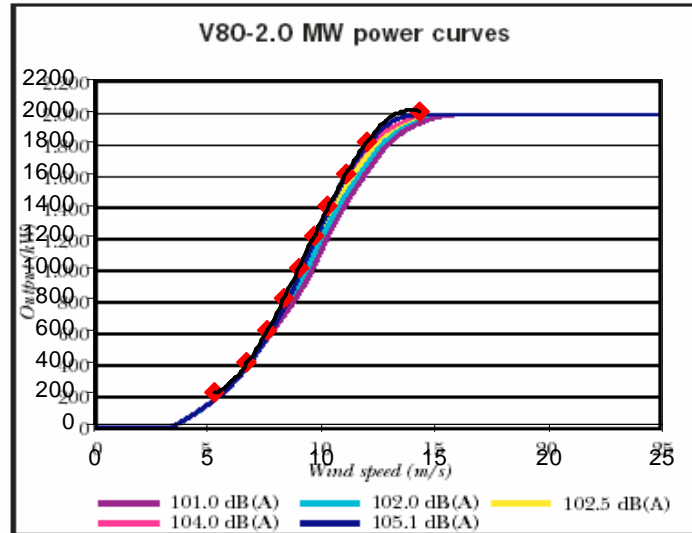


Figure 10: Vestas V80 power curves (lines) vs. hub height wind speed, and best fit to 105.1dB(A) curve (diamonds)

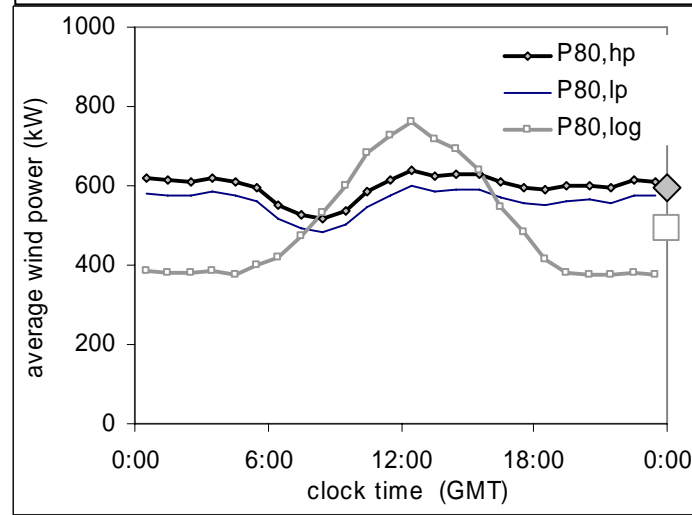


Figure 11: hourly averaged real and estimated wind power at 80 m height per clock hour in 1987

In the calculations it was implicitly assumed that the wind speed gradient over the rotor was the same as at the time the power production was determined as a function of hub height wind speed. In stable conditions however, the higher wind gradient causes a non-optimal angle of attack at the blade tips when the tips travel far below and above the hub. This will involve some loss, which is not determined here.

B. Effect on sound production

Figure 12 shows 'theoretical' sound power levels for the Vestas turbine [15, 16]; in fact for $V_h > 8$ m/s measured levels are somewhat less, for $V_h > 8$ m/s somewhat higher [16]. To calculate the sound power level L_W as a function of hub height wind speed V_h the factory '105.1dB(A)' power curve is approximated with a fourth power polynome:

$$L_W = -0.0023 \cdot V_h^4 + 0.146 \cdot V_h^3 - 2.82 \cdot V_h^2 + 22.6 \cdot V_h + 39.5 \text{ dB(A)} \tag{5}$$

for $4 < V_h < 12$ m/s and 107 dB(A) for $V_h > 12$ m/s. In figure 13 the result per clock hour is plotted when using actual and extrapolated (from 10 m) wind speeds. Averaged over the same hours over all 1987 sound power level in daytime is overestimated by appr. 0.5 dB, but at night underestimated by appr. 1.5 dB. In the '101.0dB(A)' low power curve setting (with a best fourth power polynomial fit $L_W = -0.022 \cdot V_h^4 + 0.781 \cdot V_h^3 - 9.98 \cdot V_h^2 + 55.3 \cdot V_h - 12.3$ dB(A)) sound power levels are 3 dB lower.

The year averages do not show the hourly differences between actual and logarithmically predicted sound power levels. This is shown in figure 14 for two days each in January and July 1987 (also shown in figure 2) where actual and predicted half-hour sound power levels are plotted as a function of 10-m wind speed. On both winter days and at wind speeds $V_{10} > 5.5$ m/s actual sound power agree within 1 dB with the predicted sound power, but at lower 10-m wind speeds actual levels are rather higher for most of the time. On both summer days 10-m wind speeds are lower than in winter, but sound power level is more often higher than predicted and can reach near maximum levels even at very low (2.5 m/s) 10-m wind speeds (when at

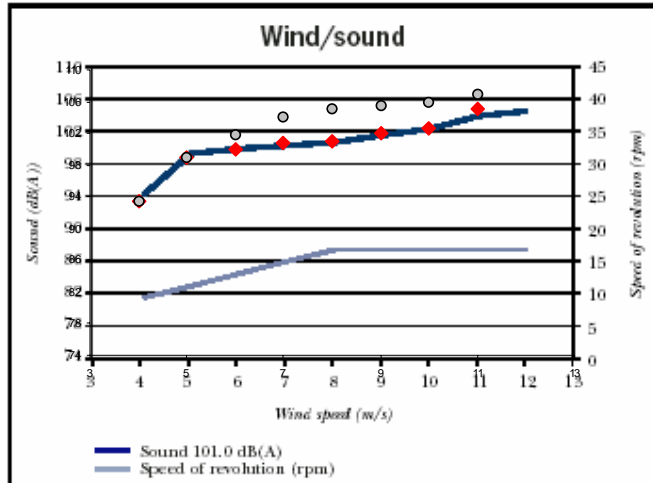


Figure 12: Vestas V80 sound power level at '101.0dB(A)' power curve (diamonds and upper line) and '105.1dB(A)' power curve (circles), and speed of rotation (lower line) vs. hub height wind speed

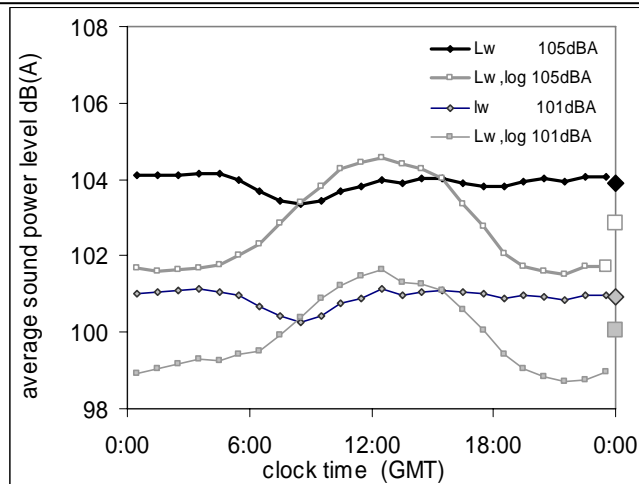


Figure 13: hourly averaged real and estimated (log) sound power level at '105.1dB(A)' and '101.0dB(A)' power curve settings

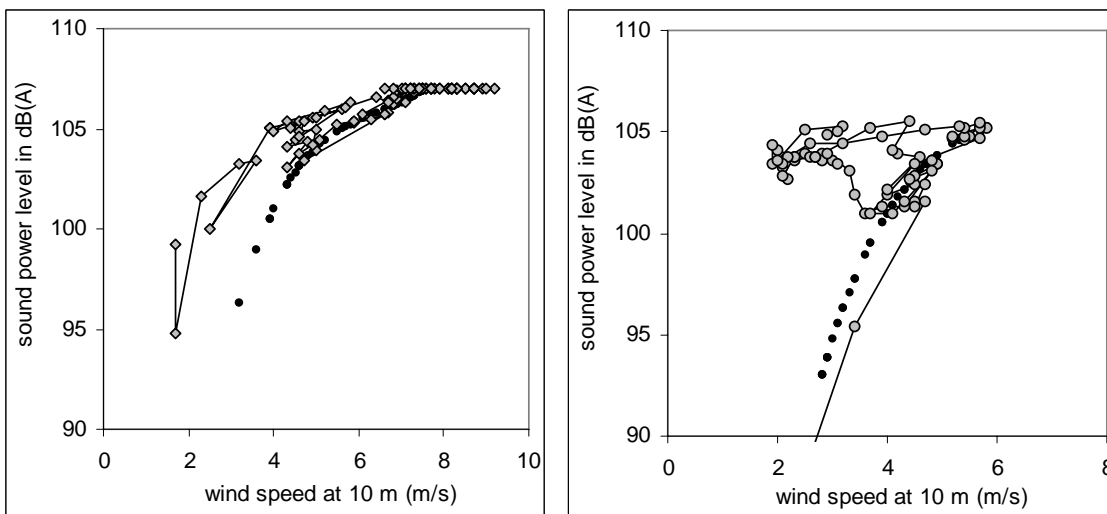


Figure 14: half-hourly progress of actual (grey diamonds) and logarithmically predicted (black dots) sound power level plotted vs. 10-m wind speed over 498 hours; left: January 13-14; right: July 2-3

ground level people will probably feel no wind at all). In these conditions residents in a quiet area will perceive the highest contrast: hardly or no wind induced sound in vegetation, while the turbine(s) are rotating at almost top speed. In these conditions also an increased fluctuation strength (strong ‘blade swish’) of the turbine sound will occur [8], making the sound more conspicuous.

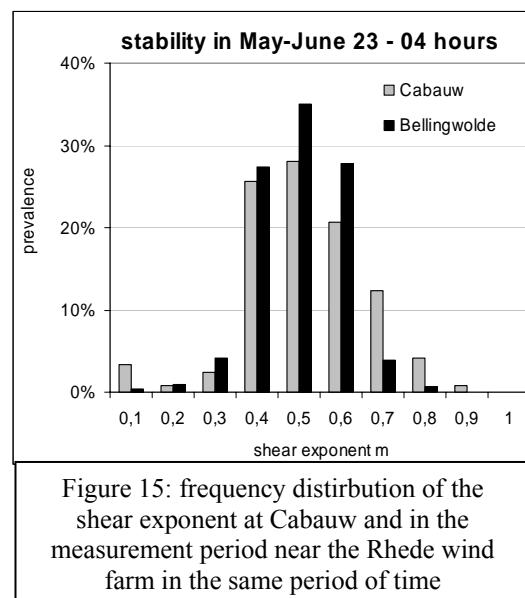
7. Other onshore results

Values of wind shear have been reported by various authors, and show similar results. Pérez et al [4] measured wind speeds up to 500 m above an 840 m altitude plateau north of Valladolid, Spain, for every hour over sixteen months. The shear exponent, calculated from the wind speed at 40 m and 220 m, varied from 0.05 to 0.95, but was more usual between 0.1 and 0.7. High shear exponents occurred more often than in Cabauw: $m > 0.48$ for 50% of the time. This is likely the result of the more southern position: insolation is higher, causing bigger temperature differences between day and night, and the atmosphere above the plateau is probably drier causing less reflection of infrared radiation at night. There was a distinct seasonal pattern, with little day-night differences in January, and very pronounced differences in July.

Smith et al [5] used data from wind turbine sites in the US Midwest over periods of 1.5 to 2.5 years and calculated shear exponents for wind speeds between a low altitude of 25 - 40 m and a high altitude of 40 – 123 m. At four sites the hourly averaged night time (22:00 – 6:00) shear exponent ranged from 0.26 to 0.44, in daytime from 0.09 to 0.19. The fifth station was exceptional with a day and night time wind shear below 0.17.

Archer et al [6] investigated wind speeds at 10 m and 80 m from over 1300 meteorological stations in the continental USA. No shear statistics are given, but for 10 stations the ratio V_{80}/V_{10} is plotted versus time of day. At all these stations the ratio is 1.4 ± 0.2 in most of the daytime and 2.1 ± 0.3 in most of the night time. Using equation 1, it follows that the shear exponent varies between 0.15 ± 0.07 and 0.35 ± 0.07 , respectively.

From the measurements in Bellingwolde at the Rhede wind farm [7] the shear exponent could be calculated from the 10-m and 100-m wind velocity, the latter determined from the sound level and the relation between sound power level and hub height (100 m) wind speed. This was done for all (892) five minute periods when wind turbine sound was dominant between 23:00 and 04:00 hours within the measurement period (May and June; location A in [7]). From the Cabauw data the same period and time was selected and all values of the half-hour shear exponent $m_{10,80}$ were determined. For both locations the resulting frequency distributions of the shear exponent are plotted in figure 15. The distributions are rather similar, though at Cabauw very high wind shear occurred more often than at Bellingwolde.



8. Conclusion

High altitude night time wind speeds have been underestimated by neglecting the influence of atmospheric stability. In recent years more attention is being paid to stability as it has a large impact on wind power production, especially at the height of modern, tall turbines.

Results from various landward areas show that the shear exponent in the lower atmospheric boundary layer (< 200 m) in daytime is 0.1 to 0.2, corresponding to a wind speed ratio V_{80}/V_{10} of 1.25 to 1.5. This wind profile is comparable to the profile predicted by the well-known logarithmic wind profile for low roughness lengths (low vegetation).

At night the situation is quite different and in various landward areas the shear exponent has a much wider range with values up to 1, but more usually between 0.25 and 0.7. Near the Rhede wind farm, where long term measurements have been performed [7, 8], the same range of wind shear occurred, showing that the site indeed was suitable to study the effect of atmospheric stability on wind turbine performance and representative for many other locations.

A shear exponent $0.25 < m < 0.7$ means that the ratio V_{80}/V_{10} varies between 1.7 and 4.3. High altitude wind speeds are thus (much) higher than expected from logarithmic extrapolation of 10-m wind speeds.

The underestimate of high altitude night time wind speed has been compensated partly by the overestimate of high altitude daytime wind speed, which partly explains why, until recently, atmospheric stability was not been recognized as an important determinant for wind power. To assess wind turbine electrical and sound power production the use of a neutral wind profile should be abandoned as it yields data that are not consistent with reality.

References

- 1: Troen and E.L. Petersen: "European Wind Atlas", Risø National Laboratory, Roskilde (1989)
- 2: M. Motta, R. J. Barthelmie, P. Vølund: "The influence of non-logarithmic wind speed profiles on potential power output at Danish offshore sites", *Wind Energy* 8, 219 – 236 (2005)
- 3: A. Smedman, U. Högström and H. Bergström: "Low level jets – A decisive factor for off-shore wind energy siting in the Baltic Sea", *Wind Engineering* 20 (3), 137-147 (1996)
- 4: I.A. Pérez, M.A. García, M.L. Sánchez and B. de Torre: "Analysis and parameterisation of wind profiles in the low atmosphere", *Solar Energy* 78 (6), 809 (2005)
- 5: K. Smith, G. Randall, D. Malcolm, N. Kelly and B. Smith: "Evaluation of wind shear patterns at Midwest wind energy facilities", National Renewable Energy Laboratory NREL/CP-500-32492, USA (2002)
- 6: C.L. Archer and M.Z. Jacobson: "Spatial and temporal distributions of U.S. winds and wind power at 80 m derived from measurements", *J. Geophys. Res.* 108 (D9) (2003)
- 7: G.P. van den Berg: "Effects of the Wind Profile at Night on Wind Turbine Sound", *J. Sound Vib.* 277 (4-5), 955-970 (2004)
- 8: G.P. van den Berg: "The beat is getting stronger: the effect of atmospheric stability on low frequency modulated sound of wind turbines", *Journal of Low Frequency Noise, Vibration And Active Control*, Vol. 24 (1), 1-24 (2005)
- 9: E. Pedersen and K. Persson Waye: "Perception and annoyance due to wind turbine noise – a dose-response relationship", *J. Acoust. Soc. Am* 116 (6), 3460-3470 (2004)
- 10: J.R. Garrat, "The atmospheric boundary layer", Cambridge University Press (1992)
- 11: IEC International Standard 61400-11, Wind Turbine Generator Systems - Part 11: Acoustic Noise Measurement Techniques, IEC 61400-11:1998(E)
- 12: www.knmi.nl/research/atmospheric_research/pagina_1_Cabauw.html
- 13: Van Ulden, A.P. and J. Wieringa, "Atmospheric boundary-layer research at Cabauw", *Boundary-layer Meteorology*, 78, 39-69 (1996)
- 14: 6: "Klimatologische gegevens van Nederlandse stations; no.8: Frequentietabellen van atmosferische stabiliteit", ("Climatological data from Dutch stations; no. 8: frequency tables of atmospheric stability"), KNMI, De Bilt (1972)
- 15: Vestas brochure, "V80-2.0 MW", 10/03
- 16: Jorgensen HK, "Wind turbine power curve and sound – measurement uncertainties", REGA (Renewable Energy Generators Australia Ltd) Forum 2002, Coffs Harbour, Australia (2002)

**First International Meeting
on
Wind Turbine Noise: Perspectives for Control
Berlin 17th and 18th October 2005**

**Public opinion of a proposed wind farm situated close
to a populated area in New Zealand: results from a
cross-sectional study**

Charmaine A. WATTS

Faculty of Health and Environmental Sciences, Auckland University of
Technology, Private Bag 9006, Auckland 1020, NEW ZEALAND.

Email: c.watts@ps.gen.nz

Philip J. SCHLUTER

Faculty of Health and Environmental Sciences, Auckland University of
Technology, Private Bag 9006, Auckland 1020, NEW ZEALAND.

Email: philip.schluter@aut.ac.nz

Roger WHITING

Faculty of Health and Environmental Sciences, Auckland University of
Technology, Private Bag 9006, Auckland 1020, NEW ZEALAND.

Email: roger.whiting@aut.ac.nz

Correspondence and reprints:

Charmaine Watts

282 Gleeson Rd

Waipipi

Auckland

NEW ZEALAND

Tel: +64-9-235 5082

Mob: +64-027 679 4044

Email: c.watts@ps.gen.nz

Abstract

Background: In 2003, electricity generating company, Genesis Energy, began informing the public of their intention to apply for consent to build a wind farm on the Awhitu Peninsula coast, New Zealand, as they are obliged to do under New Zealand's Resource Management Act 1991. A number of community groups claiming to represent the majority of the community opposed the application and in September 2004 consent was declined.

Aim: This study was undertaken to investigate the attitudes of members within the local community to the proposed wind farm.

Methods: A postal survey with pre-paid return envelopes was mailed to a sample of 500 Franklin residents, systematically selected from the local 2004/2005 telephone directory. Two articles appeared in the local free Franklin County News informing and prompting selected participants to return completed questionnaires.

Results: 40 questionnaires were returned undelivered. Of the remaining 460, completed questionnaires were returned from 211 (46%). Most, 145 (70%), residents supported a wind farm being built in their area, with 35 (17%) neutral and only 28 (13%) against the farm. There was no difference in attitude between gender ($P=0.49$), age ($P=0.71$) or proximity to the farm ($P=0.69$). Attitudes varied little to questions eliciting attitudes to the visual impact of the wind turbines from participants' properties. Noise pollution was listed as the main perceived disadvantage for 44 (21%) respondents, ranking behind visual unsightliness (24%) but ahead of wildlife disadvantages (15%), location (12%) and space requirements (11%).

Conclusion: Contrary to the assertions of several lobby groups, results of this study suggest that in fact the majority of the residents in the area are in favour of the wind farm being built. However, perceptions about noise pollution are real for a sizeable proportion of the community. Education is required to alleviate this and other concerns before wind farms will be welcomed into Franklin and other similar local communities.

Keywords: Wind farm, community attitudes, cross-sectional study, noise pollution, perception

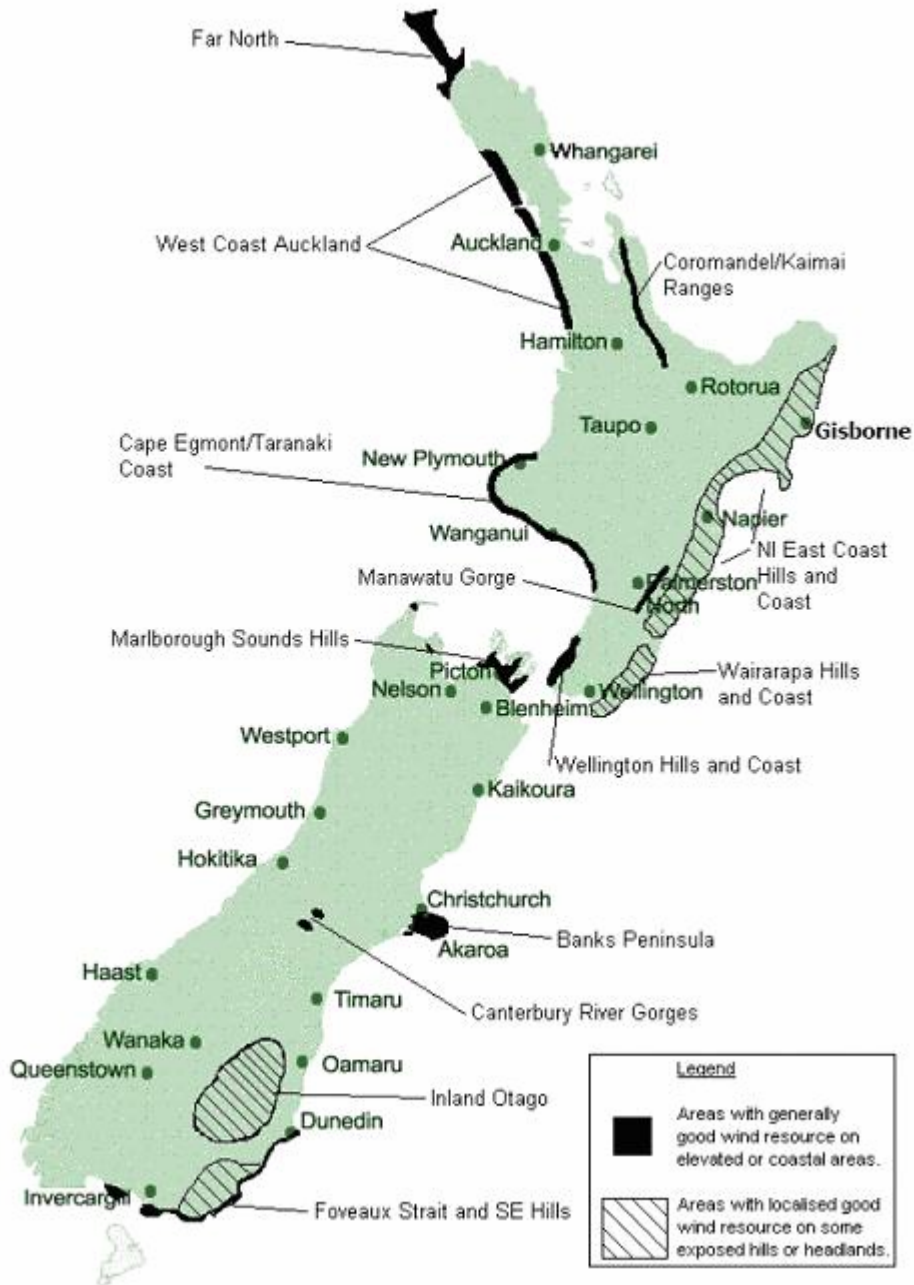
Introduction

The demand for electricity in New Zealand has steadily increased since 1974, particularly in the North Island north of Lake Taupo¹. Since the commissioning of the Clyde hydroelectric power station in 1993, thermal plants have provided the bulk of the increase in electricity generation required². In order to meet the current and predicted demand growth in electricity demand rates, it is estimated that 150 to 320 megawatts (MW) of new electricity generation capacity will be required annually¹. Advances in energy demand efficiencies and savings through better electricity utilization are included in the estimate. This increased demand has prompted efforts throughout New Zealand to seek new and alternative generation options. These efforts include new wind farms in the Tararua Ranges, possible re-commissioning of the oil fired Marsden Power Station and various other projects³. In 2004, Meridian Energy, New Zealand's largest electricity generator⁴, abandoned its plans to develop a hydro generation scheme in the South Island (Project Aqua), previously considered as New Zealand's largest new renewable generation option⁵. Instead, Meridian Energy began focusing on developing two wind farms, one in each of the North and South Islands of New Zealand, with a total capacity of approximately 280 MW⁶. This choice was made because New Zealand has a significant wind energy resource, and is well suited to wind energy development with relatively strong winds throughout the year (see Figure 1)⁷.

Wind farms are a relatively new phenomenon to New Zealand and there is little statistical information on public opinion on these farms and even less on public opinion on the proposed development of such farms. To date there are two studies which have explored the public opinion of New Zealanders to wind energy and the existing Tararua wind farm^{8,9}. The Omnibus Wind Survey in 2004 found that wind power is the public's preferred generation option to meet New Zealand's future electricity need, with two thirds of respondents expressing some level of support for building a wind farm in their local area⁸. The main reason cited for favouring the building of a local wind farm was the perceived benefit for the environment. Conversely, the main reason cited for opposing the building of a local wind farm was the perceived visual and auditory impact. Another New Zealand study found that arguments used to oppose the Tararua Wind Farm were predominantly anticipated adverse effects such as a noise, electromagnetic interference (EMI), visual intrusion and land devaluation⁹. These National studies compare with International studies, where the most prominent long-term impact that people would consider a problem is the visual effect on the landscape¹⁰⁻¹². In Scotland, twice as many people think a local wind farm has had a positive impact as think it has a negative impact¹⁰. In a UK community, three quarters of local residents support the wind farm, the most frequently mentioned benefit is that the wind farm is good for the environment and non-polluting¹¹. While US study of a yet to be developed wind farm in the Appalachian Mountains found that Western North Carolinians were favourably disposed toward the development of a wind energy industry, for those that opposed a wind energy

industry the overwhelming problem noted was aesthetics¹².

Figure 1. Locations in New Zealand believed to be most suitable for wind energy development⁷.



In New Zealand, an area within the Franklin district, situated on West Coast Auckland, a second site (known as the Awhitu wind farm site) was identified as having significant wind energy generation potential and ideally located being proximal to Auckland, a heavy electricity using centre. The Awhitu wind farm proposed by Genesis Energy is located within a privately owned farm,

approximately 6km west of the township of Waiuku. The 19 wind turbine structures will have a maximum overall height (including the rotor) of 90 metres from the base of the structure and a maximum hub height (excluding the rotor) of 62 metres from the base of the structure. The turbines will have a nominal capacity of between 600 and 1500 kilowatts each, while the total installed capacity for the new development is expected to be within the range of 15 to 25 MW. An assessment of environmental effects from the Awhitu wind farm was submitted by Genesis Energy at the resource and subsequent environment court hearings, these effects included, visual, natural character, traffic, noise, archaeological, radio service, property value, birds, turbine safety, public health and effects on animals¹³. Individuals and groups opposing the wind farm, made submissions on environmental effects which included cultural (tangata whenua), bird kill, erosion, shadow flicker, traffic, radio services, decommissioning, health, noise and emissions¹⁴. One key element of the submissions was the claim that a significant majority of the local population opposed the construction of the wind farm¹⁵. As a consequence of these submissions, the consent was declined in September 2004.

Upon close scrutiny, the surveys purporting to be statistical studies reflecting public opinion on wind farms¹⁶⁻¹⁸ appeared to be seriously flawed and likely to produce biased findings. Antidotal evidence suggested that the pattern of response was likely to be substantially different from that tabled at the resource and Environment Court hearing. In an effort to fully understand public opinion on this matter, this study was instigated. In particular, using robust statistical methods and sound epidemiological principles we sought to measure public opinion on the proposed Awhitu wind farm from residents living in close proximity to the site.

Methods

Study population

Franklin district residents listed in the Franklin 2004/2005 local telephone directory.

Study design

A cross-sectional survey of 500 sampled residents was undertaken. Residents were selected using a randomized systematic approach. Specifically, the directory contains approximately 16,000 phone and address listings. A starting point page number was randomly selected using random number tables, and then every 30th residential listing was selected for the survey. A covering letter describing the survey (and giving a \$50 dollar incentive to return the completed questionnaire), the questionnaire and the self-addressed prepaid envelopes were mailed to the 500 selected residents. Two articles appeared in the local free Franklin County News informing and prompting selected participants to return completed questionnaires, one timed when the questionnaire were initially mailed and the second two-weeks later. Any household resident over the age of 18

years was invited to complete the questionnaire.

Survey instrument

The questionnaire contained seven groups of questions relating to wind farm attitudes and perceptions, in addition to gender and age range (elicited in five age-bands), over two pages. Among the questions, participants were asked if that had visited a wind farm with more than one turbine (Yes/No), how they felt about a wind farm being built in the Waiuku area (responses on a 5-point Likert scale from strongly against to strong in favour), the perceived main advantages of the wind farm: environmental friendliness, low cost, renewable resource, employment opportunities, well-suited to New Zealand (each option having a No/Yes/Not sure option and room for additional comments), the perceived main disadvantages of the wind farm: unsightly, requires too much space, noise pollution, disadvantage to wildlife, bad location (each option having a No/Yes/Not sure option and room for additional comments), feelings about the Waiuku wind farm under the following conditions (with responses on a 5-point Likert scale from strongly against to strongly in favour): If you can't see or hear the wind turbines from your property; If you can't hear the wind turbines but can see them as distinct features from your property; If you can't hear the wind turbines but can see them as an obvious feature from your property. Lastly, respondents were asked "which of the following factors has most influenced your views about the proposed Awhitu wind farm?" with response options: environmental friendliness, low cost, renewable resource, employment opportunities, well-suited to New Zealand, unsightly, requires too much space, noise pollution, disadvantage to wildlife, bad location, other.

Statistical analyses

Frequencies and percentages were reported for all categorical variables. Comparisons of categorical variables between groups was made using Fisher's exact test. A significance level of $P\text{-value} < 0.05$ was used to define statistical significance. All data was analyzed using statistical software package MINITAB Release 14.

Ethics

The local AUT Research Ethics Committee provided clearance for this study (clearance number: 04-153).

Results

Overall, 500 household residents were posted questionnaires but 40 (8%) were returned by New Zealand Post with the message return to sender. Of the remaining 460, completed questionnaires were returned from 211 (46%). Responder demographics included 98 (49%) females and had age distribution 18-25 years, 7 (3%); 26-39 years, 29 (14%); 40-55 years, 76 (38%); 55-70 years, 60 (30%); and 70+ years, 29 (14%). Only 50 (24%) had ever visited a wind farm with more than one turbine in the past.

Where possible, the data were partitioned by whether respondents resided outside or within the Waiuku region, the vicinity of the proposed farm. Sufficient contact details were available from 149 survey forms to allocate their geographical location, 107 outside the Waiuku region and 42 from within Waiuku.

Attitudes to a wind farm being built in the Waiuku area

The distribution of Franklin resident's attitudes towards the proposed wind farm being built in the Waiuku area appears in Table 1. Overall, 145 (70%) Franklin residents support a wind farm being built with the majority 116 (56%) declaring strong support. A further 35 (17%) of Franklin residents were neutral (neither for nor against) and only 28 (13%) residents were against the building of the proposed farm.

Table 1. Distribution of response to the question "How do you feel about a wind farm being built in the Waiuku area?" and partitioned by whether respondents lived within or outside the Waiuku region.

Response	Overall	Resident outside	Resident within
	(N=208)	Waiuku region	Waiuku region
	n (%)	(N=105)	(N=42)
	n (%)	n (%)	n (%)
Strongly against	20 (10)	8 (8)	6 (14)
Weakly against	8 (4)	4 (4)	2 (5)
Neutral	35 (17)	16 (15)	5 (12)
Weakly in favour	29 (14)	18 (17)	5 (12)
Strongly in favour	116 (56)	59 (56)	24 (57)

There was no difference in the distribution of attitude between responders across gender ($P=0.49$) or age ($P=0.71$) groups. Moreover, no statistically significant difference emerged in the pattern of response from those participants residing within or outside the Waiuku area ($P=0.69$), see Table 1.

Attitudes to seeing and hearing wind turbines from respondent's properties

Participants were next asked to respond to a series of scenarios pertaining to their attitude about seeing and hearing wind turbines from their property. Table 2 summarizes the pattern of response to these questions.

Many Franklin residents declared that they supported a wind farm in the Waiuku area, even as an obvious feature from their property, 126 (62%); with a majority 91 (45%) declaring strong support. A further 37 (18%) of Franklin residents were neutral (neither for nor against) a wind farm as an obvious feature and only 40 (20%) respondents were against. Again, there were no significant differences in the pattern of response for any of these three scenarios across gender, age, or place of residence (all $P>0.05$).

Table 2. Pattern of response for attitudes to a wind farm being built in the Waiuku area under three auditory and visual scenarios.

	Cannot see or hear wind turbines from your property (N=205)	Cannot hear but see in the distance wind turbines from your property (N=204)	Cannot hear but see as an obvious feature wind turbines from your property (N=203)
	n (%)	n (%)	n (%)
Strongly against	16 (8)	21 (10)	25 (12)
Weakly against	6 (3)	7 (3)	15 (7)
Neutral	35 (17)	34 (17)	37 (18)
Weakly in favour	21 (10)	27 (13)	35 (17)
Strongly in favour	127 (62)	115 (56)	91 (45)

Respondents perceived advantages and disadvantages of the proposed wind farm
Tables 3 houses the pattern of response to a list of perceived advantages and disadvantages associated with the Awhitu wind farm.

Table 3. Pattern of response to participants perceived main advantages and disadvantages of the proposed Awhitu wind farm.

	No n (%)	Yes n (%)	Not sure n (%)	No response n (%)
<i>Perceived main advantages</i>				
Environmental friendliness	18 (9)	161 (76)	16 (8)	16 (8)
Low cost (comparable to coal/oil/gas)	16 (8)	137 (65)	43 (20)	15 (7)
Renewable resource	6 (3)	173 (82)	15 (7)	17 (8)
Increased employment opportunities	43 (20)	83 (39)	57 (27)	28 (13)
Well suited to New Zealand	10 (5)	164 (78)	20 (9)	17 (8)
<i>Perceived main disadvantages</i>				
Unightly	108 (51)	51 (24)	31 (15)	21 (10)
Requires too much space	121 (57)	24 (11)	36 (17)	30 (14)
Noise pollution	91 (43)	44 (21)	55 (26)	21 (10)
Disadvantages to wildlife	118 (56)	32 (15)	38 (18)	23 (11)
Bad location	117 (55)	26 (12)	36 (17)	32 (15)

Respondents ranked the renewable resource advantages of the proposed wind farm the highest, 173 (83%), closely followed by the suitability of such farm to New Zealand, 164 (78%), and the perceived environmental friendliness, 161 (76%). Unsightliness was the highest ranked main perceived disadvantage of the proposed wind farm for nearly a quarter of respondents, 51 (24%), followed by noise pollution, 44 (21%). Only 26 (12%) residents thought the location of an Awhitu wind farm was a main disadvantage against 117 (55%) residents did not consider this a main disadvantage. Again, there were no significant differences in

the pattern of response across gender, age, or location of residence in relation to the Waiuku area (all $P > 0.05$).

Discussion

A clear majority (70%) of Franklin residents support the proposed wind farm in the Waiuku area. Indeed, only 13% of residents were opposed to the proposal. These results are consistent with a recent Environmental Efficiency Conservation Association (EECA) nation-wide omnibus survey⁸ which found that 60% of respondents were in favour of having a wind farm built in their local area. Sub-group analysis revealed no statistically significant or important differential pattern in the support of the wind farm across gender, age categorization or whether respondents lived in the Waiuku area (close in proximity to the proposed farm) or outside this area. The sub-group analyses are important in determining whether the wind farm support is general or sex, age or proximity specific.

The majority of Franklin residents (62%) support a wind farm in the Waiuku area even if it was an obvious feature from their properties. A specific question about noise being heard was not included in the scenarios determining attitudes to seeing and hearing wind turbines, as the likelihood of noise being generated by the Awhitu wind farm was considered negligible. Leventhall's report¹⁹ on low frequency noise from wind turbines with special reference to the Awhitu wind farm, describes the noise associated with wind turbines and the negligible noise anticipated with the proposed Awhitu wind farm in particular¹³. However, nearly a quarter of respondents considered noise pollution to be a perceived problem. This could be due to perception of noise pollution associated with wind turbines rather than actual noise from wind turbines being a problem especially as the majority of respondents (76%) had not visited a wind farm in the past. It might be anticipated that if the wind farm is granted resource consent then the level of respondents who consider noise pollution associated with wind turbines will drop. Education on the 'nature' of noise from wind turbines and how people hear 'noise' would go some way to helping people understand that noise from today's modern turbines is negligible.

The main advantage of an Awhitu wind farm identified by 82% of Franklin residents was that it is a renewable resource. This contrasts with the Omnibus Survey findings where 25% of respondents considered this the main benefit of wind power⁸. Franklin residents also thought an Awhitu wind farm was well suited to New Zealand, along with environmental friendliness being identified as the second main advantage with 78% and 76% respectively. Groups opposing wind farms often ascribe the attributes of unsightliness, noise pollution and disadvantages to wild life. However in this study the majority of Franklin residents did not associate this with the Awhitu wind farm. In addition Franklin residents did not consider the space required or the location to be issues.

Strengths of this study include the methodological rigor in design, using robust

probability sampling methods and the relatively large yet targeted sample size. However, the study also suffers from weaknesses including a moderate response rate (46%). It may be argued that this response rate implies that the findings lack representation and cannot be generalized across the population. We assert that this is not the case. The age and gender distributions of the respondents have good representation and are similar to the demographics determined from the 2001 Census for this region. Moreover, individuals with stronger opinions, either negative or positive, tend to be more motivated to respond surveys and thus it can be assumed that non-responders are likely to be more neutral²¹. The positive pattern of response was emphatically from our findings and consistent with those previously determine⁸. Thus, we argue that these results have both utility and can be generalized across the population²² and are important in describing the public's perception of wind farms.

Further research will examine the change in attitudes of the Franklin residents should the proposed wind farm gain resource consent and be constructed. We intend to investigate changes in the public's perception over time to determine whether the strong support garnered in this survey is further strengthened or if it fluctuates in some way.

In conclusion, the results of this survey indicate that the majority of residents support the construction of the wind farm in the area even when it is an obvious feature from their property. The majority of Franklin residents feel the advantages of a wind farm are its status as a renewable resource, environmental friendliness, low cost, well suited to New Zealand and employment opportunities. The majority of Franklin residents do not believe that the Awhitu wind farm is unsightly, requires too much space, produces noise pollution, and is disadvantageous to wildlife or that it is a bad location. The difference between the results of this survey and those of a convenience sample presented to the resource hearing and the Environment Court emphasizes the need for rigorous statistical conduct and review before statements about a community's 'majority view' can be appropriately declared.

Acknowledgements

We would like to thank Neil Binnie and Owen Young for their assistance in designing the questionnaire.

References

1. Leyland B. *New Zealand's Load Growth from 1974 and Expected Demand to 2025*. Auckland: Centre for Advanced Engineering, University of Auckland; 2004.
2. Ministry of Economic Development. Energy Database 2005. *Ministry of Economic Development*. Available at: www.med.govt.nz/ers/en_stats/edfonlin/edfjan2005/index.html. Accessed 28 July, 2005.
3. Ministry of Economic Development. Submission on the Marsden B Power

- Station Re-Powering Project. *Ministry of Economic Development*. Available at: www.med.govt.nz/ers/environment/energy-submissions/marsden/marsden-02.htm. Accessed 28 July, 2005.
4. Meridian Energy. About Us. *Meridian Energy*. Available at: <http://www.meridianenergy.co.nz/aboutus/default.htm>. Accessed 29 July, 2005.
 5. Meridian Energy. Project Aqua at a Glance. *Meridian Energy*. Available at: www.meridianenergy.co.nz/ProjectAqua/project+aqua+at+a+glance/default.htm. Accessed 28 July, 2005.
 6. Meridian Energy. Wind Power. *Meridian Energy*. Available at: <http://www.meridianenergy.co.nz/WindProjects/>. Accessed 28 July, 2005.
 7. Environmental Efficiency Conservation Association (EECA). *A Review of New Zealand's Wind Energy Potential to 2015*. Wellington: EECA; 2001.
 8. Environmental Efficiency Conservation Association (EECA). *Omnibus survey on the knowledge and interest in methods of generation, preferred methods of generation and views on wind power*. Wellington: UMR Research; 2004.
 9. Berg C. *Minimising Community Opposition to Wind Farm Developments in New Zealand* [Master of Science]. Wellington: Faculty of Science, Victoria University; 2003.
 10. Brauholtz S. *Public Attitudes to Wind Farms. A Survey Of Local residents In Scotland*. Edinburgh: MORI Scotland; 2003.
 11. RBA Research. *Lambrigg Residents Survey, Lambrigg Wind Farm*. Leeds: RBA Research; 2002.
 12. O'Grady D. Public Attitudes Toward Wind Energy in Western North Carolina, A Systematic Survey. Paper presented at: The 2002 N C Wind Summit; 9 December, 2002; Boone, NC.
 13. Genesis Energy Ltd. *Awhitu Wind Farm Resource Consent Application and Assessment of Environmental Effects*. Wellington: Genesis Energy Ltd; 2004.
 14. Genesis Energy Ltd, Franklin District Council. *Document 1.654-1.665. Resource Management Act 1991, Section 96 making of submissions to notified applications for resource consent between Genesis Power and Franklin District Council*. Wellington: Genesis Energy Ltd & Franklin District Council; 2004.
 15. Waiuku Wind Farm Information Group. *Public Notice*. Franklin: WWIG; 2004.
 16. Waiuku Wind Farm Information Group. *Kohekohe-Karioitahi Rd Survey People Supporting or Against Wind Farm Proposal, Awhitu Wind Farm Resource Consent Application Submission*. Franklin: WWIG; 2004.
 17. Environment Court. Statement of Evidence of Diane Jean Lucas on behalf of the Karioitahi Equestrian Environmental Protection Society (KEEPS) Incorporated and the Waiuku Wind farm Information Group Incorporated. In: Environment Court ENV A 376/04 and 392/04 between Genesis Power Limited and the Energy Efficiency and Conservation Authority (Appellants) and Franklin District Council (Respondent). Auckland: Environment Court; 2004.

18. Hobbs M. *Makara Survey on Wind Energy*. Wellington: MP, New Zealand Governmnet; 2004.
19. Leventhall G. *Notes on Low Frequency Noise from Wind Turbines with special reference to the Genesis Power Ltd Proposal, near Waiuku NZ*. Ashtead Surrey 2004.
20. Statistics New Zealand. Waiuku Community Profile. *Statistics New Zealand*. Available at: <http://www2.stats.govt.nz/domino/external/web/CommProfiles.nsf/FindInfobyArea/526101-au>. Accessed 27 July, 2005.
21. Kish L. *Survey Sampling*. New York: Wiley; 1965.
22. Rothman K, Greenland S. *Modern Epidemiology*. 2nd ed. Philadelphia: Lippincott-Raven; 1998.